**Faculty of Science and Engineering**
**Department of Applied Geology**

# Late Quaternary Evolution of Western Australian Continental Shelf Sediment Systems

**Giada Bufarale**

**This thesis is presented for the Degree of**
**Doctor of Philosophy**
**of**
**Curtin University**

**December 2018**

# Declaration

To the best of my knowledge and belief this thesis contains no material previously published by any other person except where due acknowledgment has been made.

This thesis contains no material which has been accepted for the award of any other degree or diploma in any university.

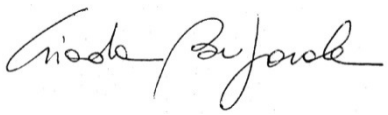

Giada Bufarale

Date: Perth, 12/12/2018

# Abstract

The western coast of Australia is characterised by a north-south trending continental margin, extending from 35° S to 13.5° S and spanning a temperate regime in the south to a tropical regime in the north. The mainland coastline and offshore islands have a total length of over 20,000 kilometres. This geographic extent has resulted in a range of climatic, oceanographic, environmental and geological regimes that have greatly influenced the geomorphic and sedimentological evolution of the continental shelves and coastlines during the Quaternary.

This thesis aimed to provide a comprehensive investigation of the sedimentary and geomorphic development and evolution of the Western Australia (WA) coastline and inner continental shelf, during the Late Quaternary. This period experienced major fluctuations in global climate and sea level, with continental shelves becoming exposed during glacial periods and then flooded, as the Earth warmed and ice sheets collapsed. The most recent deglaciation (18,000 to 8,000 years Before Present, BP) saw sea levels rise ~120 m, flooding the shelf with coastlines retreating tens to hundreds of km to their present positions.

Four important but under-investigated settings, encompassing a range of depositional environments, were selected for this study, including (1) the tropical Southern Kimberley coast, (2) the subtropical meta/hypersaline Shark Bay, (3) the Swan River estuary and (4) the temperate Geographe Bay. Whilst a multidisciplinary approach to data collection and analysis was taken in each area, geophysical (shallow seismic) techniques were the fundamental method of data gathering, as they represent an excellent tool to map surficial geomorphological and sub-surficial geological and sedimentary features. The choice of the investigation methods was usually site specific. In Shark Bay, a parametric sub-bottom profiler was the most appropriate technique for penetrating a 10 m-section of moderately soft sediments, within very shallow-water settings. A more powerful seismic source (boomer sub-bottom profiler) was needed in order to penetrate and analyse the carbonate platform and coral reef systems in the Kimberley region, the estuarine environment of the Swan River and the indurated limestone shelf in Geographe Bay. In these cases, the goal was to acquire relatively deep sedimentary horizons and hence a stronger vertical penetration was required.

Generally, in each sedimentary system considered, seismic profiles were combined with high-resolution remote sensing imagery (Light Detection and Ranging – LiDAR bathymetry and high-resolution satellite and aerial photos) and sedimentological information (where available), in order to correlate surficial sediment bodies, internal architecture and lithofacies. By integrating these data with age information (such as radiocarbon dating), models of system evolution have been then proposed for each of these logistically and scientifically challenging locations.

The following section summarises the key findings achieved for the investigated environments, which can be considered geographic and scientific frontiers.

## Kimberley

The inner shelf Kimberley Bioregion (northwest Australia) is characterised by a macrotidal setting where prolific coral reef growth has developed around a complex drowned landscape. High-resolution shallow seismic studies were conducted across various reef settings in the Buccaneer Archipelago, Montgomery and Molema Islands to evaluate stratigraphic evolution, morphological patterns and reef distribution. Reef sites were chosen to assess most of the reef types present, particularly high intertidal planar reefs and fringing reefs. The internal acoustic reflectors of the reefs were identified according to their shape, stratigraphic position and characteristics. Two main seismic horizons were identified marking the boundaries between Holocene reef (Marine Isotope Stage 1, MIS 1, last 12 ky), commonly 10-20 m thick, and MIS 5e (Last Interglacial, LIG, ~125 ky, up to 12 m thick) and Proterozoic rock foundation over which Quaternary reef growth occurred.

This research achieved the first regional geophysical study of the Kimberley reefs. Sub-bottom profiles demonstrated that the surveyed reefs are characterised by a multiple reef build-up, indicating that coral reef growth occurred in the Kimberley during previous sea level highstands. The data also showed that antecedent substrates and regional subsidence have influenced and controlled the amount of accommodation available for reef growth and control the morphology of the successive reef building stages. In addition, the study showed that in spite of macrotidal conditions, high-turbidity and frequent high-energy cyclonic events, corals have exhibited prolific reef growth during the Holocene, developing significant reef accretionary structures.

## Shark Bay

The analysis of seismic stratigraphy and remote sensing analysis, combined with core sampling and radiocarbon dating, has demonstrated the interconnection between sediment body morphologies, seagrass related substrates and pre-existing topography within the Faure Sill channel-bank complex (Shark Bay). Sea-level fluctuations appear to have largely controlled the evolution of the bank and can be summarised in the following three main stages. 1) After 8.5 – 8 ky BP, when sea level was ~11 m below the present, in a transgressive setting, seagrass establishment progressively contributed to initiating bank growth, by binding and trapping sediments and producing muddy carbonate deposits. 2) Around 6800 years BP, the bank elevation reached its apex, in conjunction with a +2 m highstand of sea level. 3) During the Late Holocene, following a decline of sea level to present, the bank vertical growth slowed down but the sedimentation continued filling channels and topographic lows. Average accumulation rates of the bank (1.3 m/ky) conform to previous estimates derived for seagrass banks but rates are strongly facies dependent, attesting to the dynamic nature of this channel-bank complex. The extensive seagrass meadows have been and remain essential for the Shark Bay area. For instance, not only are seagrasses particularly important for the entire shallow benthic ecosystem (by providing shelter and food for numerous species), but they also had a major role in determining the development of oolitic shoals, stromatolites and microbial mats in Hamelin Pool and L'Haridon Bight, by limiting the

water exchange between the southern basins and the open ocean and hence contributing to the onset of hypersaline conditions, associated with these facies.

## Swan River

High-resolution seismic profiles were conducted across the metropolitan area of the Swan River estuary (Perth, Western Australia) to explore the sub-surficial stratigraphic architecture, down to a depth of about 40 m below the river bed. The acoustic profiles revealed a complex system of palaeochannels where three main unconformities bound as many seismic units over the acoustic basement. Integrating these data with sediment borehole analysis, LiDAR data and the available literature of the geology and stratigraphy of the area, it was possible to determine the development of these stratigraphic units, in response to Late Pleistocene and Holocene sea-level fluctuations and conditioned by pre-existing topography and depositional palaeoenvironments during the last ~130,000 years.

The deepest unit is interpreted as the Perth Formation, which consists of interbedded sediments that were deposited in a large palaeo-valley that incised into the underlying acoustic basement (bedrock: Tamala Limestone and Kings Park Formation), under a fluvial to estuarine setting, existing between ~130 and 80 ky BP (in the Last Interglacial). The middle unit, composed of heterogenic fluvial (possibly lacustrine) and estuarine sediments, represents the Swan River Formation. Similarly to the Perth Formation, the formation infills channels incised in older formations and reflects the hydrogeological conditions linked with sea-level fluctuation changes during the Last Glacial low-stand. Holocene (last ~10 ky) fluvial and estuarine deposits form the shallowest unit. These sediments have a highly variable internal structure, ranging from stratified deposits to hard and chaotic units, atop pre-existing topographic highs.

This research represents the first environmental high-resolution acoustic investigation in the middle reach of the Swan River estuary. The data indicated that, like several other examples around the world, for instance Burrill Lake (NSW, Australia) and Arcachon Lagoon (Aquitaine, France), the geomorphic record of Late Pleistocene and Holocene sea-level fluctuations in the metropolitan area of the Swan River is characterised by a series of palaeochannels, which developed during glacial lowstands of sea level, and related channel-fill deposits which formed during interglacial highstands.

## Geographe Bay

High-resolution shallow seismic profiles collected along the inner shelf in Geographe Bay (south-west Australia) exposed a highly-variable buried sedimentary architecture. Three main acoustic units have been inferred, corresponding to different geological facies, deposited under various sea level conditions. The acoustic basement (Unit B) belongs to the Early Cretaceous Leederville Formation; the middle unit is attributable to Tamala Limestone (Unit P, Late-Mid Pleistocene) and the top unit (Unit H) is Holocene in age. Combining the seismic data with high-resolution bathymetry and sediment grabs, several surficial and buried

morphological features are revealed, including sandbars, palaeochannels and ridges.

The shore-oblique sandbars have been directly influenced by local hydrodynamics including wave direction and currents, seagrass and sediment size. The palaeochannels (buried and surficial) are the expression of previous sea level lowstands. Two sets of shore-parallel, low-relief ridges, located at a depth of ~7 m and ~20 m, are relict landforms that are most likely regressive beach ridges and sub-littoral deposits (paleo-dunes), belonging to the Tamala Limestone formation. These geomorphological structures were formed during Late Pleistocene relatively high sea level stages (late Marine Isotope Stage 5e and 5c, respectively), cemented when the sea level was lower and subsequently subject to transgressive erosion.

The newly acquired seismic datasets established that the inner shelf is mainly covered by a thin veneer of sediments, above the Pleistocene hard surface, with the exception of the sandbars, where the sediment build-up can be up to 6 m in thickness.

## Summary

Together these regional studies highlight that the WA coast and shelf has significant morphological complexity with clear regional patterns controlled by:

1) Late Pleistocene and Holocene sea-level fluctuations (two marine transgressions and a major regression) which are recorded in multiple stages of reef build-up in the Kimberley and various seabed features, such as palaeochannels, submerged ridges and several distinct erosional and depositional features.
2) Pre-existing topography (weathered substrates, terranes and various stratigraphic and geological structures) that shaped the initial sedimentation, with highs and channels, and provided relict sediments, especially siliciclastic, that have been reworked into the systems today.
3) The local physical characteristics and processes that influenced the sediment production and distribution, in particular seagrass, local tides and currents.

Each of the regions studied during this thesis represents an iconic and geologically unique environment, with little published data describing the submerged landscapes, seascapes and sedimentary environments. None of these logistically and scientific challenging sites have been previously investigated using seismic equipment. Therefore, this study can be regarded as guidance for fieldwork and seismic acquisition strategies in analogous scenarios. The research provides a variety of pioneering datasets which can be considered as analogues for sedimentological and stratigraphic analysis of carbonate-siliciclastic settings, in WA and internationally. In addition, the knowledge gained from this project can assist in the formulation or enhancement of geological modelling for depositional settings, sequence stratigraphy and characteristics of potential or discovered hydrocarbon reservoirs, having comparable depositional, palaeogeographic and diagenetic histories.

# Acknowledgements

Many people have supported me, taught me and encouraged me during these years that have been studded with laughs and tears, gains and losses, achievements and failures.

I will start thanking my Mentor, the late Prof. Lindsay Collins, for me just *Professor*. An excellent scientist, an inspiring educator, a "*Rock" Legend*. Every word that I wrote, every data that I analysed and every conclusion that I draw has been inspired by my *Professor* and what he taught me. Thanks for everything and beyond.

I feel privileged to have been supported, supervised and inspired by Dr Mick O'Leary, my supervisor. With your contagious passion for geomorphology and marine science, you have always been able to give me the cleverest advises, with patient and genuineness. I am sure this thesis and all the accomplishments that I have achieved wouldn't have been the same without your help.

My colleague Alexandra Stevens…my friend Alex. I truly don't know how I could thank you for everything that you have done for me in the last …9 years (and counting)! Thanks for your English, ArcGIS tips, your data management...but most of all thank you for keeping me sane, inside and outside the office!

I am grateful for the supervision that Prof. Chris Elders has given me since 2015.

I would like to acknowledge the contribution of an Australian Government Research Training Program Scholarship in supporting this research.

This work wouldn't have been possible without the collaboration of many colleagues, in particular Ricardo Jahnert, Moataz Kordi Tubagus Solihuddin. Thanks for your muscles, brain and eyes during the field trips around our amazing coast (and back in Uni). Every survey has also been possible thanks to many people that helped me. Special thanks are in the acknowledgements of each chapter/manuscript. However, thank you again for your time, efforts and unconditioned help!

Working in the field has been truly amazing, but my time in the office has been as much wonderful, thanks to many office and department colleagues. The list is long but I would like to thank in particular Therese Morris (your geological knowledge is endless…like your friendship!), Mehrooz Aspandiar, Annette Labrooy and Andy Wieczorek (for your constant administrative and logistic help), Sira Tecchiato, Milo Barham, Jane Cunneen, Sam McHarg, Tanya Claridge, Gretchen Benedix-Bland, and Prof. Krishna Sappal.

A special acknowledgement goes to the Society of Underwater Technology, in particular Dr Liz Lawlor, my fellow committee members and the staff in Perth office. I feel I won much more than a scholarship and what I have learnt with you is priceless.

I would like to thank Kathy Deubert for her smiles, sweetness and being unique.

I have many people that helped and encouraged me before, during (and after) this thesis, from Italy to Australia (through Dubai!). It would be impossible to name all of them, but thanks for making my life better.

I have always known that I would be a scientist when I grew up. I also know it would have been impossible without the encouragement, faith and everlasting love of my parents Ivana and Mario. I have to thank in particular my father that shared with me the passion for ocean and rocks, that first took me to the sea when I was a toddler, that scuba-dived with me during my MSc thesis. I am sure you watched over this thesis too.

Finally, my most heartfelt thanks go to my husband Giovanni De Vita. In every manuscript I thanked you “for your technical advises”, but you did so much more. You pushed me to do this PhD, you taught me every single secret of seismic acquisition, you have been (and still are) my 24/7 technical support. You instilled in me the importance to be meticulous (or picky), triple check always everything, do many backups. And for all of this, I will always be grateful. My life would never have been so full (and wonderful) without you Vanni (and our little ball of fur Reef)…but I’ll say the rest in Italian…

“The sea is everything. It covers seven tenths of the terrestrial globe. Its breath is pure and healthy. It is an immense desert, where man is never lonely, for he feels life stirring on all sides. The sea is only the embodiment of a supernatural and wonderful existence. It is nothing but love and emotion; it is the Living Infinite. ”
(Jules Verne, 20,000 Leagues under the Sea)

*I dedicate this thesis to my husband Vanni that has shared with me all the joys and sorrows and*
*to my father Mario and my Professor Lindsay that couldn't see the end of this journey…*

# List of publications included as a part of this thesis

This dissertation compiles a collection of research papers that were either published, in press or under review at the time of writing this thesis document. The objectives and relationship amongst the various papers are described in the *Introduction* chapter.

The *Discussion* chapter summarises the papers and place the outcomes in a wider context (Western Australia).

The final chapter *Conclusions* presents the key outcomes obtained during this PhD research and summarise the main findings.

The research papers contained within this thesis are the following (see in Appendix A):

**Bufarale, G.**, Collins, L.B., 2015. Stratigraphic architecture and evolution of a barrier seagrass bank in the mid-late Holocene, Shark Bay, Australia. Mar. Geol. 359, 1–21. https://doi.org/10.1016/j.margeo.2014.11.010

**Bufarale, G.**, Collins, L.B., O'Leary, M.J., Stevens, A., Kordi, M., Solihuddin, T., 2016. Quaternary onset and evolution of Kimberley coral reefs (Northwest Australia) revealed by high-resolution seismic imaging. Cont. Shelf Res. 123, 80–88. https://doi.org/10.1016/j.csr.2016.04.002

**Bufarale, G**., O'Leary, M., Stevens, A. and Collins, L.B., 2017. Sea level controls on palaeochannel development within the Swan River estuary during the Late Pleistocene to Holocene. CATENA, 153, pp.131-142. https://doi.org/10.1016/j.catena.2017.02.008

# List of additional relevant publications

The publications listed below were either not prepared and published during the time of this thesis, peer reviewed or I was not the first author, and so do not form part of the main thesis.

## Papers (peer-reviewed, see in Appendix B)

Collins, L.B., O'Leary, M., Stevens, A., **Bufarale, G.**, Kordi, M., Solihuddin, T., 2015. Geomorphic patterns, internal architecture and reef growth in a macrotidal, high-turbidity setting of coral reefs from the Kimberley bioregion. Aust. J. Marit. Ocean Aff. 7, 12–22. DOI:10.1080/18366503.2015.1021411

Solihuddin, T., **Bufarale, G.**, Blakeway, D. and O'Leary, M.J., 2016. Geomorphology and late Holocene accretion history of Adele Reef: a northwest Australian mid-shelf platform reef. Geo-Marine Letters, pp.1-13. DOI 10.1007/s00367-016-0465-3

**Bufarale, G.**, O'Leary, M., Collins, L.B., Stevens, A., Kordi, M., Solihuddin, T., 2016. Geomorphology and Holocene Evolution of Kimberley Coral Reefs. Proceedings of the 13th International Coral Reef Symposium - Coral reef records of sea level, climatic and environmental changes: a tribute to Lucien Montaggioni, Honolulu: 243-253.

## Conference presentations and extended abstracts

Growth history of Faure Sill seagrass bank, Shark Bay, during changing sea levels: oral presentation at Coast to Coast Conference, Mandurah, Australia, October 2014. Extended abstract published in Conference Proceedings: Coast to Coast Conference 2014: Coastal Knowledge for Coastal Change. ISBN-10: 0994357206, p 1-5.

Subbottom profiling and growth patterns of Kimberley coral reefs, North West Australia: poster presentation at Coast to Coast Conference Mandurah, Australia, October 2014. Best Poster Award.

Subbottom profiling and growth patterns of Kimberley coral reefs, North West Australia: oral presentation at Royal Society of WA Postgraduate Student Conference, Crawley, Australia, 2014. Extended abstract published in: WA Science, Volume 98, part 1, June 2015.

Mid-Late Holocene evolution of a carbonate-clastic barrier bank, during changing sea levels (Shark Bay, Western Australia): poster presentation at the IGSC, Prague, Czech Republic, 2015. Best Poster Award. Extended abstract published in Conference Proceedings: 6IGSC Prague: Crossing the Boundaries, p 55-57.

Late Quaternary sea level effects on coral reef evolution and growth in Southern Kimberley, North West Australia: oral presentation at the 6IGSC, Prague, Czech Republic, 2015. Extended abstract published in Conference Proceedings: 6IGSC Prague: Crossing the Boundaries, p 25-27.

Mid-Late Holocene Development of the Mixed Carbonate Clastic System of the Faure Channel-Bank Complex and Wooramel Delta (Shark Bay, Australia): poster presentation at the 2015 ICE AAPG/SEG, Melbourne, Australia, 2015. Extended abstract published in in Conference Proceedings: AAPG/SEG International Conference and Exhibition: Energy for the Next Fifty Years.

Late Pleistocene and Holocene Reef Growth in Southern Kimberley, North West Australia: oral presentation at the 2015 ICE AAPG/SEG, Melbourne, Australia, 2015. Extended abstract published in in Conference Proceedings: AAPG/SEG International Conference and Exhibition: Energy for the Next Fifty Years

Stratigraphic architecture and evolution of a barrier seagrass bank in the mid-late Holocene, Shark Bay, Australia: oral presentation at the Royal Society of WA Postgraduate Symposium, Murdoch, Australia, 2015. Extended abstract published in: WA Science, Volume 98, part 2, December 2015.

Stratigraphic architecture and evolution of a barrier seagrass bank in the mid-late Holocene, Shark Bay, Australia: oral presentation at the SEG / AAPG International Conference & Exhibition (ICE), Barcelona, Spain, 2016.

Geomorphology and Holocene evolution of Kimberley coral reefs: oral presentation at the 13$^{th}$ International Coral Reef Symposium (ICRS), Honolulu, USA, 2016.

New insights into the geomorphic evolution of Geographe Bay, South-West Australia: oral presentation at the 1st State NRM and Coastal Conference, Bentley, Australia, 2017.

Sea-level controls on buried geomorphology within the Swan River Estuary during the Late Quaternary: poster presentation at the 18$^{th}$ International Association for Mathematical Geosciences (IAMG) Conference, Fremantle, Australia, 2017

## Reports

Collins, L.B., **Bufarale, G.**, and Rajah-Kanagasabai, S., 2014. Shark Bay Analogues Project: evolution of the Faure Sill. Report 2014/03. Prepared for Woodside Energy Limited.

Collins, L.B., O'Leary, M., Stevens, A., **Bufarale, G.**, Kordi, M., Solihuddin, T., 2015. Final Report of Project 1.3.1 of the Kimberley Marine Research Program Node of the Western Australian Marine Science Institution, WAMSI, Perth, Western Australia, 246 pp.

# Statement of contributions of others

This thesis was supported by Curtin University through Australian Postgraduate Award (APA), Curtin Research Scholarship (CRS) and Faculty Postgraduate Award (FPA). Several institutions and private organisations also funded this research program, including Western Australia Marine Science Institution (Kimberley, Chapter 2), Woodside and the Browse Joint Venture partners (Shark Bay, Chapter 3), Swam River Trust (Swan River estuary, Chapter 4) and Department of Transport (Geographe Bay, Chapter 5).

Field excursions, especially seismic surveys, undertaken for this doctoral thesis were carried out in collaboration with colleagues and supervisors listed in each chapter. However as the primary author of this thesis, and related published manuscripts, I have been responsible for the acquisition, analysis and post-processing of the data, and their interpretation. A written statement of co-authors contribution is provided in Appendix C.

Student : Mrs Giada Bufarale

Signature : 

Date : 19/02/2018

Supervisor : Dr Michael J. O'Leary

Signature : 

Date : 19/02/2018

Co-Supervisor : Professor Chris Elders

Signature : 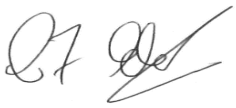

Date : 19/02/2018

# Table of Contents

# List of Figures

# List of Tables

# Chapter 1

# Introduction

"We are all visitors to this time, this place. We are just passing through. Our purpose here is to observe, to learn, to grow, to love, and then we return home"
(Aboriginal proverb)

## 1. Rationale

Continental shelves are defined as "flat or gently sloping regions adjacent to a continent or around an island that extend from the low water line to a depth, generally about 200 m, where there is a marked increase in downward slope" (IHO, 2013. Page 26). Their width and depth can vary considerably according to their processes of origin (Figure 1.1), but generally they extend from the shoreline, gently dipping to the edge of the outer margin, marked by the shelf break (continental slope. Niedoroda, 2005; Larcombe, 2007). Plate tectonics and geodynamics are the fundamental processes (called *endogenous*) that controls the mean continental shelf width and slope, with the passive margins (like the Western Australian one) being the most extensive shelves, where thick sediment accumulations, supplied by broad drainage systems, are developed seaward (Larcombe, 2007). Shelf geomorphology is also influenced by *exogenous* processes including glaciations and related glacio-eustatic sea level changes (also comprising glacial erosion and glacio-isostatic processes), fluvial and biogenic sediment supplies (including coral reef growth) and hydrodynamic processes influencing the erosion and transport of sediments (Harris and Macmillan-Lawler, 2016).

Australia's Indian Ocean continental shelf and coast, from Geographe Bay to the Southern Kimberley, are located along a passive margin (Falvey and Mutter, 1981). Due to this position, away from the Indian Ocean's spreading centre, Western Australia (WA) can be considered relatively tectonically relatively stable since marine isotope stage (MIS) 5e (~1.0 m of tectonic uplift around Cape Cuvier and ~15 m of subsidence in the Southern Kimberley. Szabo, 1979; Baker et al., 2005, Collins et al., 2006; O'Leary et al., 2008; Solihuddin et al., 2015). In addition, since Australia's western border is located far enough from the former glacial maximum ice sheets, the vertical displacement as a result of glacio-isostatic processes can also be considered small (~1.0 m. Stirling et al., 1995; O'Leary et al., 2013, Murray-Wallace and Woodroffe, 2014; Lambeck et al., 2014).

Inland WA is occupied by hot and arid deserts and the West Coast covers several climatic regimes, including tropical, grassland and temperate (BoM, 2005). This variety of climatic conditions greatly impacts the types of rivers and waterways along the coast. Whilst in the tropical Kimberley, relatively large rivers (such as the Fitzroy

River) have a reasonable annual discharge (up to 9,000 gigalitres. DoE-WA, 2004) and represent a significant source of terrigenous sedimentation into the ocean, the majority of the WA coast lacks major drainage systems (i.e. average annual flows: Blackwood River, 740 gigalitres; Gascoyne River, 766 gigalitres; Swan River, 506 gigalitres. DoE-WA, 2004), and hence the shelf can be considered sediment-starved, in terms of allochthonous terrigenous sediment supply (McMahon and Finlayson, 2003; Brooke et al., 2017). In contrast, WA continental shelf has an extensive carbonate production, dominated by coralline algae, bryozoans, molluscs and foraminifers, in mid-latitude, cool waters, and coral reefs in high-latitude, warm waters, resulting in a carbonate-dominated shelf (James and Bone, 2011; Brooke et al., 2017).

The WA continental shelf is very broad and relatively shallow (up to 250 m of depth), with a width ranging from several hundred kilometres in the North West to less than 10 km off Ningaloo Reef (Brooke et al., 2017).

In this context of tectonic stability, scarcity of terrigenous input and low-gradient morphology, the shoreline and shelf morphology have been preserved and represent potential archives of Late Quaternary sea level changes and seascape evolution (Brooke et al., 2017). Thus, the study of these elements, by employing high-resolution remote sensing and seismic imaging and sediment analysis, will help to better understand the mechanisms governing deposition along the western margin of Australia and evaluate the impacts that sea level rise and fall had on the coast and inner shelf (from the shore-line to about ~10 km seaward), since MIS 5e.

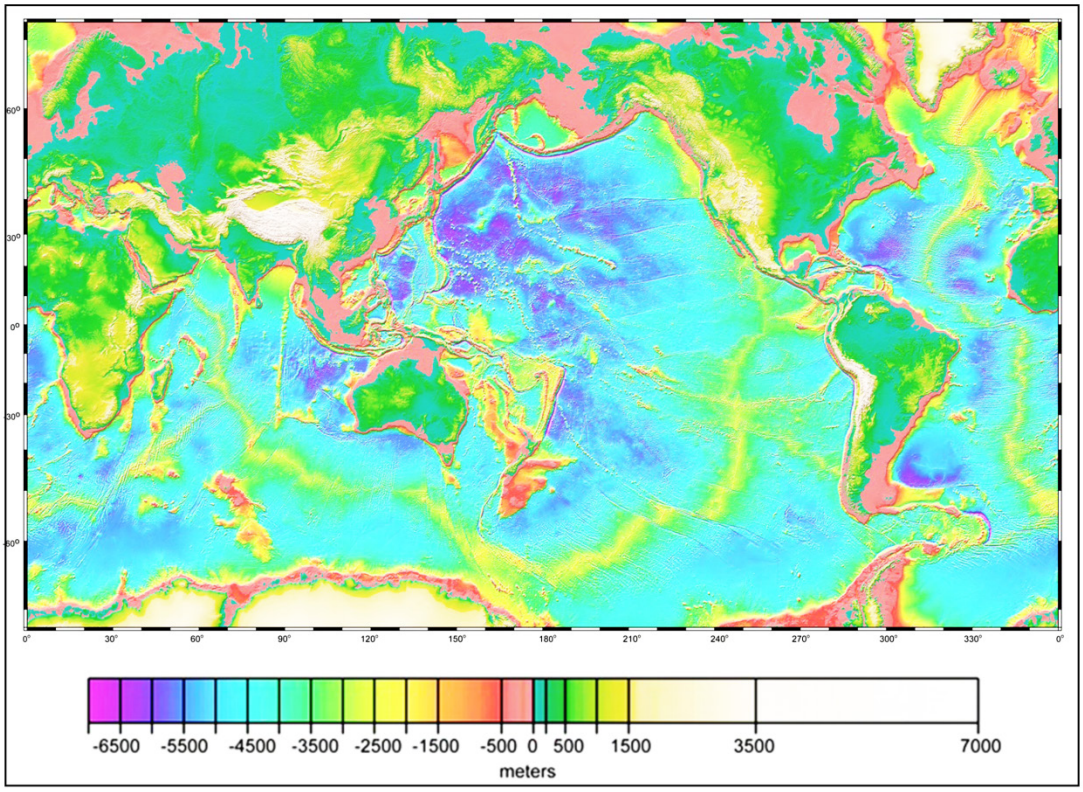


**Figure 1.1. Global topography (land elevation and ocean depths, in metres) with modern continental shelves marked in pink (from 0 to -200 m below mean sea level). Modified after**

**Smith and Sandwell, 1997 and https://www.ceoe.udel.edu/research/affiliated-programs/wind-power-program/mapping-resources/world, 30 October 2017.**

## 2. Aims and research objectives

The main research objective of this doctorate was to investigate how the sea level and climate changes over a single glacial cycle (from ~130 thousand years ago to present) have controlled the evolution of Australia's Indian Ocean continental shelf into its modern form.

The research thesis is divided into four sub-projects, focusing on the following contrasting marine environments: the coral reefs of the Southern Kimberley coast, the mixed carbonate-clastic system of the Faure Sill (Shark Bay), the Swan River estuary and the inner continental shelf in Geographe Bay. Each of these regions represents a geologically unique environment; with little published data describing the submerged landscape, the buried architecture and depositional history of these sedimentary settings, the outcomes of this research have generated a better knowledge of the local sedimentological and sequence stratigraphy.

This investigation takes a multidisciplinary approach that required the collection, analysis and combination of a varied range of datasets:

1. Remote sensing images, to establish the regional surficial geomorphology and substrate distribution patterns;
2. High-resolution seismic imaging, using different sub-bottom profiling systems, to determine the seabed architecture below the seafloor;
3. Sediment sampling and analysis, including dating, to obtain the chronology and climate history of the studied sedimentary systems.

This approach first required the interpretation and reconstruction of the antecedent shelf substrate, which includes the landforms existing prior to post-glacial flooding, such as ancient river valleys, plateaus, estuaries and coastal ridges. The second step was to characterise the marine landforms and habitats that have developed over this topography, like coral reefs, sand shoals, seagrass banks, channels, etc. Lastly, it was possible to examine, in coral reefs for instance, the timing of reef initiation, grow rates and style and how this related back to changes in climate and sea level which followed the flooding of the shelf.

## 3. Thesis structure

This dissertation comprises 8 main chapters, including:

**Chapter 1:** *Introduction*. This chapter introduces the aims and the research objectives for the study and provides a brief literature review of the state-wide coastal settings, including geology, climate and marine ecosystems. In each of the following chapters, more detailed local aspects are included.

**Chapters 2 to 5:** *Body of the thesis*. Each chapter is a stand-alone manuscript and includes aspects of the regional setting, methods, discussions of new findings, conclusion and cited references. The chapters are presented in geographic order, from tropical North to temperate South, and copies of the published papers can be found in the Appendix A at the end of the thesis manuscript, together with their

Copyright Clearance. The Kimberley study (Chapter 2. http://www.sciencedirect.com/science/article/pii/S0278434316301893) is published in *Continental Shelf Research*; the Shark Bay research (Chapter 3. http://www.sciencedirect.com/science/article/pii/S0025322714003557) is published in *Marine Geology*; Swan River investigation (Chapter 4. http://www.sciencedirect.com/science/article/pii/S0341816217300607) is published in *CATENA*.

**Chapter 6:** *Methods*. This chapter reviews and explains with a more technical approach the methods used during the data acquisition and post-processing, in particular the geophysical methodologies as they represent the primary data collection method used.

**Chapter 7:** *Discussion*. The purpose of this chapter is to put the Australia's Indian Ocean continental margin into an international context, critically acknowledge gaps in the data and understanding, and describe how the work has advanced the field. In addition, the analysis and the outcomes of the results obtained (Ch. 2 to 5) were compared to find common controlling parameters and draw conclusions about the Late Pleistocene and Holocene development of the continental shelf.

**Chapter 8:** *Conclusion*. This conclusive chapter summarises the major achievements of this thesis investigation and the new outcomes about the Late Quaternary evolution of each marine (or estuarine) area reported.

## 4. WA coastal setting

Following, there is a summary of the WA geological and climatic evolution and the metocean and biological conditions, in order to put each studied environment in a state-wide context.

### 4.1. Geology

The geological evolution of WA has a long history, spanning more than 4200 million years (Ma. GSWA, 1990). Archean and Proterozoic rocks dominate the mainland geology, with the Yilgarn Craton ranging from 3000 to 2500 Ma (Sircombe and Freeman, 1999) and the Pilbara Craton older than 3500 Ma (Buick at al., 1995). During this extensive period of time, long episodes of relative tectonic stability were interrupted by relatively short episodes of intense crustal growth (GSWA, 1990), including extensive eruption of basaltic volcanics, collisions forming orogenic belts and intense tectonic and magmatic activity. The intense weathering and erosion of the Kings Leopold and Halls Creek Orogens, which occurred between 2000 and 400 Ma, formed the sandstones that, with shales and basalts, infilled the Kimberley Basin (Short, 2005). Since the beginning of the Phanerozoic, nine more main basins have been established: Perth, Carnarvon, Canning, Browse, Bonaparte, Ord, Officer, Eucla and Bremer Basins, with the first three covering much of the western border of Australia (and the study areas considered in this thesis. Veevers, 1971. Figure 1.2).

The Perth, Carnarvon, Canning basins become progressively younger southward and go from entirely marine deposits in the north (Canning Basin), through the

mixed Carnarvon Basin to non-marine in the south (Perth Basin). The divergence in age and sedimentary facies reflects different positions of the basins in Gondwanaland (Figure 1.2 and Figure 1.3. Veevers, 1971; GSWA, 1974).

In the Early Jurassic, the Gondwanan supercontinent developed grabens and faults, separating India from WA and opening up the Indian Ocean (GSWA, 1990). The rifting initiated in the north western corner of the modern WA and progressed anticlockwise during the entire Cretaceous, forming proto- western (140-65 Ma) and southern coastlines of Australia (from 120 Ma. Short and Woodroffe, 2009). While drifting and moving northward, the WA climate changed significantly, going from mainly moist in the Late Cretaceous – Paleogene (temperate to tropical) to arid during the Neogene, alternating arid and humid during the Plio-Pleistocene (due to the glacial and interglacial cycles), to the modern relatively dry conditions (GSWA, 1990).

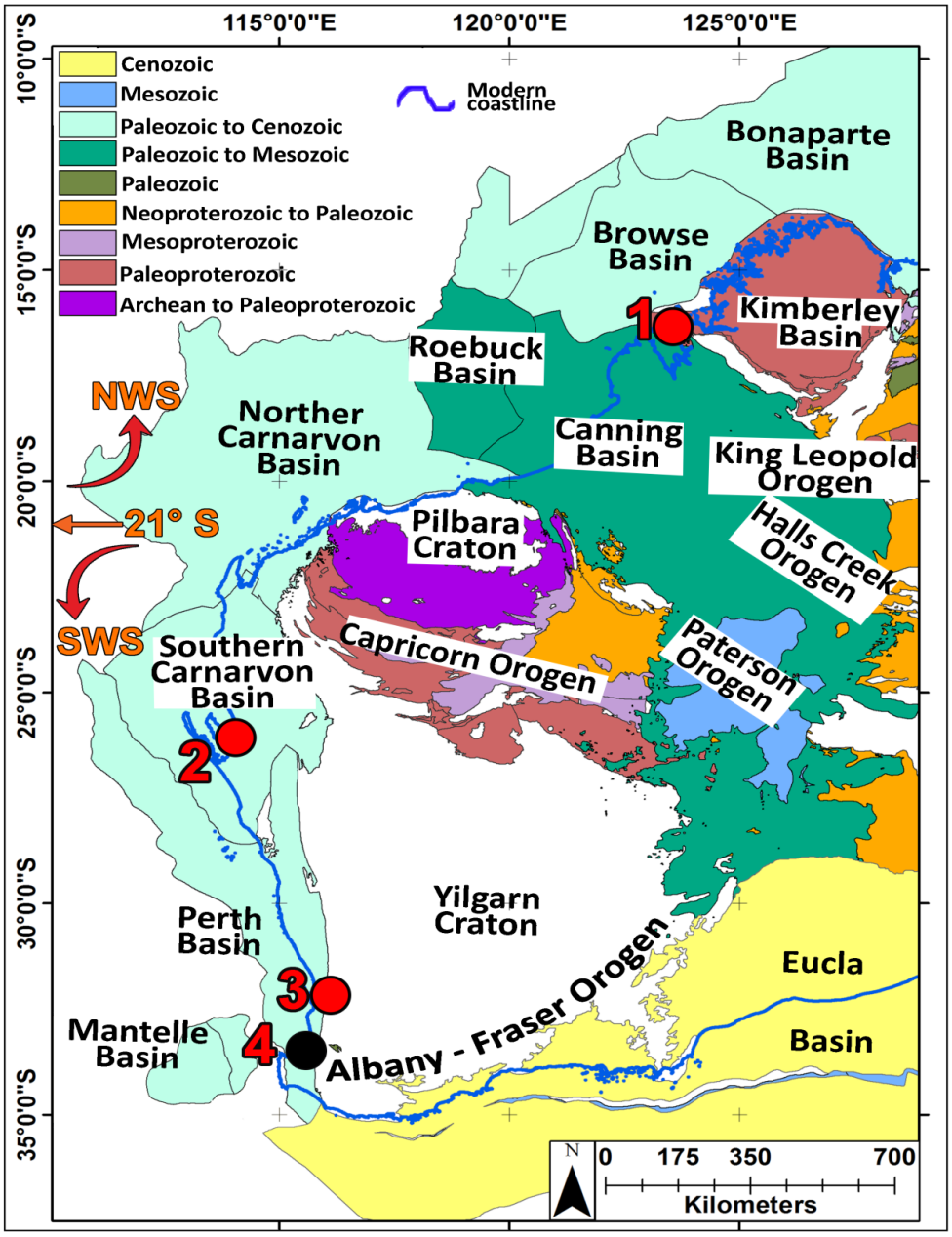

**Figure 1.2 (previous page). Distribution of cratons, main orogens and principal coastal and offshore basins of Western Australia. Note, names of inland basins are not shown (modified after GSWA, 1990. Metadata are from http://www.ga.gov.au/metadata-gateway/metadata/record/74371/). Red dots indicate the locations of the environmental systems studied. From north to south: 1 Southern Kimberley, 2 Shark Bay, 3 Swan River, 4 Geographe Bay. NWS: North West Shelf; SWS: South West Shelf.**

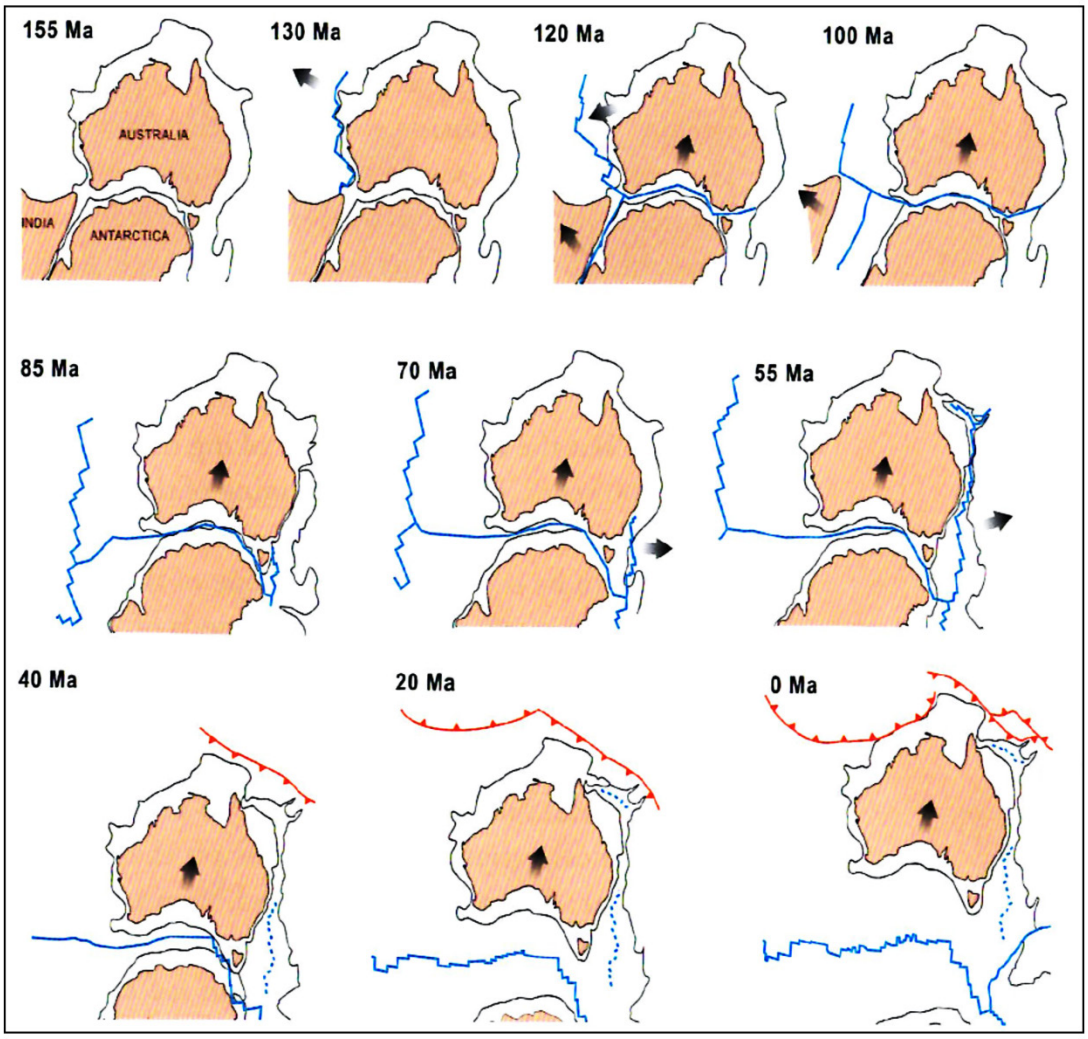


**Figure 1.3. Breakup and evolution of Gondwanaland to the modern settings. Arrows indicate the main movement direction of the continents; blue lines show active marine spreading (dashed lines: inactive); red lines represent the subduction zones; black lines mark the edge of the continental shelves and plates (Short and Woodroffe, 2009).**

## 4.2. Quaternary climate and sea-level fluctuations

The Quaternary has been characterised by several orbitally-induced variations of the global climate, at different latitudes, that affected the temperature and, consequently, the growth or melting of ice sheets. During glacial periods, a transfer of water mass from oceans to high latitude ice sheets (in addition to the permanent Antarctica and Greenland ice sheets. Pirazzoli, 1997) caused a relative fall in global sea level and a shoreline transgression outward across the continental shelf (Woolfe et al., 1998; Lambeck et al., 2002). The dry conditions associated with the glacial periods corresponded also to a dryer and windier global climate (Short, 2009). Aeolian processes became gradually more important, leading to the formation of

extensive aeolian dunes and silt and dust transport (Collins, 1987; Blewett et al., 2012). Conversely, during interglacial periods (as at present), the global climate was wetter and warmer, leading to a partial melting of the ice sheets. As the water returned to the oceans, the sea level progressively started rising, inundating the continental shelves (Pirazzoli, 1997).

The Quaternary climate and the induced sea level fluctuations (Figure 1.4), together with the modern climatic settings have contributed to the formation of the present near-shore environments.

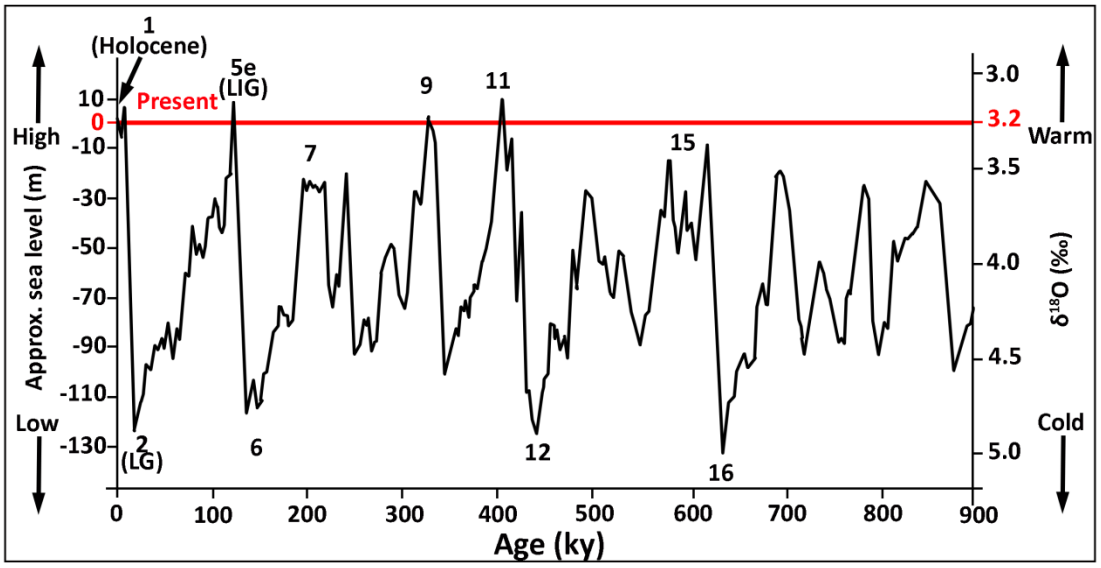


**Figure 1.4. Global changes in sea level height (based on the oxygen isotope index) for the last 900 ky. LG: Last Glacial, LIG: Last Interglacial. The numbers represent different Marine Isotope Stages (MIS). Modified after Saqab and Bourget (2015) and Blewett et al. (2012).**

## 4.3. Modern climate and metocean conditions

The wide latitudinal range of the western continental margin of Australia strongly influences the climatic conditions across the state; as a result, the latitudes indirectly control some of the factors that help influencing the coastal shape, such as wind and wave regimes, weathering processes and vegetation onset (like seagrasses, etc. Bird, 2011). The latitude 21° marks the boundaries between two distinct regions: the North West Shelf (NWS) and the South West Shelf (SWS or South West. Figure 1.2). These two distinct sections are reflection of major climatic and geological conditions. The climatic regimes span from tropical in NWS (including the entire Kimberley region), characterised by summer monsoons, to temperate in the South West, with Mediterranean-type seasonal cycles (Figure 1.5, based on the Köppen classification system. BoM, 2005).

The average rainfall and temperature patterns vary considerably, in relation to the climatic regimes and latitudinal gradation (Short, 2005). The tropical northwest and the temperate southwest are humid, with annual rainfall up to 600 mm; in contrast, the central area (from Shark Bay to the southern border of the Kimberley) is largely arid and dry, receiving between 25 and 200 mm of rain, per annum. There is also a marked contrast of wet/dry seasons, between north and south. In the Kimberley, the

summer months (from December to February) are considerably wet, associated with the cyclone season. From Ningaloo Reef, southward, the rainy season spans instead from June to August (BoM, 2005; Short, 2005; BoM, 2010; Bird, 2011. Figure 1.6).

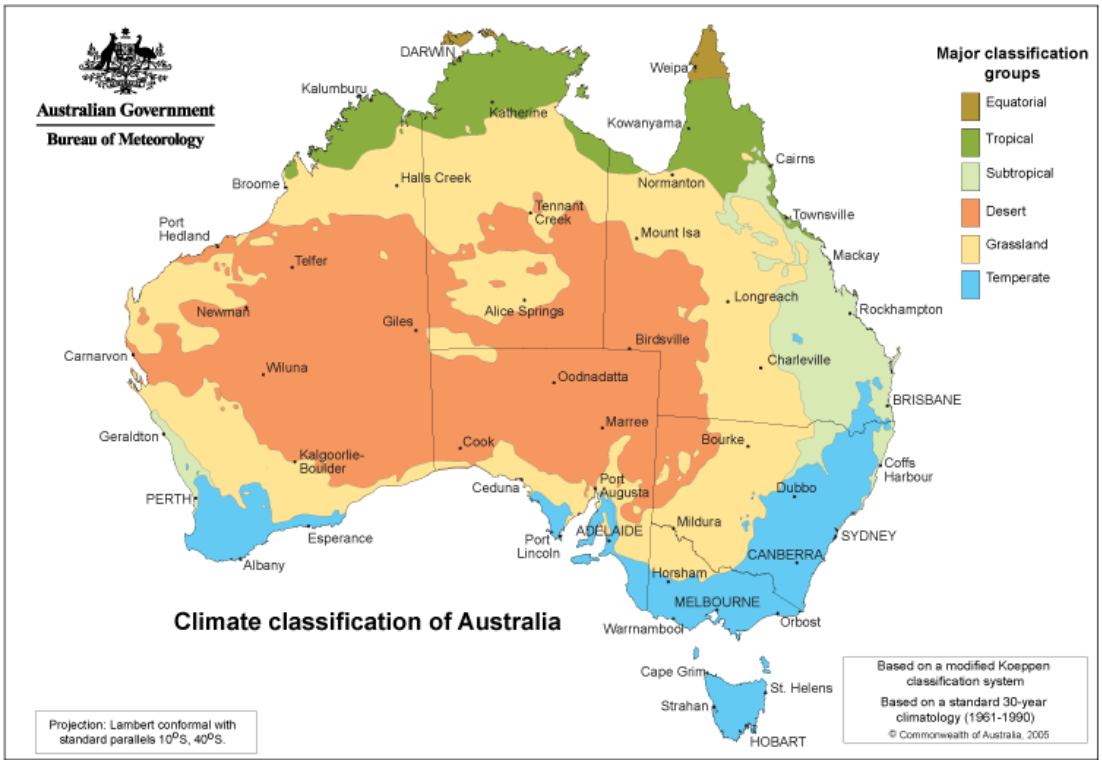


**Figure 1.5. Climate classification map of the Australian mainland based on the Köppen classification scheme (according to the native vegetation that characterises each zone. From BoM, 2005).**

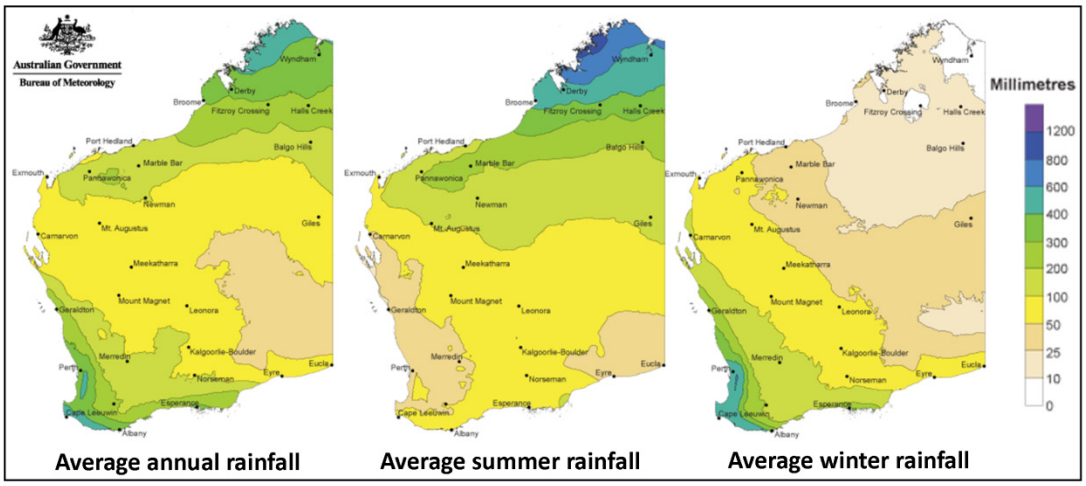


**Figure 1.6. WA rainfall patterns (from BoM, 2010).**

The annual and seasonal temperature patterns are illustrated in Figure 1.7. Similarly to the rainfall and climatic conditions, the temperatures also change with the latitude. On average, the Kimberley is 9 to 12 degrees warmer than the South West,

throughout the year. The temperatures are quite high in summer and mild to relatively cool in winter (above 10° C state-wide. Short, 2005).

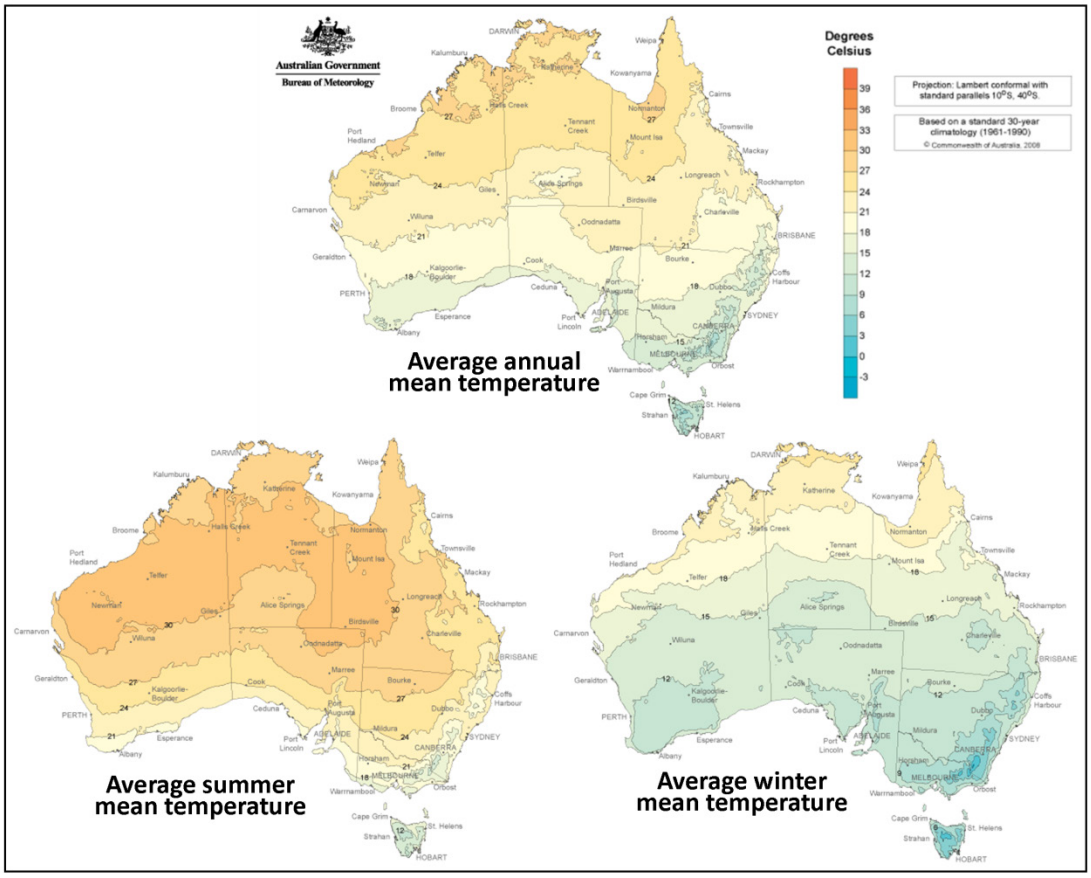


**Figure 1.7. Australian temperature variability (from BoM, 2008).**

The great climatic variability also controls the variations in water temperature, currents and winds (Evans et al., 2017).

The South-West and central regions, up to Shark Bay, are significantly influenced by the warm, low-density Leeuwin Current that flows southward on the ocean surface (Figure 1.8). The Leeuwin Current has an impact on the average sea surface temperature, resulting in relatively warm waters (20.8°C on average. Feng et al., 2003). The nutrient-depleted waters of the Leeuwin Current result in higher levels of light penetration, leading to high diversity of algal and seagrass species and benthic communities (Evans et al., 2017).

From Shark Bay to the Northern Kimberley, the coastal environments are instead greatly affected by the Indonesian Throughflow, a warm, low-nutrient, low-salinity oceanic current that originates along the Indonesian archipelago (Figure 1.8). The Indonesian Throughflow has a seasonal regime, flowing weaker during the Australian summer, contributing to the formation of cyclones (Evans et al., 2017). The central-northern section of WA coast is characterised by warmer waters (ranging from 22 to 28°C nearshore. Pearce and Griffiths, 1991).

Local winds and sea breezes have a significant influence on the local hydrodynamics of the inner continental shelf (usually on the order of ~15 km

seaward. Niedoroda, 2005; Larcombe, 2007), such as velocity and direction of coastal waves and currents, and these physical effects have impacts also on coastal sediment budget and nutrient transfer (Gallop et al., 2012). South-south westerly sea breezes are predominant in summer (Gallop et al., 2012); in winter, winds are generally northerly in the South-West and easterly in the North-West, producing a weaker sea breeze (Short, 2005; Gallop et al., 2012).

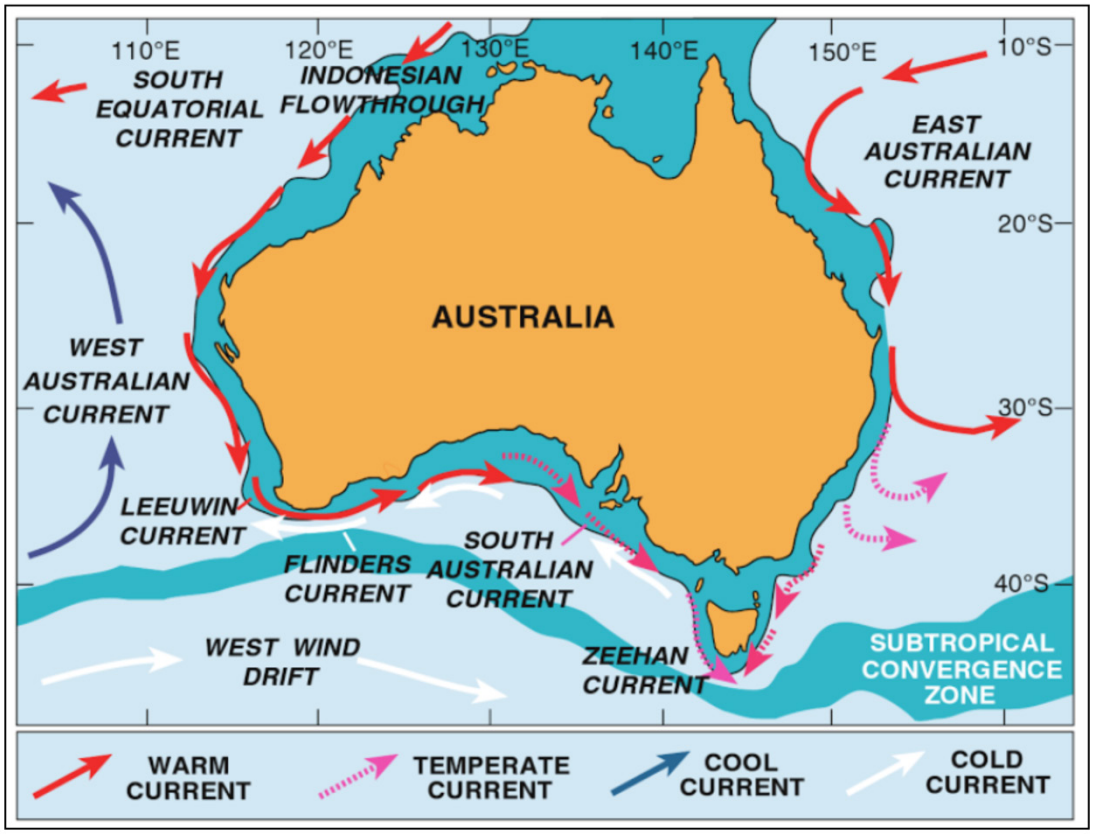


**Figure 1.8. Major currents surrounding Australian oceans (James and Bone, 2011).**

The tidal ranges also vary considerably from north and south WA (Figure 1.9). Ningaloo Reef and the Exmouth Gulf mark the separation between micro-tidal ranges (< 2 m) at higher latitudes, and mid- to macro-tidal ranges (2-4 m and > 6 m, respectively) in the tropics. The South-West is characterised by very low tidal ranges, with spring tides that varies between 0.6 and 1.4 m (Short, 2005). The tidal range increases northward, culminating in the Kimberley, in particular in King Sound, where with a maximum spring tide of 12.5 m, the tidal ranges are the highest in Australia and amongst the highest ocean tides in the world (Wolanski and Spagnol, 2003; Purcell, 2002).

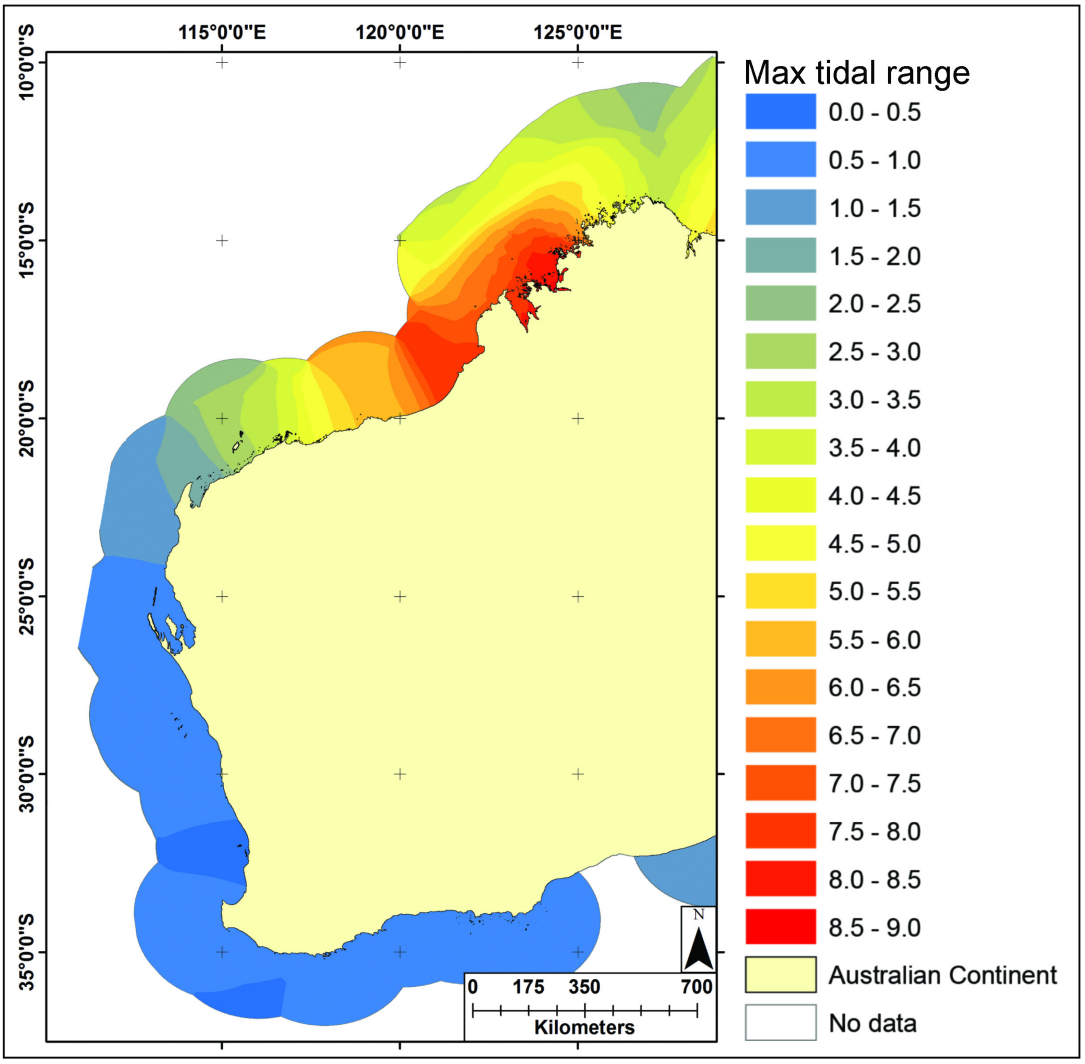


**Figure 1.9. Map of maximum tidal range around the WA coast. The legend colours show the tidal ranges. The data were obtained from CSIRO (2015).**

## 4.4. Marine sedimentation regime and ecosystems

The variety of climate and metocean conditions also influences the coastal and inner shelf development and sediment production and distribution regime.

In the Kimberley and NWS, inner and mid-shelf sediments are mainly a mixture of Holocene bioclasts (including coral fragments) and foraminifera, fine lithoclastics and laterite (primarily found nearshore), post-Last Glacial Maximum ooids and peloids, and relicts (Collins, 2011). In the South West inner shelf zone, bryozoans, encrusting coralline algae and benthic foraminifers and molluscs become more dominant at increasingly higher latitudes, with abundant ubiquitous relict material (skeletal and lithic intraclasts). Deep-water sediments (> 200 m below sea-level BSL) are mostly pelagic, with limited phosphate accumulations (Collins, 2011). Localised reefal carbonates can be found offshore the Kimberley coast, bordering the continental shelf. This zone includes a number of isolated reef platforms, islands and submerged banks (i.e. Rowley Shoals, Scott Reef, Seringapatam Reef, Oceanic

Shoals, Ashmore and Cartier Reefs), formed during past stages of lower sea-levels, in overall subsiding conditions (Collins, 2011).

Influenced by the wide latitudinal range and particularly relevant to the sedimentation are the subtidal and intertidal marine ecosystems, such as seagrass meadows, reefs, mangroves and salt marshes (Short, 2005).

Western Australia has the largest and the most diverse seagrass beds in the world (Kirkman, 1997). Seagrass meadows provide a wide range of services, including protection and control of coastal erosion, by stabilising the sediments and producing *in situ* bioclasts (like coralline algae, foraminifera and molluscs), that can be reworked and contribute to beach sediments (Short, 2005; Barbier et al., 2011).

Similarly to seagrasses, reef systems also act as coastal protection by attenuating waves and assisting beach and shoreline preservation (Barbier et al., 2011).

The coral communities of coastal WA include four main reef systems:

1) Houtman Abrolhos Islands (28°-29°S, one of the highest latitude coral reefs in the world, often referred as the Abrolhos. Abdo et al., 2012),
2) Ningaloo Reef (21°-23°S),
3) Dampier Archipelago (20°S),
4) Kimberley coast and neighbouring islands (10°-18°S).

Mangroves and salt marshes are more extensive in tropical and sub-tropical WA, but also occur along the south-west estuaries (Short and Woodroffe, 2009). These intertidal ecosystems are able to reduce the impacts of incoming waves and storms, and hence have a key role in coastal protection (Wolanski, 2007; Barbier et al., 2011). In addition, they are able to stabilise sediments, reducing shoreline erosion (Wolanski, 2007; Barbier et al., 2011).

Moreover, it must be noted that in terms of coastal and beach nourishment, the contribution given by a number of hard-bodied organisms, including molluscs, red algae, encrusting bryozoans, that live along the shelf and after their death, provide bioclasts that can be reworked and washed onto beaches by waves (Short, 2005).

## References

Abdo, D.A., Bellchambers, L.M. and Evans, S.N., 2012. Turning up the heat: increasing temperature and coral bleaching at the high latitude coral reefs of the Houtman Abrolhos Islands. PLoS One, 7(8), p.e43878.

Baker, R.G., Haworth, R.J. and Flood, P.G., 2005. An oscillating Holocene sea level? Revisiting Rottnest Island, Western Australia, and the Fairbridge eustatic hypothesis. Journal of Coastal Research, pp.3-14.

Barbier, E.B., Hacker, S.D., Kennedy, C., Koch, E.W., Stier, A.C. and Silliman, B.R., 2011. The value of estuarine and coastal ecosystem services. Ecological monographs, 81(2), pp.169-193.

Bird, E.C., 2011. Coastal geomorphology: an introduction. John Wiley & Sons.

Blewett, R.S., Kennet, B.L.N., Huston, D.J., 2012. Australia in time and space. In: Shaping a nation: A geology of Australia. Geoscience Australia and ANU E-Press.

Brooke, B.P., Nichol, S.L., Huang, Z. and Beaman, R.J., 2017. Palaeoshorelines on the Australian continental shelf: Morphology, sea-level relationship and applications to environmental management and archaeology. Continental Shelf Research, 134, pp.26-38.

Buick, R., Thornett, J.R., McNaughton, N.M. and Smith, J.B., 1995. Record of emergent continental crust approximately 3.5 billion years ago in the Pilbara Craton of Australia. Nature, 375(6532), p.574.

Bureau of Meteorology (BoM), 2005. Climate classification maps. 26 Sept. 2017 http://www.bom.gov.au/jsp/ncc/climate_averages/climate-classifications/index.jsp?maptype=kpngrp#maps

Bureau of Meteorology (BoM), 2008. Average mean temperature. 30 October 2017 http://www.bom.gov.au/jsp/ncc/climate_averages/temperature/index.jsp?maptype=6&period=an#maps

Bureau of Meteorology (BoM), 2010. Mean rainfall. 30 October 2017 http://www.bom.gov.au/jsp/ncc/climate_averages/rainfall/index.jsp?period=win&area=wa#maps

Collins, L.B.,1987. Geological evolution of the Swan-Canning estuarine system. In John, Jacob. (Ed.), The Swan River estuary ecology and management. Bentley, Curtin University of Technology. Pp.9-20.

Collins, L.B., Zhao, J.X. and Freeman, H., 2006. A high-precision record of mid–late Holocene sea level events from emergent coral pavements in the Houtman Abrolhos Islands, southwest Australia. Quaternary International, 145, pp.78-85.

Collins, L.B., 2011. Geological setting, marine geomorphology, sediments and oceanic shoals growth history of the Kimberley region. Journal of the Royal Society of Western Australia, 94(2), p.89.

CSIRO, 2015. Tidal Dataset - CAMRIS - Maximum Tidal Range. v1. CSIRO. Data Collection. http://doi.org/10.4225/08/551485767777F

Department of Environment Western Australia (DoE-WA), 2004. The Importance of Western Australia's Waterways. 30 October 2017 http://www.water.wa.gov.au/__data/assets/pdf_file/0007/3211/85861.pdf

Evans, K., Bax, N. & Smith, D.C., 2017. Australia state of the environment 2016: marine environment, independent report to the Australian Government Minister for the Environment and Energy, Australian Government Department of the Environment and Energy, Canberra.

Falvey, D.A., & Mutter, J.C., 1981. Regional plate tectonics and the evolution of Australia's passive continental margins. BMR J. Aust. Geol. Geophys., 6, 1-29

Feng, M., Meyers, G., Pearce, A. and Wijffels, S., 2003. Annual and interannual variations of the Leeuwin Current at 32 S. Journal of Geophysical Research: Oceans, 108(C11).

Gallop, S.L., Verspecht, F. and Pattiaratchi, C.B., 2012. Sea breezes drive currents on the inner continental shelf off southwest Western Australia. Ocean Dynamics, 62(4), pp.569-583.

Geological Survey of Western Australia (GSWA), 1974, Geology of Western Australia. West. Australia Geol. Survey, Mem. 2, 541 p.

Geological Survey of Western Australia (GSWA), 1990. Geology and Mineral Resources of Western Australia: Western Australia Geological Survey, Memoir 3, 827p.

Harris, P.T. and Macmillan-Lawler, M., 2016. Global Overview of Continental Shelf Geomorphology Based on the SRTM30_PLUS 30-Arc Second Database. In Seafloor Mapping along Continental Shelves (pp. 169-190). Springer International Publishing.

James, N.P. and Bone, Y., 2010. Neritic carbonate sediments in a temperate realm: southern Australia. Springer Science & Business Media.

Kirkman, H. 1997. Seagrasses of Australia. State of the Environment Technical Paper Series (Estuaries and the Sea). Canberra, Australia: Department of the Environment.

IHO, International Hydrographic Organization (2013). Standardization of undersea feature names: guidelines proposal for terminology: Draft. Publication B-6 Edition 4.1.0, xxxx 2013 English/French Version, Monaco. 26 September 2017 <https://www.iho.int/iho_pubs/draft_pubs/B-6_e4.1.0_2013_v2_20130510.pdf>.

Lambeck, K., Esat, T. M., & Potter, E. K.,2002. Links between climate and sea levels for the past three million years. Nature, 419(6903), 199-206.

Larcombe, P., 2007. Continental shelf environments. In: Perry, C. and Taylor, K. eds., 2007. Environmental sedimentology. John Wiley & Sons. Pp 351-388.

Niedoroda, A., W., 2005. Continental shelves. In: Schwartz, M., Encyclopedia of Coastal Science. Encyclopedia of Earth Sciences Series. Springer, 2005. 26 September 2017 <http://www.myilibrary.com?ID=41174>. Pp 337-339.

O'Leary, M., Hearty, P. J. & McCulloch, M. T., 2008. Geomorphic evidence of major sea-level fluctuations during marine isotope substage-5e, Cape Cuvier, Western Australia. Geomorphology 102, 595–602.

O'Leary, M.J., Hearty, P.J., Thompson, W.G., Raymo, M.E., Mitrovica, J.X. and Webster, J.M., 2013. Ice sheet collapse following a prolonged period of stable sea level during the last interglacial. Nature Geoscience, 6(9), pp.796-800.

Pearce, A. F., Griffiths, R. W., 1991. The Mesoscale Structure of the Leeuwin Current: A Comparison of Laboratory Models and Satellite Imagery. J. Geophys. Res., 96(C9), 16739-16757.

Pirazzoli, P.A., 1997. Sea-level changes: the last 20 000 years. Oceanographic Literature Review, 8(44), p.785.

Purcell, S. P., 2002. Intertidal reefs under extreme tidal flux in Buccaneer Archipelago, Western Australia. Coral Reefs, 21(2), 191-192.

Saqab, M.M., Bourget, J., 2015. Controls on the distribution and growth of isolated carbonate build-ups in the Timor Sea (NW Australia) during the Quaternary. Mar. Pet. Geol. 62, 123–143. doi:10.1016/j.marpetgeo.2015.01.014.

Short, A.D., 2005. Beaches of the Western Australian Coast: Eucla to Roebuck Bay: A guide to their nature, characteristics, surf and safety. Sydney University Press.

Short, A.D. and Woodroffe, C.D., 2009. The coast of Australia. Cambridge University Press.

Sircombe, K.N. and Freeman, M.J., 1999. Provenance of detrital zircons on the Western Australia coastline—Implications for the geologic history of the Perth basin and denudation of the Yilgarn craton.

Smith, W., and Sandwell, D., 1997. Measured and Estimated Seafloor Topography, World Data Service for Geophysics, Boulder Research Publication RP-1, poster, 34" X 53". Geology, 27(10), pp.879-882.

Solihuddin, T., Collins, L. B., Blakeway, D., O'Leary, M. J., 2015. Holocene coral reef accretion and sea-level in a macrotidal, high turbidity setting: Cockatoo Island, Kimberley Bioregion, northwest Australia. Marine Geology, 359, 50–60.

Stirling, C.H., Esat, T.M., McCulloch, M.T., Lambeck, K., 1995. High-precision U-series dating of corals from Western Australia and implications for the timing and duration of the Last Interglacial. Earth Planet. Sci. Lett. 135, 115e130.

Szabo, B.J., 1979. Uranium-series age of coral reef growth on Rottnest Island, Western Australia. Mar. Geol. 29, M11eM15.

Veevers, J.J., 1971. Phanerozoic history of Western Australia related to continental drift. Journal of the Geological Society of Australia, 18(2), pp.87-96.

Wolanski, E., Spagnol, S., 2003. Dynamics of the turbidity maximum in King Sound, tropical Western Australia. Estuarine Coastal and Shelf Science, 56(5-6), 877-890.

Wolanski, E. 2007. Estuarine ecohydrology. Elsevier, Amsterdam, The Netherlands.

Woolfe, K.J., Larcombe, P., Naish, T., Purdon, R/G., 1998. Lowstand rivers need not incise the shelf: An example from the Great Barrier Reef, Australia, with implications for sequence stratigraphic models Geology, January 26, p. 75-78.

# Chapter 2

# Southern Kimberley

"When you can hear Kimberley calling
Then you know that it's time to get moving."
(Kimberley Calling, Dan Sultan)

## Quaternary onset and evolution of Kimberley coral reefs (Northwest Australia) revealed by high-resolution seismic imaging

Giada Bufarale[1, 3], Lindsay B. Collins[1, 3], Michael J. O'Leary[2, 3], Alexandra Stevens[1, 3], Moataz Kordi[1, 3], Tubagus Solihuddin[1, 3]

1 Department of Applied Geology, Curtin University, GPO Box U1987, Perth, WA 6845, Australia

2 Department of Environment and Agriculture, Curtin University, Bentley, Western Australia, 6102

3 The Western Australian Marine Science Institution, Floreat, Western Australia, 6014

This article is published in Continental Shelf Research, Volume 123, 15 July 2016, Pages 80-88.

doi.org/10.1016/j.csr.2016.04.002 and reprinted with permission in Appendix A.

## Abstract

The inner shelf Kimberley Bioregion of northwest Australia is characterised by a macrotidal setting where prolific coral reefs growth has developed around a complex drowned landscape and is considered a biodiversity "hotspot". High-resolution shallow seismic studies were conducted across various reef settings in the Kimberley (Buccaneer Archipelago, north of Dampier Peninsula, latitude: between 16° 40' S and 16° 40' S) to evaluate stratigraphic evolution, interaction with different substrates, morphological patterns and distribution. Reef sites were chosen to assess most of the reef types present, particularly high intertidal planar reefs and fringing reefs. Reef internal acoustic reflectors were identified according to their shape, stratigraphic position and characteristics. Two main seismic horizons were identified marking the boundaries between Holocene reef (Marine Isotope Stage 1, MIS 1, last 12 ky), commonly 10 – 20 m thick, and MIS 5 (Last Interglacial, LIG, ~120 ky, up to 12 m thick) and Proterozoic rock foundation over which Quaternary reef growth occurred. Within the Holocene Reef unit, at least three minor internal reflectors, generally discontinuous, subparallel to the reef flat were recognised and interpreted as either growth hiatuses or a change of the coral framework or sediment matrix. The LIG reefs represent a new northernmost occurrence along the Western Australian coast.

The research presented here achieved the first regional geophysical study of the Kimberley reefs. Sub-bottom profiles demonstrated that the surveyed reefs are characterised by a multi-stage reef build-up, indicating that coral growth occurred in the Kimberley during previous sea level highstands. The data show also that antecedent substrate and regional subsidence have contributed, too, in determining the amount of accommodation available for reef growth and controlling the morphology of the successive reef building stages. Moreover, the study showed that in spite of macrotidal conditions, high-turbidity and frequent high-energy cyclonic events, corals have exhibited prolific reef growth during the Holocene developing significant reef accretionary structures. As a result coral reefs have generating habitat complexity and species diversity in what is a biodiversity hotspot.

## 1. Introduction

The Kimberley is located in the Australia's northwest continental margin and, primarily due to its remote geographical location, published scientific investigations of the region are scarce compared to other marine and coastal ecosystems in Australia (Wilkinson, 2008; McKenzie et al., 2009; Wilson, 2013). A recent remote sensing study by Moataz et al. (2016) recognised the Kimberley has hosting a major reef system, the largest in Western Australia, and second only to the Great Barrier Reef in terms of total reefal area and number of reef islands. Despite been recognised as a major biodiversity hotspot of international significance (Chin et al., 2008; Wilkinson, 2008; Department of the Environment, 2014; Pepper and Scott Keogh, 2014), the coral reefs of the Kimberley coast remain relatively understudied when compared with other relatively well-known a reef systems along the Western Australian coast, such as the Houtman Abrolhos islands, Ningaloo fringing reef and some isolated oceanic atoll-like reefs (e.g., Scott Reef, Rowley Shoals. Eisenhauer et al., 1993; Collins et al., 2003; Collins et al., 2006; Collins et al., 2011. See reviews

in Montaggioni, 2005 and Collins, 2011). In particular, Collins (2011) and Wilson (2013) noted a significant information gap on the geomorphology, evolution and development of reefs of the Kimberley Bioregion. Until recently, when Solihuddin et al. (2015) accomplished the first detailed geological account of Holocene reef growth in Cockatoo Island (Kimberley Bioregion), it was not known whether reefs are thin veneers over rock platforms or significant long-lived accretionary structures. The paper showed in fact that, at least at this one location, the Holocene reef consists of a thick reef framework, up to 15 m thick. The Cockatoo study also showed that the initiation of Holocene reef occurred soon after flooding of the continental shelf over older Pleistocene reef surface, which was found between 20 and 30 m below sea level, with reefs growing in *catch-up* mode reaching base level around 3000 years ago. This is a significant finding as it suggests corals are able to persist and grow significant accretionary structured in what might be considered challenging or extreme environmental conditions, including extreme macrotidal range (Wilson, 2013), high-turbidity (Brooke, 1997; Wilson et al., 2011; Solihuddin et al., 2015), frequent cyclones (Wilson, 2013). The Solihuddin et al. (2015) study now raises a series of further questions about the reefs in the Buccaneer Archipelago:

- Is the reef morphology of Cockatoo Island a result of a unique local oceanographic effect or do most Kimberley reef exhibit a similar morphology and growth history?
- The northernmost occurrence of Last Interglacial (LIG) reef along the Western Australian coast is found at Cape Range (Ningaloo Reef. O'Leary et al., 2008); does the discovery of LIG reef within the open cut mine Cockatoo represent a broader occurrence of LIG reefs throughout the Kimberley?
- What role has the antecedent topography in terms of structural control of on reef growth during the Holocene?

This project presents the first detailed seismic study across a range of reef morphotypes in order to (1) provide insights into the internal reef architecture and structures, (2) determine the thickness of the Holocene reef and pre-existing reef build-ups, and (3) establish the growth-controlling factors and their role on the Quaternary reef evolution. This paper presents a detailed description of reef morphologies and provides a better understanding of the past reef growth history of inner reefs of the Kimberley (Buccaneer Archipelago. **Figure 2.1**).

## 2. Environmental setting and geology

The Kimberley region occupies a land area of about 424,000 km$^2$ (O'Faircheallaigh, 2013) and extends from Cape Keraudren (southern end of Eighty Mile Beach) to the border of Western Australia / Northern Territory, for a length exceeding 5000 km (Brocx and Semeniuk, 2011; Kordi et al., 2016. **Figure 2.1**). The Kimberley south of Cape Leveque (Dampier Peninsula) is situated within the Phanerozoic Canning sedimentary Basin and is characterised by a simple relatively straight coastline, however the Kimberley north of Cape Leveque is situated within the Proterozoic Kimberley block and is characterised by complex coastal highly indented coastline (Chin et al., 2008; Collins, 2011; Tyler et al., 2012). The coastal and marine habitats include extensive archipelagos, with more than 2400 islands, bays, capes, tidal

plains, mangroves and a broad variety of coral reefs rich in diversity (at least 850 where mapped by Kordi et al., 2016).

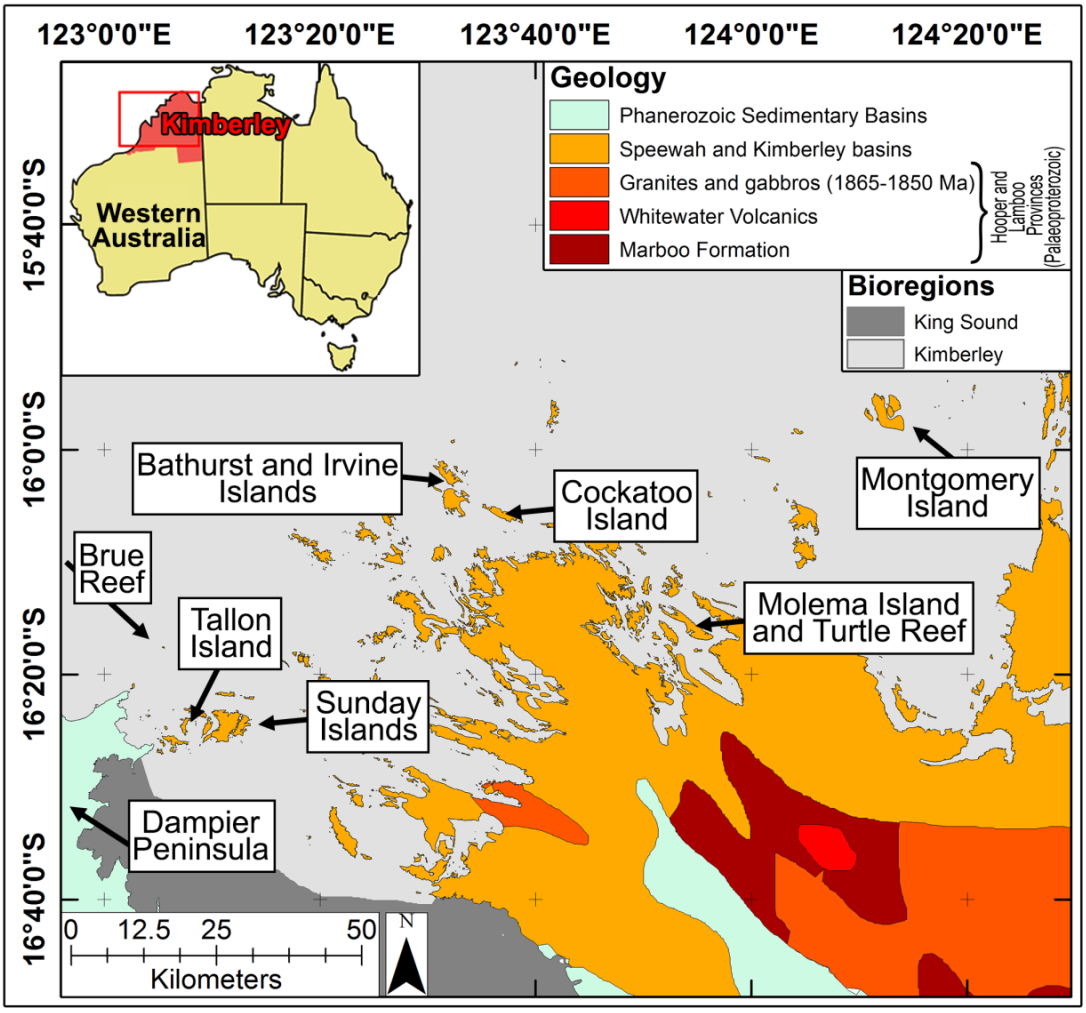


**Figure 2.1. Map of the reef in the Buccaneer Archipelago, Kimberley, showing the geology of the region (after Tyler et al., 2012) and the marine bioregions (Integrated Marine and Coastal Regionalisation of Australia, IMCRA, v4.0. Commonwealth of Australia, 2006). The reefs seismically surveyed in this study are labelled.**

These complex environments are strongly influenced by macrotidal conditions, high-turbidity, tropical monsoonal climate and proximity to the Indo – Pacific Throughflow (ITF) and the Leeuwin Current (e.g., Wolanski and Spagnol, 2003; Condie and Andrewartha, 2008; Collins and Testa, 2010; Brocx and Semeniuk, 2011; Wilson, 2013).

Situated in a semi-arid to sub-humid climate zone, the Kimberley experiences seasonal rainfall (between November and March) that influences local freshwater and sediment drainage from the hinterland to the coast (Parkinson, 1986; Brocx and Semeniuk, 2011). A tidal range of 12 m during springs and less than 3 m during some neaps has resulted in an extensive intertidal zone (Cresswell and Badcock, 2000). These tidal motions can result in tidal currents of 2 m/s, which can remobilise and resuspend fine particles with the result being coral reefs can become invisible from the surface at high tide and at low tide, the reefs appear partially covered by

mud (Wilson et al., 2011). The turbidity increases in wet season when the rates of river runoff are higher (Wolanski and Spagnol, 2003).

The Kimberley marine environment is strongly influenced by an ancient geological history and it is characterised by complex structural and tectonic settings. The intricate coastal geomorphology is structurally controlled by ancient folded and faulted Proterozoic metasedimets and volcanics (**Figure 2.1**. Tyler et al., 2012). Since the Miocene tectonic subsidence (Sandiford, 2007), has resulted in a drowned ria-style coast which has likely influenced the style and development of coral reef growth on the North West Shelf. During the last glacial, the inner shelf reefs experienced subsidence of around 0.11 m/ky (Solihuddin et al., 2015).

## 2.1. Geomorphic Classification of Reefs in the Kimberley Bioregion

Due to the macrotidal conditions, most reef flats in the Kimberley are exposed during low tide and are, therefore, intertidal in character (Figure 2.2). Reefs which have not yet grown to sea level are permanently subtidal, and many small patch reefs and most shoals are of this type. A specialised type of high intertidal reef recognised by Wilson et al. (2011) and Wilson (2013) is characterised by a high, flat topped surface that may be several metres above mean low water springs (MLWS) tide level, and experiences significant subaerial exposure during the tidal cycle. These reefs have unique surface characteristics, including lithified algal ridges, terraced reef platforms, and coralline algae (rhodolith banks), as well as *Porites* microatolls. In order to capture a range of reef typologies this study utilised a revised reef geomorphic classification scheme developed by Collins et al. (2015) and Kordi et al. (2016) for the Kimberley Bioregion, which was adapted from the Great Barrier Reef Geomorphic classification scheme by Hopley et al. (2007).

Fringing reefs are widespread in the Kimberley (Kordi et al., 2016) with morphologies influenced by the complex embayment and island coastal morphology, both as mainland and island associated features. In this study of the Kimberley, five main types of fringing reefs were essentially described: Bay Head, Inter-island, Circum-island, Headland and Narrow-beach Base.

Planar reefs are large isolated features characterised by flat topped platforms that are usually emergent only at low tide. Examples are Montgomery Reef, the Adele group of reefs (Adele and Churchill) and Brue Reef (see **Figure 2.1** for location).

There are many patch reefs and shoals scattered throughout the Kimberley Bioregion (see Wilson, 2013 for examples). These reefs usually grow on isolated topographic highs suitable for colonisation by coral growth and are common on exposed margins of fringing reefs. They are usually intertidal to subtidal features and are often small. These features were not studied in detail in this project which focused on the larger and more diverse reefs.

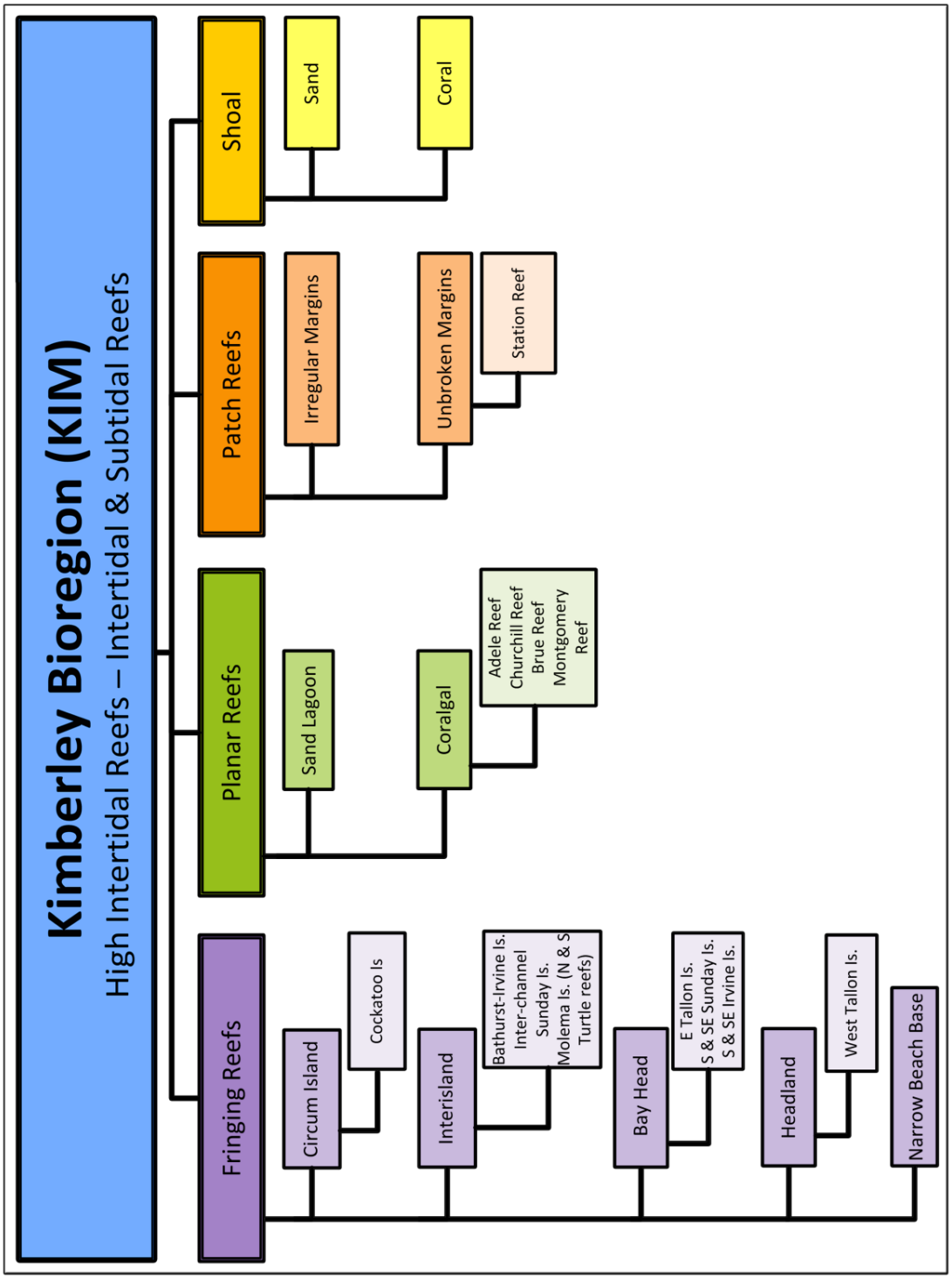


**Figure 2.2. Geomorphic classification scheme for the Kimberley reefs, based on adaptation of Hopley (2007) Collins (2015), Kordi et al., 2016 and data from this study.**

## 3. Methods

The surveyed reef sites (**Figure 2.1**) were chosen in order to capture a broad range of reef morphotypes (Figure 2.2) and included almost 300 km of sub-bottom profiler (SBP) lines. The geophysical survey was limited to the Buccaneer Archipelago and Montgomery Island and designed to target the orientation, internal architecture and morphology of the reefs. Profiles perpendicular to the reef allowed capture of the

reef growth axis, transects parallel to the reef crest and crossing tie lines permitted a correlation during the interpretation and creation a three-dimensional perspective of the acoustic units' framework.

The surveys were conducted using an AA201 boomer system (Applied Acoustic Engineering Limited, Great Yarmouth, UK). Accurate positioning was obtained with a dual frequency Differential Global Positioning System (DGPS). Data were digitally recorded using SonarWiz 5 (Chesapeake Technology Inc., Mountain View, CA) as acquisition and post-processing software. The seismic profiles were postprocessed to improve the signal to noise ratio by tracking the bottom and applying standard signal processing procedures such as bandpass filter and user defined gain/attenuation.

Sub-bottom profiling survey provided information on reef architecture, Holocene thickness and foundation, as well as earlier Pleistocene reef growth events. Stratigraphy and geochronology of Holocene, Pleistocene Reef and Proterozoic basement exposed in the Cockatoo mine pit (Solihuddin et al., 2015) were used to interpret and ground truth the major seismic horizons recorded over the modern Cockatoo reef flat (see Solihuddin et al., 2015; Collins et al., 2015 and in the further sections). The reliability of this correlation was verified by laterally tracing the key seismic surfaces onto the neighbouring reefs, demonstrating a regional consistency of the stratigraphic pattern of two stages of reef growth (Holocene and Pleistocene).

# 4. Results and discussion

## 4.1. Seismic facies analysis

Two significant seismic reflectors R1 and RF were identified and defined on the basis of their (1) relative position, (2) acoustic reflection and (3) architectural characters (Table 2.1 and seismic profiles). Between R1 and the seabed, many profiles also exhibit minor acoustic horizons, named H1, H2 and H3.

**R1 Reflector.** R1 is a high-energy reflector, which represents the top of the Pleistocene calcretised reef limestone unit recognised by Solihuddin et al. (2015. Table 2.1 and depicted in green colour in the seismic profiles). Occasionally R1 is masked by seabed multiple echoes or by a thick and hard overlying substrate. The R1 follows a similar topographic profile to the modern reef flat seabed in exhibiting a quasi-horizontal reef flat that steeply dips at the forereef slope matching the modern forereef slope. The seismic unit bounded by the sea floor/modern reef flat and R1 represents the Holocene reef/sediment build-up.

**Table 2.1. Characteristics and acoustic features of seismic units identified in the profiles.**

| Facies Unit | Thickness | Limits | Age | Internal Structure | Morphology | Interpretation | Example |
|---|---|---|---|---|---|---|---|
| Holocene | Variable: 7-22 m | **Top:** seabed **Bottom:** unconformity R1 (top LIG unit) | Last 12 ky | Moderate to low amplitude. Local discontinuous, sub-parallel reflectors (H1, H2 and H3) | Reef flat, crest, forereef slope. Local pinnacle reef | Reef facies | 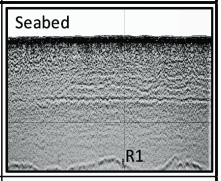  |
| | | | | Well-layered, locally parallel to subparallel prograded. Minor disconformities | Channel fill. Sediment mounds or drapes | Sediment Bodies | 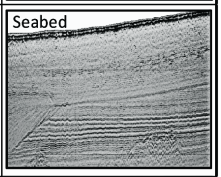  |
| LIG (MIS 5e) | Variable: 7-12 m | **Top:** unconformity R1 (top LIG unit) **Bottom:** unconformity RF (top Rock Foundation unit) | ~ 120 ky | Weak to moderate amplitude with discontinuous, subparallel minor reflectors | Reef flat, crest, forereef slope. Local pinnacle reef | Reef facies | 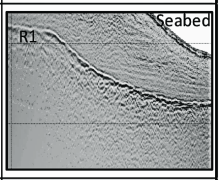  |
| Rock Foundation | Basement | **Top:** RF (top Rock Foundation unit) **Bottom:** NA | Proterozoic (2000 My) | Chaotic, low-amplitude. Acoustic basement | Local deep valley-like depressions and ridges | Folded metamorphics, conglomerates and sandstones (Kimberley Group) | 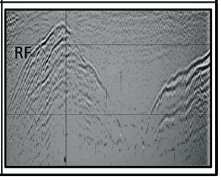  |

**H Reflectors.** The Holocene unit is characterised by a series of internal discontinuous, subparallel reflectors of moderate to low amplitude (H1, H2 and H3, represented in shades of orange colour in the seismic profiles). H1 is the shallowest reflector, found in the first 5 metres from the seafloor surface. In some profiles, it is not recognisable, due to very high impedance of the seafloor reflector masking the first few metres of substrate. H2 can be usually found between 5 and 8 metres from the seabed and H3, where identified, is generally 3 to 7 metres above the R1. These reflectors could be interpreted as hiatuses or a change of the coral framework (possibly from muddy to sandy matrix), according to the observation of Solihuddin et al. (2015).

**RF Reflector.** The post-processing and interpretation of the acoustic profiles across the area define the RF reflector as the deepest seismic horizon identified in the surveyed reefs and locally forms deep valley-like depressions and ridges (Table 2.1 and depicted in blue colour in the seismic profiles). The RF caps a chaotic, low amplitude unit that can be considered on the basis of the profile analysis and correlation with the data derived from a mine pit in Cockatoo Island as the Proterozoic rock foundation, and represents the acoustic basement of the reefs in the Buccaneer Archipelago. The terrestrial expression of this unit is represented by folded metamorphics, conglomerates and sandstones of the Kimberley Group. The seismic unit bounded by the R1 and RF represents an older, Pleistocene reef unit, which belongs to the Last Interglacial (LIG) sea level highstand. The LIG section has been diagenetically altered and consists of calcretised, muddy branching coral framestone containing recrystallised corals (Solihuddin et al., 2015).

## 4.2. Internal architecture of Southern Kimberley Reefs

A number of reef typologies have been identified in the Kimberley (see Figure 2.2). These include a range of fringing reef morphologies, with reef flat elevations that fall within two primary categories, high inertial and intertidal. The internal architecture of a variety of reef types were investigated and compared, through the analysis of seismic profiles.

### *4.2.1. Fringing reefs*

*Circum-island reef: Cockatoo Island*

The Buccaneer Archipelago (see **Figure 2.1** for location) is characterised by a highly discordant coastline resulting from the partial submergence of a structurally controlled geological landscape with anticlinal features forming the region's islands and coastal headlands.

Cockatoo Island is located less than 6 km from the mainland coastline and consists of strongly folded and trending NW – SE Palaeoproterozoic metamorphic and igneous rocks of the King Leopold Orogen (Wright, 1964). The Cockatoo Island reef is a high intertidal, circum-island fringing reef, species-rich, with branching corals that dominate the modern forereef slope and persist to depths of 10 m below mean sea level (Solihuddin et al., 2015). Tides of up to 12 m provide the main physical energy.

The seismic profiles were mainly confined to the reef flat and forereef slope in front of the mine pits (insert in Figure 2.3. Survey lines marked in red). The profiles on the southern-eastern margin of the reef flat reveal the structure of the reef overlying Proterozoic rocks (below RF horizon, in blue colour) and confirm the stratigraphy mapped by Solihuddin et al., 2015 in the mine pits. An initial reef building phase of LIG reefs (below R1 horizon, in green colour) of 5 – 10 m thickness overlies the Proterozoic substrate. Thereafter Holocene reef comprises the reef flat and is 15 – 20 m thick. Up to 25 m of well-laminated fine sediment mound is located in front of the reef flat (Figure 2.3B). This massive sediment body is about 2.5 km long and directly overlies the LIG reef building phase.

*Inter-island reefs: Bathurst Island – Irvine Island*

Interisland reefs are defined by joining two separate islands, and are commonly found in the Buccaneer Archipelago and some appear to coalesce to form inter-island reefs where two islands are located in close proximity. One such inter-island reef is located between Bathurst and Irvine Islands (**Figure 2.1**).

This inter-island fringing reef is characterised by a deep elongate depression, 30 to 35 m deep, which cuts across the platform (Figure 2.4), and it has been suggested by Wilson (2013) that this indicates the partial coalescence of two fringing reefs, which left a residual gap in the platform as a function of incomplete reef growth, as opposed to a single platform with an elongate karst depression. The platform surface is frequently emergent, with a transverse sand sheet, shallow reef flat pools containing corals and fields of *Porites* microatolls present, features in common with other high intertidal reefs.

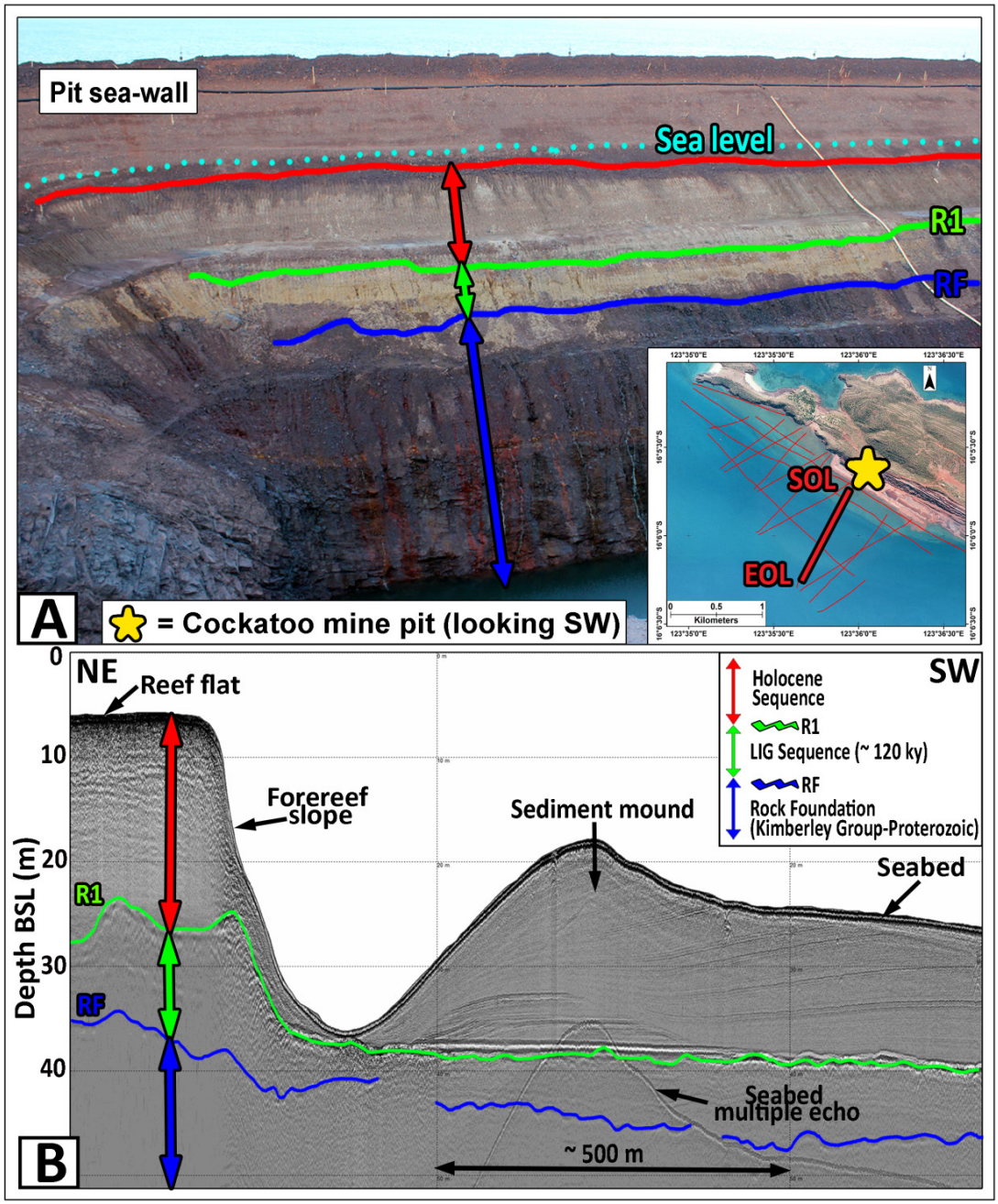


**Figure 2.3. A) Cockatoo mine pit section (Photo credit: Solihuddin T., 2013). Insert: Landgate aerial photography provided by the Department of Parks and Wildlife (DPaW); SBP lines are marked in red. SOL: start of line; EOL: end of line. B) Cross-section of a seismic profile collected adjacent to mapped mine pit sections of Solihuddin et al. (2015) established position of Proterozoic foundation (RF, blue), Last Interglacial reef (R1, green) and overlying Holocene reef across the fringing reef. Note the sediment mound in front of the reef flat. Modified after Collins et al., 2015.**

The internal structure of the Bathurst – Irvine reef in west – east section (Figure 2.4) reveals its growth that occurred on relatively flat Proterozoic bedrock 30 – 40 m below mean sea level (MSL). Within the reef platform, the reflector R1 is approximately horizontal and the LIG sequence is around 10 – 12 m thick. Within the 15 m of Holocene reef build-up, there are 3 minor acoustic reflectors H1, H2, and H3, which are interpreted as either hiatuses or temporary pauses in reef growth,

changes in the type of sediment matric (sand *vs* mud) or change in coral facies (branching to massive).

Seismic traverses across the pool in the middle of the Bathurst-Irvine interisland reef reveal a thin (5 m thick) LIG reef unit present close to the modern sea bed, overlying the Proterozoic substrate. Within the pool Holocene pinnacle reefs up to 10 m high grow from the base of the pool (Figure 2.4B).

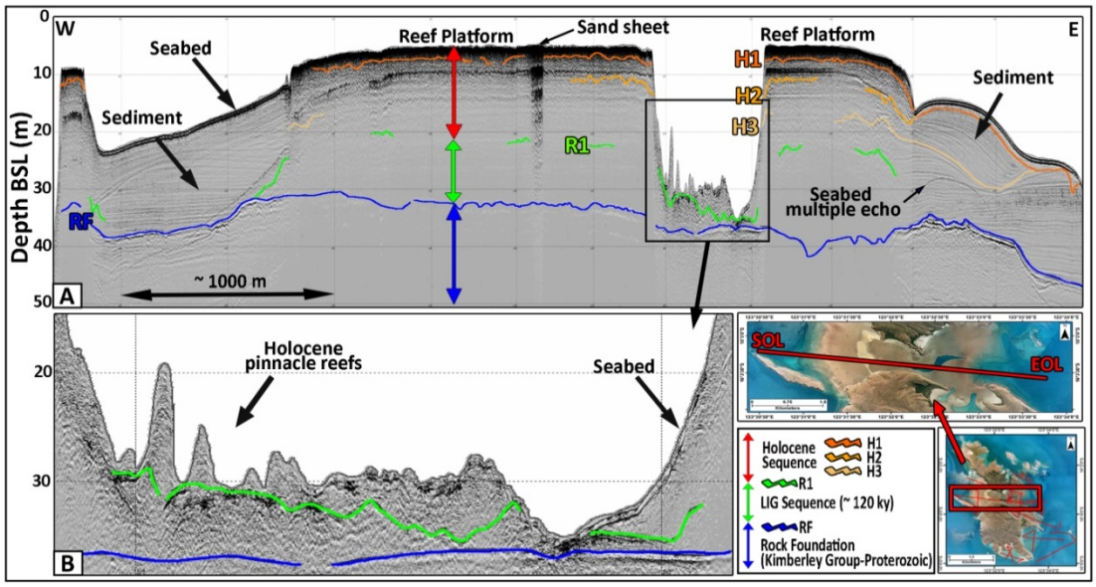


**Figure 2.4. A) W – E section of the Bathurst – Irvine high intertidal fringing reef (width 7 km), showing two stages of platform growth, marginal sediment bodies, drowned reefs (insert, B) in the central elongate pool and basement topography.**

Both margins of the reef flat have well-developed bedded sediment lobes, up to 20 m thick. Longitudinal and transversal seismic profiles have shown that the bodies have a complex internal architecture (Figure 2.4 and Figure 2.5), composed of surficial seaward prograding layers, in discordant relationship with the deeper and more horizontal ones. Similarly for the Holocene discontinuities (H1, H2, and H3), the internal beds could also be linked to possible non-deposition. Based on a qualitative interpretation of the seismic data, the drapes are composed by fine to medium grained sediments and, according to the local geomorphology and the collected samples, the sediment supply could be a combination of clastic influx coming from the surrounding islands and from suspension (from the mainland), and bioclastic carbonate deposits derived from the reefs. The western sediment mound Figure 2.4A) is likely a result of ebb tides flowing off the reef platforms and bottom current dynamics, resulting in filling of pre-existing accommodation space.

A north – south profile (Figure 2.5) of the platform shows a similar stratigraphy for the reef platform, with 25 m of Holocene sediment infilling the adjacent small lagoon to the south of the platform. Holocene and LIG thicknesses are similar to those already recorded in the W – E profile of the platform. Topographic changes in the Proterozoic surface, as it rises to the north, have influenced the position of the platform by providing suitable elevated substrate which was colonised by LIG reef growth. Within the sediment body, the internal geological pattern is almost completely obscured by an acoustic turbidity anomaly. This seismic signature,

named *curtain*, is associated with fluid escape through the sediment (Baltzer et al., 2005). It is noteworthy that Traditional Owners have reported freshwater springs in the general area. The presence of the two shallow pools along north east Irvine Island could be linked to upward migration of fresh water into the seawater. The mixed brackish waters could have been a significant control on reef growing processes, limiting the Holocene (and possibly LIG) build-up in the area.

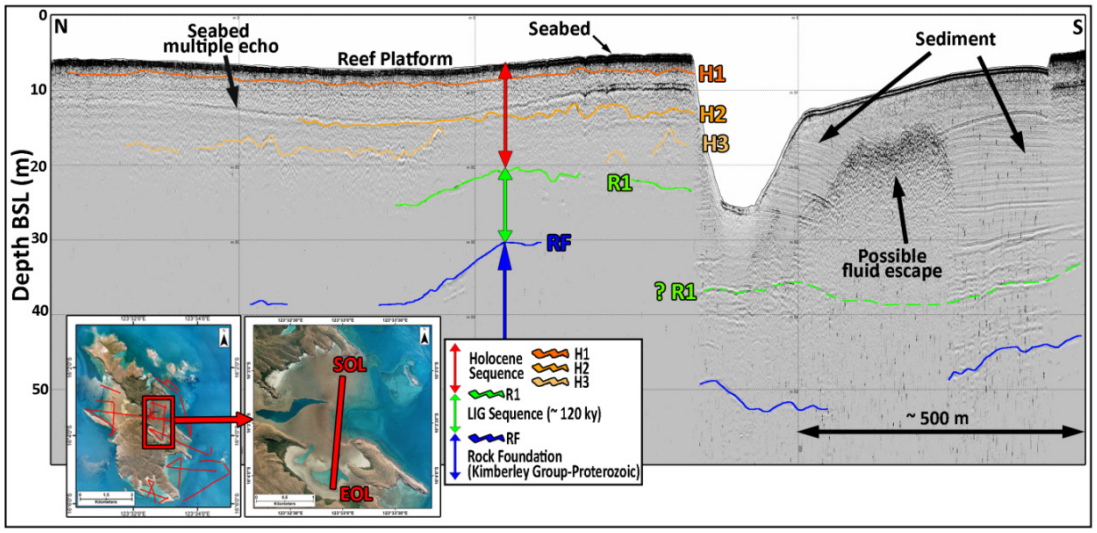


**Figure 2.5. N – S section of Bathurst – Irvine Reef and adjacent embayment substrate. Note influence of platform elevation in the location of platform building; 2 stages (LIG and Holocene) of reef growth, and the 25 m thick bedded sediment pile filling the embayment to the S, with an internal signal probably representing fluid escape.**

### *Bay head reefs: South Sunday Island*

Fringing bay head reefs are mainly developed in the southern and south-eastern sectors of the Sunday Islands (Figure 2.6). The reef flats are sheltered and elongate along the coastline, with an approximate width between 500 m and 1500 m. The acoustic profiles cover only the external edges of the platform, due to the tidal conditions during the survey. The data available reveal that the pre-existing Proterozoic topography (RF) rises from 30 m to 10 – 15 m below the seafloor, significantly attenuating the reef development. Both the Last Interglacial and the Holocene reefs are relatively thin, with a similar internal architecture. Whereas the Proterozoic rock foundation presents irregularities, such as channels or depressions, the LIG reef growth tends to level the topography (see Figure 2.6B). For this reason, it is problematic to establish an average thickness of this unit. The overlying Holocene reef build-up is about 7 m thick on a mostly flat pre-existing LIG surface.

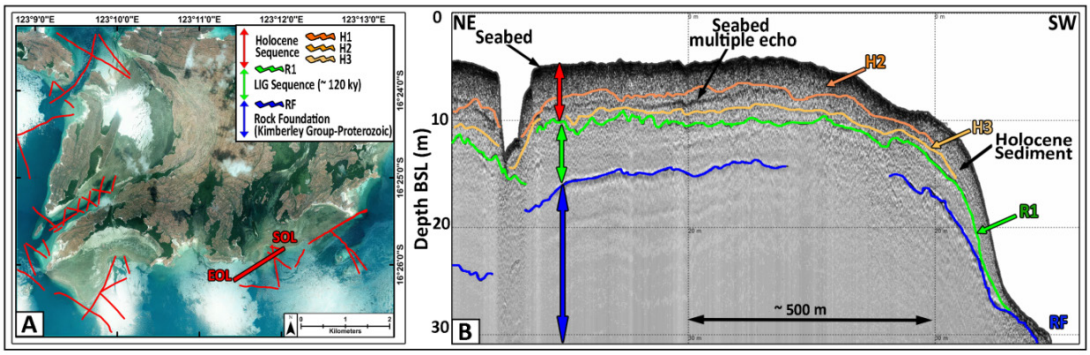


**Figure 2.6. Sunday Islands. A) Landgate aerial photography provided by DPaW; track plot of seismic profiles are marked with thin red lines. B) Seismic profile. These Proterozoic islands are separated by deep depressions (probably structurally controlled), with both Holocene and LIG reef growth as fringing reefs. Irregular topography of Kimberley Group is partially blanketed by 2 stages of reef growth.**

### *4.2.2. Planar, coralgal reefs*

*Montgomery Island*

Montgomery Island is located approximately 23 km west of the coastline (**Figure 2.1**). It is bordered by a large high intertidal reef which is a planar coralgal reef, and contains a central Proterozoic island (Wilson, 2013). Montgomery Reef is known to have a unique set of reef substrates on the platform, in particular rhodolith dominated substrates and associated crustose coralline algae forming a distinctive reef crest, and at least 2 terraces described by Wilson (2013) as upper and lower lagoons. Shallow pools with internal coral growth characterise parts of the reef flat. The well-developed Proterozoic central island is surrounded by sand cays and vegetated by mangroves and grasses (Wilson, 2013). Reef flats are dominated by sand and coral rubble with small living corals in shallow pools. The platform is very shallow and emergent at low tide with distinctive waterfall cascades across the reef crest. Spring tidal range is 12 m, and the platform margin is exposed by a few metres at low tide. A prominent north – south trending spine protruding from the main platform on its western side is called “The Breakwater”.

Due to the extreme shallowness of water on the platform in all parts of the tidal cycle, except during high water spring tides, seismic transects could only be obtained at the platform margins. Good quality profiles were collected on east and west sides of the Breakwater.

The Breakwater appears to have developed as a northward prograding feature, with seismic data showing a distinct pattern of development. There are many pinnacle reefs and significant sediment cover in places along with occasional palaeochannels. Two stages of pinnacle growth can be frequently recognised, with a thicker LIG build-up under a thin Holocene reef substrate. In some cases, pinnacle reefs occur above a deep basal unconformity, interpreted as the Proterozoic surface, capped by sediment cover terminating at 10 m MSL on the eastern side of the Breakwater (Figure 2.7). Three stages of reef development are present, with different level of maturity going from juvenile in the north and mature in the south. An axial section across the northern tip of the Breakwater (profile 1, Figure 2.7A) confirms an initial ridge of LIG coalescent pinnacle reefs that was followed by

sediment cover during the Holocene. The N – S axis of the Breakwater apparently follows a bathymetric ridge with the same trend which controlled the reef initiation and provided a favourable template for an initial reef growth. A similar west – east profile, situated just to the north eastern extremity of the Breakwater (profile 2, Figure 2.7B) endorses the pattern of LIG coalescent pinnacle growth on the Proterozoic, then pinnacle reef recolonization during the Holocene accompanied by infill of depressions by active sedimentation. On the south-western margin of the Breakwater, in a N – S section, a series of pinnacle reefs occurs above the basal unconformity with a sediment blanket between pinnacles. The pinnacles are buried by the sediment and, in some cases, protrude through the sediment cover demonstrating contemporaneous infill and active Holocene reef building. These pinnacles usually colonised an earlier (probably LIG) stage of pinnacle growth (see profile 3, Figure 2.7C).

Together these profiles show a different level of maturity, establishing the current surface morphology as a spine-like protuberance northward from the Montgomery platform. First (south), a mature stage is characterised by a ridge of LIG coalescent pinnacles, overlain by Holocene reef. In the central region, an intermediate phase is constituted by an incipient regrowth on LIG pinnacles by Holocene reefs. And finally, in the relatively young reef sequence (north), a continuous reef flat is near emergent.

At its south western corner, the Montgomery Reef platform margin has distinctive morphology of a subtidal reef terrace with a near-vertical fore reef slope (Figure 2.8). The littoral terrace is characterised by a barren zone lacking spur and groove morphology, with occasional sand sheets; a lower littoral reef front ramp, with slope 5 – 10 degrees, high-energy tidal flow, encrusted by coralline algal ridges; a mid-littoral reef crest with 100 m wide rhodolith banks and lacking a boulder zone; and finally a lower and upper reef flat dominated by rhodoliths and small pools containing corals. Two reef build-ups are present overlying Proterozoic basement; a 10 m thick LIG reef and a 22 m thick Holocene reef, immediately underlying the platform margin (Figure 2.8). The distinctive terracing of the steep forereef is controlled by the boundary between these two reef building events.

Reef building processes in and around Montgomery platform include both phases of reef building and buried sedimentary sequences, however it is clear that the Holocene build-up phase of the main platform is significant. In shallow platform conditions, the internal structure of the platform is difficult to determine due to prominent ringing in the profiles and lack of penetration. It is likely that reef thickness declines toward the central island as the Proterozoic topography rises.

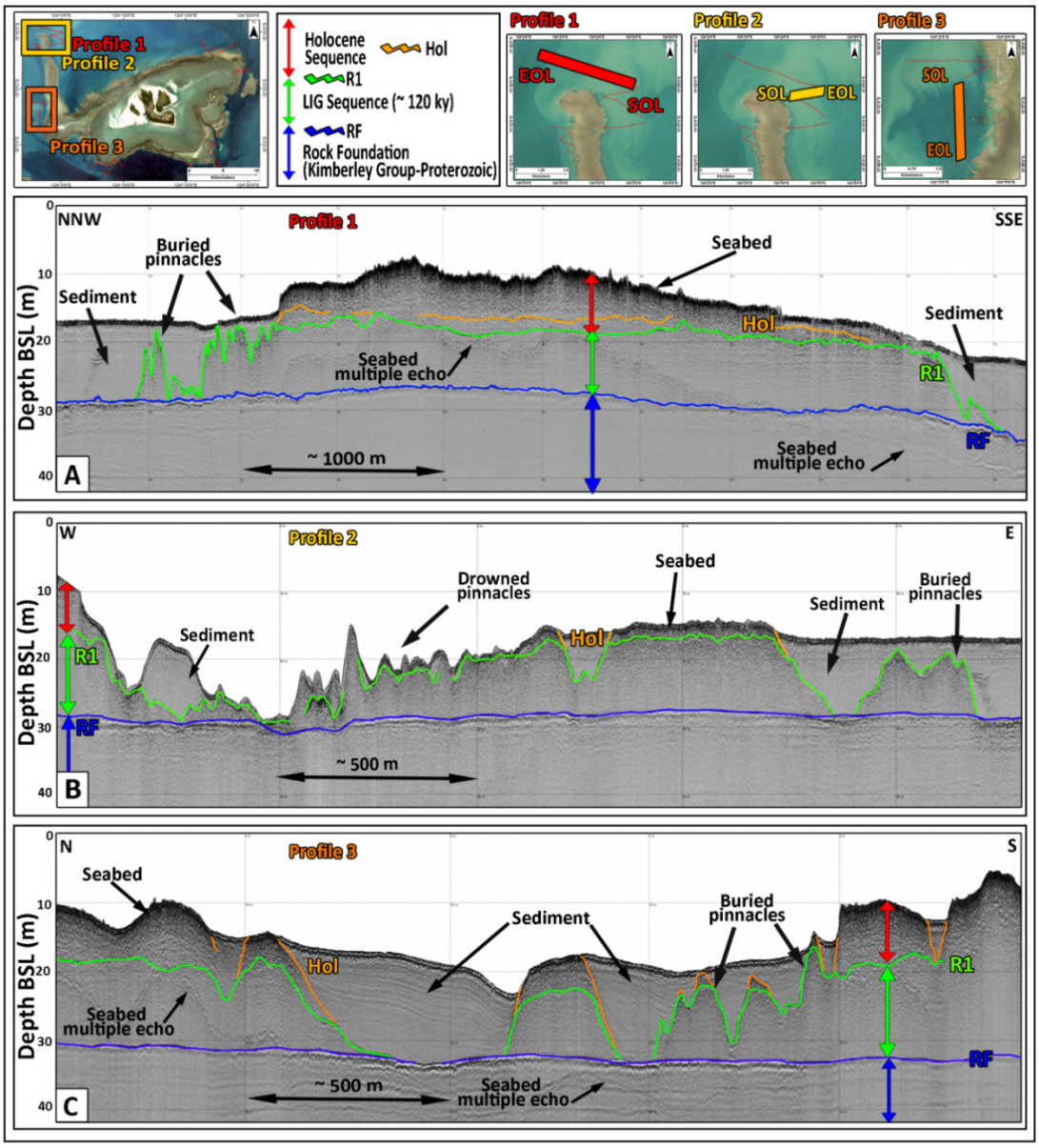


**Figure 2.7. History of reef growth for the Breakwater from seismic profiles. A) Profile 1. Cross section of the Breakwater along its distal submerged northern margin reveals an initial LIG ridge composed of marginal pinnacles and central coalescent pinnacle architecture, overlain by Holocene coral reef with small surficial pinnacle reefs; note thickening of sediment drapes at margins of the ridge structure. B) Profile 2. A similar history is shown by this profile of the east margin of the Breakwater at its northern extremity. Note incipient colonisation of LIG pinnacle reefs by Holocene reefs, and influx of Holocene sediments. C) Profile 3. N – S view of the south western seaward margin of the Breakwater. Proterozoic surface (RF, blue) with two stacked generations of pinnacle reef development (LIG and Holocene), with bedded sediment infilling the reef terrain and overwhelming reef growth, proximal to and near the point of attachment to the Montgomery platform.**

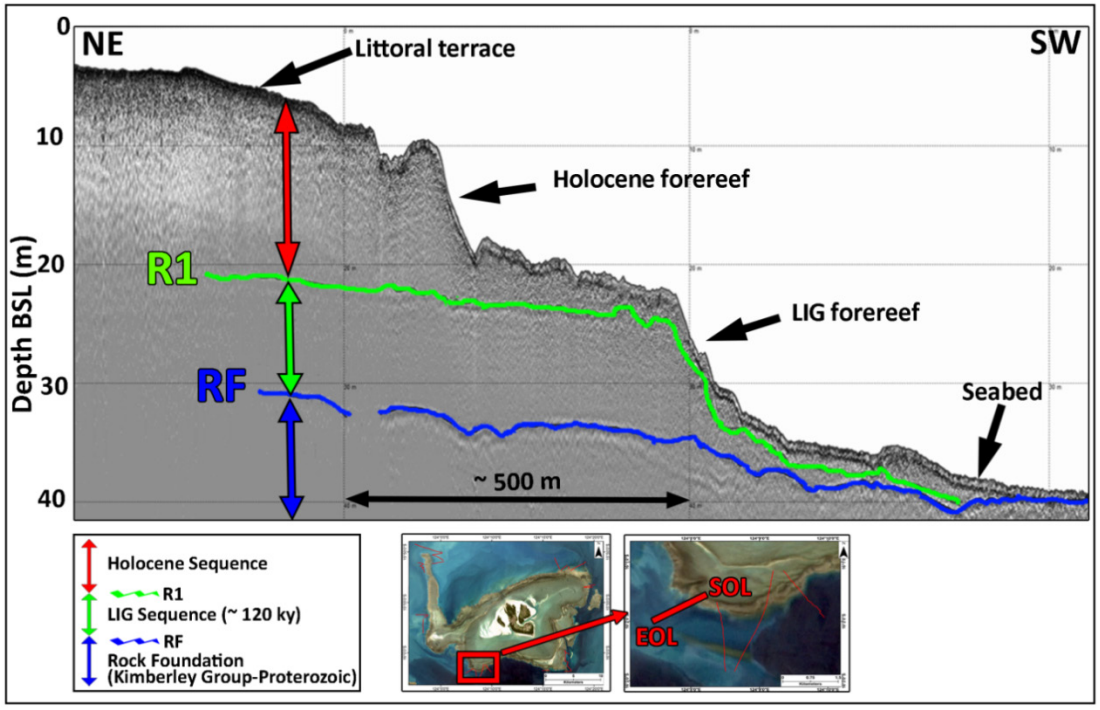


**Figure 2.8. Seismic sections showing structure of the SW margin of Montgomery Reef. Note terraced morphology of forereef is controlled by the boundary of LIG and Holocene reef build-up events. The lower level of basement substrate (RF, blue) under the crest of Montgomery Reef allowed for 2 stages of reef growth, LIG, and Holocene separated by an unconformity (R1, green).**

## 5. Conclusion

The study presented here has achieved the first regional geophysical study of the Kimberley reefs. By developing an understanding of seismostratigraphic events, it has been possible to document the subsurface evolution and growth history of diverse reef systems for a range of reef types mapped in the Buccaneer Archipelago. The seismic data demonstrate the long term resilience of the Kimberley reefs, their capacity to thrive in challenging environmental circumstances, including high-turbidity and other high-energy events throughout the Holocene. Evidences of Last Interglacial reefs also suggest that reef growth was not an opportunistic event during the Holocene but reef growth has occurred in the region during earlier highstand events.

High-resolution seismic data demonstrated that:

- The surveyed reefs in the Buccaneer Archipelago have a similar reef morphology and growth history as in Cockatoo Island. Seismically, all reefs exhibit a multistage reef build-up, correlated to late Pleistocene sea level highstand events. Inter-island fringing reefs appear to have formed by progradation and coalescence of fringing reefs attached to adjacent islands. Where coalescence has not gone to completion, deep inter-reef channels or elongate depressions still remain between adjacent fringing reefs or within intertidal platform reefs (e.g. Bathurst and Irvine reef). Within few reef systems, linked pinnacle reefs up to 15 m thick, are present.

- The study also documented the first widespread occurrence of last interglacial coral reefs north of Cape Range (Exmouth latitude: 21° 55' S). However unlike the emergent reef terraces which intermittently outcrop along the coast between Dongara (latitude: 29° 15' S) and Exmouth, LIG reefs occur at depth of between 20 and 35 m would suggest that the coastal Kimberley region has undergone or is still undergoing subsidence at least since the Last Interglacial. A subsiding coast can explain the complex ria coastline and numerous islands which is s characteristic of the Northern Kimberley coast.

- Pre-existing topography and substrate depth control the amount of accommodation available for reef growth and stacking of reef building events. From the seismic profiles, it appears evident that the elevation of the Proterozoic rock foundation represents a major factor in determining the thickness and location of the reefs and controlling their vertical accretion. Pre-existing topographic highs, like hills or ridges were possibly inundated several hundred years later than the adjacent valleys or palaeochannels. Also the substrate represents a controlling factor in reef development. Corals are not able to grow on mobile unconsolidated sediments, hence where there is this kind of foundation, no reefs build-up is present. Subsidence of the LIG substrates must also be taken into consideration. The Kimberley coast is considered to represent a subsiding landscape. This hypothesis is supported by the seismic data obtained during this study. As a consequence, a greater accommodation space has become available, being an important control factor of the overall Holocene morphology.

Combining this information with reef chronology and measurements of accretion rates (from Solihuddin et al., 2015), the data indicate that the interaction between Quaternary global sea-level fluctuations and the complex, subsiding Kimberley landscape has been of primary importance in controlling the longer term evolutionary patterns of coral reef development and growth, the available accommodation for and timing of multiple events of reef growth over geological timescales.

## Acknowledgements

The Kimberley Reef Geomorphology Project 1.3.1 is funded by the Western Australian State Government through the Western Australian Marine Science Institution. This research was assisted by the Bardi Jawi, Mayala and Dambimangari people, the Traditional Owners of these lands, through essential assistance and guidance in part of the field work. The authors wish to thank: Cygnet Bay Marine Research Station staff (in particular James Brown and Dr Erin McGinty) that provided vessel support for marine operations and access to research facilities at Cygnet Bay; Mark Hardman (Fugro Satellite Positioning Pty Ltd) for supplying the DGPS; Neil MacDonald (Applied Acoustic Engineering Ltd) and Western Advance (Malaga, Western Australia) for the equipment support; Giovanni De Vita for his technical advice; Richard Costin and Annabelle Sandes (Kimberley Media). The authors would like to thank Dr Piers Larcombe for his valuable comments and suggestions to improve the manuscript.

It must be noted that the Aboriginal history of climate, land and environment is based on thousands of years of residence and rich culture: it is important to consider this broad understanding alongside the modern science completed here.

The authors wish to dedicate this project to the late Professor L. B. Collins who left us before the publication of this manuscript.

## References

Baltzer, A., Tessier, B., Nouzé, H., Bates, R., Moore, C., & Menier, D., 2005. Seistec seismic profiles: a tool to differentiate gas signatures. Marine Geophysical Researches, 26(2-4), 235-245.

Brocx, M., and Semeniuk, V., 2011. The global geoheritage significance of the Kimberley coast, Western Australia. Journal of the Royal Society of Western Australia 94, 57-88.

Brooke, B., 1997. Geomorphology of the north Kimberley coast, in: Walker D. (Ed.), Marine biological survey of the central Kimberley coast.Western Australia. University of Western Australia, Perth, unpublished report, W.A. Museum Library No. UR377, pp. 13–39.

Chin, A., Sweatman, H., Forbes, S., Perks, H., Walker, R., Jones, G., Williamson, D., Evans, R., Hartley, F., Armstrong, S., Malcolm, H., Edgar, G., 2008. Status of the coral reefs in Australia and Papua New Guinea, in: Wilkinson, C. (Ed), Status of Coral Reefs of the World. Global coral reef monitoring network. Reef and Rainforest Research Centre, pp 159 – 176.

Condie, S.A., Andrewartha, J., 2008. Circulation and connectivity on the Australian North West Shelf. Continental Shelf Research 28, 14: 1724 – 1739.

Collins, L. B., Zhu, Z. R., Wyrwoll, K. H., & Eisenhauer, A., 2003. Late Quaternary structure and development of the northern Ningaloo Reef, Australia. *Sedimentary Geology*, *159*(1), 81-94.

Collins, L. B., Zhao, J. X., & Freeman, H., 2006. A high-precision record of mid–late Holocene sea-level events from emergent coral pavements in the Houtman Abrolhos Islands, southwest Australia. Quaternary International, 145, 78-85.

Collins, L. B., Testa V., 2010. Quaternary development of resilient reefs on the subsiding Kimberley continental margin, northwest Australia. Brazilian Journal of Oceanography 58, 1 – 13.

Collins, L.B., Testa, V., Zhao, J., Qu, D., 2011. Holocene growth history of the Scott reef carbonate platform and coral reef. Journal of the Royal Society of Western Australia 94(2), 239 – 250.

Collins, L. B., 2011. Geological setting, marine geomorphology, sediments and oceanic shoals growth history of the Kimberley Region. Journal of the Royal Society of Western Australia 94(2), 89 – 105.

Collins, L. B., O'Leary, M., Stevens, A., Bufarale, G., Kordi, M., & Solihuddin, T., 2015. Geomorphic patterns, internal architecture and reef growth in a macrotidal, high-turbidity setting of coral reefs from the Kimberley bioregion. Australian Journal of Maritime & Ocean Affairs, 7(1), 12-22.

Commonwealth of Australia, 2006. A guide to the integrated marine and coastal regionalisation of Australia Version 4.0. Department of the Environment and Heritage, Canberra, Australia.

Cresswell, G. R., Badcock, K. A., 2000. Tidal mixing near the Kimberley coast of NW Australia. Marine Freshwater Research 51, 641 – 6.

Department of the Environment, 2014. Australia's 15 National Biodiversity Hotspots. Australian Government, Canberra. Available at: http://www.environment.gov.au/node/13909

Eisenhauer, A., Wasserburg, G. J., Chen, J. H., Bonani, G., Collins, L. B., Zhu, Z. R., & Wyrwoll, K., 1993. Holocene sea-level determination relative to the Australian continent: U/Th (TIMS) and $^{14}C$ (AMS) dating of coral cores from the Abrolhos Islands. Earth and Planetary Science Letters, 114(4), 529-547.

Kordi, M.N., Collins, L.B., O'Leary, M., and Stevens, A., 2016. ReefKIM: an integrated geodatabase for sustainable management of the Kimberley Reefs, NW Australia. Ocean & Coastal Management, 119: 234-243.

Hopley, D., Smithers, S., Parnell, K., 2007. The Geomorphology of the Great Barrier Reef: development, diversity, change. Cambridge.

McKenzie, N.L., Start, A.N., Burbidge, A.A., Kenneally, K.F., Burrows, N.D., 2009. Protecting the Kimberley: a synthesis of scientific knowledge to support conservation management in the Kimberley region of Western Australia. Department of Environment and Conservation, Perth, WA.

Montaggioni, L. F., 2005. History of Indo-Pacific coral reef systems since the last glaciation: Development patterns and controlling factors. Earth – Science Reviews 71 (1 – 2), 1 – 75.

O'Faircheallaigh, C., 2013. Extractive industries and Indigenous peoples: a changing dynamic?. Journal of Rural Studies 30, 20 – 30.

O'Leary, M.J, Hearty, P.J. & McCulloch, M.T., 2008b. Geomorphic evidence of major sea-level fluctuations during marine isotope substage-5e, Cape Cuvier, Western Australia. Geomorphology 102(3-4), pp.595–602.

Parkinson, G., 1986. Atlas of Australian Resources, Third Series, Volume 4: Climate. Division of National Mapping, Canberra.

Sandiford, M., 2007. The tilting continent: a new constraint on the dynamic topographic field from Australia. Earth and Planetary Science Letters 261 (1 – 2), 152–163.

Solihuddin, T., Collins, L.B., Blakeway, D., O'Leary, M.J., 2015. Holocene Reef Growth and Sea Level in a Macrotidal, High Turbidity Setting: Cockatoo Island, Kimberley Bioregion, Northwest Australia. Marine Geology 359, 50–60.

Tyler, I. M., Hocking, R. M., & Haines, P. W., 2012. Geological evolution of the Kimberley region of Western Australia. Episodes – Newsmagazine of the International Union of Geological Sciences 35(1), 298.

Wilson, B., S. Blake, D. Ryan, J. Hacker., 2011. Reconnaissance of species-rich coral reefs in a muddy, macro-tidal, enclosed embayment, Talbot Bay, Kimberley, Western Australia. Journal of the Royal Society of Western Australia 94, 251 – 265.

Wilson, B., 2013. The Biogeography of the Australian North West Shelf, environmental change and life's response. Elsevier, 1st Edition.

Wolanski, E., Spagnol, S., 2003. Dynamics of the turbidity maximum in King Sound, tropical Western Australia. Estuarine Coastal and Shelf Science, 56(5-6), 877-890.

Wright, R.L., 1964. Geomorphology of the west Kimberley area. CSIRO Land Res. Ser. 9, 103–118.

# Chapter 3

# Shark Bay

"Yandani Gutharraguda –
Welcome to Shark Bay"
(Nhanda and Malgana Aboriginal People)

## Stratigraphic architecture and evolution of a barrier seagrass bank in the mid-late Holocene, Shark Bay, Australia

Giada Bufarale and Lindsay B. Collins

Department of Applied Geology, Curtin University, GPO Box U1987, Perth, WA 6845, Australia

This article is published in Marine Geology, Volume 359, 1 January 2015, Pages 1-21.

doi.org/10.1016/j.margeo.2014.11.010 and reprinted with permission in Appendix A.

## Abstract

Within the Faure Sill complex (Shark Bay, Western Australia), a combination of remote sensing analysis, seismic stratigraphy and cores to ground truth, together with radiocarbon dating, demonstrate the interconnection between sediment body morphologies, seagrass related substrates and pre-existing topography and reveal the system as a channel – bank complex. Sea-level fluctuations appear to have largely controlled the hydrodynamic conditions of the bank, contributing to each stage of its evolution. 1) Not earlier than 8.5 – 8.0 ky BP, in a lowstand period, after an erosive event of underlying palaeosurfaces, seagrass establishment progressively contributed to initiating bank growth. 2) Around 6800 years BP, bank accumulation reached its apex, in conjunction with a rapid sea transgression. 3) During the Late Holocene, succeeding a slow decline to present sea level, bank growth continued to fill available accommodation space and a number of hiatuses, indicating temporal and spatial discontinuities within the process of bank building, are recognised. Average depositional rates of bank building (1.3 m/ky) conform to previous estimates derived for seagrass banks but rates are strongly facies dependent, attesting to the dynamic nature of this channel – bank complex. The extensive seagrass meadows are essential for a wide range of aspects of the environment of the Shark Bay area. Not only are they particularly important for the entire shallow benthic ecosystem, but they also had a major role in the partial closure of the southern basins and hence determining the development of hypersaline conditions and associated oolitic microbial and evaporitic facies in Hamelin Pool and L'Haridon Bight. Moreover, this system has a critical role in producing, sequestering and storing organic carbon.

## 1. Introduction

Registered as a World Heritage Property in 1991 on the basis of its "natural heritage" values (Hancock et al., 2000), Shark Bay is located approximately 800 km north of Perth on the west coast of Australia (Figure 3.1). It has a "W" shape, open to the Indian Ocean to the north and divided by the Peron Peninsula into two narrow gulfs: Freycinet Basin on the western side and L'Haridon Bight and Hamelin Pool, to the east (Figure 3.1B). Faure Sill, a seagrass bank, is one of Shark Bay's most notable structures, lying approximately between 25° 45' S and 26°30' S and 113° 40' E and 114° 15' E (Figure 3.2), orientated east – west across the axis of the Hamelin and L'Haridon hypersaline basins and covering an area of around 1000 km2 (Davies, 1970a). The bank extends from Kopke Point (Gladstone Embayment / Wooramel Complex) to Faure Island, Petit Point (Nanga Peninsula) and to Dubaut Point (southern part of Peron Peninsula); it is nearly emergent at Faure and Pelican Islands and it is characterised by shallow water and relatively deep and broad channels, mainly north – south oriented (Figure 3.2).

The two most prominent natural assets of Shark Bay are stromatolites and seagrass. Stromatolites are common in fossil sequences, widely recorded back to the Precambrian (Schopf, 1993; Allwood et al., 2006), but rare in modern waters, where their occurrence is limited to some locations in Western Australia, in the Bahamas and in a few other places elsewhere (e.g. Cohen et al, 1993; Dravis, 1983; Moore and Burne, 1994; Jahnert and Collins, 2013).

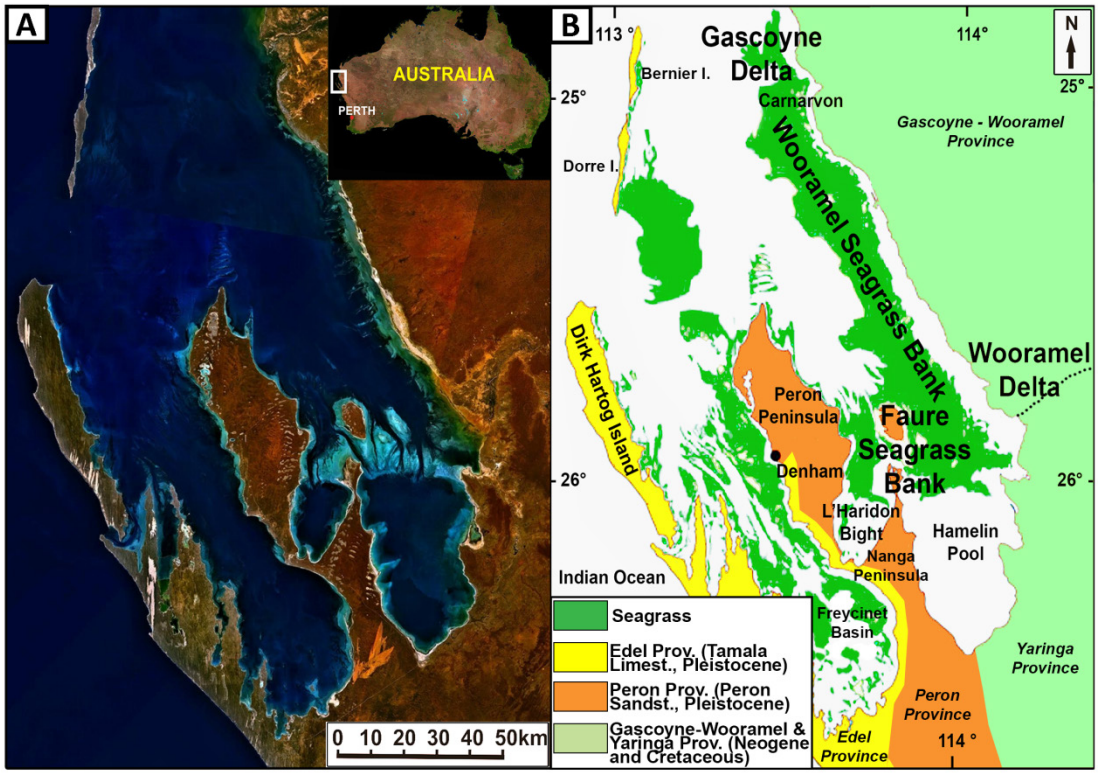


**Figure 3.1. A) Aerial view of the area from Geoscience Australia. B) Simplified map of Shark Bay, with seagrass distribution. The two most notable banks are the Faure and Wooramel seagrass banks, adjacent to the Wooramel and Gascoyne Deltas (modified from Walker et al., 1988; Jahnert and Collins, 2013; Playford et al., 2013 and www.sharkbay.org).**

It is well known that seagrass communities provide a wide range of services (Duarte, 2002; Gibb et al., 2014). They are fundamental in controlling fluid dynamics across the bank where they reside (Fonseca et al., 1982; Belperio et al., 1984; Verduin and Backhaus, 2000; Koch et al., 2006). The extensive seagrass meadows at Shark Bay, the largest reported assemblage in the world (Walker, 1990), has had a significant control during Holocene time on the sedimentary regime and the growth of the bank, leading to major environment changes, which have caused a partial closure of the southern basins of Hamelin Pool and L'Haridon Bight (Davies, 1970b; Logan et al., 1970a; Logan et al., 1970b; Hagan and Logan, 1974; Read, 1974; Walker, 1985; Walker et al., 1988a; Walker et al., 1988b; Jahnert and Collins, 2013; Collins and Jahnert, 2014). Its role in reducing the rate of water flowing through the sill has resulted in a decrease or loss of sediment movement, which is trapped and bound by the roots and rhizomes, stabilising and enhancing the accretion of the seabed (Walker et al., 1999). The thick meadow acts as protection from cyclones and other severe conditions and, as well, prevents erosion of the seafloor (Walker, 1990; Duarte, 2002). Moreover, epiphytes and other organisms (such as molluscs

and foraminifera), which live in their rhizomes, produce a significant amount of calcium carbonate and play an important role in the deposition and accumulation of sediment (Logan and Hagan, 1974; Walker and Woelkerling, 1988). Barrier banks, climatic conditions and restricted tidal exchange control the salinity of the enclosed waters (Logan and Cebulski, 1970), creating unique environments with metahaline to hypersaline conditions, which provide a basis for the development of a variety of biogenic and physical structures such as microbial communities (stromatolites) and oolitic shoals (Jahnert and Collins, 2013). Thus, explaining the evolution of the seagrass banks is crucial to understanding the development of the hypersaline facies association in basins to the south.

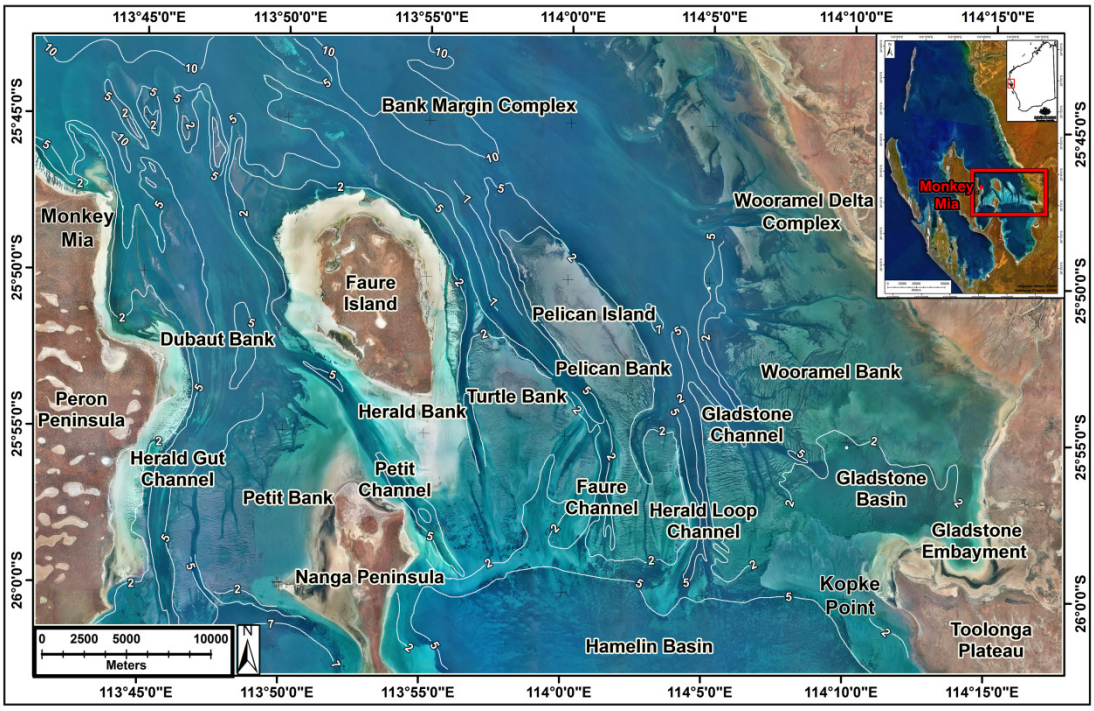


**Figure 3.2. Locality map showing the study area and the locations mentioned in sections 4 and 5. Locality names are from Hagan and Logan, 1974. Simplify bathymetric contours are shown. Aerial view of the Faure Sill is a mosaic of photos from Landgate (Western Australia). Insert image from Geoscience Australia.**

During the 1970's, pioneering research was described in two American Association of Petroleum Geologists Memoirs (Logan et al., 1970b; Logan et al., 1974) and subsequent work undertaken by Playford and Cockbain, 1976; Playford, 1990; Chivas et al., 1990. Recent research has provided the first detailed regional evaluation of the subtidal microbial system and tidal flat evolution (Jahnert and Collins, 2011; 2012; 2013; Collins and Jahnert, 2014).

Besides these local values, seagrass banks provide global ecosystem services. For instance, seagrass meadows are involved in producing, sequestering and storing organic carbon (Duarte, 2002; Grimsditch et al., 2012; Lavery et al., 2013; Duarte et al, 2013) and significantly contributing to carbon, nitrogen and phosphorus cycles in the ocean (Fourqurean et al., 2012). Moreover, the wider Gascoyne Delta – Wooramel Bank – Wooramel Delta – Faure Sill system (Figure 3.1B) has potential

as an analogue for some Browse Basin hydrocarbon reservoirs in the North West Shelf, Western Australia (Barber et al., 2003; Tovaglieri and George, 2014).

To investigate the Holocene development of the Faure channel – bank complex, remote sensing imagery analysis, acoustic profiles and sedimentological information were combined, in order to correlate internal architecture, sediment bodies and lithofacies. Integrating these data with radiocarbon dating, information about the accumulation rates was obtained, together with an estimated age of bank onset. This paper reports the analyses conducted on the Faure Sill and new insights and understanding of its evolution, growth and chronology, by considering morphostratigraphic elements, channel architecture and geometry, and linking traditional research with newly developed facies associations and stratigraphic relationships.

## 2. Geology and environmental setting

The landscape of Shark Bay has been significantly controlled by tectonism (Butcher et al., 1984). Fold and fault systems have been shaping the geography of the area since the Palaeozoic (Van de Graaff et al., 1976, Hocking et al., 1987). Anticlinal folds, oriented NNW – SSE, are responsible for the formation of peninsulas and islands and synclines are associated with the gulfs and bays (Butcher et al., 1984, Playford et al., 2013). A regional normal fault system oriented N – S has operated in the region and some reverse faults are associated with the anticlines (Butcher et al., 1984; Playford et al., 2013).

The Shark Bay region can be divided into four main physiographic provinces (Figure 3.1; Logan et al., 1970a; Hancock et al., 2000):

1) At the eastern margin of inland Shark Bay, Neogene and Cretaceous limestone units compose the *Yaringa Province* (Playford et al., 2013).

*2)* The *Gascoyne – Wooramel Province* is the wide alluvial coastal plain that stretches between the Gascoyne and Wooramel Rivers (Logan et al., 1970a).

3) The *Peron Province* is located in the central part of Shark Bay. During the latter part of the Quaternary, Shark Bay was characterised by three distinct marine transgressions (Logan at al., 1974; O'Leary at al., 2008; Jahnert and Collins, 2011). The first phase led to the formation of the Peron Sandstone (Logan, 1968; Logan et al., 1970a), a red, quartz rich sandstone, exposed on the Peron and Nanga Peninsulas and in Faure and Pelican Islands (Table 3.1).

4) The western Edel Province comprises Edel Land, Dirk Hartog Island and the Bernier – Dorre Islands. The main formation exposed in the area is the Tamala Limestone (Logan, 1968; Logan et al., 1970a; Playford et al., 1976), a pale, off white calcarenite (cemented calcareous dune sand) which developed as a result of a second phase of coastal dune formation (Logan et al., 1970a).

The Faure bank complex sits at a focal point between the coastal strip along the western margin of the Gascoyne – Wooramel Province and the eastern shores and hinterland of the Yaringa Province and Peron Provinces (Peron and Nanga Peninsulas and Faure Island; Hancock et al., 2000).

Although the principal Pleistocene units in the area are the eolianites of the Tamala Limestone and Peron Sandstone, there are also a few outcrops of Pleistocene marine formations: Dampier Limestone (and its member the Carbla Oolite), Bibra Limestone and Depuch Sandstone (Playford et al., 2013).

The Dampier Limestone (Logan et al., 1970a; van de Graaff et al., 1983) is the oldest marine dominated unit recognised in the Shark Bay area (Table 3.1). Dated as Middle Pleistocene, it was deposited in shallow marine (less than 3 m) tidal channel flats, storm beaches, and beach ridge environments (Hocking. et al., 1987). It outcrops in the coastal areas of the Edel and Peron Provinces. In east Hamelin Pool, the marine carbonate rocks of the Carbla Oolite member of the Dampier Limestone are exposed (Logan et al., 1970a; Playford et al., 2013).

**Table 3.1. Stratigraphic nomenclature for Shark Bay (modified from O'Leary at al., 2008). Note the position of acoustic reflectors HR1 and HR2 within the stratigraphy (top Bibra and top Dampier Limestones respectively, further discussed in later in the text). Tamala Limestone (Middle – Lower Pleistocene) and Depuch Limestone (Late Pleistocene) are also present in Shark Bay, but they have been excluded from the table since there is no evidence of their occurrence in the study area.**

| Series/Epoch | Formation | MIS | Sedimentation |
|---|---|---|---|
| Holocene | Holocene - Recent *Unit 1* | MIS 1 | Sill development |
| | | | HR1 |
| Upper Pleistocene | Bibra Limestone *Unit 2* | MIS 5a-5e | Marine deposits |
| | | | HR2 |
| Middle Pleistocene | Dampier Limestone *Unit 3* | MIS 9/11 (poorly dated) | Marine deposits |
| | | | HR3 |
| | Carbla Oolite Member *Unit 4 ?* | | Marine deposits |
| | | | HR4 |
| Middle - Lower Pleistocene | Peron Sandstone *Unit 5 ?* | MIS 11>37 | Transgressive system. Dune development |

The *Bibra Limestone* (Logan et al., 1970a; van de Graaff et al., 1983) is a thin intertidal deposit of bioclasts and corals, widespread in outcrops in Shark Bay (Logan et al., 1970a; Playford et al., 2013). It is estimated to have been deposited during the marine phase of the late Pleistocene interglacial (Marine Isotope Stage 5) high sea level stand (van de Graaff et al, 1983; Hocking et al., 1987; O'Leary et al., 2008). The last marine transgression (MIS 1) is referred to as the Holocene marine phase (Table 3.1).

The Depuch Limestone (Logan et al., 1970a) is a red brown, strongly cemented calcarenite and calcirudite derived by erosion and reworking of the Tamala Limestone (Playford et al., 2013) and can be found in Edel Province.

The presence of well-developed barrier banks associated with a semiarid to arid climate (1:10 ratio of rainfall / evaporation) and a restricted tidal exchange produced and preserves the hypersaline (56 – 70) conditions in the Hamelin Pool and L'Haridon Bight embayments (Logan and Cebulski, 1970; Logan et al., 1974; Walker et al., 1988; CALM, 1996, Hancock et al., 2000). Predominant southerly winds, 1 – 2 metre tidal range and large salinity and temperature gradients also strongly control the dynamics of the entire bay (Logan et al., 1974; Nahas et al, 2005).

## 3. Materials and methods

Initially, Faure Sill was mapped by delineating geomorphic and habitat boundaries. GIS Software (Geographic Information System; ArcGIS® by Esri) and datasets formed the basis of the descriptive analysis of seafloor features. High resolution (50 cm/pixel) orthophotos and aerial photos (1:25,000 scale) provided by the Department of Parks and Wildlife (DPaW) and sourced from Landgate (Western Australia), combined with ground truth data were used in order to draft detailed 2 maps (sediments and benthic substrates map and morphological elements map). Ground truth information was drawn from existing literature, particularly from Logan (1970) and Logan et al. (1974), from information collected as part of the Curtin Shark Bay Project (Jahnert and Collins, 2011, 2012 and 2013) and from the present project (32 cores and surficial sediment samples along the seismic lines). Two full coverage GIS based maps were created for Faure Sill.

A follow up shallow geophysical survey provided useful information on the thickness and seismic characteristics of the sediment packages and geometry of the seismic reflectors, giving good quality data on the Holocene and Pleistocene stratigraphic features of bank growth, down to a depth of about 15 m below the seafloor. The survey was carried out using a nonlinear (parametric) sub-bottom profiler (SBP) SES2000 Compact System (Innomar Technologie GmbH; Rostock, Germany), mounted vertically on the port side of the survey vessel. A Sokkia GSR2650 LB Differential Global Position System (DGPS) antenna was mounted on the top of the pole supporting the SBP, to provide an accurate position. During the survey, about 270 km of tracks were acquired, mainly oriented east – west and north – south. The penetration of the SBP varied across the survey area depending on the subsurface conditions. The processing software used was Innomar ISE version 2.9 (Interactive Sediment layer Editor) and SonarWiz 5 (Chesapeake Technology Inc.); the interpretation of the seismic sections has been performed based on a velocity of sound in sediments of 1600 m/s. Seismic velocity was chosen in accordance with the lithology of the area, which can be generalised as loose sand, very soft clay and medium dense to dense sand and gravel (see Hamilton, 1970; Leighton and Robb, 2008).

Lastly, during the stratigraphic survey, a vibracorer was used (from Quaternary Resources, Australia). To integrate and assess the results obtained with the seismic survey, 32 sediment cores were collected. A Sokkia GSR2650 LB DGPS, interfaced

with a laptop computer running OpenCPN 2.5.0 (open source navigation software), was used to position the vessel on the pre-established core location coordinates. Later, each core was cut into 1 metre sections of and relocated to the Sedimentology Laboratory in the Department of Applied Geology, at Curtin University (Western Australia). Then, after splitting each section, cores were photographed and studied. Core logging included an evaluation of colour (using the Munsell Soil Chart – Munsell, 1954), bioturbation, texture and lithology and a record of any major stratigraphic changes. Finally, samples were collected for further analyses, such as X-Ray diffraction (XRD), foraminiferal identification (Parker, 2009) and radiocarbon AMS $^{14}C$ dating.

Dating values derived from four cores were used to assess the age of reflectors and facies and to calculate accumulation rates in the bank and delta areas. The dating was conducted by the Radiocarbon Dating Centre (Australian National University, ACT), using the accelerator mass spectrometer method (AMS). One species of foraminifera (*Amphisorus hemprichii*, Ehrenberg, 1839) was targeted and picked for dating. 20 mg of sample was the minimum weight required for dating (Fallon et al., 2010). Reworked, abraded or micritised specimens were excluded, since they could lead to unreliable dates and outliers in data. The quantity of *Amphisorus* in some intervals was scarce, limiting the choice of specimens. The conventional ages and their error, rounded to the nearest year (Fallon et al., 2010), are expressed in radiocarbon years using the Libby half-life of 5568 years and following the conventions of Stuiver and Polach (1977). The curve Marine09 was used as a calibration dataset to convert conventional ages into calibrated years, assuming a delta R of 70 ± 50. The marine calibration incorporates a time dependent global ocean reservoir correction of about 400 years (Stuiver and Reimer, 1993; Stuiver et al., 2005).

# 4. Results

## 4.1. Morphology and substrate mapping

A sediments and benthic substrates map and a morphological elements map were derived through an initial remote sensing analysis of the Sill. Superficial sediment facies, geomorphic features and bedforms reveal the composite nature of the complex.

### *4.1.1. Sediments and benthic substrates of the Faure Sill System*

Sediments and benthic substrates were grouped according to their tidal zone position: hinterland, supratidal, intertidal and subtidal (Figure 3.3). The hinterland is dominated by eolian Pliocene and Pleistocene deposits of the Peron Sandstone (quartz sandstone) and “birridas”, which are interdune depositional basins of granular gypsum and quartz sediment fills (Jahnert and Collins, 2012) to the west, while to the east, Cretaceous Limestone (Toolonga Calcilutite), Quaternary alluvial and colluvial deposits of the Wooramel Delta and quartz sand dominate (Jahnert and Collins, 2012). Supratidal and intertidal facies include evaporites, hypersaline coquinas, microbial mats, stromatolites and sandy sediments. Nearshore, subtidal substrates are mainly microbial deposits (stromatolite and cryptomicrobial

structures, also lithified microbial pavement and bivalve coquinas). The Faure Bank consists of mobile mixed bioclastic quartz sands at surface.

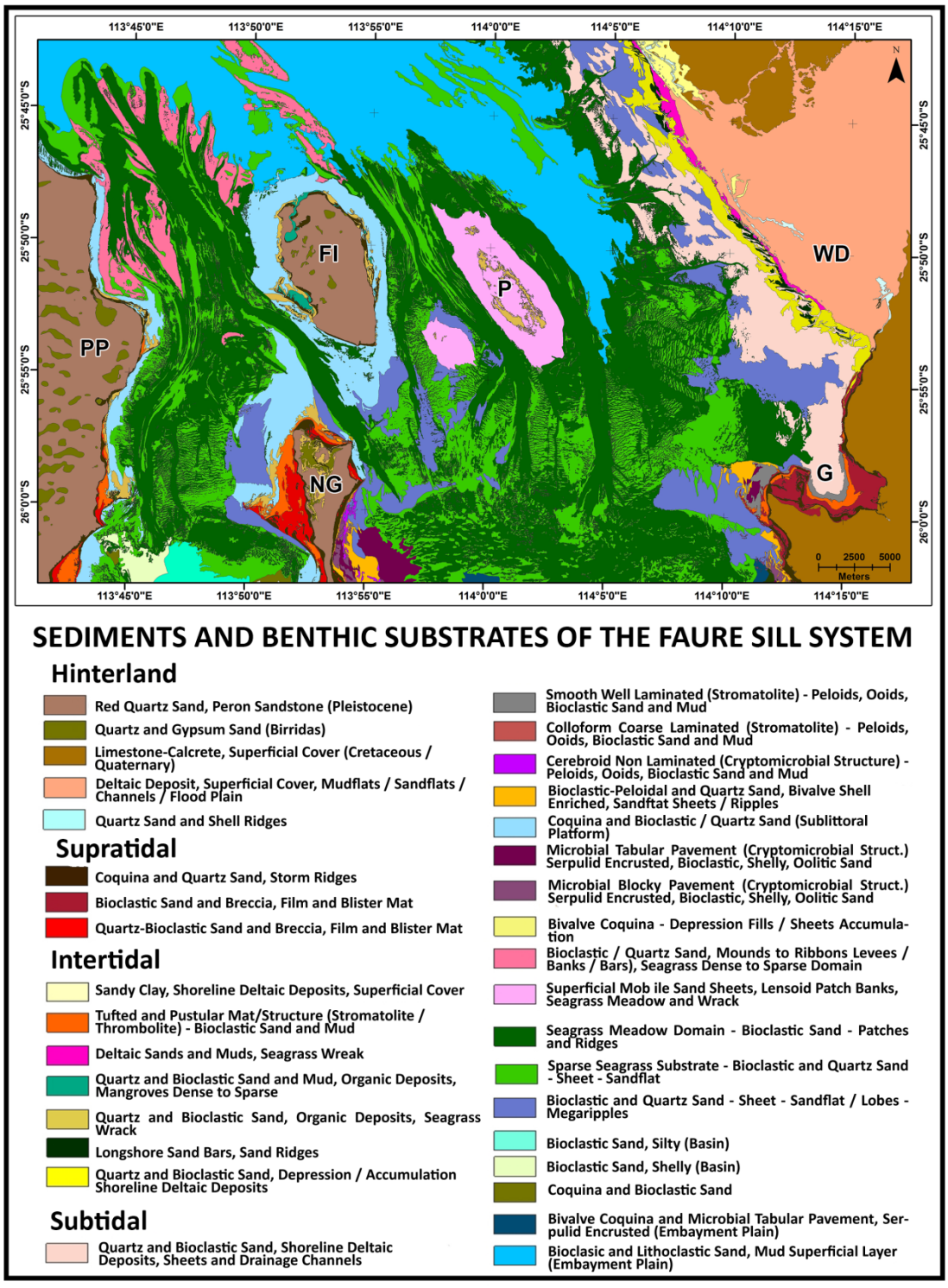


**Figure 3.3. Sediments and benthic substrates of the Faure Sill System. Note the preponderance of light and dark green, associated with substrates related to the presence of seagrass. PP= Peron Peninsula; NG= Nanga Peninsula; FI= Faure Island; P= Pelican Island; WD= Wooramel Delta; G= Gladstone Embayment.**

In the south, the embayment plain of Hamelin Pool comprises bivalve coquina, serpulids and algae with a superficial veneer of microbial organic material (Jahnert

and Collins, 2012); while in L'Haridon Bight the basin is mainly composed of bioclastic, silty sand (Collins and Jahnert, 2014). Bioclastic and lithoclastic sand, covered by a muddy layer, occupies the northern side of Faure Bank. Bioclastic particles are mainly seagrass epiphytes, including coralline algae, foraminifera and other constituents, together with small bivalves. Seagrass is sparse over the bank surface but relatively dense on channel margins, and is mainly *Amphibolis antarctica (Labillardière)* Sonder & Ascherson ex Ascherson 1868 (Walker, 1990).

### *4.1.2. Morphological elements of the Faure Sill System*

The morphological elements of the Faure Sill System (Figure 3.4) consist of channel and tidal fan associated features (longitudinal and lateral bars, flood and ebb tide fans and levees) and bank elements, including patch, fringing and barrier banks, with surficial sand sheets, usually with ripples or megaripples.

L'Haridon, Hamelin and Gladstone basins enclose the southern side of the bank and an embayment plain flanks the northern border. In the hinterland of the delta complex, numerous abandoned channels are present, evidence that the Wooramel River has switched its path during Pleistocene and Holocene time. The sublittoral platform which fringes the southern coast of Faure Sill includes oolite shoals and lithified pavement.

## 4.2. Acoustic classification of sediment bodies

Post processing and interpretation of SBP data provided useful information on the thickness, lateral distribution and internal architecture of sediments, up to 15 m below the seafloor.

A number of significant acoustic reflectors were identified and considered on the basis of their position and acoustic impedance. From top to bottom the identified horizons are Seafloor, HR1, HR2, HR3 and HR4 (Table 3.1). Age data is based upon the work of Logan et al. (1970) and O'Leary et al. (2008). The profiles show further minor discontinuities, located in the Holocene sediment package, between Seafloor and HR1.

Seismic reflectors from HR1 to HR4 are acoustically quite similar and sometimes can be discerned only by analysing their stratigraphic position and horizontal distribution. They mainly appear as irregular surfaces, generally flat and not always well defined, due to signal penetration or amplitude anomalies; these are primarily located where the seagrass is particularly dense. Air bubbles, originating from the plants' photosynthetic activity, can have a strong impact on the propagation of sound in water, causing a stronger scattering and reflection (Wilson et al., 2012). In some areas, generally where the water was very shallow, the acoustic penetration was very limited due to harder bottom or seabed multiple echoes which masked the data.

HR4 is the deepest horizon found in the profiles acquired and can be considered the acoustic basement of the area. It has been detected only close to the Wooramel Delta and at the eastern side of Monkey Mia, where it deepens to 8.5 m below the seabed (12.1 m below sea level). HR4 caps Unit 5 (Peron Sandstone, see Table

3.1) whose base has not been recorded, either on seismic data or in any core sample.

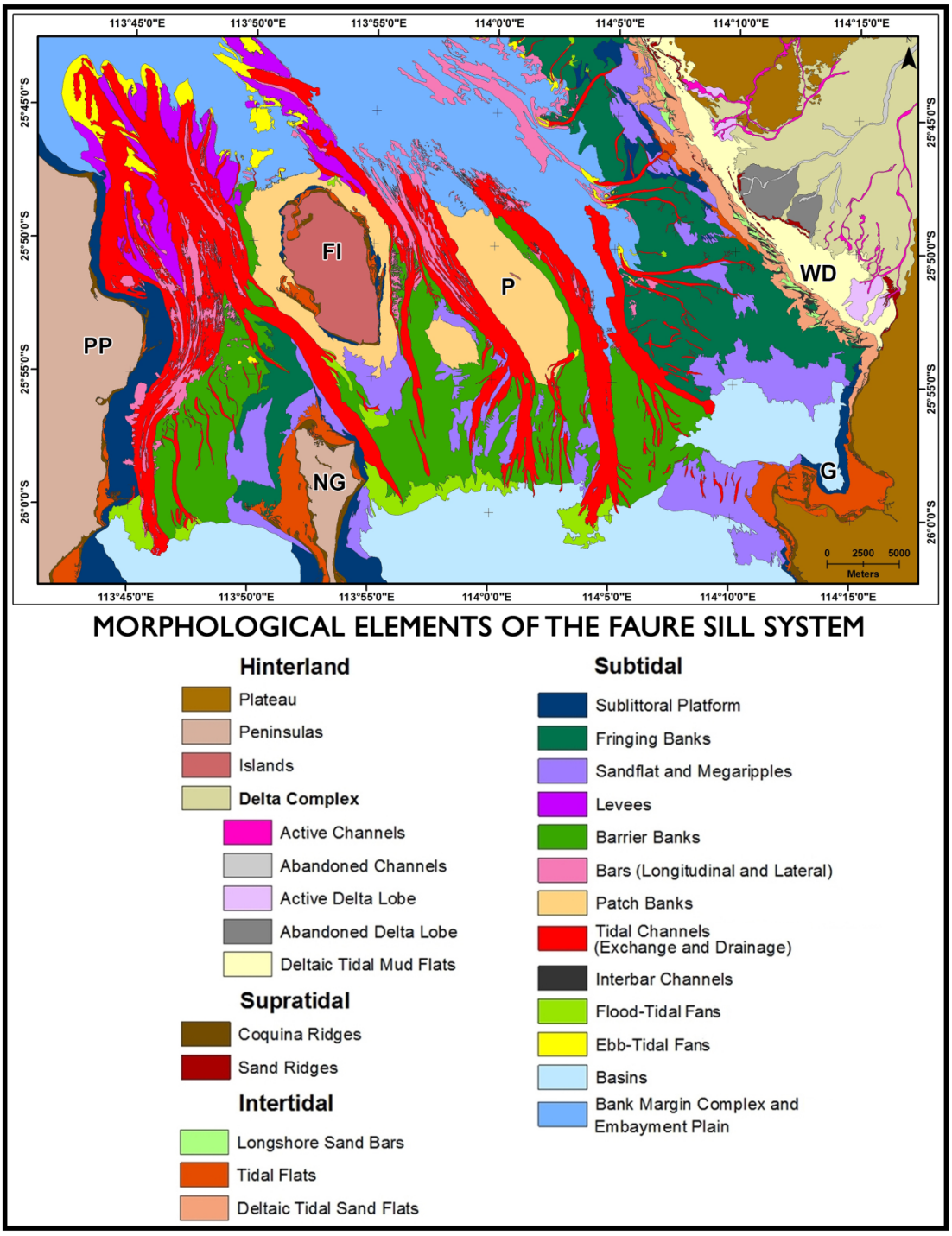


**Figure 3.4. Morphological Elements of the Faure Sill System. Note the well-developed channels (in red). Fringing and barrier banks are colour coded in dark greens. Ebb tidal fans are mainly located in the north – western side of the Faure Sill, but at smaller scale they are present also along the margins of the Wooramel Delta. Flood tidal fans (light green) are along the southern bank margin. PP= Peron Peninsula; NG= Nanga Peninsula; FI= Faure Island; P= Pelican Island; WD= Wooramel Delta; G= Gladstone Embayment.**

More continuous and observable in Dubaut and Wooramel banks is the horizon HR3, which, from the profiles, has a depth that ranges from 1.4 to 11.4 m below the

seafloor (5.0 to 13.3 below sea level). Unit 4 (identified as Carbla Oolite) is below the discontinuity HR3 and above the acoustic basement HR4. From a stratigraphic point, the deepest reflector that can be followed beneath almost all the bank is HR2 (top Dampier Limestone, Unit 3). In the middle of the central bank, it can be detected as deep as 9.3 m below the seafloor (approximately 12.7 m below sea level). Where top and base reflectors are resolved, it is possible to calculate the thickness, which ranges from a few centimetres to a maximum of more than 4.7 m between Herald Loop and Gladstone Channel (refer to Figure 3.2 for location), averaging 1 m. A clear and marked acoustic response derives from HR1 (top Bibra Limestone), which can be considered the main acoustic reflector in the area. This horizon occurs at a depth that ranges between 1.9 and 11.5 m below sea level and can be interpreted as an erosional surface that separates Bibra Limestone (Unit 2) and the Holocene sequence (Unit 1). Unit 2 is bounded by HR1 and HR2 and its thickness can reach up to 4 m, but more commonly it is around 1 m.

Above the reflector HR1, the Holocene sedimentary package is well represented (Unit 1). Its thickness ranges between 0.10 m and about 8 m and SBP profiles reveal a complex internal structure within this unit, with many relict features, such as numerous oblique to sigmoid prograding acoustic reflectors, often truncated. An intra-Holocene horizon is identifiable in the whole bank. It is a probable palaeo-topographic surface, often expressed as buried channels, later infilled with softer sediments and it may indicate lowstand erosion within the Holocene sequence of generally rising sea levels and vertical bank growth.

A classification system for sediment bodies based on acoustic characteristics and distribution and the morphological features of the bank was developed and includes five main types: 1. Bank top sediment bodies; 2.Channel associated sediment bodies; 3. Tidal fan associated sediment bodies; 4. Shoreline attached sediment lobes; 5. Patch banks, Fringing Banks and Barrier Banks. Characteristics of these sand bodies are summarised in Table 3.2.

The internal architecture of selected Holocene sediment bodies is illustrated in Figure 3.5.

1a) Bank Top – Linear Ridges: the central and shallowest areas of the Faure Sill are characterised by elongate seagrass ridges, having an east – west linear trend. They are well stabilised, mainly composed of *Amphibolis*, and represent an important surface aspect of the bank where seagrass has vegetated and stabilised tidally generated linear bedforms. In Figure 3.5A, the high rate of deposition is clearly evident. The first metre of sediment is characterised by intense progradation, with a north – south direction. The surficial sediment is sandy, allowing a penetration of the signal to 4 – 6 m below the seafloor (cf Figure 3.3). At this depth a strong and continuous reflector (HR1), harder than the overlying sediment, is recorded. A second weaker and more discontinuous reflector (HR2) is documented between 6 m and 7 m below the seabed.

**Table 3.2. Sediment body types of the Faure Sill, based on shallow geology investigation.**

| Sediment body type | Morphology | Scale | Biota/internal architecture/facies | Example |
|---|---|---|---|---|
| 1) Bank top: linked with the presence of seagrass and pre-Holocene topographic highs | | | | |
| a. Linear ridges | Elongate E–W; tidally generated seagrass stabilised. | H = 1–2 m<br>L = 000s of m | *Amphibolis* ribbons; bivalve lags. Intense progradation. Sandy top. | Central and shallower areas across the Sill (Fig. 5A). |
| b. Flat topped sand sheets | Flats; sheet to wedge like. | H = 1–3 m<br>L = 00s of m | Sparsely populated by seagrass. Progradation. Muddy bioclastic sand on top and sandy bioclastic mud. | South-western edge of Faure Island, northern part of the Nanga Peninsula, western side of the Faure Sill. |
| 2) Channel associated: five exchange channels branching off in many minor drainage channels | | | | |
| a. Longitudinal channel bars | Present in every major channel; elongate along the main stream flow; channel parallel | H = 2 m<br>W = 00s of m<br>L = 000s of m | Moderate density seagrass cover (*Amphibolis*). Homogeneous internal architecture. Quartzose sand. | Associated with all major channels (e.g. Herald Bight and Herald Gut). (Fig. 5B). |
| b. Lateral spill over sheets | Sheet like, elongate N–S along bank/channel margins. | H = 0.5 m<br>L = 00s of m | Bare muddy sand carbonate facies. | Associated with all major channels and tidal fans. |
| c. Interdistributary channels | Flat topped, triangular bars, flare down current. | H = 1–2 m<br>L = 000s m | Minor seagrass. Distinct sets of palaeochannels. Laminated silty sand and sandy mud. | Variably distributed along the southern part of the bank (Fig. 5C). |
| 3) Tidal fan associated: terminal prograding flood and ebb tidal fans | | | | |
| a. Distributary mouth bars (flood tidal fans) | Deltoid to lobate terminal bars, frequently coalescing, prograding basinward. | H = 1–4 m<br>L = 000s of m | Bare sandy top, overlying carbonate mud. Frequently cross bedded, oblique to sigmoid acoustic reflectors. | Southern edge of the Faure Sill, between Nanga Peninsula and Gladstone Embayment (Fig. 5D). |
| b. Ebb tidal fans | Main channel, flanked by linear bars, terminating with a seaward sloping lobe. | H = 1–2 m<br>L = 0–00s of m | Bivalves and small foraminifera, no seagrass. Silty sand with fine to medium, well-rounded quartz. | North west bank, close to Monkey Mia, at the end of Herald Gut and Petit Channels. Along the margins of the Wooramel Delta. |
| c. Levees | Channel margin spill over banks, Flat surface. | H = 1–4 m | Seagrass stabilised along the margins. Reflector free. Muddy sand on top and sandy mud downward. | Herald Loop fan delta, Herald Gut ebb tide delta. |
| 4) Shoreline attached sand lobes | | | | |
| Shoreline attached sand lobes | Sheet like, basin ward prograding, megaripples. | H = up to 1.5 m<br>Wavelength ≈ 25–30 m,<br>L = 000s<br>Thickness = 7 m | Bare sandflat, intense progradation. Laminated sands and carbonate muddy apron facies. | Close to Gladstone Embayment (Kopke Point). (Fig. 5E). |
| 5) Patch Banks, Fringing Banks, Barrier Banks | | | | |
| Patch banks, fringing banks, barrier banks | Surrounding or associated with topographic highs. | Variable<br>H = 1–7 m | Seagrass and bioclastic sand (top) and sandy bioclastic mud at base. | Herald, Petit and Dubaut Fringing Banks, Pelican and Turtle Patch Banks, Wooramel Bank. |

1b) *Bank Top – Flat Topped Sand Sheets*: sand flats and sand sheets border Faure Island and the northern part of the Nanga Peninsula with their maximum extent found in the south and south – east parts of the island. They are sparsely populated by seagrass and are morphologically flat.

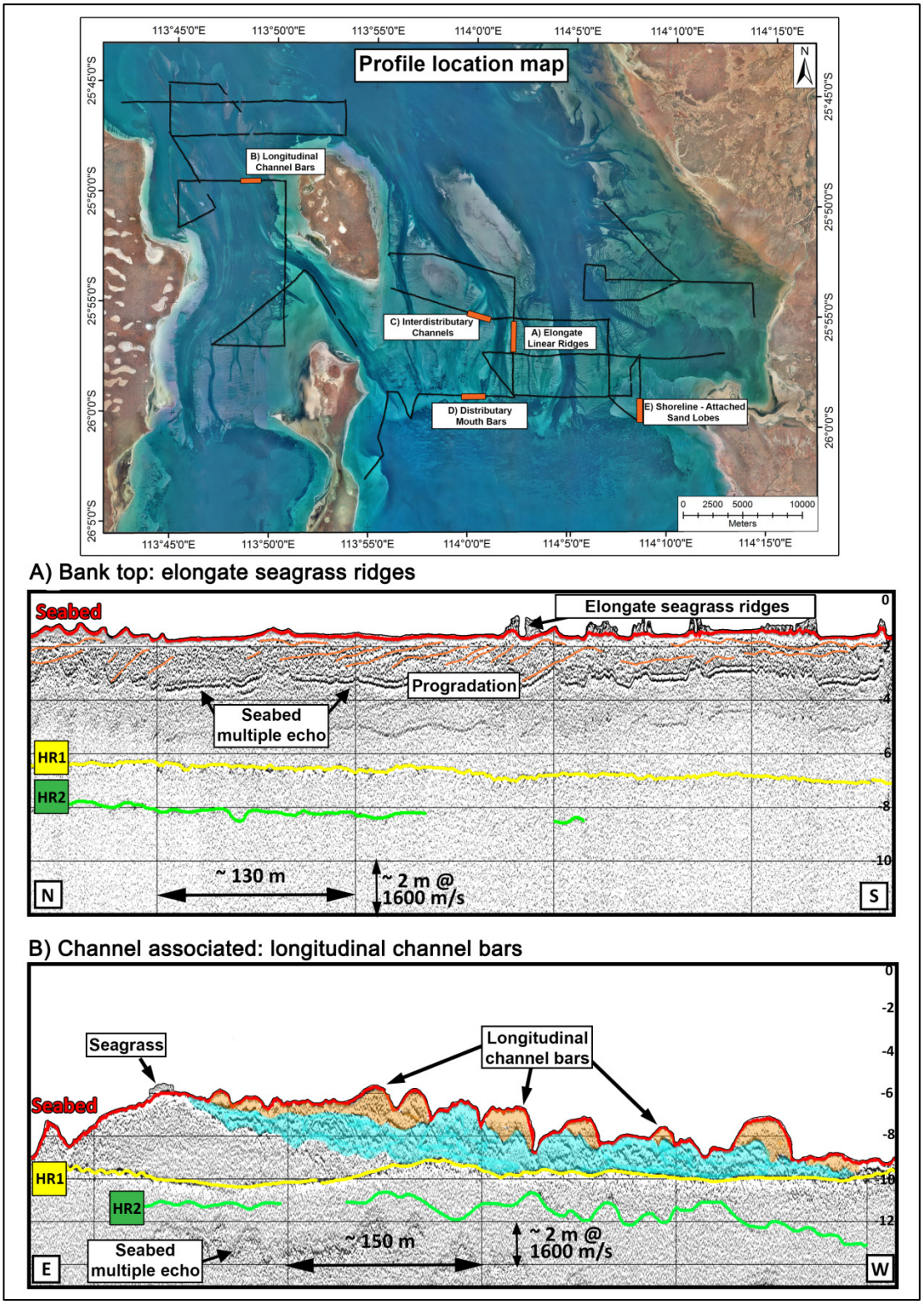


**Figure 3.5. Examples of stratigraphic profiles of sediment bodies. Main acoustic reflectors have been illustrated to highlight their occurrence. In green: reflector HR2; in yellow: reflector HR1; in blue and orange: palaeosurfaces in Late Holocene sedimentary package; in red: seafloor. Vertical axes represent the depth below sea level (every profile starts at 0 m). A) 1a: Bank top – elongate linear ridges vegetated by seagrass. The first metres of sediment are characterised by intense progradation of bank sediments, with a south – north direction and a high rate of deposition. The surficial sediment is sandy. B) 2a: Channel associated – longitudinal channel bars (orange) are homogeneous and without internal structure. The underlying sediments (blue) are about 1 – 2 m thick, with a wedge shape and bar like morphology.**

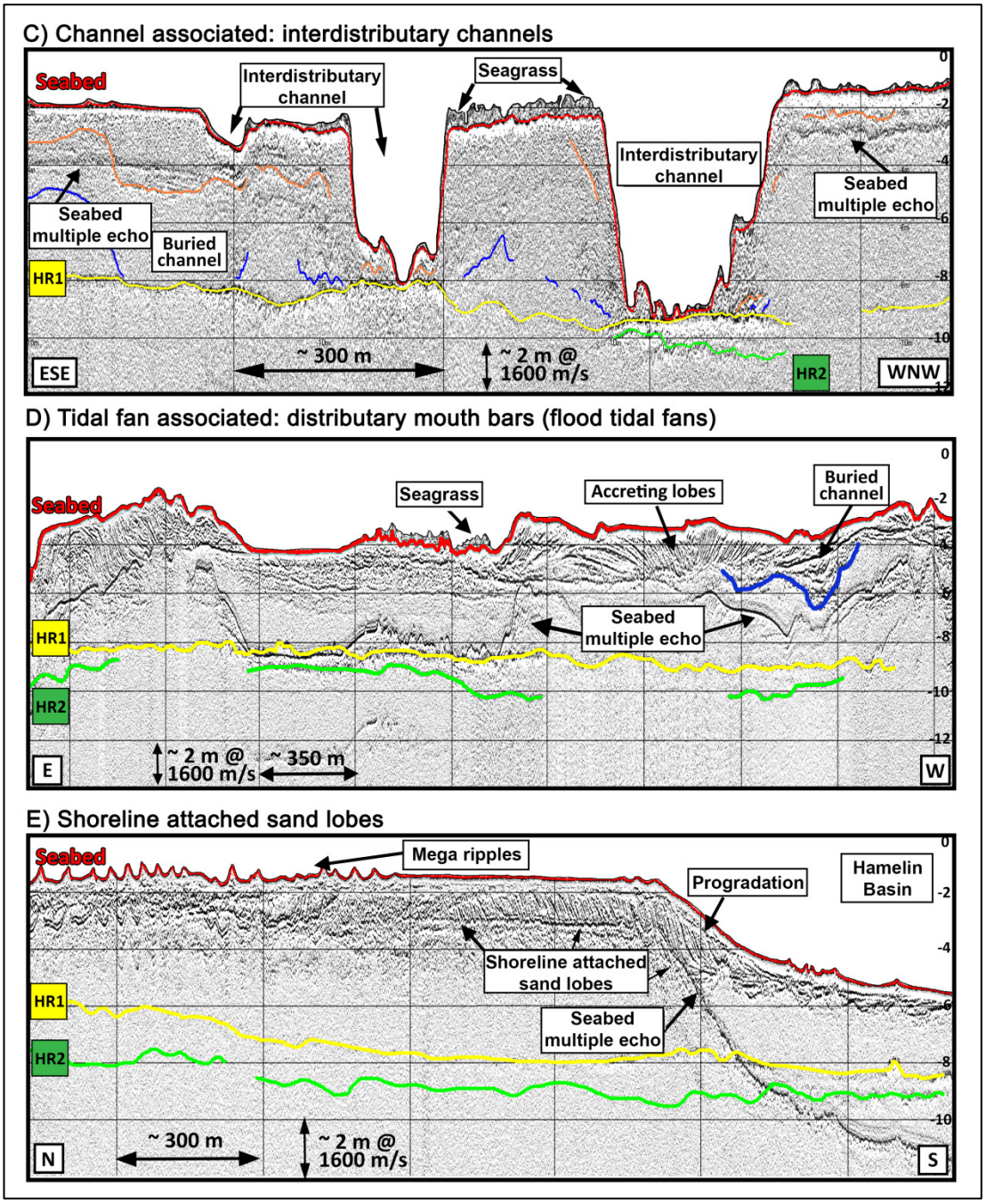


**Figure 3.5 (continued). C) 2c: Channel associated – interdistributary channels. Some profiles reveal distinct sets of palaeodistributary channels that characterise a buried morphology within the tidal fan areas. D) 3a: Tidal fan associated – distributary mouth bars. The lateral accretion pattern within coalescing distributary mouth bar lobes characterises the flood tidal complex along the southern bank margin. E) 4: Shoreline attached sand lobes. Note progradation towards Hamelin Pool to the south. Megaripples are several hundred metres long, with a wavelength about 25 – 35 m, east – west oriented.**

2a) *Channel Associated – Longitudinal Channel Bars*: longitudinal channel bars are present in every major channel. They are morphologically elongate north – south and mainly channel parallel. In Figure 3.5B, longitudinal channel bars are highlighted in orange; they do not have any particular internal architecture, which indicates the material is homogeneous. The underlying sediments (in blue) are

about 1 – 2 m thick, with a wedge shape. Both the top and the bottom (HR1) are good reflectors, but there are numerous, weaker and very irregular internal reflectors within this earlier generation of a bar complex. Between HR1 and the sediment highlighted there is an earlier package of sediments, where very little internal reflection is recognisable.

2b) *Channel Associated – Lateral Spillover Sheets*: spillover packages involve lateral accretion near channel margins and upward bank growth. This sand body type is associated with all major channels and tidal fans and they are often associated with small buried channels, filled with 1 – 2 m of sediments, usually parallel to the modern channel, but significantly narrower.

2c) *Channel Associated – Interdistributary Channels*: besides the main tidal channels, which permit an exchange of water between Hamelin Pool and L'Haridon Bight and the rest of the bay, there are several drainage channels, variably distributed along the southern part of the bank. Some profiles reveal distinct sets of palaeodistributary channels that characterise a buried morphology within the tidal fan areas (Figure 3.5C).

3a) *Tidal Fan Associated – Distributary Mouth Bars*: east – west profiles show well-defined accreting lobes within distributary mouth bars, between the embayment plain of Hamelin Basin and the Faure bank. These features are about 2 – 5 m thick and are interrupted by occasional buried channels. North – south seismic lines confirm the oblique reflection configuration that occurs with the progradation pattern on the bank margin. The lateral accretion pattern within coalescing distributary mouth bar lobes is clearly shown in Figure 3.5D in a flood tidal complex along the southern bank margin. The horizon HR1 is not recognisable throughout due to seabed multiple echoes which are particularly strong in these profiles. Where visible, it is flat and about 5 m below the seafloor.

3b) *Tidal Fan Associated – Ebb tidal fans*: mainly situated in the North West bank, close to Monkey Mia, well-developed ebb tidal fans consist of bare thin Holocene sediments, terminating with a seaward sloping lobe. Although the major terminal fans can be found at the end of Herald Gut and Petit Channels, minor fans occur also along the margins of the Wooramel Delta, at the mouths of Wooramel active channels (mapped in yellow in Figure 3.4).

3c) *Tidal Fan Associated – Levees*: the area between Dubaut Bank and the Herald Gut ebb tide fan is characterised by the presence of subtidal shallow levees and channel margin spill over sheets. They are well developed structures, stabilised by thick seagrass on top. The internal architecture is poorly defined and almost reflector free, probably due to seagrass cover impeding penetration. The surface morphology is essentially flat.

4) S*horeline – Attached Sand Lobes*: between Gladstone Basin and Hamelin Pool (Kopke Point), a shallow sand lobe complex is present. Bare sand flats and megaripples cover the surface. The seismic profiles reveal a distinct progradation throughout the margins of the complex. In the south, a flood tide progradation prevails, and in the northern margin ebb tide progradation is present. The lobes are

characterised by a complex reflector configuration, with numerous oblique to sigmoid reflectors in N – S section. Progradation is controlled by tidal currents with lesser wind driven circulation. Megaripples (i.e.: subaqueous dunes according to Ashley, 1990) are several hundred metres long, with a wavelength about 25 – 35 m (Figure 3.5E).

5) *Patch Banks, Fringing Banks, Barrier Banks*: some banks present difficulties for profiling due to extremely shallow water over bank surface. Turtle and Pelican patch banks border the Faure Channel, and the topographic highs of the Peron Sandstone control the bank thickness. Based on the position of the HR2 reflector, Faure Channel was likely formed in the lowstand following Dampier time, and this has also determined its position during Bibra and Holocene time.

## 4.2. Composition and mineralogy of bank lithofacies

The nature and occurrence of the acoustic reflectors and units recognised in the seismic analysis were ground truthed with a follow up core study (Figure 3.6). Core logging and successive analyses have assisted with the interpretation of the results obtained with the seismic, allowing a lithological understanding of particular sediment packages. Although minor differences in terms of position and frequency occur, seismic reflectors correspond well to actual changes in facies and lithology in the cores.

The Faure Sill is composed of three different types of sediment: sand, mud and clay (Figure 3.3 and Figure 3.6). Bioclastic muddy sediments are by far the most common bank lithofacies. Bioclastic, quartzose, sandy facies are associated with *terminal ebb tidal fans*, in the north – western area of the Faure Sill (Figure 3.4 and Figure 3.6). Bioclastic, sandy facies are also common in the upper part of *terminal prograding flood tidal fans***,** located in the southern portion of the bank, bordering the northern Hamelin Pool basin (Figure 3.4 and Figure 3.6). The sand size ranges from coarse (generally cross bedded) to fine (frequently thinly laminated). Seagrass peats and skeletal particles are also a significant component. Shelly facies are typically associated with buried palaeochannels. Bioclastic, muddy facies are associated with lower *terminal prograding flood tidal fans and carbonate bank* and with delta related sediments Figure 3.4 and Figure 3.6). Kaolinite clays are found in the channel base unit of the *Wooramel Delta* area (Figure 3.6). In general, coarsening upward sequences characterise cores of bank build-up. Whereas muddy bioclastic facies are found in lower parts of the bank, likely reflecting dense seagrass cover of *Posidonia spp*, an efficient trapping of fine sediment, more sandy bioclastic sediments are found in upper parts of the bank and its terminal fans, where seagrass cover is sparse *Amphibolis* and tidal and wave reworking increases with bank shoaling (see Figure 3.6).

In a previous work, Hagan and Logan (1974, p. 73) have found that the dominant skeletal constituents of the bank are coralline algal particles and whole and fragmented foraminifers and molluscs. Nonskeletal sediment components are commonly quartz, lithoclasts and ooids.

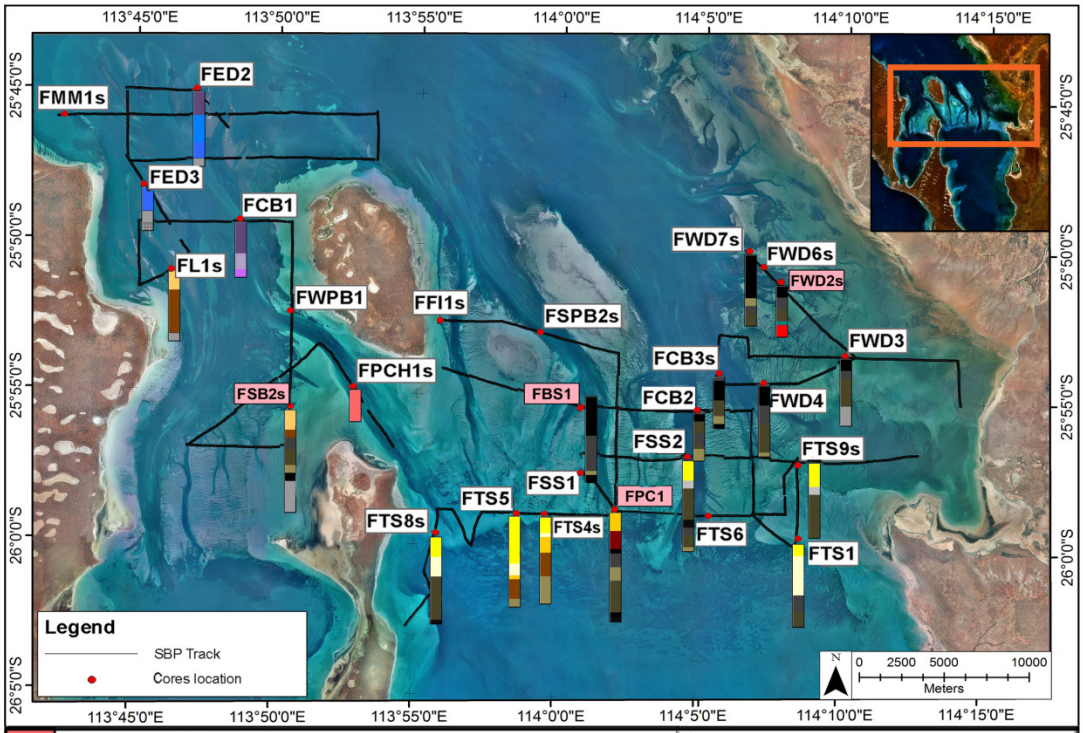


| | | |
|---|---|---|
| | Coarse Shelly Bioclastic Sand | Shelly facies, associated with paleo-channel |
| | Coarse-grained Cross-bedded Bioclastic Sand | Bioclastic - sandy facies, associated with upper **terminal prograding flood-tidal fans** |
| | Moderately Bioclastic Quartzose Silty Sand | |
| | Fine-grained Silty Bioclastic with Thinly laminated Mud and Seagrass Peats | |
| | Fine-grained Silty/Muddy Sand with Very Thinly Bedded Muddy Seagrass Peats | |
| | Medium Muddy Bioclastic Sand | |
| | Thickly laminated to Thinly Bedded Silty Bioclastic Sand and Weakly Bioclastic Mud | Bioclastic - muddy facies, associated with lower **terminal prograding flood-tidal fans and carbonate bank** |
| | Sandy Bioclastic Mud | |
| | Weakly Bioclastic Burrow Mottled Carbonate Mud | |
| | Strongly Bioclastic Carbonate Mud | |
| | Weakly bioclastic Sandy Carbonate Mud, Clayey | |
| | Moderately bioclastic Sandy Carbonate Mud, Clayey | |
| | Disseminated Pyrite Kaolinite Clay | **Wooramel Delta** associated kaolinite clay (channel base unit) |
| | Goethite Kaolinite Clay | |
| | Weakly Bioclastic Quartzose Sand | Bioclastic, quartzose, sandy facies, associated with **terminal ebb-tidal fans** |
| | Mildly Bioclastic Silty Quartzose Sand | |
| | Shelly Bioclastic Silty Quartzose Sand | |
| | Bioclastic Cross-bedded Quartzose Sand | |
| | Fine-grained Moderately Planar-bedded Bioclastic Quartzose Sand | |
| | Medium-grained Silty Quartzose Sand | **Pleistocene** |
| | Coarse-grained Shelly Sand | |

**Figure 3.6. Core interpretation with sub-bottom profiler track plot lines. Lithofacies are colour coded and grouped into major facies units in the legend. The cores sampled for dating and further analyses are highlighted in pink.**

Three cores were subsampled for XRD analysis. Core FPC1 was collected in the middle of the bank and cores FWD2s and FWD7s are from the Wooramel Delta area (refer to Figure 3.6 for their location).

Bank sediments are strongly bioclastic (from 42.7% to 75.15%), and are mainly composed of calcareous seagrass epiphytes. With the exception of sandy, bioclastic, bank top sediments, muddy carbonates in the lower and middle part of the sequence make up most of the package. Quartz content is locally significant where the underlying Peron Sandstone experienced channel erosion or where

topographic highs of Peron Sandstone shed quartz to the surrounding seagrass banks as erosion proceeded. The "amorphous" group in Figure 3.7 is a mixture of poorly ordered terrigenous clay minerals representing about 20 – 40% of the sediment in each sample, rising to 54% near the Wooramel Delta.

| | Core and Water Depth (m) | | wt% Carbonates | wt% Quartz | wt% Amorphous | |
|---|---|---|---|---|---|---|
| FPC1 | 0.02 | 3.22 | 73.05 | 1.78 | 25.17 | Bioclastic Sands |
| | 0.20 | 3.40 | 70.18 | 1.55 | 28.28 | |
| | 0.45 | 3.65 | 59.84 | 0.93 | 39.24 | |
| | 0.60 | 3.80 | 69.56 | 1.16 | 29.28 | |
| | 1.00 | 4.20 | 67.96 | 1.73 | 30.31 | Bank Muds |
| | 1.30 | 4.50 | 66.44 | 1.39 | 32.18 | |
| | 1.55 | 4.75 | 75.15 | 1.21 | 23.64 | |
| | 1.65 | 4.85 | 67.60 | 1.37 | 31.03 | Bioclastic Sands |
| | 2.75 | 5.95 | 48.70 | 15.37 | 35.93 | |
| | 3.60 | 6.80 | 70.06 | 1.19 | 28.76 | Bank Muds |
| | 4.42 | 7.62 | 74.38 | 1.48 | 24.14 | |
| FWD2s | 0.05 | 4.15 | 51.15 | 2.24 | 46.62 | Delta Muds |
| | 0.60 | 4.70 | 68.70 | 2.13 | 29.17 | |
| | 0.90 | 5.00 | 62.40 | 1.78 | 35.82 | |
| | 1.15 | 5.25 | 74.58 | 1.72 | 23.70 | |
| | 1.30 | 5.40 | 59.41 | 2.31 | 38.29 | |
| | 1.70 | 5.80 | 48.12 | 4.86 | 47.02 | |
| | 1.80 | 5.90 | 2.83 | 4.08 | 93.09 | Clays |
| | 2.30 | 6.40 | 2.69 | 4.16 | 93.15 | |
| FWD7s | 0.05 | 1.51 | 63.73 | 1.64 | 34.64 | Delta Muds |
| | 0.15 | 1.61 | 46.04 | 2.00 | 51.96 | |
| | 0.80 | 2.26 | 44.45 | 2.02 | 53.53 | |
| | 1.10 | 2.56 | 43.69 | 2.29 | 54.02 | |
| | 1.80 | 3.26 | 44.13 | 2.25 | 53.62 | |
| | 2.50 | 3.96 | 57.51 | 2.62 | 39.87 | |
| | 2.85 | 4.31 | 42.72 | 3.13 | 54.15 | |
| | 3.45 | 4.91 | 52.27 | 3.29 | 44.44 | |
| | 3.50 | 4.96 | 58.73 | 2.06 | 39.21 | |

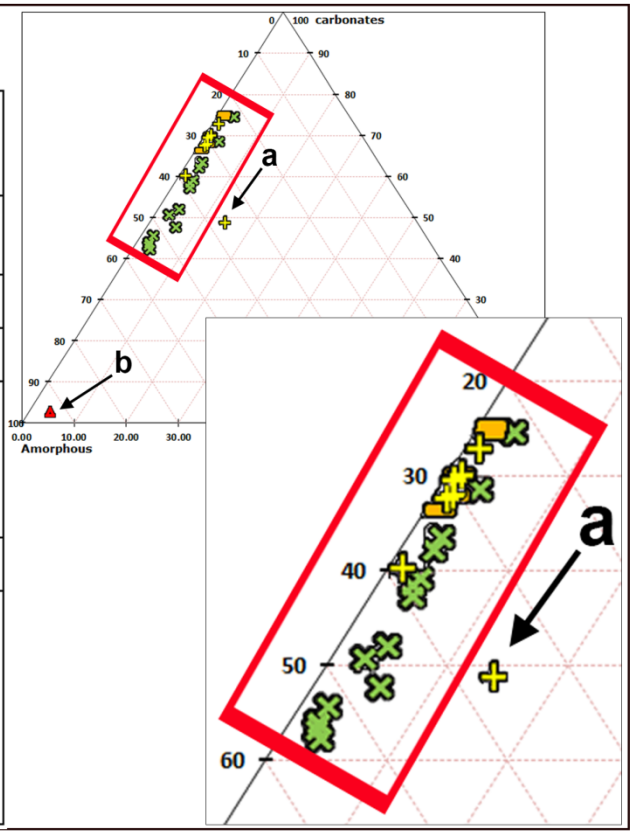


**Figure 3.7. Results of XRD analysis, expressed in % of weight. Triangular diagram summarises the XRD results for the cores. In green = delta muds (FWD2s and FWD7s); yellow = bank sands (FPC1); orange = bank muds (FPC1) and red = clay (FWD2s). The "amorphous" group represents mixed disordered terrigenous clays. The value indicated by the "a" arrow corresponds to the base of the palaeochannel in FPC1 (2.75 m from TOC). The "b" arrow shows the Wooramel channel base unit.**

## 4.3. Age model and sediment accumulation rates

Radiocarbon dating was used to assess the age of reflectors and facies and to calculate accumulation rates in the bank and delta areas, in particular the timing of channel infill and abandonment.

Four cores (FSB1, FSB2s, FWD2s, FPC1, refer to Figure 3.6 for location) were chosen for Radiocarbon AMS $^{14}C$ dating, based on morphological elements and facies association in the bank. The samples were selected assuming that intervals close to a contact between sedimentary units may represent an erosional event, a change in depositional energy or the dominant process, or in sediment supply.

Moreover, samples between sedimentary contacts give information about long term sediment accumulation rates. In Table 3.3 the age results and their error, rounded to the nearest year (Fallon et al., 2010), are presented, together with the depths of the samples below sea level and seafloor. Accumulation rates derived from radiocarbon

ages combined with sediment thicknesses obtained through seismic data were used to estimate the age of Faure Sill onset and other bank events.

**Table 3.3. Depths for each sample (from seafloor and from sea level, in metres) and the conventional and calibrated ages, obtained with $^{14}C$ AMS dating. Column 9: Dh (m) = length in metres of the interval. Colum 10: Dt (y) = difference between the highest and lowest age in the corresponding interval. Last column reports the growth rates for different sections in the cores. Apparent growth rates were calculated from the difference between the highest and the lowest age of the corresponding section. The gaps in the cores indicate erosional intervals and are highlighted in the table in red.1) Gap = 2445 ± 59 y (transition mud to sand). 2) Gap = 1878 ± 53 y (transition weakly bioclastic mottled mud to moderate bioclastic clayey mud). 3) Transition Pleistocene to Holocene sediments, 4) Gap = 658 ± 50 y (base buried channel). 5) Gap = 3319 ± 60 y (transition strongly to moderately bioclastic clayey carbonate mud). 6) Gap = 2307 ± 68 y (transition weakly to strongly bioclastic mud). 7) Gap = 1737 ± 59 y (transition sandy mud to clayey mud). 8) Gap = 1102 ± 71 y (transition clayey mud to sandy mud). Note that gaps 1 and 7 are overlain by sandy (rather than muddy) bank sediments which become dominant. Further discussion is in this section.**

| Sample | Depth from seafloor (m) | Depth from sea level (m) | Conventional $^{14}C$ age (years) | Error ± (years) | Calibrated ages (marine reservoir effect) 68.2% probability (years) | Error ± (years) | Section | Dh (m) | Dt (yr) | Dh/Dt (m/ka) | |
|---|---|---|---|---|---|---|---|---|---|---|---|
| FSB2s-CD1 | 0.05 | 2.27 | 1135 | 25 | 646 | 26 | 1 | 0.58 | 979 | 0.59 | |
| FSB2s-CD2 | 0.63 | 2.85 | 2110 | 30 | 1625 | 54 | | | | | → 1 |
| FSB2s-CD3 | 1.05 | 3.27 | 4105 | 30 | 4070 | 64 | | | | | → 2 |
| FSB2s-CD4 | 2.00 | 4.22 | 5630 | 30 | 5948 | 43 | 2 | 0.63 | 347 | 1.82 | |
| FSB2s-CD5 | 2.63 | 4.85 | 5290 | 35 | 5601 | 39 | | | | | → 3 |
| FSB2s-CD6 | 3.00 | 5.22 | 34180 | 430 | 38418 | 646 | Pleistocene | | | | |
| FSB2s-CD7 | 3.20 | 5.42 | 33660 | 400 | 37971 | 585 | | | | | |
| FSB2s-CD8 | 3.30 | 5.52 | 34110 | 420 | 38341 | 610 | | | | | |
| FSB2s-CD9 | 3.50 | 5.72 | 32860 | 370 | 36954 | 432 | | | | | |
| FSB2s-CD10 | 3.55 | 5.77 | 32060 | 330 | 36026 | 530 | | | | | |
| FSB2s-CD11 | 3.70 | 5.92 | 31680 | 320 | 35760 | 509 | | | | | |
| FSB2s-CD12 | 4.66 | 6.88 | 30190 | 280 | 34414 | 343 | | | | | |
| FPC1-CD1 | 0.05 | 3.25 | >MODERN | NA | >MODERN | NA | 1 | 2.70 | 390 | 6.93 | |
| FPC1-CD2 | 0.50 | 3.70 | 385 | 40 | 33 | 23 | | | | | |
| FPC1-CD3 | 0.78 | 3.98 | 505 | 35 | 92 | NA | | | | | |
| FPC1-CD4 | 1.45 | 4.65 | 680 | 25 | 273 | 28 | | | | | |
| FPC1-CD5 | 1.60 | 4.80 | 650 | 35 | 216 | 69 | | | | | |
| FPC1-CD6 | 1.85 | 5.05 | 810 | 30 | 390 | 56 | | | | | |
| FPC1-CD7 | 2.30 | 5.50 | 755 | 45 | 346 | 55 | | | | | |
| FPC1-CD8 | 2.75 | 5.95 | 705 | 40 | 306 | 55 | | | | | → 4 |
| FPC1-CD9 | 3.75 | 6.95 | 1480 | 35 | 964 | 45 | 2 | 1.00 | 659 | 1.52 | → 5 |
| FPC1-CD10 | 3.90 | 7.10 | 4240 | 40 | 4280 | 76 | | | | | → 6 |
| FPC1-CD11 | 4.15 | 7.35 | 6210 | 40 | 6587 | 60 | 3 | 0.25 | 121 | 2.07 | |
| FPC1-CD12 | 4.40 | 7.60 | 6315 | 40 | 6708 | 58 | | | | | |
| FSB1-CD1 | 0.20 | 3.03 | 645 | 30 | 213 | 66 | 1 | 3.8 | 1686 | 2.25 | |
| FSB1-CD2 | 3.02 | 5.85 | 1405 | 30 | 890 | 46 | | | | | |
| FSB1-CD3 | 4.00 | 6.83 | 2345 | 35 | 1899 | 53 | | | | | |
| FWD2s-CD1 | 0.05 | 4.15 | 1790 | 30 | 1285 | 34 | 1 | 0.55 | 705 | 0.78 | |
| FWD2s-CD2 | 0.60 | 4.70 | 2425 | 30 | 1990 | 55 | | | | | → 7 |
| FWD2s-CD3 | 0.90 | 5.00 | 3835 | 30 | 3727 | 63 | 2 | 0.25 | 305 | 0.82 | |
| FWD2s-CD4 | 1.15 | 5.25 | 4080 | 35 | 4032 | 65 | | | | | → 8 |
| FWD2s-CD5 | 1.30 | 5.40 | 5605 | 35 | 5934 | 43 | 3 | 0.35 | 800 | 0.44 | |
| FWD2s-CD6 | 1.65 | 5.75 | 4890 | 30 | 5134 | 78 | | | | | |

In Figure 3.8, the Holocene ages for all the four cores are plotted against depth (below sea level, in metres). The regional Holocene sea level curve has been compiled from coral reef data derived from Collins et al, 2006; Twiggs and Collins, 2010 and coquina ridge data from Jahnert and Collins, 2013. Based on inspection of Figure 3.8 and Table 3.3 every core sampled has its own peculiar accumulation pattern, with different rates within the same core, as shown in the last four columns of Table 3.3. The sedimentation record consists of both depositional and hiatal intervals.

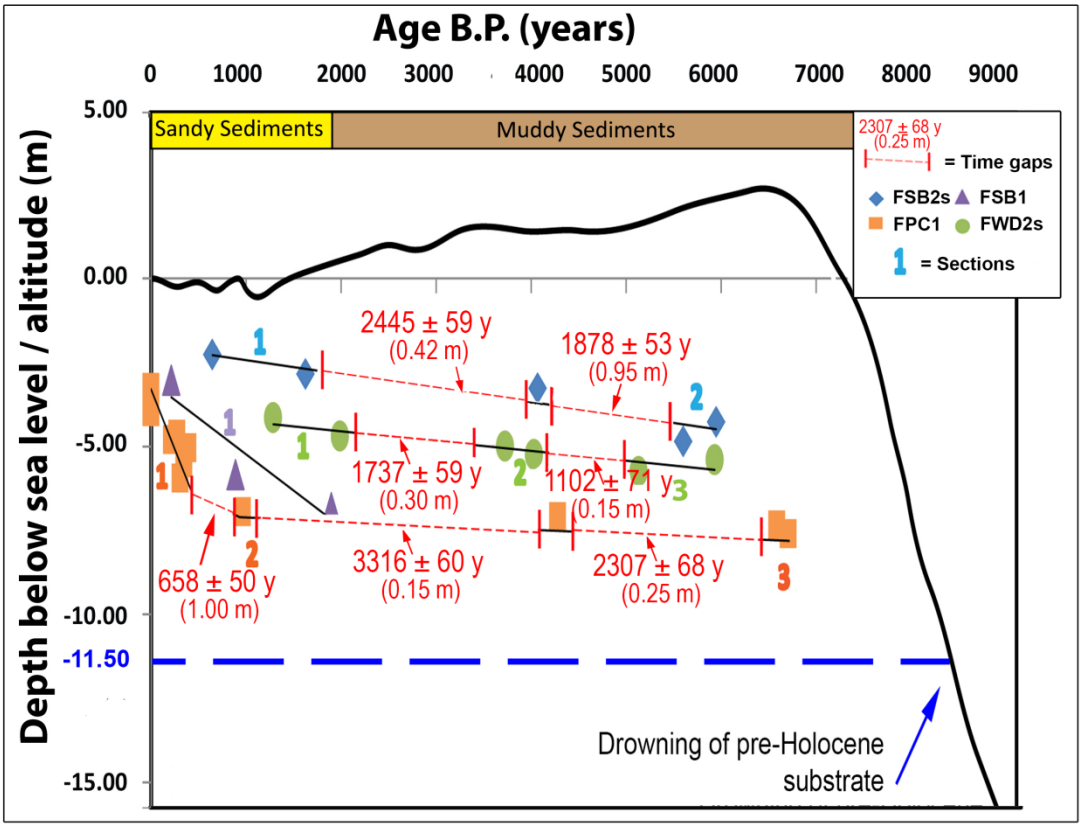


**Figure 3.8. Bank accumulation curves plotted with Holocene sea level curve. The numbers indicate sections described in this paper and time gaps (in red) are missing (erosional?) intervals. In the graph, pre-Holocene samples have been omitted. Note onset and continuation of sandy sediments in last 2000 years BP. The sea level curve is based mainly on coral reef records and sediment from Collins et al., 2006; Twiggs and Collins, 2010; Jahnert and Collins, 2013. Bank ages are based on AMS $^{14}$C dating (this study).**

Core FSB2s (Figure 3.9A), located in the eastern part of the complex, is the only core sample where pre-Holocene sediments were reached and dated, below 3 m. FSB2s can be subdivided into two sections. Section 1 (see Figure 3.8), corresponding to the surficial sand body, has a very slow rate of accumulation (averaging 0.59 m of deposition in 1000 years), if compared with the deeper and older muddy sediments (Section 2), where the accumulation rate surpasses 1.80 m/ky. In Section 2 and elsewhere age inversions are present, the oldest date of the section has been considered, in order to reduce errors caused by the inverse correlation between estimated accumulation rate and duration (cf. Sadler, 1981 and Cohen et al, 1993). The foraminiferal sample collected at 1.05 m (from the top of the core and 3.27 m BSL) is between two consecutive time gaps of sediments, respectively of 2445 years from the upper sampling point (at 0.63 m) and 1878 years from the lower sample (at 2.00 m). Channel migration and erosion are likely within this area, resulting in hiatuses in the accumulation record. The change in accumulation rates from the shallower sandy portion of the core to the deeper section can be plausibly linked with the density of seagrass. Depositional rates for muddy sediments associated with seagrass are significantly greater than for quartz sands, commonly derived from erosion of the Peron Sandstone.

Core FPC1 (Figure 3.9B) is situated between a terminal prograding flood tidal fan and the carbonate bank. The core intersects an abandoned distributary channel of the Faure Channel, indicated by the dating combined with the seismic dataset. Similarly to FSB2s, the growth rates of FPC1 can be divided into sections. Section 1 (Figure 3.8), corresponding to the first 2.75 m of the core (from the top of the core and 5.95 m below sea level), represents infill of a palaeochannel, recognisable from the seismic profile. It has some inversions of ages, with older foraminiferal samples situated above younger ones, interpreted as resulting from reworking of multiple sediment sources or downward mixing and activities of burrowing organisms. The oldest age of this section (390 years BP) has been used when calculating the accumulation rate. During the last 390 years BP, a significant amount of sediment was deposited in this location, with an accumulation rate of about 6.93 m/ky. The high rate represents very rapid deposition of prograding sandy and laminated infill in the most recent part of bank growth. Between 2.75 and 3.75 m of depth below the seafloor (5.95 and 6.95 m BSL), in Section 2, the rate drops to 1.52 m/ky. Radiocarbon dating has revealed two hiatuses between two consecutive depths of sampling. Between 3.75 and 3.90 m (6.95 and 7.10 m BSL), more than 3300 years of sediment is absent and between 3.90 and 4.15 m of depth (7.10 and 7.35 BSL), there is a second hiatus of approximately 2300 years. The hiatuses are recognisable also in the core logging and most likely characterise erosional phases in bank development, during active channel migration in a distributary region. Section 3, representing the last two samples dated, at the bottom of the core, has an accumulation rate slightly higher than Section 2, corresponding to 2.07 m/ky. Sections 2 and 3 are similar to the rate found in the other central bank core FSB1.

Core FSB1 (Figure 3.9C) is located in the middle of the Faure Sill, in the north central part of the carbonate bank. Its accumulation trend is very regular, with a constant depositional rate from the top to the bottom of the core. The total recovery for this core sample was 4.01 m and it covers a time span of 1686 ± 53 years, equivalent to a mean accumulation rate of ~2.25 m/ky. The radiocarbon dating indicates that the sedimentation is mainly confined to the late Holocene.

Core FWD2s (Figure 3.9D) is located in the eastern part of the complex, in the carbonate bank associated with the Wooramel Delta. The first dating sample, taken at 0.05 m of depth, is 1285 years BP. The core was taken on the edge of a channel, marking an erosive event or a subsidence of sediment to the bottom of the channel, a possible cause of the lack of sediment near the top of the core. The accumulation rate of the core has three distinct intervals with different slopes. In Section 1, till 0.60 m of depth (4.15 m BSL), the surficial sediment has a rate of growth of 0.78 m/ky. Similarly to FSB2s, a time gap also occurs in this location; between 0.60 and 0.90 m of depth, there is a hiatus of almost 1740 years. It follows a period of deposition (0.82 m/ky in Section 2) and another gap of more than 1100 years between Section 2 and Section 3, the last portion of the muddy carbonate sediment, which has an accumulation rate of approximately 0.44 m/ky. Although the recovered core is 2.47 m long, it has not been possible to date the deeper grey green and red clayey sediment (about 0.6 m thick), found near the base of the core, due to an absence of *Amphisorus* for dating.

Accumulation rates varied in time and magnitude during the Holocene, suggesting that bank growth fluctuated in different settings, in accordance with organism productivity in seagrass, local tidal conditions, water depth and facies. When the conditions changed, bank growth rate responded. In the case of the cut-and-fill channel in core FPC1 (Figure 3.9B), the growth was significantly accelerated. In other circumstances, a limitation or interruption to growth resulted. However, with a switch in conditions these areas reactivated. Such changes are reflected in cores FPC1, FSB2s and FWD2s, where there are more “breaks” than “beds” represented in the cores in chronological terms.

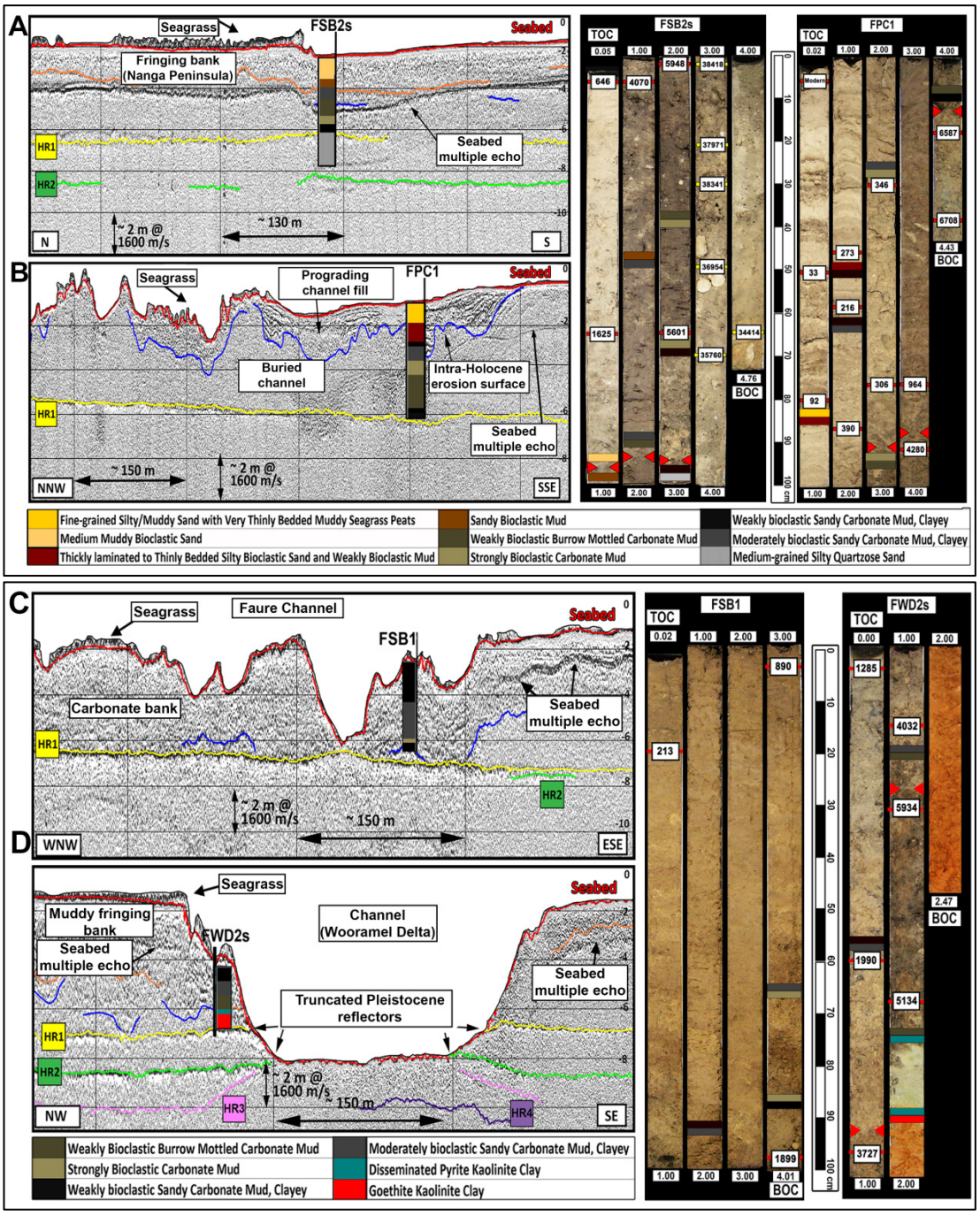


**Figure 3.9 Seismic profiles (see Figure 3.5 for colour code of depicted reflectors and Figure 3.6 for locations and colour scheme) and relative photos of the cores chosen for dating. Each**

**number on top of a red bar represents the position and the age (cf. Table 3.3) of the sample. The red triangles mark hiatus boundaries. A) FSB2s: shallow fringing bank (NW Nanga Peninsula). The first metre of core is mainly sandy. Then, the percentage of mud increases till 2.6 m (from TOC) where it becomes clayey mud, with only a small fraction of sand. Note that about 1.7 m of Pleistocene sediment has been collected, starting at 3.3 m. B) FPC1: rapid infill of eroded bank topography (palaeochannel). From TOC to 2.90 m, the core intersected a palaeochannel. The sediments are intensely layered, where seagrass peats alternate with fine bioclastic sand. Below the palaeochannel boundary, the sediment transits to interbedded grey muds and silty sand with dark grey mud beds. C) FSB1: channel dissected, seagrass vegetated, shallow carbonate bank. Located in the middle of the Faure complex, it is dominated by muddy carbonate and weakly bioclastic muds. D) FWD2s: fringing bank and channel, delta associated. Situated in the subtidal portion of the Wooramel Delta, the core is characterised by the presence of a goethite and kaolinite clay interval at the base.**

# 5. Discussion

## 5.1. Shallow stratigraphy

Generally, the main acoustic reflectors in the seismic profiles coincide with an abrupt variation of sediment types, which is evident from the sediment core analyses. Based on stratigraphic position, lithology and radiocarbon age, the seismic reflector HR1 can be confidently identified as the top of pre-Holocene Bibra Limestone. The underlying seismic reflector HR2 has been intersected by only one core (FED3, Figure 3.6) and no dating has been performed, but, on the basis of its stratigraphic position and lithological information, including calcrete clasts at the contact, it is considered to be the top of the Dampier Limestone. Both the pre-Holocene units have generally similar subsurface expression and lithology (with calcarenite concretions at contacts) and the seismic reflectors represent surfaces of impedance contrast beneath the Holocene bank build-up. No core reached the horizons HR3 and HR4; consequently their identification is on the basis of their stratigraphic position and the available literature (Logan et al., 1970a; Kendrick et al., 1991; O'Leary et al., 2008). Found only close to Wooramel Delta and around the topographic highs (Peron Peninsula, Faure Island, Nanga Peninsula), the reflectors could indicate two pre-Dampier (Middle and Lower Pleistocene) units. HR3 could represent the top of an earlier pre-Dampier marine phase or could be a marine equivalent of the Carbla Oolite member (MIS Stage 9/11, but poorly dated, O'Leary et al., 2008). Consequently, the identification of HR4 and its underlying unit is uncertain. Based on its geometry and stratigraphic position it could be part of the Peron Sandstone. Discontinuities seen in outcropping Peron Sandstone could be expressed as HR3 and HR4. These surfaces may have provided a template for later deposition, including location of channels over pre-existing topographic lows, control of the depositional topography of the Bibra and Dampier Limestones, determination of Holocene build-up patterns, distribution and thickness, and nucleation of bank growth around topographic highs.

The Holocene stratigraphic sequence within the Faure Sill has a thickness that ranges from a few centimetres to about 8 metres. With the exception of the areas close to topographic highs and the main channels, the Holocene sediments in the central area of the bank are 4 – 7 m thick. In the eastern and western regions (respectively Petit and Dubaut Banks and Wooramel Bank), the base of the Holocene is more surficial, deepening, on average, from 2 to 4 m from the seafloor.

The Holocene stratigraphic sequence not only presents a broad variety of internal geometries, but also has different sedimentological characteristics.

## 5.2. Morphostratigraphic elements and facies associations

The Faure channel – bank complex can be broadly subdivided into 5 regions (Figure 3.10). Each shares similar morphological elements, lithology and stratigraphy, as follows: 1) Terminal ebb tidal fans, 2) Fringing bank and flood tidal channels, 3) Carbonate bank, 4) Terminal prograding flood tidal fans, with shoreline attached sandflat, 5) Delta associated fringing bank (Wooramel Delta).

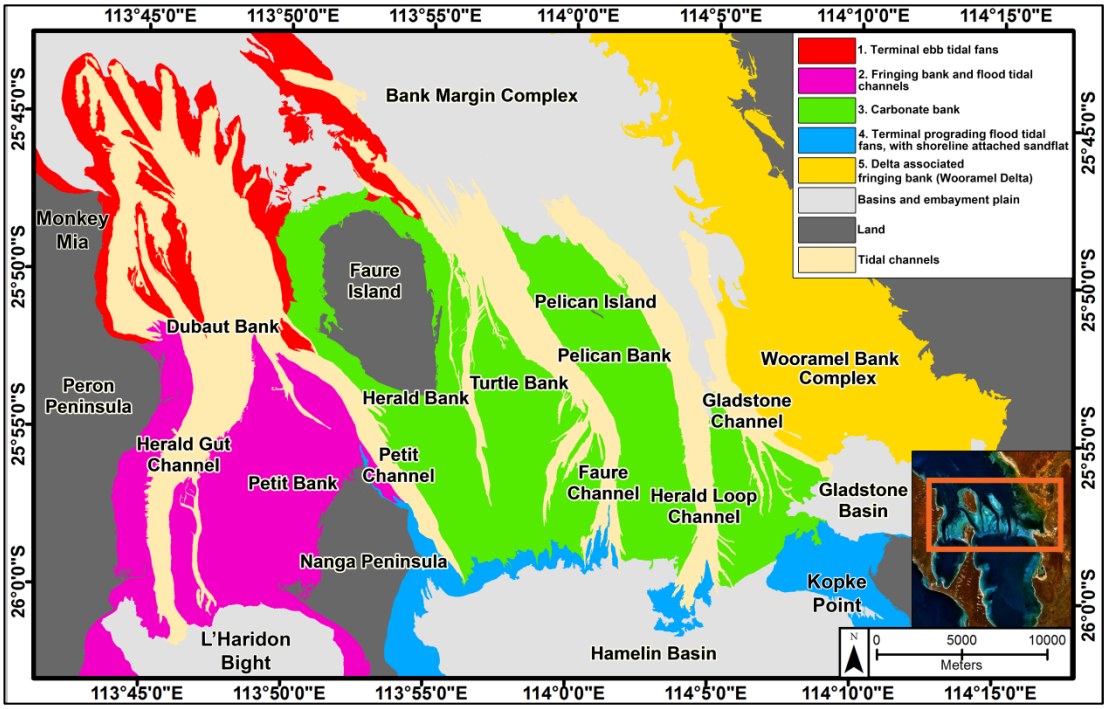


**Figure 3.10. Faure channel – bank complex can be subdivided into five regions (see 1 to 5 in legend) based on morphological elements, lithology and stratigraphy. In the figure, basins and embayment plain, land and tidal channels are also marked.**

1) *Terminal ebb tidal fans* occur in the north western area of the bank, approximately between Monkey Mia and Faure Island (Figure 3.2). Morphologically, they can be compared with the ebb delta model described by Hayes (1980), where a main ebb channel, flanked on either side by channel margin linear bars, terminates with a seaward sloping terminal lobe of sand. In Dubaut Bank (Figure 3.2), the main associated channel is Petit Channel. It is expressed in the northernmost portion as several minor channels, separated by levee deposits and broad sheets of sand (Figure 3.4). In the southern part, it coalesces with Herald Gut Channel. Within the channel complex, longitudinal channel bars run parallel to the main stream Figure 3.5B). At least four terminal lobes, prograding seaward, produce a large scale coalescent ebb tidal fan (Figure 3.4).

An idealised facies association for this subcomplex has been developed, based on the core data (Figure 3.6). The basal unit, above the pre-Holocene basement, is fine grained, silty quartzose sand, with bivalves and small foraminifera. The quartz component of the sediments is likely derived from the underlying Peron Sandstone.

The unit is overlain by silty sand with fine to medium, well-rounded quartz. In contrast to the basal unit, the middle unit lacks bivalves and is coarser. The uppermost unit is composed of weakly bioclastic cross bedded quartzose sand. The idealised vertical stratigraphic sequence describes the growth and development of this area of the bank in terms of energy conditions, fluctuation in accommodation and source material. In the lower part of the unit, clustered bivalve beds were most likely deposited by tidal currents. The bivalves are in a horizontal position, with the concavity downward and in a coarser grained mix, likely indicating a strong directional current flow. The lithology of the channel bars differ from the idealised facies association for the terminal ebb tidal complex. They are predominantly quartz dominated, with a minor bioclastic component, displaying an upward coarsening and an increase in quartzose material (cf. Figure 3.5B).

2) *Fringing bank and flood tidal channels* have their best expression in the western side of the bank, between the south western edge of Faure Island and the north eastern edge of the Nanga Peninsula (Figure 3.2). The main channels are Petit Channel and Herald Gut Channel, which are two of the deepest exchange channels in the bank, also branching into many minor drainage channels. Herald Gut Channel is the only connection that L'Haridon Bight has with the open ocean while Petit Channel flows into Hamelin Pool. In terms of facies assemblage, this sub-complex is mostly composed of bioclastic carbonate mud with mottled burrow traces, transitioning to sandy bioclastic mud and topped by medium grained muddy bioclastic sand (as in core FSB2s, Figure 3.9A). The channel sediments are predominantly composed of quartzose sand, with well-rounded to sub-rounded grains and occasional darker pigmented particles. They are generally weakly bioclastic and foraminifera and calcareous algae are present. The channels have a critical role in controlling the depositional patterns in the terminal ebb and flood part of the western lobe of the bank. During the growth of the bank, material from the surrounding Plio-Pleistocene highs has been eroded, deposited into the channels and distributed at either ends of the ebb and flood tidal fans. Evidence of Holocene channel migration between Faure Island and Nanga Peninsula is discernible within the seismic profiles and core collected in Petit Channel (see Figure 3.5C and Figure 3.9B). The presence of levees and longitudinal channel bars confirms this migration.

3) *Carbonate bank* morphologies can be found over the entire central complex. Small to medium scale ripples cover the entire bank and run subparallel to seagrass stabilised ridges, with an east – west direction (Figure 3.3). All around the southern side of the topographic highs of Turtle and Pelican Banks, linear ridges represent an important surface aspect of the bank where seagrass has vegetated and stabilised tidally generated linear bedforms (Figure 3.5A). Besides the main tidal channels, which cut the bank and permit an exchange of water between Hamelin Pool and the open ocean, there are several drainage channels, variably distributed along the southern part of the bank. Some profiles reveal distinct sets of palaeodistributary channels recognisable in both seismic and sedimentological data (cf. Figure 3.5C and Figure 3.9B core FPC1). It does appear therefore, that during the Holocene, the channels most likely experienced periods of migration and abandonment through the bank, with different palaeocurrent directions and several phases of erosional and depositional events (cut and fill). From the top to the bottom of the bank the

following facies are found: 1) weakly bioclastic sandy carbonate mud, clayey, 2) moderately bioclastic, sandy, carbonate mud, clayey and 3) strongly bioclastic carbonate mud. The facies' occurrence is mainly linked with the presence of seagrass but is also related to the pre-Holocene topographic highs, which the carbonate bank facies have grown around. Data from core logging have shown also that the central eastern carbonate bank experienced the influx of some terrigenous derived material and clays. These deposits could be related to storm or cyclone events which caused flooding of the Wooramel River.

4) *Terminal prograding flood tidal fans, with shoreline attached sandflat* form a well-defined subcomplex situated in the southern edge of the Faure Sill, between Nanga Peninsula and Gladstone Embayment. Morphologically, it displays a continuous belt of coalescent flood tidal fan lobes (terminal submarine fans of Davies, 1970b), up to 2.5 km long, running parallel to the entire slope length between the bank and Hamelin Basin. Faure Channel and Herald Loop Channel break the continuity of the belt with numerous bifurcated minor channels. Longitudinal seismic profiles show that the lobes have a complex internal structure, composed of surficial cross bedded or prograding layers, becoming more horizontal with deepening in the sequence (Figure 3.5D). Transverse seismic lines confirm the oblique configuration that occurs with the basinward progradation pattern on the bank margin. In a few areas of the subcomplex, Holocene carbonate sand lobes have a flat topped geometry in a discordant relationship with the underlying inclined beds, possibly as a consequence of non-deposition (with minor erosion) linked to sea level height. In very shallow water conditions, the updip deposition is obstructed resulting in successive beds built out and prograding basinward. Linear ridges of seagrass, running in an east – west direction, characterise the northern portion of the fan (cf. Figure 3.5A). The deposits are characterised by coarsening upward sandy units, generally cross bedded, up to 2 metre thick, overlaying a fine grained sandy unit, with thin seagrass peats and a minor muddy component. The deepest units have the typical facies association found in the bank; carbonate mud with variable fractions of sand and bioclasts. The development of fan lobes is indicative of a prevalent basinward flow.

Close to Gladstone Embayment (Kopke Point), there is a prominent shoreline attached sandflat, where the water shallows (to < 3 m) and stronger currents develop, generating ripples and megaripples (Figure 3.5E). These tidally – produced features can be up to 1.5 m high and several hundred metres long, with a wavelength of 25 – 35 m. The seismic profiles reveal a distinct progradation throughout the margins of the complex. In the south, a flood tide progradation prevails, and in the northern margin ebb tide progradation is present. Progradation is controlled by tidal currents with lesser wind driven circulation. In the deepest areas of the channels (> 4.5 m), lenticular to elongate sets of sand bars are bounded by flood oriented cross bedding. Facies analysis showed that the composition of the sediments collected along the terminal bars and lobes varies from coarse to medium grained bioclastic sands (top of the cores) to silty fine grained laminated sands and to carbonate muddy apron facies (bottom of the cores). In the cores, evidence of an internal architecture is clear, with overall excellently preserved cross bedding. Dark pigmented grains emphasise these features. The transitional contact between the

surficial carbonate sands and the underlying sediment occasionally lacks distinctness, due to a strong bioturbation.

5) *Delta associated fringing bank (Wooramel Delta)* occupies the easternmost part of the Faure Sill and is strongly influenced by the Wooramel River and the Wooramel seagrass bank (Figure 3.4. Logan et al., 1970a). The semiarid Wooramel River has a limited influence on sedimentation, with sandy fluvial sediments confined to the deltaic wedge. Terrigenous clay periodically spread across the bank following discharge events associated with occasional (usually cyclone associated) runoff activity (Davies, 1970a). The delta progrades southward into Gladstone Embayment and seaward over Holocene carbonate sediments of the intertidal and subtidal zones (Davies, 1970a). North – west longshore currents created by tidal and wind regimes, redistribute the sediment in subparallel longshore sand bars and sand ridges. Numerous tidal channels, linked to the Wooramel River, cut the intertidal and subtidal zones of the delta. The delta front, which in the southern part is more than 10 km from the hinterland, has a steep slope before flattening offshore, at depths greater than 5 m.

Four cores were collected and logged in the delta region (Figure 3.6). The units and facies in these cores show a clear terrigenous influence (Figure 3.6 and Figure 3.9D). The sediments are mainly clay rich carbonate mud. The upper section, which is up to 2 metres thick, consists of clayey, weakly bioclastic sandy carbonate mud. Deepening, the sediment becomes slightly more bioclastic, with bioturbation and burrow mottled mud (Figure 3.6). In core FWD2s, the lower section abruptly changes from dark brown clay rich mud to green grey kaolinite clay (layer thickness of 15 cm) and then, at the base of the core, sharply becomes orange dark red clay, with an organic component and no texture or colour variations over the interval. The middle clayey layer could indicate that a rapid terrigenous input into the delta occurred as pulses into the bank, forced by possible storm surges and flooding (Figure 3.9D). Davies (1970a, p.148) described a similar submarine core, collected a few kilometres north, in a submarine levee. He considered that the red alluvium at the base of the section grading upward into reduced green clayey sand, marks the transgressive Holocene unconformity between Holocene bank sediments and Plio-Pleistocene alluvium. The sequence seen near the Wooramel Delta can be considered as a possible result of events that influenced the amount of terrigenous material in the bank. Terrigenous sediments are concentrated in the vicinity of the Wooramel River (Logan et al., 1970a, and this study); therefore bank cores, located close to the delta appear to be more affected by major storm events and run-off from flooding.

## 5.3. Holocene bank growth and accumulation

Radiocarbon dating assisted linking the sedimentological data to the Holocene event chronology and calculating the bank accumulation rate. This new information has revealed a highly dynamic geological record and appears to be broadly consistent with previous onset and evolution data (Davies, 1970a; Logan et al, 1970a, 1974; Hagan and Logan, 1974; Walker and Woelkerling, 1988), whilst adding significantly to seismic, facies and geological understanding.

The Holocene bank accumulation rates vary by more than an order of magnitude, ranging from 0.44 m/ky in the lowest Holocene section in the Wooramel Delta to 6.93 m/ky in the upper section of core FPC1, where a rapid deposition of prograding and laminated sand filled a palaeochannel (Table **3.3**). Table 3.4 summarises the average accumulation rates for each facies considered. These values are comparable with the rates of vertical accretion estimated by Davies (1970a, p. 161). Rao (1996) stated that in Australian carbonate environments, the maximum accumulation rates are from about 1.5 m/ky in tropical waters to 1.0 m/ky in cold water. In general terms, the Faure Sill is 7 m thick and has a basal age of close to 7 ky, giving an approximate accumulation rate of 1 m/ky. Excluding the "outlier" filled channel rate (see Table 3.4) the average accumulation rate for all dated cores was 1.3 m/ky. However, rates obtained are facies dependent (see Table 3.4).

**Table 3.4. Range and average accumulation rate in the analysed facies, based on four dated cores.**

| Facies | Range of accumulation rate (m/ka) | Average accumulation rate (m/ka) |
|---|---|---|
| Bank | 0.59–2.25 | 1.7 |
| Filled channel | ?–6.9 | 6.9 |
| Delta | 0.44–0.82 | 0.7 |
| Maximum range and average accumulation rate | 0.44–6.9 | 3 |
| Average for all facies (filled channel excluded) | – | 1.3 |

Considering the Holocene accumulation curves plotted in the context of the regional Holocene sea level trend (Figure 3.8), the cores in the central area of the bank (FPC1 and FSB1) have a similar trend and the two marginal cores (FSB2s and FWD2s) are comparable with each other. After the end of the Last Ice Age, in Late Pleistocene – Early Holocene time, under the input of water derived by the melting of ice sheets, sea level rose about 130 m from ~18000 to ~6800 years BP, culminating in a highstand of 2.5 m above the present level (Lambeck, 1990; Lambeck and Nakada, 1990). An initial post drowning erosional phase of pre-Holocene substrates would have accumulated before establishment of pioneer seagrass and epiphyte communities became significant, possibly over several hundred years duration. Within the bank, this date approximately coincides with the oldest determined Holocene date (6708 ± 58 years, in FPC1) but because the core didn't reach the pre-Holocene surface (HR1; see Figure 3.9), bank initiation could be significantly older than this date. Based on seismic profiles, the most recent pre-Holocene reflector HR1 (interpreted as top of the Bibra Limestone) can be found at depths of at least 11.5 m below the present sea level, and would have been submerged by 8500 years BP (Figure 3.8 and Figure 3.11.1). Initial erosion of topographic highs of the Peron Sandstone is likely to have shed quartz dominated sand sheets over the drowning substrate.

The first seagrass communities started their colonisation and contribution at the onset of a protobank, trapping and binding sediments (cf. Scoffin, 1970) and

producing *in situ* sediments, such as coralline algal fragments, other calcareous epiphytes (Walker and Woelkerling, 1988) and bioclastic remains. During the transgressive period, until the highstand at ~2.5 m above the present sea level, the bank continued to develop. By 6800 years BP, bank build-up had advanced but lagged significantly behind sea level (Figure 3.11.2). Thereafter declining sea level is likely to have caused a base level fall of 2 m (Figure 3.8) with possible bank erosion (expressed as hiatuses in $^{14}C$ dating).

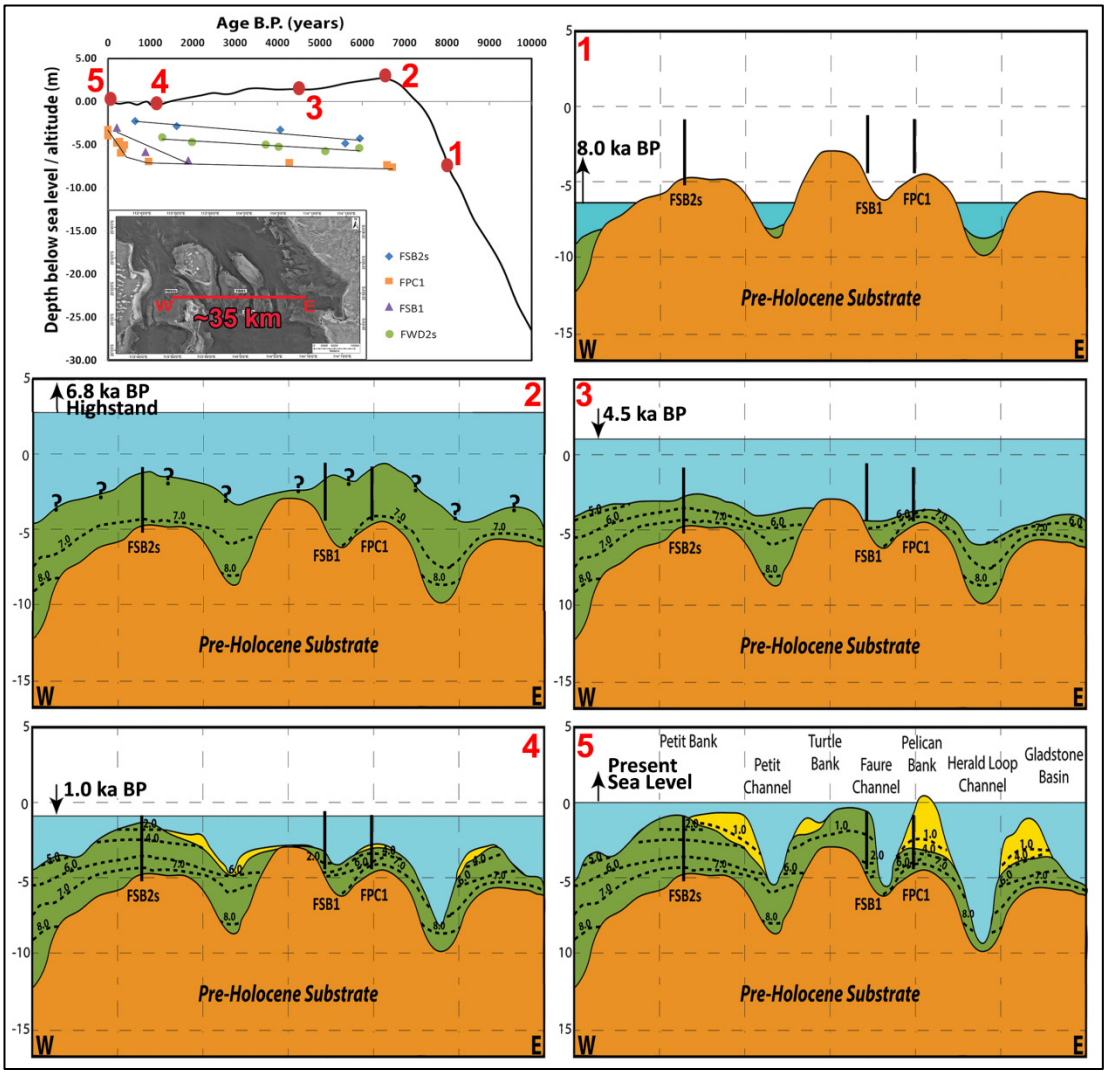


**Figure 3.11. Reconstruction of the Holocene chronology of the Faure Sill, based on the data from this study. Dashed lines represent isochrones. The colours are a generalisation of the lithology: orange = pre-Holocene substrate, green = bioclastic carbonate mud, yellow = bioclastic sand. The arrows refer to the trend of the sea level (fall or rise). FSB1, FPC1 and FSB2s are three cores described in the text. Heights of sediments on cores are based on radiocarbon dating levels obtained (Table 3.3); uncertainty exists on height of bank growth (panel 2) prior to erosional events (panel 3). The profile is not to scale, but is a simplification of the main topography. The transect length is about 35 km, W – E oriented. On the vertical axis, the scale is in metres, 0 corresponds to the present sea level. Sea level data are based on the composite sea level curve in Figure 3.8. 1) Early Holocene. The pre-Holocene substrate was largely exposed, with a sparse cover of bioclastic sand to mud. 2) Middle Holocene. The sea rapidly rose till reaching the highstand level and completely flooding the bank region. During this period, the seagrass meadows were at their apex, playing a significant role in trapping sediments and producing muddy carbonate deposits *in situ*. 3) Late Holocene. The irregular downward trend of sea level has been responsible for several distinct erosional and depositional events. 4) Most recent part of Holocene. The sea level dropped till reaching the**

**lowstand level. Sandy bank top facies were initiated (yellow). 5) Present conditions of the bank. Note the culmination of sandy bank top sediments, now fully developed.**

Based on $^{14}C$ dating of coquina ridges near Telegraph Station (south Hamelin Pool, Shark Bay) Jahnert and Collins (2013) estimated that sea level generally fell by about 1 m in less than 2200 years, standing at ~1.5 m above the present sea level, at ~4.5 ky BP (Figure 3.11.3). Such a fall could be associated with the hiatuses found in the dating of the cores FSB2s, FPC1 and FWD2s (Figure 3.8 and Table **3.3**). In both the marginal cores (FSB2s and FWD2s), about 2000 years of sediments (from ~4.0 to ~5.9 ky BP) are missing in the stratigraphic record, suggesting the possible occurrence of an erosive event, amplified in shallow water areas and associated with a decreased accumulation in deeper parts. In a regressive context, a brief and moderate sea level increase followed, accompanied by minor deposition.

Generally, declining sea level continued until a lowstand at about 1000 years BP, when the sea level was about 1 m below the present. Jahnert and Collins (2013) found evidence of an exposure surface (1040 – 940 $^{14}C$ years BP) in a lithified carbonate pavement in Garden Point and Rocky Point (Shark Bay). The results of the core dating show that the bioclastic sands, characterising the surficial sediments in the terminal prograding flood tidal fan, are very recent (from 964 ± 45 years BP to present). This suggests fan sedimentation is continuing in the very recent history of the bank.

In the present day bank, narrow linear ridges, parallel to the predominant currents, have taken the place of the dense seagrass meadows which gradually disappeared from the shallowest areas. Between the bank and the deep basins and channels, where the slopes are relatively steep, the seafloor is bare or has only occasional scattered seagrass. Deposition in such environments is mostly tidal current dominated, and only particles with a larger diameter, such as coarse grained sands, are deposited. In contrast to the carbonate mud found where the seagrasses are more developed, the bioclastic sands are usually found in cross bedded fans, prograding outward from the bank with clinoform geometry. Sedimentation and deposition has adjusted downward and basinward as the sea level dropped. This is confirmed by the upward coarsening sequences seen in the sandy fan and bank top trend from silty fine grained sands to coarse grained cross bedded bioclastic sands.

## 5.4. Role of the seagrass banks in Shark Bay

Shark Bay has distinctive and exceptional examples of active geological and biological processes and ecosystems. Faure Sill, with its peculiar hydrological structure, is an area where seagrass meadows, carbonate deposits and sediments create highly dynamic and diverse environments. It is recognised worldwide that seagrass meadows are fundamentally involved in modifying a coastal marine environment, in its physical, chemical, geological and biological aspects (Walker, 1989; Gibbs et al., 2014). In Shark Bay, particularly within the Faure Sill, since their appearance in the early Holocene, seagrasses have had a primary role in reshaping and transforming the geomorphology and ecosystems of the area. Production and deposition of a significant amount of bioclastic and epiphytic sediments is strictly linked with the seagrass presence. Accumulation rates of seagrass associated sediment are higher than adjacent sedimentary environments. While the calcareous

epiphytes represent a significant component, roots, rhizomes and leaves also reduce the speed of currents facilitating deposition, trapping fine sediments (Walker, 1990). With the formation of a sill between the open ocean and the embayment waters, together with the semiarid climatic condition of the area, the southern embayments of Hamelin Pool and L'Haridon Bight have become meta- to hyper-saline (Logan and Cebulski, 1970; Logan et al, 1974). These environments, incompatible with the growth of seagrass are instead suitable for the establishment of unique microbial systems, stromatolites, oolitic and coquina systems, particularly of *Fragum erugatum,* Tate, 1889 (Jahnert and Collins, 2011, 2012, 2013).

Seagrasses perform a range of services (Gibb et al., 2014). They provide shelter and food for numerous species of molluscs, crustaceans and fish, including many commercially valuable species, like *Pagrus auratus* Bloch & Schneider, 1801 (Heithaus, 2004). Shark Bay supports an internationally significant population of dugongs (*Dugong dugon* Muller, 1776) which feed on *Amphibolis antarctica* (Walter, 1989) and it has the largest breeding population of loggerhead turtles in Western Australia (*Caretta caretta* Linnaeus, 1758. Preen et al., 1997). The seagrass is important also for small and large cetaceans. Particularly, Monkey Mia is famous worldwide for the contact between humans and some members of the local population of bottlenose dolphins (*Tursiops truncates* Montagu, 1821. Preen et al., 1997). Tiger sharks (*Galeocerdo cuvier* Péron & Lesueur, 1822) are linked too with the shallow seagrass ecosystem, as the local fauna represent their most common prey items (Heithaus, 2001). Seagrass meadows are not only essential for an entire shallow benthic ecosystem, but they play a critical role in producing, sequestering and storing organic carbon (Grimsditch et al., 2012; Lavery et al., 2013; Duarte et al, 2013) and considerable contribution to carbon, nitrogen and phosphorus cycles in the ocean (Fourqurean et al., 2012). Fourqurean et al., 2012 established that the total storage of organic carbon and nutrients in the seagrass linked sediments of Shark Bay is on average 243.0 Mg $C_{org}$ ha $^{-1}$, substantially higher than the median values for the world's seagrass ecosystems (139.7 Mg $C_{org}$ ha $^{-1}$). Moreover they believe there is a positive correlation between surficial $C_{org}$ and salinity: $C_{org}$ is higher in hypersaline environments, as the hypersalinity coincides with a decrease of energy (Fourqurean et al., 2012). This hypothesis is supported by Lavery et al. (2013). These recent insights highlight the importance of the Shark Bay seagrass communities in carbon sequestration, potentially providing a globally significant climate change mitigation benefit (Grimsditch et al., 2012).

## 6. Conclusions

Through shallow seismic and sedimentological analysis, this investigation has been able to characterise the Faure Sill in terms of its seismic architecture, facies, chronology and growth history, and to determine its relationship to the adjacent Wooramel Delta, providing new insights and a better understanding of the sedimentological facies and geomorphological features of the bank.

Traditionally, evolution of the Shark Bay banks has been described in terms of fringing banks with a coalescence of patch banks, forming barrier banks such as the Faure Sill. The Faure channel – bank complex is an example of a system characterised by the presence of tidal channels with ebb tidal and flood tidal fan

morphologies at bank margins and frequent channel associated sediment bodies. Morphostratigraphic elements and facies associations are indicative of sediment supply, accommodation and fluid dynamics changes (tides, currents and waves) as a function of the variation of the sea level over the time.

- During the Early Holocene, the pre-Holocene substrate was largely exposed, then a flooding event (not earlier than 8.5 – 8.0 ky BP) could have caused erosion of the palaeosurfaces and quartz shedding from eroding pre-existing topography. After this initial lag phase seagrass bank establishment progressively contributed bioclastic sediment, initiating the early stages of bank growth. In Middle Holocene time, the transgressing seas rapidly rose until reaching the +2 m highstand level around 6800 years BP, with bank accumulation accelerating. During this period, the seagrass meadows reached their apex, playing a significant role in binding and trapping sediments and producing muddy carbonate deposits. During the succeeding slow decline to present sea level (Late Holocene), bank growth continued to fill available accommodation and channel – bank morphology continued to develop. Seismic profiles and geochronology reveal abandoned channels, rapid infill of eroded bank regions, progradation of terminal fans, and distinct erosional and depositional events, with one prominent hiatus of up to 2000 years duration recorded. Nevertheless, the bank continued to fill the available accommodation, with development of sandy, bank top sediment bodies. The latest Holocene to present, the bank is nearly emergent at low tide, with depths of 0.5 m commonly recorded, and relatively sparse seagrass cover in shallow areas. Tidally generated bedforms are widespread, however prolific seagrass growth continues in intervening channels.

- The growth of the bank has been controlled by three major factors: 1) the pre-Holocene topography which, with its highs and channels, shaped the accommodation for the sediments during the Holocene onset; 2) the seagrass that not only acted as a sediment trap, but also by suppling habitats for organisms, provided a large volume of biogenic carbonate deposits, generated *in situ*; 3) sea-level fluctuations that largely controlled the hydrodynamic conditions, such as the amount of tidally oscillating waters and their velocity, influencing erosion, transportation and deposition, and the channel – bank morphology.

- The system of deltas and banks represented by the Gascoyne and Wooramel Deltas and the Wooramel and Faure seagrass banks contains juxtaposed clastic and carbonate facies and stretches along 200 km of the coastal Carnarvon Basin (Figure 3.1). To the south, the mixed carbonate – clastic system consisting of the Faure channel – bank complex and Wooramel Delta grades into the hypersaline microbial, oolitic, coquina and evaporite systems in Hamelin Pool within Shark Bay. This system could be regarded as a partial analogue for the Plover Formation, in the Browse Basin (North West Shelf, Western Australia). The Plover Formation is an important hydrocarbon reservoir which comprises Early to Middle Jurassic coastal plain

and fluviodeltaic deposits, with marine carbonate and igneous and volcaniclastic intervals (Blevin et al, 1998; Longley et al, 2003; Barber et al. 2003; Tovaglieri and George, 2014).

## Acknowledgments

Woodside and the Browse Joint Venture partners are thanked for providing research funding to Curtin Applied Geology for this project. Authors wish to thank the following: Landgate Imagery and DPaW for digital aerial photos; DPaW Denham, particularly Wayne Moroney for vessel support during the seismic surveys; the Department of Spatial Sciences (Curtin University) for supplying the DGPS; Bobbie Rice and Darren Skene (Quaternary Resources); Blue Lagoon Pearls for providing and operating the vessel P2 for the vibracoring survey, the facilities for the initial cutting of the cores and valuable help in many aspects of the field work; Cleve Flottman (DWG Consulting), Westarc Welders and Mark Winstanley (Department of Applied Physics, Curtin University) for designing and constructing the coring A frame. Thanks to Shashi Rajah Kanagasabai (Applied Geology) for his assistance during the vibracoring survey, core logging, XRD analysis and preliminary interpretation during his honours degree thesis; Alexandra Stevens (Applied Geology) for her help with paper review, Giovanni De Vita for his technical advices and Sira Tecchiato (Applied Geology) during the seismic survey.

## References

Allwood, A.C., Walter, M.R., Kamber, B.S., Marshall, C.P., Burch, I.W., 2006. Stromatolite reef from the Early Achaean era of Australia. Nature 441, 714 – 718.

Ashley, G., 1990. Classification of large scale subaqueous bedforms: a new look at an old problem. Journal of Sedimentary Petrology 60, 160-172.

Belperio, A. P., Hails, J. R., Gostin, V. A. and Polach, H. A. 1984. The stratigraphy of coastal carbonate banks and Holocene sea levels of northern Spencer Gulf, South Australia. Marine Geology 61, 297– 313.

Blevin, J.E., Struckmeyer, H.I.M., Cathro, D.L., Totterdell, J.M., Boreham, C.J., Romine, K.K., Loutit, T.S., Sayers, J., 1998. Tectonostratigraphic framework and petroleum systems of the Browse Basin, North West Shelf. In: Purcell, P.G. and Purcell, R.R. (eds), The Sedimentary Basins of Western Australia 2: Proceedings of the Petroleum Exploration Society of Australia Symposium, Perth, 1998, 369–395.

Butcher, B.P., Van de Graaff, W.J.E., Hocking, R.M., 1984. Shark Bay – Edel, Western Australia: Geological Survey of Western Australia, 1:250 000 Geological Series Explanatory Notes, 1 – 21.

Chivas, A.R., Torgensen, H.A., Polach, A., 1990. Growth rates and Holocene development of stromatolites from Shark Bay, Western Australia. Australian Journal of Earth Sciences 37, 113 – 121.

Cohen, A.S., Soreghan, M.I., Scholz, C.A., 1993. Estimating the age of formation of lakes – an example from Lake Tanganyika, east African rift system. Geology 21(6), 511 – 514.

Collins, L., B., Jahnert, R., J., 2014. Stromatolite Research in the Shark Bay World Heritage Area. Journal of the Royal Society of Western Australia, 97: 189 – 219.

Davies, G.R., 1970a. Carbonate bank sedimentation, Eastern Shark Bay, Western Australia: Carbonate sedimentation and environments, Shark Bay, Western Australia. In: Logan, B.W., Davies, G.R., Read, J.F., Cebulski, D.E (Eds.),Carbonate sedimentation and environments, Shark Bay, Western Australia. American Association of Petroleum Geologists Memoirs 13, 85 – 168.

Davies, G.R., 1970b. Algal laminated sediments, Gladstone Embayment, Shark Bay, Western Australia. Carbonate sedimentation and environments, Shark Bay, Western Australia. In: Logan, B.W., Davies, G.R., Read, J.F., Cebulski, D.E (Eds.),Carbonate sedimentation and environments, Shark Bay, Western Australia. American Association of Petroleum Geologists Memoirs 13, 169 – 205.

Dravis, J. J. 1983. Hardened subtidal stromatolites, Bahamas. Science 219, 385–386.

Duarte, C.M., 2002. The future of seagrass meadows. Environmental Conservation 02, pp 192 – 206.

Duarte, C., Kennedy, H., Marbà, N., Hendriks, I., 2013. Assessing the capacity of seagrass meadows for carbon burial: current limitations and future strategies. Ocean and Coastal Management 83, 32 – 38.

Fallon, S.J., Fifield, L.K., Chappell, J.M., 2010. The next chapter in radiocarbon dating at the Australian National University: Status report on the single stage AMS, Nuclear Instruments and Methods in Physics Research. B 268, 898 – 901.

Fonseca, M.S., Fisher, J.S., Zieman, J.C., Thayer, G.W., 1982. The role of current velocity in structuring seagrass meadows. Estuarine, Coastal and Shelf Science, 17, 367–380.

Fourqurean, J. W., Kendrick, G. A., Collins, L. S., Chambers, R. M., Vanderklift, M. A., 2012. Carbon, nitrogen and phosphorus storage in subtropical seagrass meadows: examples from Florida Bay and Shark Bay. Marine and Freshwater Research 63, 967 – 983.

Grimsditch, G., Alder, J., Nakamura, T., Kenchington, R., Tamelander, J., 2012. The blue carbon special edition – Introduction and overview. Ocean and Coastal Management, iFirst, 1 – 4.

Jahnert, R.J, Collins, L.B., 2011. Significance of subtidal microbial deposits in Shark Bay, Australia. Marine Geology 286, 106 – 111.

Jahnert, R.J. and Collins, L.B., 2012. Characteristics, distribution and morphogenesis of subtidal microbial systems in Shark Bay, Australia, Marine Geology 303 – 306,115 – 136.

Jahnert, R.J, Collins, L.B., 2013. Controls on microbial activity and tidal flat evolution in Shark Bay, Western Australia. Sedimentology 60 (4), 1071 – 1099.

Kendrick, G. W., Wyrwoll, K. – H., Szabo, B.J., 1991. Pliocene – Pleistocene coastal events and history along the western margin of Australia. Quaternary Science Reviews 10, 419 – 439.

Koch, E. W., Ackerman, J. D., Verduin, J., van Keulen, M., 2006. Fluid Dynamics in Seagrass Ecology – from Molecules to Ecosystems. In: Larkum, A.W.D., Orth, R.J., Duarte, C.M. (Eds) Seagrasses: biology, ecology and conservation. 193 – 225.

Hagan, G. M. and Logan, B. W., 1974. Development of carbonate banks and hypersaline basins, Shark Bay, Western Australia. American Association of Petroleum Geologists, Memoir 22, 61 – 139.

Hamilton, E.L., 1970. Sound velocity and related properties of marine sediments, North Pacific. Journal of Geophysical Research 75, 23

Hancock, S., Brown, P., Stephens, B., 2000. Shark Bay Terrestrial Reserves Management Plan 2000 – 2009. Department of Conservation and Land Management for the National Parks and Nature Conservation Authority Perth, Western Australia.

Hayes, M.O., 1980. General morphology and sediment patterns in tidal inlets. Sedimentary Geology 26, 139 – 156.

Heithaus, M.R., 2001. The Biology of Tiger Sharks, *Galeocerdo Cuvier*, in Shark Bay, Western Australia: Sex Ratio, Size Distribution, Diet, and Seasonal Changes in Catch Rates. Environmental Biology of Fishes 61(1), 25 – 36.

Heithaus, M.R., 2004. Fish communities of subtropical seagrass meadows and associated habitats in Shark Bay, Western Australia. Bulletin of Marine Science 75 (1), 79 – 99(21).

Hocking, R. M., Moors, H. T., Van De Graaff W. J. E., 1987. Geology of the Carnarvon Basin Western Australia. Geological Survey of Western Australia Bulletin 133, 289.

Lavery PS, Mateo M – A, Serrano O, Rozaimi M, 2013. Variability in the carbon storage of seagrass habitats and its implications for Global Estimates of Blue Carbon Ecosystem Service. PLoS ONE 8(9).

Leighton, T.G., Robb, G.B.N., 2008. Preliminary mapping of void fractions and sound speeds in gassy marine sediments from sub-bottom profiles. Journal of Acoustical Society of America 124 (5), 313 – 320.

Logan, B. W., 1968. Western Australia: in Quaternary shorelines research in Australia and New Zealand. Edited by ED GILL: Australian Journal of Science 31, 110.

Logan, B. W., Read, J. F., Davies, G. R., 1970a. History of carbonate sedimentation, Quaternary Epoch, Shark Bay, Western Australia. In Carbonate sedimentation and environments, Shark Bay, Western Australia. Logan, B.W., Davies, G.R., Read, J.F., Cebulski, D.E (Eds.),Carbonate sedimentation and environments, Shark Bay,

Western Australia. American Association of Petroleum Geologists Memoir 13, pp 38–84.

Logan, B. W., Davies, G. R., Read, J. F., Cebulski, D.E., 1970b. Carbonate sedimentation and environments, Shark Bay, Western American Association of Petroleum Geologists, Memoir 13, 223.

Logan, B.W., Cebulski, D.E., 1970. Sedimentary environments of Shark Bay, Western Australia. In: Logan, B.W., Davies, G.R., Read, J.F., Cebulski, D.E (Eds.),Carbonate sedimentation and environments, Shark Bay, Western Australia. American Association of Petroleum Geologists Memoirs 13, 1–37.

Logan, B.W., Read, J.F., Hagan, G.M., Hoffman, P., Brown, R.G., Woods, P.J., Gebelein, C.D., 1974. Evolution and diagenesis of quaternary carbonate sequences, Shark Bay, Western Australia. American Association of Petroleum Geologists Memoir 22, 358.

Longley, I.M., Buessenschuett, C., Clydsdale, L., Cubitt, C.J., Davis, R.C., Johnson, M.K., Marshall, N.,M., Murray, A.P., Somerville, R., Spry, T.B., Thompson, N.B., 2002. The North West Shelf of Australia e a Woodside perspective. In: Purcell, P.G., Purcell, R.R. (Eds.), The Sedimentary Basins of Western Australia: Proceedings of the Petroleum Exploration Society of Australia 3. Perth, pp. 27 – 88.

Moore, L.S., Burne, R.V., 1994. The Modern Thrombolites of Lake Clifton, Western Australia. Phanerozoic Stromatolites II, pp 3 – 29.

Munsell, A. H., 1954. Munsell Soil Color Chart. U.S Dept. Agriculture. Soil Survey Manual 2009 Edition Munsell Soil Chart.

Nahas, E. L., Pattiaratchi, C. B., Ivey, G. N., 2005. Process controlling the position of frontal systems in Shark Bay, Western Australia. Estuarine, Coastal and Shelf Science 65, 463 – 474.

O'Leary, M. J., Hearty, P. J., McCulloch, M. T., 2008. U – series evidence for widespread reef development in Shark Bay during the last interglacial. Palaeogeography, Palaeoclimatology, Palaeoecology 259: 424 – 435.

Parker, J.H., 2009. Taxonomy of Foraminifera from Ningaloo Reef, Western Australia. Association of Australasian Palaeontologists. Canberra. Memoir 39.

Playford, P. E., Cockbain, A. E., 1976. Modern algal stromatolites at Hamelin Pool, a hypersaline barred basin in Shark Bay, Western Australia. In: Walter, M.R. (Ed.), Developments in Sedimentology, 20. Elsevier Scientific Publishing Company, pp. 389–411.

Playford, P. E., 1990. Geology of the Shark Bay area, Western Australia. In: Berry, P.F., Bradshaw, S.D., Wilson, B.R. (Eds) Research in Shark Bay: Report of the France – Australe bicentenary expedition committee, Western Australian Museum, Perth, pp. 13–31

Playford, P. E., Cockbain, A. E., Berry, P. F., Roberts, A. P., Haines, P. W. and Brooke, B. P. 2013. The geology of Shark Bay: Geological Survey of Western Australia, Bulletin 146 pp 281.

Preen, A. R., Marsh, H., Lawler, I. R., Prince, R. I. T., Shepherd, R., 1997. Distribution and Abundance of Dugongs, Turtles, Dolphins and other Megafauna in Shark Bay, Ningaloo Reef and Exmouth Gulf, Western Australia. Wildlife Research 24(2), 185 – 208

Rao, C. P., 1996. Modern Carbonates: Tropical, Temperate and Polar, Introduction to Sedimentology and Geochemistry. Tasmania, Australia. 206 pp.

Read, J. F., 1974. Carbonate bank and wave built platform sedimentation, Edel Province, Shark Bay, Western Australia. In: Logan, B.W., Read, J.F., Hagan, G.M., Hoffman, P., Brown, R.G., Woods, P.J., Gebelein, C.D., (Eds). Evolution and diagenesis of quaternary carbonate sequences, Shark Bay, Western Australia. American Association of Petroleum Geologists Memoir 22, 250 – 282.

Sadler, P.M., 1981. Sediment Accumulation Rates and the Completeness of Stratigraphic Sections. Geology 89 (5), 569 – 584.

Scoffin, T P., 1970. The trapping and binding of subtidal carbonate sediments by marine vegetation in Bimini Lagoon, Bahamas. Journal of Sedimentary Petrology 40, 249 – 273.

Schopf, J.W., 1993. Microfossils of the Early Archean Apex chert: new evidence of the antiquity of life. Science 260, 640 – 646.

Stuiver, M., Polach, H. A., 1977. Discussion: Reporting of $^{14}C$ data. Radiocarbon 19: 355 – 363.

Stuiver, M., Reimer, P. J., 1993, Extended $^{14}C$ database and revised CALIB radiocarbon calibration program. Radiocarbon 35, 215 – 230.

Stuiver, M., Reimer, P.J., Reimer, R.W., 2005. Calib 5.0 program and documentation. URL: http://radiocarbon.pa.qub.ac.uk/calib/.

Tovaglieri, F., George, A.D., 2014. Stratigraphic architecture of an Early – Middle Jurassic tidally influenced deltaic system (Plover Formation), Browse Basin, Australian North West Shelf. Marine and Petroleum Geology 49, 59 – 83.

Twiggs, E. J., Collins, B. C., 2010. Development and demise of a fringing coral reef during Holocene environmental change, eastern Ningaloo Reef, Western Australia. Marine Geology 275, 20–36.

van de Graaff, W. J. E., Hocking, R. M., Butcher, B. P., 1983, Yaringa, Western Australia: Geological Survey of Western Australia, 1:250 000 Geological Series Explanatory Notes, 23p.

Verduin, J.J., Backhaus, J.O., 2000. Dynamics of plant flow interactions for the seagrass *Amphibolis antarctica*: field observations and model simulations. Estuarine, Coastal and Shelf Science 50 (2), 185–204.

Walker, D.I., 1985. Correlations between salinity and growth of the seagrass *Amphibolis antarctica* (labill.) Sonder & Aschers., in Shark Bay, Western Australia, using a new method for measuring production rate. Aquatic Botany 23 (1), 13–26.

Walker, D.I., Kendrick, G. A.,McComb, A. J., 1988a.The distribution of seagrass species in Shark Bay, Western Australia, with notes on their ecology. Aquatic Botany 30, 305 – 317.

Walker, D. I. and Woelkerling, Wm. J., 1988b. Quantitative study of sediment contribution by epiphytic coralline red algae in seagrass meadows in Shark Bay, Western Australia. Marine Ecology – Progress Series 43, 71–77.

Walker, D. I., 1990. Seagrass in Shark Bay, Western Australia. In: Berry, P.F., Bradshaw, S.D., Wilson, B.R. (Eds) Research in Shark Bay: Report of the France – Australe bicentenary expedition committee. Western Australia Museum, Perth, Australia, pp101 – 106.

Walker, D.I, Dennison, G.E., 1999. Status of Australian seagrass research and knowledge. In: Butler A. and Jernakoff, P. (Eds). Seagrass in Australia. Strategic Review and Development of an R & D Plan. CSIRO Cataloguing – in – Publication pp 1 – 24.

Wilson, C. J., Wilson, P. S., & Dunton, K. H.,2012. An acoustic investigation of seagrass photosynthesis. Marine Biology *159* (10), 2311 – 2322.

# Chapter 4

# Swan River

"A river cuts through rock, not because of its power, but because of its persistence"
(James N. Watkins)

## Sea level controls on palaeochannel development within the Swan River Estuary during the Late Pleistocene to Holocene

Giada Bufarale[1], Michael J. O'Leary[2], Alexandra Stevens[2], Lindsay B. Collins[1]

1 Department of Applied Geology, Curtin University, GPO Box U1987, Perth, WA 6845, Australia

2 Department of Environment and Agriculture, Curtin University, Bentley, Western Australia, 6102

This article is published in CATENA, Volume 153, June 2017, Pages 131-142.

doi.org/10.1016/j.catena.2017.02.008 and reprinted with permission in Appendix A.

## Abstract

High-resolution seismic profiles were conducted across the metropolitan area of the Swan River estuary (Perth, Western Australia) to explore the sub-surficial stratigraphic architecture, down to a depth of about 40 m below the river bed. The acoustic profiles revealed a complex system of palaeochannels where three main unconformities (R1, R2, R3) bound as many seismic units (U1, U2, U3), over the acoustic basement.

Integrating these data with sediment borehole analysis, LiDAR data and available literature of the geology and stratigraphy of the area, it was possible to determine the development of these stratigraphic units, in response to Late Pleistocene and Holocene sea-level fluctuations and conditioned by pre-existing topography and depositional palaeoenvironments during the last ~130,000 years.

The deepest unit (U3) can be interpreted as the Perth Formation, which consists of interbedded sediments that were deposited in a large palaeo-valley downcutting into the underlying acoustic basement (bedrock: Tamala Limestone and Kings Park Formation), under a fluvial to estuarine setting, existing between ~130 and 80 ky BP (in the Last Interglacial).

The middle unit (U2), composed of heterogenic fluvial (possibly lacustrine) and estuarine sediments, represents the Swan River Formation. Similarly to the Perth Formation, the formation infills channels incised in older formations and reflects the hydrogeological conditions linked with sea level fluctuation changes during the Last Glacial lowstand.

Holocene (last ~10 ky) fluvial and estuarine deposits form the shallowest unit (U1). These sediments have a highly variable internal structure, ranging from heavily layered, filling palaeochannels, to hard and chaotic, atop pre-existing topographic highs.

The wave-dominated Swan River system shares several similarities with a number of estuaries worldwide, such as Burril Lake (NSW, Australia) and Arcachon Lagoon (Aquitaine, France).

This research represents the first environmental high-resolution acoustic investigation in the middle reach of the Swan River estuary.

## 1. Introduction

Understanding the geomorphic development and sedimentary evolution of riverine, estuarine and deltaic environments under the high amplitude sea level changes that characterise the Pleistocene and Holocene Epochs has been the focus of a number of studies worldwide.

For instance, research performed along the lower Murray River (South Australia) and the adjacent Lacepede Shelf revealed that the stratigraphic and structural architecture of the area is the product of both climate and sea level variations throughout the Pleistocene and the Holocene, resulting in formation of dunes, karst features and ancient infilled channels and lagoons (i.e. Bourman at al., 2000; Hill et

al., 2009). Similarly, sea level fluctuations, together with palaeo-topography, have controlled the Quaternary sequence stratigraphy of the Brisbane River (Queensland, Australia. Evans et al., 1992). Palaeochannels and cut-and-fill structures, formed as a response to sea level changes during the Late Pleistocene and Holocene, have also been widely recognised across Europe, America and Asia, for example along the Atlantic French and Spanish coasts (Chaumillon et al., 2010; Menier et al., 2011; Blanco et al., 2015), the Gulf of Mexico (Anderson et al., 2014), in Tokyo Lowland (Tanabe et al., 2015), and beneath the Mekong River and Red River deltas in Cambodia and Vietnam, respectively (Tamura et al., 2009; Hori et al., 2004).

Here we investigate the role that sea level oscillations, hydrodynamic conditions and pre-existing geomorphological settings had in controlling the development and evolution of the Swan River (SW Australia) during the past ~130 thousand years (ky). The study area differs from the previously mentioned studies in that the immediate coastal region is characterised by a mixed carbonate siliciclastic sedimentary system.

This study aims to construct a more detailed picture of Late Pleistocene and Holocene sequence stratigraphy and sedimentary architecture of the middle reach (Melville Waters) of the Swan River, using high-resolution shallow seismic data, ground truthed with geotechnical borehole data, in order to better understand how changing sea level driven fluctuations (base level) have influenced the evolution of the estuary throughout this period.

## 1.1. Previous work

The Swan River estuary is located in the south west of Western Australia and flows westward through the Perth Metropolitan area, into the Indian Ocean, at the City of Fremantle. Baker (1956) carried out the first scientific study of the Quaternary sedimentation in the Perth Basin, including the Swan River. He produced seven geological cross-sections using borehole data in various bridge and wharf sites (Figure 4.1, highlighted in pink). On the basis of these cross-sections and further geotechnical studies (Jones and Marsh, 1965; Ove Arup, 2001; Coffey Geosciences, 2002), Gordon (2003a, 2012) proposed an inferred location of three palaeoriver channel systems within the upper reach and Perth Waters of the Swan River estuary (Figure 4.1). In addition, a number of recent geotechnical studies (i.e. Golder Associated Pty Ltd, 2008, 2012) took place along the northern shore of the Swan middle reach (Perth Waters, between the Narrows Bridge and Barrack Square jetties, see Figure 4.2) as part of the Elizabeth Quay development, a major waterfront project that involved the construction of an extensive artificial inlet. Boreholes and localised geophysical investigations (sub-bottom profiling, seismic refraction and electrical resistivity imaging) identified potential palaeochannel structures and a total of three primary seismic reflectors above the bedrock.

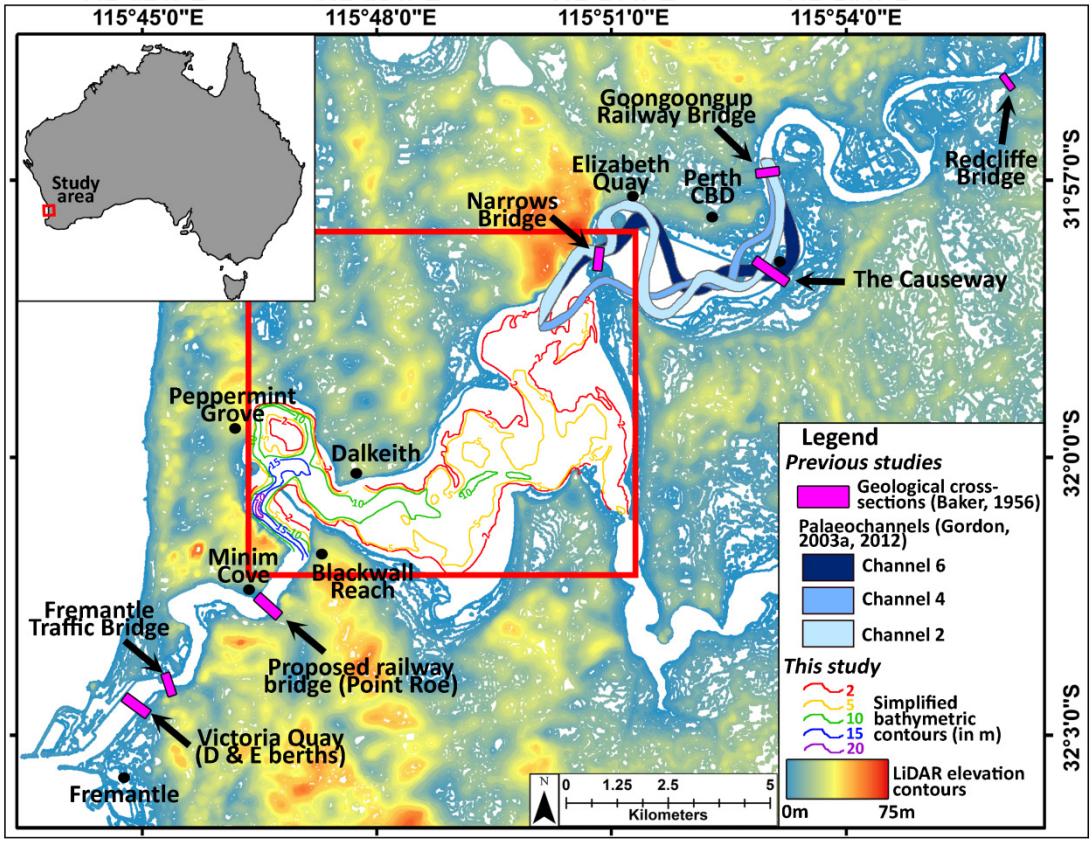


**Figure 4.1. Locality map showing the study area and locations mentioned in the paper. Simplified palaeochannels proposed by Gordon (2003a, 2012) are represented by 3 shades of blue, representing 3 cutting events. Baker's (1956) cross section locations are highlighted in pink. This study focused on the wide, underfilled middle reach of the Swan estuary, whereas Gordon's studies were restricted to the upper reach of the estuary. Simplified bathymetric contours, limited to the studied area, are also shown (source: Department of Transport).**

These palaeoriver channels represent the geomorphological and sedimentary response of the Swan River estuary to orbitally driven changes in sea level, spanning ~130 ky to present. This period captured the peak of the Last Interglacial (MIS 5e; 127 to 116 ky) with sea levels between 3 and 6 metres above present. The period between 110 ky and 80 ky saw sea level oscillating between -10 and -30 metres below present (MIS 5d, c, b and a). After 40 ky global cooling saw sea levels fall to around -125 m at the Last Glacial Maximum (LGM), which peaked around 18 ky years BP. Global deglaciation after 18 ky years saw rapidly rising sea levels reaching near present elevations around 7 ky BP (Bufarale et al., 2015).

Thus, sea level-driven changes in base level and the influence this had on fluvial sediment dynamics, together with the pre-existing geomorphology, likely played a major role in controlling the development of the Swan River estuary during the Last Glacial cycle (Churchill, 1959, cf. geological heritage in Chaumillon et al., 2010; Menier et al., 2011).

The sedimentology and geology of the Swan River and its estuary have, so far, been principally studied in a geotechnical context for planning and construction of bridges and harbour works and mainly limited to the middle reach and mouth of the Swan estuary. Much of this data remains largely unpublished, or is present in the

form of state government and consultancy reports (e.g. Australian Hydrographic Services, 1971; McKimmie Jamieson & Partners, 1987; Main Roads Western Australia, 1998; Ove Arup, 2001; Coffey Geosciences, 2002; Coffey Geosciences, 2010; Golder Associated Pty Ltd, 2008).

## 2. Geological and regional setting

The Perth Region is located in the south west of Western Australia and stretches between 31° 20' S (Gingin Brook and Moore River) and 32° 35' S (South Dandalup River), covering an area of about 4000 km2 (Davidson, 1995). The region is largely occupied by the 30 km wide Swan Coastal Plain, bound to the west by the Indian Ocean and to the east by the north-south orientated Darling, Gingin and Dandaragan Scarps. These scarps represent the western margin of the Darling Plateau, a weathered Archaean crystalline low-relief plain (Davidson, 1995).

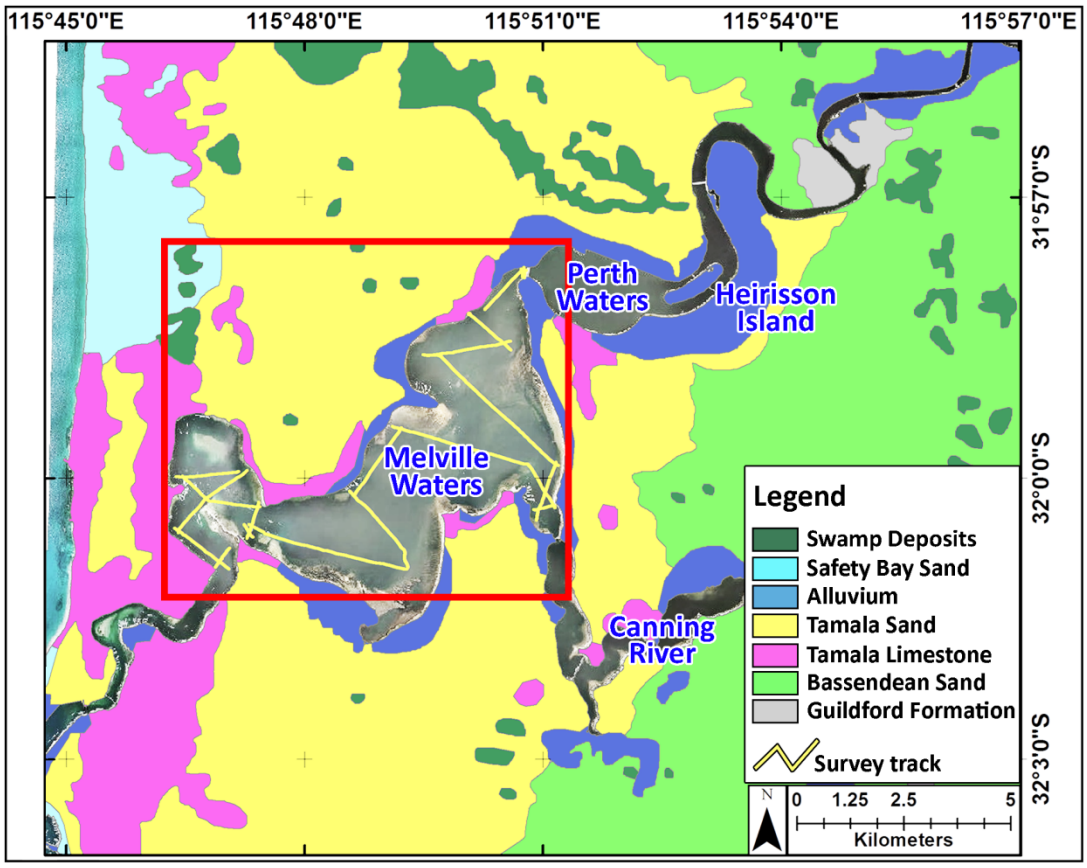


**Figure 4.2. Simplified surface geology (redrawn after Davidson, 1995 and Gozzard, 2007a), superimposed on Landgate (Western Australia) aerial image. Formation ages are included in Table 4.1. Geophysical survey track plot and survey boundaries are also marked, in yellow.**

The Swan Coastal Plain lies along a passive continental margin and, together with the Rottnest Shelf, represents the surficial sediments of the Perth Basin. Formed as a north-south rift valley during the Phanerozoic, the 1000 km long Perth sedimentary basin is infilled by a 15 km thick sequence of continental and marine sediments, from Permian to Late Cretaceous in age (Playford et al., 1976; Kendrick et al., 1991, Commander, 2003). The geological history relevant to the study started in the Early Tertiary, when a Cretaceous river valley or submarine canyon system was inundated and infilled with Palaeocene and Eocene shallow marine to estuarine

sediments of the Kings Park Formation (Table 4.1. Collins, 1987; Hudson-Smith and Grinceri, 2007; Mathew, 2010). Overlaying the Kings Park Formation (onshore) is the >150 m thick Plio-Pleistocene age Kwinana group sediments which comprise marine, fluvial, aeolian, alluvial and lacustrine sediments and record the periodic sea-level fluctuations and flooding of the inner shelf and Swan Coastal Plain. The outcropping formations present within the survey area are reported in Figure 4.2.

The Swan Coastal Plain is fed from six main drainage basins, the largest of which is the Swan River and includes three major tributaries: the Canning, Avon and Helena Rivers.

The Swan River estuary covers a large portion of Perth's northern and eastern urban areas (~ 40 km2) flowing westward through the Perth Metropolitan area and into the Indian Ocean at the City of Fremantle. In the estuary, the surficial sediments are mainly clastic, ranging from mud (low energy areas, such as the deep central portion of the basin) to sand (higher energy zones, sand flats and beaches. Quilty and Hosie, 2006). A bioclastic component is also present, composed of faecal pellets, foraminifera, whole and fragmented molluscs and other benthic invertebrates (Quilty and Hosie, 2006). Seagrass (Halophila ovalis), which covers between 75% and 99% of the shallow waters (less than 2 m, in the lower reaches of the Estuary), is often associated with coarse, shelly sediments (Hillman et al., 1995).

The Swan River estuary has an open connection to the Indian Ocean and is influenced by local wind-driven waves and, to a smaller extent, by tides (diurnal microtidal range of 0.4 m. Eliot et al., 2006). This system can be regarded as a wave-dominated estuary (Radke et al., 2004). Like the majority of the coastal waterways along the southwestern coast of Australia, the Swan River estuary conforms reasonably well to the wave-dominated estuary facies model (Dalrymple et al., 1992; Radke et al., 2004). In accordance with the Dalrymple et al.'s model (1992), the Swan estuary is composed of three different morphological components: upper reach, narrow and highly sinuous (river-dominated), middle reach, with a wide and partially filled central basin (mixed energy), and funnel-like shape lower reach (marine -dominated). The reaches are separated by topographic sills which, like in many wave-dominated estuaries (Dalrymple et al., 1992), affect local hydrodynamics, salt wedge propagation and water exchange with the ocean (Stephens and Imberger, 1996; Stephens and Imberger, 1997).

The region is characterised by a dry Mediterranean climate, with precipitation mostly confined to the autumn and winter months (Kennewell and Shaw, 2008). Consequently, the Swan system exhibits a strongly seasonal streamflow with events occurring between May and September, when the rainfall and runoff are higher (Rehman and Saleem, 2014). Marine saline waters can reach up to 35 km upstream but, being mainly controlled by barometric effects, tidal dynamics, storm surge and wind, the penetration of the salt wedge can be observed up to 60 km upstream, under exceptional climatic circumstances (Stephens and Imberger, 1996). Weather conditions also play a very important role in the circulation and main changes in the mean water level of the estuary.

**Table 4.1. Stratigraphic column (modified after Smith et al., 2012) and geological formations of the Swan Coastal Plain present within the survey boundaries (refer to Figure 4.2 for the surface geology). Note 1: Tamala Sand is the result of weathering and remobilisation of relict material of the Tamala Limestone which has been blown eastward. Note 2: The Swan River Formation can be found along the middle and lower sections of the Swan and Canning Rivers. The development of this formation can be linked to the fluctuations of sea level. The Swan River Formation subcrops the modern Swan River Holocene estuarine and floodplain clays and sands. Note 3: The Perth Formation reflects the complex palaeoclimate and sea level oscillations that characterised the Last Interglacial period. Three main lithological units (sand, silt and clay) were deposited into a palaeochannel eroded during the earlier lower sea level conditions (Penultimate Glacial period) by the ancestral Swan River, into the Kings Park Formation.**

| Stratigraphic Column | Formation/Deposit | Lithology | Depositional Environment | Age | Notes | References |
|---|---|---|---|---|---|---|
| | Alluvial and swamp deposits | Peat and peaty sand, high clay | Alluvial and Swamp | Holocene | | Commander, 2003 |
| | Fluvial deposits | Silt sand, with clay | Fluvial and estuarine | Holocene | | Commander, 2003 |
| | Safety Bay Sand | Fine-medium sand | Near-shore/eolian | Holocene | | Davidson, 1995 |
| | Tamala Sand | Sand, with clay and silt | Near-shore/eolian | 25 to 15 ky BP | See Note 1 in table caption | Bastian, 1996; Gozzard, 2007a |
| | Swan River Fm | Sand, silt and clay | Heterogenic fluvial and estuarine | 75 to 18 ky BP | See Note 2 in table caption | Gozzard, 2007a |
| | Perth Fm | Interbedded sand, silt and clay | Estuarine to fluvial | 130 to 80 ky BP | See Note 3 in table caption | Gozzard, 2007a |
| | Tamala Limestone | Coarse to medium-grained, mostly cross-bedded calcarenite, with minor lenses of clay and gravel-sized lithoclasts | Eolianites, beachrocks, shallow marine beds, coral reefs and marl | Strongly diachronous; Mid-Late Pleistocene to Holocene | The Tamala Limestone has several members and within the study area, the marine units of Minim Cove Member and Peppermint Grove Member outcrop along the foreshore of the Swan River estuary near Point Roe | Murray-Wallace and Kimber, 1989; Brooke, 2001; Gordon, 2003b |
| | Bassendean Sand | Sand, with lens of clay | Fluvial to estuarine | Middle to Late Pleistocene | Bassandean Sand interfingers to the east with Guildford Fm | Gozzard, 2007b |
| | Gnagara Sand | Very poorly sorted sand | Fluvial to estuarine | Middle Pleistocene | Stratigraphic equivalent of the Guildford Formation | Gozzard, 2007a |
| | Ascot Fm | Shelly calcarenite, silty clay | Marine prograding shoreline | Late Pliocene to Early Pleistocene | Some sections contain fresh-water gastropods (proximity of lake/swamp?) | Kendrick et al, 1991 Gozzard, 2007a |
| | Guildford Fm | Mainly clay and silt, with also lenses of poorly sorted sand and conglomerate | Fluvial, with shallow-marine and estuarine lenses | Early Pleistocene to about 130 ky BP | General fining-upwards sequence, almost without interruption | Davidson, 1995; Gozzard, 2007a; Gozzard, 2007b |
| | Kings Park Fm | Shale, calcareous sandstone and minor limestone | Shallow marine to estuarine deposits | Early Tertiary Palaeocene - Lower Eocene | 600 m thick valley-fill. The marine shale facies may be related to an old submarine canyon that converged in the ancestral Swan River | Quilty, 1974; Collins, 1987; Hudson-Smith and Grinceri, 2007; Mathew, 2010 |

## 2.1. Estuary morphology

Two shallow sills (< 5 m depth), one at the Fremantle Traffic Bridge and the other between the Narrows and The Causeway bridges (see Figure 4.1 for location), divide the system into three main segments, the upper reach, middle reach and lower reach:

Upper Reach – In the upper section of the estuary, upstream from Heirisson Island (see Figure 4.2), the tidal river is narrow and sinuous, with a depth ranging from less than 2 metres to about 6 metres (Chalmer et al., 1976; Atkinson and Klemm, 1987).

Middle Reach – The middle sector of the estuary includes Perth Waters and Melville Waters (see Figure 4.2). Between the Narrows and The Causeway bridges (Perth Waters), the Swan River estuary is wide and very shallow, with an average lowest water level of less than 1 m. From the Narrows bridge to Blackwall Reach (Melville Waters), the river is more extensive, with a central basin (that according to Dalrymple et al., 1992 can be called unfilled estuary) that deepens seaward, reaching 24 m of depth, and marginal shallow sand flats and spits fringing the shoreline (see Figure 4.2. Chalmer et al., 1976; Collins, 1987; Quilty and Hosie, 2006).

Lower Reach – The lower segment, downstream from Blackwall Reach to the Fremantle Traffic Bridge, was defined by Quilty and Hosie (2006) as a “coastal dune limestone corridor”. In this last section, the Swan estuarine passage is characterised by a narrow straight that follows the joints and structures in the limestone, forming right angles and cliffs through the Tamala Limestone. In contrast to the middle reach, this portion of the estuary shallows seaward, to less than 5 m, at the Fremantle Harbour.

Although the exact geological nature of these sills is unknown (no seismic data was collected along these features and pre-existing literature is scarce), it is likely that they formed under a combination of pre-existing topography and more recent sediment accumulations (as in Dalrymple et al., 1992; Dalrymple and Choi, 2007).

It must be noted that harbour development, dredging and foreshore reclamation, dating back to the end of the 19$^{th}$ Century (Tutton, 2003), have significantly changed many areas of the Swan River estuary (Chalmer et al., 1976; Collins, 1987; Radke et al., 2004). The removal of sediment build-up and rocky outcrops, especially at the estuary mouth, caused an increase in marine water intrusion, tidal exchange and salinity, resulting in a proliferation of marine aquatic plants (Hodgkin and Hesp, 1998). Urbanisation and agriculture have also had an impact on the sediment transport and composition, causing significant changes in runoff and inputs of salt, nutrients and sediments in the estuary (Atkinson and Klemm, 1987; Hamilton et al., 2001).

# 3. Methods

About 30 km of high-resolution shallow seismic profiles have been collected, processed and analysed along the Swan River estuary, between the Narrows Bridge and Blackwall Reach (Figure 4.2, survey track plot sketched in yellow). Survey run lines were devised to capture a range of substrate architectures and geometries, to

a maximum depth of 40 m below the river bed. Transects perpendicular to the river course revealed the location and width of buried palaeochannels. Profiles along the strike of the river permitted the correlation and interpretation of acoustic horizons.

The seismic data were acquired using an AA201 boomer system (Applied Acoustic Engineering Limited, Great Yarmouth, UK). A hand-held GARMIN eTrex Global Positioning System (GPS) was employed to obtain and record position (accuracy: typically less than 4 m). The seismic data were digitally recorded in SegY format (Rev 1), using SonarWiz 5 (V5006.0032. Chesapeake Technology Inc., Mountain View, CA) as acquisition and post-processing software.

Acoustic reflectors have been interpreted, where possible, through sedimentary analysis and correlation of borehole logs, which were drilled by a number of agencies primarily for geotechnical investigations (Main Roads Western Australia, 1998; Golder Associated Pty Ltd, 2008; see Gordon, 2012). The most recent of these were 4 boreholes cored near Dalkeith for the Perth Flying Squadron Yacht Club by Coffey (Coffey Geosciences, 2010; see Figure 4.1 for location and Figure 4.3). The data was also correlated with the information provided by two geophysical surveys, undertaken by Australian Hydrographic Services (1971) and McKimmie Jamieson & Partners (1987) as part of a proposed dredging and reclamation project, in the Outer and Inner Harbour in Fremantle.

Formations and sediment ages were acquired from literature, in particular Murray-Wallace and Kimber (1989), Hearty (2003), Gozzard (2007a), Gordon (2012), and Brooke et al. (2014). Due to the characteristics, scope and planning of the core drilling, we were unable to carry out any radiocarbon dating specific to this project.

Palaeomorphology reconstruction of the Last Glacial Swan River was performed with ArcGIS 10.2 software (Esri) using a combination of seismic profiles and bathymetric data of the modern river floor (from Swan and Canning River 2010-2011 Hydrographic Surveys, Department of Transport).

# 4. Results and interpretation

The seismic analysis of the sub-bottom profiles shows that the shallow architecture underneath the Swan River estuary is dominated by palaeochannels. The seismic profiles contain numerous acoustic reflectors, some of which have distinctive features and can be recognised across the study area, and others which are discontinuous and only recorded in some locations. Four main reflectors (river bed, R1, R2 and R3) were identified, which define three acoustic units (U1, U2 and U3), which sit atop of the acoustic basement (Table 4.2). In some places, there was no penetration beyond the river bed surface.

## 4.1. Seismic units and sedimentary facies

*Seismic Unit U1.* Sub-bottom profiles reveal an irregular but laterally continuous, strong reflector, here defined as R1. The sediments bound between the river bed and R1 form seismic unit 1 (U1). U1 has a variable thickness ranging from being barely discernible to up to 14 m thick and is characterised by a number of different seismic features. Where thicker than 2.5 m, U1 is intensely bedded and typically

infills palaeochannels. The layers are parallel to subparallel and pinch out updip (divergent fill), converging against pre-existing highs. Minor reflector R1a runs sub-parallel to the seafloor and is useful to subdivide U1. The strata of the upper sub-unit are thinner (up to 0.30 m of thickness), more laminated and laterally more continuous than in the lower sub-unit (up to 1 m). The Dalkeith boreholes (Coffey Geosciences, 2010) show the upper sub-unit to be mainly composed of thinly bedded unconsolidated silty sand, with mainly horizontal or gently undulated laminations (Figure 4.3). In contrast, the lower sub-unit consists of thick bedded clay units, which are horizontally layered over the pre-existing topographic lows, such as channels or depressions. In the zones where unit U1 is thinner than 2.5 m, the substrate appears to be harder and more cemented, with no internal layering.

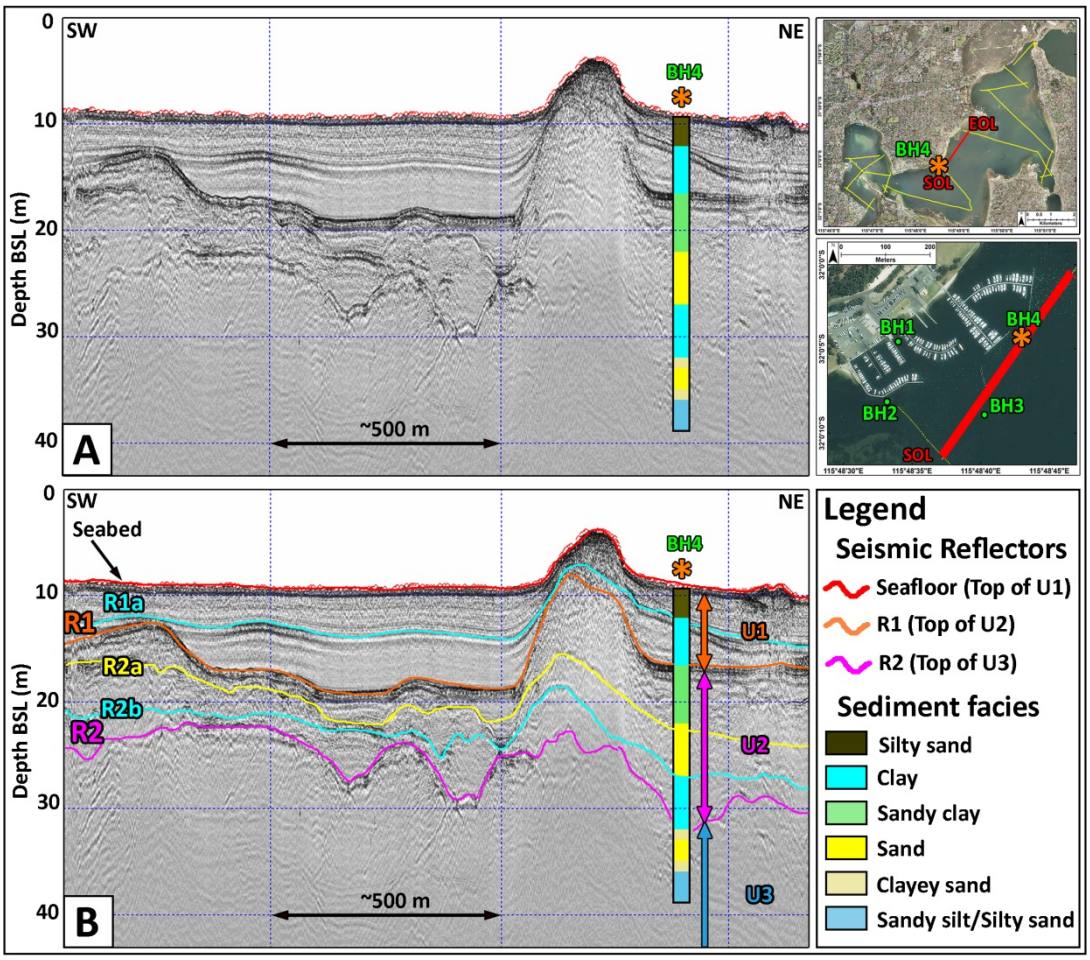


**Figure 4.3. Seismic profile adjacent to the Perth Flying Squadron Yacht Club (Dalkeith), showing two sets of palaeochannels. A: uninterpreted seismic profile, with schematic core. B: interpreted seismic profile. R1 represents the main reflector, at the base of intensely bedded deposits (U1). R2 has been incised into an older substrate and covered by tripartite sediments (U2). From this seismic profile it is not possible to depict the base of the unit (U3) underlying the acoustic reflector R2. Aerial photo images provided by Landgate (Western Australia). Depths are in metres, below the sea level.**

*Seismic Unit U2*. From the seismic profiles, a second and deeper seismic reflector, which is here defined as R2, can be observed. It has an irregular surface, mostly forming depressions, separated by areas of hill-like undulating bathymetry; flat areas are rare. Bounded between reflectors R1 and R2, is an older sequence, named here

seismic unit U2, and directly underlies seismic unit U1. U2 is inhomogeneous, characterised by a series of internal, moderate to strong acoustic reflectors, which are locally discontinuous (Figure 4.3). Based on the borehole data (Coffey Geosciences, 2010), seismic unit U2 can be subdivided into three sub-units. This tripartition is evident also in the seismic profiles, where 2 sub-reflectors (R2a and R2b) can be recognised (Figure 4.3). The lower sub-unit (between R2b and R2) is composed of parallel, partially continuous strata of firm to stiff clay (Coffey Geosciences, 2010), with traces of sand, fills minor stream channels and cuts into the underlying older deposits. Locally, this deeper sub-unit is capped by a poorly defined sequence where compacted sand is the main component (middle sub-unit, bound by R2a and R2b). This sub-unit is partially truncated by the overlaying, semi-horizontal sandy clayey deposits (upper sub-unit, bound by R1 and R2a). The three sub-units are intermittently visible in the seismic profiles, but this absence may be more ambiguous than real, possibly due to a lack of velocity contrast between their lithologies.

In some areas, R1 and R2 (and relative acoustic units) have been locally depicted as inferred reflectors (i-R1 and i-R2, see further in Section 5.1), since their seismic pattern was masked by an acoustic wipe-out on the sub-bottom profiler record. This type of signal has been recorded also in tie lines, confirming that this pattern is a real feature in the sediments.

**Table 4.2. Facies identified in the seismic profiles.**

| Seismic unit | Limits | Max Thickness | Internal structure | Lithology | Interpretation (see further for more details) |
|---|---|---|---|---|---|
| U1 | River bed to R1 | 14 m | From heavily layered, filling palaeochannels, to hard and chaotic, atop of pre-existing topographic highs | From silty sand to clay | Holocene, fluvial channel-fill deposits |
| U2 | R1 to R2 | 27 m | Inhomogeneous (beds or without internal structure) | Sand, silt and clay | Swan River Fm. |
| U3 | R2 to R3 | 21 m | Interbedded | Sand, silt and clay | Perth Fm. |
| Acoustic basement | Top: R3 | NA | Laminated to massive | - | Tamala Limestone/Kings Park Formation |

*Seismic Unit U3.* Due to equipment limitation and lack of acoustic contrast in the local lithology, the substrate below the reflector R2 is less definite. There are several discontinuous internal reflectors that cannot be accurately depicted as they are intermittent and quite irregular. Between Dalkeith and Blackwall Reach, a gently undulating third acoustic reflector (here name R3) is definite enough to be depicted (Figure 4.4). The geotechnical data (Coffey Geosciences, 2010) regards the

deposits between reflectors R2 and R3, which form the seismic unit U3, to include interbedded horizons of silt, sand and clay. U3 is characterised by discontinuous and irregular minor internal reflectors; concave-up, onlapping strata are also locally recognisable.

*Acoustic basement.* The acoustic basement lies below seismic unit U3. Capped by the reflector R3, the acoustic basement is characterised by minor seismic reflectors that disappear progressively with depth, indicating a strong absorption of the acoustic energy, likely suggesting a hard and compacted lithology.

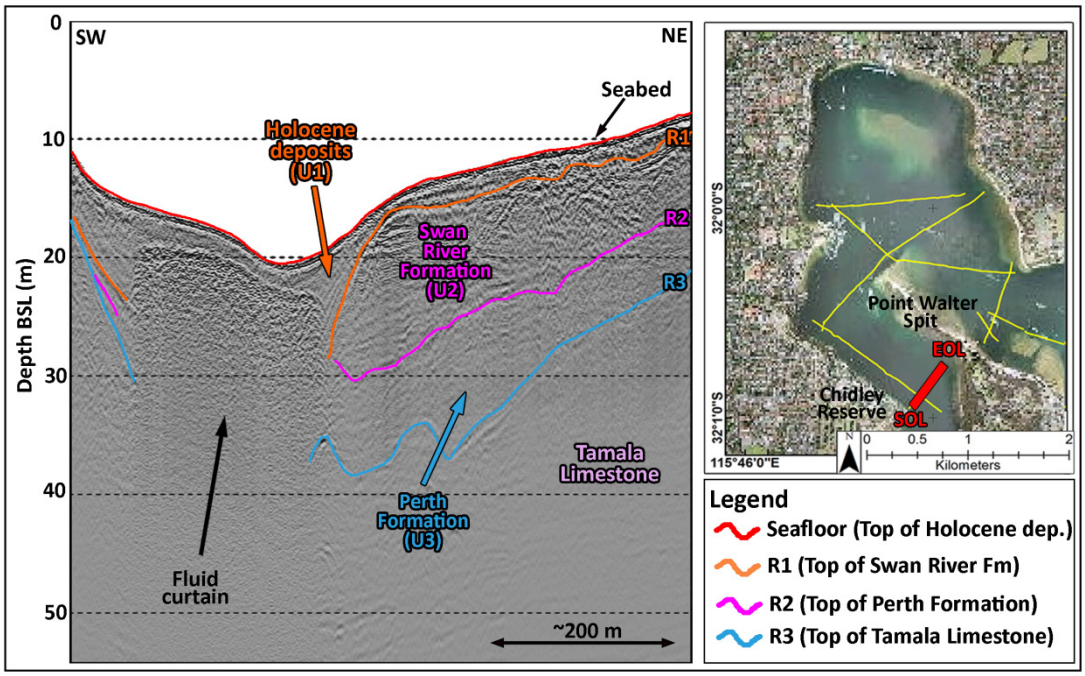


**Figure 4.4. Seismic profile showing the top of the acoustic basement (Tamala Limestone) forming a topographic low, successively partially infilled by more recent formations. Tamala Limestone outcrops on both the shores of the Swan River (Chidley Reserve and Point Walter Spit) and the upper limit can be picked also along the seismic profiles. The channel-like geometry of the basement has conditioned the modern bathymetry. Note the fluid curtain rising from Tamala Limestone (see further discussion on the nature of these fluids in Section 5.1). Aerial photo images provided by Landgate (Western Australia). Depths are in metres, below the sea level. SOL: start of line, EOL: end of line.**

## 4.2. Interpretation of the seismic data

High-resolution sub-bottom profiles have revealed a complex buried palaeochannel network within the middle reach of the Swan River estuary, allowing for a detailed analysis of the architecture of the palaeodrainage within the study area.

Based on these newly acquired seismic profiles, available sedimentary analysis (Coffey Geosciences, 2010) and literature of the geology and stratigraphy of the area (Gordon, 2003a; Gozzard, 2007a; Gordon, 2012; technical reports: McKimmie Jamieson & Partners, 1987; Golder Associated Pty Ltd, 2008, 2012), the depositional history of the Swan River estuary from Late Pleistocene to present comprises three phases, resulting in three 3 different lithostratigraphic units, from the oldest to most recent the 1) Perth Formation (U3), 2) Swan River Formation (U2), and 3) the Holocene (U1).

A number of studies have demonstrated that sea-level fluctuations linked with Glacial and Interglacial periods are the primary control in the sedimentary development and evolution of fluvio-estuarine depositional environments (Blum and Törnqvist, 2000; Lambeck and Chappell, 2001; Blum et al., 2013). The impact of repeated sea level oscillations has also had a major influence in the development of the Swan River estuary, as evidenced in the subaerial landscape and buried features along the present river course (Hearty, 2003).

### *4.2.1. Acoustic basement*

There are two sedimentary units that form the acoustic basement of the study area: Tamala Limestone (western part of the survey area) and the Kings Park Formation (eastern part of the survey area). In the western portion of the Melville Waters, where the Swan River estuary narrows and the water depth increases (from 5 to more than 20 m), Tamala Limestone is observed outcropping along both the river banks. On the western bank (SOL, Figure 4.4) the cliff of Chidley Reserve is more than 20 degrees steep and the limestone cliff continues below the water level. On the eastern bank (EOL, Figure 4.4) the shore has, instead, a gentle slope, outcropping in the Point Walter Spit. This morphology is reflected in the bathymetry (see Figure 4.2) and the sub-bottom profiles acquired in the area corroborate this observation. In Figure 4.4, reflector R3 (top of Tamala Limestone) is in fact shallow, at the start and at the end of the line (17 and 21 m, below sea level, respectively), and progressively deepens to almost 40 m below sea level in the central part of the profile, forming a topographic low, partially infilled by the more recent formations.

A few kilometres upstream, near the Narrow Bridge, the incised shales/siltstones of the Kings Park Formation are found under the Perth Formation (Coffey Geosciences, 2002; Golder Associated Pty Ltd, 2008, 2012).

From the seismic profiles, the horizontal extent and upper and lower contacts of Tamala Limestone and the Kings Park Formation are not detectable.

### *4.2.2. Perth Formation*

The deepest palaeochannel identified in the Swan River seismic profiles was interpreted as a downcutting, into the underlying Tamala limestone and Kings Park formations (acoustic basement). Although it is not possible to depict this erosional surface (acoustic reflector R3) for the entire study area, the log data from the drilling between Goongoongup Bridge and Victoria Quay Berths confirms that it deepens uniformly from Guildford to Fremantle (Baker, 1956; Gordon, 2012).

At the onset of the Last Interglacial (LIG), between 135 and 127 ky, the sea level swiftly rose about 100 m and reached at least 2 m above the present sea level by 127 ky BP (Stirling et al., 1995; O'Leary et al., 2008). The riven downcutting experienced during the previous Glacial period ceased with the rise of base level and onset of estuarine sedimentation (net deposition). The incised palaeovalley was infilled with at least 20 m of interbedded estuarine sand, silt and clay deposits. According to Gozzard (2007a), Mathew (2010) and confirmed by the lithological facies analysis from the boreholes collected by Coffey Geosciences (2010) in Dalkeith, and the other available geotechnical information (Golder Associated Pty Ltd, 2008, 2012), it is likely that the deposits between the reflector R2 and R3

represent the Perth Formation (U3). This fluvial and estuarine complex constitutes the fill of a palaeovalley, aligned with the present Swan River estuary. The basal part of the Perth Formation, consisting mainly of clay sediments, was deposited in the lower portion of the palaeochannel. The middle portion is dominated by sandy and coarser sediments, indicating a greater energy and volume of the palaeo-Swan River. In the upper and younger section, the Perth Formation is composed of silt and clay, deposited in a quieter estuarine environment. Mathew (2010), through X-ray Diffraction (XRD) analysis and Scanning Electron Microscope (SEM) imaging, showed that the upper deposits of this formation have a large amount of iron-stained grains of kaolinite and quartz, possibly derived from the erosion, transport and successive deposition of the granite forming the Darling Scarp during warm and humid climate conditions.

Gozzard (2007a) assigned an age of ~130-80 ky to the Perth Formation, by correlating it to previous studies (Murray-Wallace and Kimber, 1989; Kendrick et al., 1991) that dated the marine fauna sampled from exposures along the middle and lower reaches of the Swan River, which can be can be considered the marine equivalent of the estuarine Perth Formation .

### *4.2.3. Swan River Formation*

The peak of the Last Interglacial (sub-stage MIS-5e; c. 127-116 ky) was followed by ~40 ky (from MIS 5d until MIS 5a, about 80 ky ago) of general cooling (Lambeck et al., 2002; Hearty, 2003; Woodroffe and Webster, 2014). This progressive reduction of the temperatures culminated about 18 ky BP, when the sea level reached its lowest stand at -130 m below the present sea level (Last Glacial Maximum, LGM. Hearty at al., 2007; Lambeck et al., 2014). During this lowstand period, the ancestral Swan River had another episode of downcutting (Figure 4.5A). The seismic profiles revealed the presence of a second palaeochannel, incising into the Kings Park and Perth Formations. The morphology and pattern of the palaeo-riverine bottom, where detectable, appear to be quite different from that of the present river floor. The river gradient was significantly higher than the present following the termination of the LIG and prior to the onset of the LGM, extending in the study area, from -9 m below the present river level to -40 m, with a difference in height of ~30 m, versus less than 25 m in the present time (the deepest surveyed point is 24 m, between Peppermint Grove and Minim Cove). This difference can be explained as a typical fluvial response to sea level changes (i.e., change in base level): the palaeochannel had a higher gradient due to the fact that sea level was lower over the Last Glacial cycle with the palaeo-Swan River incising into underlying strata in order to maintain a balance with a lower than the present base (sea) level (cf. Schumm, 1993; Blum and Törnqvist, 2000).

During the LGM, fluviatile heterogenic deposits of sand, silt and clay were deposited under various hydrological settings. From the borehole data (Coffey Geoscience, 2010), the complex nature of the sediments composing the seismic unit U2 is clear and can be referred to Gozzard's description (2007a) of the Swan River Formation (Figure 4.5B).

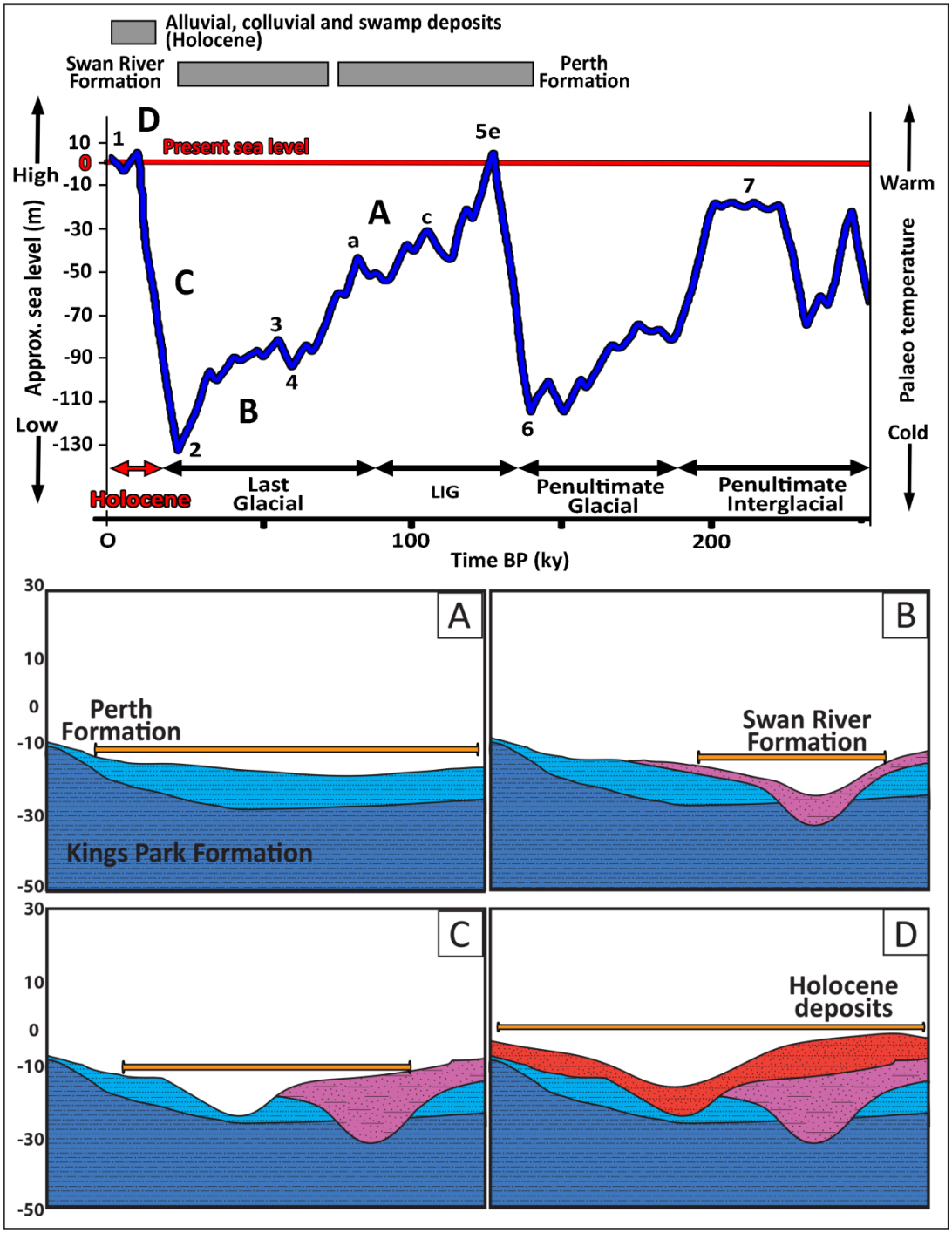


**Figure 4.5. Top: Sea level curve in the past 250 ky. Odd numbers refer to Interglacial Marine Isotope Stages (MIS) and even numbers indicate the Glacial MIS (modified after Lisiecki and Raymo, 2005; Berger, 2008 and Saqab and Bourget, 2015). Bottom: Schematic cross-section showing the evolution of the morpho-stratigraphy in the middle reach of the Swan River (Melville Waters) through the Late Quaternary, based on seismic profiles and Gozzard (2007a). Horizontal axis: ~ 3 km; vertical axis: depth/elevation values are in metres, referred to the present sea level. Orange lines represent the width of active valley. A) During the Last Glacial period, a deep inset valley cut the pre-existing Kings Park Formation and Perth Formation, during a low sea level stand. B) Changes in sea level caused by fluctuations in the climate during the last 50-70 ky of this Glacial period resulted in an alternation of erosion and deposition during which the palaeochannel was filled with the variegate sediments of the Swan River Formation. C) Last Glacial Maximum (MIS 2, ~ 18 ky BP). As the sea level reached its lowest point, the most recent palaeochannel was cut and successively (D) infilled with fluvial deposits through the Holocene interglacial conditions.**

The sequence of the Swan River Formation consists of a series of three stacked interbedded deposits, at least 22 m thick (in the survey area), formed in a riverine, estuarine and marine setting (bottom to top). Sand and gravel sediments dominate the upper section of the river (between Guildford and Perth/The Causeway). In the middle reaches, the content of finer sediment (silt and clay in lenses) increases. In the lower portion (in Fremantle) sand, silt and clay take over (Gozzard, 2007a).

### *4.2.4. Holocene deposits*

At the peak of the LGM sea level reached its lowest point around 130 m below the present sea level (e.g. Lambeck and Nakada, 1990; Lambeck et al., 2014). The coastline is reasoned to have been at least 12 km westward from Rottnest Island, located 18 kilometres west of Fremantle. The palaeo-Swan River joined the submarine Perth Canyon, approximately 22 km northwest of Rottnest (Playford, 1977), incising into the underlying formations. Due to a greater longitudinal profile gradient, the river started to cut down into the generally horizontally deposited estuarine sediments of the Swan River Formation, down to a depth of 30 m below the present sea level (as determined from the seismic profiles acquired for this study). The morphology of the channel where the Swan River was flowing at the Late Glacial and Early Holocene (Channel 2, Figure 4.6) is easily recognised in the seismic profiles along the whole survey area. At the termination of the LGM, the sea level rose and the valley became an estuary; the flow velocity slowed and up to 14 m of deposits was trapped as a palaeovalley-fill along the Swan River. Based on the lowest depth of Channel 2, it is likely that the accumulation of these sediments (unit U1) started to take over around 10 ky ago, when the sea level reached a depth of at least 30 m below the present sea level. U1 represents the most recent deposits of the survey area, formed during the Holocene.

## 5. Geomorphic evolution of the Swan River Estuary

During the Last Glacial cycle, the main channel of the palaeo-Swan River (Channel 2, Figure 4.6) was deeper and significantly narrower than the present, with the modern shallow areas adjacent to South Perth, Crawley, Ardross and Bicton probably forming emergent fluvial terraces. This palaeoriver was likely to be very fast-flowing, with transport exceeding deposition, resulting in a channel mostly free of finer sediment (at least, in the middle reach). Two shallow islands were probably present (Figure 4.6A), linked to buried topographic highs that were overstepped by the river in the Mid-Holocene. Similarly to the modern setting, a palaeo-Canning River flowed into the Swan River (Figure 4.6A). Channel 2 is in line with the modern thalweg (Figure 4.6A), demonstrating that the sedimentation subsequent to the Holocene sea level rise has only partially filled it. The seismic profiles also show evidence of a distributary channel separating southward from the main stream (Figure 4.6B). The abandoned palaeochannel was about 300 m wide and up to 12 m deep. The base has a clear erosional contact, indicating that the channel was active and cutting into the underlying Swan River Formation. During Holocene sea level rise (around 10 ky BP), the first areas to be flooded were the old channels, with sediments that started to infill these palaeochannels, levelling the river bed. Similarly to the profile in Figure 4.3, there is a subdivision of the Holocene infilling sediment. The lower portion (5-7 m thick) appears to be composed of clay, arranged in thick layers and could indicate a phase when the channel was partially abandoned,

causing a reduction of the water flow. The upper sediments (~5 m of thickness) appear to be constituted by unconsolidated sandy silty and thinly laminated, possibly corresponding to a stage of intermittent flow, progressively converted to channel abandonment. Considering the amount of deposition, it is likely that a substantial volume of water was flowing in the tributary channel, capable of carrying a large quantity of sediments, until the palaeo-waterway become inactive.

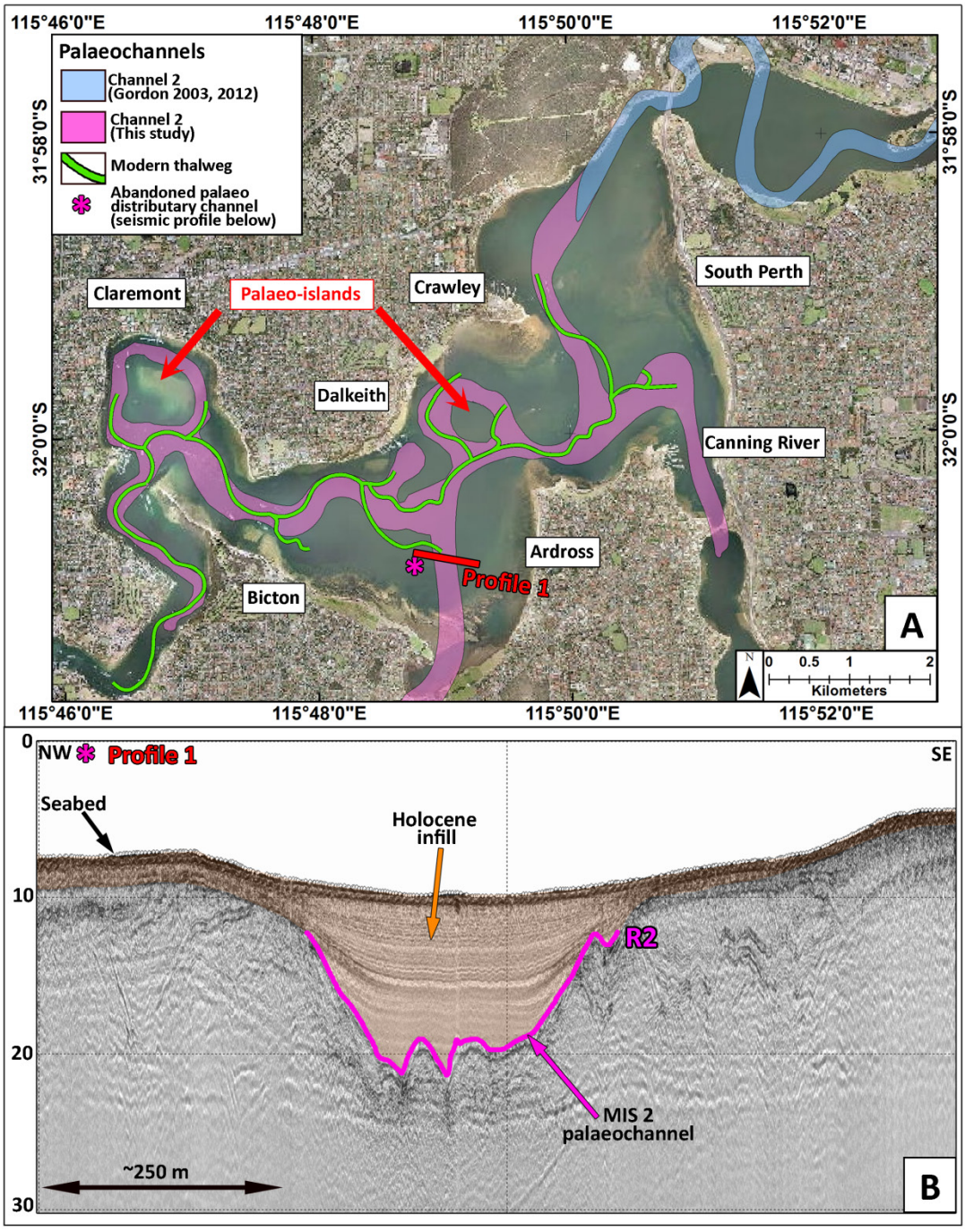


**Figure 4.6. A: Sketch map of the palaeomorphology of Channel 2. The modern thalweg is marked in green. Although the modern and palaeo Swan River have a similar trend, the MIS 2 palaeochannel was likely significative narrower than the contemporary one. Aerial photo provided by Landgate (Western Australia). B: Acoustic profile of the abandoned tributary. Depths are in metres, below the sea level.**

Based on high-resolution topographic (elevation) data of the region (see Figure 4.2), it is not possible to locate the alternative pattern of the ancestral tributary channel across the Swan Coastal Plain due to the large aeolian dune build-up and extensive urbanisation; however, with a further seismic survey along the coastline, it may be possible to detect where the palaeochannel extended towards the shelf.

## 5.1. Fluid blankets

In some locations, seismic units U1, U2 and U3 appeared partially concealed by an acoustic wipe-out (Figure 4.7). The masking is likely to have been caused by absorption of the seismic signal due to fluid escape from underlying deposits. This pattern, called fluid blankets or fluid curtains in relation to the volume of fluid content, is associated with thick sediment deposits in valley bottoms, palaeochannels or buried depressions (Baltzer et al., 2005). The origin and processes of this fluid-flow is still poorly understood, but it could possibly be linked to a combination of the thickness and nature of the sedimentary deposits in the Swan Coastal Plain and the presence of a high water table.

From the seismic profiles, this kind of structure can be found only in association with the bottom of palaeochannels, masking their base. Plotting the distribution of these features in the coastal dune systems map, they appear to be approximately aligned with the three interdune wetland belts, which run sub-parallel, with a north-south direction in the coastal plain, both north and south of Perth (Figure 4.7A). It is likely that the buried fluid-escape structures are linked with freshwater springs, rising from the unconfined, superficial aquifer that, in the Swan estuarine system, rests on the Kings Parks Formation and Tamala Limestone (Davidson, 1995). In addition, it is worth mentioning that Aboriginal people and early European settlers reported running freshwater springs in the area, especially west of the Narrows Bridge (Kennedy Fountain), where the Old Swan Brewery was built and the permanent high quality water was, in the past, used during beverage production (Vinnicombe, 1992). Considering that the survey was carried out at the end of the winter (September), it is expected that, having been recharged by the seasonal rainfall, the water table had risen creating a water pressure gradient that may have initiated a shallow groundwater flow into subaqueous springs or seeps (Figure 4.7B).

This kind of acoustic signature could also be linked with the presence of a biogenic gas, such as methane, derived by the decomposition of organic matter, typical in estuarine environments (Baltzer et al., 2005). It is possible that in the area, a combination of the two occurrences is the cause of the limited imaging of the buried sediment structures. Evidence of fluid rise within the sediments have been found also during a seismic investigation carried out in 2008 along the Perth CBD Foreshore (Golder Associated Pty Ltd, 2008), where the presence of gas prevented the imaging of the sediments in approximately 50% of the study area.

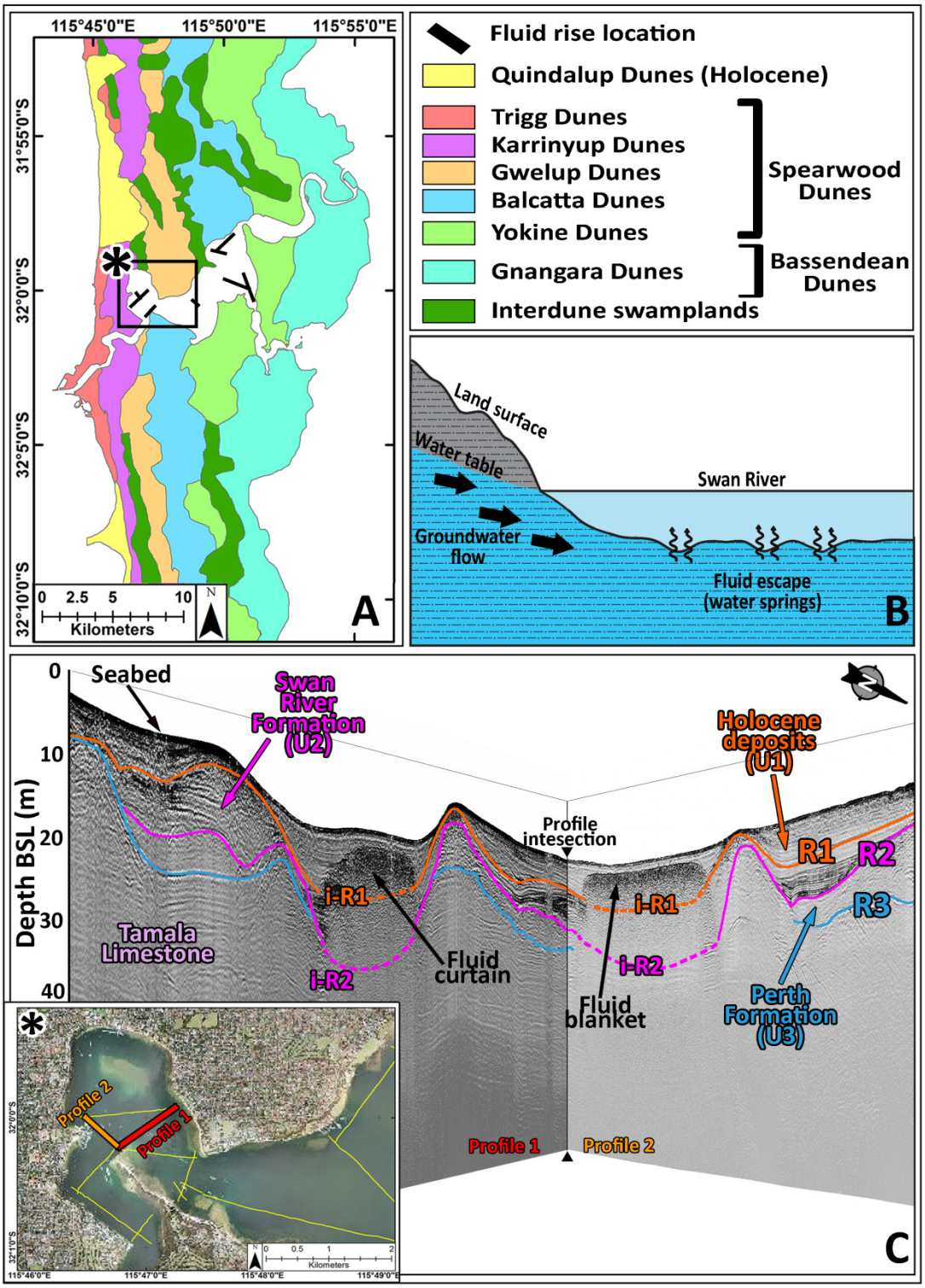


**Figure 4.7. A: Dune systems in the Swan Coastal Plain (re-drawn after Bastian, 1996). Note the north-south trend of the dune system. The locations where fluid rise was recognised in the seismic profiles are marked in black. The rectangle indicates the inset area in panel C. B: Schematic diagram illustrating the formation of fluid escape in the hypothesis of the presence of subaqueous springs (profile not to scale). In late winter, after heavy rainfall, the water table is higher. These conditions result in the groundwater having a greater pressure of and consequent formation of seepage that flows into the Swan River. Details are discussed in the text. C: Intersecting cross-section between Profiles 1 (length: ~ 1000 m) and Profile 2 (Length: ~ 650 m). Areas where there is a fluid escape are depicted with dash lines. In this reach, the**

**acoustic basement is likely to be Tamala Limestone. Inset: aerial photo provided by Landgate (Western Australia).**

## 6. Comparisons with other palaeo-estuarine systems

The Swan River system fits reasonably well to Dalrymple et al.'s model (1992) of a wave-dominated estuary: a funnel-shaped geometry (differing from the model only at the river mouth, where the pre-existing topography significantly controls its shape), a straight-meandering-straight channel morphology (from the source, going seaward) and a tripartite zonation, as a function of water depth and hydrodynamic conditions, that is reflected in the facies distribution. At present, submerged sandy barriers across the river mouth, typical of a wave-dominated system, are not found in the Swan River estuary, as they were dredged for the Fremantle Harbour reclamation during the Nineteenth century (Tutton, 2013).

The Swan River estuary shares several similarities with a number of estuaries worldwide. Table 4.3 and Figure 4.8 compare the Swan River with analogous environments in Australia (Burril Lake, NSW) and France (Arcachon Lagoon, Bay of Biscay). Despite diversities in size and shape, the three estuarine water bodies have similar environmental settings, lying on a tectonically stable, wave-dominated coastline, with low tidal ranges (micro- to mesotidal). High-resolution seismic profiles carried out in the three locations revealed a complex internal architecture, characterised by three main episodes of cut-and-fill (Sloss et al., 2005; Allard et al, 2009; this study), that record as many transgressive and regressive events (lowstand and high stand stages of sea level). Noteworthily, fluid rise is also present in each location. Sets of palaeochannels are clearly recognisable in the seismic data of the Swan River and Arcachon Lagoon, but not identifiable in Burril Lake. This may be due to the fact that the latter is the narrowest of the considered environments (Figure 4.8C), therefore the lowstand river channel has remained confined and could not migrate during the time.

The main differences include the thickness and the age of the sediments over the bedrock.

Arcachon Lagoon has the thinnest sediment package. With only ca 10 m section (Allard et al, 2009), the deposits on top of the rock foundation are about 1/3 thinner than in the other 2 locations (Table 4.3). This difference can be explained by combining annual rates of coastal retreat and relative sea level rise (Klingebiel and Gayet, 1995). According to Klingebiel and Gayet (1995), coastal erosion along the Arcachon Bay is about 1 to 2 m/year, therefore sediments deposited during recent transgressive events may have not be preserved. In addition, dating of sediment cores have shown that from 5.0 to 2.5 ky BP, the sea level in the area was about at -5 to -4 m below the present, then increased to -2 to -1 m below present sea level in the following 1.5 ky, before slowly stabilising at present time (Klingebiel and Gayet, 1995). Conversely, along the Australian coasts, evidence of a Late Holocene highstand is present, with a sea level about 1 m higher than the present, at 6 ky BP, in both the Swan River and Burril Lake areas (Lambeck and Nakada, 1990). It is likely that sedimentation has been greater and perpetuated for longer in these locations, resulting in thicker deposits.

**Table 4.3. Summary of characteristics of three wave-dominated estuaries: Burril Lake (NSW, Australia), Arcachon Lagoon (Aquitaine, France) and Swan River (WA, Australia).**

| | Swan River, south western Australia (this study) | Burrill Lake, south eastern Australia (Sloss et al., 2006) | Arcachon Lagoon, south western France (Allard et al., 2009) |
|---|---|---|---|
| Estuary type<br>Tidal regime<br>Morphology | Wave-dominated barrier estuary<br>Microtidal<br>Meandering valley upstream, with a wide central basin and narrow corridor downstream | Wave-dominated barrier estuary<br>Microtidal<br>Relatively shallow and narrow bilobate valley, connected to the ocean by a shoaled sinuous channel | Lagoon<br>Mesotidal<br>Equilateral triangular shape, with 20-km-long sides and connected to the ocean by a tidal inlet |
| Bedrock | Calcarenite and calcareous siltstone | Permian quartz sandstone and monzonite rock | Mesozoic–Cenozoic sedimentary rocks (Leorri and Cearreta, 2004) |
| Total catchment area | ~120,000 $km^2$ (Swan-Avon catchment. Viney and Sivapalan, 2001) | 80 $km^2$ | 4140 $km^2$ (Castel et al., 1996) |
| Sand barrier at the mouth | Dredged | Yes | Yes |
| Tectonic conditions | Stable | Stable | Relatively stable (Klingebiel and Gayet, 1995) |
| Sediment thickness (over bedrock) | From <1 m to at least 27 m (with limitation from acoustic penetration) | From 2 to up to 30 m | ~10 m |
| Sedimentary succession | *Basal unit* (130 to 80 ky BP): interbedded sand, silt and clay<br>*Middle unit* (75 to 18 ky BP): sand, silt and clay<br>*Top unit* (Holocene): silt sand, with clay | *Basal unit* (Late Pleistocene): quartzose sand.<br>*Middle unit* (Holocene): bipartite. Base: quartzose carbonate-rich sand (7.8 and 7.0 ky BP); top: quartzose sand (4.5 ky BP).<br>*Top unit* (ca. 1000 years to present): sand, with seagrass (downstream); estuarine silty clay, with considerable organic material (central basin); organic-rich sandy mud deposits and seagrass (upstream). | *Basal unit* (older than 7.500 ky BP): coarse-grained sand.<br>*Middle unit* 1 (7.5–5.5 ky BP): coarse sand.<br>*Middle unit* 2 (5.5–2.8 ky BP): sand with shells and clay.<br>*Top unit* 1 (2.8–1.5 ky BP): silt and sand, with shell lags.<br>*Top unit* 2 (1.5 ky BP-present): silts and organic debris |

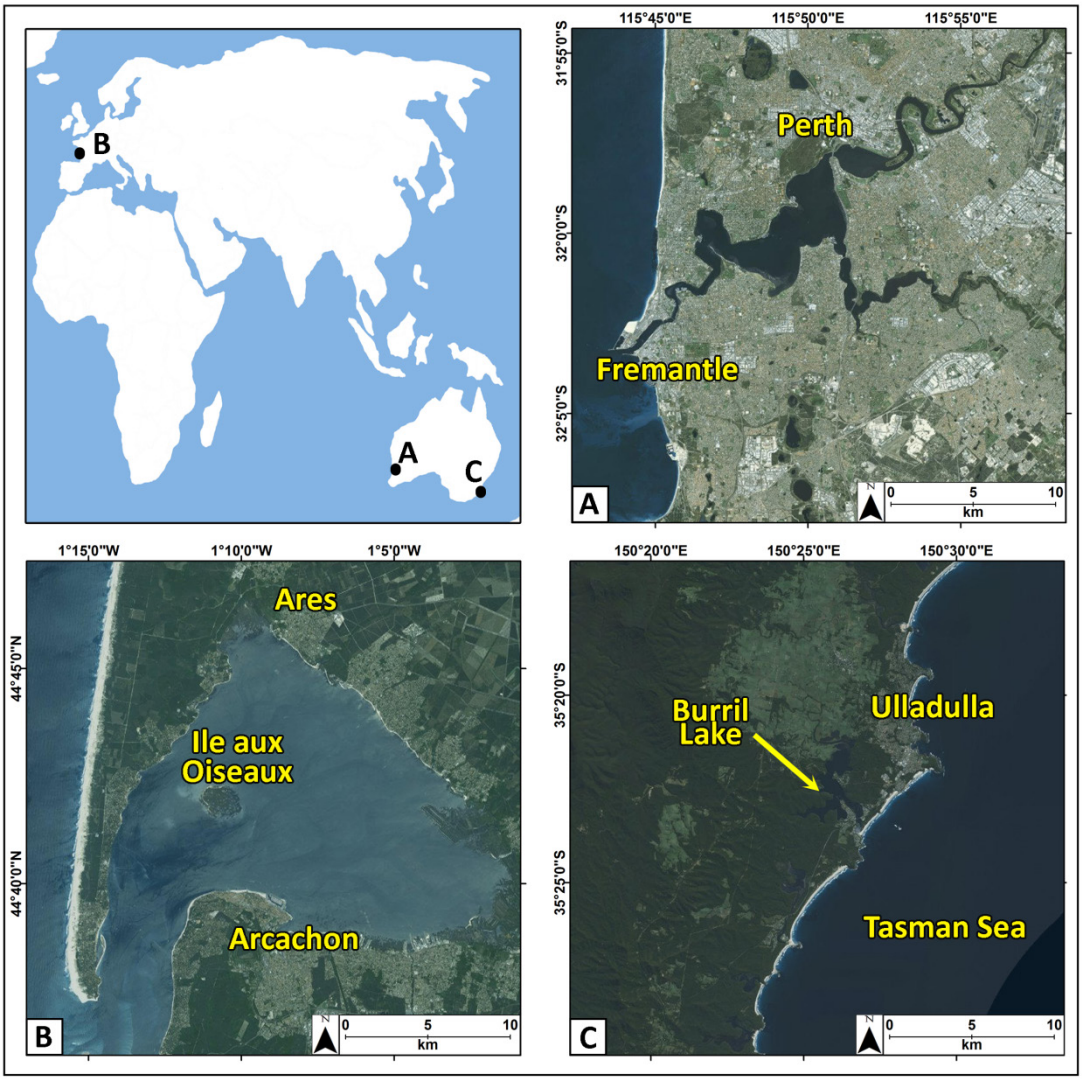


**Figure 4.8. Wave-dominated estuaries of B) Arcachon Lagoon (south western France) and C) Burril Lake (south eastern Australia) considered for a comparison with the A) Swan River. Note the three locations have been shown with the same scale in order to appreciate better their difference in shape and size, especially between B and C.**

## 7. Conclusions

This paper reports the results and new insight of the first environmental high-resolution seismic investigation in the middle reach of the Swan River estuary (Melville Waters). Three major acoustic reflectors and 4 seismic units can be recognised within the survey area, forming complex buried cut-and-fill systems (palaeochannels). Combining this data with terrestrial LiDAR data, pre-existing literature and sedimentological analysis, it has been possible to characterise the buried palaeochannels in terms of their seismic architecture, geomorphology and facies, providing a better understanding of the development and evolution of the estuary, as primarily driven by sea level rise and fall during the Late Pleistocene and Holocene. Relative ages of depositional episodes were determined from pre-existing literature and analysis of the sea level curve.

1) Pre-LIG (Mid–Late Pleistocene lowstand): the palaeo-Swan River flowed through a large valley (acoustic reflector R3), downcutting into the underlying

bedrock (acoustic basement), which comprises Tamala Limestone, to the western part of the survey area, and Kings Park Formation, to the east.

2) LIG to LGM: a rapid sea level rise (135-127 ky BP, sub-stage MIS-5e) marked the transition from riverine to estuarine setting, with a consequent increment of sediment deposition. The incised palaeovalley was infilled with tripartite deposits of Perth Formation (U3. From bottom to top: clay, silt and alluvial sand). Following the termination of the Last Interglacial highstands (127 to 80 ky, until MIS 5a), an orbitally driven reduction in global temperatures (Last Glacial period) caused a drop in sea level, during which the ancestral Swan River had another episode of downcutting. A narrow and deep palaeochannel incised the Perth Formation and the underlying bedrock (R2) and was successively infilled with estuarine and alluvial deposits of the Swan River Formation (U2), until the sea level reached its lowest position at -130 m below present (LGM), by 21 ky BP.

3) LGM to Holocene. During the Last Glacial Maximum, a further palaeochannel (Channel 2, R1) was cut. Through the following transgression, when the sea level was at least 30 m below the present level (~10 ky BP), deposition of Holocene sediments (U1) started to infill Channel 2, till reaching the present conditions and becoming an estuary.

Like several other examples around the world, for instance Burril Lake (NSW, Australia) and Arcachon Lagoon (Aquitaine, France), the geomorphic record of Late Pleistocene and Holocene sea-level fluctuations in the metropolitan area of the Swan River is characterised by a series of palaeochannels, which developed during glacial low sea level stands, and related channel-fill deposits which formed during interglacial highstands.

## Acknowledgments

The Swan River Trust and Dr Sue Osborne are thanked for approving the survey and providing the vessel support for marine operations; CMST researchers (Curtin University), in particular Chella Armstrong and Chandra Salgado Kent (Marine Mammal Observers), Iain Parnum and Malcolm Perry; Neil MacDonald (AAEngineering Ltd) and Western Advance for the equipment support; Moataz Kordi and Tubagus Solihuddin (Curtin University) during the seismic survey; Dario Vallini (Fremantle Port Authority), Brendan Wright (Golder Associates Pty Ltd) for allowing access to the previous survey results; Hery Setiawan (Department of Transport, WA) for providing bathymetric datasets; Giovanni De Vita for his technical advice.

This manuscript was considerably improved by comments from Catena editor Gert Verstraeten, Dr David Menier and two anonymous reviewers.

This research did not receive any specific grant from funding agencies in the public, commercial, or not-for-profit sectors.

## References

Allard, J., Chaumillon, E. and Féniès, H., 2009. A synthesis of morphological evolutions and Holocene stratigraphy of a wave-dominated estuary: The Arcachon lagoon, SW France. Continental Shelf Research, 29(8), pp.957-969.

Anderson, J.B., Wallace, D.J., Simms, A.R., Rodriguez, A.B. and Milliken, K.T., 2014. Variable response of coastal environments of the northwestern Gulf of Mexico to sea-level rise and climate change: Implications for future change. Marine Geology, 352, pp.348-366.

Atkinson, R.P., Klemm, V.V., 1987. The effects of discharges, effluents and urbanisation of the Swan River, in Jacob, J., (Ed.), The Swan River estuary ecology and management. Curtin University of Technology, Bentley, pp.296-313.

Australian Hydrographic Services (AHS), 1971. Western Australia Fremantle Harbour and approaches, Final report of survey, job no. h.325. Unpublished.

Baker, G.F.U., 1956. Some aspects of Quaternary sedimentation in the Perth Basin W.A. M.Sc Thesis University of Western Australia.

Baltzer, A., Tessier, B., Nouzé, H., Bates, R., Moore, C., Menier, D., 2005. Seistec seismic profiles: A tool to differentiate gas signatures. Mar. Geophys. Res. 26, 235–245. doi:10.1007/s11001-005-3721-x.

Bastian, L. V., 1996. Residual soil mineralogy and dune subdivision, Swan Coastal Plain, Western Australia. Aust. J. Earth Sci. 43, 31–44. doi:10.1080/08120099608728233.

Berger, W.H., 2008. Sea level in the Late Quaternary: Patterns of variation and implications. Int. J. Earth Sci. 97, 1143–1150. doi:10.1007/s00531-008-0343-y.

Blanco, G.F., Rodríguez, G.F., González, L.A.P. and Abanades, J., 2015. Morphodynamics, sedimentary and anthropogenic influences in the San Vicente de la Barquera estuary (North coast of Spain). Geologica acta, 13(4), pp.279-295.

Blum, M.D., Tornqvist, T.E., 2000. Fluvial responses to climate and sea-level change: a review and look forward. Sedimentology 47, 2–48. doi:10.1046/j.1365-3091.2000.00008.x.

Blum, M., Martin, J., Milliken, K. and Garvin, M., 2013. Paleovalley systems: insights from Quaternary analogs and experiments. Earth-Science Reviews, 116, pp.128-169.

Bourman, R.P., Murray-Wallace, C.V., Belperio, A.P. and Harvey, N., 2000. Rapid coastal geomorphic change in the River Murray Estuary of Australia. Marine Geology, 170(1), pp.141-168.

Brooke, B.P., Olley, J.M., Pietsch, T., Playford, P.E., Haines, P.W., Murray-Wallace, C. V., Woodroffe, C.D., 2014. Chronology of Quaternary coastal aeolianite deposition and the drowned shorelines of southwestern Western Australia - a reappraisal. Quat. Sci. Rev. 93, 106–124. doi:10.1016/j.quascirev.2014.04.007.

Bufarale, G. and Collins, L.B., 2015. Stratigraphic architecture and evolution of a barrier seagrass bank in the mid-late Holocene, Shark Bay, Australia. Marine Geology, 359, pp.1-21.

Castel, J., Caumette, P. and Herbert, R., 1996. Eutrophication gradients in coastal lagoons as exemplified by the Bassin d'Arcachon and the Étang du Prévost. Hydrobiologia, 329(1-3), pp.ix-xxviii.

Chalmer, P.N., Hodgkin, E.P., Kendrick, G.W., 1976. Benthic faunal changes in a seasonal estuary of south-western Australia. Rec. West. Aust. Mus. 4, 383–410.

Chappell, J., Shackleton, N.J., 1986. Oxygen isotopes and sea level. Nature 324, 137–140.

Churchill, D.M.,1959. Late Quaternary Eustatic Changes in the Swan River District. Royal Society of Western Australia, 42(2): 53-55.

Chaumillon, E., Tessier, B., Reynaud, J-Y., 2010. Stratigraphic records and variability of incised valleys and estuaries along French coasts 75–85.

Coffey Geosciences, 2002. Perth Urban Rail Development South West Metropolitan Railway Geotechnical Desk Study. Unpublished.

Coffey Geosciences, 2010. Perth Flying Squadron Yacht Club Geotechnical Desk Study. Unpublished.

Collins, L.B.,1987. Geological evolution of the Swan-Canning estuarine system, in Jacob, J., (Ed.), The Swan River estuary ecology and management. Curtin University of Technology, Bentley, pp. 9-20.

Commander, P., 2003. Outline of the geology of the Perth region. Aust. Geomech. 38, 7–16.

Davidson, W. A., 1995. Hydrogeology and groundwater resources of the Perth Region, Western Australia: Western Australia Geological Survey, Bulletin 142.

Dalrymple, R.W., Zaitlin, B.A. and Boyd, R., 1992. Estuarine facies models: conceptual basis and stratigraphic implications: perspective. Journal of Sedimentary Research, 62(6).

Dalrymple, R.W., Choi, K., 2007. Morphologic and facies trends through the fluvial – marine transition in tide-dominated depositional systems : A schematic framework for environmental and sequence-stratigraphic interpretation 81, 135–174. doi:10.1016/j.earscirev.2006.10.002.

Eliot, M.J., Travers, A., Eliot, I., 2006. Morphology of a Low-Energy Beach, Como Beach, Western Australia. J. Coast. Res. 221, 63–77. doi:10.2112/05A-0006.1.

Evans, K.G., Stephens, A.W., Shorten, G.G., 1992. Quaternary sequence stratigraphy of the Brisbane River delta, Moreton Bay, Australia. Mar. Geol. 107, 61–79. doi:10.1016/0025-3227(92)90069-T.

Golder Associated Pty Ltd, 2008. Geotechnical investigation, Perth Waterfront Project, Perth Foreshore. Western Australia. Unpublished.

Golder Associated Pty Ltd, 2012. Interpretive Report, Phase 2 Geotechnical Studies, Perth Waterfront Development, Western Australia. Unpublished.

Gordon, F.R., 2003a. Sea level change and paleochannels in the Perth area. Aust. Geomech. 38, 85–90.

Gordon, F.R., 2003b. Coastal Limestones. Aust. Geomech. 38, 7–24.

Gordon, F.R., 2012. Geology of quaternary coastal limestones of Western Australia. Thesis (Ph.D.), Curtin University.

Gozzard, J.R., 2007a. A reinterpretation of the Guildford Formation. Australian Geomechanics, 42(3).

Gozzard, J.R., 2007b. Geology and landforms of the Perth region. Geological Survey of Western Australia, p126.

Hamilton, D.P., Chan, T., Robb, M.S., Pattiaratchi, C.B. and Herzfeld, M., 2001. The hydrology of the upper Swan River Estuary with focus on an artificial destratification trial. Hydrological Processes, 15(13), pp.2465-2580.

Hearty, P.J., 2003. Stratigraphy and timing of eolianite deposition on Rottnest Island, Western Australia. Quat. Res. 60, 211–222. doi:10.1016/S0033-5894(03)00063-2.

Hearty, P.J., Hollin, J.T., Neumann, A.C., O'Leary, M.J., McCulloch, M., 2007. Global sea-level fluctuations during the Last Interglaciation (MIS 5e). Quat. Sci. Rev. 26, 2090–2112. doi:10.1016/j.quascirev.2007.06.019.

Hill, P.J., De Deckker†, P., von der Borch, C., Murray-Wallace, C. V., 2009. Ancestral Murray River on the Lacepede Shelf, southern Australia: Late Quaternary migrations of a major river outlet and strandline development. Aust. J. Earth Sci. 56, 135–157. doi:10.1080/08120090802546993.

Hillman, K., McComb, A.J. and Walker, D.I., 1995. The distribution, biomass and primary production of the seagrass Halophila ovalis in the Swan/Canning Estuary, Western Australia. Aquatic Botany, 51(1), pp.1-54.

Hodgkin, E.P., Hesp P., 1998. Estuaries to salt lakes: Holocene transformation of the estuarine ecosystems of south-western Australia. Marine and Freshwater Research 49(3): 183–201.

Hori, K., Tanabe, S., Saito, Y., Haruyama, S., Nguyen, V. and Kitamura, A., 2004. Delta initiation and Holocene sea-level change: example from the Song Hong (Red River) delta, Vietnam. Sedimentary Geology, 164(3), pp.237-249.

Hudson-Smith, E., Grinceri, M., 2007. Ground conditions and building protection for the New MetroRail City Project, Perth. Aust. Geomech. 42, 33–58.

Jones, P.H., Marsh, J.G., 1965. Some problems in the construction of embankments for the Mitchell Freeway, Perth W.A. Institution of Engineers Australia Journal Vol. CE 7 No. 2.

Kendrick, G.W., Wyrwoll, K.-H., Szabo, B.J., 1991. Pliocene–Pleistocene coastal events and history along the western margin of Australia. Quaternary Sci. Rev., 10(5), pp. 419–439.

Kennewell, C., Shaw, B.J., 2008. Perth, Western Australia. Cities 25, 243–255. doi:10.1016/j.cities.2008.01.002.

Klingebiel, A. and Gayet, J., 1995. Fluvio-lagoonal sedimentary sequences in Leyre delta and Arcachon bay, and Holocene sea level variations, along the Aquitaine coast (France). Quaternary International, 29, pp.111-117.

Lambeck, K. and Nakada, M., 1990. Late Pleistocene and Holocene sea-level change along the Australian coast. Palaeogeogr. Palaeoclimatol. Palaeoecol. 89, 143–176.

Lambeck, K. and Chappell, J., 2001. Sea level change through the last glacial cycle. Science, 292(5517), pp.679-686.

Lambeck, K., Esat, T.M., Potter, E.-K., 2002. Links between climate and sea levels for the past three million years. Nature 419, 199–206. doi:10.1038/nature01089.

Lambeck, K., Rouby, H., Purcell, A., Sun, Y., Sambridge, M., 2014. Sea level and global ice volumes from the Last Glacial Maximum to the Holocene. Proc. Natl. Acad. Sci. U. S. A. 111, 15296–303. doi:10.1073/pnas.1411762111.

Leorri, E. and Cearreta, A., 2004. Holocene environmental development of the Bilbao estuary, northern Spain: sequence stratigraphy and foraminiferal interpretation. Marine Micropaleontology, 51(1), pp.75-94.

Lisiecki, L.E., Raymo, M.E., 2005. A Pliocene-Pleistocene stack of 57 globally distributed benthic δ18O records. Paleoceanography 20, 1–17. doi:10.1029/2004PA001071.

Main Roads Western Australia (MRWA), 1998. Narrows Bridge widening project report on survey of existing documents possibly relevant to foundation conditions. Unpublished.

Mathew, G.V., 2010. Analysis and interpretation of ground and building movements due to EPB tunnelling. PhD Thesis, University of Western Australia.

Mccomb, K.H.A.J., Walker, D.I., 1995. Aquatic botany The distribution , biomass and primary production of the seagrass Halophila ovalis in the Swan / Canning Estuary, Western Australia 51, 1–54.

McKimmie Jamieson & Partners (Aust) Pty Ltd, 1987. Fremantle Port Authority Geophysical investigation. Unpublished.

Menier, D., Tessier, B., Dubois, A., Goubert, E. and Sedrati, M., 2011. Geomorphological and hydrodynamic forcing of sedimentary bedforms-Example of Gulf of Morbihan (South Brittany, Bay of Biscay). Journal of Coastal Research, (64), p.1530.

Murray-Wallace, C. V., Kimber, R.W.L., 1989. Quaternary marine aminostratigraphy: Perth Basin, Western Australia. Aust. J. Earth Sci. 36, 553–568. doi:10.1080/08120098908729509.

O'Leary, M.J., Hearty, P.J., McCulloch, M.T., 2008. Geomorphic evidence of major sea-level fluctuations during marine isotope substage-5e, Cape Cuvier, Western Australia. Geomorphology 102, 595–602. doi:10.1016/j.geomorph.2008.06.004.

Ove Arup, 2001. Geotechnical Perth Convention Centre Desk Study Report to Multiplex Constructions Pty. Ltd. Unpublished.

Playford, P.E., Cockbain, A.E. and Low, G.H. 1976. Geology of the Perth Basin Western Australia, Geol. Soc. West. Austr., Bulletin 124.

Playford, P.E., 1977. Part 1, Geology and groundwater potential, in: Playford, P.E., Leech, R.E.J., (Eds.), Geology and Hydrology of Rottnest Island. Geol. Surv. West. Aust., 6: 1-53.

Quilty, P., 1974. Tertiary stratigraphy of Western Australia. J. Geol. Soc. Aust. 21, 37–41. doi:10.1080/00167617408728853.

Quilty, P.G., Hosie, G., 2006. Modern Foraminifera, Swan River Estuary, Western Australia: Distribution and Controlling Factors. J. Foraminifer. Res. 36, 291–314. doi:10.2113/gsjfr.36.4.291.

Rehman, S.U. and Saleem, K., 2013. Forecasting scheme for swan coastal river streamflow using combined model of IOHLN and Niño 4. Asia-Pacific J. Atmos. Sci. 50, 1–9. doi:10.1007/s13143-014-0009-61.

Roe, G.H., Stolar, D.B. and Willett, S.D., 2006. Response of a steady-state critical wedge orogen to changes in climate and tectonic forcing. Geological Society of America Special Papers, 398, pp.227-239.

Saqab, M.M., Bourget, J., 2015. Controls on the distribution and growth of isolated carbonate build-ups in the Timor Sea (NW Australia) during the Quaternary. Mar. Pet. Geol. 62, 123–143. doi:10.1016/j.marpetgeo.2015.01.014.

Schumm, S.A., 1993. River response to baselevel change: implications for sequence stratigraphy. The Journal of Geology, pp.279-294.

Sloss, C.R., Jones, B.G., McClennen, C.E., de Carli, J. and Price, D.M., 2006. The geomorphological evolution of a wave-dominated barrier estuary: Burrill Lake, New South Wales, Australia. Sedimentary Geology, 187(3), pp.229-249.

Smith, A.J., Massuel, S., Pollock, D.W., 2012. Geohydrology of the Tamala Limestone Formation in the Perth Region: Origin and Role of Secondary Porosity. CSIRO: Water for a Healthy Country National Research Flagship, 63 pp.

Stephens, R. and Imberger, J., 1996. Dynamics of the Swan River Estuary: The seasonal variability. Mar. Freshw. Res. 47, 517. doi:10.1071/MF9960517.

Stephens, R. and Imberger, J., 1997. Intertidal motions within deep basin of Swan River estuary. Journal of Hydraulic Engineering, 123(10), pp.863-873.

Stirling, C.H., Esat, T.M., Mcculloch, M.T., Lambeck, K., 1995. High-precision U-series dating of corals from Western Australia and implications for the timing and duration gradients in the North Atlantic Ocean (321 to 721N) during the Last Interglacial period. Paleoceanography 14, 23–33. doi:10.1016/0012-821X(95)00152-3.

Radke, L.C., Prosser, I.P., Robb, M., Brooke, B., Fredericks, D., Douglas, G.B. and Skemstad, J., 2004. The relationship between sediment and water quality, and riverine sediment loads in the wave-dominated estuaries of south-west Western Australia. Marine and Freshwater Research, 55(6), pp.581-596.

Tamura, T., Saito, Y., Sieng, S., Ben, B., Kong, M., Sim, I., Choup, S., Akiba, F., 2009. Initiation of the Mekong River delta at 8 ka : evidence from the sedimentary succession in the Cambodian lowland. Quat. Sci. Rev. 28, 327–344. doi:10.1016/j.quascirev.2008.10.010

Tanabe, S., Nakanishi, T., Ishihara, Y. and Nakashima, R., 2015. Millennial-scale stratigraphy of a tide-dominated incised valley during the last 14 kyr: Spatial and quantitative reconstruction in the Tokyo Lowland, central Japan. Sedimentology, 62(7), pp.1837-1872.

Tutton, M., 2003. Engineering geology of Fremantle harbour. Australian Geomechanics, 38(4), pp.91-102.

Viney, N.R. and Sivapalan, M., 2001. Modelling catchment processes in the Swan–Avon river basin. Hydrological Processes, 15(13), pp.2671-2685.Vinnicombe, P., 1992. An Aboriginal site complex at the foot of Mount Eliza which includes the old Swan Brewery building. Historic Environment, 9(1/2), p.53.

Woodroffe, C.D., Webster, J.M., 2014. Coral reefs and sea-level change. Mar. Geol. 352, 248–267. doi:10.1016/j.margeo.2013.12.006

# Chapter 5

# Geographe Bay

"Look deep into nature, and then you will
understand everything better"
(Albert Einstein)

## Sea level controls on the geomorphic evolution of Geographe Bay, South-West Australia.

Giada Bufarale[1], Michael J. O'Leary[2], Julien Bourget[3]

1 Department of Applied Geology, Curtin University, GPO Box U1987, Perth, WA 6845, Australia

2 Department of Environment and Agriculture, Curtin University, Bentley, Western Australia, 6102

3 Centre for Energy Geoscience, School of Earth Sciences, University of Western Australia, Crawley, Western Australia 6009, Australia

## Abstract

High-resolution shallow seismic profiles collected along the inner shelf in Geographe Bay (south-west Australia) exposed a highly-variable buried architecture. Three main acoustic units, separated by unconformities, correspond to different geological facies, deposited under various sea level conditions. The acoustic basement (Unit B) belongs to the Early Cretaceous Leederville Formation; the middle unit is attributable to Tamala Limestone (Unit P, Late-Mid Pleistocene) and the top unit (Unit H) is Holocene in age. Combining the seismic data with high-resolution bathymetry and sediment grabs, several surficial and buried morphological features are revealed, including sandbars, palaeochannels and ridges.

The shore-oblique sandbars have been directly influenced by local hydrodynamics including mean wave direction and currents, seagrass and sediment size. The palaeochannels (buried and surficial) are the expression of previous sea level lowstands. Two sets of shore-parallel, low-relief ridges, located at a depth of ~7 m and ~20 m, are relict landforms that are most likely regressive beach ridges and sub-littoral deposits (paleo-dunes), belonging to Tamala Limestone. These geomorphological structures were formed during Late Pleistocene relatively high sea level stages (late Marine Isotope Stage 5e and 5c, respectively), cemented when the sea level was lower and subsequently subject to transgressive erosion.

The newly acquired seismic datasets showed that the inner shelf is mainly covered by a thin veneer of sediments, above the Pleistocene hard surface, with the exclusion of the sandbars, where the sediment build-up can be up to 6 m in thickness. This information is extremely valuable to estimate the sedimentary resources in Geographe Bay.

## 1. Introduction

Geographe Bay is located between Cape Naturaliste and the city of Bunbury, in the south-western corner of Western Australia (WA) and, like much of the WA coastline, lacks major fluvial sediment input and is considered sediment starved (McMahon and Finlayson, 2003; Brooke et al., 2017). Consequently, much of the sediment available for shoreline nourishment is sourced by the remobilisation of relict siliciclastic sediments deposited on the inner shelf during sea level lowstands, and from carbonate organisms, such as coralline algae, molluscs, foraminifera, bryozoans which are produced in and around the extensive seagrass banks that characterise Geographe Bay (James and Bones, 2010; Brooke et al., 2014). These relict siliciclastic grains, currently located on the inner shelf can be considered a finite resource with the volume of sediment available for transport onshore currently limited by wave energy, water depth and grain size (Whitehouse, 2007). Carbonate grains on the other hand are continually being produced and can potentially provide a sediment resource for coastal nourishment. However, the supply of carbonate sediments to the coast is limited by the rates of carbonate production which can be influenced by changing environmental parameters such as sea surface temperature, nutrient availability, and habitat change (James and Bone, 2010), as well as hydrodynamic processes.

The Geographe Bay coastline is backed by a series of low relief coastal aeolianites and dunes (Brooke et al., 2014), with sections of the coast presently experiencing coastal erosion, the cause of which is still poorly understood (Geographe Catchment Council, 2008; Barr and Eliot, 2011, Barr et al., 2017). Thus there is a need to better characterise the offshore sediment resources as a potential reservoir of high-quality sand for coastal nourishment and shoreline restoration, particularly in a context of the coastal response of a sediment-starved coast under rising sea levels and changing wave climates.

The aim of this study was to better understand local coastal evolution, the sediment resource potential of Geographe Bay, and the influence that geomorphology, hydrodynamics and habitat have on sediment mobility and onshore transport. During this study, an integrated approach was adopted, combining high-resolution bathymetry, sedimentological analysis, hydrodynamic data and high-resolution reflection seismic images, conducted between Busselton and Port Geographe (Geographe Bay, Rottnest Shelf, south-west Western Australia).

## 2. Regional settings

### 2.1. Coastal physiography

Geographe Bay is a 90 km long, J-shaped bay with a WNW aspect in the north and NW through to NE aspect in the south (Figure 5.1). The nearshore bathymetry is relatively simple with a shallow dipping seabed reaching 30 m depth, about 15 km from the coast. However, the south westernmost section between Dunsborough and Cape Naturaliste is characterised by fairly steep nearshore bathymetry with water depths reaching 40 m within 1 km of the coast (Figure 5.1).

The region is characterised by a Mediterranean climate, warm and dry between November and March (summer) and cool and wet in winter (Bureau of Meteorology - Australia, 2011). There is only one permanent river (Capel River) that discharges directly into the ocean, the other waterways are ephemeral or seasonal and flow mainly into drains (White and Comer, 1999. Figure 5.1). Extensive seagrass meadows (*Posidonia sinuosa* and *Amphibolis antarctica*) represent the major benthic habitat within the Bay, covering more than 90% of the seabed between 0 m and 10 m below sea level (Van Niel et al., 2009). The seagrass coverage decreases progressively northward and with depth, down to 30 m below sea level (BSL. Oldham et al., 2010).

Geographe Bay, like in the rest of south-western Australia, experiences a diurnal microtidal regime with a spring tidal amplitude on the order of 0.6 m (CSIRO, 2015). Winds are mainly seasonal: the summer period is dominated by a relatively light to moderate S to SW offshore sea breezes (up to 15 m/s, in the afternoon) while strong W to NW winds (up to 25 – 30 m/s) associated with cold fronts occur periodically during the winter months (Fahrner and Pattiaratchi, 1994; Oldham et al., 2010). The wave regime is mainly dominated by the seasonal winds, with waves typically reaching heights of up to 2 m in winter and less than 1 m in summer (near the shoreline. Fahrner and Pattiaratchi, 1994; Oldham et al., 2010). The surface waves are also influenced by oceanic SW swell, with Cape Naturaliste refracting the waves

into Geographe Bay, protecting the coast from the prevailing long period ground swell (Fahrner and Pattiaratchi, 1994; Oldham et al., 2010).

Coastal currents and water circulation patterns are mainly induced by wind-driven effects, including storm waves, sea breezes, Coriolis force and local bathymetry (Fahrner and Pattiaratchi, 1994; Oldham et al., 2010). These metocean processes generate eastward to north-eastward longshore currents that influence sediment transport, control the seafloor sediment characteristics and are ultimately reflected in the sedimentary record (Paul and Searle, 1978; Hamilton and Collins, 1997; Oldham et al., 2010).

The seagrass meadows also have a significant role in the overall hydrodynamic conditions of the Bay, attenuating wave and current energy and sediment particle transport (McMahon et al., 1997; Oldham et al., 2010).

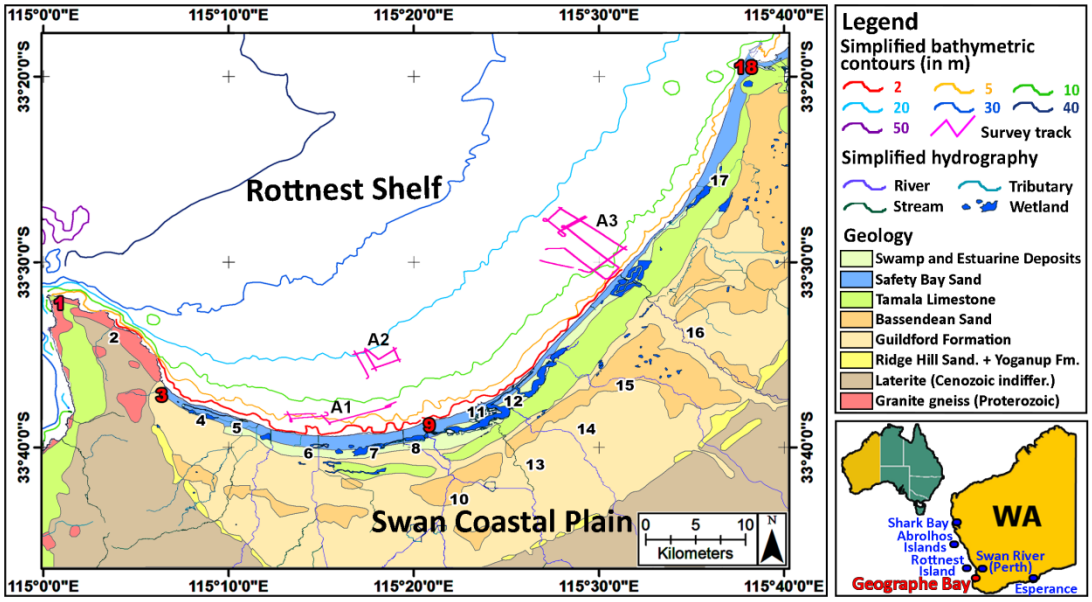


**Figure 5.1. Geographe Bay map showing simplified surface geology (redrawn after Playford at al. 1976), localities (red labels) and bodies of water (black labels). 1 Cape Naturalist, 2 Jingarmup Creek, 3 Dunsborough, 4 Toby Inlet, 5 Toby drain, 6 t, 7 New River, 8 Vasse-Diversion drain, 9 Busselton and Busselton Jetty, 10 Vasse River, 11 Port Geographe Marina, 12 Vasse-Wonnerup Estuary, 13 Sabina River, 14 Abba River, 15 Lundlow River, 16 Capel River, 17 Mile Brook diversion, 18 Point Casuarina (Bunbury). A1, A2 and A3 are the seismic survey locations. Geophysical survey track plot are also marked. Hydrography: Linear (Hierarchy) (DOW-029) (29-10-2008 12:18:04) from Shared Location Information Platform (SLIP) (WMS Server: https://www2.landgate.wa.gov.au/ows/wmspublic?; Service Name: SLIP Public Web Map Service (ISO 19115 Categories)). Simplified bathymetric contours are shown (source: Department of Transport).**

## 2.2. Coastal Geology and Geomorphology

Geographe Bay is located along the SW Australian continental shelf margin (Fairbridge, 1961; Baker et al., 2005), and situated within the southern Perth Basin, a Phanerozoic, intensely faulted half-graben, infilled with a 15 km thick sedimentary sequence of Palaeozoic to Early Cretaceous clastics, and Early Cretaceous to Holocene carbonates (Collins and Baxter, 1984). The area has been relatively tectonically stable since the Mid-Pleistocene (Playford et al. 1976, Szabo, 1979; Kendrick et al., 1991; Stirling et al., 1995; Baker et al., 2005; Brooke et al., 2014).

The Early Cretaceous *Leederville Formation*, which consists of fine- to medium-grained quartz sandstone, interbedded with shale, is believed to be mainly non-marine, with occasional marine or shallow near-shore marine horizons (Playford et al., 1976; Deeney, 1989; Hirschberg, 1989; Schafer et al., 2008). This formation is unconformably overlaid by Quaternary superficial formations, predominantly sand and limestone in the west, and lacustrine clays in the east (Deeney, 1989; Hirschberg, 1989). The superficial deposits, collectively known as the Kwinana Group form the Swan Coastal Plain, a narrow strip (10–15 km wide) of reworked Quaternary sediments that comprise shallow marine and littoral deposits and associated fossil aeolian dunes that run sub-parallel to the coastline (Collins, 1988; Commander, 2003). Fluvial, alluvial and lacustrine deposits are also present (Playford et al., 1976; Hirschberg, 1989). This shoreline succession becomes progressively youner and decreases in elevation westward and comprises the Early Pleistocene Ridge Hill Shelf (*Ridge Hill Sandstone*), the Middle Pleistocene Yoganup Shoreline deposits (*Yoganup Formation*), the Bassendean, Spearwood and Quindalup Dune Systems, respectively *Bassendean Sand*, aeolian limestone and yellow sand of *Tamala Limestone* (both Middle to Late Pleistocene in age) and Holocene marine and aeolian parabolic dunes and sands of *Safety Bay Sand*, all described by Playford at al. (1976) and Commander (2003. Figure 5.1).

The *Rottnest Shelf,* defined by Carrigy and Fairbridge (1954), forms the marine equivalent of the Swan Coastal Plain and can be subdivided into three main bathymetric provinces: the *Inner Shelf*, which extends from 0 to 100 m in depth, where submerged terraces and ridges formed during past periods of low sea level are observed (Figure 5.1), the *Outer Shelf* that ends with the shelf-slope break at 170 m, and the *Upper Continental Slope* (Collins, 1988). Traces of subaerial erosion are recognisable in remnant subaqueous features such as reefs, shore-parallel ridges and barrier dune systems (Collins, 1988; Playford, 1997; Brooke et al., 2010).

# 3. Methods

## 3.1. Seafloor mapping

In 2016, the Department of Transport (DoT, WA) acquired and processed bathymetric datasets, during multiple LiDAR (Light Detection and Ranging), multibeam and Laser surveys (Coastal Information, DoT, 2016). The high-resolution data have a horizontal sounding density of 5 m x 5 m and cover the nearshore seafloor up to about 30 m of water depth (Coastal Information, DoT, 2016).

During this study, a map of the main seafloor features was produced through a visual interpretation of the bathymetry, using ESRI's ArcGIS Desktop 10.5. The geomorphological features were manually outlined at a 1:10,000 scale and include sandbars, palaeochannels and ridges.

The morphological information was used to determine the areas within the Bay to carry out the following seismic survey, based on different characteristics of the seafloor.

Three distinct areas were selected for detailed seismic investigation and sediment sampling (Figure 5.1):

- Area 1 (A1), located in the westernmost portion of the investigation area, is characterised by a high concentration of sandbars, oblique to the shoreline.
- Area 2 (A2), situated 6 km seaward from the Busselton Jetty, has numerous deep-water (~20 m) ridges and palaeochannels.
- Area 3 (A3), located in front of the Capel River mouth, is distinguished by several shallow-water (<10 m) ridges and palaeochannels.

## 3.2. High-resolution shallow seismic data acquisition

A total of 71 km of high-resolution reflection seismic profiles were acquired, between the mouths of Buayanup drain and Capel River (A1, A2 and A3. Figure 5.1). The main track orientations were parallel and perpendicular to the coastline, to capture most elements of the sub-seafloor morphology. In A1, the seismic survey covered 16 km, mainly oriented NNE-SSW, from a water depth of 5 m to 10 m. A total of 15 km of seismic profiles were collected within A2, in relatively deep waters (~15-22 m). A3 comprises 40 km of seismic tracks, mainly orthogonal to the coastline, between ~8 and 22 m of water depth.

The seismic survey was undertaken using an Applied Acoustic Boomer System (Applied Acoustic Engineering Limited, Great Yarmouth, UK), comprising an energy source (CSP-P 300) and a sound source (AA201 boomer plate), mounted on a surface tow catamaran. An 8-element hydrophone streamer was employed as receiver. A GNSS (Global Navigation Satellite System) receiver Trimble NetR9 was interfaced to the acquisition workstation, broadcasting NMEA string to the geophysical software (SonarWiz 6 V6.01.0024, Chesapeake Technology Inc.). Data was digitally recorded in Seg-Y format, and a real time quality control (QC) was done during data collection.

SonarWiz 6 was also employed as post processing software. The first step of post processing was bottom tracking, which is used to digitise the seafloor reflector that represents the altitude of the receiver from the sea bottom (essentially the water depth). In the second step, standard signal processing procedures, such as application of an automatic gain correction algorithm (from tracked seabed downwards) and enhancing the contrast within the seismic profiles, were applied to improve the signal to noise ratio. In the final step, sub-bottom horizons were digitised with manual picking. The following stratigraphic interpretation was performed using pre-existing literature as no dating has been undertaken for this research. Based on the local geology and previous studies on speed of sound in sediments (see Whiteley and Stewart, 2008; Duncan et al., 2009; Duncan and Gavrilov, 2012), the depth below the seafloor and the sediment thickness values were converted from milliseconds to metres, using an estimated propagation velocity of 2000 m/s, with a margin of error of the order of ± 50 m/s, which translates as a vertical error of 0.5 m.

### 3.3. Sediment sampling and analysis

A pipe dredge was used to collect 17 unconsolidated surficial sediment samples along areas A1 (10 samples) and A2 (7 samples). Sampling location coordinates were recorded directly into SonarWiz 6, using the same positioning system used for the seismic survey.

The samples were dried and sieved using a mechanical shaker, over 63 μm, 125 μm, 250 μm, 500 μm, 1 mm and 2 mm, and examined using a stereoscopic light microscope (Leica EZ4). Analysis of the sediments included an evaluation of colour using the Munsell Soil Chart (Munsell, 1954), estimation of shape (roundness/sphericity of individual grains) and identification of the mineral and biogenic components.

## 4. Results

### 4.1. Shallow stratigraphy

The shallow seismic survey allowed the characterisation of the internal architecture of the sub-surface succession and identification of stratigraphic features, down to a depth of approximately 30-40 m below the seafloor. The sub-surface succession can be divided into three discrete seismic units (from bottom to top: B, P and H), bounded between two main acoustic reflectors (TB and TP, respectively. Figure 5.2). Two minor reflectors (TP1 and TP2) have been also detected along the survey area, within Unit P. Following, acoustic and geometrical characters of reflectors and units are described.

#### *4.1.1. Unit B*

TB (depicted in green, during the seismic interpretation. Figure 5.2) is the deepest reflector recognised in the study area, ranging between ~27 m BSL (below sea level) in A2 and ~47 m BSL in A3. Where detected, TB appears to be mostly relatively flat. In A2 and A3, where profiles orthogonal to the coastline are longer (between 2.5 and 6 km of length), TB is clearly seen deepening offshore, laying sub-parallel to the modern seafloor. In several coastal-parallel profiles, channel incisions are recognised. No other main seismic reflectors can be recognised below TB, for this reason, TB can be considered the top boundary of the acoustic basement (Unit B).

#### *4.1.2. Unit P*

Reflector TP (shown in orange. Figure 5.2) is well resolved in area A1 and in the profiles close to shore in A3. This horizon is undulated to irregular, with several depressions and incisions and marks the top of Unit P, which is bounded between TP and TB. The internal structure of Unit P varies across the survey area and ranges from chaotic or reflection-free, to poorly or moderately stratified. Two minor reflectors can be occasionally recognised within this unit (TP1 and TP2). TP1 is mostly recognisable near shore, especially in A3 (depicted in yellow in the seismic interpretation. Figure 5.2). This secondary reflector is generally flat, with occasional channel-like depressions, up to 250 m wide and 11 m deep. TP2 is mainly observable in A2 and A3 (highlighted in pink in the interpreted seismic profiles.

Figure 5.2) and, similarly to TP1, it appears relatively flat, with occasional depressions (up to 7 m deep. Figure 5.2C).

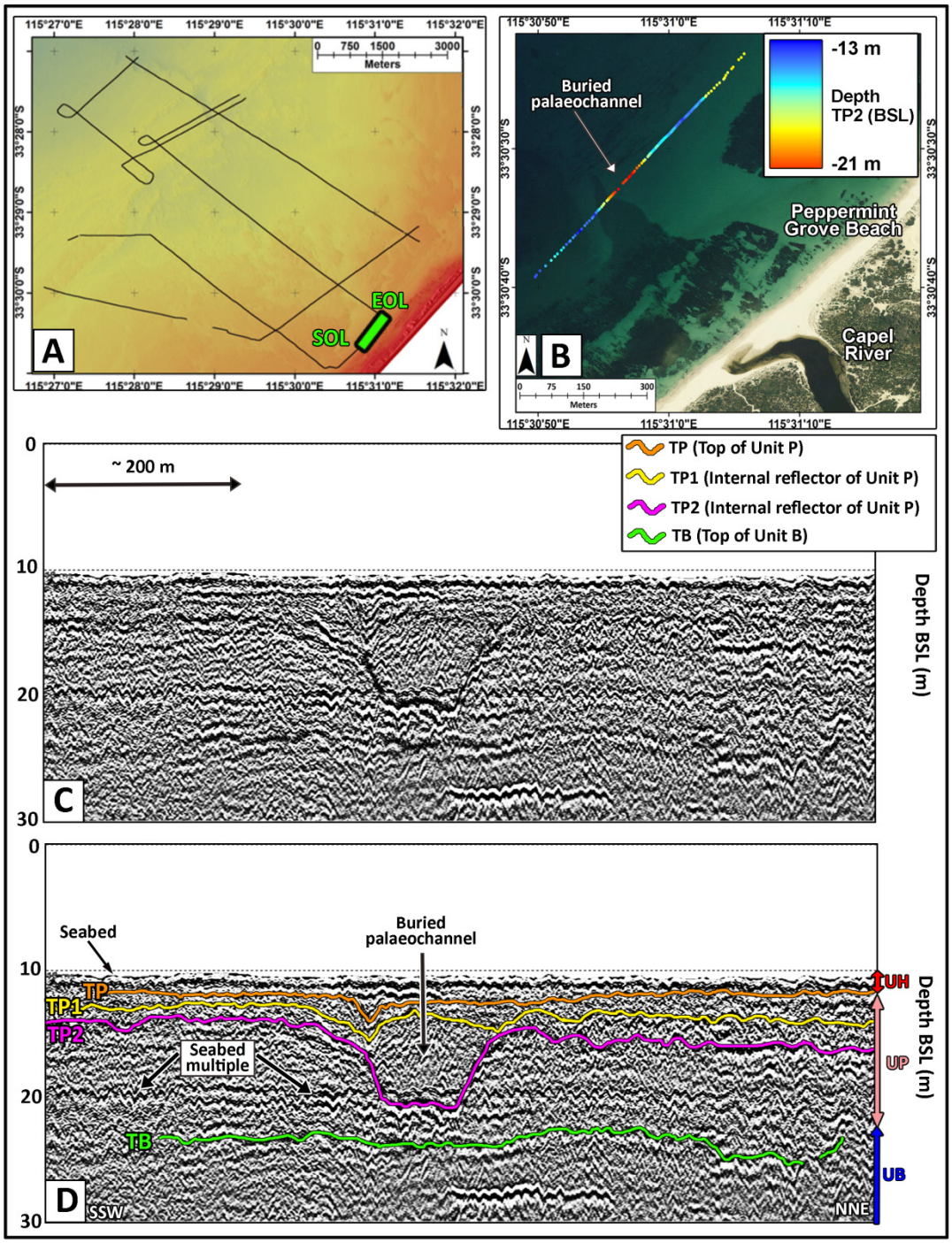


**Figure 5.2. Example of seismic profile, showing the two main seismic reflectors depicted in the survey area (TP and TB) and two secondary reflectors (TP1 and TP2). It is not possible to depict the base of Unit B underlying the acoustic reflector TB and, for this reason, it can be considered the acoustic basement of the survey area. A: Seismic tracks for Area 3. The location of the profile reported in C-D is highlighted in green (SOL: start of line, EOL: end of line). B: Ortophoto from SLIP (Shared Land Information Platform) Enabler portal, Landgate Imagery Bunbury 2031 Oct Nov 2010 Mosaic). The buried palaeochannel is clearly visible when plotting the depth of the reflector TP2 (from sea level). C-D: uninterpreted and interpreted seismic profile. Note the well-defined buried palaeochannel. The vertical axis corresponds to the depth BSL and the scale is in metres. The sound velocity in the sediments is equivalent to ~2000 m/s. The horizontal axis represents the distance covered by the vessel and the scale is in metres.**

### 4.1.3. Unit H

Unit H is bounded between the seafloor and the reflector TP. Where TP is detected, it is possible to calculate the thickness of this surficial unit, which ranges from less than 50 cm to a maximum of about 6 m, averaging between 1 and 3 m. A strong return signal of the seafloor, seabed multiples and local poor imaging mask this unit (and consequently the ability to detect the underlying horizons TP and TB). In addition, it is likely that in some areas, especially in the offshore profiles, Unit H is too thin to be detected with the equipment used (vertical resolution of the boomer is approximately 30 cm) or not present at all; these uncertainties made the interpretation of Unit H potentially ambiguous. Occasionally, parallel stratified reflections can be identified within Unit H.

## 4.2. Seabed features

High-resolution bathymetry highlighted three main geomorphic features that characterise the seabed morphology in Geographe Bay, these are sandbars, palaeochannels and ridges (Figure 5.3).

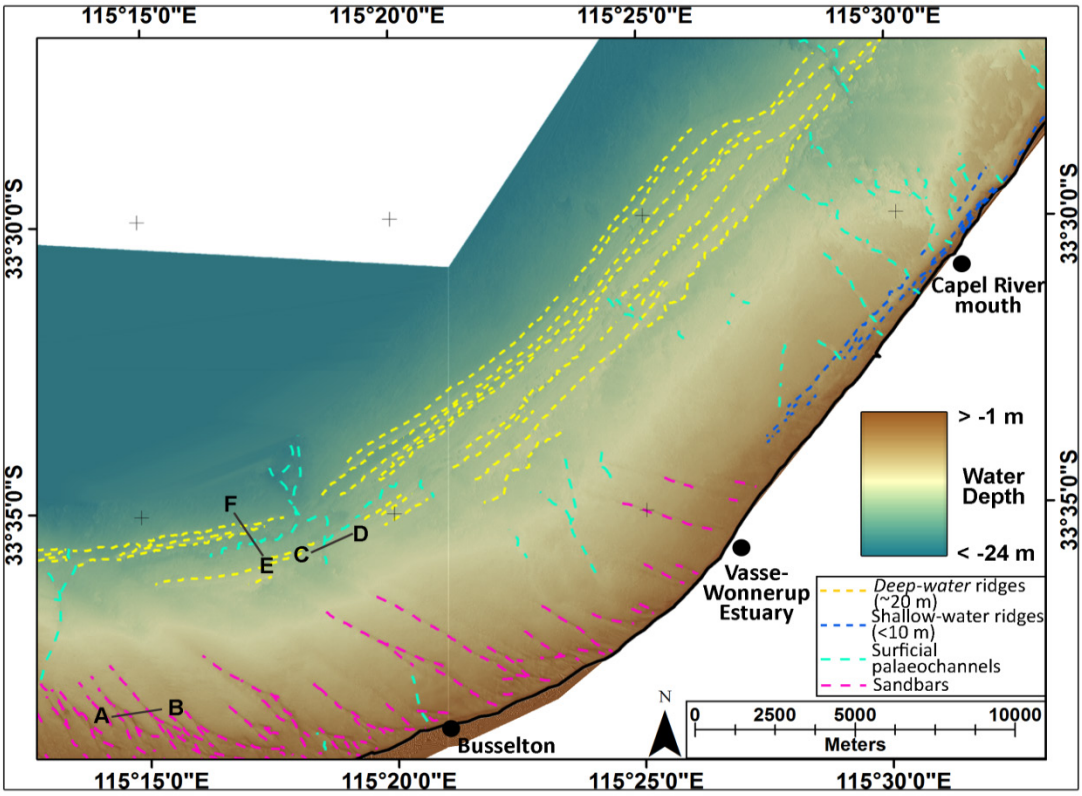


**Figure 5.3. Composite bathymetric data (from DoT) overlaid by seabed features. White areas: no data. Profile A-B: see Figure 5.4. Profile C-D: see Figure 5.5. Profile E-F: see Figure 5.6.**

### 4.2.1. Sandbars

The sandbars and associated swales are near-continuous linear features that extend obliquely (acute angle to the shoreline of 15-30 degrees) from nearshore, up to ~6 km seaward (between Geographe and West Busselton), to a depth of 10 m. They are mainly located in the south-western portion of the bay, with the easternmost sandbar lying in front of the northern tip of Vasse-Wonnerup Estuary (location 12 in Figure 5.1 and Figure 5.3). The distance between successive

sandbars increases in a north-easterly direction, ranging from about 250 m to more than 1.5 km. These sandbars greatly vary in size, ranging between about 100 to 300 m in width, with a relief above the seabed of up to ~3 m, thinning seaward. They are generally asymmetrical, with an almost bare stoss flank and a vegetated lee side (Figure 5.4).

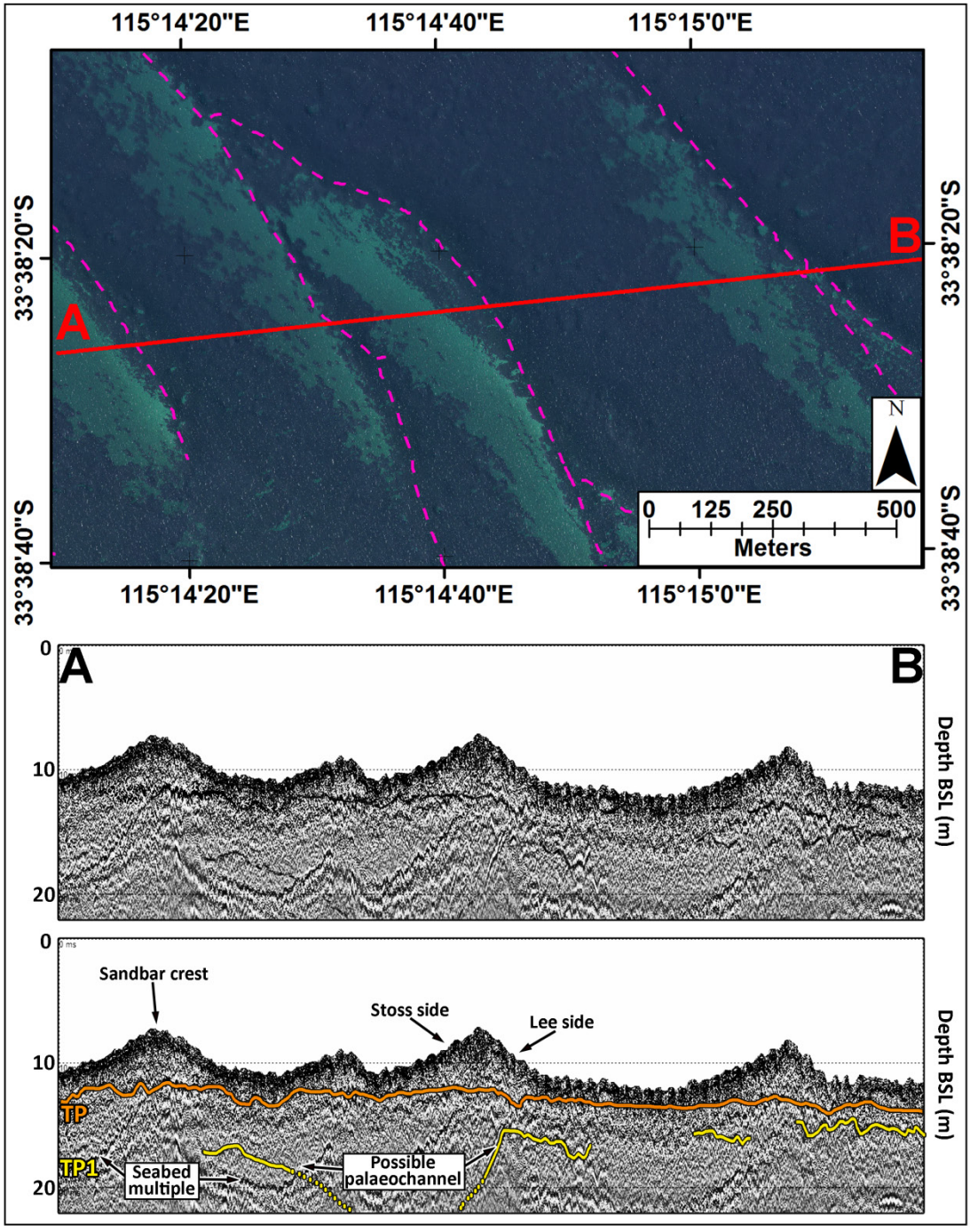


**Figure 5.4. Profile A-B: sandbars, for location refer to Figure 5.3. Length: ~1755 m. Top: orthophoto from SLIP Enabler portal (Landgate Imagery). Darker colours represent areas covered with seagrass meadow. Pink dash line depicts the crest of the sandbars. Bottom: uninterpreted and interpreted seismic profile showing the buried architecture below the sandbars. The reflector TP is almost flat; conversely, reflector TP1 is irregular with a possible palaeochannel, marked with dash line. Refer to Section 4.1 for more information about these reflectors.**

### 4.2.2. Palaeochannels

The high-resolution bathymetric and seismic images revealed the presence of several buried and surficial palaeochannels, assembled predominantly around Area 1 and Area 3, respectively (see surficial palaeochannels marked in light blue in Figure 5.3 and Figure 5.5). The surficial features have a variable length, from a few hundred metres to ~6 km, and are generally perpendicular to the coastline and quite shallow, with an average depth ~1 m below the surrounding seabed.

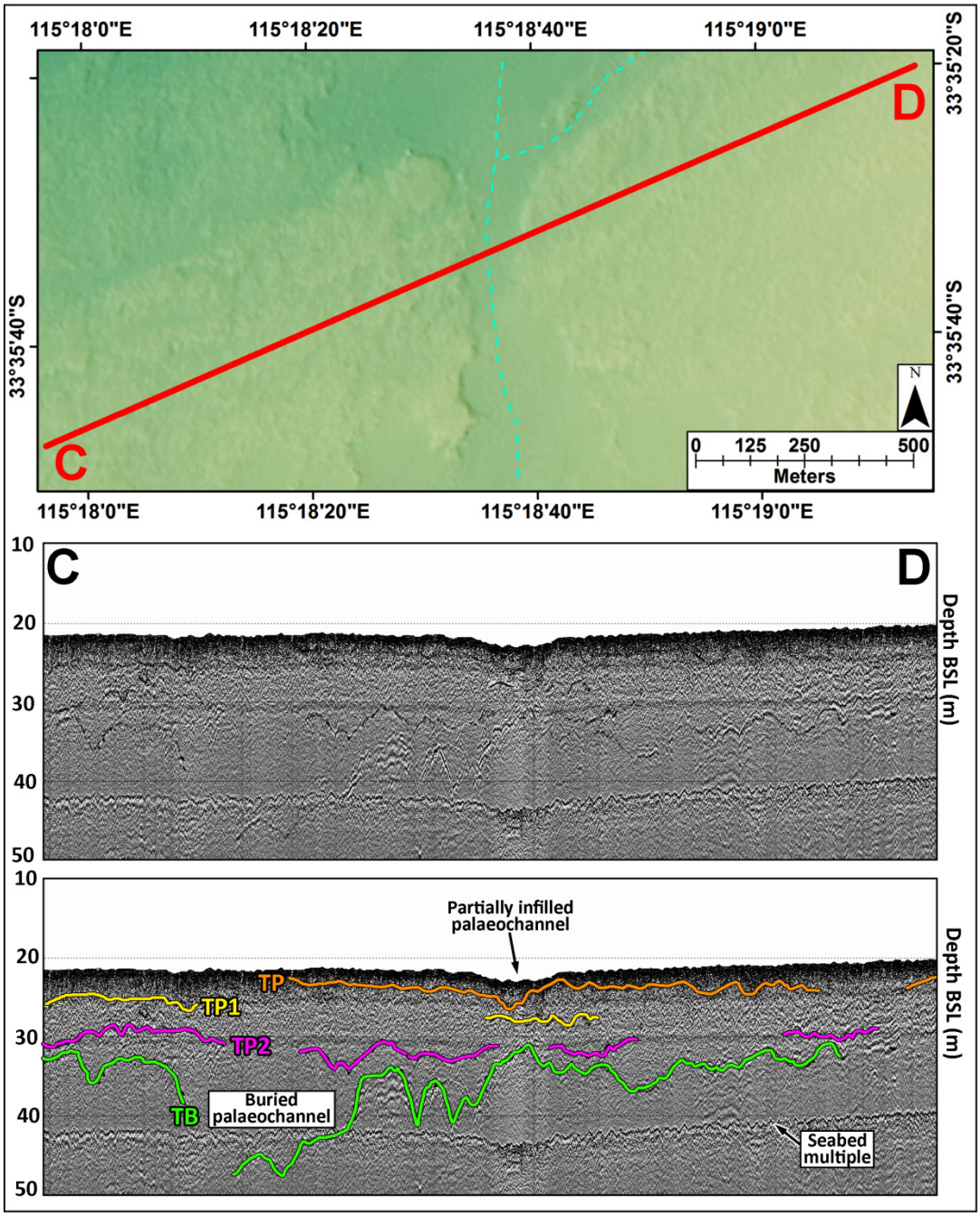


**Figure 5.5. Profile C-D: palaeochannels, for location refer to Figure 5.3. Length: ~2175 m. Top: composite bathymetric data (from DoT) through the offshore channel. The light blue dash line depicts the thalweg of the surficial channel. Bottom: uninterpreted and interpreted seismic profile revealing a deeper buried palaeochannel. In addition, it is also evident that the palaeochannel recognisable from the bathymetric data is almost entirely infilled with sediments belonging to Unit H (refer to Section 4.1.3 for more information about these reflectors).**

### 4.2.3. Low-relief ridges

Further significant geomorphic features that characterise the seabed in Geographe Bay are the linear, shore-parallel, low-relief ridges (Figure 5.6).

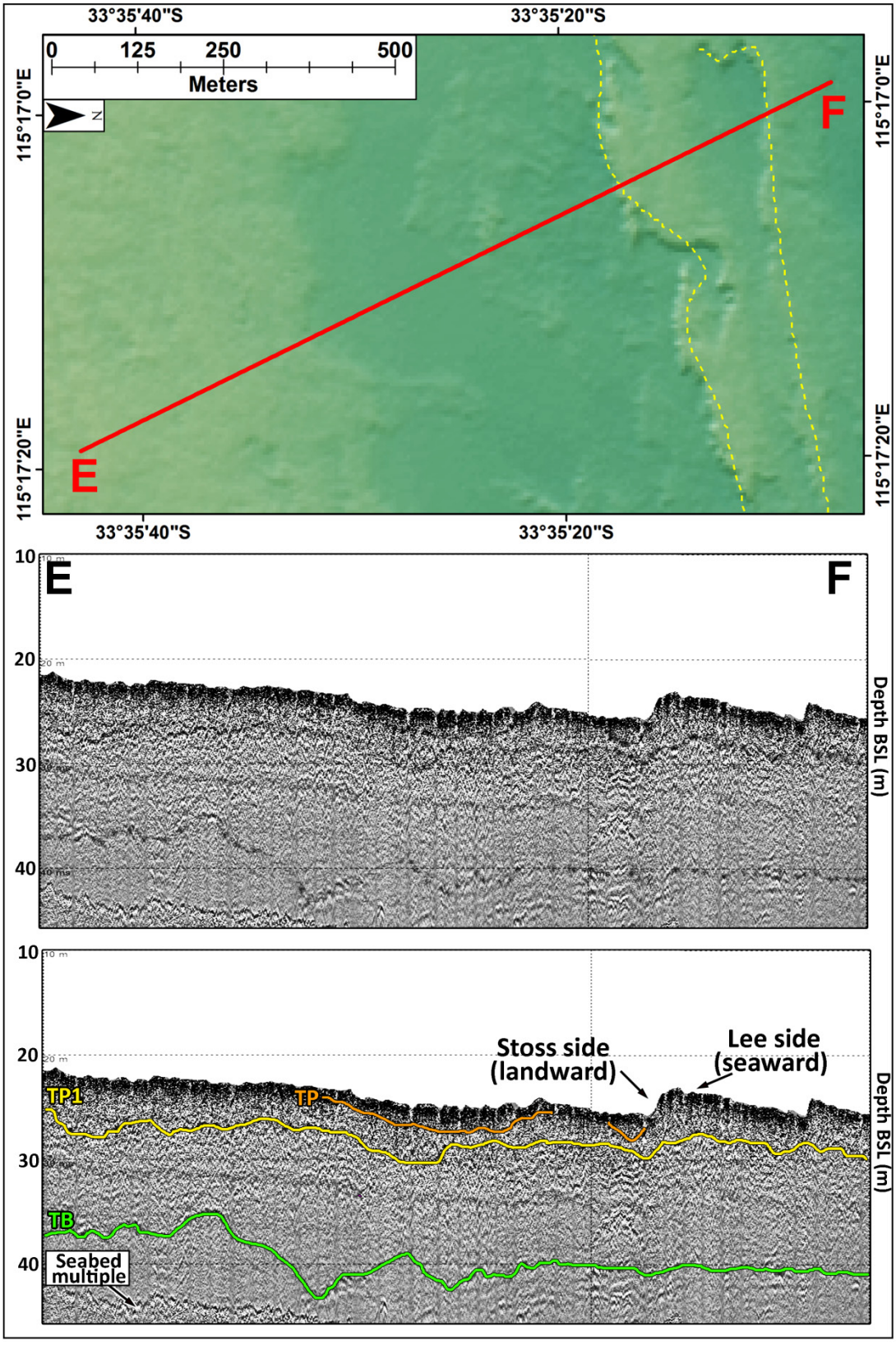

**Figure 5.6 (Previous page). Profile E-F: ridges, for location refer to Figure 5.3. Length: 1215 m. Top: composite bathymetric data (from DoT). Yellow dash line depicts the crest of the ridges. Note: the layout of the map has been rotated by an angle of 270° to match the orientation of the seismic profile. The north arrow has been adjusted accordingly. Bottom: uninterpreted and interpreted seismic profile displaying the sub-surficial architecture; note Units P and H are not clearly discernible, probably due to the fact that H is too thin for the equipment capabilities (refer to Section 4.1 for more information about the seismic reflectors).**

Two distinct groups are observed: the *deep-water ridges*, that lie between 6 and 9.5 km from the shoreline, at a depth of ~15 to 20 m, and the *shallow-water ridges* which are found only in the north-eastern portion of the Bay and are located within 1 km from the coast, in water depth < 7 m (Figure 5.3). Cross-section transects indicate that the ridges have an uneven profile, with an almost flat top, a steep stoss end landward and a gentle lee slope seaward (Figure 5.6), with a relief of less than 3 m. The deep-water ridge crests are between 200 and 900 m apart, while the shallow-water ridges are more closely spaced, and their crests are between 100 and 500 m apart.

## 4.3. Sediment distribution

In A1, the samples collected along the sandbars range mainly from coarse (1-0.5 mm, in green) to medium size (0.5-0.25 mm; purple fraction in Figure 5.7). Very coarse material (> 2 mm) is entirely constituted by biogenic skeletal grains that are highly variable in size (up to 3.5 cm in diameter) and consist of mainly fragments or whole gastropods, but also including bivalves, foraminifera and scaphopoda. Overall, the sediments are pale yellow (Munsell colour: 10YR, 8/3 to 7/4). The mineral composition is mixed carbonate-silicate sands, dominated by quartz, which reaches ~60% of each bulk sample. In the finer fraction, quartz is dominant, representing about 85-90% of the sediments having grain dimensions < 1 mm. The quartz grains generally display a medium to low sphericity and are predominantly sub-angular to rounded in shape. They are mainly white (clear, translucent to frosted), often with crescentic impact marks, but occasionally, they appear frosted and yellow, orange to light brown. The remaining sediments comprise bioclasts (especially in samples 3, 4 and 6), minor feldspar, rock fragments, possible red/brown garnet and black heavy minerals, particularly in finer grains.

Finer siliciclastic sediments (medium to fine sand) are more dominant on top of the sandbars. Coarse and very coarse material, generally bioclastic in origin, tends to accumulate in the swales between sandbars, such as in samples 3, 4 and 6 (Figure 5.7).

In A2, the sediments sampled from the top of the deep-water ridges are coarser and contain a larger amount of quartz than along the sandbars (Figure 5.8) in which finer particles are also present. The quartz grains range from colourless, yellow, red to brown in colour and they are generally translucent to transparent, sub-rounded to well-rounded, with variable sphericity. The biogenic fragments include broken mollusc shells, foraminifera and coralline algae. Bryozoans and larger lithified fragments are also present; the latter consists of a mixture of detrital quartz and sand-sized biogenic fragments, with carbonate cement (calcite), indicating the calcarenite origin of the hard surface close to the seafloor. The biggest piece of this

calcarenite (10 x 6 x 1.5 cm) was collected in sample 14. No plant remains were found in these deep-water samples.

Grain size of sediments around the deep-water ridges decreases seaward, where medium sand content increase (for instance, sample 11, Figure 5.8). The availability of unconsolidated sediments also diminishes further offshore; in fact several attempts at sediment sampling were made, but were unsuccessful, due to the indurated nature of the seafloor. Like the sandbars, material with a larger grain size is found in depressions (samples 12, 15, 16 and 17) and finer material on top of topographic elevations (i.e. sample 14).

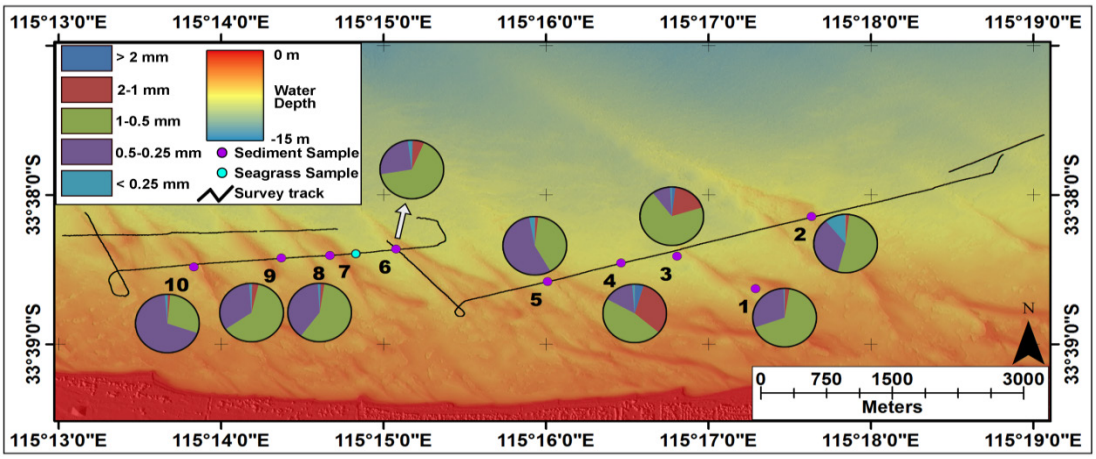


**Figure 5.7. Surficial sediment distribution superimposed on composite bathymetric data (from DoT). Each pie chart illustrates different grain size distribution in the sediments collected in Area 1. Sediments range mainly from coarse sands (1-0.5 mm, in green) and medium sands (0.5-0.25 mm, in purple). Note: sample 7 included only seagrass specimens.**

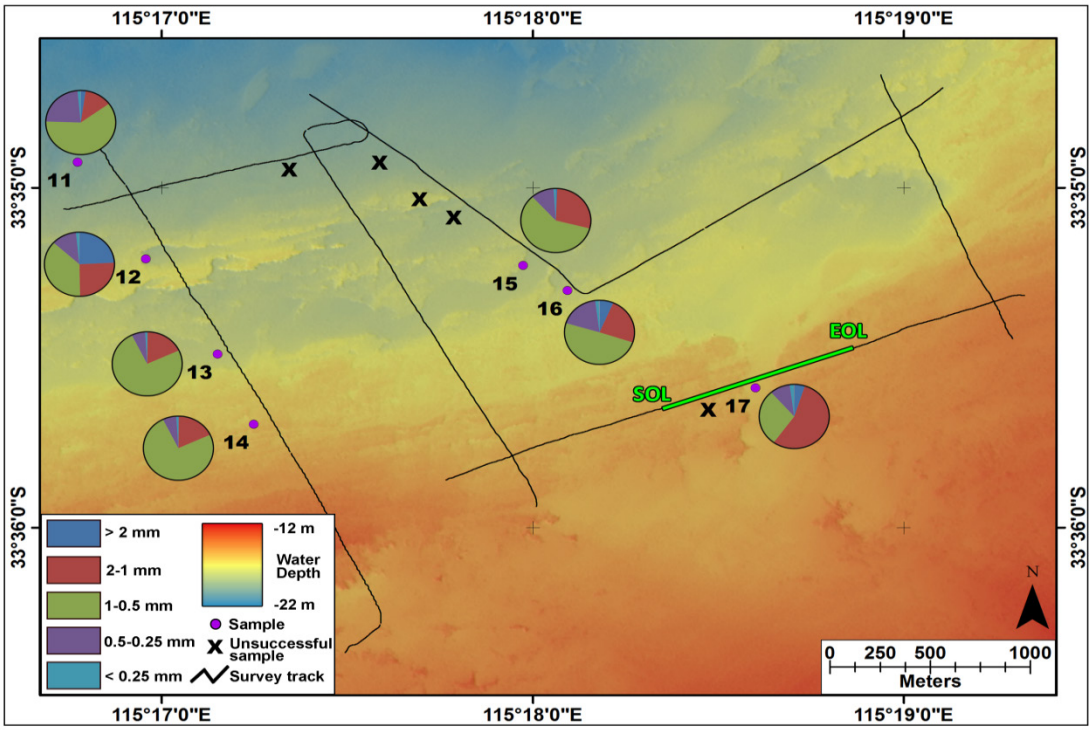


**Figure 5.8. Surficial sediment distribution superimposed on composite bathymetric data (from DoT). Like in Figure 5.7, each pie chart illustrates different grain size distribution in the**

**sediments. In Area 2, sediments range mainly from very coarse sands (1-2 mm, in red) and coarse sands (1-0.5 mm, in green). The black cross symbols represent stations where sampling was unsuccessful due to the hard substrate. The green line marks the location of the seismic profile depicted in Figure 5.12. SOL: Start of Line; EOL: End of Line.**

# 5. Discussion

In several places, no reflectors could be identified beyond the seafloor due to a combination of factors that significantly reduced the quality of the seismic imaging. Hard bottoms and lack of velocity contrast between the buried lithologies are believed to be the main causes of signal attenuation and scarce penetration; in addition, dense seagrass is likely to have affected the propagation of the signal, causing scattering and consequent deterioration of the quality in the acquired profiles. Presence of multiples of the seabed represents an additional issue in some profiles as the reflections mask the deep reflectors (refer to Kearey et al., 2002).

While no coring or dating has been performed for this specific study, the nature and age of the buried geology and the low-relief ridges have been inferred by analysing previous works and investigations that have been carried out along the inner shelf and Swan Coastal Plain between Geographe Bay and Rottnest Island (including Probert, 1967, Playford et al., 1976; Wharton, 1981; Commander, 1982; Wharton, 1982; Deeney, 1989; Hirschberg, 1989; Collins and Baxter, 1984; Hamilton and Collins, 1997; Johnson, 2002; Schafer et al., 2008; Brooke et al., 2010; Brooke et al., 2014. See Figure 5.1 for localities geographic position). Interpretation of the geomorphological features has been supported by the findings of Brooke et al. (2010; 2014). These authors carried out an extensive investigation of the morphostratigraphy of shore-parallel relict barriers and ridges, between Hillarys (30 km north of Rottnest Island) and Cockburn Sound (up to 50 km south of Rottnest Island), using bathymetric and topographic digital relief models and previously acquired dating (from Price et al. 2001 and Hearty, 2003). The findings of Skene et al. (2005), about 100 km north of the survey area (in Cockburn Sound), from several shallow cores (up to 6 m long), provide valuable insights into the sub-seafloor deposits of south west Australia and were used to support the interpretation of shallow stratigraphy proposed in this study. Finally, of fundamental importance for the inferred chronostratigraphy of the survey area, are the geotechnical, sedimentological and palynological data obtained through the “Quindalup borehole line project” and the “Busselton shallow-drilling project”, carried out along the Swan Coastal Plain, between Dunsborough and Capel (refer to Figure 5.1 for the location of these areas), as part of an assessment of the groundwater resources of the Perth Basin (Wharton, 1981; Wharton, 1982; Hirschberg, 1989). Although the majority of these studies were investigating groundwater aquifers, the findings derived by collecting terrestrial borehole sediments can be extended to the marine nearshore area, due to their proximity to the coastline. In Wharton (1981), Wharton (1982) and Hirschberg (1989), three boreholes were drilled near the shoreline adjacent to Area 1 (just west of Busselton, Figure 5.1 and Figure 5.9) and showed that the shallow stratigraphy, up to 50 m below the Australian Height Datum (AHD) includes three different units, from the oldest to most recent 1) the Early Cretaceous *Leederville Formation* (Unit B, basement), 2) the Pleistocene *Tamala Limestone* (up to 15 m thick) and the 3) *Holocene* deposits (maximum thickness of 10 m. Figure 5.9).

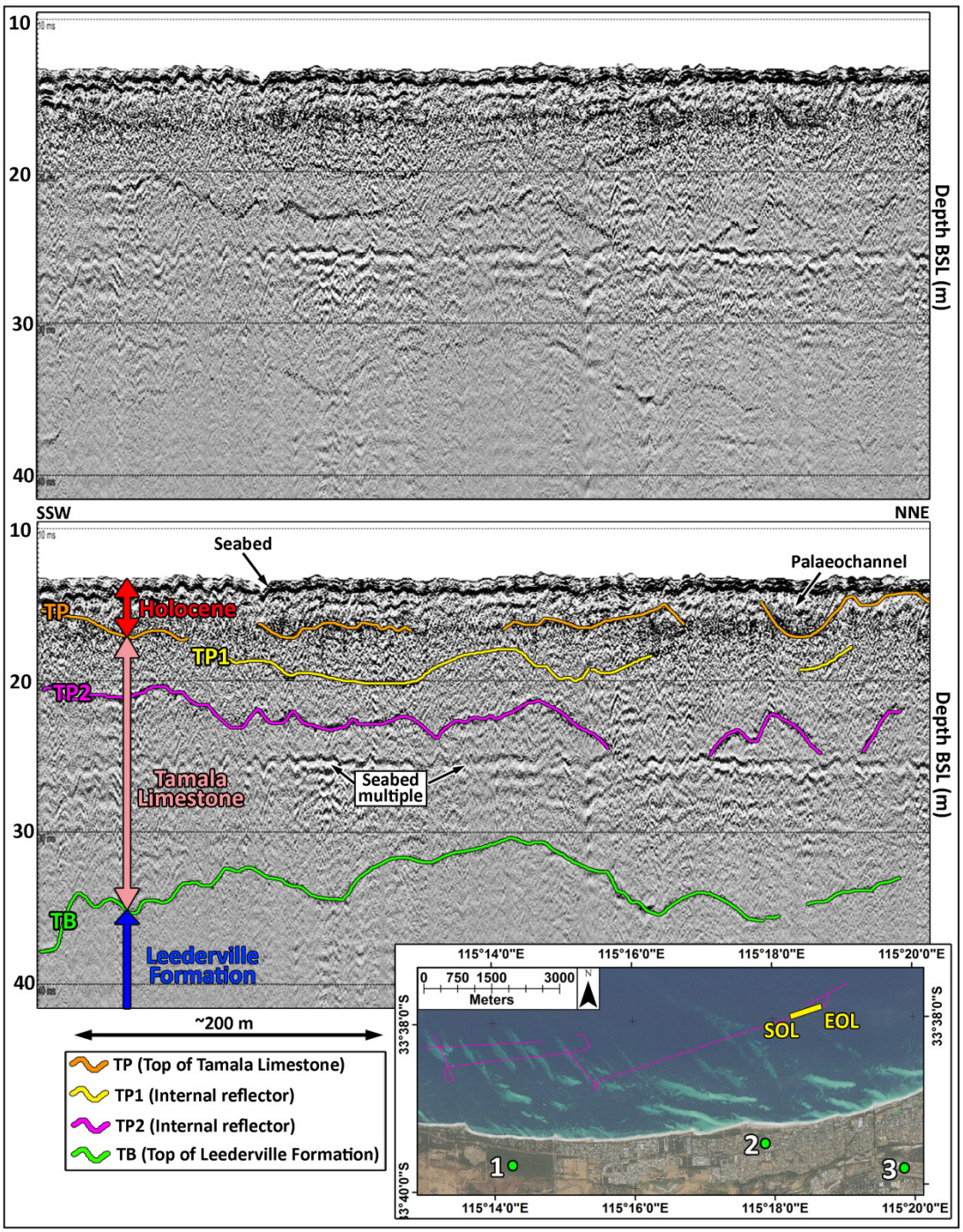


**Figure 5.9. Top: uninterpreted seismic profile. Bottom: interpreted seismic profile. The vertical axis corresponds to the depth below sea level and the scale is in metres. The sound velocity in the sediments is equivalent to 2000 m/s. The horizontal axis represents the distance covered by the vessel and the scale is in metres; in the insert location of the line, recorded in Area 1. The dots represent the boreholes collected by Wharton (1981), Wharton (1982) and Hirschberg (1989). Orthophoto section from SLIP (Shared Land Information Platform) Enabler portal, Landgate Imagery (Busselton Shire Jan 2016 Mosaic).**

## 5.1. Unit B: Leederville Formation

Based on the sedimentological records, the newly acquired seismic data and the literature available (e.g. Probert, 1967, Wharton, 1981; Wharton, 1982; Deeney, 1989; Hirschberg, 1989; Collins and Baxter, 1984; Hamilton, N.T.M. and Collins,

L.B., 1997), the intensely scoured Unit B is reasoned to belong to the *Leederville Formation*, an Early Cretaceous sequence of interbedded sandstone with siltstone and claystone (Cockbain and Playford, 1973; Playford et al., 1976). In Figure 5.9, three of the numerous boreholes analysed by Wharton (1982) and Hirschberg (1989) are reported. These authors described the sequence of this formation as weakly consolidated, fine to coarse sandstone interbedded with silty dark carbonaceous shales. Accessory minerals, including heavy minerals, feldspar and pyrite, are common (Wharton, 1981; Wharton, 1982; Hirschberg, 1989). It is likely that the heavy minerals found in the surficial sediments, collected in Area 1 and Area 2, are derived from the erosion of the Leederville Formation, during the Plio-Pleistocene, when several cycles of sea level variation have controlled the deposition and reworking of these minerals, especially along the shoreline (Collins and Baxter, 1984).

The borehole logs also showed that the Leederville Formation is unconformably overlain by the Pleistocene formation of Tamala Limestone (Wharton, 1981; Wharton, 1982; Hirschberg, 1989).

## 5.2. Unit P: Tamala Limestone

Based on the findings of Wharton (1981), Wharton (1982) and Hirschberg (1989), it is possible to assume that Unit P corresponds to *Tamala Limestone*. These authors described the formation as light-brown to orange, fine to coarse, bioclastic sand and limestone. Several other studies that have investigated the sub-surficial geology of Geographe Bay and adjacent areas, support the proposed interpretation of Unit P, including Paul and Searle (1978), Searle and Semeniuk (1985), Collins (1988) and Skene et al. (2005). The latter carried out an extensive coring program in Cockburn Sound and intersected the top of Tamala Limestone in several cores.

Tamala Limestone lies in a coastal strip, roughly parallel to the present shoreline, up to 10 km wide toward the inland and 30 km offshore (inner shelf, Brooke et al., 2010) and outcrops for several hundred kilometres along the WA coast (more than 1000km), from the South West to Shark Bay in the north (see Figure 5.1, right bottom corner for place location). This formation represents a series of shorelines and associated aeolianite build-ups (cemented dunes), composed of coastal carbonates and quartzose sand (Brooke et al., 2010), deposited during Pleistocene marine transgression events (Brooke et al., 2014).

Since Tamala Limestone is strongly diachronous, with a deposition time spanning from Mid-Late Pleistocene to Early Holocene (Murry-Wallace and Kimber, 1989; Brooke et al., 2014; Gozzard, 2007) the minor reflectors within Unit P (TP1 and TP2) likely represent different periods of deposition, diagenesis and erosion of this formation and reflect different stages of sea level; features such as palaeochannels are the confirmation of these oscillations. Palaeochannels have been, incised during lowering sea level and successively infilled by more recent sediments and are common within Unit P (see Figure 5.2).

## 5.3. Unit H: Holocene unit

It can be assumed that the sediments belonging to Unit H are a thin blanket of Holocene deposits, over Tamala Limestone.

Several authors have investigated the marine Holocene deposits along WA, in order to understand the timing of the coastal flooding. For instance, Baker et al. (2005) dated relict formations of inter-tidal serpulid tubeworms (vertical resolution as sea-level indicators: ±25 cm. Baker and Haworth, 1997, Baker and Haworth, 2000; Baker et al., 2001) from 21 locations along southern WA, from Rottnest Island to Esperance (see Figure 5.1 for their location). Their research demonstrated that sea level peaked about 2.0 m above present between 6600 and 6800 years Before Present (BP), followed by an uneven fall to the present. Notably, a similar timing and elevation of the peak Holocene sea level was identified by Jahnert and Collins (2013) and Bufarale and Collins (2015) in Shark Bay. According to the composite Holocene sea level curve for the Houtman Abrolhos Islands (WA, Collins et al., 2006. Location in Figure 5.1), it is likely that the sea inundated the inner shelf in Geographe Bay during the Early Holocene, around 10 thousand years (ky) ago, when the base (sea) level reached the modern isobath of 20 m.

From the sediment analysis, it is possible to conclude that the deposits are a mixture of relict siliciclastics, with a variable component of biogenic grains. Relict quartz grains have been deposited on the shelf by fluvial systems during lowstand and remobilised nearshore forming sandbars, during transgression and through the Holocene; the thin ferruginous coating on the grains in Area 2 suggests that the sediments are reworked material of the Cooloongup Sand, a unit derived from the residual material of Tamala Limestone (Lipar and Webb, 2014). The light yellow to cream quartzose sediments in Area 1 may have originated from the reworking of the Burragenup Member, a Holocene unit of the Safety Bay Sand, composed of remnants of cemented dunes (Lipar and Webb, 2014). The carbonate grains are instead more recent and linked with the development of the seagrass meadows. It is important to recognise that seagrasses not only produce *in situ* biogenic deposits, but also represent significant trapping and binding agents of the unconsolidated sediments (Hendriks et al., 2008; Gibbes et al., 2014; Bufarale and Collins, 2015).

Unit H cannot be clearly recognised in deeper water (in A2 and part of A3, between 15 and 20 m BSL), using a seismic device. This is an important observation suggesting a very limited Holocene sediment reservoir at depths. In an essentially sediment-starved environment like Geographe Bay, where the riverine input of siliciclastic sediments is limited, it is possible to credit the importance of seagrass as a key-feature in sediment production and deposition. This remark is in apparent contrast with the results of the sediment analysis, which saw quartz as the dominant component. In practice, it is likely that hydrodynamic sorting affects the lithology distribution. Bioclasts and quartz have in fact, significant hydrodynamic differences: carbonates are less dense, platy and have a greater surface area, therefore easily subject to a hydrodynamic sorting, whereas quartz grains are denser and less prone to be transported (Longhitano, 2011; Chiarella et al., 2012). As a result, the carbonate sediments are reworked and transported onshore by waves (Brooke et

al., 2014), and siliciclastic grains, instead, remain trapped within the sandbars, which act as a primary sediment sink, in the inner continental shelf.

# 6. Geomorphological features

The end of the MIS 5e climatic optimum (~118 ky BP) was characterised by a rapid marine regression, coinciding with an insolation minimum and cooler global temperatures (Lambeck and Chappell, 2001; Lambeck et al., 2002; Bianchi and Gersonde, 2002; Hearty et al. 2007). For the following ~110 ky, up to ~ 7 ky BP, the sea level was lower than the present (Collins et al., 2006; Jahnert and Collins, 2013; Bufarale et al., 2017). During this time, Capel and other river systems in the region deposited siliciclastic sediments on the shelf, and waves and currents mobilising terrigenous grains longshore, trapping some in Geographe Bay. The coarse river gravel remained mainly confined in the palaeochannels or topographic lows and the finer grain sediments were deposited on the palaeo-shoreface and then worked along the coast. During the sea level oscillations that characterised the late Pleistocene/Early Holocene, the siliciclastic material has been intensively reworked (and rounded) and being transported seaward by fluvial and aeolian processes under falling sea level and landward by waves and currents under rising sea levels.

Around 10 ky BP, the marine transgression led to significant changes in terms of sediment erosion, transport and deposition in Geographe Bay. The inner shelf became submerged and waves and currents started to mobilise the unconsolidated siliciclastic grains, forming longitudinal sandbars, which are presently aligned with prevailing wave direction and partially covered with seagrass. Conversely from the ridges, these features are likely to have a quartz-dominated core, with a veneer of carbonate material. It must be noted that, although the sediment directly beneath the seagrasses was not sampled, samples from the exposed stoss side showed that the bar is quartz-dominated, confirming this interpretation.

## 6.1. Sandbars

In Geographe Bay, the oblique sandbars, first described by Paul and Searle (1978), are all subparallel to each other (Figure 5.10). Superimposing the sandbar map distribution (from Figure 5.10) to the mean wave direction chart (Figure 5.11), the interaction between these elements is highlighted, with the sandbars laying perpendicular to the mean wave direction. The mean wave direction chart shows how the south-westerly storm waves are refracted around Cape Naturaliste toward Geographe Bay coast (Pattiaratchi and Wijeratne, 2011), clearly playing a significant role in mobilising the sediments and creating the sandbars. These observations have been investigated by Pattiaratchi et al. (2011, 2015, 2017) to review the effect that the construction of Port Geographe had on the local shoreline evolution. Using a computer program simulating waves, flow and sediment transport, coupled with bathymetric and LiDAR data, these researches confirmed that sandbars, storm wave and currents have a strong mutual interaction.

In addition, being a sediment-starved shelf, with medium to coarse grained sand dominating the unconsolidated sediment nearshore (as revealed from the sediment analysis; see Figure 5.7 and Figure 5.8), it is likely that, further north (i.e. in front of Capel River mouth), the finer sediment is kept in suspension above the seabed and

swept by waves and currents towards the southern part of the Bay, where due to a combination of coastal morphology, seagrass and hydrodynamic controls it is rearranged in linear sandbars, oblique to the coastline. This phenomenon has been noticed and described in several regions around the world, including in North Carolina (USA. Murray and Thieler, 2004) and New Zealand (Green et al., 2004), and interpreted as an association of longshore currents and large waves, with coarse material on the seafloor.

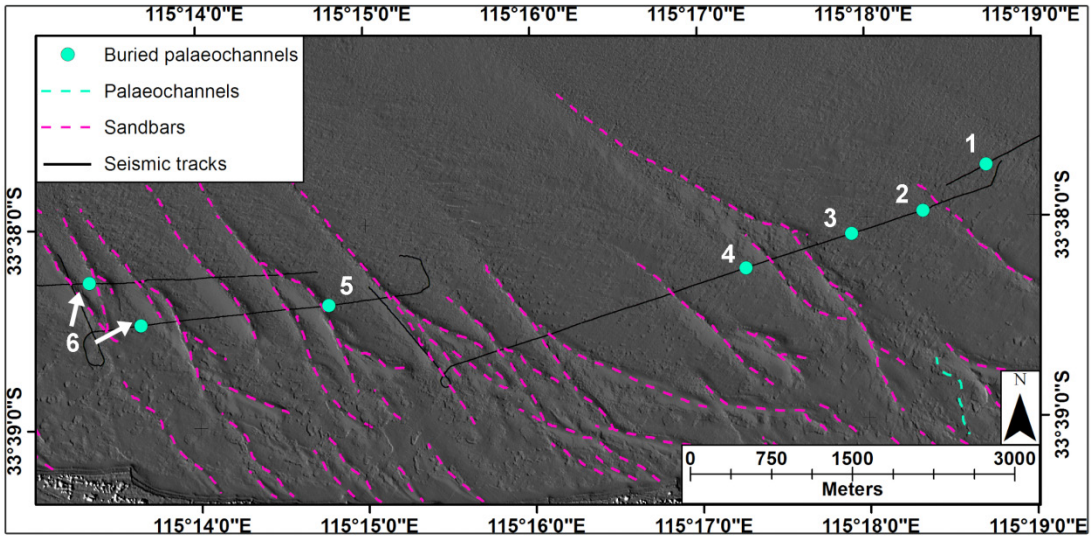


**Figure 5.10. Location of sandbars (pink dashed line) and buried palaeochannels (identified with the seismic profiles, marked in light blue dots) in area A1. Surficial palaeochannel incisions are also delineated (light blue dashed line).**

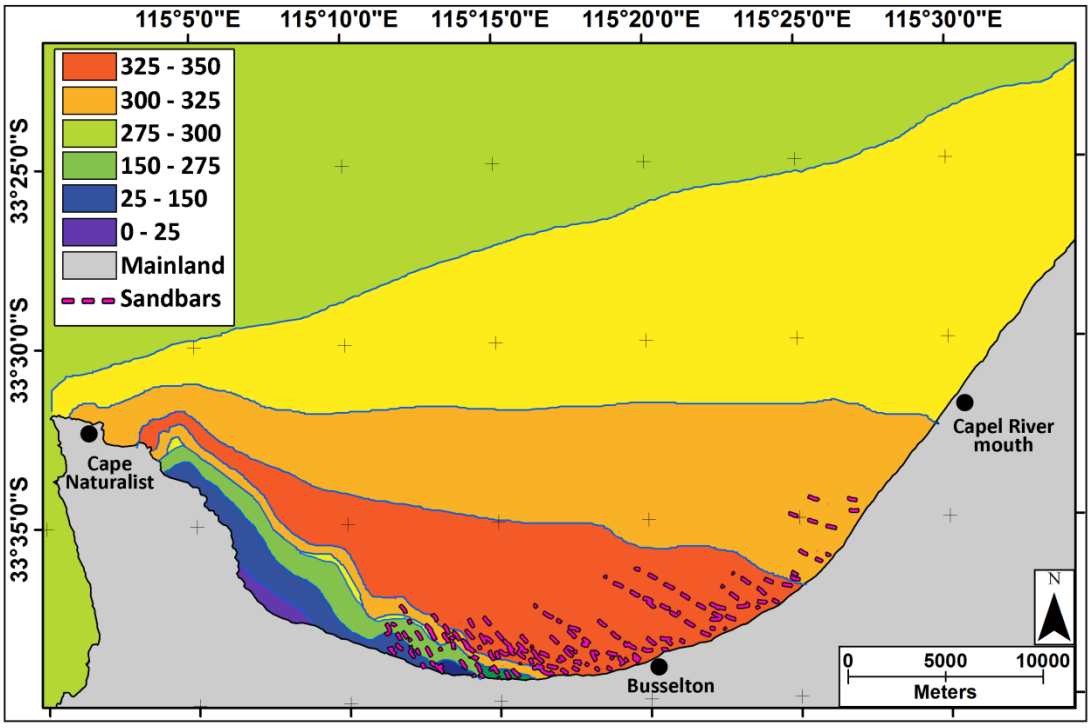

**Figure 5.11 (Previous page). Predicted mean wave direction during storm events (redrawn after Pattiaratchi and Wijeratne, 2011) with superimposed sandbar tracks. Note that the sandbars shift to a different angle according to the prevalent wave direction.**

## 6.2. Palaeochannels

Surficial and buried incisions have been described in detail in several studies worldwide, using different methods, including bathymetric and seismic data. Ryan et al. (2007), for example, employed various bathymetric datasets to detect several palaeochannels between the Burdekin and Fitzroy Rivers (north-eastern Australia). Bufarale et al. (2017) mapped three sets of palaeochannels under the modern Swan River (Perth CBD, Western Australia) using a boomer system. Similarly, underwater seismic refraction was employed by Whiteley and Stewart (2008) to identify a major palaeochannel under the modern Lane Cove River (Sydney, New South Wales). McNinch and several other authors (McNinch, 2004; Browder and McNinch, 2006; Schupp at al., 2006; McNinch and Miselis, 2012; Thieler et al., 2014) have described buried palaeochannels and oblique sandbars, along North Carolina and Virginia (U.S. central Atlantic coast) using seismic profiles, combined with swath bathymetry and side-scan sonar images.

Within the study area, several surficial and buried palaeochannels have been detected through high-resolution bathymetric and seismic datasets. Buried palaeochannels are mainly found in A1, where 6 incisions can be depicted in the seismic profiles (Figure 5.10). In A2 and A3, 4 and 3 main buried palaeochannels can be respectively recognised. In area A2, the westernmost buried palaeochannels appear to be the prolongation of channel 1 and 2 (Figure 5.10) seaward. In Area 3, a deep incision is clearly observed in the seismic profiles close to the shoreline (Figure 5.2). The palaeochannel is directly in line with the modern mouth of the Capel River, evidence that an ancient Capel River was active also in the past. At present, the incision is ~ 5 m deep, but considering that erosion of the upper part of the unit is likely to have happened, this channel and related palaeoriver might have been more significant, in terms of dimension, discharge and flow than the modern one.

The buried and surficial palaeochannels typically follow the same course, indicating that the pre-existing topography may have shaped and influenced successive morphological features (Figure 5.12).

Surficial incisions, recognisable in the high-resolution bathymetric composite images, are more numerous in Area3. The discrepancy is attributable to different Holocene thicknesses between the north-eastern A3 and the south-western A1. In the latter, where the Holocene unit is well-developed and a large amount of sediment is trapped along the sandbars, the palaeochannels have been infilled and covered up, and hence not recognisable within the bathymetric data, only in seismic profiles (Figure 5.13). In A3, on the other hand, strong coastal currents (Fahrner and Pattiaratchi, 1994) and an almost bare (from seagrass) seafloor (McMahon et al., 1997; Oldham et al., 2010) have limited the deposition of the sediments that have been instead transported and deposited further south, leaving the surficial incisions more evident.

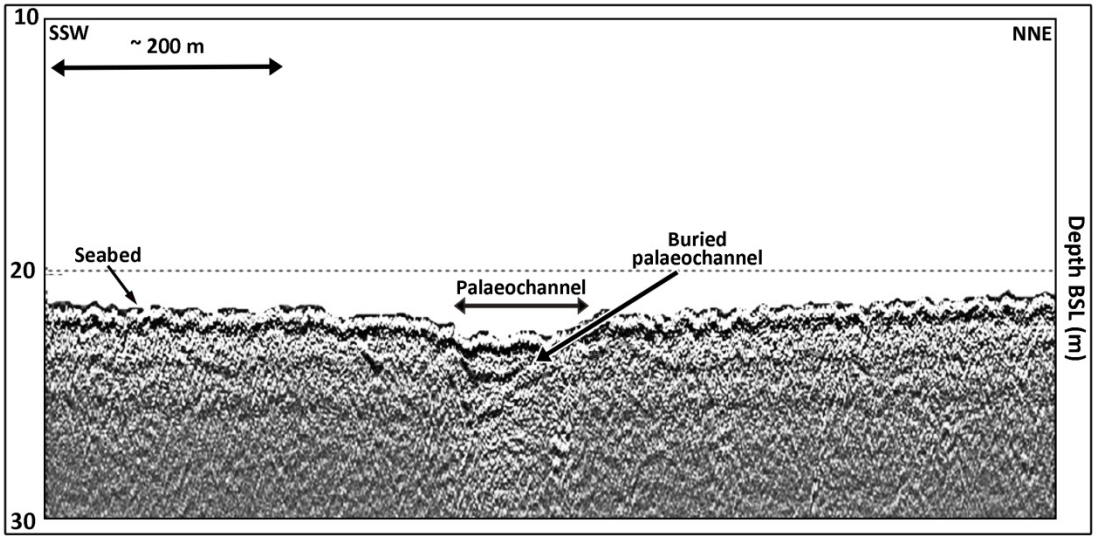


**Figure 5.12. Seismic profile in A2 (for location see Figure 5.8) showing a seafloor palaeochannel that is the surficial expression of a buried incision, located underneath.**

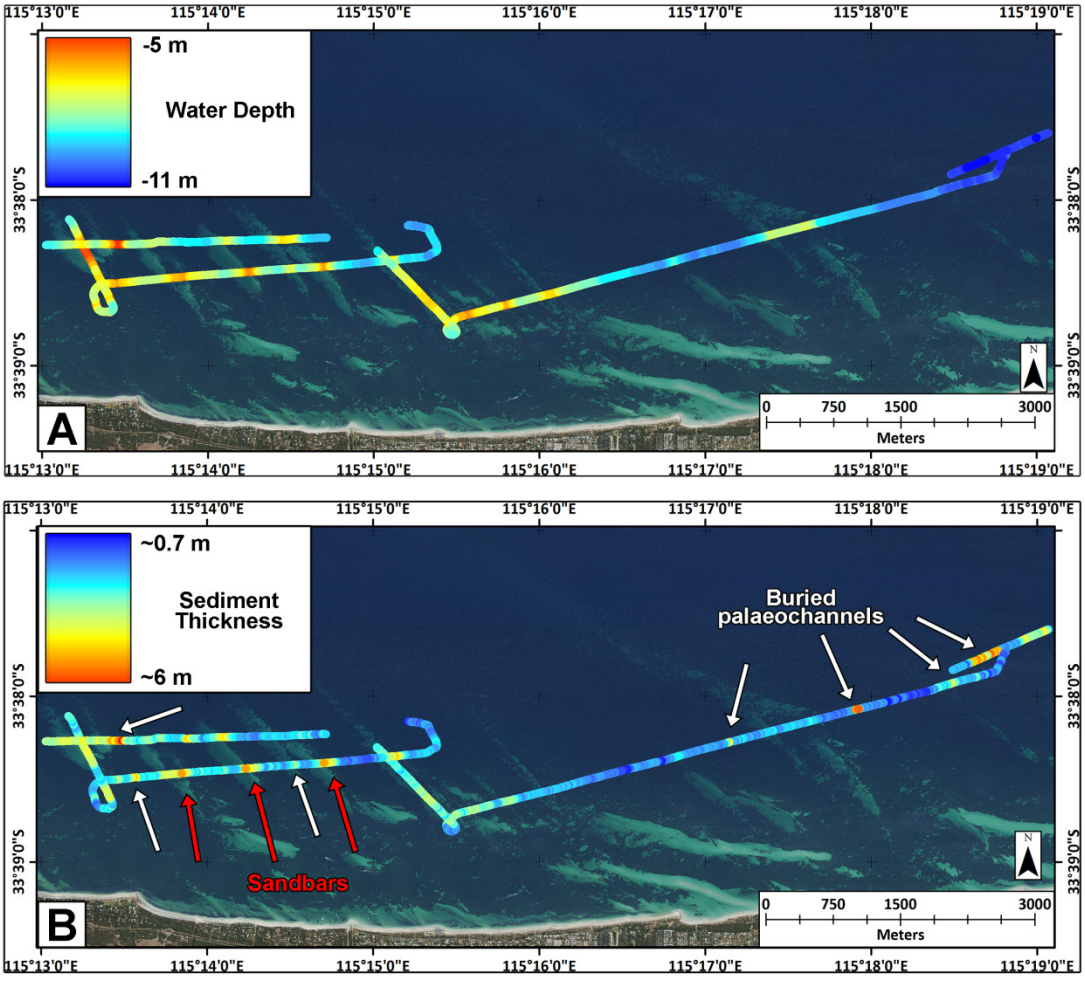


**Figure 5.13. Water depth and Unit H sediment thickness in Area 1. Orthophoto is from SLIP Enabler portal, Landgate Imagery (Busselton Shire Jan 2016 Mosaic). A) The water depth is shallower along the oblique sand bars and deepens eastward. The depth is in metres and calculated approximating the sound velocity in the water equivalent to 1500 m/s. B). The Holocene unit is very thin in deeper water and between the sandbars. The thickness values are expressed in metres, calculated approximating the sound velocity in the sediments to 2000 m/s.**

**The thickest sediments are found along the sandbars (red arrows) and palaeochannels (white arrows).**

In central-western Geographe Bay (near study area A1), similar to along the coasts of North Carolina and Virginia (U.S.A.; Browder and McNinch, 2006) and Paraná inner shelf (southern Brazil; Oliveira, 2015), buried palaeochannels and oblique sandbars are found adjacent (Figure 5.13). However, unlike what has been described in USA and Brazil, where palaeochannels have been argued to influence the development of shore-oblique sandbars (McNinch, 2004), in Geographe Bay this relationship is not significant as hydrodynamic conditions (waves and currents) are the main process involved in the formation of bottom geomorphology (Paul and Searle, 1978; Hamilton and Collins, 1997; Oldham et al., 2010; Pattiaratchi and Wijeratne, 2011).

## 6.3. Submerged low-relief ridges

As noted using the high-resolution bathymetric composite images, and also from the seismic profiles, small ridges can be recognised, corrugating the seafloor, near the coastline and into deeper water. The ridge complexes are topped by a veneer of Holocene deposits (especially thin in deep-water and toward the northern portion of the study area, near A2 and A3, respectively), but the core of the ridges appears to belong to Tamala Limestone.

Shore parallel ridges are common structures along the Western Australian coast, both onshore (Commander, 2003) and submerged on the shelf (James et al., 1999; Twiggs and Collins, 2010; Brooke et al., 2010; Nichol and Brooke, 2011, Brooke et al., 2014), recording major past sea level changes. These geomorphological structures are relict landforms, like shoreface palaeodunes or beach ridges, which are commonly found in carbonate dominated, sediment-starved coasts (Reading, 2009; Brooke et al., 2010) and record relatively stable episodes of regressive shoreline conditions, followed by transgressive erosion. Because of their low relief above the seabed and discontinuity, it is unlikely that these ridges have acted as a barrier inhibiting or trapping onshore sediment transport.

Similar to the onshore Swan Coastal Plain, where sub-aerial coastal dune ridges become progressively younger from east to west (Commander, 2003), the submerged ridges also young in the same direction, recording Late Pleistocene relatively high sea level stages. Figure 5.14 displays a schematic cross section of the Late Quaternary geomorphological evolution from the northern portion of the study area (A3). The shallow-water ridges in the south (area A1) might have been eroded completely or covered by Holocene sediments.

The shallow-water ridges were the first ridge complex to form. Toward the end of the MIS 5e-beginning of 5d, when the sea level was about 5 to 10 m lower than the present (Chappell et al., 1996), these barriers started their development, close to the innermost palaeo shoreline (Figure 5.14A). When the sea level further dropped, leaving these features exposed, cementation commenced. Similarly, the second ridge complex (deep-water ridges) established its shape in an analogous manner, during MIS 5c, when the sea level was 20-30 m below present (Chappell et al., 1996; Creveling et al., 2017. Figure 5.14B). Up to ~10 ky BP, the inner shelf

remained mainly exposed, favouring the cementation of the ridges. When the sea level inundated the shelf (Early Holocene), erosion took place, leaving the lithified ridges asymmetric, with a flat top (Figure 5.14C).

The chronostratigraphic interpretation of these geomorphic features is supported by a number of studies that have been carried out on similar structures along the WA coast, in particular in the South West (notably Brooke et al., 2010; Brooke et al., 2014). These studies describe the chronology and the nature of three submerged ridge sets, between Rottnest Island and Cockburn Sound, from nearshore up to 50-60 m of depth BSL. The two shallow structures are equivalent to the shallow-water and deep-water ridges described in the present study and the third set of ridges represent more recent (MIS 5a) features, not included in this investigation.

Nevertheless, additional coring and dating of both the ridge complexes would help to further confirm this interpretation, also providing a better assessment of the Late Pleistocene evolution of the South West coast.

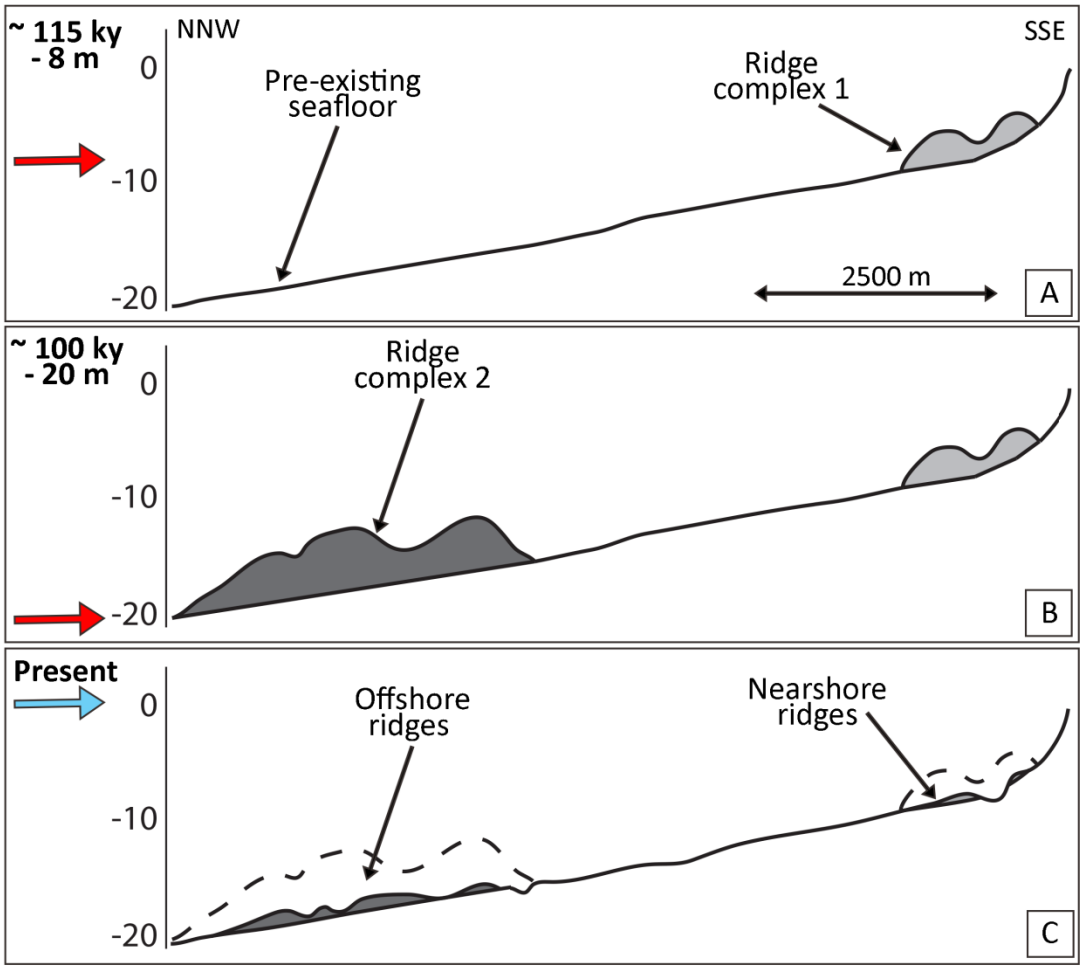


**Figure 5.14. Schematic model showing the onset and evolution of regressive beach ridges and, possibly sub-littoral deposits. The profile is a simplified cross section, located in proximity of A3, in the northern portion of the study area. Horizontal axis: ~9 km; vertical axis: depth values are in metres, referred to the present sea level (where 0 corresponds to modern mean sea level). The arrows represent the stage of sea level, in different time; red: falling sea level, blue: rising sea level. The figure has been drawn based on the data from this study and the**

**conceptual model proposed by Brooke et al. (2010) and Brooke et al. (2014) that these features described in detail.**

# 7. Conclusions

Reflection seismic data, combined with high-resolution composite bathymetric datasets and sedimentological analysis, provided the following new insights into the inner continental shelf in Geographe Bay:

1) Shallow architecture and stratigraphy has been revealed for the first time. The seismic profiles imaged three main sedimentary units, separated by unconformities and deposited under various sea level conditions, which include:
   - An acoustic basement (TB, Leederville Formation), dated back to the Early Cretaceous;
   - One intermediate unit (TP), belonging to Tamala Limestone, from Mid to Late Pleistocene;
   - A surficial unit (TH), deposited since Early Holocene, around 10 ky BP.
2) The surficial sediments of the Holocene unit are dominated by quartz but also include a percentage of carbonates and other accessory minerals and rock fragments. Finer siliciclastic sediments are more dominant on top of topographic highs and sandbars. Coarse and very coarse material, mainly carbonate, tends to accumulate in the swales and depressions. These Holocene deposits are hence the result of a combination of erosion of older formations (mainly Tamala Limestone, although heavy minerals derive from the erosion of the Leederville Formation) and *in situ* accumulation of carbonates from seagrass and other benthic communities.
3) Three main features that characterise the seabed are:
   - Several palaeochannels (buried and surficial), expression of previous sea level lowstands.
   - Near-continuous, asymmetrical sandbars and associated swales, that extend obliquely from nearshore to ~6 km seaward. These linear features are mainly located in the south-western portion of the bay and generally have an almost bare stoss flank and a lee side intensely colonised by seagrass; the sandbars are function of the a) local hydrodynamics, acting as a primary sediment sink of siliciclastic grains, with waves and currents (including longshore) influencing the geomorphology in the inner continental shelf; b) grain size and c) seagrass' effect.
   - Two sets of shore-parallel, low-relief ridges, located at a depth of <10 m and ~20 m, respectively. They represent relict landforms, probably regressive beach ridges and sub-littoral deposits (paleo-dunes), belonging to Tamala Limestone. These geomorphological structures were formed during Late Pleistocene relatively high sea level stages (end of MIS 5e-beginning of MIS 5d and 5c, respectively) and subsequently cemented and subject to successive marine (transgressive) erosion; based on the morphology of these submerged strand plains, an abrasion surface characterises the top of these

features, where the top has been cut out, leaving the core or the base of the ridges.

The data confirms that the shelf is essentially sediment-starved and the very limited Holocene sediments produced along the shelf, have then been reworked and transported onshore by waves. In terms of sediment resource potential, the sandbars are the reservoir of the sediment on the shelf, with the core likely to be quartz sand.

## Acknowledgments

The authors would like to acknowledge the DoT (Fremantle, WA) for provided the hydrographic survey vessel and the bathymetric data, in particular thanks to Kim Edwards, skipper of the hydrographic survey vessel *Alec Hansen III* and Karl Ilich. Additional funding was provided by a University of Western Australia's Research Collaboration Award.

Many thanks to John Gann and Steve Cutcomb (Chesapeake Technology, Inc.) and Giovanni De Vita for their technical support. Alexandra Stevens is acknowledged for critically reviewing the manuscript.

The first author would like to acknowledge the contribution of an Australian Government Research Training Program Scholarship in supporting this research and the support provided by the Society for Underwater Technology (SUT) through the SUT Chris Lawlor 2016 Scholarship.

## References

Baker, R.G.V., Haworth, R.J., 1997. Further evidence from relic shellcrust sequences for a late Holocene higher sea level for eastern Australia. Marine Geology 141, 1-9.

Baker, R.G.V., Haworth, R.J., 2000. Smooth or oscillating late Holocene sea-level curve? Evidence from the palaeo-zoology of fixed biological indicators in east Australia and beyond. Marine Geology 163, 367-386.

Baker, R.G.V., Haworth, R.J., Flood, P.G., 2001. Inter-tidal fixed indicators of former Holocene sea levels in Australia: a summary of sites and a review of methods and models. Quaternary International 83-85, 257-273

Baker, R.G., Haworth, R.J. and Flood, P.G., 2005. An oscillating Holocene sea level? Revisiting Rottnest Island, Western Australia, and the Fairbridge eustatic hypothesis. Journal of Coastal Research, pp.3-14.

Barr, S. and Eliot, M., 2011. Busselton coastal protection. In Coasts and Ports 2011: Diverse and Developing: Proceedings of the 20th Australasian Coastal and Ocean Engineering Conference and the 13th Australasian Port and Harbour Conference (p. 30). Engineers Australia.

Barr, S.A., Staples, O., Eliot, I., Darby, O., Abrahamse, D. and Stul, T., 2017. Adaptation to coastal inundation in a low lying, highly dynamic regional area. Australasian Coasts & Ports 2017: Working with Nature, p.1037.

Bianchi, C. and Gersonde, R., 2002. The Southern Ocean surface between Marine Isotope Stages 6 and 5d: Shape and timing of climate changes. Palaeogeography, Palaeoclimatology, Palaeoecology, 187(1), pp.151-177.

Brooke, B., Creasey, J. and Sexton, M., 2010. Broad-scale geomorphology and benthic habitats of the Perth coastal plain and Rottnest Shelf, Western Australia, identified in a merged topographic and bathymetric digital relief model. International Journal of Remote Sensing, 31(23), pp.6223-6237.

Brooke, B.P., Olley, J.M., Pietsch, T., Playford, P.E., Haines, P.W., Murray-Wallace, C.V. and Woodroffe, C.D., 2014. Chronology of Quaternary coastal aeolianite deposition and the drowned shorelines of southwestern Western Australia–a reappraisal. Quaternary Science Reviews, 93, pp.106-124.

Brooke, B.P., Nichol, S.L., Huang, Z. and Beaman, R.J., 2017. Palaeoshorelines on the Australian continental shelf: Morphology, sea-level relationship and applications to environmental management and archaeology. Continental Shelf Research, 134, pp.26-38.

Browder, A.G. and McNinch, J.E., 2006. Linking framework geology and nearshore morphology: correlation of paleo-channels with shore-oblique sandbars and gravel outcrops. Marine Geology, 231(1), pp.141-162.

Bufarale, G., Collins, L.B., 2015. Stratigraphic architecture and evolution of a barrier seagrass bank in the mid-late Holocene, Shark Bay, Australia. Mar. Geol. 359, 1–21.

Bufarale, G., O'Leary, M., Stevens, A., Collins, L.B., 2017. Sea level controls on palaeochannel development within the Swan River estuary during the Late Pleistocene to Holocene. Catena 153. doi:10.1016/j.catena.2017.02.008

Bureau of Meteorology - Australia, 2011. Climate summary statistics Busselton Shire. http://www.bom.gov.au/climate/averages/tables/cw_009515.shtml

Carrigy, M. A. and Fairbridge, R. W., 1954, Recent sedimentation, physiography and structure of the continental shelves of Western Australia. Royal Soc. West. Australia Jour., v. 38, p. 65-95.

Chappell, J., Omura, A., Esat, T., McCulloch, M., Pandolfi, J., Ota, Y. and Pillans, B., 1996. Reconciliation of late Quaternary sea levels derived from coral terraces at Huon Peninsula with deep sea oxygen isotope records. Earth and Planetary Science Letters, 141(1-4), pp.227-236.

Chiarella, D., Longhitano, S.G., Sabato, L. and Tropeano, M., 2012. Sedimentology and hydrodynamics of mixed (siliciclastic-bioclastic) shallow-marine deposits of Acerenza (Pliocene, Southern Apennines, Italy). Italian journal of geosciences, 131(1), pp.136-151.

Carruthers, T.J.B., Dennison, W.C., Kendrick, G.A., Waycott, M., Walker, D.I. and Cambridge, M.L., 2007. Seagrasses of south–west Australia: A conceptual

synthesis of the world's most diverse and extensive seagrass meadows. Journal of Experimental Marine Biology and Ecology, 350(1), pp.21-45.

Coastal Information, Department of Transport, 2016. https://catalogue.data.wa.gov.au/dataset/composite-surfaces-multibeam-lidar-laser (valid at: 22/06/2017)

Cockbain, A. E. and Playford, P. E., 1973. Stratigraphic nomenclature of Cretaceous rocks in the Perth Basin: West. Australia Geol. Survey Ann. Rept 1972, p. 26-3 1.

Collins, L.B. and Baxter, J.L., 1984. Heavy mineral-bearing strandline deposits associated with high-energy beach environments, southern Perth Basin, Western Australia. Aust. J. Earth Sci. 31, 287–292. doi:10.1080/14400958408527931

Collins, L.B., 1988. Sediments and history of the Rottnest Shelf, southwest Australia: a swell-dominated, non-tropical carbonate margin. Sedimentary Geology, 60.

Collins, L.B., Zhao, J.X. and Freeman, H., 2006. A high-precision record of mid–late Holocene sea level events from emergent coral pavements in the Houtman Abrolhos Islands, southwest Australia. Quaternary International, 145, pp.78-85.

Commander, D.P., 1982. The Bunbury shallow drilling groundwater investigation. Western ustralia Geological Survey, Professional Papers for, pp.32-52.

Commander, P., 2003. Outline of the geology of the Perth region. Aust. Geomech. 38, 7–16.

Creveling, J.R., Mitrovica, J.X., Clark, P.U., Waelbroeck, C. and Pico, T., 2017. Predicted bounds on peak global mean sea level during marine isotope stages 5a and 5c. Quaternary Science Reviews, 163, pp.193-208.

CSIRO, 2015. Tidal Dataset - CAMRIS - Maximum Tidal Range. v1. CSIRO. Data Collection. http://doi.org/10.4225/08/551485767777F

Deeney, A.C., 1989. Geology and groundwater resources of the superficial formations between Pinjarra and Bunbury, Perth Basin. Geological Survey of Western Australia, Report, 26, pp.31-57.

Department of Transport, Western Australia. https://www.transport.wa.gov.au/imarine/Cape-Peron-to-Albany.asp (valid at: 22/06/2017).

Duncan, A.J., Gavrilov, A. and Li, F., 2009. Acoustic propagation over limestone seabeds. Proceedings of Australian Acoustical Society 2009, Adelaide, South Australia.

Duncan, A.J. and Gavrilov, A., 2012. Low frequency acoustic propagation over calcarenite seabeds with thin, hard caps. Proceedings of Acoustics 2012, Fremantle Western Australia.

Fahrner, C.K. and Pattiaratchi, C.B., 1994. The physical oceanography of Geographe Bay, Western Australia. Report prepared for the Water Authority of Western Australia.

Fairbridge, R.W., 1961. Eustatic changes in sea level. Physics and Chemistry of the Earth, 4, 99-185 (London: Pergamon).

Geographe Catchment Council, 2008. Geographe Catchment Management Strategy. A Report for the Geographe Catchment Council, Water and Rivers Commission and National Heritage Trust.

Gibbes, B., Grinham, A., Neil, D., Olds, A., Maxwell, P., Connolly, R.,Weber, T., Udy, N., Udy, J., 2014. Moreton Bay and Its estuaries: a sub-tropical system under pressure from rapid population growth. In: Wolanski, E. (Ed.), Estuaries of Australia in 2050 and Beyond. Estuaries of the World, Springer, Dordrecht, pp. 203–222.

Gozzard, J.R., 2007. A reinterpretation of the Guildford formation. Aust. Geomech. 42 (3).

Green, M.O., Vincent, C.E., Trembanis, A.C., 2004. Suspension of coarse and fine sand on a wave-dominated shoreface, with implications for the developments of rippled scour depressions. Cont. Shelf Res. 24, 317–335.

Hamilton, N.T.M. and Collins, L.B., 1997. Morphostratigraphy and evolution of a Holocene composite barrier at Minninup, southwestern Australia. Aust. J. Earth Sci. 44, 113–124. doi:10.1080/08120099708728298

Hearty, P.J., 2003. Stratigraphy and timing of eolianite deposition on Rottnest Island, Western Australia. Quat. Res. 60, 211-222.

Hearty, P.J., Hollin, J.T., Neumann, A.C., O'Leary, M.J., McCulloch, M., 2007. Global sea-level fluctuations during the Last Interglaciation (MIS 5e). Quat. Sci. Rev. 26, 2090–2112. doi:10.1016/j.quascirev.2007.06.019.

Hearty, P.J. and O'Leary, M.J., 2008. Carbonate eolianites, quartz sands, and Quaternary sea level cycles, Western Australia: A chronostratigraphic approach. Quat. Geochronol. 3, 26–55. doi:10.1016/j.quageo.2007.10.001

Hendriks, I.E., Sintes, T., Bouma, T.J. and Duarte, C.M., 2008. Experimental assessment and modeling evaluation of the effects of the seagrass *Posidonia oceanica* on flow and particle trapping. Marine Ecology Progress Series.

Hirschberg, K-J B, 1989. Busselton shallow-drilling groundwater investigation, Perth Basin, Geological Survey of Western Australia, Professional Papers, Report 25, pp17–37.

Jahnert, R.J. and Collins, L.B., 2013. Controls on microbial activity and tidal flat evolution in Shark Bay, Western Australia. Sedimentology 60, 1071–1099. doi:10.1111/sed.12023

James, N.P., Collins, L.B., Bone, Y. and Hallock, P., 1999. Subtropical carbonates in a temperate realm: modern sediments on the southwest Australian shelf. Journal of Sedimentary Research, 69(6).

James, N.P. and Bone, Y., 2010. Neritic carbonate sediments in a temperate realm: southern Australia. Springer Science & Business Media.

Johnson, SL, 2002, Stratigraphy of the Leederville Formation in the western portion of the Busselton-Capel Groundwater Area, Department of Environment, Hydrogeology Report 198 (unpublished).

Kearey, P., Brooks, M. and Hill, I., 2002. An introduction to geophysical exploration. Third edition, Blackwell Scientific, Oxford, UK, pp 292.

Kendrick, G.W., Wyrwoll, K.-H., Szabo, B.J., 1991. Pliocene-Pleistocene coastal events and history along the western margin of Australia. Quat. Sci. Rev. 10, 419e439.

Lambeck, K. and Chappell, J., 2001. Sea level change through the last glacial cycle. Science, 292(5517), pp.679-686.

Lambeck, K., Esat, T.M., Potter, E.-K., 2002. Links between climate and sea levels for the past three million years. Nature 419, 199–206. doi:10.1038/nature01089.

Lipar, M. and Webb, J.A., 2014. Middle–late Pleistocene and Holocene chronostratigraphy and climate history of the Tamala Limestone, Cooloongup and Safety Bay Sands, Nambung National Park, southwestern Western Australia. Australian Journal of Earth Sciences, 61(8), pp.1023-1039.

Longhitano, S.G., 2011. The record of tidal cycles in mixed silici–bioclastic deposits: examples from small Plio–Pleistocene peripheral basins of the microtidal Central Mediterranean Sea. Sedimentology, 58(3), pp.691-719.

McMahon, K., Young, E., Montgomery, S., Cosgrove, J., Wilshaw, J., Walker, D.I., 1997. Status of a shallow seagrass system, Geographe Bay, south-western Australia. J. R. Soc. West. Aust. 80, 255–262.

McMahon, T.A. and Finlayson, B.L., 2003. Droughts and anti‐droughts: the low flow hydrology of Australian rivers. Freshwater Biology, 48(7), pp.1147-1160.

McNinch, J.E., 2004. Geologic control in the nearshore: shore-oblique sandbars and shoreline erosional hotspots, Mid-Atlantic Bight, USA. Marine Geology 211, 121–141.

McNinch, J.E. and Miselis, J.L., 2012. Geology metrics for predicting shoreline change using seabed and sub-bottom observations from the surf zone and nearshore. Int. Assoc. Sedimentol. Spec. Publ, 44, pp.99-120.

Munsell, A.H., 1954.Munsell soil color chart. U.S. Dept. Agriculture Soil Survey Manual 2009 Edition Munsell Soil Chart (1954)

Murray, A.B. and Thieler, E.R., 2004. A new hypothesis and exploratory model for the formation of large-scale inner-shelf sediment sorting and “rippled scour depressions”. Cont. Shelf Res. 24, 295–315.

Murray-Wallace, C. V. and Kimber, R.W.L., 1989. Quaternary marine aminostratigraphy: Perth Basin, Western Australia. Aust. J. Earth Sci. 36, 553–568. doi:10.1080/08120098908729509

Nichol, S.L. and Brooke, B.P., 2011. Shelf habitat distribution as a legacy of Late Quaternary marine transgressions: a case study from a tropical carbonate province. Continental Shelf Research, 31(17), pp.1845-1857.

Oldham, C., Lavery P., McMahon K., Pattiaratchi C., Chiffings T. 2010. Seagrass wrack dynamics in Geographe Bay, Western Australia. Report to Western Australian Department of Transport, and Shire of Busselton.

Oliveira, L.H.S.D., 2015. Morfologia e sedimentologia da plataforma continental interna paranaense. Doctoral Thesis. Universidade Federal do Paraná, Setor de Ciências da Terra, Programa de Pós-Graduação em Geologia. https://educapes.capes.gov.br/handle/1884/39930 (May 2017).

Pattiaratchi, C. and Wijeratne, S., 2011. Port Geographe sand and seagrass wrack modelling study, Western Australia. Report prepared for Department of Transport (WA). SESE report no. 465, School of Environmental Systems Engineering, the University of Western Australia, Perth.

Pattiaratchi CB, Wijeratne EMS & Bosserelle C., 2011. Sand and seagrass wrack modelling in Port Geographe, south-western Australia. Proceedings of Coasts and Ports 2011, Engineers Australia.

Pattiaratchi CB, Wijeratne EMS, Roncevich L & Holder J, 2015. Interaction between seagrass wrack and coastal structures: lessons from Port Geographe, southwestern Australia. Proceedings of Coasts and Ports 2015, Engineer Australia.

Pattiaratchi, C.B., Wijeratne, S., Roncevich, L. and Holder, J., 2017. The influence of nearshore sandbars on coastal stability in port geographe, South-west Australia. Australasian Coasts & Ports 2017: Working with Nature, p.865.

Paul, M.J. and Searle, J.D., 1978. Shoreline Movements Geographe Bay Western Australia. In: Fourth Australian Conference on Coastal and Ocean Engineering: Managing the Coast. Barton, A.C.T.: Institution of Engineers, Australia.

Playford, P. E., Cockbain, A. E. and Lowe, G.H., 1976. Geology of the Perth Basin. Geological Survey of Western Australia Bulletin, 124: 311p.

Playford, P.E., 1988. Guidebook to the geology of Rottnest Island. Geological Society of Australia, WA Division and the Geological Survey of Western Australia.

Playford, P.E., 1997, Geology and hydrogeology of Rottnest Island, Western Australia. In Geology and Hydrogeology of Carbonate Islands, Developments in

Sedimentology 54, L.H. Vacher and T.M. Quinn (Eds), pp. 783–810 (Amsterdam: Elsevier).

Price, D.M., Brooke, B.P., Woodroffe, C.D., 2001. Thermoluminescence dating of eolianites from Lord Howe Island and south-west Western Australia. Quat. Sci. Rev. (Quat. Geochronol.) 20, 841-846.

Probert, D.H., 1967. Groundwater in the Busselton Area: Progress Report on Exploratory Drilling. Geological Survey of Western Australia.

Reading, H.G. ed., 2009. Sedimentary environments: processes, facies and stratigraphy. John Wiley & Sons.

Ryan, D.A., Bostock, H.C., Brooke, B.P., Marshall, J.F., 2007. Bathymetric expression of the Fitzroy River palaeochannel, northeast Australia: Response of a major river to sea level change on a semi-rimmed, mixed siliciclastic-carbonate shelf. Sediment. Geol. 201, 196–211. doi:10.1016/j.sedgeo.2007.05.018

Schafer, D., Johnson, S. & Kern, A., 2008. Hydrogeology of the leederville aquifer in the western Busselton - Capel Groundwater Area. Hydrogeological record series Report HG31., s.l.: Department of Water.

Schupp, C.A., McNinch, J.E., List, J.H., 2006. Nearshore shore-oblique bars, gravel outcrops, and their correlation to shoreline change. Marine Geology 233, 63–79.

Skene, D., Ryan, D., Brooke, B., Smith, J. and Radke, L., 2005. The geomorphology and sediments of Cockburn Sound. Geoscience Australia, Record 2005/10, 88 pp.

SLIP Shared Land Information Platform - Public Web Map Service http://slip.landgate.wa.gov.au
http://catalogue.beta.data.wa.gov.au/dataset/hydrography-linear-hierarchy

Stirling, C.H., Esat, T.M., McCulloch, M.T., Lambeck, K., 1995. High-precision U-series dating of corals from Western Australia and implications for the timing and duration of the Last Interglacial. Earth Planet. Sci. Lett. 135, 115e130.

Szabo, B.J., 1979. Uranium-series age of coral reef growth on Rottnest Island, Western Australia. Mar. Geol. 29, M11eM15.

Thieler, E.R., Foster, D.S., Himmelstoss, E.A. and Mallinson, D.J., 2014. Geologic framework of the northern North Carolina, USA inner continental shelf and its influence on coastal evolution. Marine Geology, 348, pp.113-130.

Twiggs, E.J. and Collins, L.B., 2010. Development and demise of a fringing coral reef during Holocene environmental change, eastern Ningaloo Reef, Western Australia. Mar. Geol. 275, 20–36. doi:10.1016/j.margeo.2010.04.004

Van Niel, K.P., Holmes, K.W. and Radford, B., 2009. Seagrass Mapping Geographe Bay 2004-2007. Report prepared for: Southwest Catchment Council, 25 pp, University of Western Australia.

Wearne, G. R., 2000. The formation and maintenance of shoreface attached sandbars in Geographe Bay. Honours Thesis, Centre for Water Research, University of Western Australia.

Wharton, P.H., 1981. The geology and hydrogeology of the Quindalup borehole line. Western Australia Geological Survey, Annual Report for 1980, pp. 27–34.

Wharton, P.H., 1982. The geology and hydrogeology of the Quindalup borehole line in Southern Perth Basin, Western Australia. Western Australia Geological Survey, Record 1982/2.

White, K. and Comer, S., 1999. Capel River action plan. Geographe Catchment Council -Geocatch- and the Capel Land Conservation District Committee.

Whitehouse, J., 2007. Evaluation of mineral resources of the continental shelf, new South Wales. Q. Notes 124, Geol. Surv. New South Wales, 23.

Whiteley, R. J. and Stewart, S. B., 2008. Case studies of shallow marine investigations in Australia with advanced underwater seismic refraction (USR). Exploration Geophysics, 39, 34–40. doi: 10.1071/EG08009

# Chapter 6

# Materials and Methods

"Measure what is measurable, and
make measurable what is not so."
(Galileo Galilei)

This section is a discussion of the equipment utilised during this thesis; a greater emphasis has been given to the geophysical methods as they constitute the main source of data used in each study area.

Table 6.1 summarises the equipment used in each study area.

**Table 6.1. Investigation methods used for each study area.**

| Data / Study area | Seismic data | | | Ground truth data | Remote sensing |
|---|---|---|---|---|---|
| | Geophysical equipment | Navigation system | Processing and Interpretation Software | | |
| **Shark Bay** | Innomar SES-2000 Compact | DGPS SOKKIA GSR2650 LB (using OmniSTAR service correction) | ISE 2.9 | Coring | High-resolution aerial photographs and orthophotos |
| **Kimberley Reef** | AA201 boomer system (Applied Acoustic Engineering Limited) | Dual frequency DGPS | SonarWiz 5 | Grab sampling | NA |
| **Swan River** | AA201 boomer system (Applied Acoustic Engineering Limited) | Hand-held GARMIN eTrex GPS | SonarWiz 5 | Coring | NA |
| **Geographe Bay** | AA201 boomer system (Applied Acoustic Engineering Limited) | Trimble NetR9 Global Navigation Satellite System (GNSS) positioning system | SonarWiz 6 | Grab sampling | High-resolution marine LiDAR bathymetry |

## 1. Geophysics and geophysical methods

The term geophysics has been defined in many ways, using numerous approaches. Sheriff, in his Encyclopedic Dictionary of Applied Geophysics (2002), provided one of the most broad and commonly used definitions: "*Geophysics is the application of physical principles to studies of the Earth*". This terminology embraces several branches, like seismology, geothermometry, gravity, geodesy, magnetism, physical oceanography, meteorology, geochronology, etc.

In this thesis, the term *geophysics* has a much narrower definition. In particular, geophysics has been used as a complement to geology, to determine the internal structure of a feature beneath the seafloor and provide indications on the nature of the processes that produced the observed conditions (Matzner, 2001).

Geophysical exploration techniques have benefits and limits. It is possible to measure physical properties and remotely make observations about the vertical and

lateral distribution of subsurfacial changes. These measurements are generally minimally invasive, relatively quick and more cost-effective and versatile than direct sampling and analysis (like drilling boreholes and cores. Mussett and Khan, 2000). The amount of acquired data is higher, thus subsurface anomalies and local features are more likely to be identified (Benson, 2005). In addition, geophysical techniques can be employed in a wide range of investigations, at different scales and studies, from crustal and upper mantle investigations to local engineering, environmental or archaeological surveys (Kearey et al., 2002). However, geophysical methods have some limitations: they provide evidence only of the present conditions (with the exception of geochronology and palaeomagnetism. Mussett and Khan, 2000); since they measure physical properties, a target, a specific geological feature or a geophysical anomaly cannot be detected if there is no measurable contrast with the background conditions or they are too small (Benson, 2005). In geophysical surveying, the interpretation of the data contains a certain degree of ambiguity, the conclusion can be non-unique (Kearey et al., 2002) and can suffer from noise or artefacts. Despite the intrinsic uncertainty in the interpretation, these survey methods represent an important tool in geological research (Kearey et al., 2002).

The choice of a geophysical device is not standard but mainly site specific and linked to the scope of work. When planning a survey, it is crucial to choose the correct methods, taking into consideration the local conditions (geology, oceanography, physical parameters, logistics, etc.) and the features that have to be investigated (size, depth, resolution, etc. Benson, 2005; Felix et al., 2013). Where possible, different geophysical technologies are used in combination, in a number of stages, and also complemented by geological studies (ground truth, such as bore holes and coring), to enhance the investigation and reduce the ambiguity that may arise with only one method (Mussett and Khan, 2000; Kearey et al., 2002; Murray et al., 2005).

Geophysical methods are generally classified as *passive* or *active*. Survey techniques included in the first group utilise natural fields of the Earth (gravitational, magnetic, electrical and electromagnetic fields) to search for buried geological features. Active methods require an artificially-generated energy source to provide information on the near-surface or deep geology (Kearey et al., 2002).

Each technique measures a specific physical property that allows the detection and characterisation of a particular geological feature (Kearey et al., 2002). Table 6.2 summaries various common geophysical methods, outing the physical parameters and properties measured during the study, the range and the main field of application. The investigation depth varies greatly with respect to the operation.

**Table 6.2. Selected geophysical methods, related physical properties and commercial applications (from van Blaricom, 1992; Hoover et al., 1995; Kearey et al., 2002). A: active; P: passive.**

| Method | | Physical parameter measured | Relevant physical property | Typical source of anomaly | Depth of investigation | Applications | |
|---|---|---|---|---|---|---|---|
| | | | | | | Direct detection | Indirect detection |
| Seismic | *Reflection (A)* | Travel time of seismic waves<br>Seismic energy | Velocity of P and S waves<br>Dynamic modulus | Contrasts of density and velocity<br>Markers at variable depth<br>Fissured rocks | All | Buried channels<br>Faults<br>Basement topography | Heavy minerals<br>Oil<br>Underground fluids |
| | *Refraction (A)* | | | | | | |
| **Gravity (P)** | | Variations in Earth's gravity field (vertical attraction of anomalies and gravitational field gradient) | Density | Rock density contrasts | All | Deposits of heavy ores<br>Salt domes<br>Basement rocks | Karstic cavities<br>Structures<br>Basement topography |
| **Magnetic (P)** | | Gradient of Earth's magnetic field | Magnetic susceptibility and remanent magnetisation | Contrasts of magnetisation or remanence contrasts<br>Magnetite content of the minerals | Surface to Curie isotherm | Magnetite<br>Pyrrhotite<br>Titano-magnetite | Iron and copper ores<br>Kimberlites<br>Chromite |
| Electrical | *Resistivity (A)* | Vertical and lateral variation of the electric field | Resistivity | Lateral or vertical variations in resistivity<br>Faults, shear zones<br>Conductive veins, sedimentary layers, volcanic intrusion | About 2 km | Massive sulfides<br>Oil shales<br>Clays<br>Geothermal reservoirs | Bulk material<br>Base metals |
| | *Induced polarization (A)* | Decay of voltage in the ground and resistivity changes | Interface ionic and electronic conduction | Metallic lustre minerals and pore water | About 2 km | Conductive material (sulfides, oxides) | Associated minerals (zinc, gold, silver…) |
| | *Self-potential (P)* | Natural potentials | Conductivity<br>Oxydability | Mineralization differences, ground water flow, electro-chemical action, geothermal | A few hundred meters | Sulfides (pyrite, copper)<br>Mn ore | Associated minerals (zinc, gold, lead…) |
| | *Electro-magnetic (A)* | Dependent on method; ratio of electric and magnetic fields | Conductivity and inductance | Lateral or vertical changes in Earth conductivity | From shallow to deep (10 m – 10 km) | Conductive material (sulfides, oxides) | Kimberlites<br>Associated minerals (nickel, lead…) |

## 1.1. Geophysical methods used at sea

The two most common marine seismic techniques used are *seismic refraction* and *seismic reflection*. In both methods, the time elapsed between a generation of a sound event, emitted by a sound source, and its reception (sensed by a receiver) is recorded (Lekkerkerk et al., 2006). The main difference between the two methods is that in refraction surveys, the times recorded represent the difference between the first and the following arrivals, corresponding to the time that the acoustic waves take to travel through the sedimentary substrata and back to the receiver; whereas in reflection surveying, the time values that are measured correspond to the interval between the sound wave generation and the signal arrival at the receiver, after being reflected by subsurface layers.

During this research work two types of seismic equipment that measure reflected waves have been employed.

In Shark Bay, where higher resolution images, particularly in the shoal areas, were required, a nonlinear (parametric) sub-bottom profiler (SBP) was used. In the other study areas (the Kimberley, Swan River and Geographe Bay), a boomer SBP system was employed, providing a much deeper penetration with a partial loss of resolution.

Both the SBPs were run at typical survey speeds of 3-5 knots (5.5-7.41 km/h) and the survey run lines were devised to capture a broad range of sub-seafloor architecture and geomorphological structures. Tracks parallel to the coastline revealed the location and width of features such as buried palaeochannels. Orthogonal profiles allowed the growth direction of morphological elements, like reefs or sandbars, to be captured and permitted their correlation during the interpretation of acoustic horizons and creation of a three-dimensional perspective of the acoustic units' framework.

### *Nonlinear (parametric) SBP*

In Shark Bay, the seismic survey was carried out using a nonlinear (parametric) SBP SES2000 Compact System (Innomar Technologie GmbH;Rostock, Germany), mounted vertically on the port side of the survey vessel.

A nonlinear (parametric) SBP combines the parametric effect with high frequency echo sounding. The parametric effect occurs when two slightly different sound frequencies f1 and f2 (called *primary frequencies* $f1<f2$; $f2/f1\approx1$) are broadcast at the same time, at high pressure; the transmitted acoustic waves then interact in the water, generating a new frequency $F=|f2-f1|$, called a *secondary frequency* (Wunderlich and Müller, 2003).

The primary frequency f2 used during the Shark Bay survey was about 100 kHz and determined the water depth, as the seismic signal did not penetrate the seabed. The secondary frequency (adjustable 5, 6, 8,10,12,15 kHz) was instead low enough to penetrate the sediment, up to a depth of about 10-15 m (Figure 6.1).

Using Innomar ISE (Interactive Sediment Layer, version 2.9) software, the seismic profiles were later post-processed to improve the signal to noise ratio (S/N). The first step was *bottom tracking* to digitise the seafloor reflector and represents the altitude of the receiver from the sea bottom (essentially the water depth). Next, standard signal processing procedures, such as bandpass filter and application of an automatic gain correction algorithm, enhanced the contrast within the seismic profiles. Sub-bottom horizons were then digitised with manual picking and identified based on their acoustic properties.

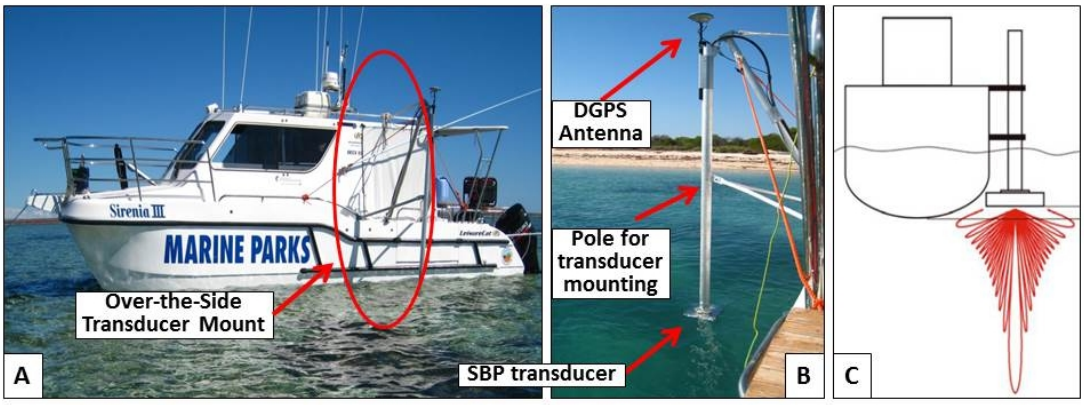


**Figure 6.1. A: Sub-bottom Profiler Innomar SES-2000 Compact system mounted "over the side". B: salient characteristics of the SBP installation. The DGPS used was a SOKKIA GSR2650 LB (with OmniSTAR service correction). C: The transducer has a small beam-width, which combined with a high frequency-bandwidth and absence of side lobes, results in a better bottom detection with a lower signal to noise ratio (Wunderlich and Müller, 2003. Modified) The SBP system consists of a main system unit with a transducer array used as non-linear transmitter and linear receiver of the signals.**

### *Boomer SBP system*

In the Kimberley, Swan River and Geographe Bay, the seismic data were acquired using an AA201 boomer system (Applied Acoustic Engineering Limited, Great Yarmouth, UK), comprising an energy source (CSP-P 300) and a sound source (AA201 Boomer Plate), mounted on a surface tow catamaran. An 8 element hydrophones streamer was employed as receiver (Figure 6.2).

Conversely from the nonlinear (parametric) SBP, the boomer is a separate source/receiver system. The boomer uses an electromechanical capacitor bank (energy source) to discharge high-voltage power that makes an electrical coil, located in the boomer plate, contract and create a mechanical sound pulse (Applied Acoustic Engineering, 2006). This sound energy consists of short pulses emitted at regular intervals, with a frequency between 500 Hz and 10 kHz. It travels through the water and the sediment and is reflected back when a change in the physical character is encountered, especially density (Applied Acoustic Engineering, 2006). The hydrophones receive the reflected sound and convert the acoustic signals into electrical signals, which are digitally recorded in SegY format (Rev 1) and displayed on a laptop, using the acquisition software (SonarWiz, Chesapeake Technology Inc., Mountain View, CA. Figure 6.2).

Various positioning systems were employed to obtain and record position (Table 6.1), by interfacing the receivers to the acquisition workstation, broadcasting a NMEA string to the geophysical software. A real time quality control was done on-board.

SonarWiz was also employed as post processing software. As with the nonlinear (parametric) SBP, the seismic profiles were post processed to improve the S/N ratio, by applying standard signal processing procedures, followed by tracking of relevant acoustic reflectors.

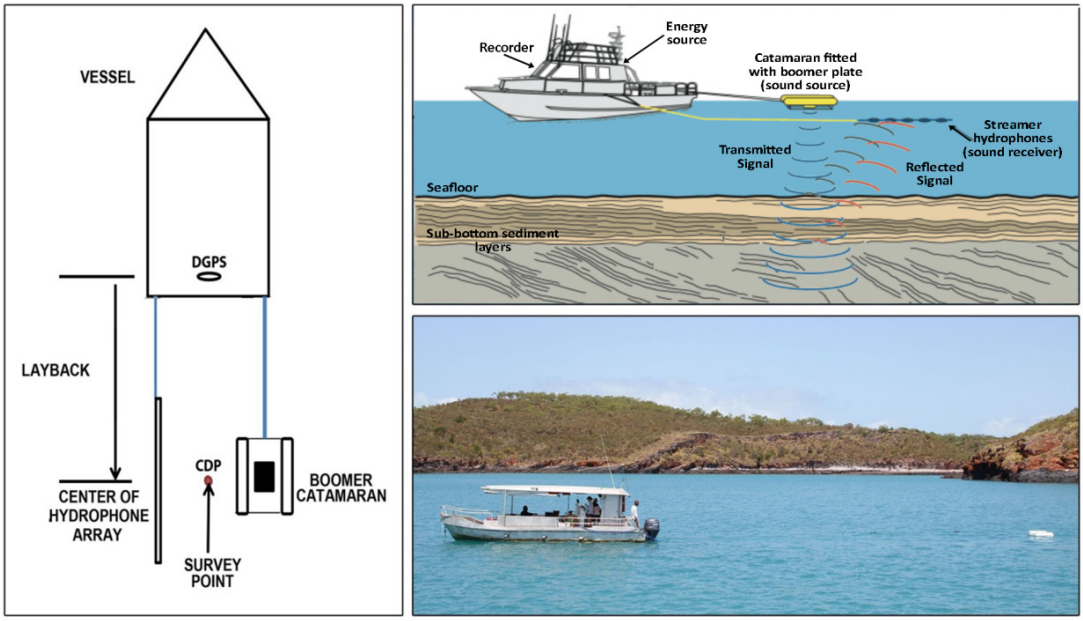


**Figure 6.2. Left: Boomer SBP survey schematic set up (from Applied Acoustic Engineering, 2006; modified); Bottom right: survey operations in the Kimberley. Top right: schematic survey operations showing sound waves from sound source (boomer plate) reflected by sub-bottom sediment layers and received by sound receiver (streamer hydrophones). From: https://coastal.er.usgs.gov/capabilities/shipboard/sonar/profiling.html (modified).**

# 2. Ground truth data

## 2.1. Vibracoring

A vibracorer system was used to take 32 sediment cores along the Faure Bank (Chapter 3).

In a vibracorer, the force of gravity is the main driver and the vibrating mechanism enhances the core tube penetration into the seafloor by liquefying a thin layer of the sediment in the immediate vicinity of the core cutter, allowing the core tube to enter the substrate (http://www.vibrocoring.com/VCconcepts.html). When the core cannot penetrate further, the vibracorer is stopped and the tube is extracted with the aid of a one-way, tulip-style core catcher that prevents sample loss. After the recovery, the core liner is removed and the core is cut into 1-m sections for on board transportation (Figure 6.3 and Table 6.3 Skene et al., 2004). This system allows a potential recovery of up to 6 m of undisturbed, *in situ* sediments for each core, giving an accurate representation of the sub-surficial sediment stratification.

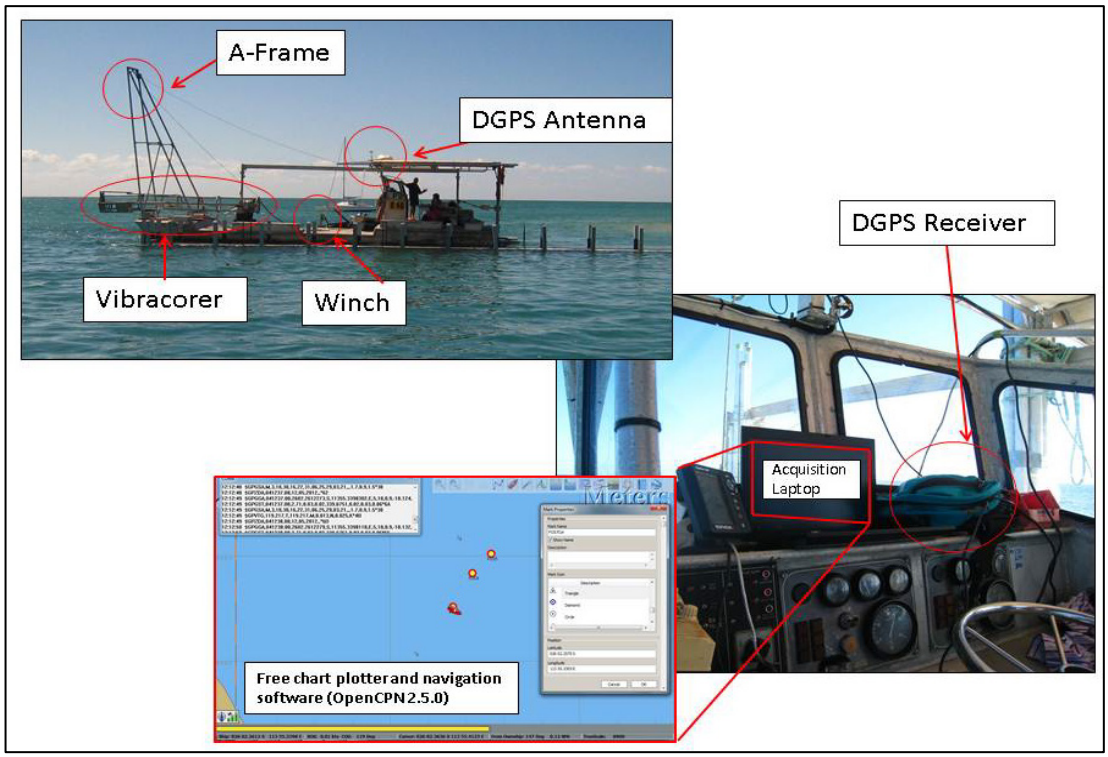


**Figure 6.3. Photo of the 13.5 m work pontoon P2 used for the survey, with configuration of the equipment.**

The following table summarises the steps performed for coring.

**Table 6.3. Coring steps.**

| Step | Description | Figure |
|---|---|---|
| 1 | Attach the barrel to the head, within the coring frame. |  |

| | | |
|---|---|---|
| 2 | Raise the rig from the deck and deploy over the stern.<br><br>A number of guide ropes, attached to the tower, stabilise the system during deployment. | 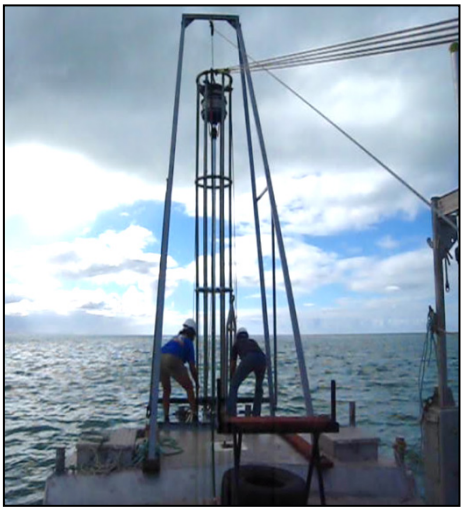 |
| 3 | Disconnect crane hook from vibracorer and deploy and secure the legs. | |
| 4 | Lower the tower into the water to allow the frame to fill with water. |  |
| 5 | Deploy and adjust the necessary length of electric cable. | |
| 6 | Allow the tower to stabilize on the seafloor in a vertical position. In softer substrates the core could start to penetrate just with the weight of the head.<br><br>Record the coordinates and the water depth at the spot.<br><br>When the gravity penetration stops, the vibracoring operation can start. | |

<table>
<tr><td>7</td><td>Turn on the generator (220 VAC 3-phase, 5 kVA required), attached to the switch gear and the vibracorer head through watertight marine connectors.<br><br>Switch on the control box.<br><br>Activate the vibration through the circuit breaker unit.<br><br>The operator can determine the progress of the penetration with the assistance of foam floating indicators attached at 1.5, 3.0 and 4.5 m to the electric cable.</td><td rowspan="2">  </td></tr>
<tr><td>8</td><td>Monitoring the vibration time and length of the supplied cable, the operator can determine when the barrel stops penetration and end the vibration as soon as possible.</td></tr>
<tr><td>9</td><td>Raise the vibracorer to the surface and collapse and secure the legs.</td><td rowspan="2">  </td></tr>
<tr><td>10</td><td>Lift, rotate and lower vibracorer back on deck.<br><br>The barrel is then removed from the tower.</td></tr>
<tr><td>11</td><td>Carefully examine the barrel:<br><br>- a scour left by the gate at the base of the tower gives information to determine the depth of the penetration.<br>- some residual material can be used to predict the type of sediment cored.</td><td>  </td></tr>
</table>

| | | |
|---|---|---|
| 12 | Label the core and way up, note down the status of the core catcher (open / closed, empty / full, dented, inverted...), cut away the empty barrel, measure and record the penetration and the initial recovery (allowing for the core catcher). | 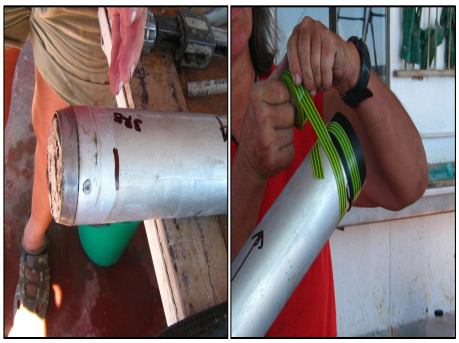 |
| 13 | Close the ends with a cap and electrical tape (yellow and green at the top of the core and white, blue or red at the bottom). | |
| 14 | Secure the core in vertical position to drain, decoupling it from the vessel using rubber, bubble wrap and ropes between the steel-to-steel connection in order to prevent disturbance from the vibrations of the vessel while moving. This step must be done as soon as possible after the collection. |  |
| 15 | At the end of the day, carefully transfer the cores to a steady place. | |

## 2.2. Seafloor sediment sampling

A pipe dredge was used to collect unconsolidated surficial sediment samples in Geographe Bay and in the Kimberley.

## 2.3. Laboratory procedures

*Core processing*

Each section of core was cut longitudinally, split into two halves and photographed. Core logging included an evaluation of colour using the Munsell Soil Chart (Munsell, 1954), bioturbation, texture and composition of the lithology and a record of any major stratigraphic changes. Finally, samples were collected from one half of the core, leaving the other one as an archived reference.

*Sediment analysis*

The sediment samples were dried and sieved using a mechanical shaker according to the Udden-Wentworth scale (Wentworth, 1922) over 63 µm, 125 µm, 250 µm, 500 µm, 1 mm and 2 mm, and examined using a stereoscopic light microscope (Leica EZ4). Analysis of the sediments included an evaluation of colour (Munsell 1954), estimation of shape (roundness/sphericity of individual grains) and identification of the mineral and biogenic components.

### *Radiocarbon dating*

The radiocarbon dating was carried out by the Australian National University-Radiocarbon Dating Centre for the Shark Bay project. One species of foraminifera (*Amphisorus hemprichii*, Ehrenberg, 1839) was targeted and picked for dating. Fallon et al. (2010) recommended 20 mg of sample as minimum weight required for dating. Reworked, abraded or micritised specimens were excluded, since they could lead to unreliable dates and outliers in data. The ages in radiocarbon years were obtained using a Libby half-life of 5568 years and following the conventions of Stuiver and Polach (1977). The curve Marine-09 was used as calibration dataset to convert conventional ages into calibrated years, assuming a delta R of 70±50. The marine calibration incorporates a time dependent global ocean reservoir correction of about 400 years (Stuiver and Reimer, 1993; Stuiver et al., 2005).

### *X-Ray Diffraction*

For the Shark Bay project, X-Ray Diffraction (XRD) Phase / Mineral Identification and Quantification were also undertaken. Samples were prepared by powdering a small quantity of sediment. Then, 0.3 g of standard (Corundum: $Al_2O_3$), assigned by the XRD laboratory was added to a representative amount of sample, equal to 3 g. Prepared samples were then micronised for 5 minutes, using a micronizing machine (McCrone Micronizing Mill) with ethanol as a grinding agent. Samples were washed out into porcelain cups to dry (Huntington et al., 2004). Each micronised sample was packed into sample holders for analysis in the diffractometer (Bruker AXS D8).

## 3. Remote sensing

The Faure Sill was mapped using high-resolution (50 cm/pixel) aerial photographs and orthophotos from Landgate (provided by the Department of Environment and Conservation, DEC, Western Australia), at scale 1:25,000, using a GIS Software (Geographic Information System; ArcGIS, Esri).

High-resolution bathymetric composite images (supplied by the Department of Transport, Western Australia) was used for the Geographe Bay study, where the main geomorphological features of the seafloor were manually outlined at scale 1:10,000, using ArcGIS Desktop 10.5. The datasets had a horizontal sounding density of 5 m x 5 m and covered the nearshore seafloor, up to about 30 m of water depth.

## References

Applied Acoustic Engineering, 2006. Fundamentals of high resolution shallow seismic surveying-CSP-1000-8005/1.

Benson, R. C., 2005. Remote sensing and geophysical methods for evaluation of subsurface conditions. In: Practical Handbook of Environmental Site Characterization and Ground-Water Monitoring, Nielsen, D. M. (Ed.). CRC Press, Florida.

Fallon, S.J., Fifield, L.K., Chappell, J.M., 2010. The next chapter in radiocarbon dating at the Australian National University: Status report on the single stage AMS, Nuclear Instruments and Methods in Physics Research. B 268 898–901.

Felix, C. A., Martins, T. S., Soares, C. H. C., Guesser, V., Demarco, L. F., Suthard, B., ... & de Mahiques, M. M., 2013. Some limitations of shallow water geophysical devices imposed by different oceanographic and geological conditions. In: Acoustics in Underwater Geosciences Symposium (RIO Acoustics), 2013 IEEE/OES (pp. 1-8), IEEE.

Kearey, P., Brooks, M., Hill, I., 2002.An introduction to geophysical exploration, 3rd Edition. Malden, MA, Blackwell Science.

Hoover, D. B., Klein, D. P. and Campbell, D. C., 1995. Geophysical methods in exploration and mineral environmental investigations. In: Preliminary compilation of descriptive geoenvironmental mineral deposit models, Du Bray, E. A. (Ed.). Denver, US Geological Survey.

Huntington, J., Mauger, A., Skirrow, R., Bastrakov, E., Connor, P., Mason, P., Keeling, J., Coward, D.,

Berman, M., Phillips, R., Whitbourn, L. and Heithersay, P., 2004. Automated mineralogical logging of core from the Emmie Bluff iron oxide copper-gold prospect, South Australia. PACRIM 2004 Congress, 19-22 September 2004, Adelaide, South Australia. AUSIMM Pub 5/2004

Lekkerkerk H. J., Van der Velden R., Roders J., Haycock T., De Vries R., Jansen P., Beemster C., 2006. Handbook of Offshore Surveying Volume 2 - Acquisition and Processing, London Clarkson Research Services Limited

Matzner, R. A., 2001. Dictionary of geophysics, astrophysics, and astronomy. CRC Press, Florida.

Munsell, A.H., 1954. Munsell soil color chart. U.S. Dept. Agriculture Soil Survey Manual 2009 Edition Munsell Soil Chart (1954)

Murray, C. J., Last, G. V., Truex, M. J., 2005. Review of Geophysical Techniques to Define the Spatial Distribution of Subsurface Properties or Contaminants. Pacific Northwest National Laboratory.

Mussett, A. E. and Khan, M. A., 2000. Looking into the Earth. Cambridge: Cambridge University Press.

Skene, D., Ryan, D. and Brooke, B., 2004. Sub-bottom Profiling, Surface Sediment Sampling, Vibracoring and Mapping with Sidescan and Multibeam Sonar Systems in

the Fitzroy River Estuary and Keppel Bay. Coastal CRC Coastal Water Habitat Mapping Project Coastal Geomorphology Subproject, Milestone Report CG04.01.

Sheriff, R. E. 2002. Encyclopedic Dictionary of Applied Geophysics, 4th Edition. Society of Exploration Geophysics. Tulsa, OK.

Stuiver, M., and Polach, H. A., 1977. Discussion: Reporting of $^{14}C$ data, Radiocarbon 19: 355-363.

Stuiver, M., and Reimer, P. J., 1993. Extended $^{14}C$ database and revised CALIB radiocarbon calibration program. Radiocarbon 35:215-230.

Stuiver, M., Reimer, P.J., Reimer, R.W., 2005. Calib 5.0 WWW program and documentation. URL: http://radiocarbon.pa.qub.ac.uk/calib/.

van Blaricom, R., & Northwest Mining Association (Eds.), 1992. Practical geophysics II for the exploration geologist. Northwest Mining Association.

Wunderlich, J., Müller, S., 2003. High-resolution sub-bottom profiling using parametric acoustics. Conference abstract. International Ocean Systems 2003.

# Chapter 7

# Discussion

"There are no facts,
only interpretations."
(Friedrich Nietzsche)

## 1. Introduction

Chapters 2 to 5 report the analysis and outcomes of four investigations carried out on selected sedimentary systems along the WA coast and inner shelf. The factors and processes that have influenced the Late Quaternary evolution of each marine (or estuarine) area are also reported.

The purpose of this chapter is to review and compare the results obtained from these local patterns, find controlling parameters and draw general considerations about the Late Pleistocene and Holocene development of Australia's Indian Ocean continental shelf and coast, from Geographe Bay to the Southern Kimberley.

Table 7.1 reports the main observations of the controlling mechanisms from each area analysed during this doctorate thesis. Comparing the leading factors in controlling the regional evolution of each sedimentary system, it appears evident that coastline development has been controlled by:

- Late Pleistocene and Holocene sea level fluctuations,
- Pre-existing topography,
- The local physical characteristics and processes.

**Table 7.1. Summary of main mechanisms involved in controlling the evolution of sedimentary systems analysed in Chapters 2 to 5.**

| Study area | Controlling mechanisms | | |
|---|---|---|---|
| Kimberley | Sea level fluctuations | Pre-existing topography | Macrotides and metocean conditions, turbidity, climate |
| Shark Bay | Sea level fluctuations | Pre-existing topography | Seagrass, metocean conditions, climate |
| Swan River | Sea level fluctuations | Pre-existing topography | Estuary physical characteristics (waves) |
| Geographe Bay | Sea level fluctuations | Pre-existing topography | Waves and winds, currents, seagrass |

In the following sections, I will discuss in detail the importance and the implications that each mechanism had in controlling the local environments.

# 2. Controlling mechanisms

## 2.1. Sea level fluctuations

Since the end of the Penultimate Glaciation (marine isotope stage MIS 6), the Western Australian continental shelf has experienced a rapid marine transgression (MIS 6 to MIS 5e), a gradual regression (MIS 5e to MIS 2) and a second rapid transgression (MIS 2 to 1. Figure 7.1). About 7,000 years BP, the global sea level stabilised in a relatively high position that has persisted until the present time. These sea-level fluctuations had a major role in modelling the geomorphology along the WA coast and continental shelf, controlling bathymetric and sedimentological (mineralogical and granulometric) features, resulting by the sediment reworking, which includes weathering, transport, deposition, storage, lithification.

Western Australia can be considered tectonically relatively stable since MIS 5e (Szabo, 1979; Stirling et al., 1995; Baker et al., 2005, Collins et al., 2006; O'Leary et al., 2013). Although a minor tectonic uplift (~1.0 m around Cape Cuvier, coordinates: 24°13′ S 113°22′ E. O'Leary et al., 2008; O'Leary et al., 2013) and subsidence (0.12 m/ky in the Southern Kimberley. Solihuddin et al., 2015), occurred since the Last Interglacial period (MIS 5e), it can be assumed that tectonic displacements are negligible in terms of influencing the height of the shoreline.

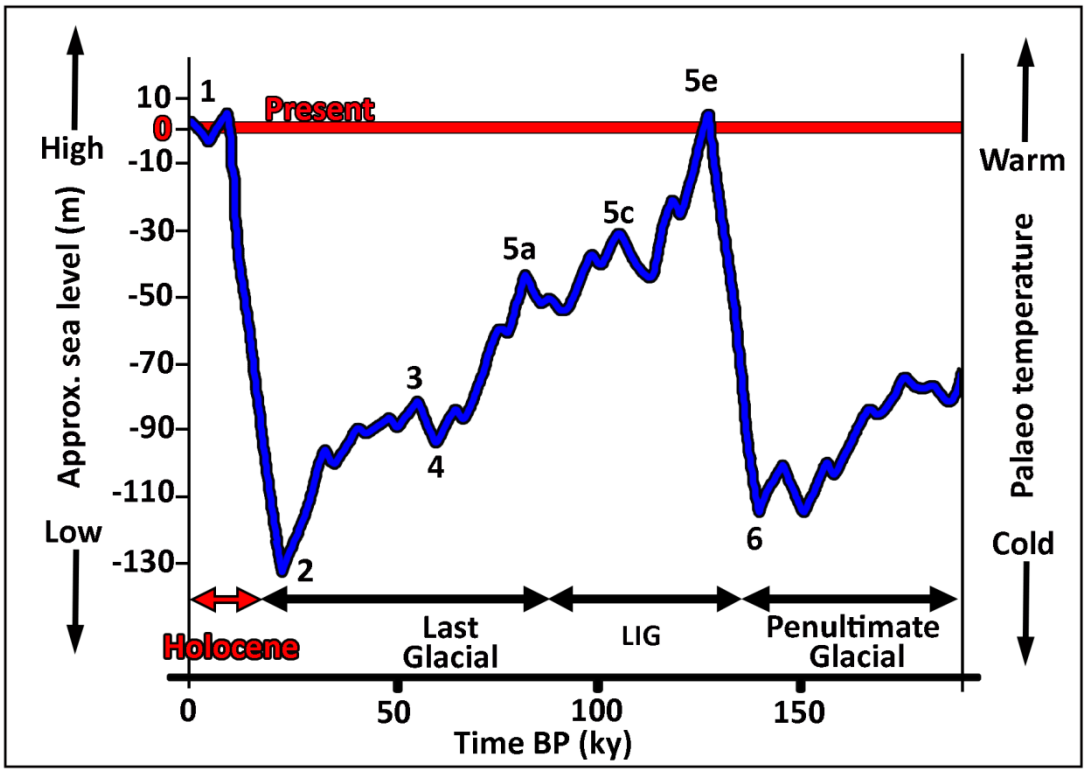


**Figure 7.1. Sea-level curve in the past ~200 ky, for Western Australia. Odd numbers refer to Interglacial Marine Isotope Stages (MIS) and even numbers indicate the Glacial MIS. The curve is based on oxygen isotope ratio $\delta^{18}O$ (modified after Saqab and Bourget, 2015 and Bufarale et al., 2017).**

### *2.1.1. Marine transgression: from MIS 6 to MIS 5e*

Defining the position of the sea level during the Penultimate Glacial Maximum (PGM, *MIS 6*) is challenging, due to the scarcity of available evidence (Murray-Wallace and Woodroffe, 2014; Rohling et al., 2017). Data from different studies, mainly based on oxygen isotope analysis, seem to agree that during the PGM the sea level was about 125 (±10) m lower than the present, comprising two sea level minima at ~155 and 140 ky BP (see Figure 7.1. Shackleton, 1987; Chappell et al., 1996; Rohling et al., 1998; Lambeck and Chappell, 2001; Rabineau et al., 2006; Hill et al., 2009; Rohling et al., 2017). In WA, there are several terrestrial examples of deposits and geomorphological features dated back to MIS 6, including the southernmost pinnacles in Nambung National Park (250 km north from Perth), belonging to the *Pinnacles Desert Member* of Tamala Limestone (Lipar and Webb, 2014; Lipar and Webb, 2015) and two aeolianite dunes in southern Kings Park (metropolitan Perth, Brooke et al., 2014). Conversely, there is a lack of literature dealing with marine examples of geomorphological evidence attributable to the PGM sea level lowstand in Western Australia, as indicators of palaeo-sea level (i.e. palaeoshoreline) are located along the continental shelf, in deep water, or have been eroded in successive time (i.e. during the Last Glacial Maximum. Figure 7.2).

Lipar et al. (2017), based on an extensive analysis of aeolianites, calcretes, microbialites and palaeosols, determined that during MIS 6, the South West climate was about 4-8 °C cooler and dryer than the present. Quantitative information on river discharges is scarce (or absent), as explained above, and this allows only a speculative glance on the sedimentary processes that could have characterised this period of time. In a glacial and dry climate, it is likely that a fluvial role in sediment supply across the shelf was of secondary importance (as noted in similar conditions by Carter and Manighetti, 2006; Bayram et al, 2007). Along south and central WA (up to Ningaloo Reef; coordinates: 22°33’ S and 113°48’ E), limited width and considerable average steepness of the submerged shelf (< 1:500, with the 100 m contour located ~ 50 km offshore) were present, with river mouths and deltas located close to the upper slope. In these conditions, it is likely that the sediment load bypassed the continental shelf, being discharged further out than at present. At lower latitudes, in northern WA, the continental shelf was wider, gently falling westward (slope angle > 1:1000). In dryer than the present-day conditions, the rivers were much smaller, flowing on exposed continental shelf and discharging their reduced sediment load nearshore, with oceanic and wind-driven currents being the major contributor to sediment distribution across the shelf. With low slope and low rainfall, it is also likely that some rivers might not have been large enough to cross the whole extensive shelf, terminating inland (internal drainage systems).

The end of the PGM (*MIS 6/5e* or *Termination II*) saw a rapid rise of the sea (from glacial collapse melting, mainly in the northern hemisphere. Gallup et al., 2002; Siddall et al., 2006) that also inundated the WA continental shelf. Several studies indicate that by 134 ky BP, the sea level increased about 100 m, standing between 4 and 12 m below the present (in Houtman Abrolhos and Grand Bahamas Islands, respectively. Zhu et al., 1993), with the final 70-80 m of rise, occurring in only 2-5 ky (Raymo, 1997; Broecker and Henderson, 1998; McCulloch, and Esat, 2000). The sediments that were deposited along the exposed continental shelves in subaerial,

lacustrine and riverine settings started to become submerged, in an increasingly deep marine environment (Emery, 1968). Transgressive erosion of relict sediments must have taken place as the water progressed landward, followed by remobilisation and transport of the deposits, under the influence of marine currents and waves (Cattaneo and Steel, 2003).

Due to global temperatures slightly higher than the present (0.5° to 2.0°C. Montoya et al., 2008; O'Leary et al., 2013), coral reefs started to colonise along most of the coast of WA, as far south as Rottnest Island (~10 km offshore Perth. Szabo, 1979; Playford, 1988), likely a result of a stronger Leeuwin Current (Collins et al., 2003; Wywroll and Miller, 2001).

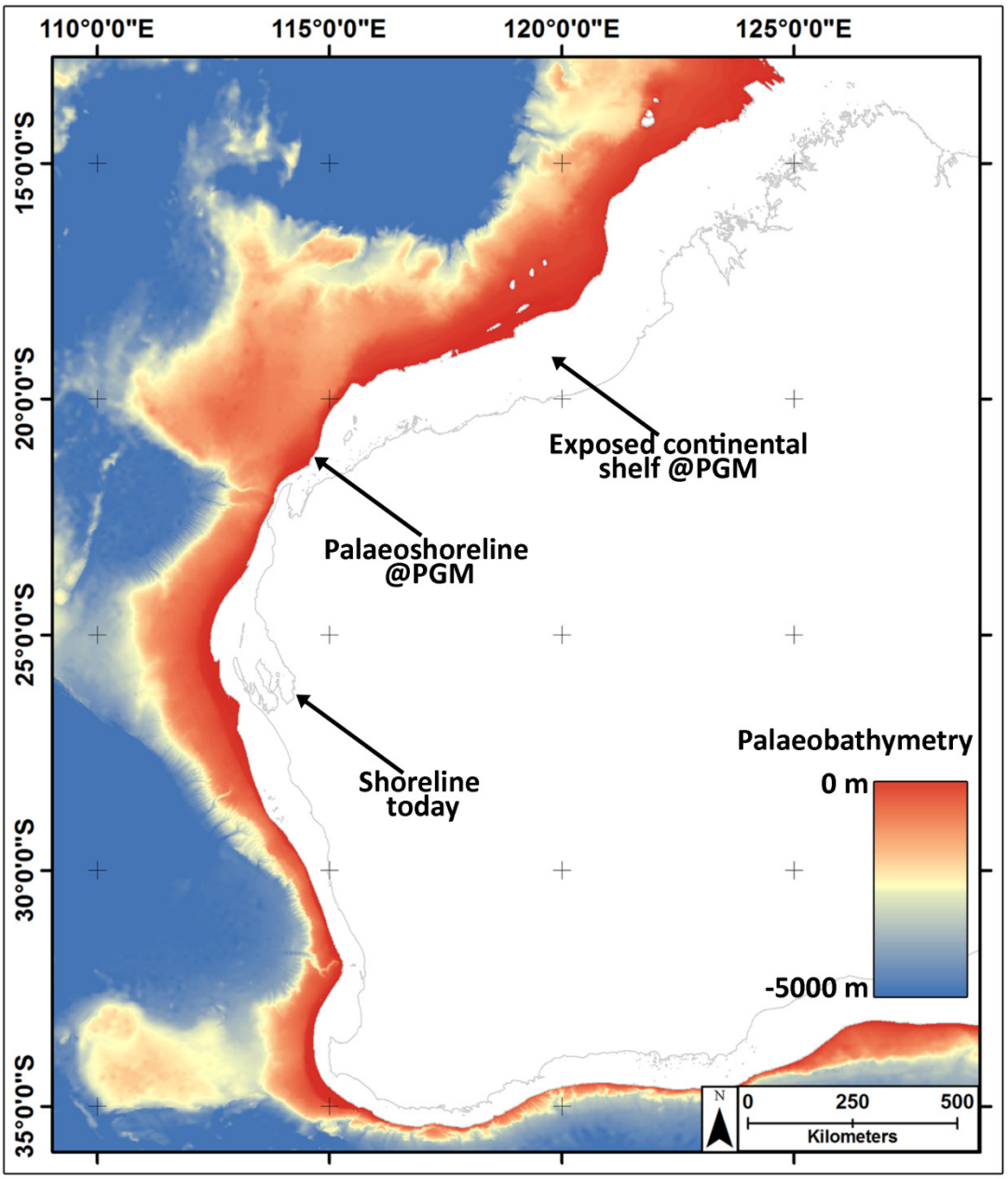


**Figure 7.2. Bathymetry of the WA coast and shelf during the PGM. Note, the palaeoshoreline corresponds to the ~125 m isobath in present time.**

### *2.1.2. Sea level highstand: Last Interglacial (LIG)*

The penultimate marine transgression terminated around 130 ky ago, when the sea level reached a relative stability, at 2 to 3 m above the present level, until 125 ky BP (Hearty et al., 2007). As WA can be considered a relatively stable "far field", the height of the sea level is not influenced by isostatic or tectonic movements, but linked mainly to the eustatic changes. During the LIG, it is estimated that the average global temperature was up to 2°C warmer than the present, enough to partially melt the West Antarctic and Greenland ice sheets and cause a significant rise of seas and oceans (O'Leary et al., 2013). After a minor regression, around 124 ky ago, the sea level started rising again, reaching a maximum around 121-119 ky BP, when the global mean sea level (MSL) peaked about 7-9 m higher than today (Hearty et al., 2007; O'Leary et al., 2013). In most of WA, there are several geomorphic features that provide indications of this past sea-level position (i.e. coral reef terraces, bioerosional notches, beach facies). Some of these structures are now exposed onshore, hence not part of the investigation. For instance, in Cape Cuvier, two distinct marine terraces (3 to 5.5 m and 5.5 to 10.5 m above the present sea level) record LIG sea level highstands (O'Leary et al., 2008). In Shark Bay, several investigations revealed the presence of widespread coral reefs during the LIG (i.e. Zhu et al., 1993; Stirling at al., 1995; Stirling at al., 1998; Hearty et al, 2007; O'Leary et al., 2008). With sea levels much higher than today, the hydrodynamic conditions of the Bay were not restricted as they are presently and the open marine settings (no hypersalinity) resulted in extensive coral reef development (O'Leary et al., 2008). Further south, in the Houtman Abrolhos Islands, Zhu et al. (1993) and Eisenhauer et al. (1996) described framestone facies at 6 m above the present sea level, dated ~124 ky BP. In addition, dating from emergent fossil corals reefs and shallow-water estuarine sediments (~+2.5 m above sea level) in Rottnest Island and in Minim Cove (Perth), respectively, indicates a LIG-MIS 5e age (Hearty, 2003; Murray-Wallace and Kimber, 1989; Brooke et al., 2014).

LIG deposits have been also found in the seismic profiles and sedimentological information collected in Shark Bay and in the Kimberley.

During the coring survey carried out in Shark Bay, the Late Pleistocene substrate, in particular the marine phase of *Bibra Limestone* (van de Graaff et al. 1983; Hocking et al.1987; Collins and Jahnert, 2014) was cored in 5 locations and has been recorded in seismic sections throughout the entire Faure Sill (Figure 7.3). This formation typically ranges between 0.5 to 1.5 m in thickness, but it reaches 3.5 m near Pelican Island and Nanga Peninsula (Figure 7.3. Refer to Bufarale and Collins, 2015 and Chapter 3 of this thesis for more seismic examples).

From the samples collected during the coring, the grey-to-white sediments belonging to Bibra Limestone are clearly distinguishable from the above Holocene muds and sands. They consist of indurated calcarenite, with bivalves and other shell fragments, foraminifers and sand-size bioclasts. Medium-grained quartzose partially cemented sand is present.

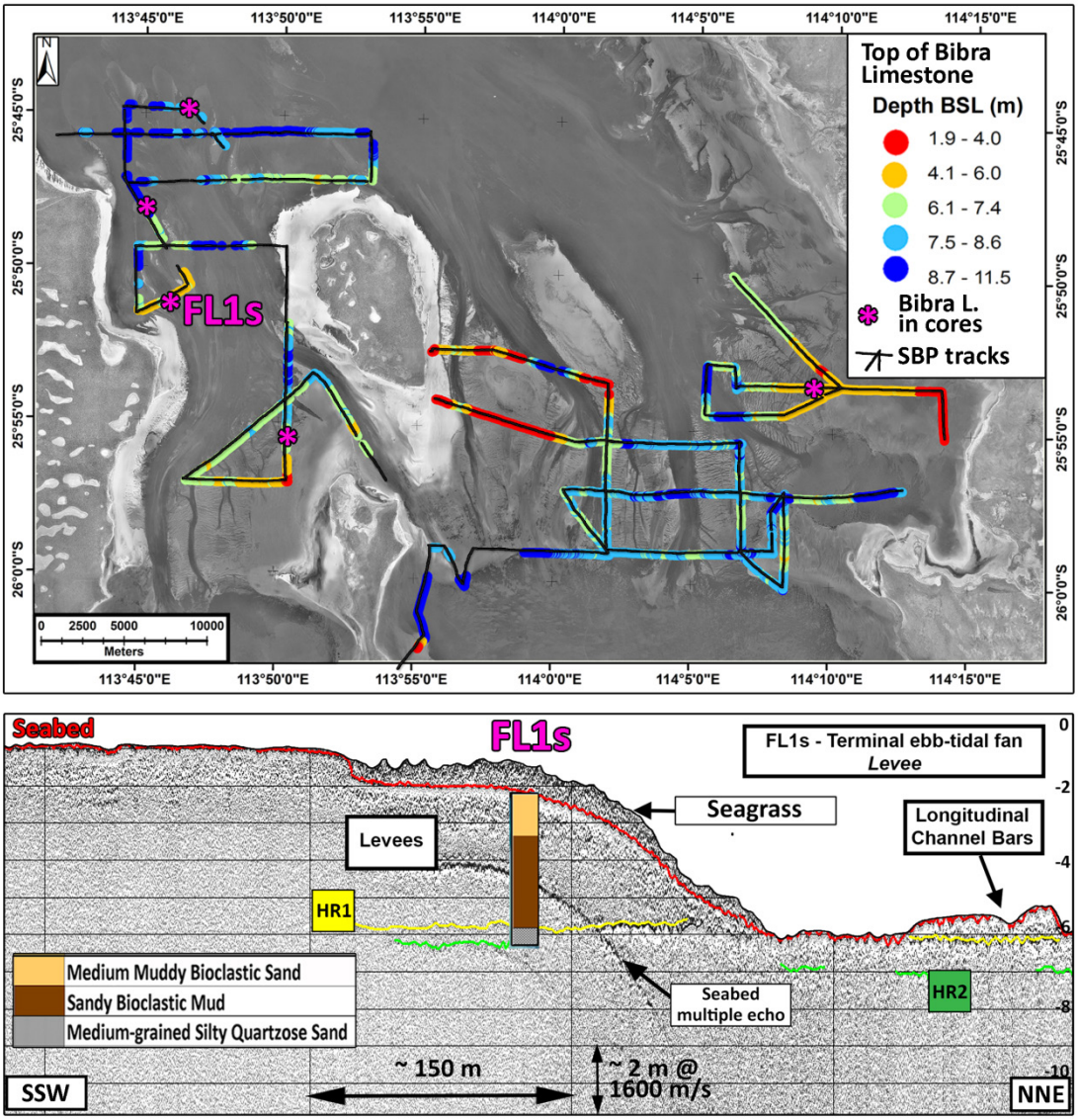


**Figure 7.3. Top: Depth of the top of shallow marine and beach-ridge deposits of Bibra Limestone. Note, the horizon could not be clearly followed through the whole bank. Hence, the gaps between the sub-bottom profiler track are due to lack of recording, multiples, poor imaging, extremely shallow water or potentially uncertain interpretation. The cores where the Late Pleistocene formation was intercepted and sampled are marked with the pink asterisk. Bottom: seismic profile crossing the western flank of a levee in the Dubaut Bank, with superimposed core schematisation. The depths have been measured considering the sound velocity in the sediments as equivalent to 1600 m/s.**

In the Kimberley (Bufarale et al., 2016 and Chapter 2), from the inner shelf (Solihuddin et al., 2015; Bufarale et al., 2016) to the outer shelf (Collins et al. 2011; Solihuddin et al., 2016), acoustic profiles acquired during a high-resolution seismic survey have shown the presence of a strong reflector, marking the basal limits of the Holocene reef. Stratigraphic investigations from the mine pit in Cockatoo Island (Solihuddin et al., 2015), and exploration well log in Adele Island (Solihuddin et al., 2016) have conclusively demonstrated this reflector is the top of a well-developed LIG reef build-up (Figure 7.4).

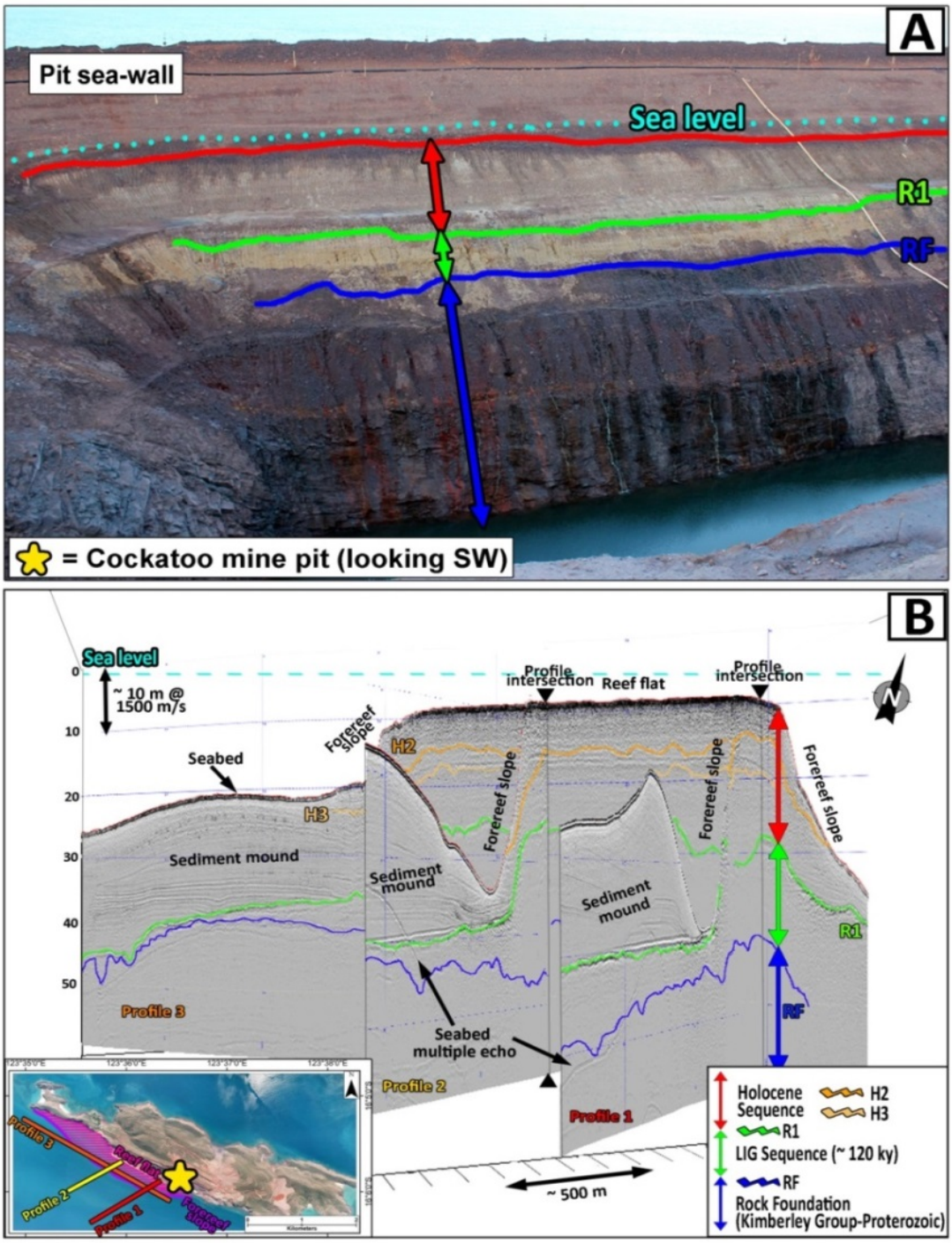


**Figure 7.4. A) Cockatoo mine pit section (Photo credit: Solihuddin T., 2013). Dotted blue line on the retaining sea-wall indicates the modern mean sea level. The sea-wall is a 13 m high structure comprising clay core and rock armour (Solihuddin et al., 2015). B) Intersecting cross-sections (Profiles 1 and 2) and distal longitudinal section (Profile 3) adjacent to mapped mine pit sections of Solihuddin et al. (2015) established position of Proterozoic rock foundation (RF, blue), top Last Interglacial reef (R1, green) and overlying Holocene reef intervals within seismic profiles collected across the fringing reef, SE Cockatoo Island. Depth values are in metres, below the sea level. Insert: location of sections Landgate aerial photography provided by the Department of Parks and Wildlife (DPaW). Modified after Collins et al (2015).**

### *2.1.3. Marine regression: from LIG to Last Glacial maximum*

According to numerous studies, global sea level receded about 140 m from LIG peak to Last Glacial maximum (LGM), dropping from 7-9 m above the modern sea level to ~130 m below the present position (i.e. Shackleton, 1987; Lambeck and Nakada, 1990; Lambeck and Chappell, 2001; Murray-Wallace and Woodroffe, 2014), leaving the continental shelves exposed. This transgression was completed in a little over 100 ky and occurred in several stages (MIS 5, 4, 3 and 2) during which cooler and relatively warm periods alternated, under the influence of an increasingly cold global climate, causing considerable fluctuations of the sea level.

The most reliable estimates of the sea level during this period are mainly derived from coral reef terraces at Huon Peninsula (Papua New Guinea), Barbados and Vanuatu (Chappell and Shackleton 1986; Chappell et al., 1996; Woodroffe and Webster, 2014), where the relatively constant tectonic uplift (about equal to the sea level fall) has allowed the preservation of several metres of reef sequences (Lambeck and Chappell, 2001).

Due to the limited tectonic movements (uplift), *marine* evidence of transgressive stages cannot be studied in modern coastal setting above present sea level, in WA. Despite this, indicators of Late Pleistocene lower sea level stands have been detected in the seismic data, buried below the sea floor.

In contrast with the mentioned scarcity of exposed marine indicators, in WA there are several *terrestrial* landforms that evidence MIS 5 sea level changes. In the mainland, carbonate aeolianites, belonging to Tamala Limestone, extensively developed during the entire MIS 5 (Brooke et al., 2014), with relict coastal dunes occupying the costal landscape, from the South West up to Carnarvon (~ 900 km north from Perth), including Rottnest Island (Hearty, 2003). A widespread development of pinnacles occurred in Nambung National Park during the warm substages MIS 5e, 5c and 5c (Lipar and Webb, 2015).

**MIS 5**

MIS 5 included the LIG (substage MIS-5e: warm, highstand peak) and a series of substages (cold: MIS 5d, 5b; moderately warm: 5c, 5a. Lambeck et al., 2002).

The end of the MIS 5e climatic optimum (~118 ky) was marked by a cooling interval, leading to *MIS 5d* cold stage (Hearty et al. 2007). A rapid regression, coinciding with an insolation minimum, culminated at about 45 m below present sea level (Lambeck and Chappell, 2001; Lambeck et al., 2002; Bianchi and Gersonde, 2002). Reef crests from the Huon Peninsula revealed that from around 105 ky BP the sea level experienced a rise of about 20-25 m in 10 ky (*MIS 5c*. Chappell et al., 1996; Esat et al., 1999; Lambeck et al., 2002). A similar timing for MIS 5c occurrence is confirmed also by Hearty and Olson (2011) from storm deposits in Bermuda. A further substage of regression followed (*MIS 5b*), culminating at 60 m below the present sea level at ~85 ky BP, as illustrated by Esat et al. (1999) and Waelbroeck et al. (2002). Records from the Huon succession show evidence that MIS 5 ended with a last highstand at 85-80 ky BP, when global sea levels were up to ~30-40 m lower than today (*MIS 5a*. Esat et al., 1999; Lambeck et al., 2002).

Unlike the Huon Peninsula, exposed marine evidence of transgressive stages is not common in WA. Despite this, seismic and sedimentological data collected during this doctorate research revealed numerous indicators linked with sea level fall during MIS 5. In the Swan River estuary (Chapter 4 and Bufarale et al., 2017), the palaeochannel formed during the PGM and cutting the older *Kings Park Formation* and *Tamala Limestone*, appears to have been infilled with fluvial and estuarine sediments of the *Perth* Formation throughout the entire length of MIS 5 (Figure 7.5).

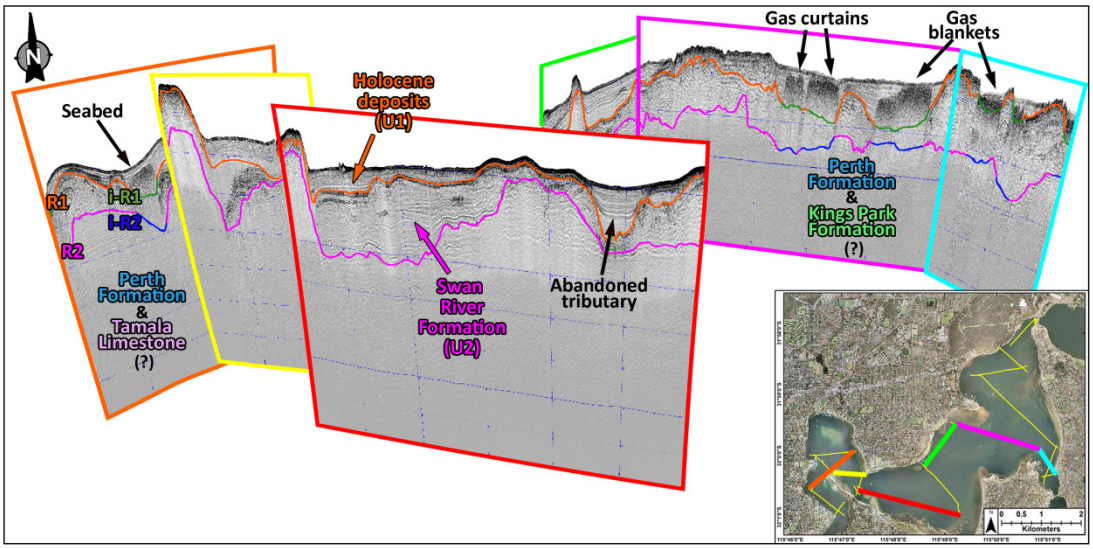


**Figure 7.5. 3D perspective view of boomer subbottom profiles across the Swan River. The three-dimensional analysis of the seismic profiles provides a remarkable tool to image with a better precision the subsurface pattern of the palaeo-incisions and expand the punctual information given by the core data (Bufarale et al., 2017). Vertical scale: 80 m BSL (western profiles) and 60 m BSL (eastern profiles); horizontal scale: variable.**

In Geographe Bay, palaeochannels have been identified in several seismic profiles (Figure 7.6) and clearly showed two sets of subparallel, laterally continuous beach ridges (Chapter 5). These buried and exposed bedforms have been formed near the shoreline, when the sea level was falling and can be followed along the Western Australian coast (James et al., 1999; Twiggs and Collins, 2010; Nichol and Brooke, 2011, Brooke et al., 2014; Murray-Wallace and Woodroffe, 2014). The submerged ridges become progressively younger from nearshore to offshore, recording the MIS 5 relatively high sea level stages (late MIS 5e-beginning of MIS 5d and MIS 5c).

In 2009, Geoscience Australia (GA) updated the existing bathymetric datasets by acquiring high-resolution bathymetry and producing a grid with a resolution of about 250 m (at the equator. Whiteway, 2009). By combining the 2009 bathymetry with the sea level curve in Figure 7.1, it is possible to estimate the position of the coastline, during the past sea level stages (Figure 7.7 and Figure 7.8 and further Figure 7.9 to Figure 7.12).

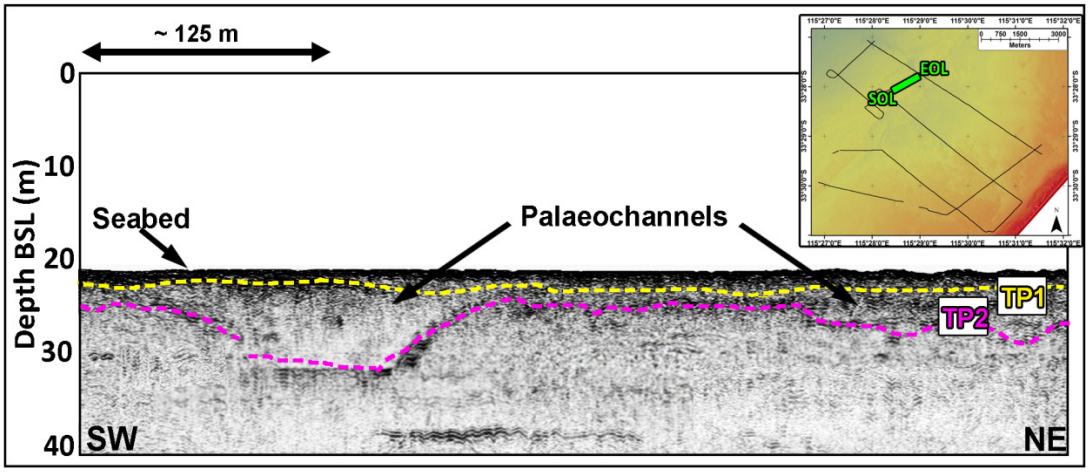


**Figure 7.6. Example of buried channels located in Busselton (Chapter 5). The location of the seismic profile reported is highlighted in green (Area 3, SOL: start of line, EOL: end of line). The vertical axis corresponds to the depth BSL and the scale is in metres. The sound velocity in the sediments is equivalent to ~2000 m/s. The horizontal axis represents the distance covered by the vessel and the scale is in metres.**

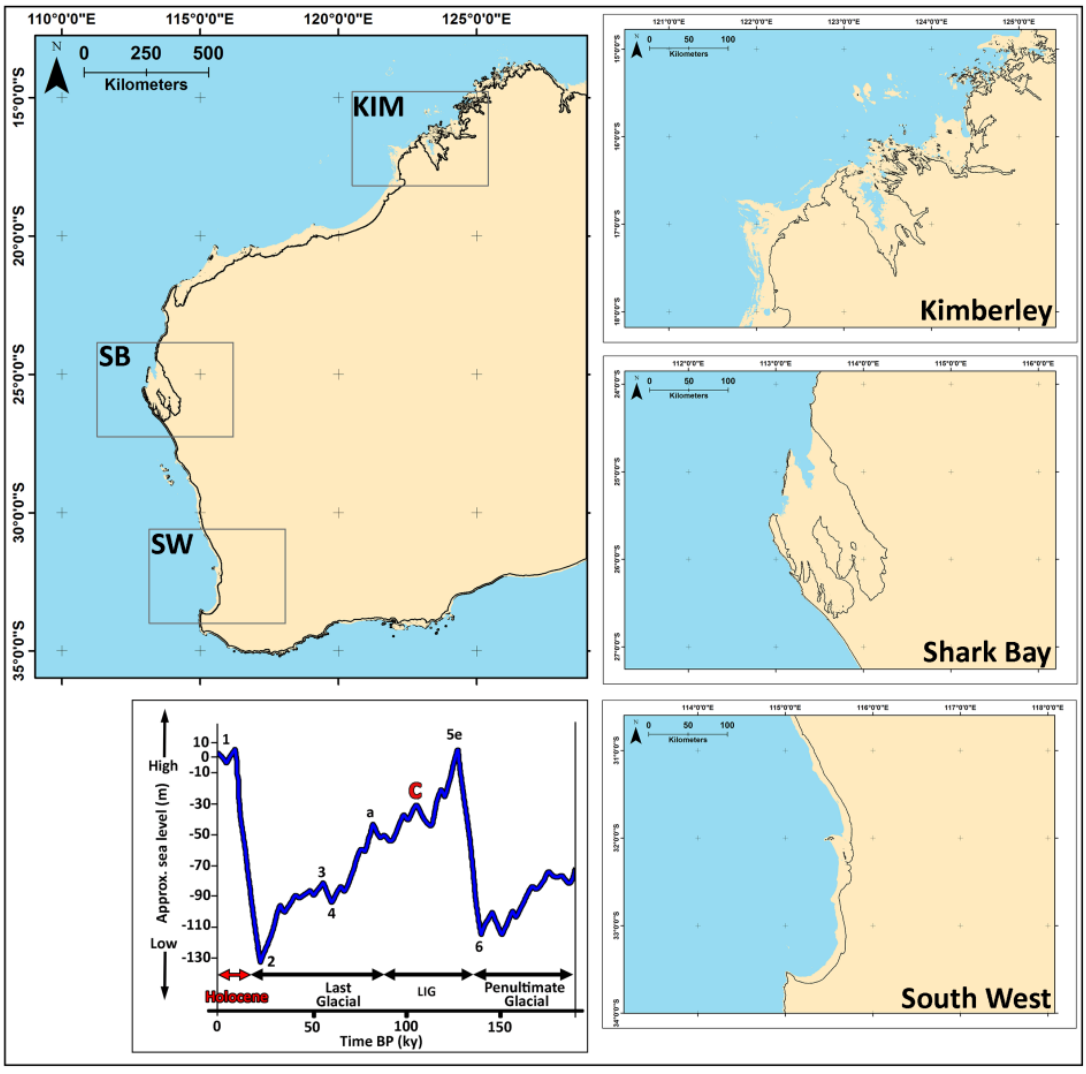


**Figure 7.7. WA continental shelf exposure, during MIS 5c, when the sea level was at ~25 m bsl. The black line marks the edge of the modern coastline.**

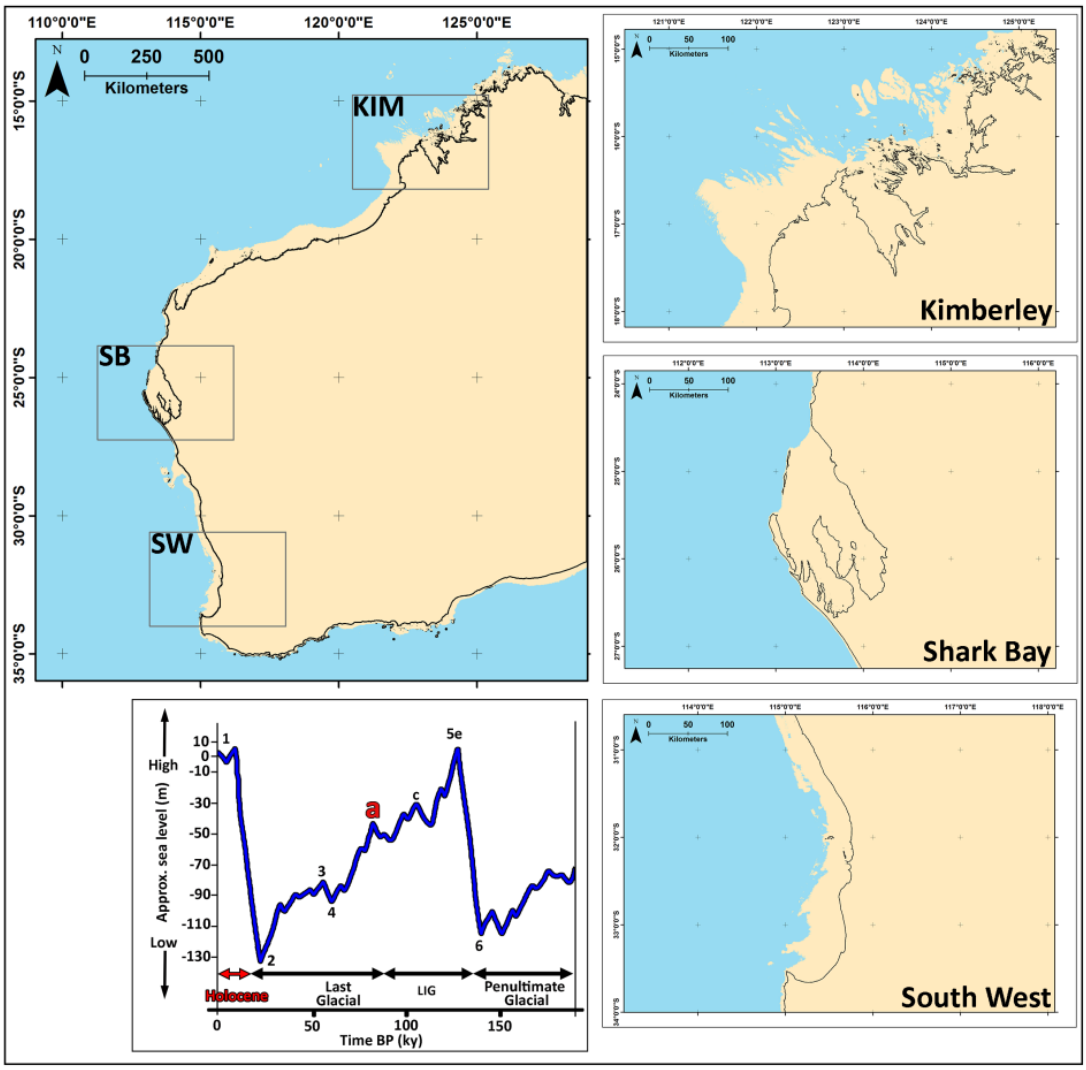


**Figure 7.8. WA continental shelf exposure, during MIS 5a, when the sea level was at ~40 m bsl. The black line marks the edge of the modern coastline.**

### MIS 4

MIS 5 was followed by a steady regression through the transition MIS 5a/4, during which the sea level had fallen almost 60 m (at MIS 4, ~70 ky BP. Figure 7.9. Cutler et al., 2003). During this lowstand period, the palaeorivers across WA had another episode of downcutting, in response to changes in base level.

During the seismic survey along the Swan River, the profiles clearly revealed the presence of a second palaeochannel, incising into the Kings Park and Perth Formations (Figure 7.5). The ancestral Swan River had a higher gradient than the modern one as it had to incise further into underlying strata in order to maintain a balance with a lower than present base (sea) level (Figure 7.10). Toward the MIS 4/3 transition, fluviatile heterogenic deposits of sand, silt and clay of the *Swan River Formation* were deposited under various hydrological settings.

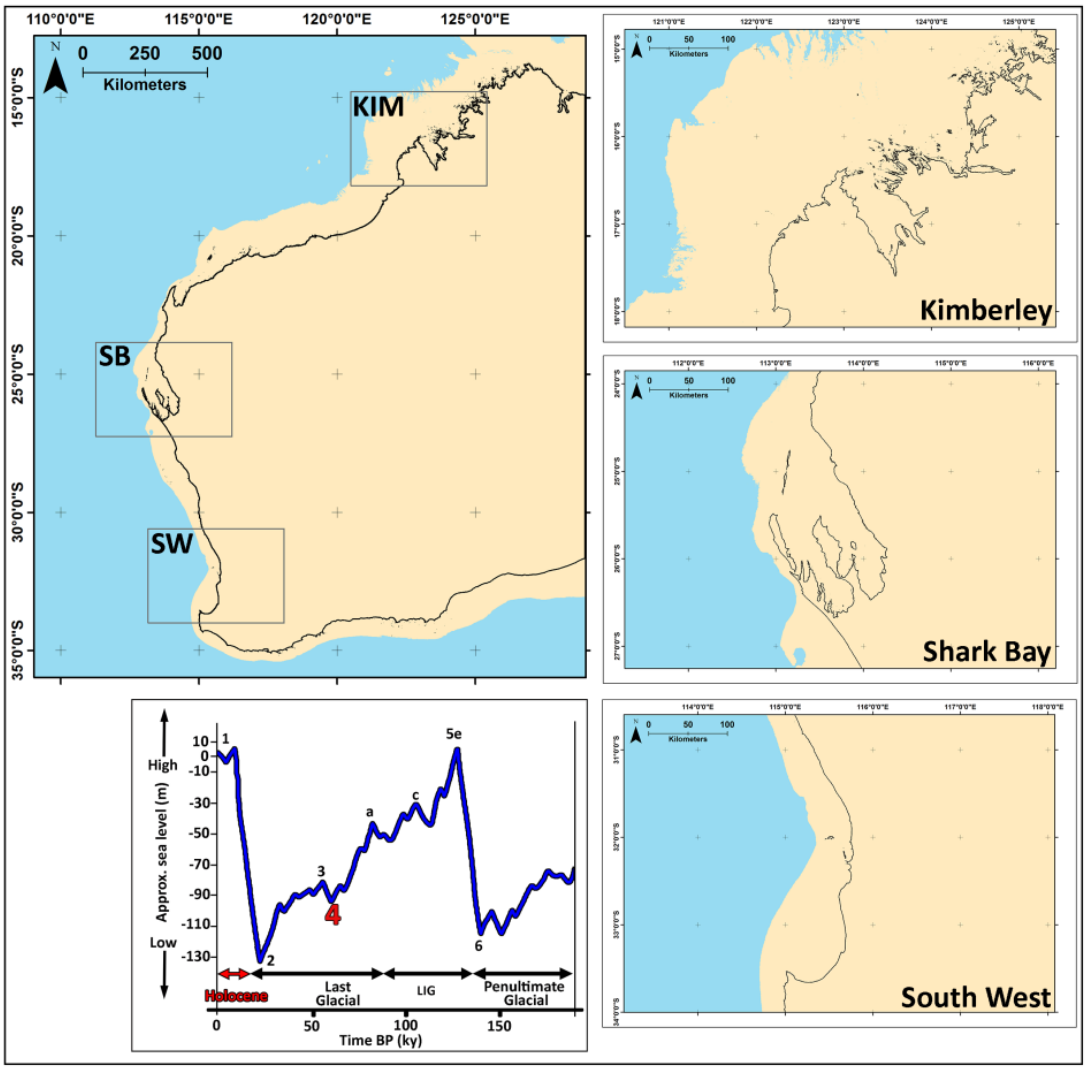


**Figure 7.9. WA continental shelf exposure, during MIS 4, when the sea level was at ~100 m below the modern sea level. The black line marks the edge of the modern coastline.**

Optically stimulated luminescence (OSL) and thermoluminescence (TL) dating, carried out by Brooke et al. (2014), revealed that Rottnest Island (Bathurst Point, north eastern part of the island) experienced a major phase of dune accumulation during MIS 4, which followed the deposition of calcarenite and LI reef accretion in MIS 5. OSL dating on the *Cooloongup Sand* also gave a MIS 4 (to MIS 2) age (Lipar and Webb, 2014). These deposits are a thin veneer (0.5-2 m thick) of quartzose sand that overlie the Tamala Limestone, intermittently along the Greater Perth region, up to the Nambung National Park. Their origin is debated but most likely they derived from earlier dissolution and karstification (mainly during high rainfall in MIS 5) of the Tamala Limestone that would have released a considerable amount of quartz sand (insoluble residue), successively redeposited during the drier and windier glacial climate of MIS 4, up to MIS 2 (Lipar and Webb, 2014).

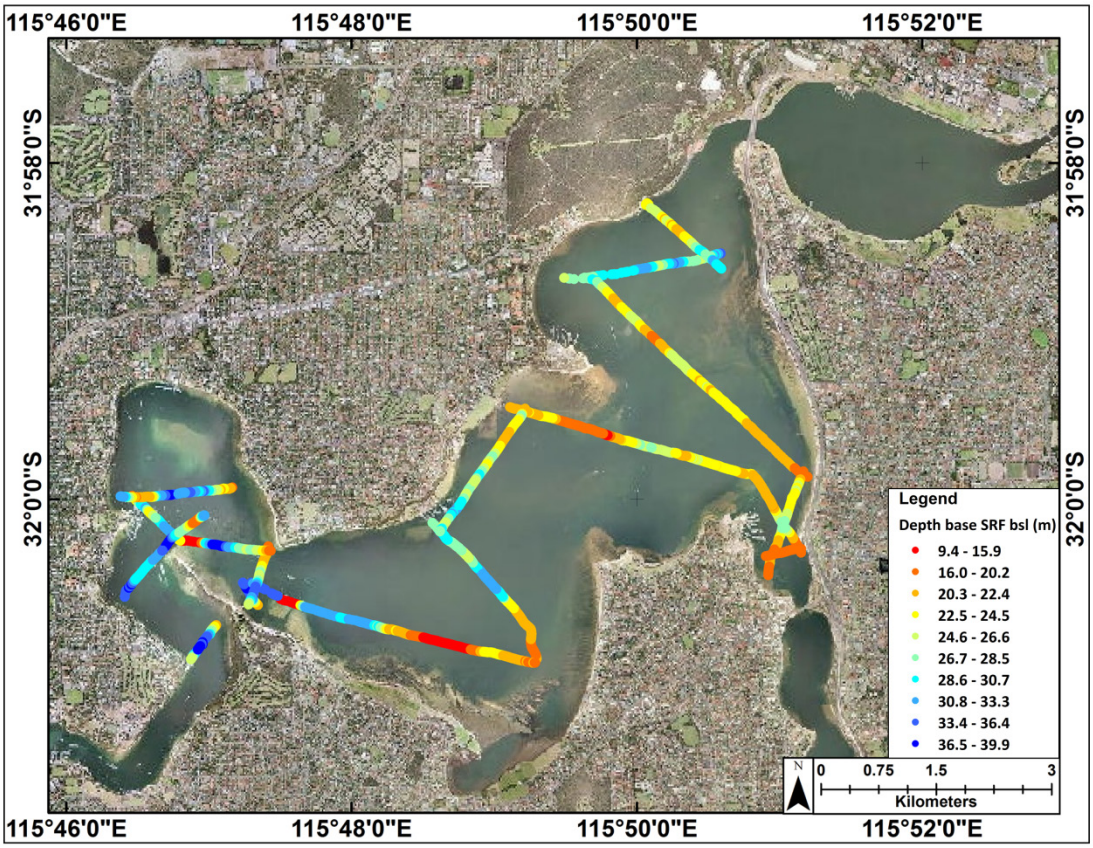


**Figure 7.10. Depth of the deep channel, below sea level, cut during the MIS 4 along the present metropolitan Swan River and infilled with the Swan River Formation. The gradient is greater than the modern one.**

### MIS 3

The rapidly uplifting Huon Peninsula has also made possible the identification and dating of coral terraces belonging to a further stage of the Late Pleistocene marine regression, called *MIS 3*. During MIS 3, sea level had a relative rise to around the modern -70 m contour, over the period 64-32 ky BP, before lowering again at ~30 ky BP (Figure 7.11. Chappell et al., 1996; Lambeck and Chappell, 2001; Cutler et al., 2002; Woodroffe and Webster, 2014). Lambeck et al. (2002) identified (from North Atlantic planktonic foraminifera) five highstands within this stage, centred on 32, 36, 44, 49-52 and 60 ky BP. Similar age and sea level elevations have been reached also by Cabioch and Ayliffe (2001), working on emerged terraces in Vanuatu.

Although no features (on the seafloor or buried underneath) have been recognised as belonging to MIS 3, within the investigations carried out for this thesis, several other authors have described various marine and terrestrial indicators of the occurrence of this stage in WA. For instance, while analysing the oceanographic controls on carbonate sedimentation, James et al. (2004) collected skeletal and lithic sediments along the mid-shelf (50-120 m of water depth) in the North West Shelf (NWS. Between the Kimberley and Ningaloo Reef) and interpreted these deposits as having formed in shallow water, during MIS 3 and 4. Brooke at al. (2014), using high-resolution and OSL and TL dating, mapped drowned barriers and dune landforms formed during MIS 3, today located at –60 to -50 m below the present sea

level. These extensive features are similar to the marine ridges in Busselton and in fact they represent younger (and deeper) sets of these shore-parallel relict landforms (likely shoreface palaeodunes or beach ridges).

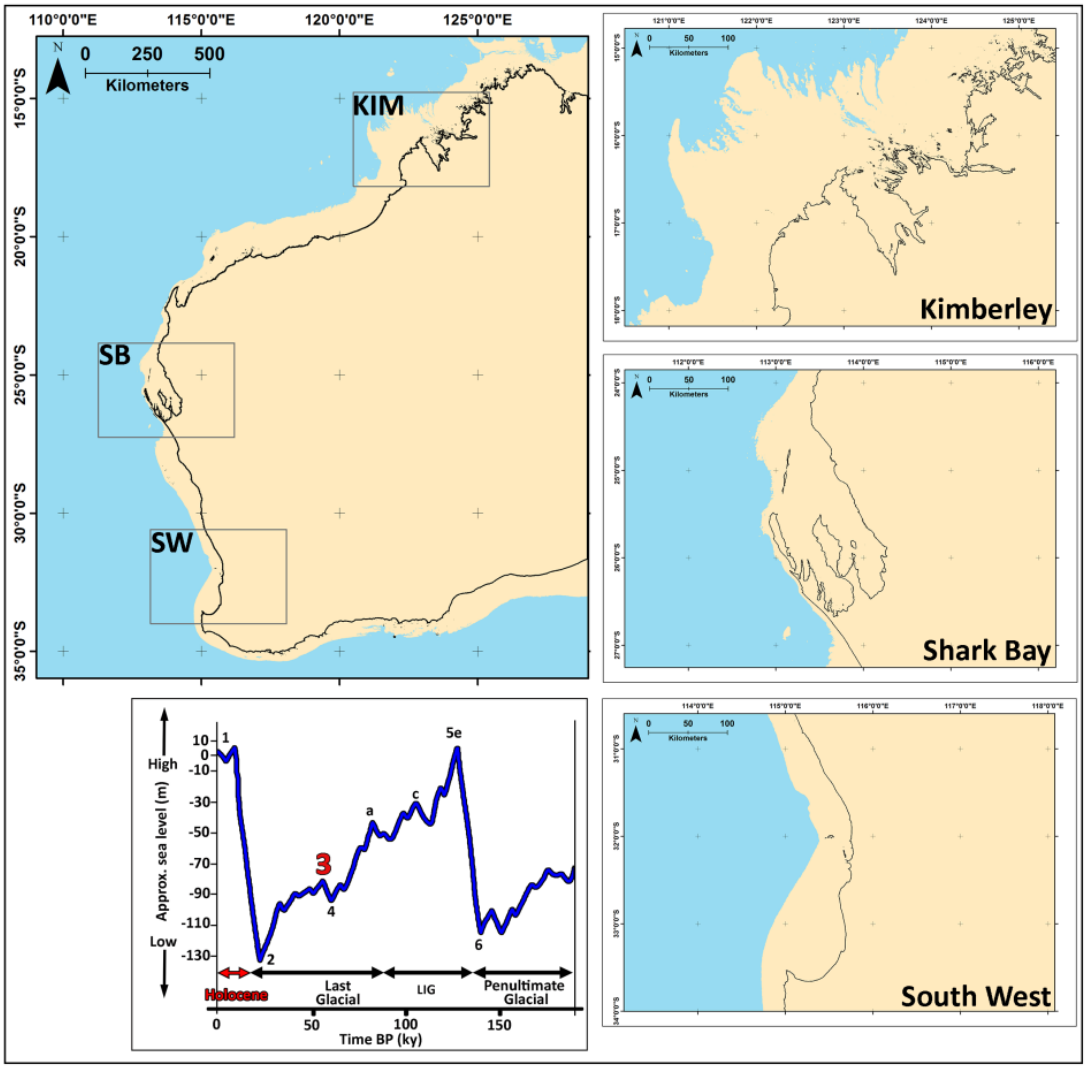


**Figure 7.11. WA continental shelf exposure, during MIS 3, when the sea level was at ~70 m below the modern level. The black line marks the edge of the modern coastline.**

### MIS 2

A successive saw-tooth pattern and relatively slow drop of the sea level, from MIS 3 to MIS 2 preceded the Last Glacial Maximum (LGM), at 22-21 ky BP. During this stage, lasting about 6 ky, the continental ice sheets reached their maximum development, leading to a drop of the global sea level to ~130 m below the present (Figure 7.12. Chappell et al., 1996; Lambeck and Chappell, 2001; Yokoyama et al., 2001; Montaggioni and Braithwaite, 2006). During this time, the width of the exposed continental shelf varied greatly, from several hundred kilometres in the North West to less than 10 km off Ningaloo Reef, and the area of the WA mainland was about ¼ larger than the present, with more than 580,000 km$^2$ of continental shelf exposed (value calculated using ArcGIS, from the Western Australia/Northern

Territory border in the north, to Western Australia/South Australia border, in the south (Figure 7.12).

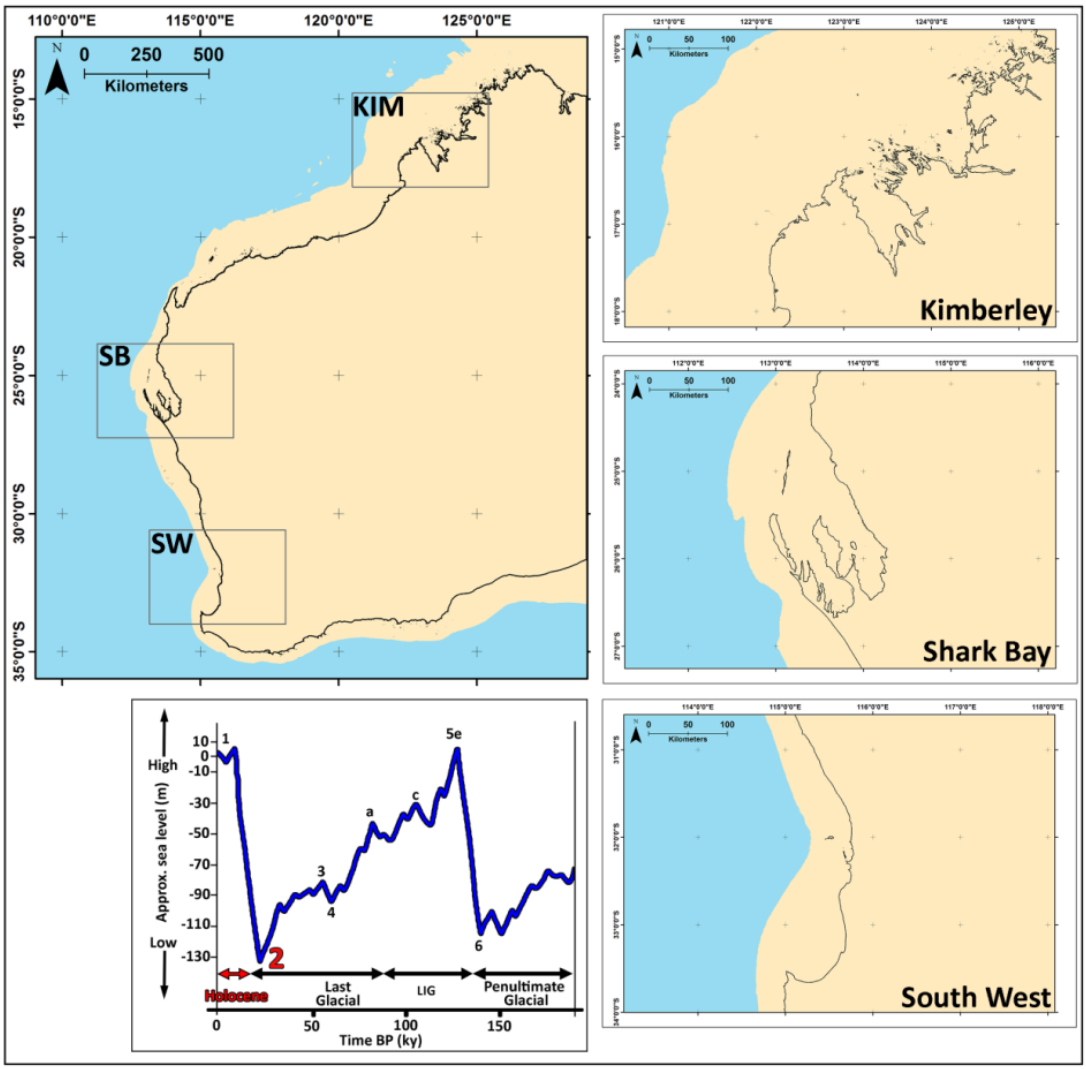


**Figure 7.12. WA continental shelf exposure at LG maximum, ~18 ky BP. It is estimated that the sea level was at 130 m below modern sea level. The total area of exposed continental shelf was about 580,000 km$^2$.The black line marks the edge of the modern coastline.**

It was beyond the scope of this research to investigate the geomorphological features in marine environments related to the LGM, as they lie in deep water (around the modern -130 m contour). Despite this, during the seismic survey in the mid-shelf reefs of the Kimberley, several deep channels, more than 80 m deep, have been recognised cutting through the mid-shelf reef platforms of Adele, Churchill and Beagle reefs (Solihuddin et al., 2016). By combining the acoustic profiles with the bathymetric grids produced by Geoscience Australia (GA, 2009), several palaeorivers (possibly tributaries of the modern Fitzroy, Isdell and Prince Regent rivers) were identified, deeply incising more than 200 km of continental shelf, left exposed by the lower sea level (Figure 7.13).

In the same geographic area (NWS), James et al. (2004) recognised and collected sediment samples from two major terraces along the outer shelf, at water depth >

120 m below the sea level and interpreted these bathymetric features as MIS 2 lowstand shoreline.

During the LGM, the sea-surface temperature (SST) was 6° to 10°C colder than MIS 5e (Wells and Wells, 1994). This cooling, together with the limited width of the exposed shelf deeply influenced the surface water circulation along WA. In conjunction with a limited longshore current regime, the Leeuwin Current (the major offshore ocean current) experienced a major decline that affected the SST, and hydrodynamic settings along the coast, especially at mid-high latitudes (from ~19°S and further south. Wells and Wells, 1994; Wywroll and Miller, 2001). Under these conditions, the weaker Leeuwin Current did not warm up the coastal area as it has done during the LI (and does today. Wells and Wells, 1994). Consequently, the rainfall was lower, with stronger winds (Spooner et al., 2011; Lipar et al., 2017) and the carbonate productivity decreased (Murray-Wallace, 2002.). This suggests that the sediment paucity that characterises the WA coast today was even more enhanced during MIS 2. In addition, Wilson (2013) argued that during the LGM, coral reefs in Ningaloo Reef and further north in the Kimberley may not have been present or as widespread as today and during MIS 5e, due to colder SST, a reduced Leeuwin Current and lower sea level (as the latter may have reduced the rocky substrate availability suitable for coral reef development).

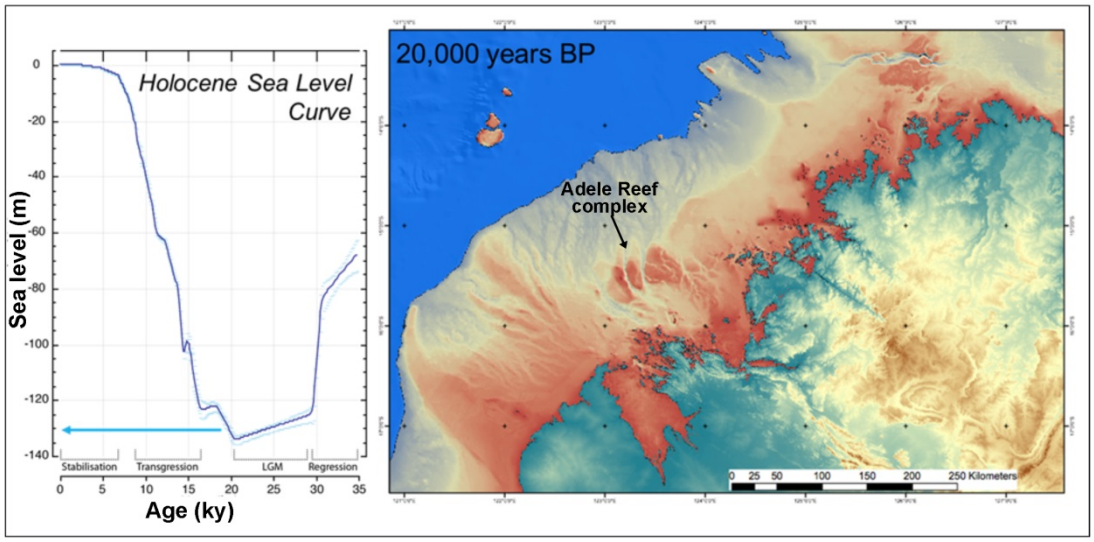


**Figure 7.13. Intensely incised continental shelf in the Kimberley, during the LGM. Credit: Dr Michael O'Leary.**

### *2.1.4. Marine transgression from MIS 2 to MIS 1 (Holocene)*

The past ~11.7 ky defines the Holocene (*MIS 1*. Walker et al., 2008), the most recent time of Earth history. The transition from MIS 2 to MIS 1 started earlier, though, around 18 ky BP, when the end of the LGM occurred, marked by a rise of the global temperature that triggered the polar ice sheets melting, and consequent rise of the sea level. In ~10 ky, it is estimated that sea level quickly rose (at 12 m/ky) until reaching a position around 2.5 m above the present, ~6.8 ky ago (Chappell and Thom,1986; Lambeck and Nakada, 1990; Baker et al., 2005; Jahnert and Collins, 2013). After a brief period of stability, at 6 ky BP, the sea level gradually receded (at ~0.2 m/ky) to the present position (Chappell and Thom, 1986; Reeves et al., 2008).

Several authors, analysing distinct records, agree that during the period from 12 to 3 ky BP, the Australian climate was wetter than the present, with more active rivers, particularly in the tropics (Nanson et al., 1989) and higher lake and estuary levels, throughout the country (Bowler et al., 1976). Cores from offshore Cape Range Peninsula (Ningaloo Reef) show an increment of clay-rich terrigenous material, indicating a greater river discharge, thus a higher rainfall (Gingele et al., 2001). The research carried out along the metropolitan reach of the Swan River also shows that around 10 ky ago, the sea level had risen enough to transform the valley into an estuary (Bufarale et al., 2017); the higher terrigenous content of the palaeo-Swan, together with a more marked oceanography (longshore currents), built obstructing sand bars at the river mouth that amplified the reduction of the flow velocity, resulting in a subsequent deposition of up to 14 m of sediments, within the basin (Hodgkin and Hesp, 1998; Bufarale et al., 2017)

12 ky BP also marks the time when the Leeuwin Current resumed flowing strongly, with a similar pattern to today, most likely influencing the precipitation rates in WA (Gingele et al., 2001).

Using pollen and charcoal analysis on marine sediments, van der Kaars and De Deckker (2002) determined that this period was also characterised by heavier summer rain than today, with a more vigorous monsoonal activity (Wywroll, and Miller, 2001).

Around 10 ky ago, the inner shelf, which had remained predominantly exposed for the preceding ~90 ky, became flooded with the rising sea level. Dramatic changes occurred in terms of sediment erosion, transport and deposition.

When sea level reached the modern -30 m contour, topographic highs and seabed features (like the ridges in Geographe Bay), which underwent an intense lithification when they were exposed (since MIS 5a), became submerged. Erosion started to occur, leaving these relict geomorphological structures asymmetric, with a flat top.

Longshore currents became increasingly stronger, forming sandbars and megaripples (i.e. in Geographe Bay and Shark Bay, respectively. Figure 7.14), tombolos and other shoreline-attached structures along the south and central coasts of Western Australia (Sanderson and Eliot, 1996; Gozzard, 2007).

In the NWS region, the sea level rise firstly initiated the deposition of ooids and peloids over extensive shallow warm-water areas (between 15.4–12.7 ky BP), then, once the Leeuwin Current began to flow (reducing the overall salinity), their sedimentation ceased (around 12 ky BP), resulting in predominantly skeletal carbonate productivity, which occurs in the present (James et al., 2004; Collins, 2011).

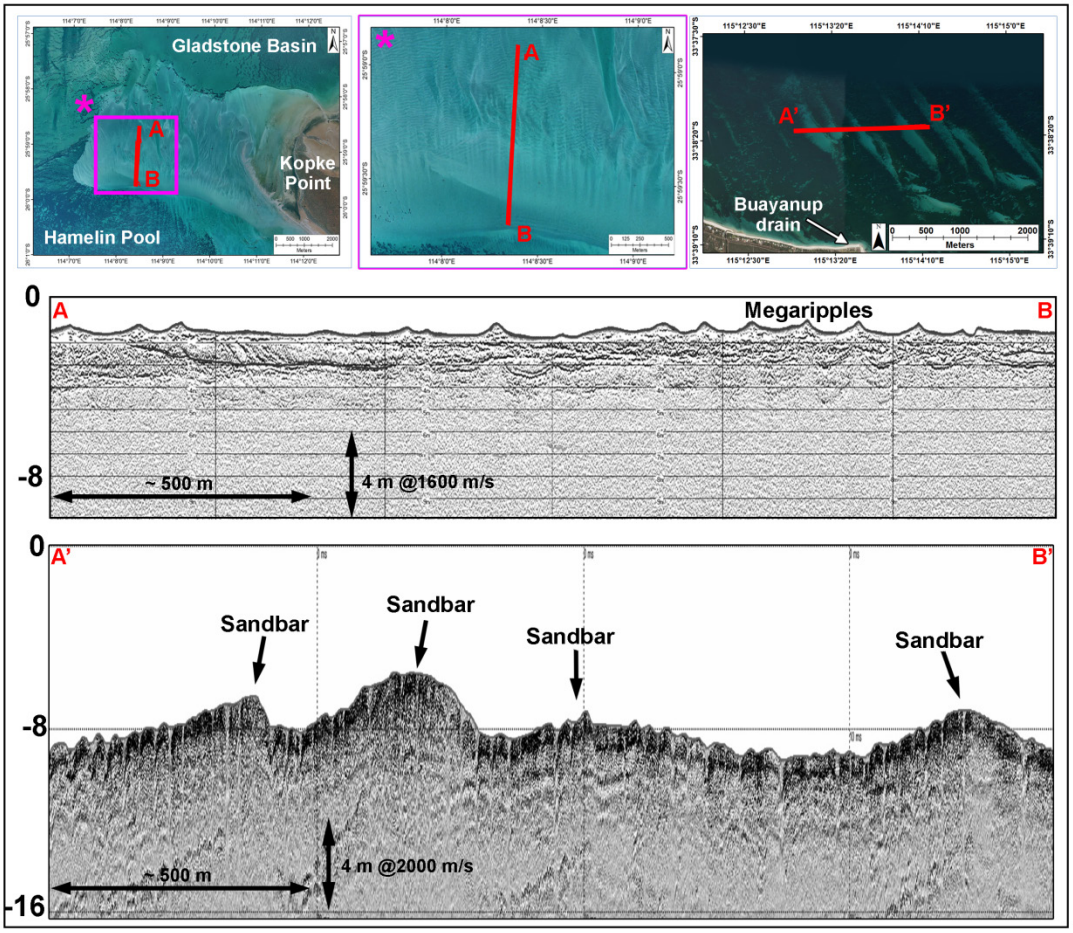


**Figure 7.14. Seismic sections showing megaripples in Shark Bay (A-B) and sandbars in Geographe Bay (A'-B'). The vertical axis corresponds to the depth BSL and the scale is in metres. The sections have the same vertical and horizontal scale. Megaripples are several hundred metres long, with a wavelength about 25 – 35 m, east – west oriented. Sandbars greatly vary in size, ranging between about 100 to 300 m in width, with a relief up to ~3 m in height. For their location refer to Figure 3.2 and Figure 5.1, respectively).**

The last 10 ky of sea level changes, until reaching the present equilibrium, also had a great impact on the development of important coastal systems, that include coral reefs, seagrass meadows and stromatolites.

Coral reefs developed as far south as the Houtman Abrolhos Islands (Collins et al., 2003; Feng et al., 2010). These high latitude reefs, sustained by the warm Leeuwin Current, grew at an overall rate of 7.7 m/ky, building up over 25 m of Holocene reef platform since 10 ky BP (leeward reefs (Collins et al., 2003). At Ningaloo Reef, due to a higher pre-existing topography (Last Interglacial reef platforms), the Holocene inundation and successive initiation of the fringing reefs occurred later, around 8.0–7.5 ky BP (Twiggs and Collins, 2010). In the Kimberley, reef growth initiated around 9000–8940 BP (on Cockatoo Island. Solihuddin et al., 2015), not long after the flooding of the pre-existing topography. Similarly, the corals of the isolated oceanic platform of Scott Reef began to build up, around 9 ky BP (Collins, 2002)

With the increasing stability of the sea level, large seagrass communities established along the western coast of Australia, especially extensive in Shark Bay

and Geographe Bay (the largest reported assemblages in the world. Walker, 1990). In Shark Bay, the first colonies of seagrasses were established by 8.0 ky BP, progressively contributing to the initiation of the Faure Sill bank growth. Around 6.8 ky BP, in conjunction with the Holocene high stand maximum, the seagrass meadows were at their apex, playing a significant role in trapping sediments and producing muddy carbonate deposits *in situ*. During the Late Holocene, when the sea level dropped to the present level, the bank stopped growing vertically and the seagrass (and loose sediments) started expanding laterally, filling the available accommodation space, such as palaeochannels and topographic lows (Bufarale and Collins, 2015).

The second most prominent natural asset of Shark Bay, after the seagrass, is the stromatolites. Prior to the sea level rise, Hamelin Pool and L'Haridon Bight (Shark Bay) sat along topographic lows in the pre-existing substrate (see Figure 7.15 and Figure 7.16). The basins were first flooded by the Holocene sea level rise and when the waters receded toward the present position, the seagrass bank of the Faure Sill and the emerged islands partially closed the two embayments. In an area where the evaporation greatly exceeds the rainfall, this closure has resulted in an intensification of the salinity levels, making these environments metahaline to hypersaline, an optimal setting for the development of microbial communities (stromatolites and microbial mats), hypersaline coquinas and oolitic shoals (Jahnert and Collins, 2013; Bufarale and Collins, 2015). The coquina ridge systems that rim the supratidal zone (3 to 6 m above MSL) of Hamelin Pool (south-east Shark Bay) provide insights into the mid-late Holocene tropical cyclone and storm record (Nott, 2011; Jahnert et al., 2012). These deposits document up to 6 ky of moderate to intense tropical cyclonic surges and storm waves. They also support the model of a reduction of the storm activity between 3.6 and 3 ky BP, suggesting that in this period the climate was likely drier than the present (Nott, 2011; Jahnert et al., 2012).

Another element confirming the progressive maturing of the shoreline along the WA coast is the widespread mangrove communities across river estuaries that formed when the relative sea level stabilised (Grindrod et al., 1999).

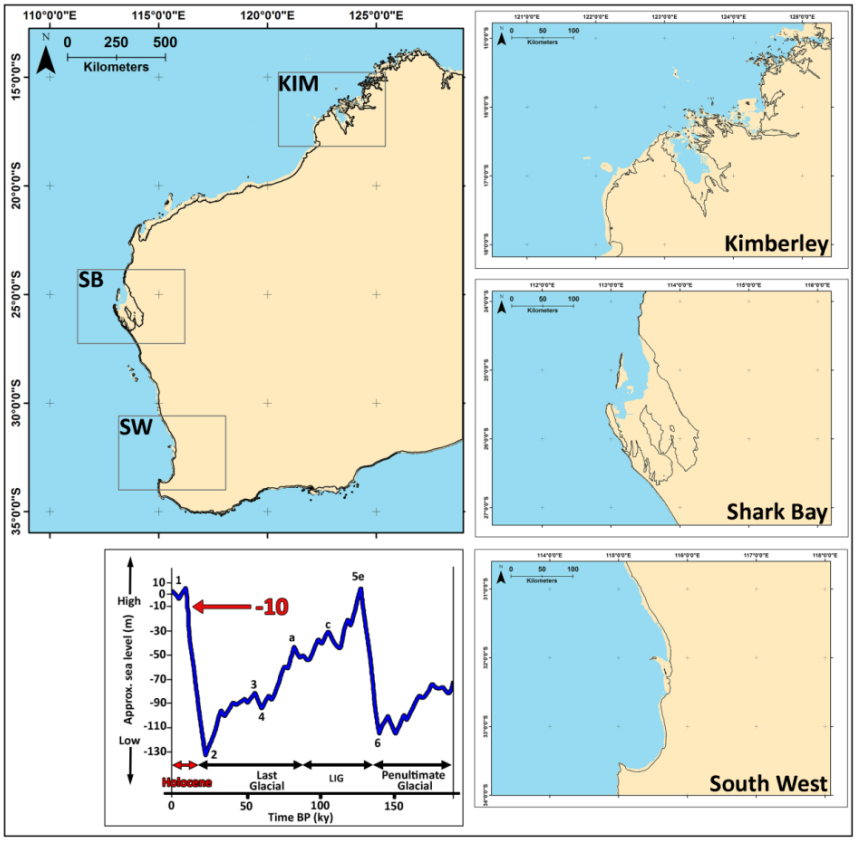


**Figure 7.15. WA continental shelf exposure when the sea level was at ~10 m bsl. The black line marks the edge of the modern coastline.**

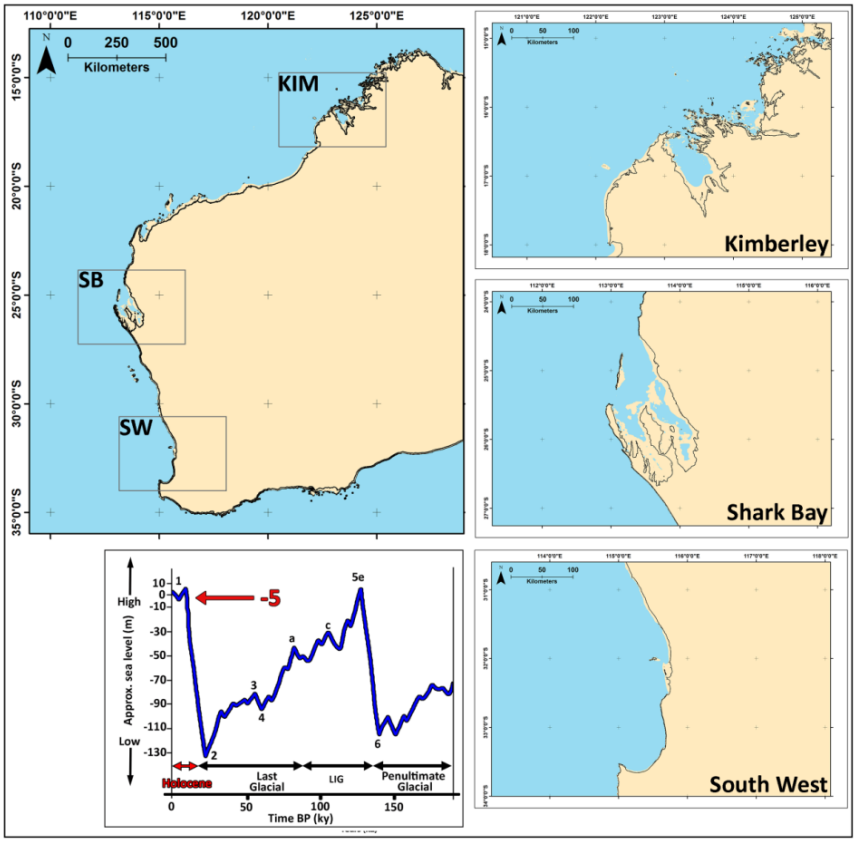


**Figure 7.16. WA continental shelf exposure when the sea level was at ~5 m bsl. The black line marks the edge of the modern coastline.**

## 2.2. Pre-existing topography

The second main factor involved in controlling the evolution of a sedimentary setting is the shape and elevation of the bedrock over which the system developed.

Palaeochannels and topographic lows represent the major depocentres, with thick sediments packages filling the depressions and levelling the surficial topography. This is particularly evident along the Swan River, where well-developed palaeo-tributaries downcut during the Late Pleistocene regression and became completely filled up in the Holocene transgression. This trend is also noticeable along the Faure Sill, where very strong hydrodynamic conditions have cut and infilled incisions along the bank, during the Holocene (Figure 7.17). In Geographe Bay, LiDAR bathymetry and seismic images revealed the presence of several palaeochannels, perpendicular to the coastline.

In contrast, topographic highs represent areas of harder substrate, where the overlying sediments are thinner, and act as sills, affecting the sediment dynamics and hydrodynamics. A significant example comes from the Swan River, where two shallow sills (<5 m depth), one at the Fremantle Traffic Bridge and the other between the Narrows and Causeway bridges (see Bufarale et al., 2017), divide the system into three main segments, the upper reach, middle reach and lower reach, greatly influencing the river channel type, transitioning from narrow and sinuous (upstream), to wide and shallow central basin and ending with a narrow straight that follows the joints and structure of the basement (*coastal dune limestone corridor*, as defined by Quilty and Hosie, 2006).

Collins et al. (2003) recognised the pre-existing substrate as one of the limiting factors for the development of the windward reef platforms in the Houtman Abrolhos Islands. The Last Interglacial reef that underlies the west side of the modern platform has a greater elevation, if compared to the east leeward side, resulting in reduced accommodation space, restricting the reef development during the Holocene.

In the Kimberley, the steady subsidence of ~0.12 to 0.2 m/ky has provided significant accommodation space, allowing the Holocene reefs to grow up to 35 m thick (Collins et al., 2011; Solihuddin et al., 2016; Bufarale et al., 2016). In contrast, the vertical development of the Holocene corals in Ningaloo Reef has been restricted by the localised uplift to a maximum thickness of ~10-15 m (Collins et al., 2003).

Different morphological features and their height play a role in controlling also the size distribution of the sediments. Medium to fine grains are more dominant on top of the ridges and mounds. Coarse and very coarse material tends to accumulate in swales, palaeochannels and depressions, as shown in Geographe Bay (Chapter 5).

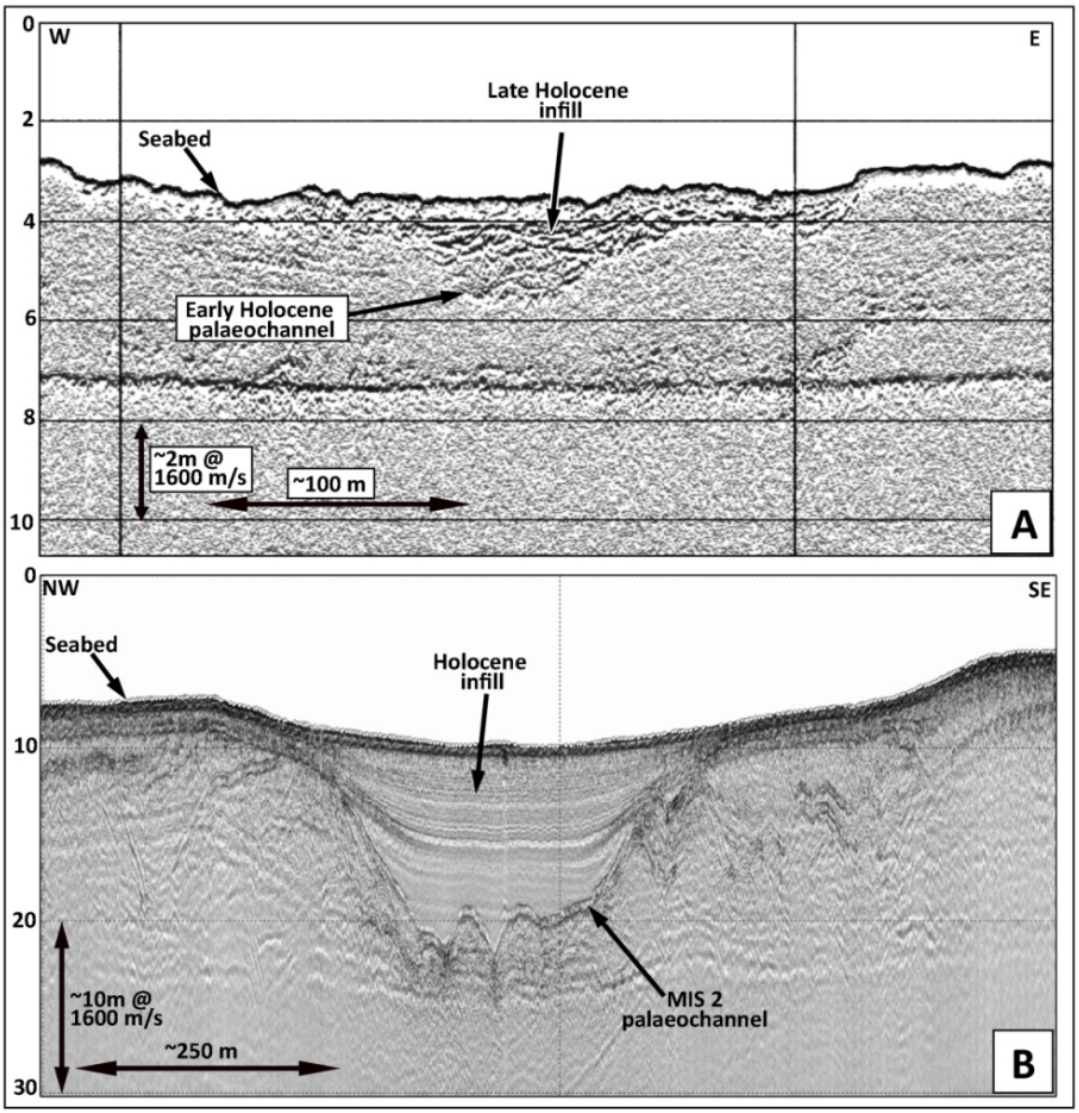


**Figure 7.17. Acoustic profiles showing cut and infill of palaeochannels in Shark Bay (A) and Swan River (B). Depths are in metres, below the sea level.**

## 2.3. Local physical characteristics and processes

WA is characterised by a total coastal length of almost 13, 000 kilometres (excluding the islands). The study areas considered in this thesis have a latitudinal distance well exceeding 2000 km, spanning from temperate regimes in the south to tropics in the north. The climatic variability, together with the local morphology and the hydrodynamic conditions, have greatly influenced the evolution, sediment distribution and lithology of each environment, resulting in a wide range of sedimentary systems.

Temperature, rainfall, tides, winds and related oceanic currents and waves control directly or indirectly the following processes that have governed the Late Quaternary deposits of WA coast:

- Erosion rates and associated terrigenous sediment supply (riverine and aeolian),

- Onset and distribution of seagrass and coral reefs, and associate biogenic sediment supply,
- Wind and currents and associated sediment distribution.

In terms of local physical characteristics and processes, the most controlled environment, within the studied locations, is the Kimberley. The coastline is extremely irregular and indented, with major rivers depositing a large amount of sediments not only nearshore but also offshore, with sediment plumes that reach the mid shelf (i.e. Adele Complex). The turbidity increases during the wet season, when cyclones are frequent. The most peculiar environmental characteristic of the area is the presence of macrotidal ranges (up to 11 m on the spring tide).

Solihuddin et al. (2015; 2016) analysed the matrix from reef cores collected in various locations in the Buccaneer Archipelago and showed that although carbonate content is dominant, terrigenous clays represents a significant percentage. This high terrigenous input is attributable to the presence of numerous rivers and creeks, including the Isdell, Lennard and Fitzroy Rivers. The latter, in particular, has the greatest mean annual discharge and the largest sediment load in WA (Epton, 2000; Department of Water, 2008). The sediment discharge increases during the wet season (from November until April) and reaches its maximum following tropical cyclonic events, resulting in extreme turbidity. Strong tidally-generated current flows keep the fine-grained terrigenous sediment in suspension until it becomes trapped and infills the open reef fabric, supporting primary framework preservation and reef accretion (Solihuddin et al., 2015).

Based on the reef-flat elevation, the reef typologies identifiable in the Kimberley fall within two primary categories, low intertidal (LIR) and high intertidal reefs (HIR), which are highly atypical coral reefs (Bufarale et al, 2015; Collins et al., 2015). Solihuddin et al. (2016) studied the phenomenon in detail, carrying out a multibeam survey across selected reefs in the Southern Kimberley, to measure elevation and width of the reef flats. Plotting the survey data in a diagram (Figure 7.18), where the Y axis, is the elevation above and below MSL and the X axis, is the frequency of a particular elevation which occurred during the survey, the resulting curves (corresponding to an individual reef flat) clearly showed the two reef categories, where the HIR include reef flats that stand between mean low water neap (MLWN) and mean high-water neap (MHWN), and the LIR that sit below the Mean Low Water Springs (MLWS). The gap between the two categories indicates that no reefs grow between MLWN and MLWS. Further differences between HIR and LIR are the reef flat width and composition, with HIR having extensive reef flats and coralline algal terraces, versus LIR where coral and sediment prevail on relatively narrow reef flats (Solihuddin et al., 2016).

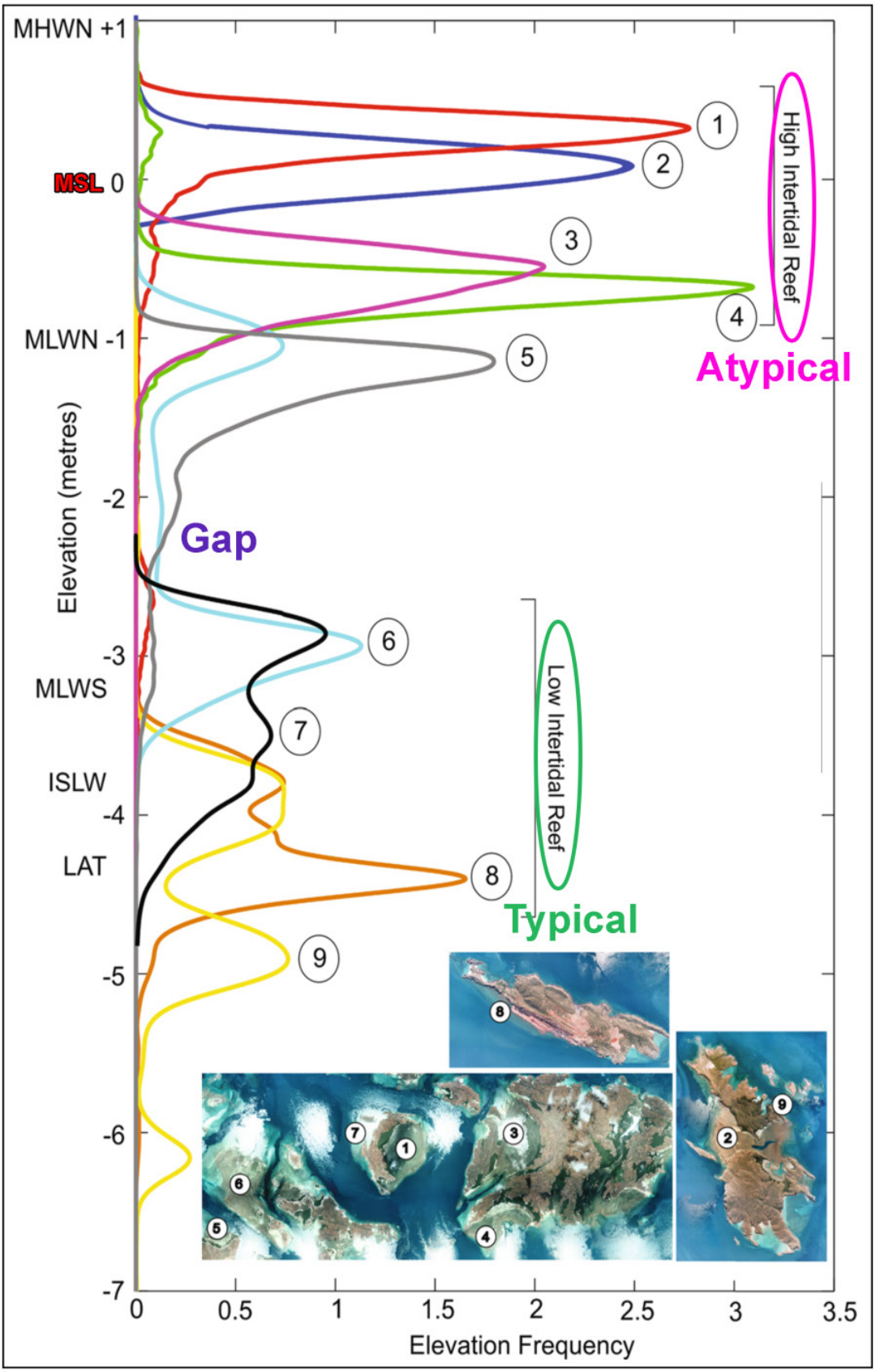


**Figure 7.18. Elevation/frequency diagram for selected reefs: 1 East Tallon, 2 Irvine-Bathurst, 3 The Pool, 4 Hancock, 5 Kolganu, 6 Waterlow, 7 West Tallon, 8 Cockatoo, 9 Bathurst. MHWN = Mean High Water Neaps; MSL = Mean Sea Level; MLWN = Mean Low Water Neaps; MLWS =**

**Mean Low Water Springs; ISLW = Indian Spring Low Water; LAT = Lowest Astronomical Tide. Modified after Solihuddin et al. (2016).**

The highest elevation recorded is in East Tallon Island, where the reef flat sits about 0.75 m above MSL, with a modal point slightly higher than the mean sea level, at 0.25 to 0.5 m (Figure 7.18 curve 1, in red). On the other hand, the multibeam results indicate that the West Tallon reef flat (Figure 7.18 curve 7, in black) belongs to the LIR. The dichotomy of the reef flats is mainly due to a strong, ebb-dominated, tidal asymmetry on East Tallon that retains seawater over the low tide and allows continued accretion (refer to Lowe et al., 2015 and Solihuddin et al., 2016 for a more detailed explanation). Reef flat widths and roughness (determined by benthic composition and biota. Lowe at al., 2015) also influence the development of high intertidal reefs: wide and “rough” reef flats, dominated by coralline algae (like East Tallon), are capable of water retention and become HIRs; conversely, in narrow and microtopographically less complex reef flats (with corals and sediments, but without coralline algae, like West Tallon), sea water is not preserved at low tide and the reefs remain low intertidal, at MLWS.

This contrast in elevation has also influenced the chronology of Holocene reef build-up. Isochrones and reef facies show that the corals started growing vertically about 7 ky ago on both sides, but stopped after reaching sea level (between 1 and 4 ky ago, on West Tallon and inner East Tallon, respectively). On mid and outer East Tallon, due to the characteristic reef geomorphology that keeps a constant film of water on top of the reef, the reef grew in an atypical way, prograding seaward, with this process still active (Solihuddin et al., 2016). The apparent absence of reef flat elevations between MLWS and MLWN is explained by Solihuddin et al. (2016) as an indication that during the Holocene, reefs with the potential to become HIR (that sit in macrotidal conditions, with wide reef flat and coralline algae coverage), have done so, while other reefs have remained low intertidal reefs.

Similarly to Tallon Island, the Abrolhos Holocene reefs have also developed a windward/leeward asymmetry (Collins et al., 2003), but in this case as a result of wave energy, rather than tides. The almost-submerged, windward margins are colonised by coralline algal-dominated build-ups and are about 9 m thick, more than 15 m thinner than the leeward reefs, where the accumulation of *Acropora cervicornis* have contributed to the build-up of a well-developed reef complex (over 26 m thick. Collins et al., 2003). The difference in thickness between the leeward and windward reef platforms can be linked to a different wave energy regime (much stronger windward) and a poorly developed pre-existing substrate (much lower elevation on the leeward side, which resulted in a greater accommodation space. Collins et al., 2003).

Shark Bay and Geographe Bay are located in sub-tropical and temperate regions and are characterised by a lower energy regime, with meso- to micro-tides. Since the mid-Holocene, no corals have grown in the cooler waters, instead dense seagrass meadows have developed in both the areas. The two settings also have in common a lack of major river systems, discharging large quantities of terrigenous into the ocean (they are hence *sediment-starved*, like most of Australia. McMahon and Finlayson, 2003; Brooke et al., 2017), and they both lie in sheltered locations,

protected from major weather events. In this context, the surficial sediments, deposited during the Holocene, are a combination of mixed carbonate-siliciclastic deposits, with relict quartz, eroded from older formations (mainly Peron Sandstone and Tamala Limestone, respectively) and bioclasts produced and trapped *in situ* by seagrasses and other benthic communities. Winds and currents, also influenced by the local topography, play a significant role in mobilising the sediments. In east Faure Sill, near the Wooramel Delta, north-westerly longshore currents created by tides and wind, redistribute the sediment in subparallel longshore sandbars and sand ridges. In Geographe Bay, storm waves, deviated and refracted by Cape Naturaliste (Pattiaratchi and Wijeratne, 2011), mobilise the finer sediment from the northern portion of the Bay (i.e. in front of the Capel River mouth) and keep it in suspension from the seabed. Waves and longshore currents then form the sediment into linear sandbars, oblique to the coastline, in the southern part of the Bay.

Since the Mid- Late Holocene, terrestrial, marine and *in situ* sediments have partially infilled the middle reach of the Swan River estuary. The sediment supply fluctuates daily and annually. The river is wave-dominated, hence the marine supply varies with the metocean conditions and, with a lesser influence, the tides. The terrestrial input changes seasonally. In summer, precipitation is limited, consequently mean discharge and the sediment load are drastically reduced. Seagrass and algae communities that prosper in the middle reach, produce and maintain bioclastic sediments.

Oceanic currents, especially the warm, southerly-flowing Leeuwin Current, have been a controlling mechanism, significantly influencing reef accretion across WA (i.e. reef growth at the Abrolhos. Collins et al., 2003).

Conversely from the Kimberley and, to minor extent, in Shark Bay, human impact in the SW has been significant, since the 19$^{th}$ century. Dredging and the construction of the Fremantle Harbour at the Swan River mouth (last ~1.5 km) caused an increase in marine water intrusion. Agriculture and consequent upstream use of the river has also had an impact on the sediment transport and composition, causing significant changes in runoff and inputs of sediments in the estuary (Atkinson and Klemm, 1987; Hamilton et al., 2001). In Geographe Bay, the extensive coastal development that occurred in the 1990s has significantly modified the natural hydrodynamics and the morphological profile of the beaches (especially in Port Geographe and Wonnerup. see Figure 5.1 for location).Numerous coastal protection structures, including groynes and seawalls, had to be installed to manage the shoreline erosion (Barr and Eliot, 2011).

## 3. Conclusions

The Late Quaternary evolution of Australia's western coast and continental shelf is the result of a series of controlling mechanisms that include sea-level fluctuations (two marine transgressions and a major regression), pre-existing topography and local physical characteristics and processes.

Since the Late Pleistocene, in a context of relative tectonic stability, drastic climatic changes resulted in major sea-level fluctuations that flooded, exposed and

inundated again the continental shelf, leading to multiple back and forth migrations of the shoreline. Seismic studies of the sub-surficial marine geology provided information on the depositional history and sedimentary patterns of four nearshore environments and showed that sea level changes are recorded as multiple stages of reef build-up (Kimberley) and various erosional and depositional features, such as palaeochannels and submerged ridges (Shark Bay, Swan River and Geographe Bay).

The current shape of the present coastline in the studied environmental systems (and by generalisation, the entire WA coast) reflects the inherited landscape. Weathered substrates, terranes and various stratigraphic structures, formed during previous geological times have played a significant role in modelling the initial sedimentation and providing relict terrigenous sediments, that have been transported, reworked and deposited into the systems today.

Considering the latitudinal vastness of WA, the resulting climatic variability has greatly contributed to the evolution and sediment distribution of its inner shelf and coast. In the tropical Kimberley, suitable climatic and oceanographic conditions have been essential for the onset of extensive coral reefs. Temperate seagrasses flourish in the shallow nearshore environments of Geographe Bay and Shark Bay. In these locations, the lack of major rivers and the consequent negligible terrigenous input from the mainland, together with a sheltered position that protects the bays from intense meteorological events, have resulted in clear and relatively calm waters, an optimal habitat for seagrass development. Seagrass meadows have been fundamentally involved in modifying the coastal marine environment, acting as a sediment trap, suppling habitats for organisms and providing a large volume of biogenic carbonate deposits, generated *in situ*. Seagrass and algal communities are also one of the sources of sediments for the wave-dominated Swan River environment, together with terrestrial and marine supplies.

## References

Bufarale, G., O'Leary, M., Stevens, A., Collins, L.B., 2017. Sea level controls on palaeochannel development within the Swan River estuary during the Late Pleistocene to Holocene. Catena 153. doi:10.1016/j.catena.2017.02.008

Baker, R.G., Haworth, R.J. and Flood, P.G., 2005. An oscillating Holocene sea level? Revisiting Rottnest Island, Western Australia, and the Fairbridge eustatic hypothesis. Journal of Coastal Research, pp.3-14.

Bayram, A., Larson, M. and Hanson, H., 2007. A new formula for the total longshore sediment transport rate. Coastal Engineering, 54(9), pp.700-710.

Barr, S. and Eliot, M., 2011. Busselton coastal protection. In Coasts and Ports 2011: Diverse and Developing: Proceedings of the 20th Australasian Coastal and Ocean Engineering Conference and the 13th Australasian Port and Harbour Conference (p. 30). Engineers Australia.

Bianchi, C. and Gersonde, R., 2002. The Southern Ocean surface between Marine Isotope Stages 6 and 5d: Shape and timing of climate changes. Palaeogeography, Palaeoclimatology, Palaeoecology, 187(1), pp.151-177.

Bowler, J.M., Hope, G.S., Jennings, J.N., Singh, G. and Walker, D., 1976. Late quaternary climates of Australia and New Guinea. Quaternary Research, 6(3), pp.359-394.Broecker, W.S. and Henderson, G.M., 1998. The sequence of events surrounding Termination II and their implications for the cause of glacial-interglacial CO2 changes. Paleoceanography, 13(4), pp.352-364.

Brooke, B.P., Olley, J.M., Pietsch, T., Playford, P.E., Haines, P.W., Murray-Wallace, C.V. and Woodroffe, C.D., 2014. Chronology of Quaternary coastal aeolianite deposition and the drowned shorelines of southwestern Western Australia–a reappraisal. Quaternary Science Reviews, 93, pp.106-124.

Bufarale, G., Collins, L.B., 2015. Stratigraphic architecture and evolution of a barrier seagrass bank in the mid-late Holocene, Shark Bay, Australia. Mar. Geol. 359, 1–21.

Bufarale, G., Collins, L.B., O'Leary, M.J., Stevens, A., Kordi, M. and Solihuddin, T., 2016. Quaternary onset and evolution of Kimberley coral reefs (Northwest Australia) revealed by high-resolution seismic imaging. Continental Shelf Research, 123, pp.80-88.

Bufarale, G., O'Leary, M., Stevens, A. and Collins, L.B., 2017. Sea level controls on palaeochannel development within the Swan River estuary during the Late Pleistocene to Holocene. CATENA, 153, pp.131-142.

Cabioch, G. and Ayliffe, L.K., 2001. Raised coral terraces at Malakula, Vanuatu, Southwest Pacific, indicate high sea level during marine isotope stage 3. Quaternary Research, 56(3), pp.357-365.

Carter, L. and Manighetti, B., 2006. Glacial/interglacial control of terrigenous and biogenic fluxes in the deep ocean off a high input, collisional margin: A 139 kyr-record from New Zealand. Marine geology, 226(3), pp.307-322.

Cattaneo, A. and Steel, R.J., 2003. Transgressive deposits: a review of their variability. Earth-Science Reviews, 62(3-4), pp.187-228.

Chappell, J., Thom, B.G., 1986. Coastal morphodynamics in North Australia: review and prospect. Australian Geographical Studies 24, 110–127.

Chappell, J., Omura, A., Esat, T., McCulloch, M., Pandolfi, J., Ota, Y. and Pillans, B., 1996. Reconciliaion of late Quaternary sea levels derived from coral terraces at Huon Peninsula with deep sea oxygen isotope records. Earth and Planetary Science Letters, 141(1-4), pp.227-236.

Collins, L.B., Zhu, Z.R., Wyrwoll, K.H., Hatcher, B.G., Playford, P.E., Eisenhauer, A., Chen, J.H., Wasserburg, G.J., Bonani, G., 1993. Holocene growth history of a reef

complex on a cool-water carbonate margin: Easter Group of the Houtman Abrolhos, Eastern Indian Ocean. Mar. Geol. 115, 29–46. doi:10.1016/0025-3227(93)90073-5)

Collins, L., 2002. Tertiary foundations and Quaternary evolution of coral reef systems of Australia's North West Shelf. In The sedimentary basins of Western Australia 3: Proceedings of the Petroleum Exploration Society of Australia Symposium, Perth, WA, 2002 (pp. 129-152). Petroleum Exploration Society of Australia.

Collins, L.B., Zhu, Z.R., Wyrwoll, K.H. and Eisenhauer, A., 2003. Late Quaternary structure and development of the northern Ningaloo Reef, Australia. Sedimentary Geology, 159(1), pp.81-94.

Collins, L.B., Zhao, J.X. and Freeman, H., 2006. A high-precision record of mid–late Holocene sea level events from emergent coral pavements in the Houtman Abrolhos Islands, southwest Australia. Quaternary International, 145, pp.78-85.

Collins, L.B., Testa, V., Zhao, J. and Qu, D., 2011. Holocene growth history and evolution of the Scott Reef carbonate platform and coral reef. Journal of the Royal Society of Western Australia, 94(2), pp.239-250.

Collins, L.B., 2011. Geological setting, marine geomorphology, sediments and oceanic shoals growth history of the Kimberley region. Journal of the Royal Society of Western Australia, 94(2), pp.89-105.

Collins, L.B., O'Leary, M., Stevens, A., Bufarale, G., Kordi, M., Solihuddin, T., 2015. Final Report of Project 1.3.1 of the Kimberley Marine Research Program Node of the Western Australian Marine Science Institution, WAMSI, Perth, Western Australia, 246 pp.

Cutler, K.B., Edwards, R.L., Taylor, F.W., Cheng, H., Adkins, J., Gallup, C.D., Cutler, P.M., Burr, G.S. and Bloom, A.L., 2003. Rapid sea-level fall and deep-ocean temperature change since the last interglacial period. Earth and Planetary Science Letters, 206(3), pp.253-271.

Department of Water, 2008. Rivers of the Kimberley. Water notes WN35 August 2008. https://www.water.wa.gov.au/__data/assets/pdf_file/0016/3364/82108.pdf (valid at: 22/09/2017)

Eisenhauer, A., Zhu, Z.R., Collins, L.B., Wyrwoll, K.H. and Eichstätter, R., 1996. The Last Interglacial sea level change: new evidence from the Abrolhos islands, West Australia. Geologische Rundschau, 85(3), pp.606-614.

Emery, K.O., 1968. Relict sediments on continental shelves of world. AAPG Bulletin, 52(3), pp.445-464.

Epton, K 2000, Rivers of the Kimberley: Their discovery and naming, Hesperian Press, Carlisle, Western Australia.

Esat, T.M., McCulloch, M.T., Chappell, J., Pillans, B. and Omura, A., 1999. Rapid fluctuations in sea level recorded at Huon Peninsula during the penultimate deglaciation. Science, 283(5399), pp.197-201.

Gallup, C.D., Cheng, H., Taylor, F.W. and Edwards, R.L., 2002. Direct determination of the timing of sea level change during Termination II. Science, 295(5553), pp.310-313.

Feng, M., Slawinski, D., Beckley, L.E. and Keesing, J.K., 2010. Retention and dispersal of shelf waters influenced by interactions of ocean boundary current and coastal geography. Marine and Freshwater Research, 61(11), pp.1259-1267.

Geoscience Australia, 2009. Australian Bathymetry and Topography Grid. Website: https://ecat.ga.gov.au/geonetwork/srv/eng/search#!a05f7892-fae9-7506-e044-00144fdd4fa6 (valid at: 22/09/2017).

Gingele, F.X., De Deckker, P. and Hillenbrand, C.D., 2001. Late Quaternary fluctuations of the Leeuwin Current and palaeoclimates on the adjacent land masses: clay mineral evidence. Australian Journal of Earth Sciences, 48(6), pp.867-874.

Grindrod, J., Moss, P. and Van der Kaars, S., 1999. Late Quaternary cycles of mangrove development and decline on the north Australian continental shelf. Journal of Quaternary Science, 14(5), pp.465-470.

Gozzard, J.R., 2007. Geology and Landforms of the Perth Region 53, 1689–1699. doi:10.1017/CBO9781107415324.004

Jahnert, R., de Paula, O., Collins, L., Strobach, E., Pevzner, R., 2012. Evolution of a coquina barrier in Shark Bay, Australia by GPR imaging: Architecture of a Holocene reservoir analog. Sediment. Geol. 281, 59–74. doi:10.1016/j.sedgeo.2012.08.009

Jahnert, R.J. and Collins, L.B., 2013. Controls on microbial activity and tidal flat evolution in Shark Bay, Western Australia. Sedimentology 60, 1071–1099. doi:10.1111/sed.12023

James, N.P., Collins, L.B., Bone, Y. and Hallock, P., 1999. Subtropical carbonates in a temperate realm: modern sediments on the southwest Australian shelf. Journal of Sedimentary Research, 69(6).

James, N.P., Bone, Y., Kyser, T.K., Dix, G.R. and Collins, L.B., 2004. The importance of changing oceanography in controlling late Quaternary carbonate sedimentation on a high-energy, tropical, oceanic ramp: north-western Australia. Sedimentology, 51(6), pp.1179-1205.

Hamilton, D.P., Chan, T., Robb, M.S., Pattiaratchi, C.B., Herzfeld,M., 2001. The hydrology of the upper Swan River Estuarywith focus on an artificial destratification trial. Hydrol. Process. 15 (13), 2465–2580.

Hearty, P.J., 2003. Stratigraphy and timing of eolianite deposition on Rottnest Island, Western Australia. Quaternary Research, 60(2), pp.211-222.

Hearty, P.J., Hollin, J.T., Neumann, A.C., O'Leary, M.J. and McCulloch, M., 2007. Global sea-level fluctuations during the Last Interglaciation (MIS 5e). Quaternary Science Reviews, 26(17), pp.2090-2112.

Hearty, P.J. and Olson, S.L., 2011. Preservation of trace fossils and molds of terrestrial biota by intense storms in mid–last interglacial (MIS 5c) dunes on Bermuda, with a model for development of hydrological conduits. Palaios, 26(7), pp.394-405.

Hodgkin, E.P. and Hesp, P., 1998. Estuaries to salt lakes: Holocene transformation of the estuarine ecosystems of south-western Australia. Marine and Freshwater Research, 49(3), pp.183-201.

Lambeck, K. and Nakada, M., 1990. Late Pleistocene and Holocene sea-level change along the Australian coast. Palaeogeography, Palaeoclimatology, Palaeoecology, 89(1-2), pp.143-176.

Lambeck, K. and Chappell, J., 2001. Sea level change through the last glacial cycle. Science, 292(5517), pp.679-686.

Lambeck, K., Esat, T.M. and Potter, E.K., 2002. Links between climate and sea levels for the past three million years. Nature, 419(6903), pp.199-206.

Lipar, M. and Webb, J.A., 2014. Middle–late Pleistocene and Holocene chronostratigraphy and climate history of the Tamala Limestone, Cooloongup and Safety Bay Sands, Nambung National Park, southwestern Western Australia. Australian Journal of Earth Sciences, 61(8), pp.1023-1039.

Lipar, M. and Webb, J.A., 2015. The formation of the pinnacle karst in Pleistocene aeolian calcarenites (Tamala Limestone) in southwestern Australia. Earth-Science Reviews, 140, pp.182-202.

Lipar, M., Webb, J.A., Cupper, M.L. and Wang, N., 2017. Aeolianite, calcrete/microbialite and karst in southwestern Australia as indicators of Middle to Late Quaternary palaeoclimates. Palaeogeography, Palaeoclimatology, Palaeoecology, 470, pp.11-29.

Lowe, R.J., Leon, A.S., Symonds, G., Falter, J.L. and Gruber, R., 2015. The intertidal hydraulics of tide-dominated reef platforms. Journal of Geophysical Research: Oceans, 120(7), pp.4845-4868.

McCulloch, M.T. and Esat, T., 2000. The coral record of last interglacial sea levels and sea surface temperatures. Chemical Geology, 169(1), pp.107-129.

Montaggioni, L.F. and Braithwaite, C.J., 2009. Quaternary coral reef systems: history, development processes and controlling factors (Vol. 5). Elsevier.

Montoya, M., Crowley, T.J., vonStorch, H., 1998. Temperatures at the last interglacial simulated by a coupled ocean–atmosphere climate model. Paleoceanography 13, 170–177.

Murray-Wallace, C.V. and Kimber, R.W.L., 1989. Quaternary marine aminostratigraphy: Perth Basin, Western Australia. Australian Journal of Earth Sciences, 36(4), pp.553-568.

Murray-Wallace, C.V. and Belperio, A.P., 1991. The last interglacial shoreline in Australia—a review. Quaternary Science Reviews, 10(5), pp.441-461.

Murray-Wallace, C.V., 2002. Pleistocene coastal stratigraphy, sea-level highstands and neotectonism of the southern Australian passive continental margin—a review. Journal of Quaternary Science, 17(5-6), pp.469-489.

Murray-Wallace, C.V. and Woodroffe, C.D., 2014. Quaternary sea-level changes: a global perspective. Cambridge University Press.

Nanson, G.C., Price, D.M., Short, S.A., Young, R.W. and Jones, B.G., 1991. Comparative uranium-thorium and thermoluminescence dating of weathered Quaternary alluvium in the tropics of northern Australia. Quaternary Research, 35(3), pp.347-366.

Nichol, S.L. and Brooke, B.P., 2011. Shelf habitat distribution as a legacy of Late Quaternary marine transgressions: a case study from a tropical carbonate province. Continental Shelf Research, 31(17), pp.1845-1857.

Nott, J., 2011. A 6000 year tropical cyclone record from Western Australia. Quaternary Science Reviews, 30(5), pp.713-722.

O'Leary, M., Hearty, P. J. & McCulloch, M. T., 2008. Geomorphic evidence of major sea-level fluctuations during marine isotope substage-5e, Cape Cuvier, Western Australia. Geomorphology 102, 595–602.

O'Leary, M.J., Hearty, P.J., Thompson, W.G., Raymo, M.E., Mitrovica, J.X. and Webster, J.M., 2013. Ice sheet collapse following a prolonged period of stable sea level during the last interglacial. Nature Geoscience, 6(9), pp.796-800.

Pattiaratchi, C. and Wijeratne, S., 2011. Port Geographe sand and seagrass wrack modelling study, Western Australia. Report prepared for Department of Transport (WA). SESE report no. 465, School of Environmental Systems Engineering, the University of Western Australia, Perth.

Playford, P.E., 1988. Guidebook to the Geology of Rottnest Island. Geological Society of Australia, Perth, and The Geological Survey of Western Australia

Quilty, P.G., Hosie, G., 2006. Modern foraminifera, Swan River Estuary, Western Australia: distribution and controlling factors. J. Foraminifer. Res. 36:291–314. http://dx.doi.org/10.2113/gsjfr.36.4.291.

Rabineau M, Berné S, Olivet JL, Aslanian D, Guillocheau F, Joseph P. 2006. Paleo sea levels reconsidered from direct observation of paleoshoreline position during Glacial Maxima (for the last 500,000 yr). Earth and Planetary Science Letters 252: 119–137.

Raymo, M.E., 1997. The timing of major climate terminations. Paleoceanography, 12(4), pp.577-585.

Reeves, J.M., Chivas, A.R., García, A., Holt, S., Couapel, M.J., Jones, B.G., Cendón, D.I. and Fink, D., 2008. The sedimentary record of palaeoenvironments and sea-level change in the Gulf of Carpentaria, Australia, through the last glacial cycle. Quaternary International, 183(1), pp.3-22.

Rohling, E.J., Fenton, M., Jorissen, F.J., Bertrand, P., Ganssen, G. and Caulet, J.P. 1998. Magnitudes of sea-level lowstands of the past 5000,000 years. Nature 394: 162-165.

Rohling, E.J., Hibbert, F.D., Williams, F.H., Grant, K.M., Marino, G., Foster, G.L., Hennekam, R., De Lange, G.J., Roberts, A.P., Yu, J. and Webster, J.M., 2017. Differences between the last two glacial maxima and implications for ice-sheet, δ 18 O, and sea-level reconstructions. Quaternary Science Reviews, 176, pp.1-28.

Sanderson, P.G. and Eliot, I., 1996. Shoreline salients, cuspate forelands and tombolos on the coast of Western Australia. Journal of Coastal Research, pp.761-773.

Saqab, M.M., Bourget, J., 2015. Controls on the distribution and growth of isolated carbonate build-ups in the Timor Sea (NW Australia) during the Quaternary. Mar. Pet. Geol. 62, 123–143. doi:10.1016/j.marpetgeo.2015.01.014.

Shackleton, N.J., 1987. Oxygen isotopes, ice volume and sea level. Quaternary Science Reviews, 6(3), pp.183-190.

Short, A.D. and Woodroffe, C.D., 2009. The coast of Australia. Cambridge University Press.

Siddall, M., Bard, E., Rohling, E.J. and Hemleben, C., 2006. Sea-level reversal during Termination II. Geology, 34(10), pp.817-820.

Solihuddin, T., Collins, L. B., Blakeway, D., O'Leary, M. J., 2015. Holocene coral reef accretion and sea-level in a macrotidal, high turbidity setting: Cockatoo Island, Kimberley Bioregion, northwest Australia. Marine Geology, 359, 50–60.

Solihuddin, T., O'Leary, M.J., Blakeway, D., Parnum, I., Kordi, M. and Collins, L.B., 2016. Holocene reef evolution in a macrotidal setting: Buccaneer Archipelago, Kimberley Bioregion, Northwest Australia. Coral Reefs, 35(3), pp.783-794.

Solihuddin, T., Bufarale, G., Blakeway, D. and O'Leary, M.J., 2016. Geomorphology and late Holocene accretion history of Adele Reef: a northwest Australian mid-shelf platform reef. Geo-Marine Letters, 36(6), pp.465-477.

Spooner, M.I., De Deckker, P., Barrows, T.T. and Fifield, L.K., 2011. The behaviour of the Leeuwin Current offshore NW Australia during the last five glacial–interglacial cycles. Global and Planetary Change, 75(3), pp.119-132.

Stirling, C.H., Esat, T.M., McCulloch, M.T., Lambeck, K., 1995. High-precision U-series dating of corals from Western Australia and implications for the timing and duration of the Last Interglacial. Earth Planet. Sci. Lett. 135, 115e130.

Stirling, C.H., Esat, T.M., Lambeck, K., McCulloch, M.T., 1998.Timing and duration of the Last Interglacial: evidence for a restricted interval of widespread coral reef growth. Earth Planet. Sci. Lett. 160, 745–762

Szabo, B.J., 1979. Uranium-series age of coral reef growth on Rottnest Island, Western Australia. Mar. Geol. 29, M11eM15.

Twiggs, E.J. and Collins, L.B., 2010. Development and demise of a fringing coral reef during Holocene environmental change, eastern Ningaloo Reef, Western Australia. Mar. Geol. 275, 20–36. doi:10.1016/j.margeo.2010.04.004

van der Kaars, S. and De Deckker, P., 2002. A Late Quaternary pollen record from deep-sea core Fr10/95, GC17 offshore Cape Range Peninsula, northwestern Western Australia. Review of Palaeobotany and Palynology, 120(1), pp.17-39.

Waelbroeck, C., Labeyrie, L., Michel, E., Duplessy, J.C., McManus, J.F., Lambeck, K., Balbon, E. and Labracherie, M., 2002. Sea-level and deep water temperature changes derived from benthic foraminifera isotopic records. Quaternary Science Reviews, 21(1), pp.295-305.

Walker, D.I., 1990. Seagrass in Shark Bay,Western Australia. In: Berry, P.F., Bradshaw, S.D., Wilson, B.R. (Eds.), Research in Shark Bay: Report of the France–Australe Bicentenary Expedition Committee.Western Australia Museum, Perth, Australia, pp. 101–106.

Wells, P.E. and Wells, G.M., 1994. Large-scale reorganization of ocean currents offshore Western Australia during the late Quaternary. Marine Micropaleontology, 24(2), pp.157-186.

Whiteway, T.G., 2009. Australian Bathymetry and Topography Grid, June 2009. Geoscience Australia Record 2009/21. 46pp.

Wilson, B., 2013. The biogeography of the Australian North West Shelf: environmental change and life's response. Newnes.

Woodroffe, C.D. and Webster, J.M., 2014. Coral reefs and sea-level change. Marine Geology, 352, pp.248-267.

Wywroll, K.-H., Miller, G.H., 2001. Initiation of the Australian summer monsoon 14,000 years ago. Quaternary International 83–85, 119–128.

Wyrwoll, K.H., Greenstein, B.J., Kendrick, G.W. and Chen, G.S., 2009. The palaeoceanography of the Leeuwin Current: implications for a future world. Journal of the Royal Society of Western Australia, 92(2), pp.37-51.

Yokoyama, Y., De Deckker, P., Lambeck, K., Johnston, P. and Fifield, L.K., 2001. Sea-level at the Last Glacial Maximum: evidence from northwestern Australia to

constrain ice volumes for oxygen isotope stage 2. Palaeogeography, Palaeoclimatology, Palaeoecology, 165(3), pp.281-297.

Zhu, Z.R., Wyrwoll, K.H., Collins, L.B., Chen, J.H., Wasserburg, G.J., Eisenhauer, A., 1993. High-precision U-series dating of Last Interglacial events by mass-spectrometry, Houtman-Abrolhos Islands, Western Australia. Earth Planet. Sci. Lett. 118, 281–293.

# Chapter 8

# Conclusions

"Science is the art of finding patterns in reality"
(Ian Sample, *Massive: The Higgs Boson and the Greatest Hunt in Science*)

My PhD research aimed to answer fundamental questions of how the WA's Indian Ocean coast and inner continental shelves evolved in response to major fluctuations in global climate and sea level, during the Late Pleistocene and Holocene, when the shelf became exposed during glacial periods and then flooded as the Earth warmed and ice sheets collapsed.

I have focused my efforts on four distinct and contrasting marine environments including the Kimberley coast and offshore islands (Chapter 2), Shark Bay (Chapter 3), the Swan River estuary (Chapter 4) and Geographe Bay (Chapter 5).

In each area, I took a multidisciplinary approach to my data collection and analysis utilising remote sensing, marine geophysics, sedimentological and geochronological methodologies.

The outcomes of each research project described in Chapters 2 to 5 of this thesis can be summarised as follows:

1) *Tropical marine reef system: Kimberley*. The Quaternary reef development in the Kimberley has been influenced by global sea level changes that provide a signal which is recorded in successive stages of the reef growth, separated by hiatuses. Two acoustic reflectors can be consistently distinguished across the inner shelf reefs, marking the boundaries between Holocene reef (last 12,000 years), commonly 10-15 m thick, and Last Interglacial reef (last 125,000 years) and an ancient Neoproterozoic rock foundation over which Quaternary reef growth occurred. Three acoustic horizons characterise the offshore reefs, highlighting multiple reef building stages.

2) S*ub-tropical seagrass bank system: Faure Sill (Shark Bay)*. The development of the Faure Sill has been critical in the initiation and persistence of the Hamelin Pool stromatolites and the entire local ecosystem. The evolution of the bank has been controlled by three mechanisms: 1) pre-Holocene topography that shaped the initial sedimentation with highs and channels; 2) the seagrass, which acts as a sediment trap and represents a consistent source of bioclastic and epiphytic sediments; 3) sea level fluctuations, that largely controlled the hydrodynamic conditions, such as the current velocities, influencing the erosion, transportation and deposition of the sediments.

3) *Temperate clastic estuarine system: Swan River.* The record of Late Quaternary sea level and climatic fluctuations in the metropolitan area of the Swan River comprises three generations of palaeochannels, indicating low sea level stands, and three related channel-fill deposits, representing high sea level periods.

4) *Temperate seagrass bank system: Geographe Bay*. As in the other studied environments, the geomorphic character of Late Quaternary sea-level fluctuations in Geographe Bay are recorded in a series of architectural features which developed during different sea level stands. High-resolution bathymetry and seismic data revealed the presence of shore-oblique sandbars, several palaeochannels (buried and surficial) and two sets of shore-parallel, low-relief ridges, located nearshore and at a depth of ~ 20 m. These last two seabed features are relict landforms, formed under different sea level stages.

In conclusion, from the investigations carried out during this research, it is possible to draw the following general considerations about the *Late Quaternary evolution of Western Australian continental shelf sediment systems:*

1) The coastline and the inner and mid shelf of Western Australia experienced two marine transgressions and a major regression since the Late Pleistocene.
   The evidence of the Last Interglacial highstand can be clearly found:
   - In the Kimberley, where pre-Holocene reef build-up can be recognised in the seismic profiles and in the mine pit in Cockatoo Island,
   - In Shark Bay, where Bibra Limestone has been cored and dated,
   - In the South West (Swan River and Geographe Bay), where Tamala Limestone has been clearly depicted in the seismic profiles.

   The marine transgression that followed the Last Interglacial highstand, peaked around 18 ky BP (Last Glacial maximum), when the palaeoshoreline occurred at a present-day depth of ~130 m on the continental shelf. During the following ~11,000 years (Early to Middle Holocene) the sea level rapidly rose till reaching the highstand level of more than 2 m above the present. In the last part of the Holocene (6800 years), the sea level slowly and irregularly dropped until the present. As a consequence of these sea level fluctuations, numerous seabed structures developed along the shelf, such as palaeochannels, submerged ridges and several distinct erosional and depositional features.

2) The antecedent landscape, which consists of a combination of weathered substrates, terranes and various stratigraphic and geological structures of the bedrock, has controlled the Holocene geometry and sediment distribution in the considered sedimentary settings by:
   - Shaping the modern depocentres, such as palaeovalleys and depressions, and topographic highs that confine these depocentres.
   - Providing relict sediments, especially siliciclastic, that have been reworked into the systems today.
3) The last component influencing the Late Quaternary stratigraphic structure of the continental shelf along the Western Australian coast includes the local physical characteristics and processes. Some of the factors that determine the sediment production and distribution comprise:

- Seagrass. In areas, such as Shark Bay and in Geographe Bay, where there is a lack of major fluvial terrigenous input, the extensive seagrass meadows have a primary role in reshaping and transforming the local sedimentary regime, by facilitating deposition, trapping fine sediments and producing a significant amount of biogenic carbonate deposits.
- Hydrodynamic processes. Tides, coastal currents and wind-driven circulation patterns influence sediment transport, control the seafloor sediment characteristics and are ultimately reflected in the sedimentary record.

Each of the regions studied during this thesis represents an iconic and geologically unique environment, with little published data describing the submerged landscapes, seascapes and sedimentary environments. None of these environments have been previously investigated using seismic equipment. Therefore, these research studies represent the first ever comprehensive sedimentological and stratigraphic analysis of these important settings.

# Chapter 9

# Bibliography

Abdo, D.A., Bellchambers, L.M. and Evans, S.N., 2012. Turning up the heat: increasing temperature and coral bleaching at the high latitude coral reefs of the Houtman Abrolhos Islands. PLoS One, 7(8), p.e43878.

Allard, J., Chaumillon, E. and Féniès, H., 2009. A synthesis of morphological evolutions and Holocene stratigraphy of a wave-dominated estuary: The Arcachon lagoon, SW France. Continental Shelf Research, 29(8), pp.957-969.

Allwood, A.C., Walter, M.R., Kamber, B.S., Marshall, C.P., Burch, I.W., 2006. Stromatolite reef from the Early Achaean era of Australia. Nature 441, 714 – 718.

Anderson, J.B., Wallace, D.J., Simms, A.R., Rodriguez, A.B. and Milliken, K.T., 2014. Variable response of coastal environments of the northwestern Gulf of Mexico to sea-level rise and climate change: Implications for future change. Marine Geology, 352, pp.348-366.

Applied Acoustic Engineering, 2006. Fundamentals of high resolution shallow seismic surveying-CSP-1000-8005/1.

Ashley, G., 1990. Classification of large scale subaqueous bedforms: a new look at an old problem. Journal of Sedimentary Petrology 60, 160-172.

Atkinson, R.P., Klemm, V.V., 1987. The effects of discharges, effluents and urbanisation of the Swan River, in Jacob, J., (Ed.), The Swan River estuary ecology and management. Curtin University of Technology, Bentley, pp.296-313.

Australian Hydrographic Services (AHS), 1971. Western Australia Fremantle Harbour and approaches, Final report of survey, job no. h.325. Unpublished.

Baker, G.F.U., 1956. Some aspects of Quaternary sedimentation in the Perth Basin W.A. M.Sc Thesis University of Western Australia.

Baker, R.G., Haworth, R.J. and Flood, P.G., 2005. An oscillating Holocene sea level? Revisiting Rottnest Island, Western Australia, and the Fairbridge eustatic hypothesis. Journal of Coastal Research, pp.3-14.

Baker, R.G.V., Haworth, R.J., 1997. Further evidence from relic shellcrust sequences for a late Holocene higher sea level for eastern Australia. Marine Geology 141, 1-9.

Baker, R.G.V., Haworth, R.J., 2000. Smooth or oscillating late Holocene sea-level curve? Evidence from the palaeo-zoology of fixed biological indicators in east Australia and beyond. Marine Geology 163, 367-386.

Baker, R.G.V., Haworth, R.J., Flood, P.G., 2001. Inter-tidal fixed indicators of former Holocene sea levels in Australia: a summary of sites and a review of methods and models. Quaternary International 83-85, 257-273

Baltzer, A., Tessier, B., Nouzé, H., Bates, R., Moore, C., Menier, D., 2005. Seistec seismic profiles: A tool to differentiate gas signatures. Mar. Geophys. Res. 26, 235–245. doi:10.1007/s11001-005-3721-x.

Barbier, E.B., Hacker, S.D., Kennedy, C., Koch, E.W., Stier, A.C. and Silliman, B.R., 2011. The value of estuarine and coastal ecosystem services. Ecological monographs, 81(2), pp.169-193.

Barr, S. and Eliot, M., 2011. Busselton coastal protection. In Coasts and Ports 2011: Diverse and Developing: Proceedings of the 20th Australasian Coastal and Ocean Engineering Conference and the 13th Australasian Port and Harbour Conference (p. 30). Engineers Australia.

Barr, S.A., Staples, O., Eliot, I., Darby, O., Abrahamse, D. and Stul, T., 2017. Adaptation to coastal inundation in a low lying, highly dynamic regional area. Australasian Coasts & Ports 2017: Working with Nature, p.1037.

Bastian, L. V., 1996. Residual soil mineralogy and dune subdivision, Swan Coastal Plain, Western Australia. Aust. J. Earth Sci. 43, 31–44. doi:10.1080/08120099608728233.

Bayram, A., Larson, M. and Hanson, H., 2007. A new formula for the total longshore sediment transport rate. Coastal Engineering, 54(9), pp.700-710.

Belperio, A. P., Hails, J. R., Gostin, V. A. and Polach, H. A. 1984. The stratigraphy of coastal carbonate banks and Holocene sea levels of northern Spencer Gulf, South Australia. Marine Geology 61, 297– 313.

Benson, R. C., 2005. Remote sensing and geophysical methods for evaluation of subsurface conditions. In: Practical Handbook of Environmental Site Characterization and Ground-Water Monitoring, Nielsen, D. M. (Ed.). CRC Press, Florida.

Berger, W.H., 2008. Sea level in the Late Quaternary: Patterns of variation and implications. Int. J. Earth Sci. 97, 1143–1150. doi:10.1007/s00531-008-0343-y.

Berman, M., Phillips, R., Whitbourn, L. and Heithersay, P., 2004. Automated mineralogical logging of core from the Emmie Bluff iron oxide copper-gold prospect, South Australia. PACRIM 2004 Congress, 19-22 September 2004, Adelaide, South Australia. AUSIMM Pub 5/2004

Bianchi, C. and Gersonde, R., 2002. The Southern Ocean surface between Marine Isotope Stages 6 and 5d: Shape and timing of climate changes. Palaeogeography, Palaeoclimatology, Palaeoecology, 187(1), pp.151-177.

Bird, E.C., 2011. Coastal geomorphology: an introduction. John Wiley & Sons.

Blanco, G.F., Rodríguez, G.F., González, L.A.P. and Abanades, J., 2015. Morphodynamics, sedimentary and anthropogenic influences in the San Vicente de la Barquera estuary (North coast of Spain). Geologica acta, 13(4), pp.279-295.

Blevin, J.E., Struckmeyer, H.I.M., Cathro, D.L., Totterdell, J.M., Boreham, C.J., Romine, K.K., Loutit, T.S., Sayers, J., 1998. Tectonostratigraphic framework and petroleum systems of the Browse Basin, North West Shelf. In: Purcell, P.G. and Purcell, R.R. (eds), The Sedimentary Basins of Western Australia 2: Proceedings of the Petroleum Exploration Society of Australia Symposium, Perth, 1998, 369–395.

Blewett, R.S., Kennet, B.L.N., Huston, D.J., 2012. Australia in time and space. In: Shaping a nation: A geology of Australia. Geoscience Australia and ANU E-Press.

Blum, M., Martin, J., Milliken, K. and Garvin, M., 2013. Paleovalley systems: insights from Quaternary analogs and experiments. Earth-Science Reviews, 116, pp.128-169.

Blum, M.D., Tornqvist, T.E., 2000. Fluvial responses to climate and sea-level change: a review and look forward. Sedimentology 47, 2–48. doi:10.1046/j.1365-3091.2000.00008.x.

Bourman, R.P., Murray-Wallace, C.V., Belperio, A.P. and Harvey, N., 2000. Rapid coastal geomorphic change in the River Murray Estuary of Australia. Marine Geology, 170(1), pp.141-168.

Bowler, J.M., Hope, G.S., Jennings, J.N., Singh, G. and Walker, D., 1976. Late quaternary climates of Australia and New Guinea. Quaternary Research, 6(3), pp.359-394.

Brocx, M., and Semeniuk, V., 2011. The global geoheritage significance of the Kimberley coast, Western Australia. Journal of the Royal Society of Western Australia 94, 57-88.

Broecker, W.S. and Henderson, G.M., 1998. The sequence of events surrounding Termination II and their implications for the cause of glacial-interglacial CO2 changes. Paleoceanography, 13(4), pp.352-364.

Brooke, B., 1997. Geomorphology of the north Kimberley coast, in: Walker D. (Ed.), Marine biological survey of the central Kimberley coast. Western Australia. University of Western Australia, Perth, unpublished report, W.A. Museum Library No. UR377, pp. 13–39.

Brooke, B., Creasey, J. and Sexton, M., 2010. Broad-scale geomorphology and benthic habitats of the Perth coastal plain and Rottnest Shelf, Western Australia, identified in a merged topographic and bathymetric digital relief model. International Journal of Remote Sensing, 31(23), pp.6223-6237.

Brooke, B.P., Nichol, S.L., Huang, Z. and Beaman, R.J., 2017. Palaeoshorelines on the Australian continental shelf: Morphology, sea-level relationship and applications

to environmental management and archaeology. Continental Shelf Research, 134, pp.26-38.

Brooke, B.P., Olley, J.M., Pietsch, T., Playford, P.E., Haines, P.W., Murray-Wallace, C.V. and Woodroffe, C.D., 2014. Chronology of Quaternary coastal aeolianite deposition and the drowned shorelines of southwestern Western Australia–a reappraisal. Quaternary Science Reviews, 93, pp.106-124.

Browder, A.G. and McNinch, J.E., 2006. Linking framework geology and nearshore morphology: correlation of paleo-channels with shore-oblique sandbars and gravel outcrops. Marine Geology, 231(1), pp.141-162.

Bufarale, G., Collins, L.B., 2015. Stratigraphic architecture and evolution of a barrier seagrass bank in the mid-late Holocene, Shark Bay, Australia. Mar. Geol. 359, 1–21.

Bufarale, G., Collins, L.B., O'Leary, M.J., Stevens, A., Kordi, M. and Solihuddin, T., 2016. Quaternary onset and evolution of Kimberley coral reefs (Northwest Australia) revealed by high-resolution seismic imaging. Continental Shelf Research, 123, pp.80-88.

Bufarale, G., O'Leary, M., Stevens, A., Collins, L.B., 2017. Sea level controls on palaeochannel development within the Swan River estuary during the Late Pleistocene to Holocene. CATENA 153. doi:10.1016/j.catena.2017.02.008

Buick, R., Thornett, J.R., McNaughton, N.M. and Smith, J.B., 1995. Record of emergent continental crust approximately 3.5 billion years ago in the Pilbara Craton of Australia. Nature, 375(6532), p.574.

Bureau of Meteorology - Australia, 2011. Climate summary statistics Busselton Shire. http://www.bom.gov.au/climate/averages/tables/cw_009515.shtml

Bureau of Meteorology (BoM), 2005. Climate classification maps. 26 Sept. 2017 http://www.bom.gov.au/jsp/ncc/climate_averages/climate-classifications/index.jsp?maptype=kpngrp#maps

Bureau of Meteorology (BoM), 2008. Average mean temperature. 30 October 2017 http://www.bom.gov.au/jsp/ncc/climate_averages/temperature/index.jsp?maptype=6&period=an#maps

Bureau of Meteorology (BoM), 2010. Mean rainfall. 30 October 2017 http://www.bom.gov.au/jsp/ncc/climate_averages/rainfall/index.jsp?period=win&area=wa#maps

Bureau of Meteorology (BoM). Climate summary statistics Busselton Shire. http://www.bom.gov.au/climate/averages/tables/cw_009515.shtml

Butcher, B.P., Van de Graaff, W.J.E., Hocking, R.M., 1984. Shark Bay – Edel, Western Australia: Geological Survey of Western Australia, 1:250 000 Geological Series Explanatory Notes, 1 – 21.

Cabioch, G. and Ayliffe, L.K., 2001. Raised coral terraces at Malakula, Vanuatu, Southwest Pacific, indicate high sea level during marine isotope stage 3. Quaternary Research, 56(3), pp.357-365.

Carrigy, M. A. and Fairbridge, R. W., 1954, Recent sedimentation, physiography and structure of the continental shelves of Western Australia. Royal Soc. West. Australia Jour., v. 38, p. 65-95.

Carruthers, T.J.B., Dennison, W.C., Kendrick, G.A., Waycott, M., Walker, D.I. and Cambridge, M.L., 2007. Seagrasses of south–west Australia: A conceptual synthesis of the world's most diverse and extensive seagrass meadows. Journal of Experimental Marine Biology and Ecology, 350(1), pp.21-45.

Carter, L. and Manighetti, B., 2006. Glacial/interglacial control of terrigenous and biogenic fluxes in the deep ocean off a high input, collisional margin: A 139 kyr-record from New Zealand. Marine geology, 226(3), pp.307-322.

Castel, J., Caumette, P. and Herbert, R., 1996. Eutrophication gradients in coastal lagoons as exemplified by the Bassin d'Arcachon and the Étang du Prévost. Hydrobiologia, 329(1-3), pp.ix-xxviii.

Cattaneo, A. and Steel, R.J., 2003. Transgressive deposits: a review of their variability. Earth-Science Reviews, 62(3-4), pp.187-228.

Chalmer, P.N., Hodgkin, E.P., Kendrick, G.W., 1976. Benthic faunal changes in a seasonal estuary of south-western Australia. Rec. West. Aust. Mus. 4, 383–410.

Chappell, J., Omura, A., Esat, T., McCulloch, M., Pandolfi, J., Ota, Y. and Pillans, B., 1996. Reconciliation of late Quaternary sea levels derived from coral terraces at Huon Peninsula with deep sea oxygen isotope records. Earth and Planetary Science Letters, 141(1-4), pp.227-236.

Chappell, J., Shackleton, N.J., 1986. Oxygen isotopes and sea level. Nature 324, 137–140.

Chappell, J., Thom, B.G., 1986. Coastal morphodynamics in North Australia: review and prospect. Australian Geographical Studies 24, 110–127.

Chaumillon, E., Tessier, B., Reynaud, J-Y., 2010. Stratigraphic records and variability of incised valleys and estuaries along French coasts 75–85.

Chiarella, D., Longhitano, S.G., Sabato, L. and Tropeano, M., 2012. Sedimentology and hydrodynamics of mixed (siliciclastic-bioclastic) shallow-marine deposits of Acerenza (Pliocene, Southern Apennines, Italy). Italian journal of geosciences, 131(1), pp.136-151.

Chin, A., Sweatman, H., Forbes, S., Perks, H., Walker, R., Jones, G., Williamson, D., Evans, R., Hartley, F., Armstrong, S., Malcolm, H., Edgar, G., 2008. Status of the coral reefs in Australia and Papua New Guinea, in: Wilkinson, C. (Ed), Status of Coral Reefs of the World. Global coral reef monitoring network. Reef and Rainforest Research Centre, pp 159 – 176.

Chivas, A.R., Torgensen, H.A., Polach, A., 1990. Growth rates and Holocene development of stromatolites from Shark Bay, Western Australia. Australian Journal of Earth Sciences 37, 113 – 121.

Churchill, D.M.,1959. Late Quaternary Eustatic Changes in the Swan River District. Royal Society of Western Australia, 42(2): 53-55.

Coastal Information, Department of Transport, 2016. https://catalogue.data.wa.gov.au/dataset/composite-surfaces-multibeam-lidar-laser (valid at: 22/06/2017)

Cockbain, A. E. and Playford, P. E., 1973. Stratigraphic nomenclature of Cretaceous rocks in the Perth Basin: West. Australia Geol. Survey Ann. Rept 1972, p. 26-3 1.

Coffey Geosciences, 2002. Perth Urban Rail Development South West Metropolitan Railway Geotechnical Desk Study. Unpublished.

Coffey Geosciences, 2010. Perth Flying Squadron Yacht Club Geotechnical Desk Study. Unpublished.

Cohen, A.S., Soreghan, M.I., Scholz, C.A., 1993. Estimating the age of formation of lakes – an example from Lake Tanganyika, east African rift system. Geology 21(6), 511 – 514.

Collins, L. B., 2011. Geological setting, marine geomorphology, sediments and oceanic shoals growth history of the Kimberley Region. Journal of the Royal Society of Western Australia 94(2), 89 – 105.

Collins, L. B., O'Leary, M., Stevens, A., Bufarale, G., Kordi, M., & Solihuddin, T., 2015. Geomorphic patterns, internal architecture and reef growth in a macrotidal, high-turbidity setting of coral reefs from the Kimberley bioregion. Australian Journal of Maritime & Ocean Affairs, 7(1), 12-22.

Collins, L.B., O'Leary, M., Stevens, A., Bufarale, G., Kordi, M., Solihuddin, T., 2015. Final Report of Project 1.3.1 of the Kimberley Marine Research Program Node of the Western Australian Marine Science Institution, WAMSI, Perth, Western Australia, 246 pp.

Collins, L. B., Testa V., 2010. Quaternary development of resilient reefs on the subsiding Kimberley continental margin, northwest Australia. Brazilian Journal of Oceanography 58, 1 – 13.

Collins, L. B., Zhao, J. X., & Freeman, H., 2006. A high-precision record of mid–late Holocene sea-level events from emergent coral pavements in the Houtman Abrolhos Islands, southwest Australia. Quaternary International, 145, 78-85.

Collins, L. B., Zhu, Z. R., Wyrwoll, K. H., & Eisenhauer, A., 2003. Late Quaternary structure and development of the northern Ningaloo Reef, Australia. Sedimentary Geology, 159(1), 81-94.

Collins, L., 2002. Tertiary foundations and Quaternary evolution of coral reef systems of Australia's North West Shelf. In The sedimentary basins of Western Australia 3: Proceedings of the Petroleum Exploration Society of Australia Symposium, Perth, WA, 2002 (pp. 129-152). Petroleum Exploration Society of Australia.

Collins, L., B., Jahnert, R., J., 2014. Stromatolite Research in the Shark Bay World Heritage Area. Journal of the Royal Society of Western Australia, 97: 189 – 219.

Collins, L.B. and Baxter, J.L., 1984. Heavy mineral-bearing strandline deposits associated with high-energy beach environments, southern Perth Basin, Western Australia. Aust. J. Earth Sci. 31, 287–292. doi:10.1080/14400958408527931

Collins, L.B., 1988. Sediments and history of the Rottnest Shelf, southwest Australia: a swell-dominated, non-tropical carbonate margin. Sedimentary Geology, 60.

Collins, L.B., Testa, V., Zhao, J. and Qu, D., 2011. Holocene growth history and evolution of the Scott Reef carbonate platform and coral reef. Journal of the Royal Society of Western Australia, 94(2), pp.239-250.

Collins, L.B., Zhao, J.X. and Freeman, H., 2006. A high-precision record of mid–late Holocene sea level events from emergent coral pavements in the Houtman Abrolhos Islands, southwest Australia. Quaternary International, 145, pp.78-85.

Collins, L.B., Zhu, Z.R., Wyrwoll, K.H., Hatcher, B.G., Playford, P.E., Eisenhauer, A., Chen, J.H., Wasserburg, G.J., Bonani, G., 1993. Holocene growth history of a reef complex on a cool-water carbonate margin: Easter Group of the Houtman Abrolhos, Eastern Indian Ocean. Mar. Geol. 115, 29–46. doi:10.1016/0025-3227(93)90073-5)

Collins, L.B.,1987. Geological evolution of the Swan-Canning estuarine system, in Jacob, J., (Ed.), The Swan River estuary ecology and management. Curtin University of Technology, Bentley, pp. 9-20.

Commander, D.P., 1982. The Bunbury shallow drilling groundwater investigation. Western ustralia Geological Survey, Professional Papers for, pp.32-52.

Commander, P., 2003. Outline of the geology of the Perth region. Aust. Geomech. 38, 7–16.

Commonwealth of Australia, 2006. A guide to the integrated marine and coastal regionalisation of Australia Version 4.0. Department of the Environment and Heritage, Canberra, Australia.

Condie, S.A., Andrewartha, J., 2008. Circulation and connectivity on the Australian North West Shelf. Continental Shelf Research 28, 14: 1724 – 1739.

Cresswell, G. R., Badcock, K. A., 2000. Tidal mixing near the Kimberley coast of NW Australia. Marine Freshwater Research 51, 641 – 6.

Creveling, J.R., Mitrovica, J.X., Clark, P.U., Waelbroeck, C. and Pico, T., 2017. Predicted bounds on peak global mean sea level during marine isotope stages 5a and 5c. Quaternary Science Reviews, 163, pp.193-208.

CSIRO, 2015. Tidal Dataset - CAMRIS - Maximum Tidal Range. v1. CSIRO. Data Collection. http://doi.org/10.4225/08/551485767777F

Cutler, K.B., Edwards, R.L., Taylor, F.W., Cheng, H., Adkins, J., Gallup, C.D., Cutler, P.M., Burr, G.S. and Bloom, A.L., 2003. Rapid sea-level fall and deep-ocean temperature change since the last interglacial period. Earth and Planetary Science Letters, 206(3), pp.253-271.

Dalrymple, R.W., Choi, K., 2007. Morphologic and facies trends through the fluvial – marine transition in tide-dominated depositional systems : A schematic framework for environmental and sequence-stratigraphic interpretation 81, 135–174. doi:10.1016/j.earscirev.2006.10.002.

Dalrymple, R.W., Zaitlin, B.A. and Boyd, R., 1992. Estuarine facies models: conceptual basis and stratigraphic implications: perspective. Journal of Sedimentary Research, 62(6).

Davidson, W. A., 1995. Hydrogeology and groundwater resources of the Perth Region, Western Australia: Western Australia Geological Survey, Bulletin 142.

Davies, G.R., 1970. Carbonate bank sedimentation, Eastern Shark Bay, Western Australia: Carbonate sedimentation and environments, Shark Bay, Western Australia. In: Logan, B.W., Davies, G.R., Read, J.F., Cebulski, D.E (Eds.),Carbonate sedimentation and environments, Shark Bay, Western Australia. American Association of Petroleum Geologists Memoirs 13, 85 – 168.

Davies, G.R., 1970. Algal laminated sediments, Gladstone Embayment, Shark Bay, Western Australia. Carbonate sedimentation and environments, Shark Bay, Western Australia. In: Logan, B.W., Davies, G.R., Read, J.F., Cebulski, D.E (Eds.),Carbonate sedimentation and environments, Shark Bay, Western Australia. American Association of Petroleum Geologists Memoirs 13, 169 – 205.

Deeney, A.C., 1989. Geology and groundwater resources of the superficial formations between Pinjarra and Bunbury, Perth Basin. Geological Survey of Western Australia, Report, 26, pp.31-57.

Department of Environment Western Australia (DoE-WA), 2004. The Importance of Western Australia's Waterways. 30 October 2017 http://www.water.wa.gov.au/__data/assets/pdf_file/0007/3211/85861.pdf

Department of the Environment, 2014. Australia's 15 National Biodiversity Hotspots. Australian Government, Canberra. Available at: http://www.environment.gov.au/node/13909

Department of Transport, Western Australia. https://www.transport.wa.gov.au/imarine/Cape-Peron-to-Albany.asp (valid at: 22/06/2017).

Department of Water, 2008. Rivers of the Kimberley. Water notes WN35 August 2008. https://www.water.wa.gov.au/__data/assets/pdf_file/0016/3364/82108.pdf (valid at: 22/09/2017)

Dravis, J. J. 1983. Hardened subtidal stromatolites, Bahamas. Science 219, 385–386.

Duarte, C., Kennedy, H., Marbà, N., Hendriks, I., 2013. Assessing the capacity of seagrass meadows for carbon burial: current limitations and future strategies. Ocean and Coastal Management 83, 32 – 38.

Duarte, C.M., 2002. The future of seagrass meadows. Environmental Conservation 02, pp 192 – 206.

Duncan, A.J. and Gavrilov, A., 2012. Low frequency acoustic propagation over calcarenite seabeds with thin, hard caps. Proceedings of Acoustics 2012, Fremantle Western Australia.

Duncan, A.J., Gavrilov, A. and Li, F., 2009. Acoustic propagation over limestone seabeds. Proceedings of Australian Acoustical Society 2009, Adelaide, South Australia.

Eisenhauer, A., Wasserburg, G. J., Chen, J. H., Bonani, G., Collins, L. B., Zhu, Z. R., & Wyrwoll, K., 1993. Holocene sea-level determination relative to the Australian continent: U/Th (TIMS) and 14C (AMS) dating of coral cores from the Abrolhos Islands. Earth and Planetary Science Letters, 114(4), 529-547.

Eisenhauer, A., Zhu, Z.R., Collins, L.B., Wyrwoll, K.H. and Eichstätter, R., 1996. The Last Interglacial sea level change: new evidence from the Abrolhos islands, West Australia. Geologische Rundschau, 85(3), pp.606-614.

Eliot, M.J., Travers, A., Eliot, I., 2006. Morphology of a Low-Energy Beach, Como Beach, Western Australia. J. Coast. Res. 221, 63–77. doi:10.2112/05A-0006.1.

Emery, K.O., 1968. Relict sediments on continental shelves of world. AAPG Bulletin, 52(3), pp.445-464.

Epton, K 2000, Rivers of the Kimberley: Their discovery and naming, Hesperian Press, Carlisle, Western Australia.

Esat, T.M., McCulloch, M.T., Chappell, J., Pillans, B. and Omura, A., 1999. Rapid fluctuations in sea level recorded at Huon Peninsula during the penultimate deglaciation. Science, 283(5399), pp.197-201.

Evans, K., Bax, N. & Smith, D.C., 2017. Australia state of the environment 2016: marine environment, independent report to the Australian Government Minister for

the Environment and Energy, Australian Government Department of the Environment and Energy, Canberra.

Evans, K.G., Stephens, A.W., Shorten, G.G., 1992. Quaternary sequence stratigraphy of the Brisbane River delta, Moreton Bay, Australia. Mar. Geol. 107, 61–79. doi:10.1016/0025-3227(92)90069-T.

Fahrner, C.K. and Pattiaratchi, C.B., 1994. The physical oceanography of Geographe Bay, Western Australia. Report prepared for the Water Authority of Western Australia.

Fairbridge, R.W., 1961. Eustatic changes in sea level. Physics and Chemistry of the Earth, 4, 99-185 (London: Pergamon).

Fallon, S.J., Fifield, L.K., Chappell, J.M., 2010. The next chapter in radiocarbon dating at the Australian National University: Status report on the single stage AMS, Nuclear Instruments and Methods in Physics Research. B 268, 898 – 901.

Falvey, D.A., & Mutter, J.C., 1981. Regional plate tectonics and the evolution of Australia's passive continental margins. BMR J. Aust. Geol. Geophys., 6, 1-29

Felix, C. A., Martins, T. S., Soares, C. H. C., Guesser, V., Demarco, L. F., Suthard, B., ... & de Mahiques, M. M., 2013. Some limitations of shallow water geophysical devices imposed by different oceanographic and geological conditions. In: Acoustics in Underwater Geosciences Symposium (RIO Acoustics), 2013 IEEE/OES (pp. 1-8), IEEE.

Feng, M., Meyers, G., Pearce, A. and Wijffels, S., 2003. Annual and interannual variations of the Leeuwin Current at 32 S. Journal of Geophysical Research: Oceans, 108(C11).

Feng, M., Slawinski, D., Beckley, L.E. and Keesing, J.K., 2010. Retention and dispersal of shelf waters influenced by interactions of ocean boundary current and coastal geography. Marine and Freshwater Research, 61(11), pp.1259-1267.

Fonseca, M.S., Fisher, J.S., Zieman, J.C., Thayer, G.W., 1982. The role of current velocity in structuring seagrass meadows. Estuarine, Coastal and Shelf Science, 17, 367–380.

Fourqurean, J. W., Kendrick, G. A., Collins, L. S., Chambers, R. M., Vanderklift, M. A., 2012. Carbon, nitrogen and phosphorus storage in subtropical seagrass meadows: examples from Florida Bay and Shark Bay. Marine and Freshwater Research 63, 967 – 983.

Gallop, S.L., Verspecht, F. and Pattiaratchi, C.B., 2012. Sea breezes drive currents on the inner continental shelf off southwest Western Australia. Ocean Dynamics, 62(4), pp.569-583.

Gallup, C.D., Cheng, H., Taylor, F.W. and Edwards, R.L., 2002. Direct determination of the timing of sea level change during Termination II. Science, 295(5553), pp.310-313.

Galparsoro, I., Borja, Á., Legorburu, I., Hernández, C., Chust, G., Liria, P., Uriarte, A., 2010. Morphological characteristics of the Basque continental shelf (Bay of Biscay, northern Spain); their implications for Integrated Coastal Zone Management. Geomorphology 118, 314–329. doi:10.1016/j.geomorph.2010.01.012

Geographe Catchment Council, 2008. Geographe Catchment Management Strategy. A Report for the Geographe Catchment Council, Water and Rivers Commission and National Heritage Trust.

Geological Survey of Western Australia (GSWA), 1974, Geology of Western Australia. West. Australia Geol. Survey, Mem. 2, 541 p.

Geological Survey of Western Australia (GSWA), 1990. Geology and Mineral Resources of Western Australia: Western Australia Geological Survey, Memoir 3, 827p.

Geoscience Australia, 2009. Australian Bathymetry and Topography Grid. Website: https://ecat.ga.gov.au/geonetwork/srv/eng/search#!a05f7892-fae9-7506-e044-00144fdd4fa6 (valid at: 22/09/2017).

Gibbes, B., Grinham, A., Neil, D., Olds, A., Maxwell, P., Connolly, R.,Weber, T., Udy, N., Udy, J., 2014. Moreton Bay and Its estuaries: a sub-tropical system under pressure from rapid population growth. In: Wolanski, E. (Ed.), Estuaries of Australia in 2050 and Beyond. Estuaries of the World, Springer, Dordrecht, pp. 203–222.

Gingele, F.X., De Deckker, P. and Hillenbrand, C.D., 2001. Late Quaternary fluctuations of the Leeuwin Current and palaeoclimates on the adjacent land masses: clay mineral evidence. Australian Journal of Earth Sciences, 48(6), pp.867-874.

Golder Associated Pty Ltd, 2008. Geotechnical investigation, Perth Waterfront Project, Perth Foreshore. Western Australia. Unpublished.

Golder Associated Pty Ltd, 2012. Interpretive Report, Phase 2 Geotechnical Studies, Perth Waterfront Development, Western Australia. Unpublished.

Gordon, F.R., 2003. Sea level change and paleochannels in the Perth area. Aust. Geomech. 38, 85–90.

Gordon, F.R., 2003. Coastal Limestones. Aust. Geomech. 38, 7–24.

Gordon, F.R., 2012. Geology of quaternary coastal limestones of Western Australia. Thesis (Ph.D.), Curtin University.

Gozzard, J.R., 2007. A reinterpretation of the Guildford formation. Aust. Geomech. 42 (3).

Gozzard, J.R., 2007. Geology and landforms of the Perth region. Geological Survey of Western Australia, p126 doi:10.1017/CBO9781107415324.004.

Green, M.O., Vincent, C.E., Trembanis, A.C., 2004. Suspension of coarse and fine sand on a wave-dominated shoreface, with implications for the developments of rippled scour depressions. Cont. Shelf Res. 24, 317–335.

Grimsditch, G., Alder, J., Nakamura, T., Kenchington, R., Tamelander, J., 2012. The blue carbon special edition – Introduction and overview. Ocean and Coastal Management, iFirst, 1 – 4.

Grindrod, J., Moss, P. and Van der Kaars, S., 1999. Late Quaternary cycles of mangrove development and decline on the north Australian continental shelf. Journal of Quaternary Science, 14(5), pp.465-470.

Hagan, G. M. and Logan, B. W., 1974. Development of carbonate banks and hypersaline basins, Shark Bay, Western Australia. American Association of Petroleum Geologists, Memoir 22, 61 – 139.

Hamilton, D.P., Chan, T., Robb, M.S., Pattiaratchi, C.B., Herzfeld,M., 2001. The hydrology of the upper Swan River Estuarywith focus on an artificial destratification trial. Hydrol. Process. 15 (13), 2465–2580.

Hamilton, E.L., 1970. Sound velocity and related properties of marine sediments, North Pacific. Journal of Geophysical Research 75, 23

Hamilton, N.T.M. and Collins, L.B., 1997. Morphostratigraphy and evolution of a Holocene composite barrier at Minninup, southwestern Australia. Aust. J. Earth Sci. 44, 113–124. doi:10.1080/08120099708728298

Hancock, S., Brown, P., Stephens, B., 2000. Shark Bay Terrestrial Reserves Management Plan 2000 – 2009. Department of Conservation and Land Management for the National Parks and Nature Conservation Authority Perth, Western Australia.

Harris, P.T. and Macmillan-Lawler, M., 2016. Global Overview of Continental Shelf Geomorphology Based on the SRTM30_PLUS 30-Arc Second Database. In Seafloor Mapping along Continental Shelves (pp. 169-190). Springer International Publishing.

Hayes, M.O., 1980. General morphology and sediment patterns in tidal inlets. Sedimentary Geology 26, 139 – 156.

Hearty, P.J. and O'Leary, M.J., 2008. Carbonate eolianites, quartz sands, and Quaternary sea level cycles, Western Australia: A chronostratigraphic approach. Quat. Geochronol. 3, 26–55. doi:10.1016/j.quageo.2007.10.001

Hearty, P.J. and Olson, S.L., 2011. Preservation of trace fossils and molds of terrestrial biota by intense storms in mid–last interglacial (MIS 5c) dunes on Bermuda, with a model for development of hydrological conduits. Palaios, 26(7), pp.394-405.

Hearty, P.J., 2003. Stratigraphy and timing of eolianite deposition on Rottnest Island, Western Australia. Quat. Res. 60, 211-222.

Hearty, P.J., Hollin, J.T., Neumann, A.C., O'Leary, M.J., McCulloch, M., 2007. Global sea-level fluctuations during the Last Interglaciation (MIS 5e). Quat. Sci. Rev. 26, 2090–2112. doi:10.1016/j.quascirev.2007.06.019.

Heithaus, M.R., 2001. The Biology of Tiger Sharks, Galeocerdo Cuvier, in Shark Bay, Western Australia: Sex Ratio, Size Distribution, Diet, and Seasonal Changes in Catch Rates. Environmental Biology of Fishes 61(1), 25 – 36.

Heithaus, M.R., 2004. Fish communities of subtropical seagrass meadows and associated habitats in Shark Bay, Western Australia. Bulletin of Marine Science 75 (1), 79 – 99(21).

Hendriks, I.E., Sintes, T., Bouma, T.J. and Duarte, C.M., 2008. Experimental assessment and modeling evaluation of the effects of the seagrass Posidonia oceanica on flow and particle trapping. Marine Ecology Progress Series.

Hill, P.J., De Deckker†, P., von der Borch, C., Murray-Wallace, C. V., 2009. Ancestral Murray River on the Lacepede Shelf, southern Australia: Late Quaternary migrations of a major river outlet and strandline development. Aust. J. Earth Sci. 56, 135–157. doi:10.1080/08120090802546993.

Hillman, K., McComb, A.J. and Walker, D.I., 1995. The distribution, biomass and primary production of the seagrass Halophila ovalis in the Swan/Canning Estuary, Western Australia. Aquatic Botany, 51(1), pp.1-54.

Hirschberg, K-J B, 1989. Busselton shallow-drilling groundwater investigation, Perth Basin, Geological Survey of Western Australia, Professional Papers, Report 25, pp17–37.

Hocking, R. M., Moors, H. T., Van De Graaff W. J. E., 1987. Geology of the Carnarvon Basin Western Australia. Geological Survey of Western Australia Bulletin 133, 289.

Hodgkin, E.P. and Hesp, P., 1998. Estuaries to salt lakes: Holocene transformation of the estuarine ecosystems of south-western Australia. Marine and Freshwater Research, 49(3), pp.183-201.

Hoover, D. B., Klein, D. P. and Campbell, D. C., 1995. Geophysical methods in exploration and mineral environmental investigations. In: Preliminary compilation of descriptive geoenvironmental mineral deposit models, Du Bray, E. A. (Ed.). Denver, US Geological Survey.

Hopley, D., Smithers, S., Parnell, K., 2007. The Geomorphology of the Great Barrier Reef: development, diversity, change. Cambridge.

Hori, K., Tanabe, S., Saito, Y., Haruyama, S., Nguyen, V. and Kitamura, A., 2004. Delta initiation and Holocene sea-level change: example from the Song Hong (Red River) delta, Vietnam. Sedimentary Geology, 164(3), pp.237-249.

Hudson-Smith, E., Grinceri, M., 2007. Ground conditions and building protection for the New MetroRail City Project, Perth. Aust. Geomech. 42, 33–58.

Huntington, J., Mauger, A., Skirrow, R., Bastrakov, E., Connor, P., Mason, P., Keeling, J., Coward, D.,

IHO, International Hydrographic Organization (2013). Standardization of undersea feature names: guidelines proposal for terminology: Draft. Publication B-6 Edition 4.1.0, xxxx 2013 English/French Version, Monaco. 26 September 2017 <https://www.iho.int/iho_pubs/draft_pubs/B-6_e4.1.0_2013_v2_20130510.pdf>.

Jahnert, R., de Paula, O., Collins, L., Strobach, E., Pevzner, R., 2012. Evolution of a coquina barrier in Shark Bay, Australia by GPR imaging: Architecture of a Holocene reservoir analog. Sediment. Geol. 281, 59–74. doi:10.1016/j.sedgeo.2012.08.009

Jahnert, R.J, Collins, L.B., 2011. Significance of subtidal microbial deposits in Shark Bay, Australia. Marine Geology 286, 106 – 111.

Jahnert, R.J. and Collins, L.B., 2012. Characteristics, distribution and morphogenesis of subtidal microbial systems in Shark Bay, Australia, Marine Geology 303 – 306,115 – 136.

Jahnert, R.J. and Collins, L.B., 2013. Controls on microbial activity and tidal flat evolution in Shark Bay, Western Australia. Sedimentology 60, 1071–1099. doi:10.1111/sed.12023

James, N.P. and Bone, Y., 2010. Neritic carbonate sediments in a temperate realm: southern Australia. Springer Science & Business Media.

James, N.P., Bone, Y., Kyser, T.K., Dix, G.R. and Collins, L.B., 2004. The importance of changing oceanography in controlling late Quaternary carbonate sedimentation on a high-energy, tropical, oceanic ramp: north-western Australia. Sedimentology, 51(6), pp.1179-1205.

James, N.P., Collins, L.B., Bone, Y. and Hallock, P., 1999. Subtropical carbonates in a temperate realm: modern sediments on the southwest Australian shelf. Journal of Sedimentary Research, 69(6).

Johnson, SL, 2002, Stratigraphy of the Leederville Formation in the western portion of the Busselton-Capel Groundwater Area, Department of Environment, Hydrogeology Report 198 (unpublished).

Jones, P.H., Marsh, J.G., 1965. Some problems in the construction of embankments for the Mitchell Freeway, Perth W.A. Institution of Engineers Australia Journal Vol. CE 7 No. 2.

Kearey, P., Brooks, M. and Hill, I., 2002. An introduction to geophysical exploration. Third edition, Blackwell Scientific, Oxford, UK, pp 292.

Kendrick, G.W., Wyrwoll, K.-H., Szabo, B.J., 1991. Pliocene–Pleistocene coastal events and history along the western margin of Australia. Quaternary Sci. Rev., 10(5), pp. 419–439.

Kennewell, C., Shaw, B.J., 2008. Perth, Western Australia. Cities 25, 243–255. doi:10.1016/j.cities.2008.01.002.

Kirkman, H. 1997. Seagrasses of Australia. State of the Environment Technical Paper Series (Estuaries and the Sea). Canberra, Australia: Department of the Environment.

Klingebiel, A. and Gayet, J., 1995. Fluvio-lagoonal sedimentary sequences in Leyre delta and Arcachon bay, and Holocene sea level variations, along the Aquitaine coast (France). Quaternary International, 29, pp.111-117.

Koch, E. W., Ackerman, J. D., Verduin, J., van Keulen, M., 2006. Fluid Dynamics in Seagrass Ecology – from Molecules to Ecosystems. In: Larkum, A.W.D., Orth, R.J., Duarte, C.M. (Eds) Seagrasses: biology, ecology and conservation. 193 – 225.

Kordi, M.N., Collins, L.B., O'Leary, M., and Stevens, A., 2016. ReefKIM: an integrated geodatabase for sustainable management of the Kimberley Reefs, NW Australia. Ocean & Coastal Management, 119: 234-243.

Lambeck, K. and Chappell, J., 2001. Sea level change through the last glacial cycle. Science, 292(5517), pp.679-686.

Lambeck, K. and Nakada, M., 1990. Late Pleistocene and Holocene sea-level change along the Australian coast. Palaeogeography, Palaeoclimatology, Palaeoecology, 89(1-2), pp.143-176.

Lambeck, K., Esat, T.M., Potter, E.-K., 2002. Links between climate and sea levels for the past three million years. Nature 419, 199–206. doi:10.1038/nature01089.

Lambeck, K., Rouby, H., Purcell, A., Sun, Y., Sambridge, M., 2014. Sea level and global ice volumes from the Last Glacial Maximum to the Holocene. Proc. Natl. Acad. Sci. U. S. A. 111, 15296–303. doi:10.1073/pnas.1411762111.

Larcombe, P., 2007. Continental shelf environments. In: Perry, C. and Taylor, K. eds., 2007. Environmental sedimentology. John Wiley & Sons. Pp 351-388.

Lavery PS, Mateo M – A, Serrano O, Rozaimi M, 2013. Variability in the carbon storage of seagrass habitats and its implications for Global Estimates of Blue Carbon Ecosystem Service. PLoS ONE 8(9).

Leighton, T.G., Robb, G.B.N., 2008. Preliminary mapping of void fractions and sound speeds in gassy marine sediments from sub-bottom profiles. Journal of Acoustical Society of America 124 (5), 313 – 320.

Lekkerkerk H. J., Van der Velden R., Roders J., Haycock T., De Vries R., Jansen P., Beemster C., 2006. Handbook of Offshore Surveying Volume 2 - Acquisition and Processing, London Clarkson Research Services Limited

Leorri, E. and Cearreta, A., 2004. Holocene environmental development of the Bilbao estuary, northern Spain: sequence stratigraphy and foraminiferal interpretation. Marine Micropaleontology, 51(1), pp.75-94.

Lipar, M. and Webb, J.A., 2014. Middle–late Pleistocene and Holocene chronostratigraphy and climate history of the Tamala Limestone, Cooloongup and Safety Bay Sands, Nambung National Park, southwestern Western Australia. Australian Journal of Earth Sciences, 61(8), pp.1023-1039.

Lipar, M. and Webb, J.A., 2015. The formation of the pinnacle karst in Pleistocene aeolian calcarenites (Tamala Limestone) in southwestern Australia. Earth-Science Reviews, 140, pp.182-202.

Lipar, M., Webb, J.A., Cupper, M.L. and Wang, N., 2017. Aeolianite, calcrete/microbialite and karst in southwestern Australia as indicators of Middle to Late Quaternary palaeoclimates. Palaeogeography, Palaeoclimatology, Palaeoecology, 470, pp.11-29.

Lisiecki, L.E., Raymo, M.E., 2005. A Pliocene-Pleistocene stack of 57 globally distributed benthic δ18O records. Paleoceanography 20, 1–17. doi:10.1029/2004PA001071.

Logan, B. W., 1968. Western Australia: in Quaternary shorelines research in Australia and New Zealand. Edited by ED GILL: Australian Journal of Science 31, 110.

Logan, B. W., Davies, G. R., Read, J. F., Cebulski, D.E., 1970. Carbonate sedimentation and environments, Shark Bay, Western American Association of Petroleum Geologists, Memoir 13, 223.

Logan, B. W., Read, J. F., Davies, G. R., 1970. History of carbonate sedimentation, Quaternary Epoch, Shark Bay, Western Australia. In Carbonate sedimentation and environments, Shark Bay, Western Australia. Logan, B.W., Davies, G.R., Read, J.F., Cebulski, D.E (Eds.),Carbonate sedimentation and environments, Shark Bay, Western Australia. American Association of Petroleum Geologists Memoir 13, pp 38–84.

Logan, B.W., Cebulski, D.E., 1970. Sedimentary environments of Shark Bay, Western Australia. In: Logan, B.W., Davies, G.R., Read, J.F., Cebulski, D.E (Eds.),Carbonate sedimentation and environments, Shark Bay, Western Australia. American Association of Petroleum Geologists Memoirs 13, 1–37.

Logan, B.W., Read, J.F., Hagan, G.M., Hoffman, P., Brown, R.G., Woods, P.J., Gebelein, C.D., 1974. Evolution and diagenesis of quaternary carbonate sequences, Shark Bay, Western Australia. American Association of Petroleum Geologists Memoir 22, 358.

Longhitano, S.G., 2011. The record of tidal cycles in mixed silici–bioclastic deposits: examples from small Plio–Pleistocene peripheral basins of the microtidal Central Mediterranean Sea. Sedimentology, 58(3), pp.691-719.

Longley, I.M., Buessenschuett, C., Clydsdale, L., Cubitt, C.J., Davis, R.C., Johnson, M.K., Marshall, N.,M., Murray, A.P., Somerville, R., Spry, T.B., Thompson, N.B., 2002. The North West Shelf of Australia e a Woodside perspective. In: Purcell, P.G.,

Purcell, R.R. (Eds.), The Sedimentary Basins of Western Australia: Proceedings of the Petroleum Exploration Society of Australia 3. Perth, pp. 27 – 88.

Lowe, R.J., Leon, A.S., Symonds, G., Falter, J.L. and Gruber, R., 2015. The intertidal hydraulics of tide-dominated reef platforms. Journal of Geophysical Research: Oceans, 120(7), pp.4845-4868.

Main Roads Western Australia (MRWA), 1998. Narrows Bridge widening project report on survey of existing documents possibly relevant to foundation conditions. Unpublished.

Mathew, G.V., 2010. Analysis and interpretation of ground and building movements due to EPB tunnelling. PhD Thesis, University of Western Australia.

Matzner, R. A., 2001. Dictionary of geophysics, astrophysics, and astronomy. CRC Press, Florida.

Mccomb, K.H.A.J., Walker, D.I., 1995. Aquatic botany The distribution , biomass and primary production of the seagrass Halophila ovalis in the Swan / Canning Estuary, Western Australia 51, 1–54.

McCulloch, M.T. and Esat, T., 2000. The coral record of last interglacial sea levels and sea surface temperatures. Chemical Geology, 169(1), pp.107-129.

McKenzie, N.L., Start, A.N., Burbidge, A.A., Kenneally, K.F., Burrows, N.D., 2009. Protecting the Kimberley: a synthesis of scientific knowledge to support conservation management in the Kimberley region of Western Australia. Department of Environment and Conservation, Perth, WA.

McMahon, K., Young, E., Montgomery, S., Cosgrove, J., Wilshaw, J., Walker, D.I., 1997. Status of a shallow seagrass system, Geographe Bay, south-western Australia. J. R. Soc. West. Aust. 80, 255–262.

McMahon, T.A. and Finlayson, B.L., 2003. Droughts and anti-droughts: the low flow hydrology of Australian rivers. Freshwater Biology, 48(7), pp.1147-1160.

McNinch, J.E. and Miselis, J.L., 2012. Geology metrics for predicting shoreline change using seabed and sub-bottom observations from the surf zone and nearshore. Int. Assoc. Sedimentol. Spec. Publ, 44, pp.99-120.

McNinch, J.E., 2004. Geologic control in the nearshore: shore-oblique sandbars and shoreline erosional hotspots, Mid-Atlantic Bight, USA. Marine Geology 211, 121–141.

Menier, D., Tessier, B., Dubois, A., Goubert, E. and Sedrati, M., 2011. Geomorphological and hydrodynamic forcing of sedimentary bedforms-Example of Gulf of Morbihan (South Brittany, Bay of Biscay). Journal of Coastal Research, (64), p.1530.

Montaggioni, L. F., 2005. History of Indo-Pacific coral reef systems since the last glaciation: Development patterns and controlling factors. Earth – Science Reviews 71 (1 – 2), 1 – 75.

Montaggioni, L.F. and Braithwaite, C.J., 2009. Quaternary coral reef systems: history, development processes and controlling factors (Vol. 5). Elsevier.

Montoya, M., Crowley, T.J., vonStorch, H., 1998. Temperatures at the last interglacial simulated by a coupled ocean–atmosphere climate model. Paleoceanography 13, 170–177.

Moore, L.S., Burne, R.V., 1994. The Modern Thrombolites of Lake Clifton, Western Australia. Phanerozoic Stromatolites II, pp 3 – 29.

Munsell, A. H., 1954. Munsell Soil Color Chart. U.S Dept. Agriculture. Soil Survey Manual 2009 Edition Munsell Soil Chart.

Murray, A.B. and Thieler, E.R., 2004. A new hypothesis and exploratory model for the formation of large-scale inner-shelf sediment sorting and “rippled scour depressions”. Cont. Shelf Res. 24, 295–315.

Murray, C. J., Last, G. V., Truex, M. J., 2005. Review of Geophysical Techniques to Define the Spatial Distribution of Subsurface Properties or Contaminants. Pacific Northwest National Laboratory.

Murray-Wallace, C. V. and Kimber, R.W.L., 1989. Quaternary marine aminostratigraphy: Perth Basin, Western Australia. Aust. J. Earth Sci. 36, 553–568. doi:10.1080/08120098908729509

Murray-Wallace, C.V. and Belperio, A.P., 1991. The last interglacial shoreline in Australia—a review. Quaternary Science Reviews, 10(5), pp.441-461.

Murray-Wallace, C.V. and Woodroffe, C.D., 2014. Quaternary sea-level changes: a global perspective. Cambridge University Press.

Murray-Wallace, C.V., 2002. Pleistocene coastal stratigraphy, sea-level highstands and neotectonism of the southern Australian passive continental margin—a review. Journal of Quaternary Science, 17(5-6), pp.469-489.

Mussett, A. E. and Khan, M. A., 2000. Looking into the Earth. Cambridge: Cambridge University Press.

Nahas, E. L., Pattiaratchi, C. B., Ivey, G. N., 2005. Process controlling the position of frontal systems in Shark Bay, Western Australia. Estuarine, Coastal and Shelf Science 65, 463 – 474.

Nanson, G.C., Price, D.M., Short, S.A., Young, R.W. and Jones, B.G., 1991. Comparative uranium-thorium and thermoluminescence dating of weathered Quaternary alluvium in the tropics of northern Australia. Quaternary Research, 35(3), pp.347-366.

Nichol, S.L. and Brooke, B.P., 2011. Shelf habitat distribution as a legacy of Late Quaternary marine transgressions: a case study from a tropical carbonate province. Continental Shelf Research, 31(17), pp.1845-1857.

Niedoroda, A., W., 2005. Continental shelves. In: Schwartz, M., Encyclopedia of Coastal Science. Encyclopedia of Earth Sciences Series. Springer, 2005. 26 September 2017 <http://www.myilibrary.com?ID=41174>. Pp 337-339.

Nott, J., 2011. A 6000 year tropical cyclone record from Western Australia. Quaternary Science Reviews, 30(5), pp.713-722.

O'Leary, M. J., Hearty, P. J., McCulloch, M. T., 2008. U – series evidence for widespread reef development in Shark Bay during the last interglacial. Palaeogeography, Palaeoclimatology, Palaeoecology 259: 424 – 435.

O'Leary, M.J., Hearty, P.J., McCulloch, M.T., 2008. Geomorphic evidence of major sea-level fluctuations during marine isotope substage-5e, Cape Cuvier, Western Australia. Geomorphology 102, 595–602. doi:10.1016/j.geomorph.2008.06.004.

O'Leary, M.J., Hearty, P.J., Thompson, W.G., Raymo, M.E., Mitrovica, J.X. and Webster, J.M., 2013. Ice sheet collapse following a prolonged period of stable sea level during the last interglacial. Nature Geoscience, 6(9), pp.796-800.

O'Faircheallaigh, C., 2013. Extractive industries and Indigenous peoples: a changing dynamic?. Journal of Rural Studies 30, 20 – 30.

Oldham, C., Lavery P., McMahon K., Pattiaratchi C., Chiffings T. 2010. Seagrass wrack dynamics in Geographe Bay, Western Australia. Report to Western Australian Department of Transport, and Shire of Busselton.

Oliveira, L.H.S.D., 2015. Morfologia e sedimentologia da plataforma continental interna paranaense. Doctoral Thesis. Universidade Federal do Paraná, Setor de Ciências da Terra, Programa de Pós-Graduação em Geologia. https://educapes.capes.gov.br/handle/1884/39930 (May 2017).

Ove Arup, 2001. Geotechnical Perth Convention Centre Desk Study Report to Multiplex Constructions Pty. Ltd. Unpublished.

Parker, J.H., 2009. Taxonomy of Foraminifera from Ningaloo Reef, Western Australia. Association of Australasian Palaeontologists. Canberra. Memoir 39.

Parkinson, G., 1986. Atlas of Australian Resources, Third Series, Volume 4: Climate. Division of National Mapping, Canberra.

Pattiaratchi, C. and Wijeratne, S., 2011. Port Geographe sand and seagrass wrack modelling study, Western Australia. Report prepared for Department of Transport (WA). SESE report no. 465, School of Environmental Systems Engineering, the University of Western Australia, Perth.

Pattiaratchi CB, Wijeratne EMS & Bosserelle C., 2011. Sand and seagrass wrack modelling in Port Geographe, south-western Australia. Proceedings of Coasts and Ports 2011, Engineers Australia.

Pattiaratchi CB, Wijeratne EMS, Roncevich L & Holder J, 2015. Interaction between seagrass wrack and coastal structures: lessons from Port Geographe, southwestern Australia. Proceedings of Coasts and Ports 2015, Engineer Australia.

Pattiaratchi, C.B., Wijeratne, S., Roncevich, L. and Holder, J., 2017. The influence of nearshore sandbars on coastal stability in port geographe, South-west Australia. Australasian Coasts & Ports 2017: Working with Nature, p.865.

Paul, M.J. and Searle, J.D., 1978. Shoreline Movements Geographe Bay Western Australia. In: Fourth Australian Conference on Coastal and Ocean Engineering: Managing the Coast. Barton, A.C.T.: Institution of Engineers, Australia.

Pearce, A. F., Griffiths, R. W. (1991). The Mesoscale Structure of the Leeuwin Current: A Comparison of Laboratory Models and Satellite Imagery. J. Geophys. Res., 96(C9), 16739-16757.

Pirazzoli, P.A., 1997. Sea-level changes: the last 20 000 years. Oceanographic Literature Review, 8(44), p.785.

Playford, P. E., 1990. Geology of the Shark Bay area, Western Australia. In: Berry, P.F., Bradshaw, S.D., Wilson, B.R. (Eds) Research in Shark Bay: Report of the France – Australe bicentenary expedition committee, Western Australian Museum, Perth, pp. 13–31

Playford, P. E., Cockbain, A. E. and Lowe, G.H., 1976. Geology of the Perth Basin. Geological Survey of Western Australia Bulletin, 124: 311p.

Playford, P. E., Cockbain, A. E., 1976. Modern algal stromatolites at Hamelin Pool, a hypersaline barred basin in Shark Bay, Western Australia. In: Walter, M.R. (Ed.), Developments in Sedimentology, 20. Elsevier Scientific Publishing Company, pp. 389–411.

Playford, P. E., Cockbain, A. E., Berry, P. F., Roberts, A. P., Haines, P. W. and Brooke, B. P. 2013. The geology of Shark Bay: Geological Survey of Western Australia, Bulletin 146 pp 281.

Playford, P.E., 1977. Part 1, Geology and groundwater potential, in: Playford, P.E., Leech, R.E.J., (Eds.), Geology and Hydrology of Rottnest Island. Geol. Surv. West. Aust., 6: 1-53.

Playford, P.E., 1988. Guidebook to the geology of Rottnest Island. Geological Society of Australia, WA Division and the Geological Survey of Western Australia.

Playford, P.E., 1997, Geology and hydrogeology of Rottnest Island, Western Australia. In Geology and Hydrogeology of Carbonate Islands, Developments in Sedimentology 54, L.H. Vacher and T.M. Quinn (Eds), pp. 783–810 (Amsterdam: Elsevier).

Preen, A. R., Marsh, H., Lawler, I. R., Prince, R. I. T., Shepherd, R., 1997. Distribution and Abundance of Dugongs, Turtles, Dolphins and other Megafauna in Shark Bay, Ningaloo Reef and Exmouth Gulf, Western Australia. Wildlife Research 24(2), 185 – 208

Price, D.M., Brooke, B.P., Woodroffe, C.D., 2001. Thermoluminescence dating of eolianites from Lord Howe Island and south-west Western Australia. Quat. Sci. Rev. (Quat. Geochronol.) 20, 841-846.

Probert, D.H., 1967. Groundwater in the Busselton Area: Progress Report on Exploratory Drilling. Geological Survey of Western Australia.

Purcell, S. P., 2002. Intertidal reefs under extreme tidal flux in Buccaneer Archipelago, Western Australia. Coral Reefs, 21(2), 191-192.

Quilty, P., 1974. Tertiary stratigraphy of Western Australia. J. Geol. Soc. Aust. 21, 37–41. doi:10.1080/00167617408728853.

Quilty, P.G., Hosie, G., 2006. Modern foraminifera, Swan River Estuary, Western Australia: distribution and controlling factors. J. Foraminifer. Res. 36:291–314. http://dx.doi.org/10.2113/gsjfr.36.4.291.

Rabineau M, Berné S, Olivet JL, Aslanian D, Guillocheau F, Joseph P. 2006. Paleo sea levels reconsidered from direct observation of paleoshoreline position during Glacial Maxima (for the last 500,000 yr). Earth and Planetary Science Letters 252: 119–137.

Radke, L.C., Prosser, I.P., Robb, M., Brooke, B., Fredericks, D., Douglas, G.B. and Skemstad, J., 2004. The relationship between sediment and water quality, and riverine sediment loads in the wave-dominated estuaries of south-west Western Australia. Marine and Freshwater Research, 55(6), pp.581-596.

Rao, C. P., 1996. Modern Carbonates: Tropical, Temperate and Polar, Introduction to Sedimentology and Geochemistry. Tasmania, Australia. 206 pp.Raymo, M.E., 1997. The timing of major climate terminations. Paleoceanography, 12(4), pp.577-585.

Read, J. F., 1974. Carbonate bank and wave built platform sedimentation, Edel Province, Shark Bay, Western Australia. In: Logan, B.W., Read, J.F., Hagan, G.M., Hoffman, P., Brown, R.G., Woods, P.J., Gebelein, C.D., (Eds). Evolution and diagenesis of quaternary carbonate sequences, Shark Bay, Western Australia. American Association of Petroleum Geologists Memoir 22, 250 – 282.

Reading, H.G. ed., 2009. Sedimentary environments: processes, facies and stratigraphy. John Wiley & Sons.

Reeves, J.M., Chivas, A.R., García, A., Holt, S., Couapel, M.J., Jones, B.G., Cendón, D.I. and Fink, D., 2008. The sedimentary record of palaeoenvironments and sea-level change in the Gulf of Carpentaria, Australia, through the last glacial cycle. Quaternary International, 183(1), pp.3-22.

Rehman, S.U. and Saleem, K., 2013. Forecasting scheme for swan coastal river streamflow using combined model of IOHLN and Niño 4. Asia-Pacific J. Atmos. Sci. 50, 1–9. doi:10.1007/s13143-014-0009-61.

Roe, G.H., Stolar, D.B. and Willett, S.D., 2006. Response of a steady-state critical wedge orogen to changes in climate and tectonic forcing. Geological Society of America Special Papers, 398, pp.227-239.

Rohling, E.J., Fenton, M., Jorissen, F.J., Bertrand, P., Ganssen, G. and Caulet, J.P. 1998. Magnitudes of sea-level lowstands of the past 5000,000 years. Nature 394: 162-165.

Rohling, E.J., Hibbert, F.D., Williams, F.H., Grant, K.M., Marino, G., Foster, G.L., Hennekam, R., De Lange, G.J., Roberts, A.P., Yu, J. and Webster, J.M., 2017. Differences between the last two glacial maxima and implications for ice-sheet, δ 18 O, and sea-level reconstructions. Quaternary Science Reviews, 176, pp.1-28.

Ryan, D.A., Bostock, H.C., Brooke, B.P., Marshall, J.F., 2007. Bathymetric expression of the Fitzroy River palaeochannel, northeast Australia: Response of a major river to sea level change on a semi-rimmed, mixed siliciclastic-carbonate shelf. Sediment. Geol. 201, 196–211. doi:10.1016/j.sedgeo.2007.05.018

Sadler, P.M., 1981. Sediment Accumulation Rates and the Completeness of Stratigraphic Sections. Geology 89 (5), 569 – 584.

Sanderson, P.G. and Eliot, I., 1996. Shoreline salients, cuspate forelands and tombolos on the coast of Western Australia. Journal of Coastal Research, pp.761-773.

Sandiford, M., 2007. The tilting continent: a new constraint on the dynamic topographic field from Australia. Earth and Planetary Science Letters 261 (1 – 2), 152–163.

Saqab, M.M., Bourget, J., 2015. Controls on the distribution and growth of isolated carbonate build-ups in the Timor Sea (NW Australia) during the Quaternary. Mar. Pet. Geol. 62, 123–143. doi:10.1016/j.marpetgeo.2015.01.014.

Schafer, D., Johnson, S. & Kern, A., 2008. Hydrogeology of the leederville aquifer in the western Busselton - Capel Groundwater Area. Hydrogeological record series Report HG31., s.l.: Department of Water.

Schopf, J.W., 1993. Microfossils of the Early Archean Apex chert: new evidence of the antiquity of life. Science 260, 640 – 646.

Schumm, S.A., 1993. River response to baselevel change: implications for sequence stratigraphy. The Journal of Geology, pp.279-294.

Schupp, C.A., McNinch, J.E., List, J.H., 2006. Nearshore shore-oblique bars, gravel outcrops, and their correlation to shoreline change. Marine Geology 233, 63–79.

Scoffin, T P., 1970. The trapping and binding of subtidal carbonate sediments by marine vegetation in Bimini Lagoon, Bahamas. Journal of Sedimentary Petrology 40, 249 – 273.

Shackleton, N.J., 1987. Oxygen isotopes, ice volume and sea level. Quaternary Science Reviews, 6(3), pp.183-190.

Sheriff, R. E. 2002. Encyclopedic Dictionary of Applied Geophysics, 4th Edition. Society of Exploration Geophysics. Tulsa, OK.

Short, A.D. and Woodroffe, C.D., 2009. The coast of Australia. Cambridge University Press.

Short, A.D., 2005. Beaches of the Western Australian Coast: Eucla to Roebuck Bay: A guide to their nature, characteristics, surf and safety. Sydney University Press.

Siddall, M., Bard, E., Rohling, E.J. and Hemleben, C., 2006. Sea-level reversal during Termination II. Geology, 34(10), pp.817-820.

Sircombe, K.N. and Freeman, M.J., 1999. Provenance of detrital zircons on the Western Australia coastline—Implications for the geologic history of the Perth basin and denudation of the Yilgarn craton.

Skene, D., Ryan, D. and Brooke, B., 2004. Sub-bottom Profiling, Surface Sediment Sampling, Vibracoring and Mapping with Sidescan and Multibeam Sonar Systems in the Fitzroy River Estuary and Keppel Bay. Coastal CRC Coastal Water Habitat Mapping Project Coastal Geomorphology Subproject, Milestone Report CG04.01.

Skene, D., Ryan, D., Brooke, B., Smith, J. and Radke, L., 2005. The geomorphology and sediments of Cockburn Sound. Geoscience Australia, Record 2005/10, 88 pp.

SLIP Shared Land Information Platform - Public Web Map Service http://slip.landgate.wa.gov.au
http://catalogue.beta.data.wa.gov.au/dataset/hydrography-linear-hierarchy

Sloss, C.R., Jones, B.G., McClennen, C.E., de Carli, J. and Price, D.M., 2006. The geomorphological evolution of a wave-dominated barrier estuary: Burrill Lake, New South Wales, Australia. Sedimentary Geology, 187(3), pp.229-249.

Smith, A.J., Massuel, S., Pollock, D.W., 2012. Geohydrology of the Tamala Limestone Formation in the Perth Region: Origin and Role of Secondary Porosity. CSIRO: Water for a Healthy Country National Research Flagship, 63 pp.

Smith, W., and Sandwell, D., 1997. Measured and Estimated Seafloor Topography, World Data Service for Geophysics, Boulder Research Publication RP-1, poster, 34" X 53". Geology, 27(10), pp.879-882.

Solihuddin, T., Bufarale, G., Blakeway, D. and O'Leary, M.J., 2016. Geomorphology and late Holocene accretion history of Adele Reef: a northwest Australian mid-shelf platform reef. Geo-Marine Letters, 36(6), pp.465-477.

Solihuddin, T., Collins, L. B., Blakeway, D., O'Leary, M. J., 2015. Holocene coral reef accretion and sea-level in a macrotidal, high turbidity setting: Cockatoo Island, Kimberley Bioregion, northwest Australia. Marine Geology, 359, 50–60.

Solihuddin, T., O'Leary, M.J., Blakeway, D., Parnum, I., Kordi, M. and Collins, L.B., 2016. Holocene reef evolution in a macrotidal setting: Buccaneer Archipelago, Kimberley Bioregion, Northwest Australia. Coral Reefs, 35(3), pp.783-794.

Spooner, M.I., De Deckker, P., Barrows, T.T. and Fifield, L.K., 2011. The behaviour of the Leeuwin Current offshore NW Australia during the last five glacial–interglacial cycles. Global and Planetary Change, 75(3), pp.119-132.

Stephens, R. and Imberger, J., 1996. Dynamics of the Swan River Estuary: The seasonal variability. Mar. Freshw. Res. 47, 517. doi:10.1071/MF9960517.

Stephens, R. and Imberger, J., 1997. Intertidal motions within deep basin of Swan River estuary. Journal of Hydraulic Engineering, 123(10), pp.863-873.

Stirling, C.H., Esat, T.M., Lambeck, K., McCulloch, M.T., 1998.Timing and duration of the Last Interglacial: evidence for a restricted interval of widespread coral reef growth. Earth Planet. Sci. Lett. 160, 745–762

Stirling, C.H., Esat, T.M., Mcculloch, M.T., Lambeck, K., 1995. High-precision U-series dating of corals from Western Australia and implications for the timing and duration gradients in the North Atlantic Ocean (321 to 721N) during the Last Interglacial period. Paleoceanography 14, 23–33. doi:10.1016/0012-821X(95)00152-3.

Stirling, C.H., Esat, T.M., McCulloch, M.T., Lambeck, K., 1995. High-precision U-series dating of corals from Western Australia and implications for the timing and duration of the Last Interglacial. Earth Planet. Sci. Lett. 135, 115e130.

Stuiver, M., and Polach, H. A., 1977. Discussion: Reporting of 14C data, Radiocarbon 19: 355-363.

Stuiver, M., and Reimer, P. J., 1993. Extended 14C database and revised CALIB radiocarbon calibration program. Radiocarbon 35:215-230.

Stuiver, M., Reimer, P.J., Reimer, R.W., 2005. Calib 5.0 program and documentation. URL: http://radiocarbon.pa.qub.ac.uk/calib/.

Szabo, B.J., 1979. Uranium-series age of coral reef growth on Rottnest Island, Western Australia. Mar. Geol. 29, M11eM15.

Tamura, T., Saito, Y., Sieng, S., Ben, B., Kong, M., Sim, I., Choup, S., Akiba, F., 2009. Initiation of the Mekong River delta at 8 ka : evidence from the sedimentary succession in the Cambodian lowland. Quat. Sci. Rev. 28, 327–344. doi:10.1016/j.quascirev.2008.10.010

Tanabe, S., Nakanishi, T., Ishihara, Y. and Nakashima, R., 2015. Millennial-scale stratigraphy of a tide-dominated incised valley during the last 14 kyr: Spatial and

quantitative reconstruction in the Tokyo Lowland, central Japan. Sedimentology, 62(7), pp.1837-1872.

Thieler, E.R., Foster, D.S., Himmelstoss, E.A. and Mallinson, D.J., 2014. Geologic framework of the northern North Carolina, USA inner continental shelf and its influence on coastal evolution. Marine Geology, 348, pp.113-130.

Thieler, E.R., Foster, D.S., Himmelstoss, E.A. and Mallinson, D.J., 2014. Geologic framework of the northern North Carolina, USA inner continental shelf and its influence on coastal evolution. Marine Geology, 348, pp.113-130.

Tovaglieri, F., George, A.D., 2014. Stratigraphic architecture of an Early – Middle Jurassic tidally influenced deltaic system (Plover Formation), Browse Basin, Australian North West Shelf. Marine and Petroleum Geology 49, 59 – 83.

Tutton, M., 2003. Engineering geology of Fremantle harbour. Australian Geomechanics, 38(4), pp.91-102.

Twiggs, E.J. and Collins, L.B., 2010. Development and demise of a fringing coral reef during Holocene environmental change, eastern Ningaloo Reef, Western Australia. Mar. Geol. 275, 20–36. doi:10.1016/j.margeo.2010.04.004

Tyler, I. M., Hocking, R. M., & Haines, P. W., 2012. Geological evolution of the Kimberley region of Western Australia. Episodes – Newsmagazine of the International Union of Geological Sciences 35(1), 298.

van Blaricom, R., & Northwest Mining Association (Eds.), 1992. Practical geophysics II for the exploration geologist. Northwest Mining Association.

van de Graaff, W. J. E., Hocking, R. M., Butcher, B. P., 1983, Yaringa, Western Australia: Geological Survey of Western Australia, 1:250 000 Geological Series Explanatory Notes, 23p.

van der Kaars, S. and De Deckker, P., 2002. A Late Quaternary pollen record from deep-sea core Fr10/95, GC17 offshore Cape Range Peninsula, northwestern Western Australia. Review of Palaeobotany and Palynology, 120(1), pp.17-39.

Van Niel, K.P., Holmes, K.W. and Radford, B., 2009. Seagrass Mapping Geographe Bay 2004-2007. Report prepared for: Southwest Catchment Council, 25 pp, University of Western Australia.

Varma, S., Turner, J., Underschultz, J., 2010. Estimation of submarine groundwater discharge into Geographe Bay, Bunbury, Western Australia. J. Geochemical Explor. 106, 197–210. doi:10.1016/j.gexplo.2010.02.003

Veevers, J.J., 1971. Phanerozoic history of Western Australia related to continental drift. Journal of the Geological Society of Australia, 18(2), pp.87-96.

Verduin, J.J., Backhaus, J.O., 2000. Dynamics of plant flow interactions for the seagrass Amphibolis antarctica: field observations and model simulations. Estuarine, Coastal and Shelf Science 50 (2), 185–204.

Viney, N.R. and Sivapalan, M., 2001. Modelling catchment processes in the Swan–Avon river basin. Hydrological Processes, 15(13), pp.2671-2685.Vinnicombe, P., 1992. An Aboriginal site complex at the foot of Mount Eliza which includes the old Swan Brewery building. Historic Environment, 9(1/2), p.53.

Waelbroeck, C., Labeyrie, L., Michel, E., Duplessy, J.C., McManus, J.F., Lambeck, K., Balbon, E. and Labracherie, M., 2002. Sea-level and deep water temperature changes derived from benthic foraminifera isotopic records. Quaternary Science Reviews, 21(1), pp.295-305.

Walker, D. I. and Woelkerling, Wm. J., 1988. Quantitative study of sediment contribution by epiphytic coralline red algae in seagrass meadows in Shark Bay, Western Australia. Marine Ecology – Progress Series 43, 71–77.

Walker, D. I., 1990. Seagrass in Shark Bay, Western Australia. In: Berry, P.F., Bradshaw, S.D., Wilson, B.R. (Eds) Research in Shark Bay: Report of the France – Australe bicentenary expedition committee. Western Australia Museum, Perth, Australia, pp101 – 106.

Walker, D.I, Dennison, G.E., 1999. Status of Australian seagrass research and knowledge. In: Butler A. and Jernakoff, P. (Eds). Seagrass in Australia. Strategic Review and Development of an R & D Plan. CSIRO Cataloguing – in – Publication pp 1 – 24.

Walker, D.I., 1985. Correlations between salinity and growth of the seagrass Amphibolis antarctica (labill.) Sonder & Aschers., in Shark Bay, Western Australia, using a new method for measuring production rate. Aquatic Botany 23 (1), 13–26.

Walker, D.I., Kendrick, G. A.,McComb, A. J., 1988a.The distribution of seagrass species in Shark Bay, Western Australia, with notes on their ecology. Aquatic Botany 30, 305 – 317.

Walker, M., Johnsen, S., Rasmussen, S.O., Popp, T., Steffensen, J.P., Gibbard, P., Hoek, W., Lowe, J., Andrews, J., Björck, S. and Cwynar, L.C., 2009. Formal definition and dating of the GSSP (Global Stratotype Section and Point) for the base of the Holocene using the Greenland NGRIP ice core, and selected auxiliary records. Journal of Quaternary Science, 24(1), pp.3-17.

Wearne, G. R., 2000. The formation and maintenance of shoreface attached sandbars in Geographe Bay. Honours Thesis, Centre for Water Research, University of Western Australia.

Wells, P.E. and Wells, G.M., 1994. Large-scale reorganization of ocean currents offshore Western Australia during the late Quaternary. Marine Micropaleontology, 24(2), pp.157-186.

Wentworth, C.K., 1922. A scale of grade and class terms for clastic sediments. The Journal of Geology 30(5): 377-392.

Wharton, P.H., 1981. The geology and hydrogeology of the Quindalup borehole line. Western Australia Geological Survey, Annual Report for 1980, pp. 27–34.

Wharton, P.H., 1982. The geology and hydrogeology of the Quindalup borehole line in Southern Perth Basin, Western Australia. Western Australia Geological Survey, Record 1982/2.

White, K. and Comer, S., 1999. Capel River action plan. Geographe Catchment Council -Geocatch- and the Capel Land Conservation District Committee.

Whitehouse, J., 2007. Evaluation of mineral resources of the continental shelf, new South Wales. Q. Notes 124, Geol. Surv. New South Wales, 23.

Whiteley, R. J. and Stewart, S. B., 2008. Case studies of shallow marine investigations in Australia with advanced underwater seismic refraction (USR). Exploration Geophysics, 39, 34–40. doi: 10.1071/EG08009

Whiteway, T.G., 2009. Australian Bathymetry and Topography Grid, June 2009. Geoscience Australia Record 2009/21. 46pp.

Wilson, B., 2013. The Biogeography of the Australian North West Shelf, environmental change and life's response. Elsevier, 1st Edition.

Wilson, B., S. Blake, D. Ryan, J. Hacker., 2011. Reconnaissance of species-rich coral reefs in a muddy, macro-tidal, enclosed embayment, Talbot Bay, Kimberley, Western Australia. Journal of the Royal Society of Western Australia 94, 251 – 265.

Wilson, C. J., Wilson, P. S., & Dunton, K. H.,2012. An acoustic investigation of seagrass photosynthesis. Marine Biology 159 (10), 2311 – 2322.

Wolanski, E. 2007. Estuarine ecohydrology. Elsevier, Amsterdam, The Netherlands.

Wolanski, E., Spagnol, S., 2003. Dynamics of the turbidity maximum in King Sound, tropical Western Australia Estuarine, Coastal and Shelf Science 56, 5 – 6.

Woodroffe, C.D., Webster, J.M., 2014. Coral reefs and sea-level change. Mar. Geol. 352, 248–267. doi:10.1016/j.margeo.2013.12.006

Woolfe, K.J., Larcombe, P., Naish, T., Purdon, R/G., 1998. Lowstand rivers need not incise the shelf: An example from the Great Barrier Reef, Australia, with implications for sequence stratigraphic models Geology, January 26, p. 75-78.

Wright, R.L., 1964. Geomorphology of the west Kimberley area. CSIRO Land Res. Ser. 9, 103–118.

Wunderlich, J., Müller, S., 2003. High-resolution sub-bottom profiling using parametric acoustics. Conference abstract. International Ocean Systems 2003.

Wyrwoll, K.H., Greenstein, B.J., Kendrick, G.W. and Chen, G.S., 2009. The palaeoceanography of the Leeuwin Current: implications for a future world. Journal of the Royal Society of Western Australia, 92(2), pp.37-51.

Wywroll, K.-H., Miller, G.H., 2001. Initiation of the Australian summer monsoon 14,000 years ago. Quaternary International 83–85, 119–128.

Yokoyama, Y., De Deckker, P., Lambeck, K., Johnston, P. and Fifield, L.K., 2001. Sea-level at the Last Glacial Maximum: evidence from northwestern Australia to constrain ice volumes for oxygen isotope stage 2. Palaeogeography, Palaeoclimatology, Palaeoecology, 165(3), pp.281-297.

Zhu, Z.R., Wyrwoll, K.H., Collins, L.B., Chen, J.H., Wasserburg, G.J., Eisenhauer, A., 1993. High-precision U-series dating of Last Interglacial events by mass-spectrometry, Houtman-Abrolhos Islands, Western Australia. Earth Planet. Sci. Lett. 118, 281–293.

# Appendices

## Appendix A: First author journal publications

***Quaternary onset and evolution of Kimberley coral reefs (Northwest Australia) revealed by high-resolution seismic imaging***

Giada Bufarale[1, 3], Lindsay B. Collins[1, 3], Michael J. O'Leary[2, 3], Alexandra Stevens[1, 3], Moataz Kordi[1, 3], Tubagus Solihuddin[1, 3]

1 Department of Applied Geology, Curtin University, GPO Box U1987, Perth, WA 6845, Australia
2 Department of Environment and Agriculture, Curtin University, Bentley, Western Australia, 6102
3 The Western Australian Marine Science Institution, Floreat, Western Australia, 6014

This article is published in Continental Shelf Research, Volume 123, 15 July 2016, Pages 80-88.

doi.org/10.1016/j.csr.2016.04.002

Continental Shelf Research 123 (2016) 80–88

Contents lists available at ScienceDirect

Continental Shelf Research

journal homepage: www.elsevier.com/locate/csr

Research papers

# Quaternary onset and evolution of Kimberley coral reefs (Northwest Australia) revealed by high-resolution seismic imaging

Giada Bufarale [a,c,*], Lindsay B. Collins [a,c], Michael J. O'Leary [b,c], Alexandra Stevens [a,c], Moataz Kordi [a,c], Tubagus Solihuddin [a,c]

[a] Department of Applied Geology, Curtin University, Bentley, Western Australia 6102, Australia
[b] Department of Environment and Agriculture, Curtin University, Bentley, Western Australia 6102, Australia
[c] The Western Australian Marine Science Institution, Floreat, Western Australia 6014, Australia

ARTICLE INFO

*Article history:*
Received 7 December 2015
Received in revised form
31 January 2016
Accepted 6 April 2016
Available online 6 May 2016

*Keywords:*
Kimberley macrotidal reefs
Sea level change
Seismic stratigraphy
Reef geomorphology
Growth history

ABSTRACT

The inner shelf Kimberley Bioregion of Northwest Australia is characterised by a macrotidal setting where prolific coral reefs growth as developed around a complex drowned landscape and is considered a biodiversity "hotspot". High-resolution shallow seismic studies were conducted across various reef settings in the Kimberley (Buccaneer Archipelago, north of Dampier Peninsula, latitude: between 16°40′S and 16°00′S) to evaluate stratigraphic evolution, interaction with different substrates, morphological patterns and distribution. Reef sites were chosen to assess most of the reef types present, particularly high intertidal planar reefs and fringing reefs. Reef internal acoustic reflectors were identified according to their shape, stratigraphic position and characteristics. Two main seismic horizons were identified marking the boundaries between Holocene reef (Marine Isotope Stage 1, MIS 1, last 12 ky), commonly 10–20 m thick, and MIS 5 (Last Interglacial, LIG, ~120 ky, up to 12 m thick) and Proterozoic rock foundation over which Quaternary reef growth occurred. Within the Holocene Reef unit, at least three minor internal reflectors, generally discontinuous, subparallel to the reef flat were recognised and interpreted as either growth hiatuses or a change of the coral framework or sediment matrix. The LIG reefs represent a new northernmost occurrence along the Western Australian coast.

The research presented here achieved the first regional geophysical study of the Kimberley reefs. Subbottom profiles demonstrated that the surveyed reefs are characterised by a multi-stage reef buildup, indicating that coral growth occurred in the Kimberley during previous sea level highstands. The data show also that antecedent substrate and regional subsidence have contributed, too, in determining the amount of accommodation available for reef growth and controlling the morphology of the successive reef building stages. Moreover, the study showed that in spite of macrotidal conditions, high-turbidity and frequent high-energy cyclonic events, corals have exhibited prolific reef growth during the Holocene developing significant reef accretionary structures. As a result coral reefs have generating habitat complexity and species diversity in what is a biodiversity hotspot.



## 1. Introduction

The Kimberley is located in the Australia's northwest continental margin and, primarily due to its remote geographical location, published scientific investigations of the region are scarce compared to other marine and coastal ecosystems in Australia (Chin et al., 2008; McKenzie et al., 2009; Wilson, 2013). A recent remote sensing study by Kordi et al. (2016) recognised the Kimberley has hosting a major reef system, the largest in Western Australia, and second only to the Great Barrier Reef in terms of total reefal area and number of reef islands. Despite been recognised as a major biodiversity hotspot of international significance (Chin et al., 2008; Department of the Environment, 2014; Pepper and Scott Keogh, 2014), the coral reefs of the Kimberley coast remain relatively understudied when compared with other relatively well-known a reef systems along the Western Australian coast, such as the Houtman Abrolhos islands, Ningaloo fringing reef and some isolated oceanic atoll-like reefs (e.g., Scott Reef, Rowley Shoals. Eisenhauer et al., 1993; Collins et al., 2003; Collins et al., 2006; Collins et al., 2011. See reviews in Montaggioni, 2005 and Collins, 2011). In particular, Collins (2011) and Wilson (2013) noted a significant information gap on the geomorphology, evolution and development of reefs of the Kimberley Bioregion. Until

* Correspondence to: Department of Applied Geology, Curtin University, GPO Box U1987, Perth, Western Australia 6845, Australia.
*E-mail address:* giada.bufarale@postgrad.curtin.edu.au (G. Bufarale).

http://dx.doi.org/10.1016/j.csr.2016.04.002
0278-4343/

recently, when Solihuddin et al. (2015) accomplished the first detailed geological account of Holocene reef growth in Cockatoo Island (Kimberley Bioregion), it was not known whether reefs are thin veneers over rock platforms or significant long-lived accretionary structures. The paper showed in fact that, at least at this one location, the Holocene reef consists of a thick reef framework, up to 15 m thick. The Cockatoo study also showed that the initiation of Holocene reef occurred soon after flooding of the continental shelf over older Pleistocene reef surface, which was found between 20 and 30 m below sea level, with Reefs growing in *catch-up* mode reaching base level around 3000 years ago. This is a significant finding as it suggests corals are able to persist and grow significant accretionary structured in what might be considered challenging or extreme environmental conditions, including extreme macrotidal range (Wilson, 2013), high-turbidity (Brooke, 1997; Wilson et al., 2011; Solihuddin et al., 2015), frequent cyclones (Wilson, 2013). The Solihuddin et al. (2015) study now raises a series of further questions about the reefs in the Buccaneer Archipelago:

- Is the reef morphology of Cockatoo Island a result of a unique local oceanographic effect or do most Kimberley reef exhibit a similar morphology and growth history?
- The northernmost occurrence of Last Interglacial (LIG) reef along the Western Australian coast is found at Cape Range (Ningaloo Reef. O'Leary et al., 2008); does the discovery of LIG reef within the open cut mine Cockatoo represent a broader occurrence of LIG reefs throughout the Kimberley?
- What role has the antecedent topography in terms of structural control of on reef growth during the Holocene?

This project presents the first detailed seismic study across a range of reef morphotypes in order to (1) provide insights into the internal reef architecture and structures, (2) determine the thickness of the Holocene reef and pre-existing reef buildups, and (3) establish the growth-controlling factors and their role on the Quaternary reef evolution. This paper presents a detailed description of reef morphologies and provides a better understanding of the past reef growth history of inner reefs of the Kimberley (Buccaneer Archipelago. Fig. 1).

## 2. Environmental setting and geology

The Kimberley region occupies a land area of about 424,000 km$^2$ (O'Faircheallaigh, 2013) and extends from Cape Keraudren (southern end of Eighty Mile Beach) to the border of Western Australia/Northern Territory, for a length exceeding 5000 km (Brocx and Semeniuk, 2011; Kordi et al., 2016. Fig. 1). The Kimberley south of Cape Leveque (Dampier Peninsula) is situated within the Phanerozoic Canning sedimentary Basin and is characterised by a simple relatively straight coastline, however the Kimberley north of Cape Leveque is situated within the Proterozoic Kimberley block and is characterised by complex coastal highly indented coastline (Chin et al., 2008; Collins, 2011; Tyler et al., 2012). The coastal and marine habitats include extensive archipelagos, with more than 2400 islands, bays, capes, tidal plains, mangroves and a broad variety of coral reefs rich in diversity (at least 850 where mapped by Kordi et al. (2016)).

These complex environments are strongly influenced by macrotidal conditions, high-turbidity, tropical monsoonal climate and proximity to the Indo – Pacific Throughflow (ITF) and the Leeuwin Current (e.g., Wolanski and Spagnol, 2003; Condie and Andrewartha, 2008; Collins and Testa, 2010; Brocx and Semeniuk, 2011; Wilson, 2013).

Situated in a semi-arid to sub-humid climate zone, the

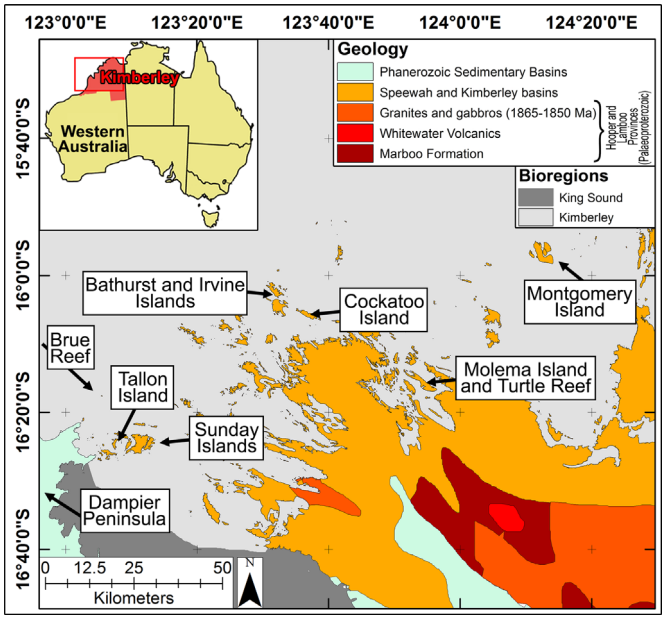


**Fig. 1.** Map of the reef in the Buccaneer Archipelago, Kimberley, showing the geology of the region (after Tyler et al., 2012) and the marine bioregions (Integrated Marine and Coastal Regionalisation of Australia, IMCRA, v4.0. Commonwealth of Australia, 2006). The reefs seismically surveyed in this study are labelled.

Kimberley experiences seasonal rainfall (between November and March) that influences local freshwater and sediment drainage from the hinterland to the coast (Parkinson, 1986; Brocx and Semeniuk, 2011). A Tidal range of 12 m during springs and less than 3 m during some neaps has resulted in an extensive intertidal zone (Cresswell and Badcock, 2000). These tidal motions can result in tidal currents of 2 m/s, which can remobilise and resuspend fine particles with the result being coral reefs can become invisible from the surface at high tide and at low tide, the reefs appear partially covered by mud (Wilson et al., 2011). The turbidity increases in wet season when the rates of river runoff are higher (Wolanski and Spagnol, 2003).

The Kimberley marine environment is strongly influenced by an ancient geological history and it is characterised by complex structural and tectonic settings. The intricate coastal geomorphology is structurally controlled by ancient folded and faulted Proterozoic metasedimets and volcanics (Fig. 1. Tyler et al., 2012). Since the Miocene tectonic subsidence (Sandiford, 2007), has resulted in a drowned ria-style coast which has likely influenced the style and development of coral reef growth on the North West Shelf. During the last glacial, the inner shelf reefs experienced subsidence of around 0.11 m/ky (Solihuddin et al., 2015).

### 2.1. Geomorphic classification of reefs in the Kimberley Bioregion

Due to the macrotidal conditions, most reef flats in the Kimberley are exposed during low tide and are, therefore, intertidal in character. Reefs which have not yet grown to sea level are permanently subtidal, and many small patch reefs and most shoals are of this type. A specialised type of high intertidal reef recognised by Wilson et al. (2011) and Wilson (2013) is characterised by a high, flat topped surface that may be several metres above mean low water springs (MLWS) tide level, and experiences significant subaerial exposure during the tidal cycle. These reefs have unique surface characteristics, including lithified algal ridges, terraced reef platforms, and coralline algae (rhodolith banks), as well as *Porites* microatolls. In order to capture a range of reef typologies this study utilized a revised reef geomorphic classification scheme developed by Collins et al. (2015) and Kordi et al. (2016) for the

Kimberley Bioregion, which was adapted from the Great Barrier Reef Geomorphic classification scheme by Hopley et al. (2007).

Fringing reefs are widespread in the Kimberley (Kordi et al., 2016) with morphologies influenced by the complex embayment and island coastal morphology, both as mainland and island associated features. In this study of the Kimberley, five main types of fringing reefs were essentially described: Bay Head, Inter-island, Circum-island, Headland and Narrow-beach Base.

Planar reefs are large isolated features characterised by flat topped platforms that are usually emergent only at low tide. Examples are Montgomery Reef, the Adele group of reefs (Adele and Churchill) and Brue Reef (see Fig. 1 for location).

There are many patch reefs and shoals scattered throughout the Kimberley Bioregion (see Wilson, 2013 for examples). These reefs usually grow on isolated topographic highs suitable for colonisation by coral growth and are common on exposed margins of fringing reefs. They are usually intertidal to subtidal features and are often small. These features were not studied in detail in this project which focused on the larger and more diverse reefs.

## 3. Methods

The surveyed reef sites (Fig. 1) were chosen in order to capture a broad range of reef morphotypes (Fig. 2) and included almost 300 km of subbottom profiler (SBP) lines. The geophysical survey was limited to the Buccaneer Archipelago and Montgomery Island and designed to target the orientation, internal architecture and morphology of the reefs. Profiles perpendicular to the reef allowed capture of the reef growth axis, transects parallel to the reef crest and crossing tie lines permitted a correlation during the interpretation and creation a three-dimensional perspective of the acoustic units' framework.

The surveys were conducted using an AA201 boomer system (Applied Acoustic Engineering Limited, Great Yarmouth, UK). Accurate positioning was obtained with a dual frequency Differential Global Positioning System (DGPS). Data were digitally recorded using SonarWiz 5 (Chesapeake Technology Inc., Mountain View, CA) as acquisition and post-processing software. The seismic profiles were postprocessed to improve the signal to noise ratio (S/N) by tracking the bottom and applying standard signal processing procedures such as bandpass filter and user defined gain/attenuation.

Subbottom profiling survey provided information on reef architecture, Holocene thickness and foundation, as well as earlier Pleistocene reef growth events. Stratigraphy and geochronology of Holocene, Pleistocene Reef and Proterozoic basement exposed in the Cockatoo mine pit (Solihuddin et al., 2015) were used to interpret and ground truth the major seismic horizons recorded over the modern Cockatoo reef flat (see Solihuddin et al., 2015; Collins et al., 2015 and further, Fig. 3). The reliability of this correlation was verified by laterally tracing the key seismic surfaces onto the neighbouring reefs, demonstrating a regional consistency of the stratigraphic pattern of two stages of reef growth (Holocene and Pleistocene).

## 4. Results and discussion

### 4.1. Seismic facies analysis

Two significant seismic reflectors R1 and RF were identified and defined on the basis of their (1) relative position, (2) acoustic reflection and (3) architectural characters (Table 1 and seismic profiles in Section 4.2). Between R1 and the seabed, many profiles also exhibit minor acoustic horizons, named H1, H2 and H3.

#### 4.1.1. R1 reflector

R1 is a high-energy reflector, which represents the top of the Pleistocene calcretised reef limestone unit recognised by Solihuddin et al. (2015). Table 1 and depicted in green color in the seismic profiles in Section 4.2. Occasionally R1 is masked by seabed multiple echoes or by a thick and hard overlying substrate. The R1 follows a similar topographic profile to the modern reef flat seabed in exhibiting a quasi-horizontal reef flat that steeply dips at the forereef slope matching the modern forereef slope. The seismic unit bounded by the sea floor/modern reef flat and R1 represents the Holocene reef/sediment buildup.

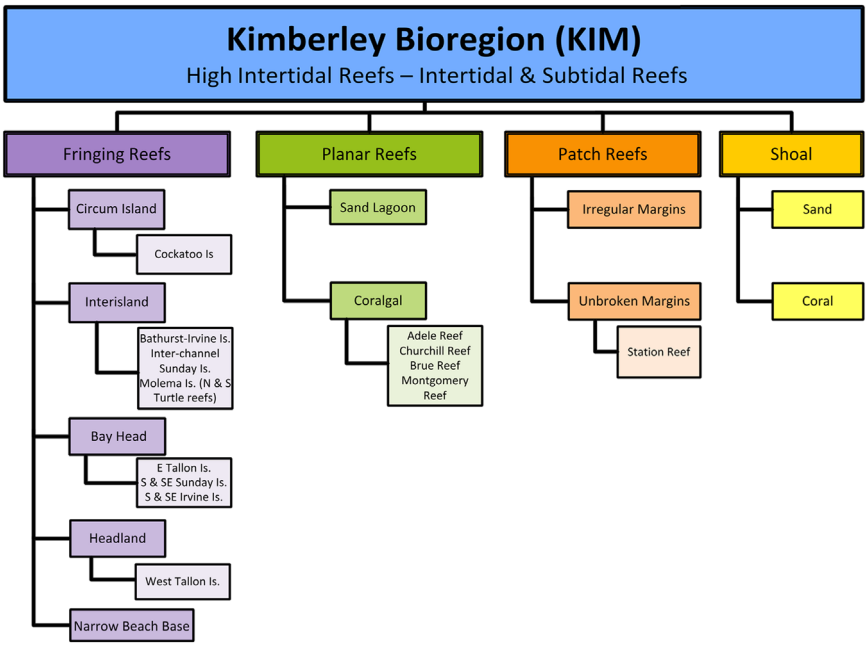


**Fig. 2.** Geomorphic classification scheme for the Kimberley reefs, based on adaptation of Hopley et al. (2007) Collins et al. (2015), and Kordi et al. (2016) and data from this study.

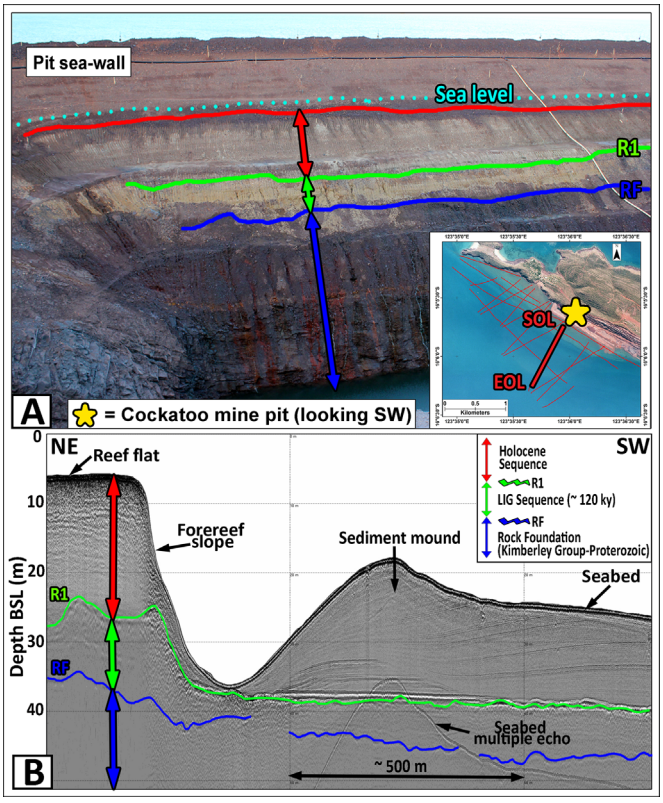


**Fig. 3.** (A) Cockatoo mine pit section (Photograph credit: Solihuddin T., 2013). Inset: Landgate aerial photography provided by the Department of Parks and Wildlife (DPaW); SBP lines are marked in red. SOL: start of line; EOL: end of line. (B) Cross-section of a seismic profile collected adjacent to mapped mine pit sections of Solihuddin et al. (2015) established position of Proterozoic foundation (RF, blue), Last Interglacial reef (R1, green) and overlying Holocene reef across the fringing reef. Note the sediment mound in front of the reef flat. Modified after Collins et al. 2015. (For interpretation of the references to color in this figure legend, the reader is referred to the web version of this article.)

#### 4.1.2. H reflectors

The Holocene unit is characterised by a series of internal discontinuous, subparallel reflectors of moderate to low amplitude (H1, H2 and H3, represented in shades of orange color in the seismic profiles in Section 4.2). H1 is the shallowest reflector, found in the first 5 m from the seafloor surface. In some profiles, it is not recognisable, due to very high impedance of the seafloor reflector masking the first few metres of substrate. H2 can be usually found between 5 and 8 m from the seabed and H3, where identified, is generally 3–7 m above the R1. These reflectors could be interpreted as hiatuses or a change of the coral framework (possibly from muddy to sandy matrix), according to the observation of Solihuddin et al. (2015).

#### 4.1.3. RF reflector

The post-processing and interpretation of the acoustic profiles across the area define the RF reflector as the deepest seismic horizon identified in the surveyed reefs and locally forms deep valley-like depressions and ridges (Table 1 and depicted in blue color in the seismic profiles in Section 4.2). The RF caps a chaotic, low amplitude unit that can be considered on the basis of the profile analysis and correlation with the data derived from a mine pit in Cockatoo Island as the Proterozoic rock foundation, and represents the acoustic basement of the reefs in the Buccaneer Archipelago. The terrestrial expression of this unit is represented by folded metamorphics, conglomerates and sandstones of the Kimberley Group. The seismic unit bounded by the R1 and RF represents an older, Pleistocene reef unit, which belongs to the Last Interglacial (LIG) sea level highstand (see further, in Section 4.2). The LIG section has been diagenetically altered and consists of calcretised, muddy branching coral framestone containing recrystallised corals (Solihuddin et al., 2015).

### 4.2. Internal architecture of Sothern Kimberley reefs

A number of reef typologies have been identified in the Kimberley (see Fig. 2). These include a range of fringing reef morphologies, with reef flat elevations that fall within two primary categories, high inertial and intertidal. The internal architecture of a variety of reef types were investigated and compared, through the analysis of seismic profiles.

#### 4.2.1. Fringing reefs

*4.2.1.1. Circum-island reef: Cockatoo Island.* The Buccaneer Archipelago (see Fig. 1 for location) is characterised by a highly discordant coastline resulting from the partial submergence of a structurally controlled geological landscape with anticlinal features forming the region's islands and coastal headlands.

Cockatoo Island is located less than 6 km from the mainland coastline and consists of strongly folded and trending NW–SE Palaeoproterozoic metamorphic and igneous rocks of the King Leopold Orogen (Wright, 1964). The Cockatoo Island reef is a high intertidal, Circum-island fringing reef, species-rich, with branching corals that dominate the modern forereef slope and persist to depths of 10 m below mean sea level (Solihuddin et al., 2015). Tides of up to 12 m provide the main physical energy.

The seismic profiles were mainly confined to the reef flat and forereef slope in front of the mine pits (inset in Fig. 3. Survey lines marked in red). The profiles on the southern-eastern margin of the reef flat reveal the structure of the reef overlying Proterozoic rocks (below RF horizon, in blue color) and confirm the stratigraphy mapped by Solihuddin et al. (2015) in the mine pits. An initial reef building phase of LIG reefs (below R1 horizon, in green color) of 5–10 m thickness overlies the Proterozoic substrate. Thereafter Holocene reef comprises the reef flat and is 15–20 m thick. Up to 25 m of well-laminated fine sediment mound is located in front of the reef flat (Fig. 3B). This massive sediment body is about 2.5 km long and directly overlies the LIG reef building phase.

*4.2.1.2. Inter-island reefs: Bathurst Island–Irvine Island.* Interisland reefs are defined by joining two separate islands, and are commonly found in the Buccaneer Archipelago and some appear to coalesce to form inter-island reefs where two islands are located in close proximity. One such inter-island reef is located between Bathurst and Irvine Islands (Fig. 1).

This inter-island fringing reef is characterised by a deep elongate depression, 30–35 m deep, which cuts across the platform (Fig. 4), and it has been suggested by Wilson (2013) that this indicates the partial coalescence of two fringing reefs, which left a residual gap in the platform as a function of incomplete reef growth, as opposed to a single platform with an elongate karst depression. The platform surface is frequently emergent, with a transverse sand sheet, shallow reef flat pools containing corals and fields of *Porites* microatolls present, features in common with other high intertidal reefs.

The internal structure of the Bathurst–Irvine reef in west – east section (Fig. 4) reveals its growth that occurred on relatively flat Proterozoic bedrock 30–40 m below mean sea level (MSL). Within the reef platform, the reflector R1 is approximately horizontal and the LIG sequence is around 10–12 m thick. Within the 15 m of Holocene reef buildup, there are 3 minor acoustic reflectors H1, H2, and H3, which are interpreted as either hiatuses or temporary pauses in reef growth, changes in the type of sediment matric (sand vs mud) or change in coral facies (branching to massive).

**Table 1**
Characteristics and acoustic features of seismic units identified in the profiles.

| Facies Unit | Thickness | Limits | Age | Internal Structure | Morphology | Interpretation | Example |
|---|---|---|---|---|---|---|---|
| Holocene | Variable: 7-22 m | **Top:** seabed **Bottom:** unconformity R1 (top LIG unit) | Last 12 ky | Moderate to low amplitude. Local discontinuous, sub-parallel reflectors (H1, H2 and H3) | Reef flat, crest, forereef slope. Local pinnacle reef | Reef facies | 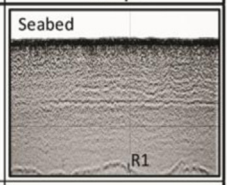  |
| | | | | Well-layered, locally parallel to subparallel prograded. Minor disconformities | Channel fill. Sediment mounds or drapes | Sediment Bodies | 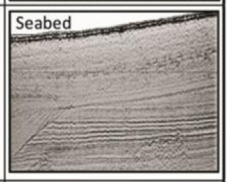  |
| LIG (MIS 5e) | Variable: 7-12 m | **Top:** unconformity R1 (top LIG unit) **Bottom:** unconformity RF (top Rock Foundation unit) | ~ 120 ky | Weak to moderate amplitude with discontinuous, subparallel minor reflectors | Reef flat, crest, forereef slope. Local pinnacle reef | Reef facies | 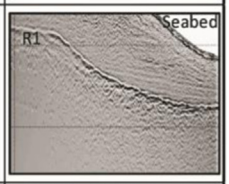  |
| Rock Foundation | Basement | **Top:** RF (top Rock Foundation unit) **Bottom:** NA | Proterozoic (2000 My) | Chaotic, low-amplitude. Acoustic basement | Local deep valley-like depressions and ridges | Folded metamorphics, conglomerates and sandstones (Kimberley Group) | 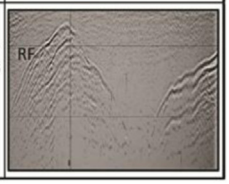  |

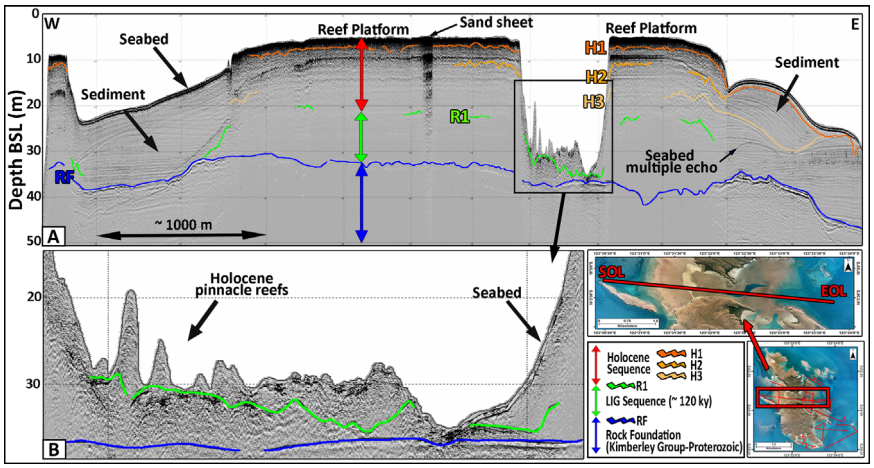


**Fig. 4.** (A) W–E section of the Bathurst–Irvine high intertidal fringing reef (width 7 km), showing two stages of platform growth, marginal sediment bodies, drowned reefs (inset, B) in the central elongate pool and basement topography.

Seismic traverses across the pool in the middle of the Bathurst-Irvine interisland reef reveal a thin (5 m thick) LIG reef unit present close to the modern sea bed, overlying the Proterozoic substrate. Within the pool Holocene pinnacle reefs up to 10 m high grow from the base of the pool (Fig. 4B).

Both margins of the reef flat have well-developed bedded sediment lobes, up to 20 m thick. Longitudinal and transversal seismic profiles have shown that the bodies have a complex internal architecture (Figs. 4 and 5), composed of surficial seaward prograding layers, in discordant relationship with the deeper and more horizontal ones. Similarly for the Holocene discontinuities (H1, H2, and H3), the internal beds could also be linked to possible non-deposition. Based on a qualitative interpretation of the seismic data, the drapes are composed by fine to medium grained sediments and, according to the local geomorphology and the collected samples, the sediment supply could be a combination of clastic influx coming from the surrounding islands and from suspension (from the mainland), and bioclastic carbonate deposits derived from the reefs. The western sediment mound Fig. 4A) is likely a result of ebb tides flowing off the reef platforms and bottom current dynamics, resulting in filling of pre-existing accommodation space.

A north–south profile (Fig. 5) of the platform shows a similar stratigraphy for the reef platform, with 25 m of Holocene sediment infilling the adjacent small lagoon to the south of the platform. Holocene and LIG thicknesses are similar to those already recorded in the W–E profile of the platform. Topographic changes in the Proterozoic surface, as it rises to the north, have influenced the position of the platform by providing suitable elevated substrate which was colonised by LIG reef growth. Within the sediment

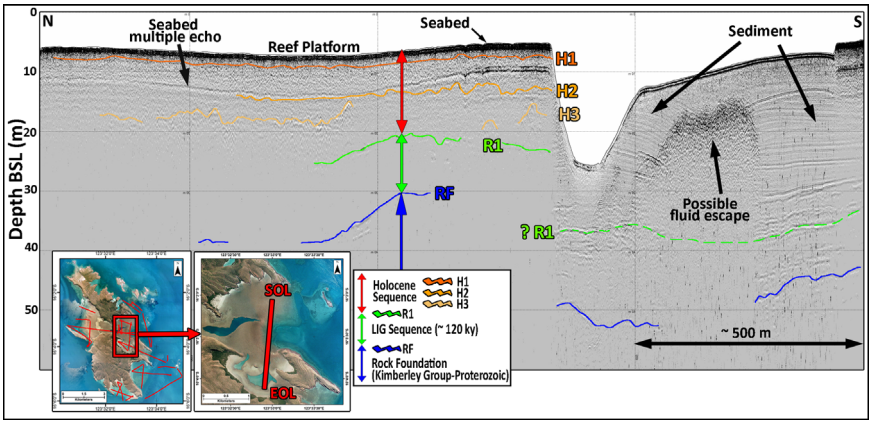


**Fig. 5.** N–S section of Bathurst–Irvine Reef and adjacent embayment substrate. Note influence of platform elevation in the location of platform building; 2 stages (LIG and Holocene) of reef growth, and the 25 m thick bedded sediment pile filling the embayment to the S, with an internal signal probably representing fluid escape.

body, the internal geological pattern is almost completely obscured by an acoustic turbidity anomaly. This seismic signature, named *curtain*, is associated with fluid escape through the sediment (Baltzer et al., 2005). It is noteworthy that Traditional Owners have reported freshwater springs in the general area. The presence of the two shallow pools along north east Irvine Island could be linked to upward migration of fresh water into the seawater. The mixed brackish waters could have been a significant control on reef growing processes, limiting the Holocene (and possibly LIG) buildup in the area.

*4.2.1.3. Bay head reefs: south Sunday Island.* Fringing bay head reefs are mainly developed in the southern and south-eastern sectors of the Sunday Islands (Fig. 6). The reef flats are sheltered and elongate along the coastline, with an approximate width between 500 m and 1500 m. The acoustic profiles cover only the external edges of the platform, due to the tidal conditions during the survey. The data available reveal that the pre-existing Proterozoic topography (RF) rises from 30 m to 10–15 m below the seafloor, significantly attenuating the reef development. Both the Last Interglacial and the Holocene reefs are relatively thin, with a similar internal architecture. Whereas the Proterozoic rock foundation presents irregularities, such as channels or depressions, the LIG reef growth tends to level the topography (see Fig. 6B). For this reason, it is problematic to establish an average thickness of this unit. The overlying Holocene reef buildup is about 7 m thick on a mostly flat pre-existing LIG surface.

*4.2.2. Planar, coralgal reefs*

*4.2.2.1. Montgomery Island.* Montgomery Island is located approximately 23 km west of the coastline (Fig. 1). It is bordered by a large high intertidal reef which is a planar coralgal reef, and contains a central Proterozoic island (Wilson, 2013). Montgomery Reef is known to have a unique set of reef substrates on the platform, in particular rhodolith dominated substrates and associated crustose coralline algae forming a distinctive reef crest, and at least 2 terraces described by Wilson (2013) as upper and lower lagoons. Shallow pools with internal coral growth characterise parts of the reef flat. The well-developed Proterozoic central island is surrounded by sand cays and vegetated by mangroves and grasses (Wilson, 2013). Reef flats are dominated by sand and coral rubble with small living corals in shallow pools. The platform is very shallow and emergent at low tide with distinctive waterfall cascades across the reef crest. Spring tidal range is 12 m, and the platform margin is exposed by a few metres at low tide. A prominent north–south trending spine protruding from the main platform on its western side is called “The Breakwater”.

Due to the extreme shallowness of water on the platform in all parts of the tidal cycle, except during high water spring tides, seismic transects could only be obtained at the platform margins. Good quality profiles were collected on east and west sides of the Breakwater.

The Breakwater appears to have developed as a northward prograding feature, with seismic data showing a distinct pattern of development. There are many pinnacle reefs and significant sediment cover in places along with occasional palaeochannels. Two stages of pinnacle growth can be frequently recognised, with a

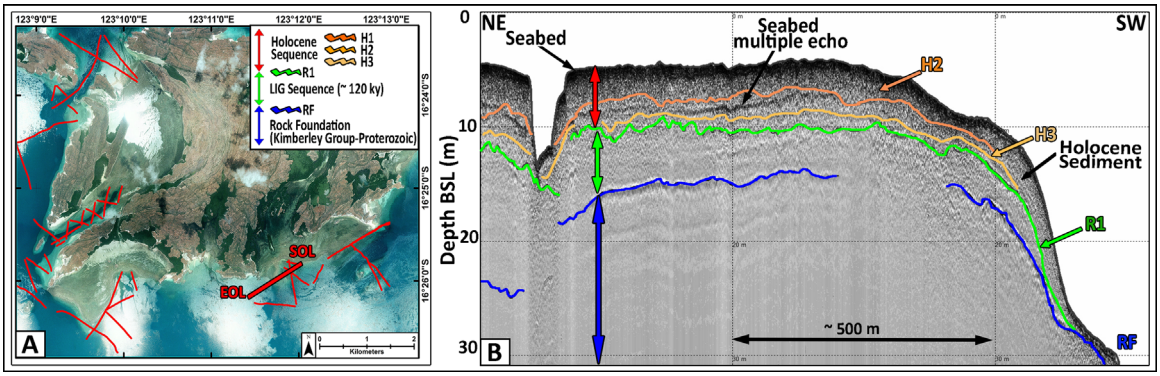


**Fig. 6.** Sunday Islands. (A) Landgate aerial photography provided by DPaW; track plot of seismic profiles are marked with thin red lines. (B) Seismic profile. These Proterozoic islands are separated by deep depressions (probably structurally controlled), with both Holocene and LIG reef growth as fringing reefs. Irregular topography of Kimberley Group is partially blanketed by 2 stages of reef growth. (For interpretation of the references to color in this figure legend, the reader is referred to the web version of this article.)

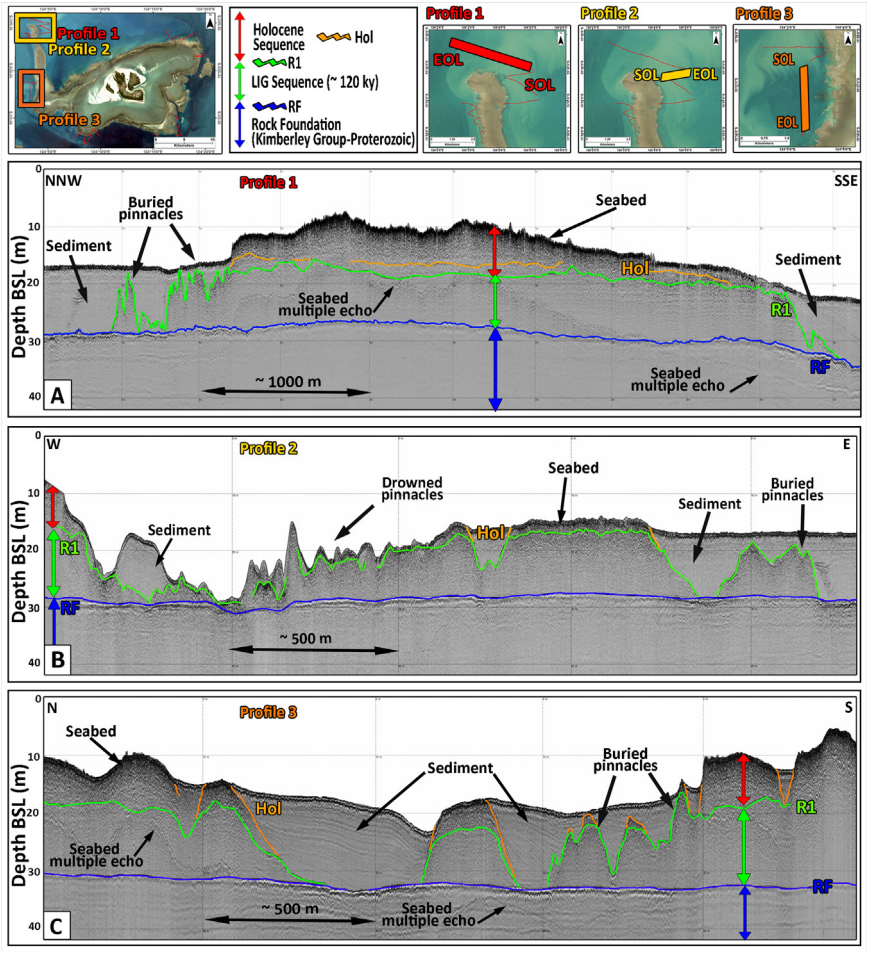


**Fig. 7.** History of reef growth for the Breakwater from seismic profiles. (A) Profile 1. Cross section of the Breakwater along its distal submerged northern margin reveals an initial LIG ridge composed of marginal pinnacles and central coalescent pinnacle architecture, overlain by Holocene coral reef with small surficial pinnacle reefs; note thickening of sediment drapes at margins of the ridge structure. (B) Profile 2. A similar history is shown by this profile of the east margin of the Breakwater at its northern extremity. Note incipient colonisation of LIG pinnacle reefs by Holocene reefs, and influx of Holocene sediments. (C) Profile 3. N–S view of the south western seaward margin of the Breakwater. Proterozoic surface (RF, blue) with two stacked generations of pinnacle reef development (LIG and Holocene), with bedded sediment infilling the reef terrain and overwhelming reef growth, proximal to and near the point of attachment to the Montgomery platform. (For interpretation of the references to color in this figure legend, the reader is referred to the web version of this article.)

thicker LIG buildup under a thin Holocene reef substrate. In some cases, pinnacle reefs occur above a deep basal unconformity, interpreted as the Proterozoic surface, capped by sediment cover terminating at 10 m MSL on the eastern side of the Breakwater (Fig. 7). Three stages of reef development are present, with different level of maturity going from juvenile in the north and mature in the south. An axial section across the northern tip of the Breakwater (profile 1, Fig. 7A) confirms an initial ridge of LIG coalescent pinnacle reefs that was followed by sediment cover during the Holocene. The N–S axis of the Breakwater apparently follows a bathymetric ridge with the same trend which controlled the reef initiation and provided a favourable template for an initial reef growth. A similar west–east profile, situated just to the north eastern extremity of the Breakwater (profile 2, Fig. 7B) endorses the pattern of LIG coalescent pinnacle growth on the Proterozoic, then pinnacle reef recolonization during the Holocene accompanied by infill of depressions by active sedimentation. On the south-western margin of the Breakwater, in a N–S section, a series of pinnacle reefs occurs above the basal unconformity with a sediment blanket between pinnacles. The pinnacles are buried by the sediment and, in some cases, protrude through the sediment cover demonstrating contemporaneous infill and active Holocene reef building. These pinnacles usually colonised an earlier (probably LIG) stage of pinnacle growth (see profile 3, Fig. 7C).

Together these profiles show a different level of maturity, establishing the current surface morphology as a spine-like protuberance northward from the Montgomery platform. First (south), a mature stage is characterised by a ridge of LIG coalescent pinnacles, overlain by Holocene reef. In the central region, an intermediate phase is constituted by an incipient regrowth on LIG pinnacles by Holocene reefs. And finally, in the relatively young reef sequence (north), a continuous reef flat is near emergent.

At its south western corner, the Montgomery Reef platform margin has distinctive morphology of a subtidal reef terrace with a near-vertical fore reef slope (Fig. 8). The littoral terrace is characterised by a barren zone lacking spur and groove morphology, with occasional sand sheets; a lower littoral reef front ramp, with slope 5–10°, high-energy tidal flow, encrusted by coralline algal ridges; a mid-littoral reef crest with 100 m wide rhodolith banks and lacking a boulder zone; and finally a lower and upper reef flat dominated by rhodoliths and small pools containing corals. Two reef buildups are present overlying Proterozoic basement; a 10 m thick LIG reef and a 22 m thick Holocene reef, immediately underlying the platform margin (Fig. 8). The distinctive terracing of the steep forereef is controlled by the boundary between these two reef building events.

Reef building processes in and around Montgomery platform include both phases of reef building and buried sedimentary

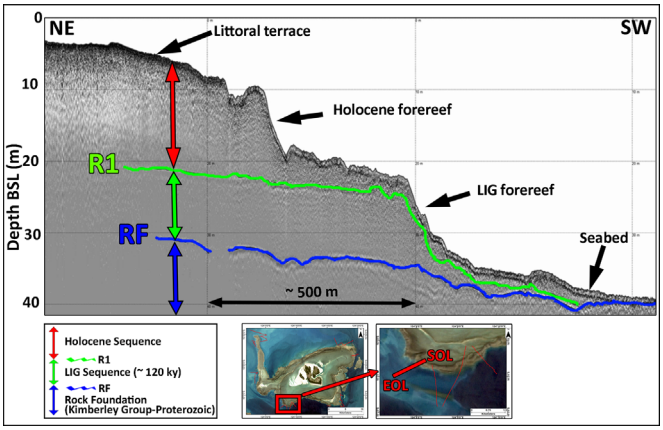


**Fig. 8.** Seismic sections showing structure of the SW margin of Montgomery Reef. Note terraced morphology of forereef is controlled by the boundary of LIG and Holocene reef buildup events. The lower level of basement substrate (RF, blue) under the crest of Montgomery Reef allowed for 2 stages of reef growth, LIG, and Holocene separated by an unconformity (R1, green). (For interpretation of the references to color in this figure legend, the reader is referred to the web version of this article.)

sequences, however it is clear that the Holocene buildup phase of the main platform is significant. In shallow platform conditions, the internal structure of the platform is difficult to determine due to prominent ringing in the profiles and lack of penetration. It is likely that reef thickness declines toward the central island as the Proterozoic topography rises.

## 5. Conclusion

The study presented here has achieved the first regional geophysical study of the Kimberley reefs. By developing an understanding of seismostratigraphic events, it has been possible to document the subsurface evolution and growth history of diverse reef systems for a range of reef types mapped in the Buccaneer Archipelago. The seismic data demonstrate the long term resilience of the Kimberley reefs, their capacity to thrive in challenging environmental circumstances, including high-turbidity and other high-energy events throughout the Holocene. Evidences of Last Interglacial reefs also suggest that reef growth was not an opportunistic event during the Holocene but reef growth has occurred in the region during earlier highstand events.

High-resolution seismic data demonstrated that:

- The surveyed reefs in the Buccaneer Archipelago have a similar reef morphology and growth history as in Cockatoo Island. Seismically, all reefs exhibit a multistage reef buildup, correlated to late Pleistocene sea level highstand events. Inter-island fringing reefs appear to have formed by progradation and coalescence of fringing reefs attached to adjacent islands. Where coalescence has not gone to completion, deep inter-reef channels or elongate depressions still remain between adjacent fringing reefs or within intertidal platform reefs (e.g. Bathurst and Irvine reef). Within few reef systems, linked pinnacle reefs up to 15 m thick, are present.
- The study also documented the first widespread occurrence of last interglacial coral reefs north of Cape Range (Exmouth latitude: 21°55′S). However unlike the emergent reef terraces which intermittently outcrop along the coast between Dongara (latitude: 29°15′S) and Exmouth, LIG reefs occur at depth of between 20 and 35 m would suggest that the coastal Kimberley region has undergone or is still undergoing subsidence at least since the Last Interglacial. A subsiding coast can explain the complex ria coastline and numerous islands which is s characteristic of the Northern Kimberley coast.
- Pre-existing topography and substrate depth control the amount of accommodation available for reef growth and stacking of reef building events. From the seismic profiles, it appears evident that the elevation of the Proterozoic rock foundation represents a major factor in determining the thickness and location of the reefs and controlling their vertical accretion. Pre-existing topographic highs, like hills or ridges were possibly inundated several hundred years later than the adjacent valleys or palaeochannels. Also the substrate represents a controlling factor in reef development. Corals are not able to grow on mobile unconsolidated sediments, hence where there is this kind of foundation, no reefs buildup is present. Subsidence of the LIG substrates must also be taken into consideration. The Kimberley coast is considered to represent a subsiding landscape. This hypothesis is supported by the seismic data obtained during this study. As a consequence, a greater accommodation space has become available, being an important control factor of the overall Holocene morphology.

Combining this information with reef chronology and measurements of accretion rates (from Solihuddin et al., 2015), the data indicate that the interaction between Quaternary global sea level fluctuations and the complex, subsiding Kimberley landscape has been of primary importance in controlling the longer term evolutionary patterns of coral reef development and growth, the available accommodation for and timing of multiple events of reef growth over geological timescales.

## Acknowledgements

The Kimberley Reef Geomorphology Project 1.3.1 is funded by the Western Australian State Government through the Western Australian Marine Science Institution. This research was assisted by the Bardi Jawi, Mayala and Dambimangari people, the Traditional Owners of these lands, through essential assistance and guidance in part of the field work. The authors wish to thank: Cygnet Bay Marine Research Station staff (in particular James Brown and Dr Erin McGinty) that provided vessel support for marine operations and access to research facilities at Cygnet Bay; Mark Hardman (Fugro Satellite Positioning Pty Ltd) for supplying the DGPS; Neil MacDonald (Applied Acoustic Engineering Ltd) and Western Advance (Malaga, Western Australia) for the equipment support; Giovanni De Vita for his technical advice; Richard Costin and Annabelle Sandes (Kimberley Media). The authors would like to thank Dr Piers Larcombe for his valuable comments and suggestions to improve the manuscript.

It must be noted that the Aboriginal history of climate, land and environment is based on thousands of years of residence and rich culture: it is important to consider this broad understanding alongside the modern science completed here.

The authors wish to dedicate this project to the late Professor L. B. Collins who left us before the publication of this manuscript.

## References

Baltzer, A., Tessier, B., Nouzé, H., Bates, R., Moore, C., Menier, D., 2005. Seistec seismic profiles: a tool to differentiate gas signatures. Mar. Geophys. Res. 26 (2–4), 235–245.

Brocx, M., Semeniuk, V., 2011. The global geoheritage significance of the Kimberley coast, Western Australia. J. R. Soc. West. Aust. 94, 57–88.

Brooke, B., 1997. Geomorphology of the north Kimberley coast. In: Walker, D. (Ed.), Marine Biological Survey of the Central Kimberley Coast. University of Western

Australia, Western Australia, Perth,
pp. 13–39 (unpublished report), Museum Library No. UR377.
Chin, A., Sweatman, H., Forbes, S., Perks, H., Walker, R., Jones, G., Williamson, D., Evans, R., Hartley, F., Armstrong, S., Malcolm, H., Edgar, G., 2008. Status of the coral reefs in Australia and Papua New Guinea. In: Wilkinson, C. (Ed.), Status of Coral Reefs of the World. Global Coral Reef Monitoring Network. Reef and Rainforest Research Centre, Townsville, Australia, pp. 159–176.
Condie, S.A., Andrewartha, J., 2008. Circulation and connectivity on the Australian North West Shelf. Cont. Shelf Res. 28 (14), 1724–1739.
Collins, L.B., Zhu, Z.R., Wyrwoll, K.H., Eisenhauer, A., 2003. Late quaternary structure and development of the northern Ningaloo Reef, Australia. Sediment. Geol. 159 (1), 81–94.
Collins, L.B., Zhao, J.X., Freeman, H., 2006. A high-precision record of mid-late Holocene sea-level events from emergent coral pavements in the Houtman Abrolhos Islands, southwest Australia. Quat. Int. 145, 78–85.
Collins, L.B., Testa, V., 2010. Quaternary development of resilient reefs on the subsiding Kimberley continental margin, Northwest Australia. Braz. J. Ocean. 58, 1–13.
Collins, L.B., Testa, V., Zhao, J., Qu, D., 2011. Holocene growth history of the Scott reef carbonate platform and coral reef. J. R. Soc. West. Aust. 94 (2), 239–250.
Collins, L.B., 2011. Geological setting, marine geomorphology, sediments and oceanic shoals growth history of the Kimberley Region. J. R. Soc. West. Aust. 94 (2), 89–105.
Collins, L.B., O'Leary, M., Stevens, A., Bufarale, G., Kordi, M., Solihuddin, T., 2015. Geomorphic patterns, internal architecture and reef growth in a macrotidal, high-turbidity setting of coral reefs from the Kimberley bioregionn. Aust. J. Marit. Ocean Aff. 7 (1), 12–22.
Commonwealth of Australia, 2006. A Guide to the Integrated Marine and Coastal Regionalisation of Australia. Department Of The Environment And Heritage, Canberra, Australia.
Cresswell, G.R., Badcock, K.A., 2000. Tidal mixing near the Kimberley coast of NW Australia. Mar. Freshw. Res. 51, 641–646.
Department of the Environment, 2014. Australia's 15 National Biodiversity Hotspots. Australian Government, Canberra (Available at) ⟨http://www.environment.gov.au/node/13909⟩.
Eisenhauer, A., Wasserburg, G.J., Chen, J.H., Bonani, G., Collins, L.B., Zhu, Z.R., Wyrwoll, K., 1993. Holocene sea-level determination relative to the Australian continent: U/Th (TIMS) and 14C (AMS) dating of coral cores from the Abrolhos Islands. Earth Planet. Sci. Lett. 114 (4), 529–547.
Kordi, M.N., Collins, L.B., O'Leary, M., Stevens, A., 2016. ReefKIM: an integrated geodatabase for sustainable management of the Kimberley Reefs, NW Australia. Ocean Coast. Manag. 119, 234–243.
Hopley, D., Smithers, S., Parnell, K., 2007. The Geomorphology of the Great Barrier Reef: Development, Diversity, Change. Cambridge.
McKenzie, N.L., Start, A.N., Burbidge, A.A., Kenneally, K.F., Burrows, N.D., 2009. Protecting the Kimberley: a Synthesis of Scientific Knowledge to Support Conservation Management in the Kimberley Region of Western Australia. Department of Environment and Conservation, Perth, WA.
Montaggioni, L.F., 2005. History of Indo-Pacific coral reef systems since the last glaciation: development patterns and controlling factors. Earth Sci. Rev. 71 (1–2), 1–75.
O'Faircheallaigh, C., 2013. Extractive industries and Indigenous peoples: a changing dynamic? J. Rural Stud. 30, 20–30.
O'Leary, M.J., Hearty, P.J., McCulloch, M.T., 2008b. Geomorphic evidence of major sea-level fluctuations during marine isotope substage-5e, Cape Cuvier, Western Australia. Geomorphology 102 (3–4), 595–602.
Parkinson, G., 1986. Atlas of Australian Resources, Third series4. Climate. Division Of National Mapping, Canberra.
Pepper, M., Scott Keogh, J., 2014. Biogeography of the Kimberley, Western Australia: a review of landscape evolution and biotic response in an ancient refugium. J. Biogeogr. 41 (8), 1443–1455.
Sandiford, M., 2007. The tilting continent: a new constraint on the dynamic topographic field from Australia. Earth Planet. Sci. Lett. 261 (1–2), 152–163.
Solihuddin, T., Collins, L.B., Blakeway, D., O'Leary, M.J., 2015. Holocene Reef growth and sea level in a macrotidal, high turbidity setting: Cockatoo Island, Kimberley Bioregion, Northwest Australia. Mar. Geol. 359, 50–60.
Tyler, I.M., Hocking, R.M., Haines, P.W., 2012. Geological evolution of the Kimberley region of Western Australia. Episodes – Newsmagazine of the International Union of Geological. Sciences 35 (1), 298.
Wilson, B., Blake, S., Ryan, D., Hacker, J., 2011. Reconnaissance of species-rich coral reefs in a muddy, macro-tidal, enclosed embayment, Talbot Bay, Kimberley, Western Australia. J. R. Soc. West. Aust. 94, 251–265.
Wilson, B., 2013. The Biogeography of the Australian North West Shelf, Environmental Change and Life's Response, 1st edition. Elsevier, New York, USA.
Wolanski, E., Spagnol, S., 2003. Dynamics of the turbidity maximum in King Sound, tropical Western Australia. Estuar. Coast. Shelf Sci. 56, 5–6.
Wright, R.L., 1964. Geomorphology of the West Kimberley Area. CSIRO Land Res. Ser. 9, 103–118.

***Stratigraphic architecture and evolution of a barrier seagrass bank in the mid-late Holocene, Shark Bay, Australia***

Giada Bufarale and Lindsay B. Collins

Department of Applied Geology, Curtin University, GPO Box U1987, Perth, WA 6845, Australia

This article is published in Marine Geology, Volume 359, 1 January 2015, Pages 1-21.

doi.org/10.1016/j.margeo.2014.11.010

Marine Geology 359 (2015) 1–21

Contents lists available at ScienceDirect

Marine Geology

journal homepage: www.elsevier.com/locate/margeo

# Stratigraphic architecture and evolution of a barrier seagrass bank in the mid-late Holocene, Shark Bay, Australia

Giada Bufarale *, Lindsay B. Collins [1]

*Department of Applied Geology, Curtin University, GPO Box U1987, Perth, WA 6845, Australia*

ARTICLE INFO

*Article history:*
Received 21 August 2014
Received in revised form 5 November 2014
Accepted 18 November 2014
Available online 27 November 2014

Communicated by J.T. Wells

*Keywords:*
Shark Bay
seagrass
Holocene sea level
bank growth
age model
sediment accumulation rate

ABSTRACT

Within the Faure Sill complex (Shark Bay, Western Australia), a combination of remote sensing analysis, seismic stratigraphy and cores to ground truth, together with radiocarbon dating, demonstrate the interconnection between sediment body morphologies, seagrass related substrates and pre-existing topography and reveal the system as a channel–bank complex. Sea level fluctuations appear to have largely controlled the hydrodynamic conditions of the bank, contributing to each stage of its evolution. 1) Not earlier than 8.5–8.0 ka BP, in a lowstand period, after an erosive event of underlying palaeosurfaces, seagrass establishment progressively contributed to initiating bank growth. 2) Around 6800 years BP, bank accumulation reached its apex, in conjunction with a rapid sea transgression. 3) During the Late Holocene, succeeding a slow decline to present sea level, bank growth continued to fill available accommodation space and a number of hiatuses, indicating temporal and spatial discontinuities within the process of bank building, are recognised. Average depositional rates of bank building (1.3 m/ka) conform to previous estimates derived for seagrass banks but rates are strongly facies dependent, attesting to the dynamic nature of this channel–bank complex. The extensive seagrass meadows are essential for a wide range of aspects of the environment of the Shark Bay area. Not only are they particularly important for the entire shallow benthic ecosystem, but they also had a major role in the partial closure of the southern basins and hence determining the development of hypersaline conditions and associated oolitic microbial and evaporitic facies in Hamelin Pool and L'Haridon Bight. Moreover, this system has a critical role in producing, sequestering and storing organic carbon.



## 1. Introduction

Registered as a World Heritage Property in 1991 on the basis of its "natural heritage" values (Hancock et al., 2000), Shark Bay is located approximately 800 km north of Perth on the west coast of Australia (Fig. 1A). It has a "W" shape, open to the Indian Ocean to the north and divided by the Peron Peninsula into two narrow gulfs: Freycinet Basin on the western side and L'Haridon Bight and Hamelin Pool, to the east (Fig. 1B). Faure Sill, a seagrass bank, is one of Shark Bay's most notable structures, lying approximately between 25° 45′ S and 26°30′ S and 113° 40′ E and 114° 15′ E (Fig. 2), orientated east–west across the axis of the Hamelin and L'Haridon hypersaline basins and covering an area of around 1000 km$^2$ (Davies, 1970a). The bank extends from Kopke Point (Gladstone Embayment/Wooramel Complex) to Faure Island, Petit Point (Nanga Peninsula) and to Dubaut Point (southern part of Peron Peninsula); it is nearly emergent at Faure and Pelican Islands and it is characterised by shallow water and relatively deep and broad channels, mainly north–south oriented (Fig. 2).

The two most prominent natural assets of Shark Bay are stromatolites and seagrass. Stromatolites are common in fossil sequences, widely recorded back to the Precambrian (Schopf, 1993; Allwood et al., 2006), but rare in modern waters, where their occurrence is limited to some locations in Western Australia, in the Bahamas and in a few other places elsewhere (e.g. Dravis, 1983; Cohen et al, 1993; Moore and Burne, 1994; Jahnert and Collins, 2013). It is well known that seagrass communities provide a wide range of services (Duarte, 2002; Gibbes et al., 2014). They are fundamental in controlling fluid dynamics across the bank where they reside (Fonseca et al., 1982; Belperio et al., 1984; Verduin and Backhaus, 2000; Koch et al., 2006). The extensive seagrass meadows at Shark Bay, the largest reported assemblage in the world (Walker, 1990), has had a significant control during Holocene time on the sedimentary regime and the growth of the bank, leading to major environment changes, which have caused a partial closure of the southern basins of Hamelin Pool and L'Haridon Bight (Davies, 1970b; Logan et al., 1970a,b; Hagan and Logan, 1974; Read, 1974; Walker, 1985; Walker and Woelkerling, 1988; Walker et al., 1988; Jahnert and Collins, 2013; Collins and Jahnert, 2014). Its role in reducing the rate of water flowing through the sill has resulted in a decrease or loss of

* Corresponding author. Tel.: +61 8 92663710.
*E-mail addresses:* giada.bufarale@postgrad.curtin.edu.au (G. Bufarale), l.collins@curtin.edu.au (L.B. Collins).
[1] Tel.: +61 8 92667977.

http://dx.doi.org/10.1016/j.margeo.2014.11.010
0025-3227/

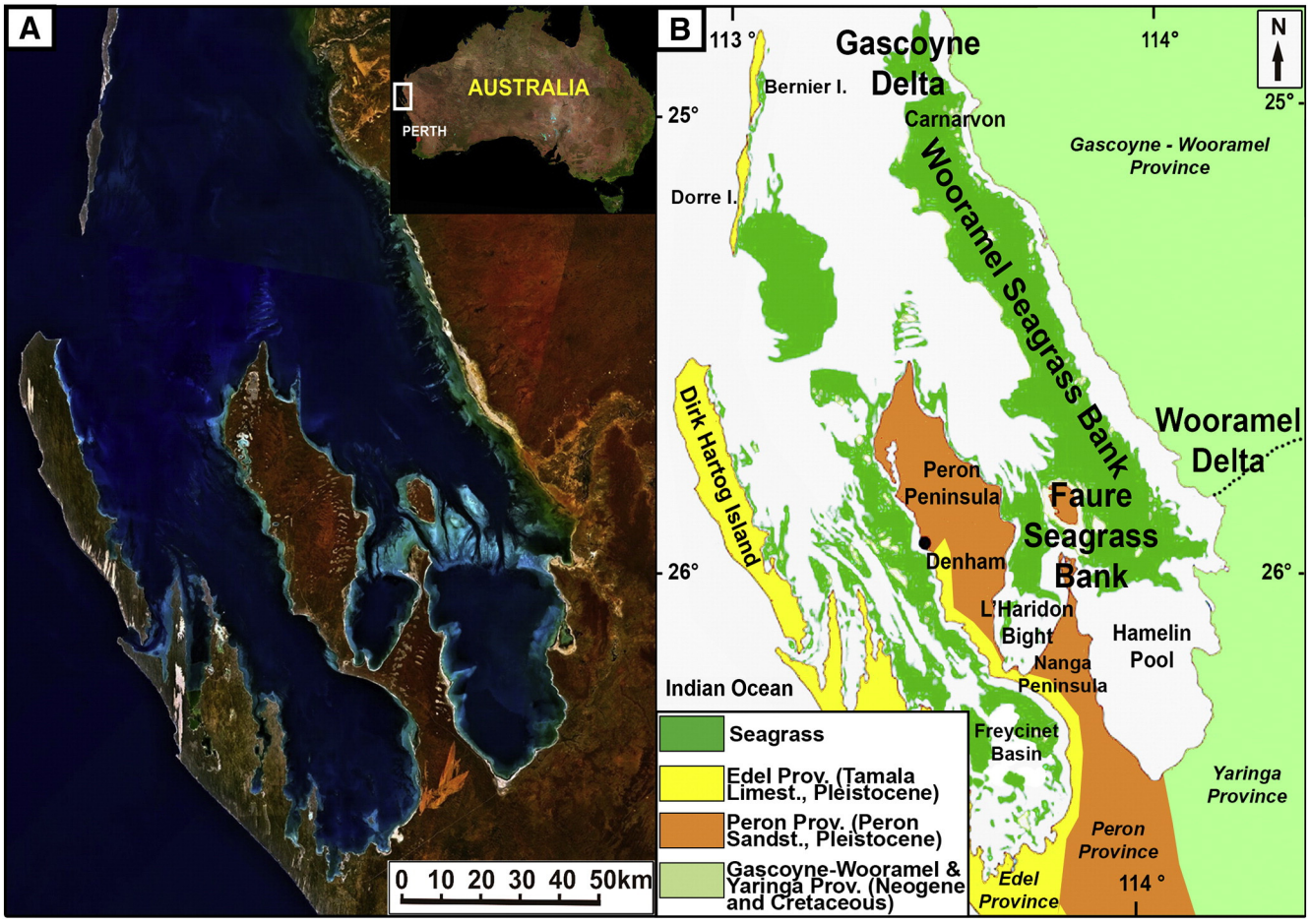


**Fig. 1.** A) Aerial view of the area from Geoscience Australia. B) Simplified map of Shark Bay, with seagrass distribution. The two most notable banks are the Faure and Wooramel seagrass banks, adjacent to the Wooramel and Gascoyne Deltas.
Modified from Walker et al. (1988), Jahnert and Collins (2013), Playford et al. (2013) and www.sharkbay.org.

sediment movement, which is trapped and bound by the roots and rhizomes, stabilising and enhancing the accretion of the seabed (Walker et al., 1999). The thick meadow acts as protection from cyclones and other severe conditions and, as well, prevents erosion of the seafloor (Walker, 1990; Duarte, 2002). Moreover, epiphytes and other organisms (such as molluscs and foraminifera), which live in their rhizomes, produce a significant amount of calcium carbonate and play an important role in the deposition and accumulation of sediment (Hagan and Logan, 1974; Walker and Woelkerling, 1988). Barrier banks, climatic conditions and restricted tidal exchange control the salinity of the enclosed waters (Logan and Cebulski, 1970), creating unique environments with metahaline to hypersaline conditions, which provide a basis for the development of a variety of biogenic and physical structures such as microbial communities (stromatolites) and oolitic shoals (Jahnert and Collins, 2013). Thus, explaining the evolution of the seagrass banks is crucial to understanding the development of the hypersaline facies association in basins to the south.

During the 1970s, pioneering research was described in two American Association of Petroleum Geologists Memoirs (Logan et al., 1970b, 1974) and subsequent work undertaken by Playford and Cockbain (1976) Playford (1990), Chivas et al. (1990). Recent research has provided the first detailed regional evaluation of the subtidal microbial system and tidal flat evolution (Jahnert and Collins, 2011, 2012, 2013; Collins and Jahnert, 2014).

Besides these local values, seagrass banks provide global ecosystem services. For instance, seagrass meadows are involved in producing, sequestering and storing organic carbon (Duarte, 2002; Grimsditch et al., 2012; Duarte et al, 2013; Lavery et al., 2013) and significantly contributing to carbon, nitrogen and phosphorus cycles in the ocean (Fourqurean et al., 2012). Moreover, the wider Gascoyne Delta–Wooramel Bank–Wooramel Delta–Faure Sill system (Fig. 1B) has potential as an analogue for some Browse Basin hydrocarbon reservoirs in the North West Shelf, Western Australia (Barber et al., 2004; Tovaglieri and George, 2014).

To investigate the Holocene development of the Faure channel–bank complex, remote sensing imagery analysis, acoustic profiles and sedimentological information were combined, in order to correlate internal architecture, sediment bodies and lithofacies. Integrating these data with radiocarbon dating, information about the accumulation rates was obtained, together with an estimated age of bank onset. This paper reports the analyses conducted on the Faure Sill and new insights and understanding of its evolution, growth and chronology, by considering morphostratigraphic elements, channel architecture and geometry, and linking traditional research with newly developed facies associations and stratigraphic relationships.

## 2. Geology and environmental setting

The landscape of Shark Bay has been significantly controlled by tectonism (Butcher et al, 1984). Fold and fault systems have been shaping the geography of the area since the Palaeozoic (van de Graaff et al., 1983; Hocking et al., 1987). Anticlinal folds, oriented NNW–SSE, are responsible for the formation of peninsulas and islands and synclines are associated with the gulfs and bays (Butcher et al., 1984; Playford et al., 2013). A regional normal fault system oriented N–S has operated in

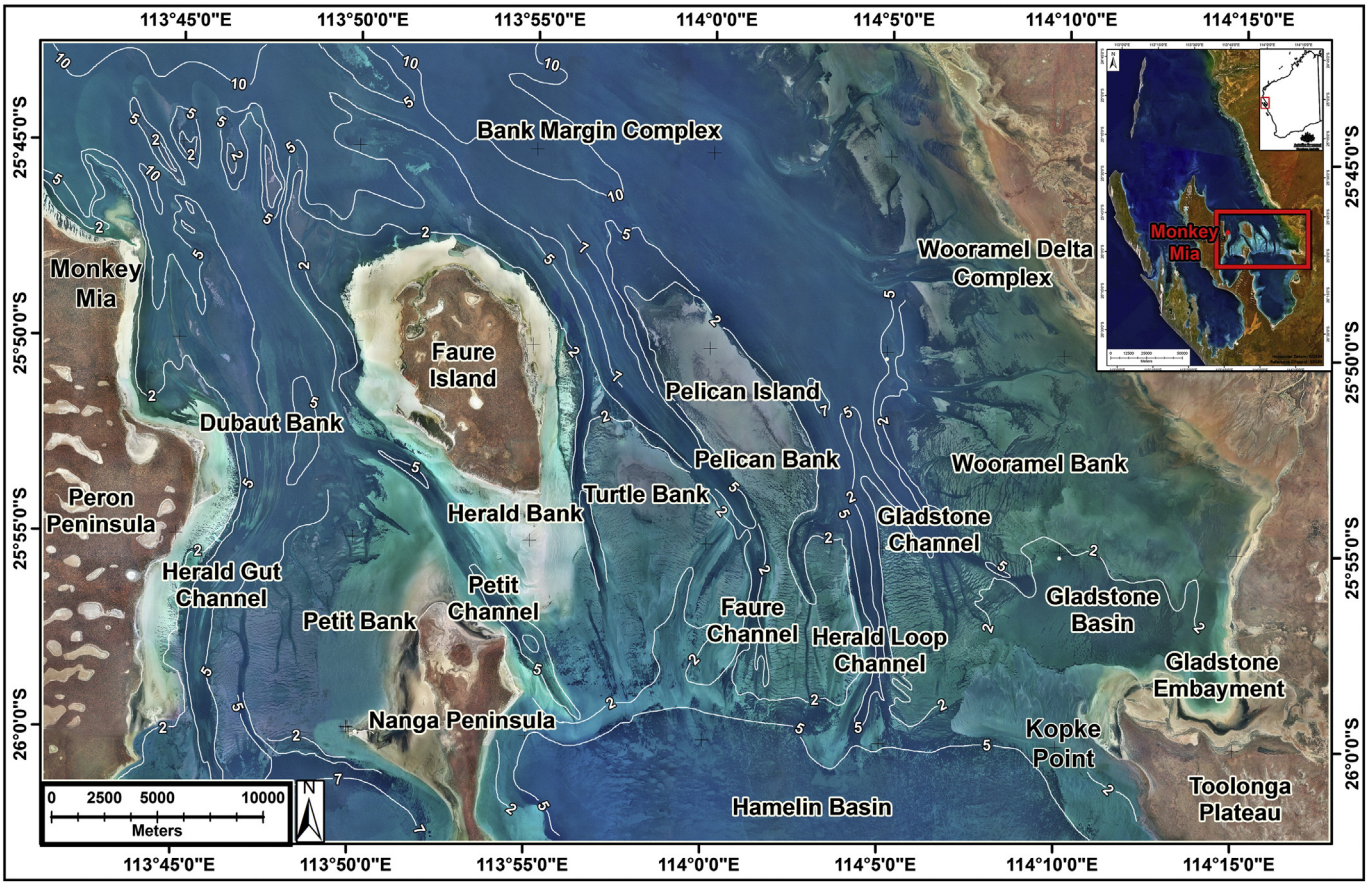


**Fig. 2.** Locality map showing the study area and the locations mentioned in Sections 4 and 5. Locality names are from Hagan and Logan, 1974. Simplify bathymetric contours are shown. Aerial view of the Faure Sill is a mosaic of photos from Landgate (Western Australia). Insert image from Geoscience Australia.

the region and some reverse faults are associated with the anticlines (Butcher et al., 1984; Playford et al., 2013).

The Shark Bay region can be divided into four main physiographic provinces (Fig. 1; Logan et al., 1970a; Hancock et al., 2000):

1) At the eastern margin of inland Shark Bay, Neogene and Cretaceous limestone units compose the *Yaringa Province* (Playford et al., 2013).
2) The *Gascoyne–Wooramel Province* is the wide alluvial coastal plain that stretches between the Gascoyne and Wooramel Rivers (Logan et al., 1970a).
3) The *Peron Province* is located in the central part of Shark Bay. During the latter part of the Quaternary, Shark Bay was characterised by three distinct marine transgressions (Logan et al., 1974; O'Leary et al., 2008; Jahnert and Collins, 2011). The first phase led to the formation of the Peron Sandstone (Logan, 1968; Logan et al., 1970a), a red, quartz rich sandstone, exposed on the Peron and Nanga Peninsulas and in Faure and Pelican Islands (Table 1).
4) The western *Edel Province* comprises Edel Land, Dirk Hartog Island and the Bernier–Dorre Islands. The main formation exposed in the area is the Tamala Limestone (Logan, 1968; Logan et al., 1970a; Playford and Cockbain, 1976), a pale, off white calcarenite (cemented calcareous dune sand) which developed as a result of a second phase of coastal dune formation (Logan et al., 1970a).

The Faure bank complex sits at a focal point between the coastal strip along the western margin of the Gascoyne–Wooramel Province and the eastern shores and hinterland of the Yaringa Province and Peron Provinces (Peron and Nanga Peninsulas and Faure Island; Hancock et al., 2000).

Although the principal Pleistocene units in the area are the eolianites of the Tamala Limestone and Peron Sandstone, there are also a few outcrops of Pleistocene marine formations: Dampier Limestone (and its member the Carbla Oolite), Bibra Limestone and Depuch Sandstone (Playford et al., 2013).

**Table 1**
Stratigraphic nomenclature for Shark Bay (modified from O'Leary et al., 2008). Note the position of acoustic reflectors HR1 and HR2 within the stratigraphy (top Bibra and top Dampier Limestones respectively, further discussed in Sections 4.2, 5.1 and 5.3). Tamala Limestone (Middle–Lower Pleistocene) and Depuch Limestone (Late Pleistocene) are also present in Shark Bay, but they have been excluded from the table since there is no evidence of their occurrence in the study area.

| Series/epoch | Formation | MIS | Sedimentation |
|---|---|---|---|
| Holocene | Holocene – Recent *Unit 1* | MIS 1 | Sill development |
| | | | HR1 |
| Upper Pleistocene | Bibra Limestone *Unit 2* | MIS 5a–5e | Marine deposits |
| | | | HR2 |
| Middle Pleistocene | Dampier Limestone *Unit 3* | MIS 9/11 (poorly dated) | Marine deposits |
| | | | HR3 |
| | Carbla Oolite Member *Unit 4 ?* | | Marine deposits |
| | | | HR4 |
| Middle – Lower Pleistocene | Peron Sandstone *Unit 5 ?* | MIS 11 > 37 | Transgressive system. Dune development |

The Dampier Limestone (Logan et al., 1970a; van de Graaff et al., 1983) is the oldest marine dominated unit recognised in the Shark Bay area (Table 1). Dated as Middle Pleistocene, it was deposited in shallow marine (less than 3 m) tidal channel flats, storm beaches, and beach ridge environments (Hocking et al., 1987). It outcrops in the coastal areas of the Edel and Peron Provinces. In east Hamelin Pool the marine carbonate rocks of the Carbla Oolite member of the Dampier Limestone are exposed (Logan et al., 1970a; Playford et al., 2013).

The Bibra Limestone (Logan et al., 1970a; van de Graaff et al., 1983) is a thin intertidal deposit of bioclasts and corals, widespread in outcrops in Shark Bay (Logan et al., 1970a; Playford et al., 2013). It is estimated to have been deposited during the marine phase of the late Pleistocene interglacial (Marine Isotope Stage 5) high sea level stand (van de Graaff et al, 1983; Hocking et al., 1987; O'Leary et al., 2008). The last marine transgression (MIS 1) is referred to as the Holocene marine phase (Table 1).

The Depuch Limestone (Logan et al., 1970a) is a red brown, strongly cemented calcarenite and calcirudite derived by erosion and reworking of the Tamala Limestone (Playford et al., 2013) and can be found in Edel Province.

The presence of well-developed barrier banks associated with a semiarid to arid climate (1:10 ratio of rainfall/evaporation) and a restricted tidal exchange produced and preserves the hypersaline (56–70) conditions in the Hamelin Pool and L'Haridon Bight embayments (Logan and Cebulski, 1970; Logan et al., 1974; Walker et al., 1988; CALM, 1996, Hancock et al., 2000). Predominant southerly winds, 1–2 metre tidal range and large salinity and temperature gradients also strongly control the dynamics of the entire bay (Logan et al., 1974; Nahas et al, 2005).

## 3. Materials and methods

Initially, Faure Sill was mapped by delineating geomorphic and habitat boundaries. GIS Software (Geographic Information System; ArcGIS® by Esri) and datasets formed the basis of the descriptive analysis of seafloor features. High resolution (50 cm/pixel) orthophotos and aerial photos (1:25,000 scale) provided by the Department of Parks and Wildlife (DPaW) and sourced from Landgate (Western Australia), combined with ground truth data were used in order to draft detailed maps (refer to Fig. 6). Ground truth information was drawn from existing literature, particularly from Logan et al. (1970a,b) and Logan et al. (1974), from information collected as part of the Curtin Shark Bay Project (Jahnert and Collins, 2011, 2012, 2013) and from the present project (32 cores and surficial sediment samples along the seismic lines). Two full coverage GIS based maps were created for Faure Sill. The sediments and benthic substrates map (Fig. 3) shows 34 different types of surficial sediment facies and for the morphological elements map, storing geomorphic features and bedforms (Fig. 4), 27 different aspects of the substrate were recognised.

A follow up shallow geophysical survey provided useful information on the thickness and seismic characteristics of the sediment packages and geometry of the seismic reflectors, giving good quality data on the Holocene and Pleistocene stratigraphic features of bank growth, down to a depth of about 15 m below the seafloor. The survey was carried out using a nonlinear (parametric) subbottom profiler (SBP) SES2000 Compact System (Innomar Technologie GmbH; Rostock, Germany), mounted vertically on the port side of the survey vessel. A Sokkia GSR2650 LB Differential Global Position System (DGPS) antenna was mounted on the top of the pole supporting the SBP, to provide an accurate position. During the survey, about 270 km of tracks were acquired, mainly oriented east–west and north–south. The penetration of the SBP varied across the survey area depending on the subsurface conditions. The processing software used was Innomar ISE version 2.9 (Interactive Sediment layer Editor) and SonarWiz 5 (Chesapeake Technology Inc.); the interpretation of the seismic sections has been performed based on a velocity of sound in sediments of 1600 m/s. Seismic velocity was chosen in accordance with the lithology of the area, which can be generalised as loose sand, very soft clay and medium dense to dense sand and gravel (see Hamilton, 1970; Leighton and Robb, 2008).

Lastly, a stratigraphic survey used a vibracorer (from Quaternary Resources, Australia). To integrate and assess the results obtained with the seismic survey, 32 sediment cores were collected. A Sokkia GSR2650 LB DGPS, interfaced with a laptop computer running OpenCPN 2.5.0 (open source navigation software), was used to position the vessel on the pre-established core location coordinates. Later, each core was cut into 1 metre sections and relocated to the Sedimentology Laboratory in the Department of Applied Geology, at Curtin University. Then, after splitting each section, cores were photographed and studied. Core logging included an evaluation of colour (using the Munsell Soil Chart — Munsell, 1954), bioturbation, texture and lithology and a record of any major stratigraphic changes. Finally, samples were collected for further analyses, such as X-ray diffraction (XRD), foraminiferal identification (Parker, 2009) and radiocarbon AMS $^{14}C$ dating.

Dating values derived from four cores were used to assess the age of reflectors and facies and to calculate accumulation rates in the bank and delta areas. The dating was conducted by the Radiocarbon Dating Centre (Australian National University, ACT), using the accelerator mass spectrometer method (AMS). One species of foraminifera (*Amphisorus hemprichii*, Ehrenberg, 1839) was targeted and picked for dating. 20 mg of the sample was the minimum weight required for dating (Fallon et al., 2010). Reworked, abraded or micritised specimens were excluded, since they could lead to unreliable dates and outliers in data. The quantity of *Amphisorus* in some intervals was scarce, limiting the choice of specimens. The conventional ages and their error, rounded to the nearest year (Fallon et al., 2010), are expressed in radiocarbon years using the Libby half-life of 5568 years and following the conventions of Stuiver and Polach (1977). The curve Marine09 was used as a calibration dataset to convert conventional ages into calibrated years, assuming a delta R of 70 ± 50. The marine calibration incorporates a time dependent global ocean reservoir correction of about 400 years (Stuiver and Reimer, 1993; Stuiver et al., 2005).

## 4. Results

### 4.1. Morphology and substrate mapping

A sediments and benthic substrates map (Fig. 3) and a morphological elements map (Fig. 4) were derived through an initial remote sensing analysis of the Sill. Superficial sediment facies, geomorphic features and bedforms reveal the composite nature of the complex.

#### 4.1.1. Sediments and benthic substrates of the Faure Sill System

Sediments and benthic substrates were grouped according to their tidal zone position: hinterland, supratidal, intertidal and subtidal (Fig. 3). The hinterland is dominated by eolian Pliocene and Pleistocene deposits of the Peron Sandstone (quartz sandstone) and “birridas”, which are interdune depositional basins of granular gypsum and quartz sediment fills (Jahnert and Collins, 2012) to the west, while to the east, Cretaceous Limestone (Toolonga Calcilutite), Quaternary alluvial and colluvial deposits of the Wooramel Delta and quartz sand dominate (Jahnert and Collins, 2012). Supratidal and intertidal facies include evaporites, hypersaline coquinas, microbial mats, stromatolites and sandy sediments. Nearshore, subtidal substrates are mainly microbial deposits (stromatolite and cryptomicrobial structures, also lithified microbial pavement and bivalve coquinas). The Faure Bank consists of mobile mixed bioclastic quartz sands at surface. In the south, the embayment plain of Hamelin Pool comprises bivalve coquina, serpulids and algae with a superficial veneer of microbial organic material (Jahnert and Collins, 2012); while in L'Haridon Bight the basin is mainly composed of bioclastic, silty sand (Collins and Jahnert, 2014). Bioclastic and lithoclastic sand, covered by a muddy layer, occupies

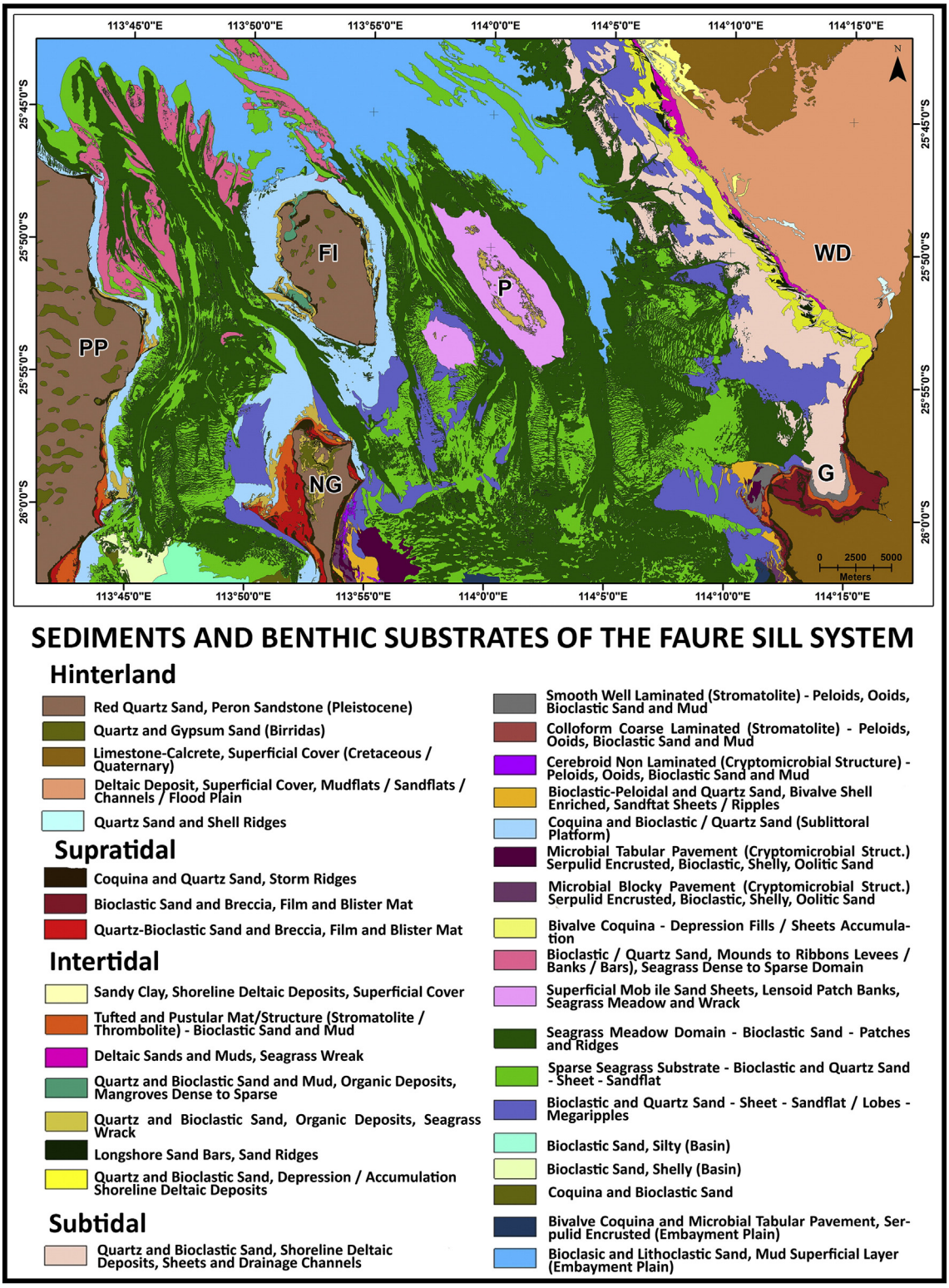


**Fig. 3.** Sediments and benthic substrates of the Faure Sill System. Note the preponderance of light and dark green, associated with substrates related to the presence of seagrass. PP = Peron Peninsula; NG = Nanga Peninsula; FI = Faure Island; P = Pelican Island; WD = Wooramel Delta; G = Gladstone Embayment.

the northern side of Faure Bank. Bioclastic particles are mainly seagrass epiphytes, including coralline algae, foraminifera and other constituents, together with small bivalves. Seagrass is sparse over the bank surface but relatively dense on channel margins, and is mainly *Amphibolis antarctica (Labillardière)* Sonder & Ascherson ex Ascherson 1868 (Walker, 1990).

*4.1.2. Morphological elements of the Faure Sill System*

The morphological elements of the Faure Sill System (Fig. 4) consist of channel and tidal fan associated features (longitudinal and lateral bars, flood and ebb tide fans and levees) and bank elements, including patch, fringing and barrier banks, with surficial sand sheets, usually with ripples or megaripples (see Fig. 5E). L'Haridon,

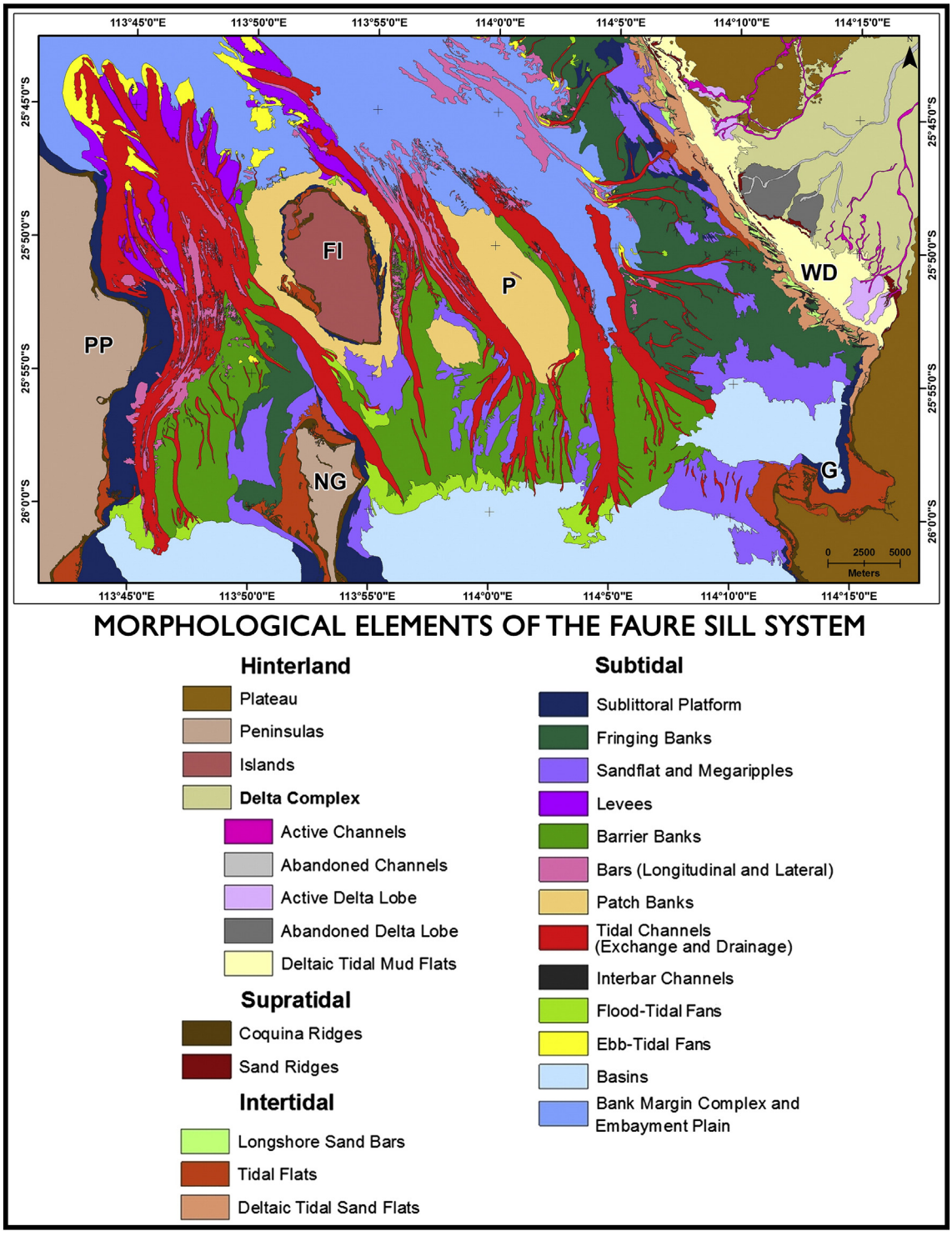


**Fig. 4.** Morphological elements of the Faure Sill System. Note the well-developed channels (in red). Fringing and barrier banks are colour coded in dark greens. Ebb tidal fans are mainly located in the north-western side of the Faure Sill, but at smaller scale they are present also along the margins of the Wooramel Delta. Flood tidal fans (light green) are along the southern bank margin. PP = Peron Peninsula; NG = Nanga Peninsula; FI = Faure Island; P = Pelican Island; WD = Wooramel Delta; G = Gladstone Embayment.

Hamelin and Gladstone basins enclose the southern side of the bank and an embayment plain flanks the northern border. In the hinterland of the delta complex, numerous abandoned channels are present, evidence that the Wooramel River has switched its path during Pleistocene and Holocene time. The sublittoral platform which fringes the southern coast of Faure Sill includes oolite shoals and lithified pavement.

### *4.2. Acoustic classification of sediment bodies*

Post processing and interpretation of SBP data provided useful information on the thickness, lateral distribution and internal architecture of sediments, up to 15 m below the seafloor.

A number of significant acoustic reflectors were identified and considered on the basis of their position and acoustic impedance. From

top to bottom the identified horizons are Seafloor, HR1, HR2, HR3 and HR4 (Table 1). Age data is based upon the work of Logan et al. (1970a, b) and O'Leary et al. (2008). The profiles show further minor discontinuities, located in the Holocene sediment package, between Seafloor and HR1.

Seismic reflectors from HR1 to HR4 are acoustically quite similar and sometimes can be discerned only by analysing their stratigraphic position and horizontal distribution. They mainly appear as irregular surfaces, generally flat and not always well defined, due to signal penetration or amplitude anomalies; these are primarily located where the seagrass is particularly dense. Air bubbles, originating from the plants' photosynthetic activity, can have a strong impact on the propagation of sound in water, causing a stronger scattering and reflection (Wilson et al., 2012). In some areas, generally where the water was very shallow, the acoustic penetration was very limited due to harder bottom or seabed multiple echoes which masked the data.

HR4 is the deepest horizon found in the profiles acquired and can be considered the acoustic basement of the area. It has been detected only close to the Wooramel Delta and at the eastern side of Monkey Mia, where it deepens to 8.5 m below the seabed (12.1 m below sea level). HR4 caps Unit 5 (Peron Sandstone, see Table 1) whose base has not been recorded, either on seismic data or in any core sample. More continuous and observable in Dubaut and Wooramel banks is the horizon HR3, which, from the profiles, has a depth that ranges from 1.4 to 11.4 m below the seafloor (5.0 to 13.3 below sea level). Unit 4 (identified as Carbla Oolite) is below the discontinuity HR3 and above the acoustic basement HR4. From a stratigraphic point, the deepest reflector that can be followed beneath almost all the bank is HR2 (top Dampier Limestone, Unit 3). In the middle of the central bank, it can be detected as deep as 9.3 m below the seafloor (approximately 12.7 m below sea level). Where top and base reflectors are resolved, it is possible to calculate the thickness, which ranges from a few centimetres to a maximum of more than 4.7 m between Herald Loop and Gladstone Channel (refer to Fig. 2 for location), averaging 1 m. A clear and marked acoustic response derives from HR1 (top Bibra Limestone), which can be considered the main acoustic reflector in the area. This horizon occurs at a depth that ranges between 1.9 and 11.5 m below sea level and can be interpreted as an erosional surface that separates Bibra Limestone (Unit 2) and the Holocene sequence (Unit 1). Unit 2 is bounded by HR1 and HR2 and its thickness can reach up to 4 m, but more commonly it is around 1 m.

Above the reflector HR1, the Holocene sedimentary package is well represented (Unit 1). Its thickness ranges between 0.10 m and about 8 m and SBP profiles reveal a complex internal structure within this unit, with many relict features, such as numerous oblique to sigmoid prograding acoustic reflectors, often truncated. An intra-Holocene horizon is identifiable in the whole bank. It is a probable palaeotopographic surface, often expressed as buried channels, later infilled with softer sediments and it may indicate lowstand erosion within the Holocene sequence of generally rising sea levels and vertical bank growth.

A classification system for sediment bodies based on acoustic characteristics and distribution and the morphological features of the bank was developed and includes five main types: 1. Bank top sediment bodies; 2. Channel associated sediment bodies; 3. Tidal fan associated sediment bodies; 4. Shoreline attached sediment lobes; 5. Patch banks, Fringing Banks and Barrier Banks. Characteristics of these sand bodies are summarised in Table 2.

The internal architecture of selected Holocene sediment bodies is illustrated in Fig. 5.

1a) Bank top — Linear ridges: the central and shallowest areas of the Faure Sill are characterised by elongate seagrass ridges, having an east–west linear trend. They are well stabilised, mainly composed of *Amphibolis*, and represent an important surface aspect of the bank where seagrass has vegetated and stabilised tidally generated linear bedforms. In Fig. 5A, the high rate of deposition is clearly evident. The first metre of sediment is characterised by intense progradation, with a north–south direction. The surficial sediment is sandy, allowing a penetration of the signal to 4–6 m below the seafloor (cf Fig. 3). At this depth a strong and continuous reflector (HR1), harder than the overlying sediment, is recorded. A second weaker and more discontinuous reflector (HR2) is documented between 6 m and 7 m below the seabed.

1b) Bank top — Flat topped sand sheets: sand flats and sand sheets border Faure Island and the northern part of the Nanga Peninsula with their maximum extent found in the south and south–east parts of the island. They are sparsely populated by seagrass and are morphologically flat.

2a) Channel associated — Longitudinal channel bars: longitudinal channel bars are present in every major channel. They are morphologically elongate north–south and mainly channel parallel. In Fig. 5B, longitudinal channel bars are highlighted in orange; they do not have any particular internal architecture, which indicates the material is homogeneous. The underlying sediments (in blue) are about 1–2 m thick, with a wedge shape. Both the top and the bottom (HR1) are good reflectors, but there are numerous, weaker and very irregular internal reflectors within this earlier generation of a bar complex. Between HR1 and the sediment highlighted there is an earlier package of sediments, where very little internal reflection is recognisable.

2b) Channel associated — Lateral spillover sheets: spillover packages involve lateral accretion near channel margins and upward bank growth. This sand body type is associated with all major channels and tidal fans and they are often associated with small buried channels, filled with 1–2 m of sediments, usually parallel to the modern channel, but significantly narrower.

2c) Channel associated — Interdistributary channels: besides the main tidal channels, which permit an exchange of water between Hamelin Pool and L'Haridon Bight and the rest of the bay, there are several drainage channels, variably distributed along the southern part of the bank. Some profiles reveal distinct sets of palaeodistributary channels that characterise a buried morphology within the tidal fan areas (Fig. 5C).

3a) Tidal fan associated — Distributary mouth bars: east–west profiles show well-defined accreting lobes within distributary mouth bars, between the embayment plain of Hamelin Basin and the Faure bank. These features are about 2–5 m thick and are interrupted by occasional buried channels. North–south seismic lines confirm the oblique reflection configuration that occurs with the progradation pattern on the bank margin. The lateral accretion pattern within coalescing distributary mouth bar lobes is clearly shown in Fig. 5D in a flood tidal complex along the southern bank margin. The horizon HR1 is not recognisable throughout due to seabed multiple echoes which are particularly strong in these profiles. Where visible, it is flat and about 5 m below the seafloor.

3b) Tidal fan associated — Ebb tidal fans: mainly situated in the North West bank, close to Monkey Mia, well-developed ebb tidal fans consist of bare thin Holocene sediments, terminating with a seaward sloping lobe. Although the major terminal fans can be found at the end of Herald Gut and Petit Channels, minor fans occur also along the margins of the Wooramel Delta, at the mouths of Wooramel active channels (mapped in yellow in Fig. 4).

3c) Tidal fan associated — Levees: the area between Dubaut Bank and the Herald Gut ebb tide fan is characterised by the presence of subtidal shallow levees and channel margin spill over sheets. They are well developed structures, stabilised by thick seagrass on top. The internal architecture is poorly defined and almost reflector free, probably due to seagrass cover impeding penetration. The surface morphology is essentially flat.

4) Shoreline-attached sand lobes: between Gladstone Basin and Hamelin Pool (Kopke Point), a shallow sand lobe complex is present. Bare sand flats and megaripples cover the surface. The seismic profiles reveal a distinct progradation throughout the

margins of the complex. In the south, a flood tide progradation prevails, and in the northern margin ebb tide progradation is present. The lobes are characterised by a complex reflector configuration, with numerous oblique to sigmoid reflectors in the N–S section. Progradation is controlled by tidal currents with lesser wind driven circulation. Megaripples (i.e.: subaqueous dunes according to

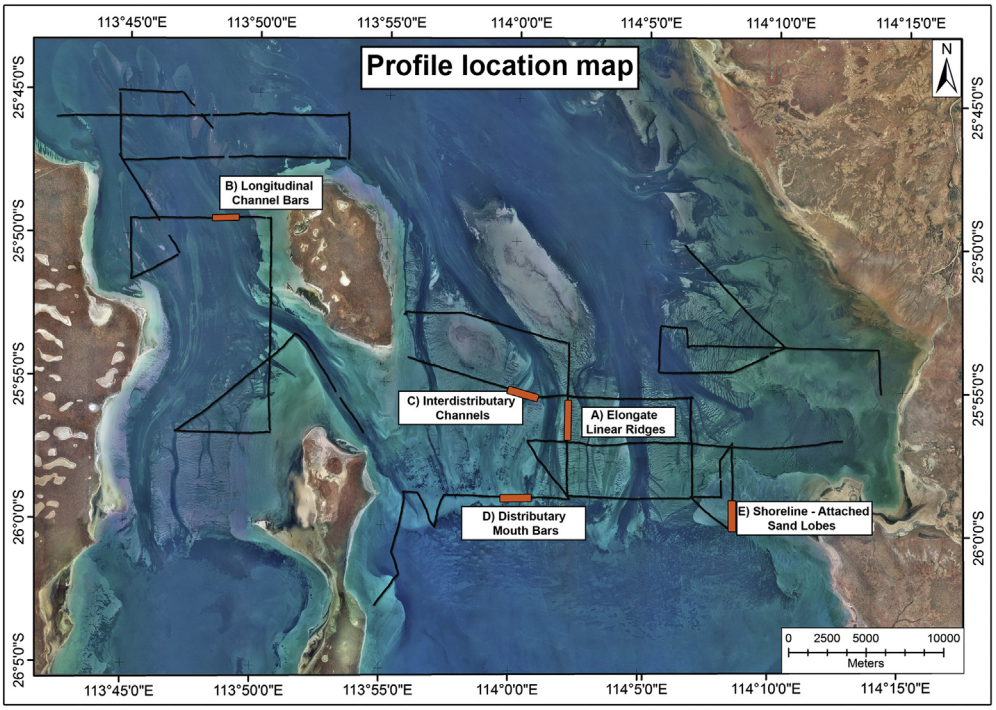


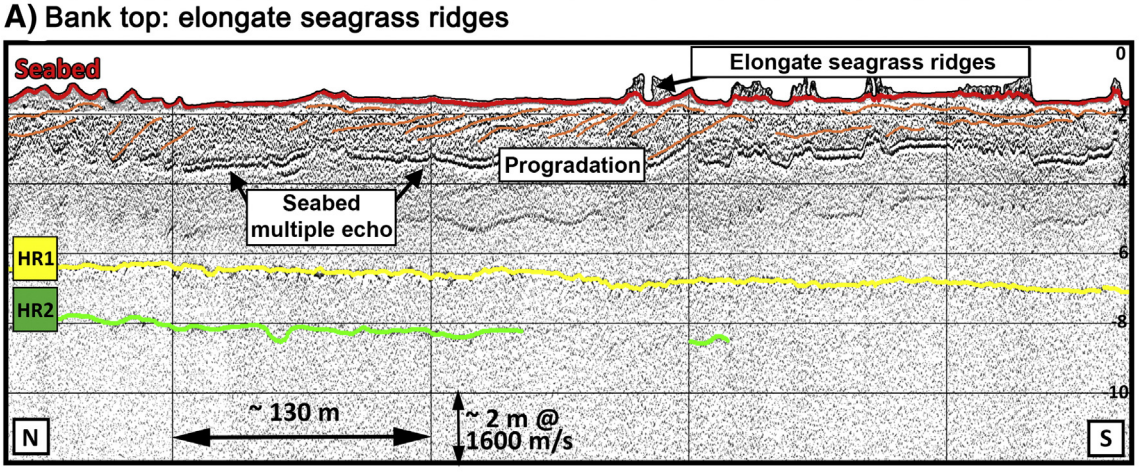


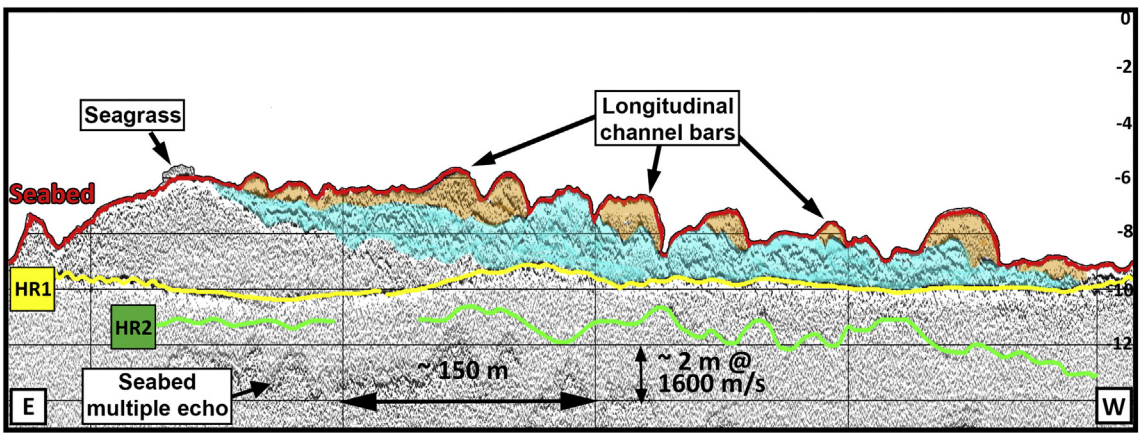

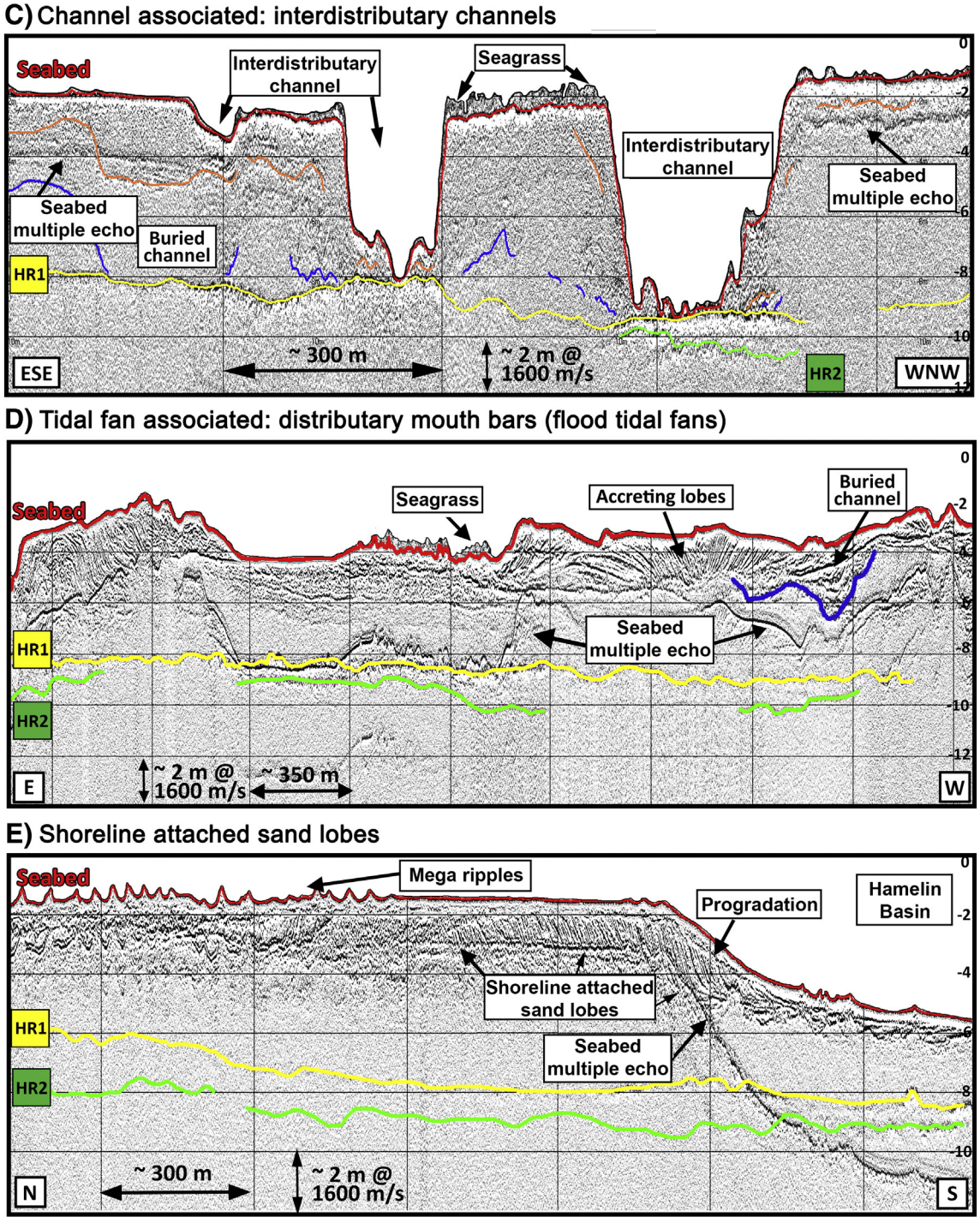


**Fig. 5.** Examples of stratigraphic profiles of sediment bodies. Main acoustic reflectors have been illustrated to highlight their occurrence. In green: reflector HR2; in yellow: reflector HR1; in blue and orange: palaeosurfaces in Late Holocene sedimentary package; in red: seafloor. Vertical axes represent the depth below sea level (every profile starts at 0 m). A) 1a: Bank top — elongate linear ridges vegetated by seagrass. The first metres of sediment are characterised by intense progradation of bank sediments, with a south–north direction and a high rate of deposition. The surficial sediment is sandy. B) 2a: Channel associated — longitudinal channel bars (orange) are homogeneous and without internal structure. The underlying sediments (blue) are about 1–2 m thick, with a wedge shape and bar like morphology. C) 2c: Channel associated — interdistributary channels. Some profiles reveal distinct sets of palaeodistributary channels that characterise a buried morphology within the tidal fan areas. D) 3a: Tidal fan associated — distributary mouth bars. The lateral accretion pattern within coalescing distributary mouth bar lobes characterises the flood tidal complex along the southern bank margin. E) 4: Shoreline attached sand lobes. Note progradation towards Hamelin Pool to the south. Megaripples are several hundred metres long, with a wavelength about 25–35 m, east–west oriented.

Ashley, 1990) are several hundred metres long, with a wavelength about 25–35 m (Fig. 5E).

5) Patch Banks, Fringing Banks, Barrier Banks: some banks present difficulties for profiling due to extremely shallow water over bank surface. Turtle and Pelican patch banks border the Faure Channel, and the topographic highs of the Peron Sandstone control the bank thickness. Based on the position of the HR2 reflector, Faure Channel was likely formed in the lowstand following Dampier time, and this has also determined its position during Bibra and Holocene time.

**Table 2**
Sediment body types of the Faure Sill, based on shallow geology investigation.

| Sediment body type | Morphology | Scale | Biota/internal architecture/facies | Example |
|---|---|---|---|---|
| 1) Bank top: linked with the presence of seagrass and pre-Holocene topographic highs | | | | |
| a. Linear ridges | Elongate E–W; tidally generated seagrass stabilised. | H = 1–2 m<br>L = 000s of m | *Amphibolis* ribbons; bivalve lags. Intense progradation. Sandy top. | Central and shallower areas across the Sill (Fig. 5A). |
| b. Flat topped sand sheets | Flats; sheet to wedge like. | H = 1–3 m<br>L = 00s of m | Sparsely populated by seagrass. Progradation. Muddy bioclastic sand on top and sandy bioclastic mud. | South-western edge of Faure Island, northern part of the Nanga Peninsula, western side of the Faure Sill. |
| 2) Channel associated: five exchange channels branching off in many minor drainage channels | | | | |
| a. Longitudinal channel bars | Present in every major channel; elongate along the main stream flow; channel parallel | H = 2 m<br>W = 00s of m<br>L = 000s of m | Moderate density seagrass cover (*Amphibolis*). Homogeneous internal architecture. Quartzose sand. | Associated with all major channels (e.g. Herald Bight and Herald Gut). (Fig. 5B). |
| b. Lateral spill over sheets | Sheet like, elongate N–S along bank/channel margins. | H = 0.5 m<br>L = 00s of m | Bare muddy sand carbonate facies. | Associated with all major channels and tidal fans. |
| c. Interdistributary channels | Flat topped, triangular bars, flare down current. | H = 1–2 m<br>L = 000s m | Minor seagrass. Distinct sets of palaeochannels. Laminated silty sand and sandy mud. | Variably distributed along the southern part of the bank (Fig. 5C). |
| 3) Tidal fan associated: terminal prograding flood and ebb tidal fans | | | | |
| a. Distributary mouth bars (flood tidal fans) | Deltoid to lobate terminal bars, frequently coalescing, prograding basinward. | H = 1–4 m<br>L = 000s of m | Bare sandy top, overlying carbonate mud. Frequently cross bedded, oblique to sigmoid acoustic reflectors. | Southern edge of the Faure Sill, between Nanga Peninsula and Gladstone Embayment (Fig. 5D). |
| b. Ebb tidal fans | Main channel, flanked by linear bars, terminating with a seaward sloping lobe. | H = 1–2 m<br>L = 0–00s of m | Bivalves and small foraminifera, no seagrass. Silty sand with fine to medium, well-rounded quartz. | North west bank, close to Monkey Mia, at the end of Herald Gut and Petit Channels. Along the margins of the Wooramel Delta. |
| c. Levees | Channel margin spill over banks, Flat surface. | H = 1–4 m | Seagrass stabilised along the margins. Reflector free. Muddy sand on top and sandy mud downward. | Herald Loop fan delta, Herald Gut ebb tide delta. |
| 4) Shoreline attached sand lobes | | | | |
| Shoreline attached sand lobes | Sheet like, basin ward prograding, megaripples. | H = up to 1.5 m<br>Wavelength ≈ 25–30 m,<br>L = 000s<br>Thickness = 7 m | Bare sandflat, intense progradation. Laminated sands and carbonate muddy apron facies. | Close to Gladstone Embayment (Kopke Point). (Fig. 5E). |
| 5) Patch Banks, Fringing Banks, Barrier Banks | | | | |
| Patch banks, fringing banks, barrier banks | Surrounding or associated with topographic highs. | Variable<br>H = 1–7 m | Seagrass and bioclastic sand (top) and sandy bioclastic mud at base. | Herald, Petit and Dubaut Fringing Banks, Pelican and Turtle Patch Banks, Wooramel Bank. |

### 4.3. Composition and mineralogy of bank lithofacies

The nature and occurrence of the acoustic reflectors and units recognised in the seismic analysis were ground truthed with a follow up core study (Fig. 6). Core logging and successive analyses have assisted with the interpretation of the results obtained with the seismic, allowing a lithological understanding of particular sediment packages. Although minor differences in terms of position and frequency occur, seismic reflectors correspond well to actual changes in facies and lithology in the cores.

The Faure Sill is composed of three different types of sediment: sand, mud and clay (Fig. 3 and Fig. 6). Bioclastic muddy sediments are by far the most common bank lithofacies. Bioclastic, quartzose, sandy facies are associated with *terminal ebb tidal fans*, in the north–western area of the Faure Sill (Figs. 4 and 6). Bioclastic, sandy facies are also common in the upper part of *terminal prograding flood tidal fans*, located in the southern portion of the bank, bordering the northern Hamelin Pool basin (Figs. 4 and 6). The sand size ranges from coarse (generally cross bedded) to fine (frequently thinly laminated). Seagrass peats and skeletal particles are also a significant component. Shelly facies are typically associated with buried palaeochannels. Bioclastic, muddy facies are associated with lower *terminal prograding flood tidal fans and carbonate bank* and with delta related sediments (Figs. 4 and 6). Kaolinite clays are found in the channel base unit of the *Wooramel Delta* area (Fig. 6).

In general, coarsening upward sequences characterise cores of bank buildup. Whereas muddy bioclastic facies are found in lower parts of the bank, likely reflecting dense seagrass cover of *Posidonia* spp., an efficient trapping of fine sediment, more sandy bioclastic sediments are found in upper parts of the bank and its terminal fans, where seagrass cover is sparse *Amphibolis* and tidal and wave reworking increases with bank shoaling (see Fig. 6).

In a previous work, Hagan and Logan (1974, p. 73) have found that the dominant skeletal constituents of the bank are coralline algal particles and whole and fragmented foraminifers and molluscs. Nonskeletal sediment components are commonly quartz, lithoclasts and ooids.

Three cores were subsampled for XRD analysis. Core FPC1 was collected in the middle of the bank and cores FWD2s and FWD7s are from the Wooramel Delta area (refer to Fig. 6 for their location). Bank sediments are strongly bioclastic (from 42.7% to 75.15%), and are mainly composed of calcareous seagrass epiphytes. With the exception of sandy, bioclastic, bank top sediments, muddy carbonates in the lower and middle part of the sequence make up most of the package. Quartz content is locally significant where the underlying Peron Sandstone experienced channel erosion or where topographic highs of Peron Sandstone shed quartz to the surrounding seagrass banks as erosion proceeded. The “amorphous” group in Fig. 7 is a mixture of poorly ordered terrigenous clay minerals representing about 20–40% of the sediment in each sample, rising to 54% near the Wooramel Delta.

### 4.4. Age model and sediment accumulation rates

Radiocarbon dating was used to assess the age of reflectors and facies and to calculate accumulation rates in the bank and delta areas, in particular the timing of channel infill and abandonment.

Four cores (FSB1, FSB2s, FWD2s, FPC1, refer to Figs. 6 and 8 for location) were chosen for Radiocarbon AMS $^{14}C$ dating, based on

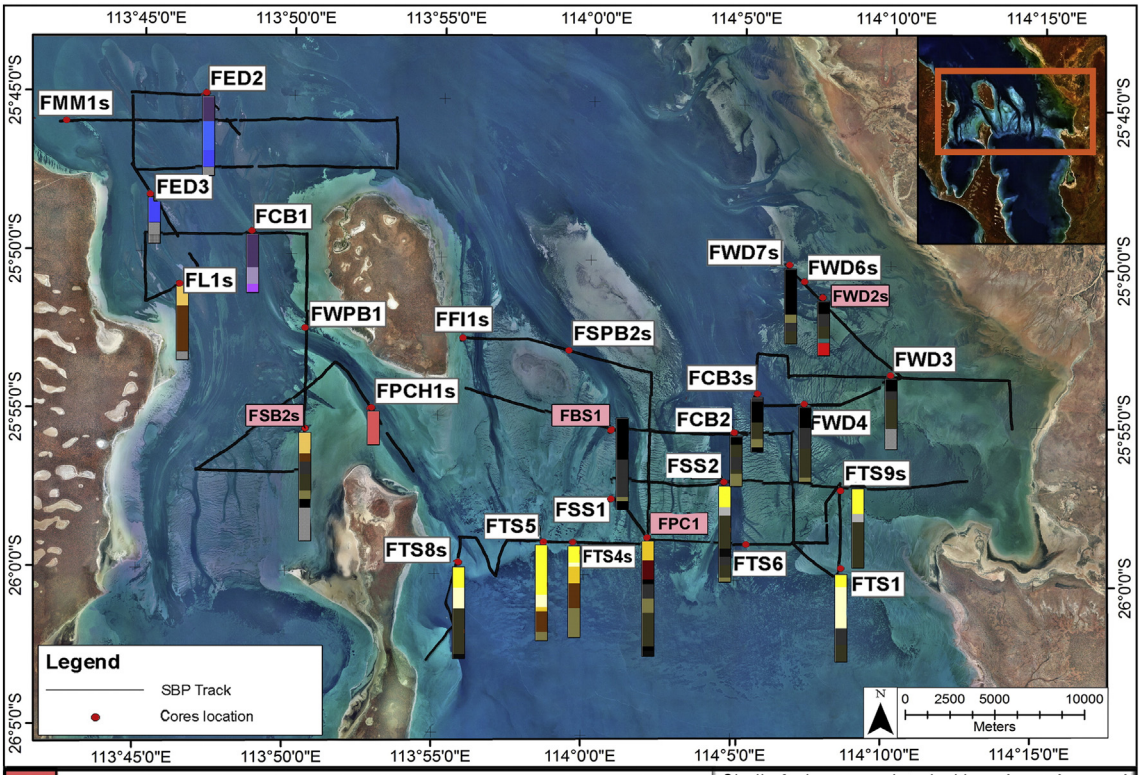


| | | |
|---|---|---|
| | Coarse Shelly Bioclastic Sand | Shelly facies, associated with paleo-channel |
| | Coarse-grained Cross-bedded Bioclastic Sand | Bioclastic - sandy facies, associated with upper **terminal prograding flood-tidal fans** |
| | Moderately Bioclastic Quartzose Silty Sand | |
| | Fine-grained Silty Bioclastic with Thinly laminated Mud and Seagrass Peats | |
| | Fine-grained Silty/Muddy Sand with Very Thinly Bedded Muddy Seagrass Peats | |
| | Medium Muddy Bioclastic Sand | |
| | Thickly laminated to Thinly Bedded Silty Bioclastic Sand and Weakly Bioclastic Mud | Bioclastic - muddy facies, associated with lower **terminal prograding flood-tidal fans and carbonate bank** |
| | Sandy Bioclastic Mud | |
| | Weakly Bioclastic Burrow Mottled Carbonate Mud | |
| | Strongly Bioclastic Carbonate Mud | |
| | Weakly bioclastic Sandy Carbonate Mud, Clayey | |
| | Moderately bioclastic Sandy Carbonate Mud, Clayey | |
| | Disseminated Pyrite Kaolinite Clay | **Wooramel Delta** associated kaolinite clay (channel base unit) |
| | Goethite Kaolinite Clay | |
| | Weakly Bioclastic Quartzose Sand | Bioclastic, quartzose, sandy facies, associated with **terminal ebb-tidal fans** |
| | Mildly Bioclastic Silty Quartzose Sand | |
| | Shelly Bioclastic Silty Quartzose Sand | |
| | Bioclastic Cross-bedded Quartzose Sand | |
| | Fine-grained Moderately Planar-bedded Bioclastic Quartzose Sand | |
| | Medium-grained Silty Quartzose Sand | **Pleistocene** |
| | Coarse-grained Shelly Sand | |

**Fig. 6.** Core interpretation with subbottom profiler track plot lines. Lithofacies are colour coded and grouped into major facies units in the legend. The cores sampled for dating and further analyses are highlighted in pink (see further in Sections 4.4 and 5.3).

morphological elements and facies association in the bank. The samples were selected assuming that intervals close to a contact between sedimentary units may represent an erosional event, a change in depositional energy or the dominant process, or in sediment supply. Moreover, samples between sedimentary contacts give information about long term sediment accumulation rates. In Table 3 the age results and their error, rounded to the nearest year (Fallon et al., 2010), are presented, together with the depths of the samples below sea level and seafloor. Accumulation rates derived from radiocarbon ages combined with sediment thicknesses obtained through seismic data were used to estimate the age of Faure Sill onset and other bank events.

In Fig. 9, the Holocene ages for all the four cores are plotted against depth (below sea level, in metres). The regional Holocene sea level curve has been compiled from coral reef data derived from Collins et al. (2006), Twiggs and Collins (2010) and coquina ridge data from Jahnert and Collins, 2013. Based on inspection of Fig. 9 and Table 3 every core sampled has its own peculiar accumulation pattern, with different rates within the same core, as shown in the last four columns of

| | Core and Water Depth (m) | | wt% Carbonates | wt% Quartz | wt% Amorphous | |
|---|---|---|---|---|---|---|
| FPC1 | 0.02 | 3.22 | 73.05 | 1.78 | 25.17 | Bioclastic Sands |
| | 0.20 | 3.40 | 70.18 | 1.55 | 28.28 | |
| | 0.45 | 3.65 | 59.84 | 0.93 | 39.24 | |
| | 0.60 | 3.80 | 69.56 | 1.16 | 29.28 | |
| | 1.00 | 4.20 | 67.96 | 1.73 | 30.31 | Bank Muds |
| | 1.30 | 4.50 | 66.44 | 1.39 | 32.18 | |
| | 1.55 | 4.75 | 75.15 | 1.21 | 23.64 | |
| | 1.65 | 4.85 | 67.60 | 1.37 | 31.03 | Bioclastic Sands |
| | 2.75 | 5.95 | 48.70 | 15.37 | 35.93 | |
| | 3.60 | 6.80 | 70.06 | 1.19 | 28.76 | Bank Muds |
| | 4.42 | 7.62 | 74.38 | 1.48 | 24.14 | |
| FWD2s | 0.05 | 4.15 | 51.15 | 2.24 | 46.62 | Delta Muds |
| | 0.60 | 4.70 | 68.70 | 2.13 | 29.17 | |
| | 0.90 | 5.00 | 62.40 | 1.78 | 35.82 | |
| | 1.15 | 5.25 | 74.58 | 1.72 | 23.70 | |
| | 1.30 | 5.40 | 59.41 | 2.31 | 38.29 | |
| | 1.70 | 5.80 | 48.12 | 4.86 | 47.02 | |
| | 1.80 | 5.90 | 2.83 | 4.08 | 93.09 | Clays |
| | 2.30 | 6.40 | 2.69 | 4.16 | 93.15 | |
| FWD7s | 0.05 | 1.51 | 63.73 | 1.64 | 34.64 | Delta Muds |
| | 0.15 | 1.61 | 46.04 | 2.00 | 51.96 | |
| | 0.80 | 2.26 | 44.45 | 2.02 | 53.53 | |
| | 1.10 | 2.56 | 43.69 | 2.29 | 54.02 | |
| | 1.80 | 3.26 | 44.13 | 2.25 | 53.62 | |
| | 2.50 | 3.96 | 57.51 | 2.62 | 39.87 | |
| | 2.85 | 4.31 | 42.72 | 3.13 | 54.15 | |
| | 3.45 | 4.91 | 52.27 | 3.29 | 44.44 | |
| | 3.50 | 4.96 | 58.73 | 2.06 | 39.21 | |

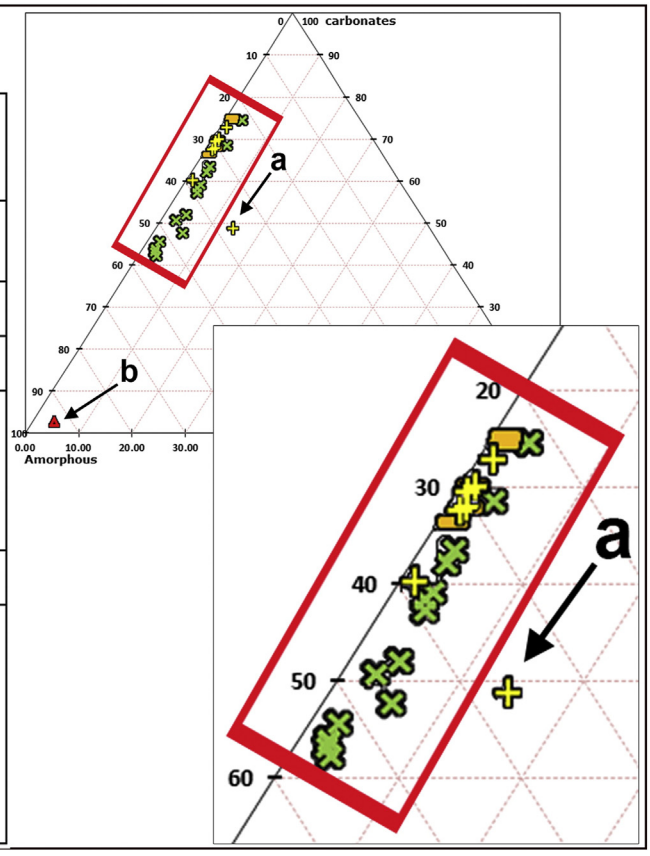


**Fig. 7.** Results of XRD analysis, expressed in % of weight. Triangular diagram summarises the XRD results for the cores. In green = delta muds (FWD2s and FWD7s); yellow = bank sands (FPC1); orange = bank muds (FPC1) and red = clay (FWD2s). The "amorphous" group represents mixed disordered terrigenous clays. The value indicated by the "a" arrow corresponds to the base of the palaeochannel in FPC1 (2.75 m from TOC). The "b" arrow shows the Wooramel channel base unit. (For interpretation of the references to colour in this figure legend, the reader is referred to the web version of this article.)

Table 3. The sedimentation record consists of both depositional and hiatal intervals.

Core FSB2s (Fig. 8A), located in the eastern part of the complex, is the only core sample where pre-Holocene sediments were reached and dated, below 3 m. FSB2s can be subdivided into two sections. Section 1 (see Fig. 9), corresponding to the surficial sand body, has a very slow rate of accumulation (averaging 0.59 m of deposition in 1000 years), if compared with the deeper and older muddy sediments (Section 2), where the accumulation rate surpasses 1.80 m/ka. In Section 2 and elsewhere age inversions are present, the oldest date of the section has been considered, in order to reduce errors caused by the inverse correlation between estimated accumulation rate and duration (cf. Sadler, 1981; Cohen et al, 1993). The foraminiferal sample collected at 1.05 m (from the top of the core and 3.27 m BSL) is between two consecutive time gaps of sediments, respectively of 2445 years from the upper sampling point (at 0.63 m) and 1878 years from the lower sample (at 2.00 m). Channel migration and erosion are likely within this area, resulting in hiatuses in the accumulation record. The change in accumulation rates from the shallower sandy portion of the core to the deeper section can be plausibly linked with the density of seagrass. Depositional rates for muddy sediments associated with seagrass are significantly greater than for quartz sands, commonly derived from erosion of the Peron Sandstone.

Core FPC1 (Fig. 8B) is situated between a terminal prograding flood tidal fan and the carbonate bank. The core intersects an abandoned distributary channel of the Faure Channel, indicated by the dating combined with the seismic dataset. Similar to FSB2s, the growth rates of FPC1 can be divided into sections. Section 1 (Fig. 9), corresponding to the first 2.75 m of the core (from the top of the core and 5.95 m below sea level), represents infill of a palaeochannel, recognisable from the seismic profile. It has some inversions of ages, with older foraminiferal samples situated above younger ones, interpreted as resulting from reworking of multiple sediment sources or downward mixing and activities of burrowing organisms. The oldest age of this section (390 years BP) has been used when calculating the accumulation rate. During the last 390 years BP, a significant amount of sediment was deposited in this location, with an accumulation rate of about 6.93 m/ka. The high rate represents very rapid deposition of prograding sandy and laminated infill in the most recent part of bank growth. Between 2.75 and 3.75 m of depth below the seafloor (5.95 and 6.95 m BSL), in

**Fig. 8.** Seismic profiles (see Fig. 5 for colour code of depicted reflectors and Fig. 6 for locations and colour scheme) and relative photos of the cores chosen for dating. Each number on top of a red bar represents the position and the age (cf. Table 3) of the sample. The red triangles mark hiatus boundaries. A) FSB2s: shallow fringing bank (NW Nanga Peninsula). The first metre of core is mainly sandy. Then, the percentage of mud increases till 2.6 m (from TOC) where it becomes clayey mud, with only a small fraction of sand. Note that about 1.7 m of Pleistocene sediment has been collected, starting at 3.3 m. B) FPC1: rapid infill of eroded bank topography (palaeochannel). From TOC to 2.90 m, the core intersected a palaeochannel. The sediments are intensely layered, where seagrass peats alternate with fine bioclastic sand. Below the palaeochannel boundary, the sediment transits to interbedded grey muds and silty sand with dark grey mud beds. C) FSB1: channel dissected, seagrass vegetated, shallow carbonate bank. Located in the middle of the Faure complex, it is dominated by muddy carbonate and weakly bioclastic muds. D) FWD2s: fringing bank and channel, delta associated. Situated in the subtidal portion of the Wooramel Delta, the core is characterised by the presence of a goethite and kaolinite clay interval at the base.

Section 2, the rate drops to 1.52 m/ka. Radiocarbon dating has revealed two hiatuses between two consecutive depths of sampling. Between 3.75 and 3.90 m (6.95 and 7.10 m BSL), more than 3300 years of sediment is absent and between 3.90 and 4.15 m of depth (7.10 and 7.35 BSL), there is a second hiatus of approximately 2300 years. The hiatuses are recognisable also in the core logging and most likely characterise erosional phases in bank development, during active channel migration in a distributary region. Section 3, representing the last two

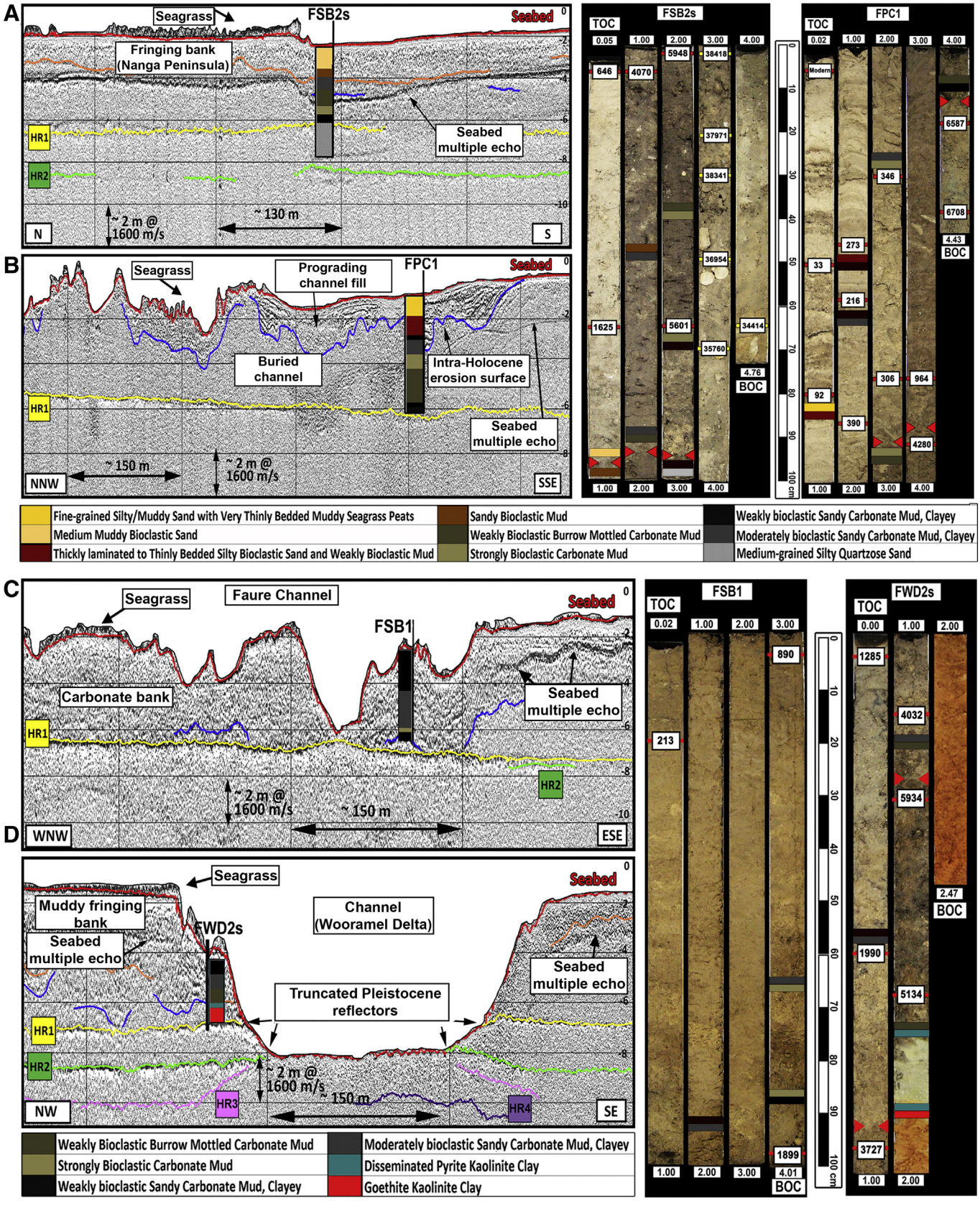

**Table 3**
Depths for each sample (from seafloor and from sea level, in metres) and the conventional and calibrated ages, obtained with $^{14}C$ AMS dating. Column 9: Dh (m) = length in metres of the interval. Colum 10: Dt (y) = difference between the highest and lowest age in the corresponding interval. Last column reports the growth rates for different sections in the cores. Apparent growth rates were calculated from the difference between the highest and the lowest age of the corresponding section. The gaps in the cores indicate erosional intervals and are highlighted in the table in red. 1) Gap = 2445 ± 59 y (transition mud to sand). 2) Gap = 1878 ± 53 y (transition weakly bioclastic mottled mud to moderate bioclastic clayey mud). 3) Transition Pleistocene to Holocene sediments, 4) Gap = 658 ± 50 y (base buried channel). 5) Gap = 3319 ± 60 y (transition strongly to moderately bioclastic clayey carbonate mud). 6) Gap = 2307 ± 68 y (transition weakly to strongly bioclastic mud). 7) Gap = 1737 ± 59 y (transition sandy mud to clayey mud). 8) Gap = 1102 ± 71 y (transition clayey mud to sandy mud). Note that gaps 1 and 7 are overlain by sandy (rather than muddy) bank sediments which become dominant. Further discussion is in this section.

| Sample | Depth from seafloor (m) | Depth from sea level (m) | Conventional $^{14}C$ age (years) | Error ± (years) | Calibrated ages (marine reservoir effect) 68.2% probability (years) | Error ± (years) | Section | Dh (m) | Dt (yr) | Dh/Dt (m/ka) | |
|---|---|---|---|---|---|---|---|---|---|---|---|
| FSB2s-CD1 | 0.05 | 2.27 | 1135 | 25 | 646 | 26 | 1 | 0.58 | 979 | 0.59 | |
| FSB2s-CD2 | 0.63 | 2.85 | 2110 | 30 | 1625 | 54 | | | | | |
| FSB2s-CD3 | 1.05 | 3.27 | 4105 | 30 | 4070 | 64 | | | | | → 1 |
| FSB2s-CD4 | 2.00 | 4.22 | 5630 | 30 | 5948 | 43 | 2 | 0.63 | 347 | 1.82 | → 2 |
| FSB2s-CD5 | 2.63 | 4.85 | 5290 | 35 | 5601 | 39 | | | | | |
| FSB2s-CD6 | 3.00 | 5.22 | 34180 | 430 | 38418 | 646 | | | | | → 3 |
| FSB2s-CD7 | 3.20 | 5.42 | 33660 | 400 | 37971 | 585 | | | | | |
| FSB2s-CD8 | 3.30 | 5.52 | 34110 | 420 | 38341 | 610 | | | | | |
| FSB2s-CD9 | 3.50 | 5.72 | 32860 | 370 | 36954 | 432 | Pleistocene | | | | |
| FSB2s-CD10 | 3.55 | 5.77 | 32060 | 330 | 36026 | 530 | | | | | |
| FSB2s-CD11 | 3.70 | 5.92 | 31680 | 320 | 35760 | 509 | | | | | |
| FSB2s-CD12 | 4.66 | 6.88 | 30190 | 280 | 34414 | 343 | | | | | |
| FPC1-CD1 | 0.05 | 3.25 | >MODERN | NA | >MODERN | NA | | | | | |
| FPC1-CD2 | 0.50 | 3.70 | 385 | 40 | 33 | 23 | | | | | |
| FPC1-CD3 | 0.78 | 3.98 | 505 | 35 | 92 | NA | | | | | |
| FPC1-CD4 | 1.45 | 4.65 | 680 | 25 | 273 | 28 | 1 | 2.70 | 390 | 6.93 | |
| FPC1-CD5 | 1.60 | 4.80 | 650 | 35 | 216 | 69 | | | | | |
| FPC1-CD6 | 1.85 | 5.05 | 810 | 30 | 390 | 56 | | | | | |
| FPC1-CD7 | 2.30 | 5.50 | 755 | 45 | 346 | 55 | | | | | |
| FPC1-CD8 | 2.75 | 5.95 | 705 | 40 | 306 | 55 | | | | | → 4 |
| FPC1-CD9 | 3.75 | 6.95 | 1480 | 35 | 964 | 45 | 2 | 1.00 | 659 | 1.52 | → 5 |
| FPC1-CD10 | 3.90 | 7.10 | 4240 | 40 | 4280 | 76 | | | | | → 6 |
| FPC1-CD11 | 4.15 | 7.35 | 6210 | 40 | 6587 | 60 | 3 | 0.25 | 121 | 2.07 | |
| FPC1-CD12 | 4.40 | 7.60 | 6315 | 40 | 6708 | 58 | | | | | |
| FSB1-CD1 | 0.20 | 3.03 | 645 | 30 | 213 | 66 | | | | | |
| FSB1-CD2 | 3.02 | 5.85 | 1405 | 30 | 890 | 46 | 1 | 3.8 | 1686 | 2.25 | |
| FSB1-CD3 | 4.00 | 6.83 | 2345 | 35 | 1899 | 53 | | | | | |
| FWD2s-CD1 | 0.05 | 4.15 | 1790 | 30 | 1285 | 34 | | | | | |
| FWD2s-CD2 | 0.60 | 4.70 | 2425 | 30 | 1990 | 55 | 1 | 0.55 | 705 | 0.78 | → 7 |
| FWD2s-CD3 | 0.90 | 5.00 | 3835 | 30 | 3727 | 63 | | | | | |
| FWD2s-CD4 | 1.15 | 5.25 | 4080 | 35 | 4032 | 65 | 2 | 0.25 | 305 | 0.82 | → 8 |
| FWD2s-CD5 | 1.30 | 5.40 | 5605 | 35 | 5934 | 43 | | | | | |
| FWD2s-CD6 | 1.65 | 5.75 | 4890 | 30 | 5134 | 78 | 3 | 0.35 | 800 | 0.44 | |

samples dated, at the bottom of the core, has an accumulation rate slightly higher than Section 2, corresponding to 2.07 m/ka. Sections 2 and 3 are similar to the rate found in the other central bank core FSB1.

Core FSB1 (Fig. 8C) is located in the middle of the Faure Sill, in the north central part of the carbonate bank. Its accumulation trend is very regular, with a constant depositional rate from the top to the bottom of the core. The total recovery for this core sample was 4.01 m and it covers a time span of 1686 ± 53 years, equivalent to a mean accumulation rate of ~2.25 m/ka. The radiocarbon dating indicates that the sedimentation is mainly confined to the late Holocene.

Core FWD2s (Fig. 8D) is located in the eastern part of the complex, in the carbonate bank associated with the Wooramel Delta. The first dating sample, taken at 0.05 m of depth, is 1285 years BP. The core was taken on the edge of a channel, marking an erosive event or a subsidence of sediment to the bottom of the channel, a possible cause of the lack of sediment near the top of the core. The accumulation rate of the core has three distinct intervals with different slopes. In Section 1, till 0.60 m of depth (4.15 m BSL), the surficial sediment has a rate of growth of 0.78 m/ka. Similar to FSB2s, a time gap also occurs in this location; between 0.60 and 0.90 m of depth, there is a hiatus of almost 1740 years. It follows a period of deposition (0.82 m/ka in Section 2) and another gap of more than 1100 years between Sections 2 and 3, the last portion of the muddy carbonate sediment, which has an accumulation rate of approximately 0.44 m/ka. Although the recovered core is 2.47 m long, it has not been possible to date the deeper grey green and red clayey sediment (about 0.6 m thick), found near the base of the core, due to an absence of *Amphisorus* for dating.

Accumulation rates varied in time and magnitude during the Holocene, suggesting that bank growth fluctuated in different settings, in accordance with organism productivity in seagrass, local tidal conditions, water depth and facies. When the conditions changed, bank growth rate responded. In the case of the cut-and-fill channel in core FPC1 (Fig. 8B), the growth was significantly accelerated. In other circumstances, a limitation or interruption to growth resulted. However, with a switch in conditions these areas reactivated. Such changes are reflected in cores

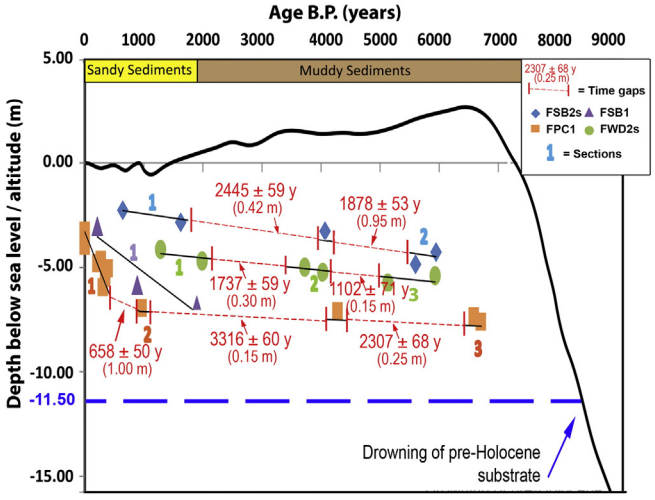


**Fig. 9.** Bank accumulation curves plotted with Holocene sea level curve. The numbers indicate sections described in this paper and time gaps (in red) are missing (erosional?) intervals. In the graph, pre-Holocene samples have been omitted. Note onset and continuation of sandy sediments in last 2000 years BP. The sea level curve is based mainly on coral reef records and sediment from Collins et al. (2006), Twiggs and Collins (2010), Jahnert and Collins (2013). Bank ages are based on AMS $^{14}$C dating (this study). (For interpretation of the references to colour in this figure legend, the reader is referred to the web version of this article.)

FPC1, FSB2s and FWD2s, where there are more "breaks" than "beds" represented in the cores in chronological terms.

## 5. Discussion

### 5.1. Shallow stratigraphy

Generally, the main acoustic reflectors in the seismic profiles coincide with an abrupt variation of sediment types, which is evident from the sediment core analyses. Based on stratigraphic position, lithology and radiocarbon age, the seismic reflector HR1 can be confidently identified as the top of pre-Holocene Bibra Limestone. The underlying seismic reflector HR2 has been intersected by only one core (FED3, Fig. 6) and no dating has been performed, but, on the basis of its stratigraphic position and lithological information, including calcrete clasts at the contact, it is considered to be the top of the Dampier Limestone. Both the pre-Holocene units have generally similar subsurface expression and lithology (with calcarenite concretions at contacts) and the seismic reflectors represent surfaces of impedance contrast beneath the Holocene bank buildup. No core reached the horizons HR3 and HR4; consequently their identification is on the basis of their stratigraphic position and the available literature (Logan et al., 1970a; Kendrick et al., 1991; O'Leary et al., 2008). Found only close to Wooramel Delta and around the topographic highs (Peron Peninsula, Faure Island, Nanga Peninsula), the reflectors could indicate two pre-Dampier (Middle and Lower Pleistocene) units. HR3 could represent the top of an earlier pre-Dampier marine phase or could be a marine equivalent of the Carbla Oolite member (MIS Stage 9/11, but poorly dated, O'Leary et al., 2008). Consequently, the identification of HR4 and its underlying unit is uncertain. Based on its geometry and stratigraphic position it could be part of the Peron Sandstone. Discontinuities seen in outcropping Peron Sandstone could be expressed as HR3 and HR4. These surfaces may have provided a template for later deposition, including location of channels over pre-existing topographic lows, control of the depositional topography of the Bibra and Dampier Limestones, determination of Holocene buildup patterns, distribution and thickness, and nucleation of bank growth around topographic highs.

The Holocene stratigraphic sequence within the Faure Sill has a thickness that ranges from a few centimetres to about 8 m. With the exception of the areas close to topographic highs and the main channels, the Holocene sediments in the central area of the bank are 4–7 m thick. In the eastern and western regions (respectively Petit and Dubaut Banks and Wooramel Bank), the base of the Holocene is more surficial, deepening, on average, from 2 to 4 m from the seafloor. The Holocene stratigraphic sequence not only presents a broad variety of internal geometries, but also has different sedimentological characteristics.

### 5.2. Morphostratigraphic elements and facies associations

The Faure channel–bank complex can be broadly subdivided into 5 regions (Fig. 10). Each shares similar morphological elements, lithology and stratigraphy, as follows: 1) Terminal ebb tidal fans, 2) fringing bank and flood tidal channels, 3) carbonate bank, 4) terminal prograding flood tidal fans, with shoreline attached sandflat, 5) delta associated fringing bank (Wooramel Delta).

1) *Terminal ebb tidal fans* occur in the north western area of the bank, approximately between Monkey Mia and Faure Island (Fig. 2). Morphologically, they can be compared with the ebb delta model described by Hayes (1980), where a main ebb channel, flanked on either side by channel margin linear bars, terminates with a seaward sloping terminal lobe of sand. In Dubaut Bank (Fig. 2), the main associated channel is Petit Channel. It is expressed in the northernmost portion as several minor channels, separated by levee deposits and broad sheets of sand (Fig. 4). In the southern part, it coalesces with Herald Gut Channel. Within the channel complex, longitudinal channel bars run parallel to the main stream (Fig. 5B). At least four terminal lobes, prograding seaward, produce a large scale coalescent ebb tidal fan (Fig. 4).
   An idealised facies association for this subcomplex has been developed, based on the core data (Fig. 6). The basal unit, above the pre-Holocene basement, is fine grained, silty quartzose sand, with bivalves and small foraminifera. The quartz component of the sediments is likely derived from the underlying Peron Sandstone. The unit is overlain by silty sand with fine to medium, well-rounded quartz. In contrast to the basal unit, the middle unit lacks bivalves and is coarser. The uppermost unit is composed of weakly bioclastic cross bedded quartzose sand. The idealised vertical stratigraphic sequence describes the growth and development of this area of the bank in terms of energy conditions, fluctuation in accommodation and source material. In the lower part of the unit, clustered bivalve beds were most likely deposited by tidal currents. The bivalves are in a horizontal position, with the concavity downward and in a coarser grained mix, likely indicating a strong directional current flow. The lithology of the channel bars differ from the idealised facies association for the terminal ebb tidal complex. They are predominantly quartz dominated, with a minor bioclastic component, displaying an upward coarsening and an increase in quartzose material (cf. Fig. 5B).
2) *Fringing bank and flood tidal channels* have their best expression in the western side of the bank, between the south western edge of Faure Island and the north eastern edge of the Nanga Peninsula (Fig. 2). The main channels are Petit Channel and Herald Gut Channel, which are two of the deepest exchange channels in the bank, also branching into many minor drainage channels. Herald Gut Channel is the only connection that L'Haridon Bight has with the open ocean while Petit Channel flows into Hamelin Pool. In terms of facies assemblage, this subcomplex is mostly composed of bioclastic carbonate mud with mottled burrow traces, transitioning to sandy bioclastic mud and topped by medium grained muddy bioclastic sand (as in core FSB2s, Fig. 8A). The channel sediments are predominantly composed of quartzose sand, with well-rounded to subrounded grains and occasional darker pigmented particles. They are generally weakly bioclastic and foraminifera and calcareous algae are present. The channels have a critical role in

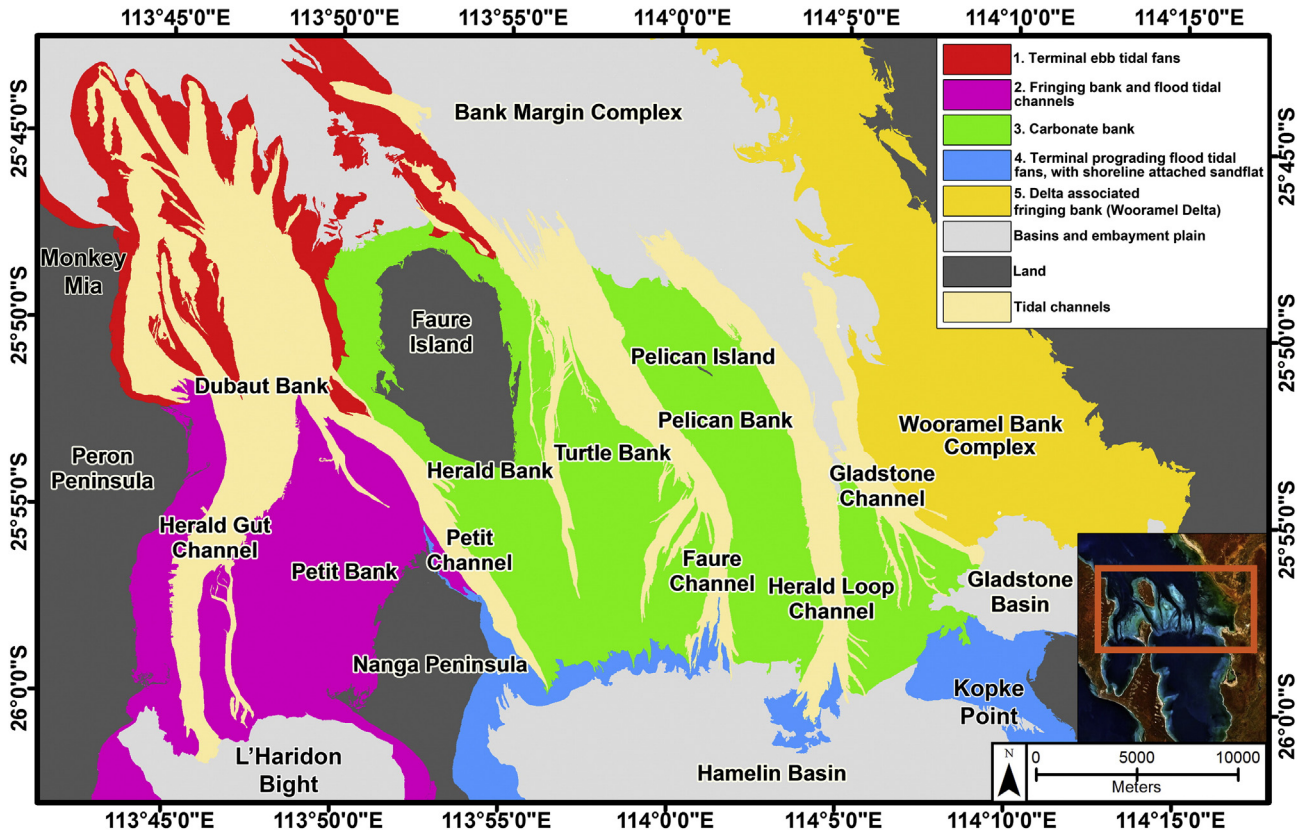


**Fig. 10.** Faure channel–bank complex can be subdivided into five regions (see 1 to 5 in legend) based on morphological elements, lithology and stratigraphy. In the figure, basins and embayment plain, land and tidal channels are also marked.

controlling the depositional patterns in the terminal ebb and flood part of the western lobe of the bank. During the growth of the bank, material from the surrounding Plio-Pleistocene highs has been eroded, deposited into the channels and distributed at either ends of the ebb and flood tidal fans. Evidence of Holocene channel migration between Faure Island and Nanga Peninsula is discernible within the seismic profiles and core collected in Petit Channel (see Figs. 5C and 8B). The presence of levees and longitudinal channel bars confirms this migration.

3) *Carbonate bank* morphologies can be found over the entire central complex. Small to medium scale ripples cover the entire bank and run subparallel to seagrass stabilised ridges, with an east–west direction (Fig. 3). All around the southern side of the topographic highs of Turtle and Pelican Banks, linear ridges represent an important surface aspect of the bank where seagrass has vegetated and stabilised tidally generated linear bedforms (Fig. 5A). Besides the main tidal channels, which cut the bank and permit an exchange of water between Hamelin Pool and the open ocean, there are several drainage channels, variably distributed along the southern part of the bank. Some profiles reveal distinct sets of palaeodistributary channels recognisable in both seismic and sedimentological data (cf. Figs. 5C and 8B core FPC1). It does appear therefore, that during the Holocene, the channels most likely experienced periods of migration and abandonment through the bank, with different palaeocurrent directions and several phases of erosional and depositional events (cut and fill). From the top to the bottom of the bank the following facies are found: 1) weakly bioclastic sandy carbonate mud, clayey, 2) moderately bioclastic, sandy, carbonate mud, clayey and 3) strongly bioclastic carbonate mud. The facies' occurrence is mainly linked with the presence of seagrass but is also related to the pre-Holocene topographic highs, which the carbonate bank facies have grown around. Data from core logging have shown also that the central eastern carbonate bank experienced the influx of some terrigenous derived material and clays. These deposits could be related to storm or cyclone events which caused flooding of the Wooramel River.

4) *Terminal prograding flood tidal fans, with shoreline attached sandflat* form a well-defined subcomplex situated in the southern edge of the Faure Sill, between Nanga Peninsula and Gladstone Embayment. Morphologically, it displays a continuous belt of coalescent flood tidal fan lobes (terminal submarine fans of Davies, 1970b), up to 2.5 km long, running parallel to the entire slope length between the bank and Hamelin Basin. Faure Channel and Herald Loop Channel break the continuity of the belt with numerous bifurcated minor channels. Longitudinal seismic profiles show that the lobes have a complex internal structure, composed of surficial cross bedded or prograding layers, becoming more horizontal with deepening in the sequence (Fig. 5D). Transverse seismic lines confirm the oblique configuration that occurs with the basinward progradation pattern on the bank margin. In a few areas of the subcomplex, Holocene carbonate sand lobes have a flat topped geometry in a discordant relationship with the underlying inclined beds, possibly as a consequence of non-deposition (with minor erosion) linked to sea level height. In very shallow water conditions, the updip deposition is obstructed resulting in successive beds built out and prograding basinward. Linear ridges of seagrass, running in an east–west direction, characterise the northern portion of the fan (cf. Fig. 5A). The deposits are characterised by coarsening upward sandy units, generally cross bedded, up to 2 metre thick, overlaying a fine grained sandy unit, with thin seagrass peats and a minor muddy component. The deepest units have the typical facies association found in the bank; carbonate mud with variable fractions of sand and bioclasts. The development of fan lobes is indicative of a prevalent basinward flow. Close to Gladstone Embayment (Kopke Point), there is a prominent shoreline attached sandflat, where the water shallows (to <3 m) and stronger currents develop, generating ripples and megaripples

(Fig. 5E). These tidally-produced features can be up to 1.5 m high and several hundred metres long, with a wavelength of 25–35 m. The seismic profiles reveal a distinct progradation throughout the margins of the complex. In the south, a flood tide progradation prevails, and in the northern margin ebb tide progradation is present. Progradation is controlled by tidal currents with lesser wind driven circulation. In the deepest areas of the channels (>4.5 m), lenticular to elongate sets of sand bars are bounded by flood oriented cross bedding. Facies analysis showed that the composition of the sediments collected along the terminal bars and lobes varies from coarse to medium grained bioclastic sands (top of the cores) to silty fine grained laminated sands and to carbonate muddy apron facies (bottom of the cores). In the cores, evidence of an internal architecture is clear, with overall excellently preserved cross bedding. Dark pigmented grains emphasise these features. The transitional contact between the surficial carbonate sands and the underlying sediment occasionally lacks distinctness, due to a strong bioturbation.

5) *Delta associated fringing bank (Wooramel Delta)* occupies the easternmost part of the Faure Sill and is strongly influenced by the Wooramel River and the Wooramel seagrass bank (Fig. 4. Logan et al., 1970a). The semiarid Wooramel River has a limited influence on sedimentation, with sandy fluvial sediments confined to the deltaic wedge. Terrigenous clay periodically spread across the bank following discharge events associated with occasional (usually cyclone associated) runoff activity (Davies, 1970a). The delta progrades southward into Gladstone Embayment and seaward over Holocene carbonate sediments of the intertidal and subtidal zones (Davies, 1970a). North–west longshore currents created by tidal and wind regimes, redistribute the sediment in subparallel longshore sand bars and sand ridges. Numerous tidal channels, linked to the Wooramel River, cut the intertidal and subtidal zones of the delta. The delta front, which in the southern part is more than 10 km from the hinterland, has a steep slope before flattening offshore, at depths greater than 5 m.

Four cores were collected and logged in the delta region (Fig. 6). The units and facies in these cores show a clear terrigenous influence (Figs. 6 and 8D). The sediments are mainly clay rich carbonate mud. The upper section, which is up to 2 m thick, consists of clayey, weakly bioclastic sandy carbonate mud. Deepening, the sediment becomes slightly more bioclastic, with bioturbation and burrow mottled mud (Fig. 6). In core FWD2s, the lower section abruptly changes from dark brown clay rich mud to green grey kaolinite clay (layer thickness of 15 cm) and then, at the base of the core, sharply becomes orange dark red clay, with an organic component and no texture or colour variations over the interval. The middle clayey layer could indicate that a rapid terrigenous input into the delta occurred as pulses into the bank, forced by possible storm surges and flooding (Fig. 8D). Davies (1970a, p. 148) described a similar submarine core, collected a few kilometres north, in a submarine levee. He considered that the red alluvium at the base of the section grading upward into reduced green clayey sand, marks the transgressive Holocene unconformity between Holocene bank sediments and Plio-Pleistocene alluvium. The sequence seen near the Wooramel Delta can be considered as a possible result of events that influenced the amount of terrigenous material in the bank. Terrigenous sediments are concentrated in the vicinity of the Wooramel River (Logan et al., 1970a, and this study); therefore bank cores, located close to the delta appear to be more affected by major storm events and run-off from flooding.

### 5.3. Holocene bank growth and accumulation

Radiocarbon dating assisted linking the sedimentological data to the Holocene event chronology and calculating the bank accumulation rate. This new information has revealed a highly dynamic geological record and appears to be broadly consistent with previous onset and evolution data (Davies, 1970a; Logan et al, 1970a, 1974; Hagan and Logan, 1974; Walker and Woelkerling, 1988), while adding significantly to seismic, facies and geological understanding.

The Holocene bank accumulation rates vary by more than an order of magnitude, ranging from 0.44 m/ka in the lowest Holocene section in the Wooramel Delta to 6.93 m/ka in the upper section of core FPC1, where a rapid deposition of prograding and laminated sand filled a palaeochannel (Table 3). Table 4 summarises the average accumulation rates for each facies considered. These values are comparable with the rates of vertical accretion estimated by Davies (1970a, p. 161). Rao (1996) stated that in Australian carbonate environments, the maximum accumulation rates are from about 1.5 m/ka in tropical waters to 1.0 m/ka in cold water. In general terms, the Faure Sill is 7 m thick and has a basal age of close to 7 ka, giving an approximate accumulation rate of 1 m/ka. Excluding the "outlier" filled channel rate (see Table 4) the average accumulation rate for all dated cores was 1.3 m/ka. However, rates obtained are facies dependent (see Table 4).

Considering the Holocene accumulation curves plotted in the context of the regional Holocene sea level trend (Fig. 9), the cores in the central area of the bank (FPC1 and FSB1) have a similar trend and the two marginal cores (FSB2s and FWD2s) are comparable with each other. After the end of the Last Ice Age, in Late Pleistocene–Early Holocene time, under the input of water derived by the melting of ice sheets, sea level rose about 130 m from ~18,000 to ~6800 years BP, culminating in a highstand of 2.5 m above the present level (Nakata and Lambeck, 1990; Lambeck and Nakada, 1990). An initial post drowning erosional phase of pre-Holocene substrates would have accumulated before establishment of pioneer seagrass and epiphyte communities became significant, possibly over several hundred years duration. Within the bank, this date approximately coincides with the oldest determined Holocene date (6708 ± 58 years, in FPC1) but because the core didn't reach the pre-Holocene surface (HR1; see Fig. 8), bank initiation could be significantly older than this date. Based on seismic profiles, the most recent pre-Holocene reflector HR1 (interpreted as top of the Bibra Limestone) can be found at depths of at least 11.5 m below the present sea level, and would have been submerged by 8500 years BP (Figs. 9 and 11.1). Initial erosion of topographic highs of the Peron Sandstone is likely to have shed quartz dominated sand sheets over the drowning substrate.

The first seagrass communities started their colonisation and contribution at the onset of a protobank, trapping and binding sediments (cf. Scoffin, 1970) and producing in situ sediments, such as coralline algal fragments, other calcareous epiphytes (Walker and Woelkerling, 1988) and bioclastic remains. During the transgressive period, until the highstand at ~2.5 m above the present sea level, the bank continued to develop. By 6800 years BP, bank buildup had advanced but lagged significantly behind sea level (Fig. 11.2). Thereafter declining sea level is likely to have caused a base level fall of 2 m (Fig. 9) with possible bank erosion (expressed as hiatuses in $^{14}C$ dating).

Based on $^{14}C$ dating of coquina ridges near Telegraph Station (south Hamelin Pool, Shark Bay) Jahnert and Collins (2013) estimated that sea level generally fell by about 1 m in less than 2200 years, standing at ~1.5 m above the present sea level, at ~4.5 ka BP (Fig. 11.3). Such a fall could be associated with the hiatuses found in the dating of the cores FSB2s, FPC1 and FWD2s (Fig. 9 and Table 3). In both the marginal

**Table 4**
Range and average accumulation rate in the analysed facies, based on four dated cores.

| Facies | Range of accumulation rate (m/ka) | Average accumulation rate (m/ka) |
|---|---|---|
| Bank | 0.59–2.25 | 1.7 |
| Filled channel | ?–6.9 | 6.9 |
| Delta | 0.44–0.82 | 0.7 |
| Maximum range and average accumulation rate | 0.44–6.9 | 3 |
| Average for all facies (filled channel excluded) | – | 1.3 |

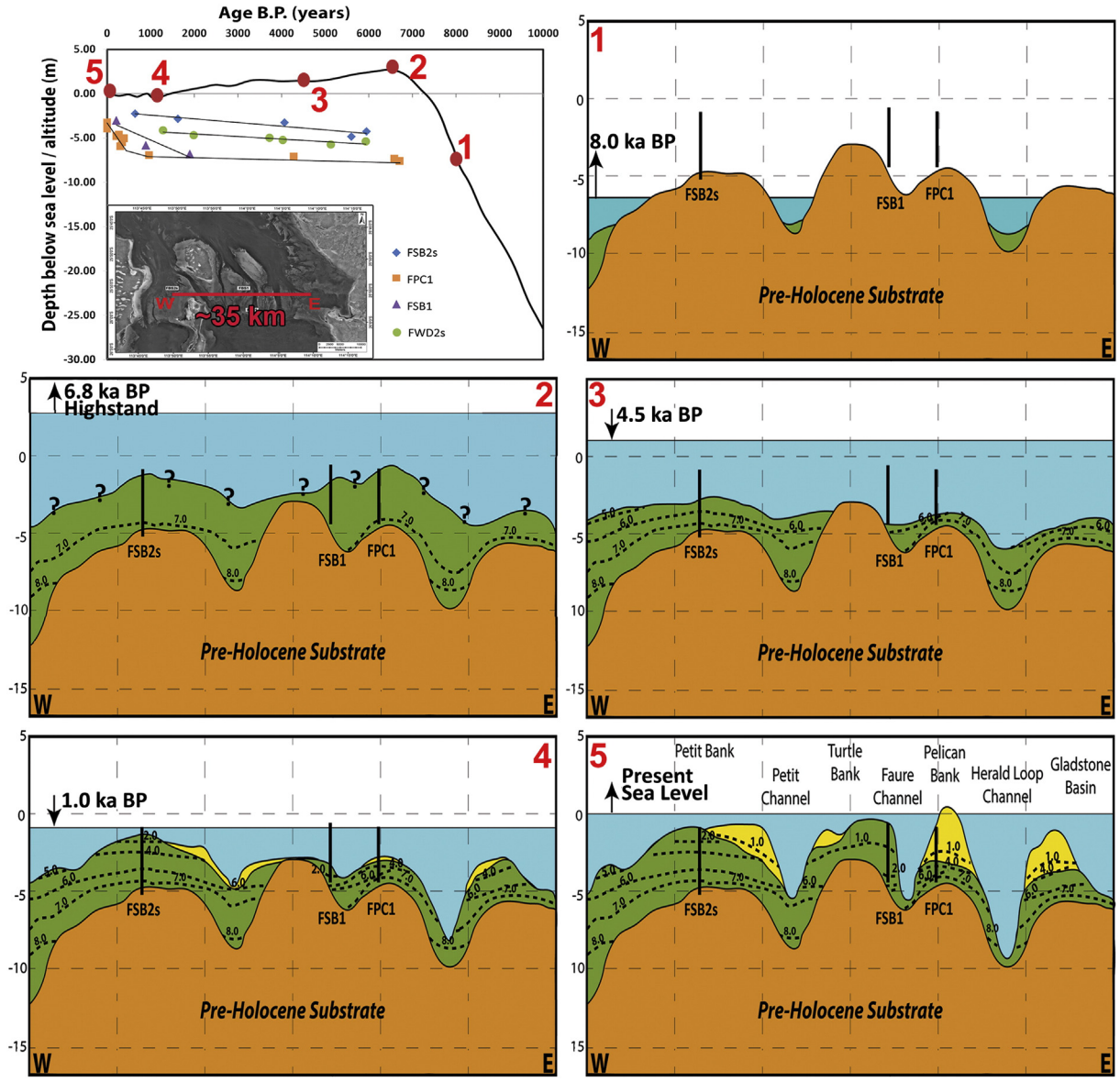


**Fig. 11.** Reconstruction of the Holocene chronology of the Faure Sill, based on the data from this study. Dashed lines represent isochrones. The colours are a generalisation of the lithology: orange = pre-Holocene substrate, green = bioclastic carbonate mud, yellow = bioclastic sand. The arrows refer to the trend of the sea level (fall or rise). FSB1, FPC1 and FSB2s are three cores described in the text. Heights of sediments on cores are based on radiocarbon dating levels obtained (Table 3); uncertainty exists on height of bank growth (panel 2) prior to erosional events (panel 3). The profile is not to scale, but is a simplification of the main topography. The transect length is about 35 km, W–E oriented. On the vertical axis, the scale is in metres, 0 corresponds to the present sea level. Sea level data are based on the composite sea level curve in Fig. 9. 1) Early Holocene. The pre-Holocene substrate was largely exposed, with a sparse cover of bioclastic sand to mud. 2) Middle Holocene. The sea rapidly rose till reaching the highstand level and completely flooding the bank region. During this period, the seagrass meadows were at their apex, playing a significant role in trapping sediments and producing muddy carbonate deposits in situ. 3) Late Holocene. The irregular downward trend of sea level has been responsible for several distinct erosional and depositional events. 4) Most recent part of Holocene. The sea level dropped till reaching the lowstand level. Sandy bank top facies were initiated (yellow). 5) Present conditions of the bank. Note the culmination of sandy bank top sediments, now fully developed.

cores (FSB2s and FWD2s), about 2000 years of sediments (from ~4.0 to ~5.9 ka BP) are missing in the stratigraphic record, suggesting the possible occurrence of an erosive event, amplified in shallow water areas and associated with a decreased accumulation in deeper parts. In a regressive context, a brief and moderate sea level increase followed, accompanied by minor deposition.

Generally, declining sea level continued until a low stand at about 1000 years BP, when the sea level was about 1 m below the present. Jahnert and Collins (2013) found evidence of an exposure surface (1040–940 $^{14}$C years BP) in a lithified carbonate pavement in Garden Point and Rocky Point (Shark Bay). The results of the core dating show that the bioclastic sands, characterising the surficial sediments in the terminal prograding flood tidal fan, are very recent (from 964 ± 45 years BP to present). This suggests that fan sedimentation is continuing in the very recent history of the bank.

In the present day bank, narrow linear ridges, parallel to the predominant currents, have taken the place of the dense seagrass meadows which gradually disappeared from the shallowest areas. Between the bank and the deep basins and channels, where the slopes are relatively steep, the seafloor is bare or has only occasional scattered seagrass. Deposition in such environments is mostly tidal current dominated, and only particles with a larger diameter, such as coarse grained sands, are deposited. In contrast to the carbonate mud found where the seagrasses are more developed, the bioclastic sands are usually found in cross bedded fans, prograding outward from the bank with clinoform geometry. Sedimentation and deposition has adjusted downward and basinward

as the sea level dropped. This is confirmed by the upward coarsening sequences seen in the sandy fan and bank top trend from silty fine grained sands to coarse grained cross bedded bioclastic sands.

### 5.4. Role of the seagrass banks in Shark Bay

Shark Bay has distinctive and exceptional examples of active geological and biological processes and ecosystems. Faure Sill, with its peculiar hydrological structure, is an area where seagrass meadows, carbonate deposits and sediments create highly dynamic and diverse environments. It is recognised worldwide that seagrass meadows are fundamentally involved in modifying a coastal marine environment, in its physical, chemical, geological and biological aspects (Walker, 1990; Gibbes et al., 2014). In Shark Bay, particularly within the Faure Sill, since their appearance in the early Holocene, seagrasses have had a primary role in reshaping and transforming the geomorphology and ecosystems of the area. Production and deposition of a significant amount of bioclastic and epiphytic sediments is strictly linked with the seagrass presence. Accumulation rates of seagrass associated sediment are higher than adjacent sedimentary environments. While the calcareous epiphytes represent a significant component, roots, rhizomes and leaves also reduce the speed of currents facilitating deposition, trapping fine sediments (Walker, 1990). With the formation of a sill between the open ocean and the embayment waters, together with the semiarid climatic condition of the area, the southern embayments of Hamelin Pool and L'Haridon Bight have become meta- to hyper-saline (Logan and Cebulski, 1970; Logan et al, 1974). These environments, incompatible with the growth of seagrass are instead suitable for the establishment of unique microbial systems, stromatolites, oolitic and coquina systems, particularly of *Fragum erugatum*, Tate, 1889 (Jahnert and Collins, 2011, 2012, 2013).

Seagrasses perform a range of services (Gibbes et al., 2014). They provide shelter and food for numerous species of molluscs, crustaceans and fish, including many commercially valuable species, like *Pagrus auratus* Bloch & Schneider, 1801 (Heithaus, 2004). Shark Bay supports an internationally significant population of dugongs (*Dugong dugon* Muller, 1776) which feed on *Amphibolis antarctica* (Walker, 1990) and it has the largest breeding population of loggerhead turtles in Western Australia (*Caretta caretta* Linnaeus, 1758), (Preen et al., 1997). The seagrass is important also for small and large cetaceans. Particularly, Monkey Mia is famous worldwide for the contact between humans and some members of the local population of bottlenose dolphins (*Tursiops truncates* Montagu, 1821), (Preen et al., 1997). Tiger sharks (*Galeocerdo cuvier* Péron & Lesueur, 1822) are linked too with the shallow seagrass ecosystem, as the local fauna represent their most common prey items (Heithaus, 2001). Seagrass meadows are not only essential for an entire shallow benthic ecosystem, but they also play a critical role in producing, sequestering and storing organic carbon (Grimsditch et al., 2012; Duarte et al, 2013; Lavery et al., 2013) and considerable contribution to carbon, nitrogen and phosphorus cycles in the ocean (Fourqurean et al., 2012). Fourqurean et al., 2012 established that the total storage of organic carbon and nutrients in the seagrass linked sediments of Shark Bay is on average 243.0 Mg $C_{org}$ $ha^{-1}$, substantially higher than the median values for the world's seagrass ecosystems (139.7 Mg $C_{org}$ $ha^{-1}$). Moreover they believe there is a positive correlation between surficial $C_{org}$ and salinity: $C_{org}$ is higher in hypersaline environments, as the hypersalinity coincides with a decrease of energy (Fourqurean et al., 2012). This hypothesis is supported by Lavery et al. (2013). These recent insights highlight the importance of the Shark Bay seagrass communities in carbon sequestration, potentially providing a globally significant climate change mitigation benefit (Grimsditch et al., 2012).

## 6. Conclusions (595)

Through shallow seismic and sedimentological analysis, this investigation has been able to characterise the Faure Sill in terms of its seismic architecture, facies, chronology and growth history, and to determine its relationship to the adjacent Wooramel Delta, providing new insights and a better understanding of the sedimentological facies and geomorphological features of the bank.

Traditionally, evolution of the Shark Bay banks has been described in terms of fringing banks with a coalescence of patch banks, forming barrier banks such as the Faure Sill. The Faure channel–bank complex is an example of a system characterised by the presence of tidal channels with ebb tidal and flood tidal fan morphologies at bank margins and frequent channel associated sediment bodies. Morphostratigraphic elements and facies associations are indicative of sediment supply, accommodation and fluid dynamics changes (tides, currents and waves) as a function of the variation of the sea level over the time.

- During the Early Holocene, the pre-Holocene substrate was largely exposed, then a flooding event (not earlier than 8.5–8.0 ka BP) could have caused erosion of the palaeosurfaces and quartz shedding from eroding pre-existing topography. After this initial lag phase seagrass bank establishment progressively contributed bioclastic sediment, initiating the early stages of bank growth. In Middle Holocene time, the transgressing seas rapidly rose until reaching the +2 m highstand level around 6800 years BP, with bank accumulation accelerating. During this period, the seagrass meadows reached their apex, playing a significant role in binding and trapping sediments and producing muddy carbonate deposits. During the succeeding slow decline to present sea level (Late Holocene), bank growth continued to fill available accommodation and channel–bank morphology continued to develop. Seismic profiles and geochronology reveal abandoned channels, rapid infill of eroded bank regions, progradation of terminal fans, and distinct erosional and depositional events, with one prominent hiatus of up to 2000 years duration recorded. Nevertheless, the bank continued to fill the available accommodation, with development of sandy, bank top sediment bodies. The latest Holocene to present, the bank is nearly emergent at low tide, with depths of 0.5 m commonly recorded, and relatively sparse seagrass cover in shallow areas. Tidally generated bedforms are widespread, however prolific seagrass growth continues in intervening channels.
- The growth of the bank has been controlled by three major factors: 1) the pre-Holocene topography which, with its highs and channels, shaped the accommodation for the sediments during the Holocene onset; 2) the seagrass that not only acted as a sediment trap, but also by suppling habitats for organisms, provided a large volume of biogenic carbonate deposits, generated in situ; 3) sea level fluctuations that largely controlled the hydrodynamic conditions, such as the amount of tidally oscillating waters and their velocity, influencing erosion, transportation and deposition, and the channel–bank morphology.
- The system of deltas and banks represented by the Gascoyne and Wooramel Deltas and the Wooramel and Faure seagrass banks contains juxtaposed clastic and carbonate facies and stretches along 200 km of the coastal Carnarvon Basin (Fig. 1). To the south, the mixed carbonate–clastic system consisting of the Faure channel–bank complex and Wooramel Delta grades into the hypersaline microbial, oolitic, coquina and evaporite systems in Hamelin Pool within Shark Bay. This system could be regarded as a partial analogue for the Plover Formation, in the Browse Basin (North West Shelf, Western Australia). The Plover Formation is an important hydrocarbon reservoir which comprises Early to Middle Jurassic coastal plain and fluviodeltaic deposits, with marine carbonate and igneous and volcaniclastic intervals (Blevin et al, 1998; Longley et al., 2002; Barber et al. 2004; Tovaglieri and George, 2014).

## Acknowledgments

Woodside and the Browse Joint Venture partners are thanked for providing research funding to Curtin Applied Geology for this project.

Authors wish to thank the following: Landgate Imagery and DPaW for digital aerial photos; DPaW Denham, particularly Wayne Moroney for vessel support during the seismic surveys; the Department of Spatial Sciences (Curtin University) for supplying the DGPS; Bobbie Rice and Darren Skene (Quaternary Resources); Blue Lagoon Pearls for providing and operating the vessel P2 for the vibracoring survey, the facilities for the initial cutting of the cores and valuable help in many aspects of the field work; Cleve Flottman (DWG Consulting), Westarc Welders and Mark Winstanley (Department of Applied Physics, Curtin University) for designing and constructing the coring A frame. Thanks to Shashi Rajah Kanagasabai (Applied Geology) for his assistance during the vibracoring survey, core logging, XRD analysis and preliminary interpretation during his honours degree thesis; Alexandra Stevens (Applied Geology) for her help with paper review, Giovanni De Vita for his technical advices and Sira Tecchiato (Applied Geology) during the seismic survey.

## References


Allwood, A.C., Walter, M.R., Kamber, B.S., Marshall, C.P., Burch, I.W., 2006. Stromatolite reef from the Early Achaean era of Australia. Nature 441, 714–718.

Ashley, G., 1990. Classification of large scale subaqueous bedforms: a new look at an old problem. Journal of Sedimentary Petrology 60, 160–172.

Barber, P.M., Carter, P.A., Fraser, T.H., Baillie, P.W., Myers, K., 2004. Under-explored Palaeozoic and Mesozoic petroleum systems of the Timor and Arafura seas, northern Australia continental margin. In: Ellis, G.K., Baillie, P.W., Munson, T.J. (Eds.), Timor Sea Petroleum Geoscience. Proceedings of the Timor Sea Symposium, Darwin, Northern Territory, 19–20 June 2003. Northern Territory Geological Survey, Special Publication 1.

Belperio, A.P., Hails, J.R., Gostin, V.A., Polach, H.A., 1984. The stratigraphy of coastal carbonate banks and Holocene sea levels of northern Spencer Gulf, South Australia. Marine Geology 61, 297–313.

Blevin, J.E., Struckmeyer, H.I.M., Cathro, D.L., Totterdell, J.M., Boreham, C.J., Romine, K.K., Loutit, T.S., Sayers, J., 1998. Tectonostratigraphic framework and petroleum systems of the Browse Basin, North West Shelf. In: Purcell, P.G., Purcell, R.R. (Eds.), The Sedimentary Basins of Western Australia 2: Proceedings of the Petroleum Exploration Society of Australia Symposium, Perth, pp. 369–395.

Butcher, B.P., Van de Graaff, W.J.E., Hocking, R.M., 1984. Shark Bay – Edel, Western Australia: Geological Survey of Western Australia, 1:250 000 Geological Series Explanatory Notes, 1 – 21.

CALM, 1996. Shark Bay Marine Reserves Management Plan 1996-2006. Management Plan No. 34. Department of Conservation and Land Management, Perth.

Chivas, A.R., Torgensen, H.A., Polach, A., 1990. Growth rates and Holocene development of stromatolites from Shark Bay, Western Australia. Australian Journal of Earth Sciences 37, 113–121.

Cohen, A.S., Soreghan, M.I., Scholz, C.A., 1993. Estimating the age of formation of lakes — an example from Lake Tanganyika, east African rift system. Geology 21 (6), 511–514.

Collins, L.B., Jahnert, R.J., 2014. Stromatolite research in the Shark Bay World Heritage area. Journal of the Royal Society of Western Australia 97, 189–219.

Collins, L.B., Zhao, J.-X., Freeman, H., 2006. A high-precision record of mid-late Holocene sea-level events from emergent coral pavements in the Houtman Abrolhos Islands, southwest Australia. Quaternary International 145–146, 78–85.

Davies, G.R., 1970a. Carbonate bank sedimentation, Eastern Shark Bay, Western Australia: carbonate sedimentation and environments, Shark Bay, Western Australia. In: Logan, B.W., Davies, G.R., Read, J.F., Cebulski, D.E. (Eds.), Carbonate Sedimentation and Environments, Shark Bay, Western Australia. American Association of Petroleum Geologists Memoirs 13, pp. 85–168.

Davies, G.R., 1970b. Algal laminated sediments, Gladstone Embayment, Shark Bay, Western Australia. Carbonate sedimentation and environments, Shark Bay, Western Australia. In: Logan, B.W., Davies, G.R., Read, J.F., Cebulski, D.E. (Eds.), Carbonate Sedimentation and Environments, Shark Bay, Western Australia. American Association of Petroleum Geologists Memoirs 13, pp. 169–205.

Dravis, J.J., 1983. Hardened subtidal stromatolites, Bahamas. Science 219, 385–386.

Duarte, C.M., 2002. The future of seagrass meadows. Environmental Conservation 02, 192–206.

Duarte, C., Kennedy, H., Marbà, N., Hendriks, I., 2013. Assessing the capacity of seagrass meadows for carbon burial: current limitations and future strategies. Ocean and Coastal Management 83, 32–38.

Fallon, S.J., Fifield, L.K., Chappell, J.M., 2010. The next chapter in radiocarbon dating at the Australian National University: status report on the single stage AMS. Nuclear Instruments and Methods in Physics Research B 268, 898–901.

Fonseca, M.S., Fisher, J.S., Zieman, J.C., Thayer, G.W., 1982. The role of current velocity in structuring seagrass meadows. Estuarine, Coastal and Shelf Science 17, 367–380.

Fourqurean, J.W., Kendrick, G.A., Collins, L.S., Chambers, R.M., Vanderklift, M.A., 2012. Carbon, nitrogen and phosphorus storage in subtropical seagrass meadows: examples from Florida Bay and Shark Bay. Marine and Freshwater Research 63, 967–983.

Gibbes, B., Grinham, A., Neil, D., Olds, A., Maxwell, P., Connolly, R., Weber, T., Udy, N., Udy, J., 2014. Moreton Bay and Its estuaries: a sub-tropical system under pressure from rapid population growth. In: Wolanski, E. (Ed.), Estuaries of Australia in 2050 and Beyond. Estuaries of the World, Springer, Dordrecht, pp. 203–222.

Grimsditch, G., Alder, J., Nakamura, T., Kenchington, R., Tamelander, J., 2012. The blue carbon special edition — introduction and overview. Ocean and Coastal Management, iFirst, pp. 1–4.

Hagan, G.M., Logan, B.W., 1974. Development of carbonate banks and hypersaline basins, Shark Bay, Western Australia. American Association of Petroleum Geologists Memoir 22, 61–139.

Hamilton, E.L., 1970. Sound velocity and related properties of marine sediments, North Pacific. Journal of Geophysical Research 75, 23.

Hancock, S., Brown, P., Stephens, B., 2000. Shark Bay Terrestrial Reserves Management Plan 2000–2009. Department of Conservation and Land Management for the National Parks and Nature Conservation Authority Perth, Western Australia.

Hayes, M.O., 1980. General morphology and sediment patterns in tidal inlets. Sedimentary Geology 26, 139–156.

Heithaus, M.R., 2001. The biology of tiger sharks, *Galeocerdo Cuvier*, in Shark Bay, Western Australia: sex ratio, size distribution, diet, and seasonal changes in catch rates. Environmental Biology of Fishes 61 (1), 25–36.

Heithaus, M.R., 2004. Fish communities of subtropical seagrass meadows and associated habitats in Shark Bay, Western Australia. Bulletin of Marine Science 75 (1), 79–99 (21).

Hocking, R.M., Moors, H.T., Van De Graaff, W.J.E., 1987. Geology of the Carnarvon Basin Western Australia. Geological Survey of Western Australia Bulletin 133, 289.

Jahnert, R.J., Collins, L.B., 2011. Significance of subtidal microbial deposits in Shark Bay, Australia. Marine Geology 286, 106–111.

Jahnert, R.J., Collins, L.B., 2012. Characteristics, distribution and morphogenesis of subtidal microbial systems in Shark Bay, Australia. Marine Geology 303–306, 115–136.

Jahnert, R.J., Collins, L.B., 2013. Controls on microbial activity and tidal flat evolution in Shark Bay, Western Australia. Sedimentology 60 (4), 1071–1099.

Kendrick, G.W., Wyrwoll, K.-H., Szabo, B.J., 1991. Pliocene — Pleistocene coastal events and history along the western margin of Australia. Quaternary Science Reviews 10, 419–439.

Koch, E.W., Ackerman, J.D., Verduin, J., van Keulen, M., 2006. Fluid dynamics in seagrass ecology — from molecules to ecosystems. In: Larkum, A.W.D., Orth, R.J., Duarte, C.M. (Eds.), Seagrasses: Biology, Ecology and Conservation, p. 193-22.

Lambeck, K., Nakada, M., 1990. Late Pleistocene and Holocene sea level change along the Australian coast. Palaeogeography Palaeoclimatology Palaeoecology 89, 143–176.

Lavery, P.S., Mateo, M.-A, Serrano, O., Rozaimi, M., 2013. Variability in the carbon storage of seagrass habitats and its implications for Global Estimates of Blue Carbon Ecosystem Service. PLoS ONE 8 (9).

Leighton, T.G., Robb, G.B.N., 2008. Preliminary mapping of void fractions and sound speeds in gassy marine sediments from subbottom profiles. Journal of Acoustical Society of America 124 (5), 313–320.

Logan, B.W., 1968. Western Australia: in Quaternary shorelines research in Australia and New Zealand. In: Gill, E.D. (Ed.), Australian Journal of Science 31, p. 110.

Logan, B.W., Cebulski, D.E., 1970. Sedimentary environments of Shark Bay, Western Australia. In: Logan, B.W., Davies, G.R., Read, J.F., Cebulski, D.E. (Eds.), Carbonate Sedimentation and Environments, Shark Bay, Western Australia. American Association of Petroleum Geologists Memoirs 13, pp. 1–37.

Logan, B.W., Read, J.F., Davies, G.R., 1970a. History of carbonate sedimentation, Quaternary Epoch, Shark Bay, Western Australia. In Carbonate sedimentation and environments, Shark Bay, Western Australia. In: Logan, B.W., Davies, G.R., Read, J.F., Cebulski, D.E. (Eds.), Carbonate Sedimentation and Environments, Shark Bay, Western Australia. American Association of Petroleum Geologists Memoir 13, pp. 38–84.

Logan, B.W., Davies, G.R., Read, J.F., Cebulski, D.E., 1970b. Carbonate sedimentation and environments, Shark Bay, Western. American Association of Petroleum Geologists Memoir 13, 223.

Logan, B.W., Read, J.F., Hagan, G.M., Hoffman, P., Brown, R.G., Woods, P.J., Gebelein, C.D., 1974. Evolution and diagenesis of quaternary carbonate sequences, Shark Bay, Western Australia. American Association of Petroleum Geologists Memoir 22, 358.

Longley, I.M., Buessenschuett, C., Clydsdale, L., Cubitt, C.J., Davis, R.C., Johnson, M.K., Marshall, N.M., Murray, A.P., Somerville, R., Spry, T.B., Thompson, N.B., 2002. The North West Shelf of Australia—a Woodside perspective. In: Keep, M., Moss, G.S.J. (Eds.), The Sedimentary Basins of Western Australia 3: Proceedings of PESA Symposium, Perth, pp. 27–88.

Moore, L.S., Burne, R.V., 1994. The modern thrombolites of Lake Clifton, Western Australia. Phanerozoic Stromatolites II, pp. 3–29.

Munsell, A.H., 1954. Munsell soil color chart. U.S. Dept. Agriculture. Soil Survey Manual 2009 Edition Munsell Soil Chart.

Nahas, E.L., Pattiaratchi, C.B., Ivey, G.N., 2005. Process controlling the position of frontal systems in Shark Bay, Western Australia. Estuarine, Coastal and Shelf Science 65, 463–474.

Nakata, M., Lambeck, K., 1990. Late Pleistocene and Holocene sea-level change in the Australian region and mantle rheology. Geophysical Journal International 96, 497–517.

O'Leary, M.J., Hearty, P.J., McCulloch, M.T., 2008. U-series evidence for widespread reef development in Shark Bay during the last interglacial. Palaeogeography, Palaeoclimatology, Palaeoecology 259, 424–435.

Parker, J.H., 2009. Taxonomy of foraminifera from Ningaloo Reef, Western Australia. Association of Australasian Palaeontologists. Canberra. Memoir 39.

Playford, P.E., 1990. Geology of the Shark Bay area, Western Australia. In: Berry, P.F., Bradshaw, S.D., Wilson, B.R. (Eds.), Research in Shark Bay: Report of the France–Australe Bicentenary Expedition Committee. Western Australian Museum, Perth, pp. 13–31.

Playford, P.E., Cockbain, A.E., 1976. Modern algal stromatolites at Hamelin Pool, a hypersaline barred basin in Shark Bay, Western Australia. In: Walter, M.R. (Ed.), Developments in Sedimentology. 20. Elsevier Scientific Publishing Company, pp. 389–411.
Playford, P.E., Cockbain, A.E., Berry, P.F., Roberts, A.P., Haines, P.W., Brooke, B.P., 2013. The geology of Shark Bay. Geological Survey of Western Australia, Bulletin 146, 281.
Preen, A.R., Marsh, H., Lawler, I.R., Prince, R.I.T., Shepherd, R., 1997. Distribution and abundance of dugongs, turtles, dolphins and other megafauna in Shark Bay, Ningaloo Reef and Exmouth Gulf, Western Australia. Wildlife Research 24 (2), 185–208.
Rao, C.P., 1996. Modern Carbonates: Tropical, Temperate and Polar, Introduction to Sedimentology and Geochemistry. Tasmania, Australia (206 pp.).
Read, J.F., 1974. Carbonate bank and wave built platform sedimentation, Edel Province, Shark Bay, Western Australia. In: Logan, B.W., Read, J.F., Hagan, G.M., Hoffman, P., Brown, R.G., Woods, P.J., Gebelein, C.D. (Eds.), Evolution and Diagenesis of Quaternary Carbonate Sequences, Shark Bay, Western Australia. American Association of Petroleum Geologists Memoir 22, pp. 250–282.
Sadler, P.M., 1981. Sediment accumulation rates and the completeness of stratigraphic sections. Geology 89 (5), 569–584.
Schopf, J.W., 1993. Microfossils of the Early Archean Apex chert: new evidence of the antiquity of life. Science 260, 640–646.
Scoffin, T.P., 1970. The trapping and binding of subtidal carbonate sediments by marine vegetation in Bimini Lagoon, Bahamas. Journal of Sedimentary Petrology 40, 249–273.
Stuiver, M., Polach, H.A., 1977. Discussion: reporting of $^{14}C$ data. Radiocarbon 19, 355–363.
Stuiver, M., Reimer, P.J., 1993. Extended $^{14}C$ database and revised CALIB radiocarbon calibration program. Radiocarbon 35, 215–230.
Stuiver, M., Reimer, P.J., Reimer, R.W., 2005. Calib 5.0 program and documentation. URL: http://radiocarbon.pa.qub.ac.uk/calib/.
Tovaglieri, F., George, A.D., 2014. Stratigraphic architecture of an Early–Middle Jurassic tidally influenced deltaic system (Plover Formation), Browse Basin, Australian North West Shelf. Marine and Petroleum Geology 49, 59–83.
Twiggs, E.J., Collins, B.C., 2010. Development and demise of a fringing coral reef during Holocene environmental change, eastern Ningaloo Reef, Western Australia. Marine Geology 275, 20–36.
van de Graaff, W.J.E., Hocking, R.M., Butcher, B.P., 1983, Yaringa, Western Australia: Geological Survey of Western Australia, 1:250 000 Geological Series Explanatory Notes, 23 pp.
Verduin, J.J., Backhaus, J.O., 2000. Dynamics of plant flow interactions for the seagrass *Amphibolis antarctica*: field observations and model simulations. Estuarine, Coastal and Shelf Science 50 (2), 185–204.
Walker, D.I., 1985. Correlations between salinity and growth of the seagrass *Amphibolis antarctica* (labill.) Sonder & Aschers., in Shark Bay, Western Australia, using a new method for measuring production rate. Aquatic Botany 23 (1), 13–26.
Walker, D.I., 1990. Seagrass in Shark Bay, Western Australia. In: Berry, P.F., Bradshaw, S.D., Wilson, B.R. (Eds.), Research in Shark Bay: Report of the France–Australe Bicentenary Expedition Committee. Western Australia Museum, Perth, Australia, pp. 101–106.
Walker, D.I., Dennison, W.C., Edgar, G., 1999. Status of Australian seagrass research and knowledge. In: Butler, A., Jernakoff, P. (Eds.), Seagrass in Australia. Strategic Review and Development of an R & D Plan, CSIRO Collingwood, pp. 1–24.
Walker, D.I., Woelkerling, Wm.J., 1988. Quantitative study of sediment contribution by epiphytic coralline red algae in seagrass meadows in Shark Bay, Western Australia. Marine Ecology — Progress Series 43, 71–77.
Walker, D.I., Kendrick, G.A., McComb, A.J., 1988. The distribution of seagrass species in Shark Bay, Western Australia, with notes on their ecology. Aquatic Botany 30, 305–317.
Wilson, C.J., Wilson, P.S., Dunton, K.H., 2012. An acoustic investigation of seagrass photosynthesis. Marine Biology 159 (10), 2311–2322.

***Sea level controls on palaeochannel development within the Swan River Estuary during the Late Pleistocene to Holocene***

Giada Bufarale[1], Michael J. O'Leary[2], Alexandra Stevens[2], Lindsay B. Collins[1]

1 Department of Applied Geology, Curtin University, GPO Box U1987, Perth, WA 6845, Australia
2 Department of Environment and Agriculture, Curtin University, Bentley, Western Australia, 6102

This article is published in CATENA, Volume 153, June 2017, Pages 131-142.

doi.org/10.1016/j.catena.2017.02.008

Catena 153 (2017) 131–142

Contents lists available at ScienceDirect

Catena

journal homepage: www.elsevier.com/locate/catena

# Sea level controls on palaeochannel development within the Swan River estuary during the Late Pleistocene to Holocene

Giada Bufarale [a,*], Michael O'Leary [b], Alexandra Stevens [b], Lindsay B. Collins [a]

[a] Department of Applied Geology, Curtin University, Bentley, WA 6102, Australia
[b] Department of Environment and Agriculture, Curtin University, Bentley, WA 6102, Australia

ARTICLE INFO

*Article history:*
Received 20 July 2016
Received in revised form 31 December 2016
Accepted 9 February 2017
Available online xxxx

*Keywords:*
Wave-dominated estuary
Late Pleistocene
Sea level fluctuations
High-resolution seismic stratigraphy
Swan River palaeochannels
Palaeodrainage evolution

ABSTRACT

High-resolution seismic profiles were conducted across the metropolitan area of the Swan River estuary (Perth, Western Australia) to explore the sub-surficial stratigraphic architecture, down to a depth of about 40 m below the river bed. The acoustic profiles revealed a complex system of palaeochannels where three main unconformities (R1, R2, R3) bound as many seismic units (U1, U2, U3), over the acoustic basement. Integrating these data with sediment borehole analysis, LiDAR data and available literature of the geology and stratigraphy of the area, it was possible to determine the development of these stratigraphic units, in response to Late Pleistocene and Holocene sea level fluctuations and conditioned by pre-existing topography and depositional palaeoenvironments during the last ~130,000 years. The deepest unit (U3) can be interpreted as the Perth Formation, which consists of interbedded sediments that were deposited in a large palaeo-valley downcutting into the underlying acoustic basement (bedrock: Tamala Limestone and Kings Park Formation), under a fluvial to estuarine setting, existing between ~130 and 80 ky BP (in the Last Interglacial).
The middle unit (U2), composed of heterogenic fluvial (possibly lacustrine) and estuarine sediments, represents the Swan River Formation. Similarly to the Perth Formation, the formation infills channels incised in older formations and reflects the hydrogeological conditions linked with sea level fluctuation changes during the Last Glacial low stand. Holocene (last ~10 ky) fluvial and estuarine deposits form the shallowest unit (U1). These sediments have a highly variable internal structure, ranging from heavily layered, filling palaeochannels, to hard and chaotic, atop pre-existing topographic highs. The wave-dominated Swan River system shares several similarities with a number of estuaries worldwide, such as Burrill Lake (NSW, Australia) and Arcachon Lagoon (Aquitaine, France). This research represents the first environmental high-resolution acoustic investigation in the middle reach of the Swan River estuary.



## 1. Introduction

Understanding the geomorphic development and sedimentary evolution of riverine, estuarine and deltaic environments under the high amplitude sea level changes that characterise the Pleistocene and Holocene Epochs has been the focus of a number of studies worldwide.

For instance, research performed along the lower Murray River (South Australia) and the adjacent Lacepede Shelf revealed that the stratigraphic and structural architecture of the area is the product of both climate and sea level variations throughout the Pleistocene and the Holocene, resulting in formation of dunes, karst features and ancient infilled channels and lagoons (i.e. Bourman et al., 2000; Hill et al., 2009). Similarly, sea level fluctuations, together with palaeo-topography, have controlled the Quaternary sequence stratigraphy of the Brisbane River (Queensland, Australia. Evans et al., 1992). Palaeochannels and cut-and-fill structures, formed as a response to sea level changes during the Late Pleistocene and Holocene, have also been widely recognised across Europe, America and Asia, for example along the Atlantic French and Spanish coasts (Chaumillon et al., 2010; Menier et al., 2011; Blanco et al., 2015), the Gulf of Mexico (Anderson et al., 2014), in Tokyo Lowland (Tanabe et al., 2015), and beneath the Mekong River and Red River deltas in Cambodia and Vietnam, respectively (Tamura et al., 2009; Hori et al., 2004).

Here we investigate the role that sea level oscillations, hydrodynamic conditions and pre-existing geomorphological settings had in controlling the development and evolution of the Swan River (SW Australia) during the past ~130 thousand years (ky). The study area differs from the previously mentioned studies in that the immediate coastal region is characterised by a mixed carbonate siliciclastic sedimentary system.

This study aims to construct a more detailed picture of Late Pleistocene and Holocene sequence stratigraphy and sedimentary architecture of the middle reach (Melville Waters) of the Swan River, using high-

* Corresponding author at: Department of Applied Geology, Curtin University, GPO Box U1987, Perth, WA 6845, Australia.
*E-mail address:* giada.bufarale@postgrad.curtin.edu.au (G. Bufarale).

http://dx.doi.org/10.1016/j.catena.2017.02.008
0341-8162/

resolution shallow seismic data, ground truthed with geotechnical borehole data, in order to better understand how changing sea level driven fluctuations (base level) have influenced the evolution of the estuary throughout this period.

### 1.1. Previous work

The Swan River estuary is located in the south west of Western Australia and flows westward through the Perth Metropolitan area, into the Indian Ocean, at the City of Fremantle. Baker (1956) carried out the first scientific study of the Quaternary sedimentation in the Perth Basin, including the Swan River. He produced seven geological cross-sections using borehole data in various bridge and wharf sites (Fig. 1, highlighted in pink). On the basis of these cross-sections and further geotechnical studies (Jones and Marsh, 1965; Ove Arup, 2001; Coffey Geosciences, 2002), Gordon (2003a, 2012) proposed an inferred location of three palaeoriver channel systems within the upper reach and Perth Waters of the Swan River estuary (Fig. 1). In addition, a number of recent geotechnical studies (i.e. Golder Associated Pty Ltd., 2008, 2012) took place along the northern shore of the Swan middle reach (Perth Waters, between the Narrows Bridge and Barrack Square jetties, see Fig. 1) as part of the Elizabeth Quay development, a major waterfront project that involved the construction of an extensive artificial inlet. Boreholes and localised geophysical investigations (subbottom profiling, seismic refraction and electrical resistivity imaging) identified potential palaeochannel structures and a total of three primary seismic reflectors above the bedrock.

These palaeoriver channels represent the geomorphological and sedimentary response of the Swan River estuary to orbitally driven changes in sea level, spanning ~130 ky to present. This period captured the peak of the Last Interglacial (MIS 5e; 127 to 116 ky) with sea levels between 3 and 6 m above present. The period between 110 ky and 80 ky saw sea level oscillating between −10 and −30 m below present (MIS 5d, c, b and a). After 40 ky global cooling saw sea levels fall to around −125 m at the Last Glacial Maximum (LGM), which peaked around 18 ky BP. Global deglaciation after 18 ky saw rapidly rising sea levels reaching near present elevations around 7 ky BP (Bufarale and Collins, 2015).

Thus, sea level-driven changes in base level and the influence this had on fluvial sediment dynamics, together with the pre-existing geomorphology, likely played a major role in controlling the development of the Swan River estuary during the Last Glacial cycle (Churchill, 1959, cf. geological heritage in Chaumillon et al., 2010; Menier et al., 2011).

The sedimentology and geology of the Swan River and its estuary have, so far, been principally studied in a geotechnical context for planning and construction of bridges and harbour works and mainly limited to the middle reach and mouth of the Swan estuary. Much of this data remains largely unpublished, or is present in the form of state government and consultancy reports (e.g. Australian Hydrographic Services, 1971; McKimmie Jamieson and Partners, 1987; Main Roads Western Australia, 1998; Ove Arup, 2001; Coffey Geosciences, 2002; Coffey Geosciences, 2010; Golder Associated Pty Ltd., 2008).

## 2. Geological and regional setting

The Perth Region is located in the south west of Western Australia and stretches between 31° 20′ S (Gingin Brook and Moore River) and 32° 35′ S (South Dandalup River), covering an area of about 4000 km$^2$ (Davidson, 1995). The region is largely occupied by the 30 km wide Swan Coastal Plain, bound to the west by the Indian Ocean and to the east by the north-south orientated Darling, Gingin and Dandaragan Scarps. These scarps represent the western margin of the Darling Plateau, a weathered Archaean crystalline low-relief plain (Davidson, 1995).

The Swan Coastal Plain lies along a passive continental margin and, together with the Rottnest Shelf, represents the surficial sediments of the Perth Basin. Formed as a north-south rift valley during the

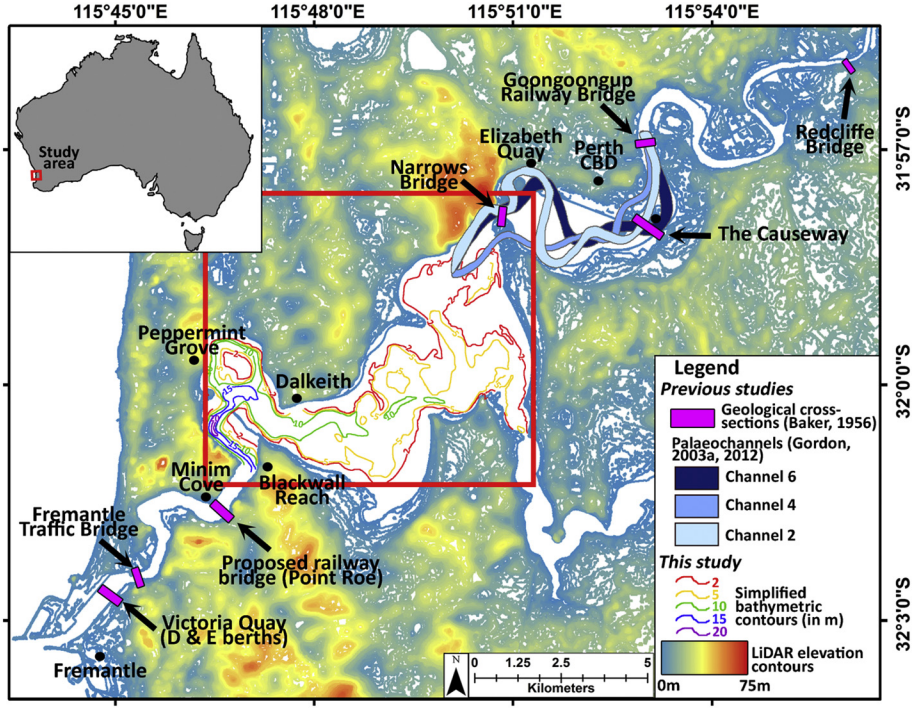


**Fig. 1.** Locality map showing the study area and locations mentioned in the paper. Simplified palaeochannels proposed by Gordon (2003a, 2012) are represented by 3 shades of blue, representing 3 cutting events. Baker's (1956) cross section locations are highlighted in pink. This study focused on the wide, underfilled middle reach of the Swan estuary, whereas Gordon's studies were restricted to the upper reach of the estuary. Simplified bathymetric contours, limited to the studied area, are also shown. (For interpretation of the references to color in this figure legend, the reader is referred to the web version of this article.)
(Source: Department of Transport).

Phanerozoic, the 1000 km long Perth sedimentary basin is infilled by a 15 km thick sequence of continental and marine sediments, from Permian to Late Cretaceous in age (Playford et al., 1976; Kendrick et al., 1991; Commander, 2003). The geological history relevant to the study started in the Early Tertiary, when a Cretaceous river valley or submarine canyon system was inundated and infilled with Palaeocene and Eocene shallow marine to estuarine sediments of the Kings Park Formation (Table 1. Quilty, 1974; Collins, 1987; Hudson-Smith and Grinceri, 2007; Mathew, 2010). Overlaying the Kings Park Formation (onshore) is the >150 m thick Plio-Pleistocene age Kwinana group sediments which comprise marine, fluvial, aeolian, alluvial and lacustrine sediments and record the periodic sea level fluctuations and flooding of the inner shelf and Swan Coastal Plain. The outcropping formations present within the survey area are reported in Fig. 2.

The Swan Coastal Plain is fed from six main drainage basins, the largest of which is the Swan River and includes three major tributaries: the Canning, Avon and Helena Rivers. The Swan River estuary covers a large portion of Perth's northern and eastern urban areas (~40 $km^2$) flowing westward through the Perth Metropolitan area and into the Indian Ocean at the City of Fremantle. In the estuary, the surficial sediments are mainly clastic, ranging from mud (low energy areas, such as the deep central portion of the basin) to sand (higher energy zones, sand flats and beaches. Quilty and Hosie, 2006). A bioclastic component is also present, composed of faecal pellets, foraminifera, whole and fragmented molluscs and other benthic invertebrates (Quilty and Hosie, 2006). Seagrass (*Halophila ovalis*), which covers between 75% and 99% of the shallow waters (<2 m, in the lower reaches of the Estuary), is often associated with coarse, shelly sediments (Hillman et al., 1995).

The Swan River estuary has an open connection to the Indian Ocean and is influenced by local wind-driven waves and, to a smaller extent, by tides (diurnal microtidal range of 0.4 m. Eliot et al., 2006). This system can be regarded as a wave-dominated estuary (Radke et al., 2004). Like the majority of the coastal waterways along the southwestern coast of Australia, the Swan River estuary conforms reasonably well to the wave-dominated estuary facies model (Dalrymple et al., 1992; Radke et al., 2004). In accordance with the Dalrymple et al.'s (1992) model, the Swan estuary is composed of three different morphological components: upper reach, narrow and highly sinuous (river-dominated), middle reach, with a wide and partially filled central basin (mixed energy), and funnel-like shape lower reach (marine-dominated). The reaches are separated by topographic sills which, like in many wave-dominated estuaries (Dalrymple et al., 1992), affect local hydrodynamics, salt wedge propagation and water exchange with the ocean (Stephens and Imberger, 1996; Stephens and Imberger, 1997).

The region is characterised by a dry Mediterranean climate, with precipitation mostly confined to the autumn and winter months (Kennewell and Shaw, 2008). Consequently, the Swan system exhibits a strongly seasonal streamflow with events occurring between May and September, when the rainfall and runoff are higher (Rehman and Saleem, 2014). Marine saline waters can reach up to 35 km upstream but, being mainly controlled by barometric effects, tidal dynamics, storm surge and wind, the penetration of the salt wedge can be observed up to 60 km upstream, under exceptional climatic circumstances (Stephens and Imberger, 1996). Weather conditions also play a very important role in the circulation and main changes in the mean water level of the estuary.

**Table 1**
Stratigraphic column (modified after Smith et al., 2012) and geological formations of the Swan Coastal Plain present within the survey boundaries (refer to Fig. 2 for the surface geology). Note 1: Tamala Sand is the result of weathering and remobilisation of relict material of the Tamala Limestone which has been blown eastward. Note 2: The Swan River Formation can be found along the middle and lower sections of the Swan and Canning Rivers. The development of this formation can be linked to the fluctuations of sea level. The Swan River Formation subcrops the modern Swan River Holocene estuarine and floodplain clays and sands. Note 3: The Perth Formation reflects the complex palaeoclimate and sea level oscillations that characterised the Last Interglacial period. Three main lithological units (sand, silt and clay) were deposited into a palaeochannel eroded during the earlier lower sea level conditions (Penultimate Glacial period) by the ancestral Swan River, into the Kings Park Formation.

| Stratigraphic column | Formation/Deposit | Lithology | Depositional environment | Age | Notes | References |
|---|---|---|---|---|---|---|
| | Alluvial and swamp deposits | Peat and peaty sand, high clay | Alluvial and Swamp | Holocene | | Commander, 2003 |
| | Fluvial deposits | Silt sand, with clay | Fluvial and estuarine | Holocene | | Commander, 2003 |
| | Safety Bay Sand | Fine-medium sand | Near-shore/eolian | Holocene | | Davidson, 1995 |
| | Tamala Sand | Sand, with clay and silt | Near-shore/eolian | 25 to 15 ky BP | See Note 1 in table caption | Bastian, 1996; Gozzard, 2007a |
| | Swan River Fm | Sand, silt and clay | Heterogenic fluvial and estuarine | 75 to 18 ky BP | See Note 2 in table caption | Gozzard, 2007a |
| | Perth Fm | Interbedded sand, silt and clay | Estuarine to fluvial | 130 to 80 ky BP | See Note 3 in table caption | Gozzard, 2007a |
| | Tamala Limestone | Coarse to medium-grained, mostly cross-bedded calcarenite, with minor lenses of clay and gravel-sized lithoclasts | Eolianites, beachrocks, shallow marine beds, coral reefs and marl | Strongly diachronous; Mid-Late Pleistocene to Holocene | The Tamala Limestone has several members and within the study area, the marine units of Minim Cove Member and Peppermint Grove Member outcrop along the foreshore of the Swan River estuary near Point Roe | Murray-Wallace and Kimber, 1989; Brooke, 2001; Gordon, 2003b |
| | Bassendean Sand | Sand, with lens of clay | Fluvial to estuarine | Middle to Late Pleistocene | Bassandean Sand interfingers to the east with Guildford Fm | Gozzard, 2007b |
| | Gnagara Sand | Very poorly sorted sand | Fluvial to estuarine | Middle Pleistocene | Stratigraphic equivalent of the Guildford Formation | Gozzard, 2007a |
| | Ascot Fm | Shelly calcarenite, silty clay | Marine prograding shoreline | Late Pliocene to Early Pleistocene | Some sections contain fresh-water gastropods (proximity of lake/swamp?) | Kendrick et al, 1991 Gozzard, 2007a |
| | Guildford Fm | Mainly clay and silt, with also lenses of poorly sorted sand and conglomerate | Fluvial, with shallow-marine and estuarine lenses | Early Pleistocene to about 130 ky BP | General fining-upwards sequence, almost without interruption | Davidson, 1995; Gozzard, 2007a; Gozzard, 2007b |
| | Kings Park Fm | Shale, calcareous sandstone and minor limestone | Shallow marine to estuarine deposits | Early Tertiary Palaeocene - Lower Eocene | 600 m thick valley-fill. The marine shale facies may be related to an old submarine canyon that converged in the ancestral Swan River | Quilty, 1974; Collins, 1987; Hudson-Smith and Grinceri, 2007; Mathew, 2010 |

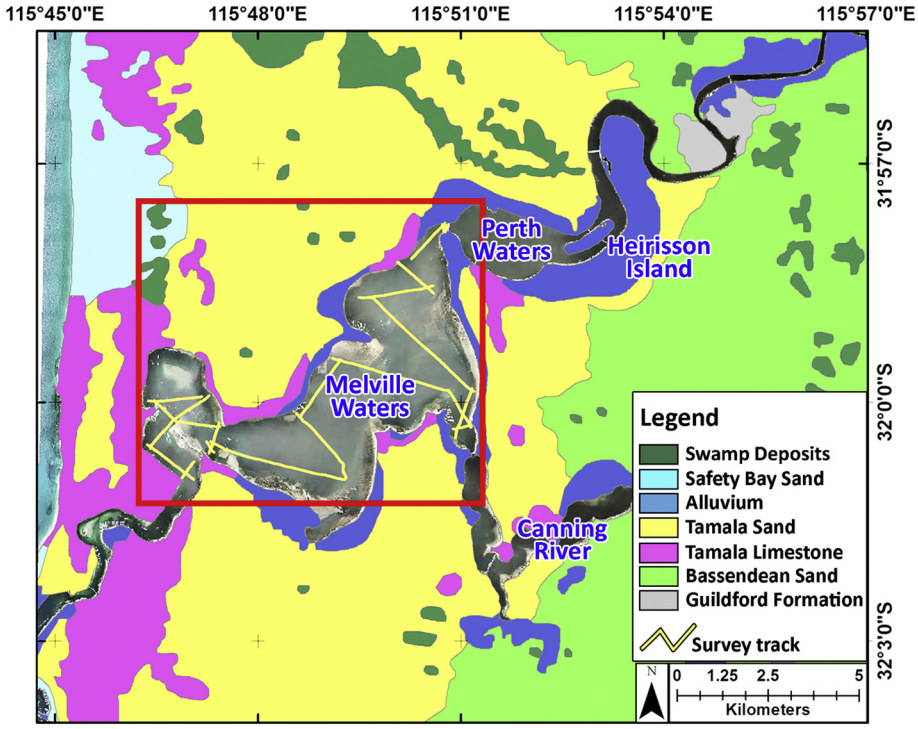


**Fig. 2.** Simplified surface geology (redrawn after Davidson, 1995 and Gozzard, 2007a), superimposed on Landgate (Western Australia) aerial image. Formation ages are included in Table 1. Geophysical survey track plot and survey boundaries are also marked, in yellow. (For interpretation of the references to color in this figure legend, the reader is referred to the web version of this article.)

### 2.1. Estuary morphology

Two shallow sills (<5 m depth), one at the Fremantle Traffic Bridge and the other between the Narrows and The Causeway bridges (see Fig. 1 for location), divide the system into three main segments, the upper reach, middle reach and lower reach:

**Upper Reach** – In the upper section of the estuary, upstream from Heirisson Island (see Fig. 2), the tidal river is narrow and sinuous, with a depth ranging from <2 m to about 6 m (Chalmer et al., 1976; Atkinson and Klemm, 1987).

**Middle Reach** – The middle sector of the estuary includes *Perth Waters* and *Melville Waters* (see Fig. 2). Between the Narrows and The Causeway bridges (Perth Waters), the Swan River estuary is wide and very shallow, with an average lowest water level of <1 m. From the Narrows bridge to Blackwall Reach (Melville Waters), the river is more extensive, with a central basin (that according to Dalrymple et al., 1992 can be called *unfilled estuary*) that deepens seaward, reaching 24 m of depth, and marginal shallow sand flats and spits fringing the shoreline (see Fig. 1. Chalmer et al., 1976; Collins, 1987; Quilty and Hosie, 2006).

**Lower Reach** – The lower segment, downstream from Blackwall Reach to the Fremantle Traffic Bridge, was defined by Quilty and Hosie (2006) as a "coastal dune limestone corridor". In this last section, the Swan estuarine passage is characterised by a narrow straight that follows the joints and structures in the limestone, forming right angles and cliffs through the Tamala Limestone. In contrast to the middle reach, this portion of the estuary shallows seaward, to <5 m, at the Fremantle Harbour.

Although the exact geological nature of these sills is unknown (no seismic data was collected along these features and pre-existing literature is scarce), it is likely that they formed under a combination of pre-existing topography and more recent sediment accumulations (as in Dalrymple et al., 1992; Dalrymple and Choi, 2007).

It must be noted that harbour development, dredging and foreshore reclamation, dating back to the end of the 19th Century (Tutton, 2003), have significantly changed many areas of the Swan River estuary (Chalmer et al., 1976; Collins, 1987; Radke et al., 2004). The removal of sediment buildup and rocky outcrops, especially at the estuary mouth, caused an increase in marine water intrusion, tidal exchange and salinity, resulting in a proliferation of marine aquatic plants (Hodgkin and Hesp, 1998). Urbanisation and agriculture have also had an impact on the sediment transport and composition, causing significant changes in runoff and inputs of salt, nutrients and sediments in the estuary (Atkinson and Klemm, 1987; Hamilton et al., 2001).

## 3. Methods

About 30 km of high-resolution shallow seismic profiles have been collected, processed and analysed along the Swan River estuary, between the Narrows Bridge and Blackwall Reach (Fig. 2, survey track plot sketched in yellow). Survey run lines were devised to capture a range of substrate architectures and geometries, to a maximum depth of 40 m below the river bed. Transects perpendicular to the river course revealed the location and width of buried palaeochannels. Profiles along the strike of the river permitted the correlation and interpretation of acoustic horizons.

The seismic data were acquired using an AA201 boomer system (Applied Acoustic Engineering Limited, Great Yarmouth, UK). A hand-held GARMIN eTrex Global Positioning System (GPS) was employed to obtain and record position (accuracy: typically <4 m). The seismic data were digitally recorded in SegY format (Rev 1), using SonarWiz 5 (V5006.0032. Chesapeake Technology Inc., Mountain View, CA) as acquisition and post-processing software.

Acoustic reflectors have been interpreted, where possible, through sedimentary analysis and correlation of borehole logs, which were drilled by a number of agencies primarily for geotechnical investigations (Main Roads Western Australia, 1998; Golder Associated Pty Ltd., 2008; see Gordon, 2012). The most recent of these were 4 boreholes cored near Dalkeith for the Perth Flying Squadron Yacht Club by Coffey

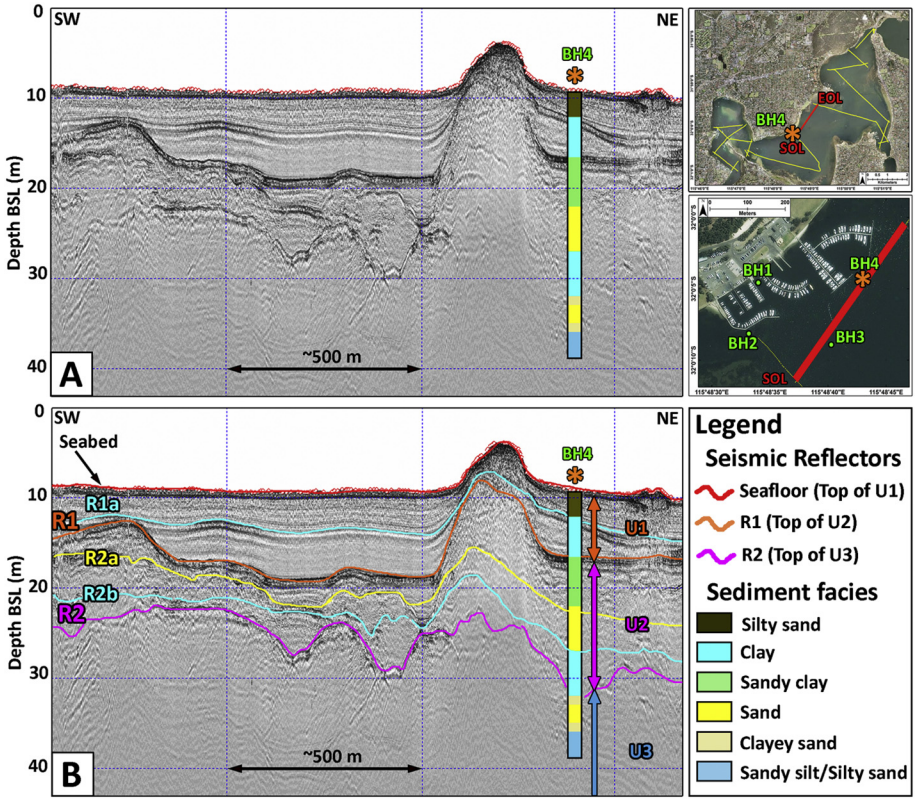


**Fig. 3.** Seismic profile adjacent to the Perth Flying Squadron Yacht Club (Dalkeith), showing two sets of palaeochannels. A: uninterpreted seismic profile, with schematic core. B: interpreted seismic profile. R1 represents the main reflector, at the base of intensely bedded deposits (U1). R2 has been incised into an older substrate and covered by tripartite sediments (U2). From this seismic profile it is not possible to depict the base of the unit (U3) underlying the acoustic reflector R2. Aerial photo images provided by Landgate (Western Australia). Depths are in metres, below the sea level.

(Coffey Geosciences, 2010; see Fig. 1 for location and Fig. 3). The data was also correlated with the information provided by two geophysical surveys, undertaken by Australian Hydrographic Services (1971) and McKimmie Jamieson and Partners (1987) as part of a proposed dredging and reclamation project, in the Outer and Inner Harbour in Fremantle.

Formations and sediment ages were acquired from literature, in particular Murray-Wallace and Kimber (1989), Hearty (2003), Gozzard (2007a), Gordon (2012), and Brooke et al. (2014). Due to the characteristics, scope and planning of the core drilling, we were unable to carry out any radiocarbon dating specific to this project. Palaeomorphology reconstruction of the Last Glacial Swan River was performed with ArcGIS 10.2 software (Esri) using a combination of seismic profiles and bathymetric data of the modern river floor (from Swan and Canning River 2010–2011 Hydrographic Surveys, Department of Transport).

## 4. Results and interpretation

The seismic analysis of the subbottom profiles shows that the shallow architecture underneath the Swan River estuary is dominated by palaeochannels. The seismic profiles contain numerous acoustic reflectors, some of which have distinctive features and can be recognised across the study area, and others which are discontinuous and only recorded in some locations. Four main reflectors (river bed, R1, R2 and R3) were identified, which define three acoustic units (U1, U2 and U3), which sit atop of the acoustic basement (Table 2). In some places, there was no penetration beyond the river bed surface.

### 4.1. Seismic units and sedimentary facies

#### 4.1.1. Seismic unit U1

Subbottom profiles reveal an irregular but laterally continuous, strong reflector, here defined as R1. The sediments bound between the river bed and R1 form seismic unit 1 (U1). U1 has a variable thickness ranging from being barely discernible to up to 14 m thick and is characterised by a number of different seismic features. Where thicker than 2.5 m, U1 is intensely bedded and typically infills palaeochannels. The layers are parallel to subparallel and pinch out updip (divergent fill), converging against pre-existing highs. Minor reflector R1a runs

**Table 2**
Facies identified in the seismic profiles.

| Seismic unit | Limits | Max Thickness | Internal structure | Lithology | Interpretation (see further details in Section 4.2) |
|---|---|---|---|---|---|
| U1 | River bed to R1 | 14 m | From heavily layered, filling palaeochannels, to hard and chaotic, atop of pre-existing topographic highs | From silty sand to clay | Holocene, fluvial channel-fill deposits |
| U2 | R1 to R2 | 27 m | Inhomogeneous (beds or without internal structure) | Sand, silt and clay | Swan River Fm. |
| U3 | R2 to R3 | 21 m | Interbedded | Sand, silt and clay | Perth Fm. |
| Acoustic basement | Top: R3 | NA | Laminated to massive | – | Tamala Limestone/Kings Park Formation |

sub-parallel to the seafloor and is useful to subdivide U1. The strata of the upper sub-unit are thinner (up to 0.30 m of thickness), more laminated and laterally more continuous than in the lower sub-unit (up to 1 m). The Dalkeith boreholes (Coffey Geosciences, 2010) show the upper sub-unit to be mainly composed of thinly bedded unconsolidated silty sand, with mainly horizontal or gently undulated laminations (Fig. 3). In contrast, the lower sub-unit consists of thick bedded clay units, which are horizontally layered over the pre-existing topographic lows, such as channels or depressions. In the zones where unit U1 is thinner than 2.5 m, the substrate appears to be harder and more cemented, with no internal layering.

*4.1.2. Seismic unit U2*

From the seismic profiles, a second and deeper seismic reflector, which is here defined as R2, can be observed. It has an irregular surface, mostly forming depressions, separated by areas of hill-like undulating bathymetry; flat areas are rare. Bounded between reflectors R1 and R2, is an older sequence, named here seismic unit U2, and directly underlies seismic unit U1. U2 is inhomogeneous, characterised by a series of internal, moderate to strong acoustic reflectors, which are locally discontinuous (Fig. 3). Based on the borehole data (Coffey Geosciences, 2010), seismic unit U2 can be subdivided into three sub-units. This *tripartition* is evident also in the seismic profiles, where 2 sub-reflectors (R2a and R2b) can be recognised (Fig. 3). The lower sub-unit (between R2b and R2) is composed of parallel, partially continuous strata of firm to stiff clay (Coffey Geosciences, 2010), with traces of sand, fills minor stream channels and cuts into the underlying older deposits. Locally, this deeper sub-unit is capped by a poorly defined sequence where compacted sand is the main component (middle sub-unit, bound by R2a and R2b). This sub-unit is partially truncated by the overlaying, semi-horizontal sandy clayey deposits (upper sub-unit, bound by R1 and R2a). The three sub-units are intermittently visible in the seismic profiles, but this absence may be more ambiguous than real, possibly due to a lack of velocity contrast between their lithologies.

In some areas, R1 and R2 (and relative acoustic units) have been locally depicted as inferred reflectors (i-R1 and i-R2, see further in Section 5.1), since their seismic pattern was masked by an acoustic wipe-out on the subbottom profiler record. This type of signal has been recorded also in tie lines, confirming that this pattern is a real feature in the sediments.

*4.1.3. Seismic unit U3*

Due to equipment limitation and lack of acoustic contrast in the local lithology, the substrate below the reflector R2 is less definite. There are several discontinuous internal reflectors that cannot be accurately depicted as they are intermittent and quite irregular. Between Dalkeith and Blackwall Reach, a gently undulating third acoustic reflector (here name R3) is definite enough to be depicted (Fig. 4). The geotechnical data (Coffey Geosciences, 2010) regards the deposits between reflectors R2 and R3, which form the seismic unit U3, to include interbedded horizons of silt, sand and clay. U3 is characterised by discontinuous and irregular minor internal reflectors; concave-up, onlapping strata are also locally recognisable.

*4.1.4. Acoustic basement*

The acoustic basement lies below seismic unit U3. Capped by the reflector R3, the acoustic basement is characterised by minor seismic reflectors that disappear progressively with depth, indicating a strong absorption of the acoustic energy, likely suggesting a hard and compacted lithology.

*4.2. Interpretation of the seismic data*

High-resolution subbottom profiles have revealed a complex buried palaeochannel network within the middle reach of the Swan River estuary, allowing for a detailed analysis of the architecture of the palaeodrainage within the study area.

Based on these newly acquired seismic profiles, available sedimentary analysis (Coffey Geosciences, 2010) and literature of the geology and stratigraphy of the area (Gordon, 2003a; Gordon, 2003b; Gozzard, 2007a; Gozzard, 2007b; Gordon, 2012; technical reports: McKimmie Jamieson and Partners, 1987; Golder Associated Pty Ltd., 2008, 2012), the depositional history of the Swan River estuary from Late Pleistocene to present comprises three phases, resulting in three 3 different lithostratigraphic units, from the oldest to most recent the 1) Perth Formation (U3), 2) Swan River Formation (U2), and 3) the Holocene (U1).

A number of studies have demonstrated that sea level fluctuations linked with Glacial and Interglacial periods are the primary control in the sedimentary development and evolution of fluvio-estuarine depositional environments (Blum and Tornqvist, 2000; Lambeck and Chappell, 2001; Blum et al., 2013). The impact of repeated sea level oscillations

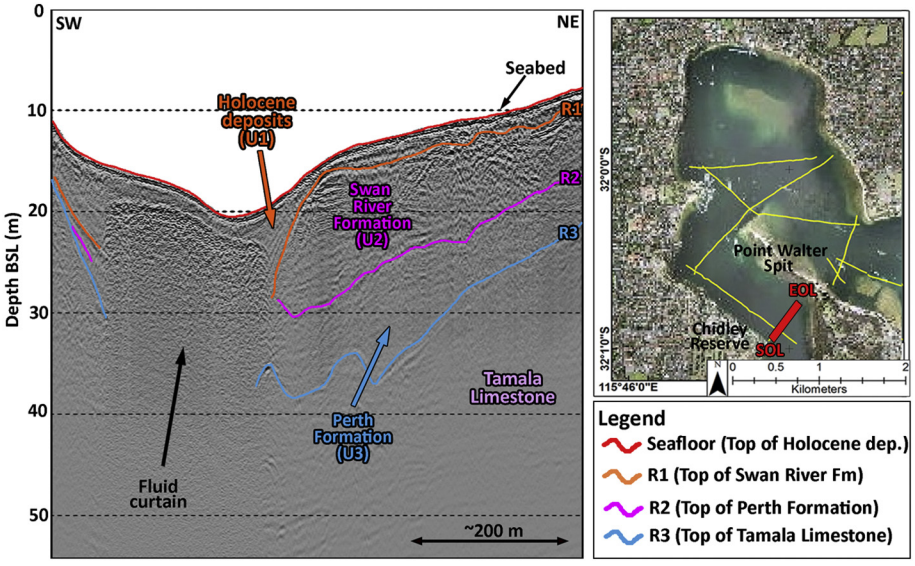


**Fig. 4.** Seismic profile showing the top of the acoustic basement (Tamala Limestone) forming a topographic low, successively partially infilled by more recent formations. Tamala Limestone outcrops on both the shores of the Swan River (Chidley Reserve and Point Walter Spit) and the upper limit can be picked also along the seismic profiles. The channel-like geometry of the basement has conditioned the modern bathymetry. Note the fluid curtain rising from Tamala Limestone (see further discussion on the nature of these fluids in Section 5.1). Aerial photo images provided by Landgate (Western Australia). Depths are in metres, below the sea level. SOL: start of line, EOL: end of line.

has also had a major influence in the development of the Swan River estuary, as evidenced in the subaerial landscape and buried features along the present river course (Hearty, 2003).

*4.2.1. Acoustic basement*

There are two sedimentary units that form the acoustic basement of the study area: Tamala Limestone (western part of the survey area) and the Kings Park Formation (eastern part of the survey area). In the western portion of the Melville Waters, where the Swan River estuary narrows and the water depth increases (from 5 to >20 m), Tamala Limestone is observed outcropping along both the river banks. On the western bank (SOL, Fig. 4) the cliff of Chidley Reserve is >20° steep and the limestone cliff continues below the water level. On the eastern bank (EOL, Fig. 4) the shore has, instead, a gentle slope, outcropping in the Point Walter Spit. This morphology is reflected in the bathymetry (see Fig. 1) and the subbottom profiles acquired in the area corroborate this observation. In Fig. 4, reflector R3 (top of Tamala Limestone) is in fact shallow, at the start and at the end of the line (17 and 21 m, below sea level, respectively), and progressively deepens to almost 40 m below sea level in the central part of the profile, forming a topographic low, partially infilled by the more recent formations.

A few kilometres upstream, near the Narrow Bridge, the incised shales/siltstones of the Kings Park Formation are found under the Perth Formation (Coffey Geosciences, 2002; Golder Associated Pty Ltd., 2008, 2012). From the seismic profiles, the horizontal extent and upper and lower contacts of Tamala Limestone and the Kings Park Formation are not detectable.

*4.2.2. Perth Formation*

The deepest palaeochannel identified in the Swan River seismic profiles was interpreted as a downcutting, into the underlying Tamala limestone and Kings Park formations (acoustic basement). Although it is not possible to depict this erosional surface (acoustic reflector R3) for the entire study area, the log data from the drilling between Goongoongup Bridge and Victoria Quay Berths confirms that it deepens uniformly from Guildford to Fremantle (Baker, 1956; Gordon, 2012).

At the onset of the Last Interglacial (LIG), between 135 and 127 ky, the sea level swiftly rose about 100 m and reached at least 2 m above the present sea level by 127 ky BP (Stirling et al., 1995; O'Leary et al., 2008). The riven downcutting experienced during the previous Glacial period ceased with the rise of base level and onset of estuarine sedimentation (net deposition). The incised palaeovalley was infilled with at least 20 m of interbedded estuarine sand, silt and clay deposits. According to Gozzard (2007a), Mathew (2010) and confirmed by the lithological facies analysis from the boreholes collected by Coffey Geosciences (2010) in Dalkeith, and the other available geotechnical information (Golder Associated Pty Ltd., 2008, 2012), it is likely that the deposits between the reflector R2 and R3 represent the *Perth Formation* (U3). This fluvial and estuarine complex constitutes the fill of a palaeovalley, aligned with the present Swan River estuary. The basal part of the Perth Formation, consisting mainly of clay sediments, was deposited in the lower portion of the palaeochannel. The middle portion is dominated by sandy and coarser sediments, indicating a greater energy and volume of the palaeo-Swan River. In the upper and younger section, the Perth Formation is composed of silt and clay, deposited in a quieter estuarine environment. Mathew (2010), through X-ray Diffraction (XRD) analysis and Scanning Electron Microscope (SEM) imaging, showed that the upper deposits of this formation have a large amount of iron-stained grains of kaolinite and quartz, possibly derived from the erosion, transport and successive deposition of the granite forming the Darling Scarp during warm and humid climate conditions.

Gozzard (2007a) assigned an age of ~130–80 ky to the Perth Formation, by correlating it to previous studies (Murray-Wallace and Kimber, 1989; Kendrick et al., 1991) that dated the marine fauna sampled from exposures along the middle and lower reaches of the Swan River, which can be can be considered the marine equivalent of the estuarine Perth Formation.

*4.2.3. Swan River Formation*

The peak of the Last Interglacial (sub-stage MIS-5e; c. 127–116 ky) was followed by ~40 ky (from MIS 5d until MIS 5a, about 80 ky ago) of general cooling (Lambeck et al., 2002; Hearty, 2003; Woodroffe and Webster, 2014). This progressive reduction of the temperatures culminated about 18 ky BP, when the sea level reached its lowest stand at −130 m below the present sea level (Last Glacial Maximum, LGM. Hearty et al., 2007; Lambeck et al., 2014). During this low stand period, the ancestral Swan River had another episode of downcutting (Fig. 5A). The seismic profiles revealed the presence of a second palaeochannel, incising into the Kings Park and Perth Formations. The morphology and pattern of the palaeo-riverine bottom, where detectable, appear to be quite different from that of the present river floor. The river gradient was significantly higher than the present following the termination of the LIG and prior to the onset of the LGM, extending in the study area, from −9 m below the present river level to −40 m, with a difference in height of ~30 m, versus <25 m in the present time (the deepest

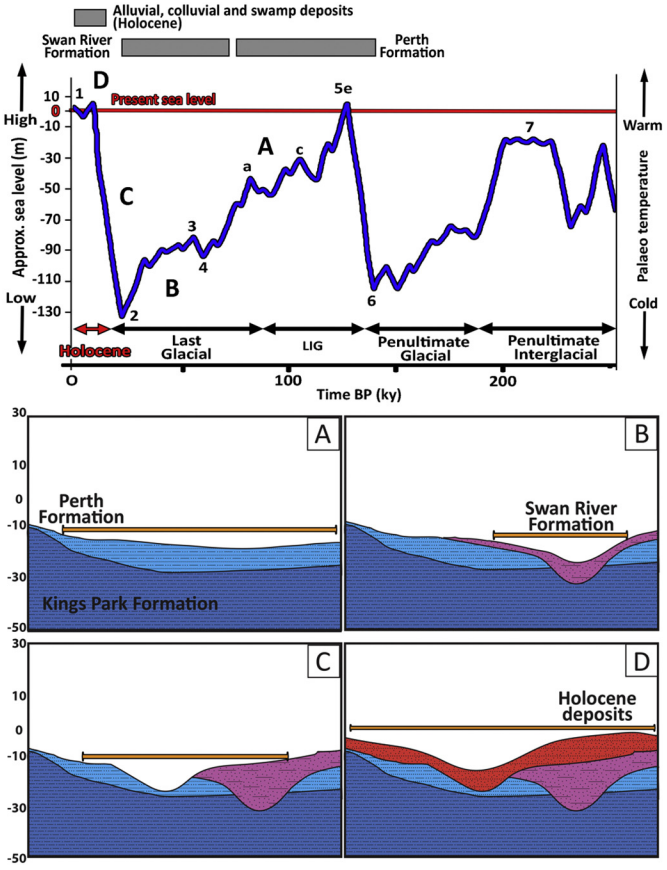


**Fig. 5.** Top: sea level curve in the past 250 ky. Odd numbers refer to Interglacial Marine Isotope Stages (MIS) and even numbers indicate the Glacial MIS (modified after Lisiecki and Raymo, 2005; Berger, 2008 and Saqab and Bourget, 2015). Bottom: schematic cross-section showing the evolution of the morpho-stratigraphy in the middle reach of the Swan River (Melville Waters) through the Late Quaternary, based on seismic profiles and Gozzard (2007a). Horizontal axis: ~3 km; vertical axis: depth/elevation values are in metres, referred to the present sea level. Orange lines represent the width of active valley. A) During the Last Glacial period, a deep inset valley cut the pre-existing Kings Park Formation and Perth Formation, during a low sea level stand. B) Changes in sea level caused by fluctuations in the climate during the last 50–70 ky of this Glacial period resulted in an alternation of erosion and deposition during which the palaeochannel was filled with the variegate sediments of the Swan River Formation. C) Last Glacial Maximum (MIS 2, ~18 ky BP). As the sea level reached its lowest point, the most recent palaeochannel was cut and successively (D) infilled with fluvial deposits through the Holocene interglacial conditions.

surveyed point is 24 m, between Peppermint Grove and Minim Cove). This difference can be explained as a typical fluvial response to sea level changes (i.e., change in base level): the palaeochannel had a higher gradient due to the fact that sea level was lower over the Last Glacial cycle with the palaeo-Swan River incising into underlying strata in order to maintain a balance with a lower than the present base (sea) level (cf. Schumm, 1993; Blum and Tornqvist, 2000).

During the LGM, fluviatile heterogenic deposits of sand, silt and clay were deposited under various hydrological settings. From the borehole data (Coffey Geoscience, 2010), the complex nature of the sediments composing the seismic unit U2 is clear and can be referred to Gozzard's (2007a) description of the *Swan River Formation* (Fig. 5B).

The sequence of the Swan River Formation consists of a series of three stacked interbedded deposits, at least 22 m thick (in the survey area), formed in a riverine, estuarine and marine setting (bottom to top). Sand and gravel sediments dominate the upper section of the river (between Guildford and Perth/The Causeway). In the middle reaches, the content of finer sediment (silt and clay in lenses) increases. In the lower portion (in Fremantle) sand, silt and clay take over (Gozzard, 2007a).

*4.2.4. Holocene deposits*

At the peak of the LGM sea level reached its lowest point around 130 m below the present sea level (e.g. Lambeck and Nakada, 1990; Lambeck et al., 2014). The coastline is reasoned to have been at least 12 km westward from Rottnest Island, located 18 km west of Fremantle. The palaeo-Swan River joined the submarine Perth Canyon, approximately 22 km northwest of Rottnest (Playford, 1977), incising into the underlying formations. Due to a greater longitudinal profile gradient, the river started to cut down into the generally horizontally deposited estuarine sediments of the Swan River Formation, down to a depth of 30 m below the present sea level (as determined from the seismic profiles acquired for this study). The morphology of the channel where the Swan River was flowing at the Late Glacial and Early Holocene (Channel 2, Fig. 6) is easily recognised in the seismic profiles along the whole survey area. At the termination of the LGM, the sea level rose and the valley became an estuary; the flow velocity slowed and up to 14 m of deposits was trapped as a palaeovalley-fill along the Swan River. Based on the lowest depth of Channel 2, it is likely that the accumulation of these sediments (unit U1) started to take over around 10 ky ago, when the sea level reached a depth of at least 30 m below the present sea level. U1 represents the most recent deposits of the survey area, formed during the Holocene.

## 5. Geomorphic evolution of the Swan River estuary

During the Last Glacial cycle, the main channel of the palaeo-Swan River (Channel 2, Fig. 6) was deeper and significantly narrower than the present, with the modern shallow areas adjacent to South Perth, Crawley, Ardross and Bicton probably forming emergent fluvial terraces. This palaeoriver was likely to be very fast-flowing, with transport exceeding deposition, resulting in a channel mostly free of finer sediment (at least, in the middle reach). Two shallow islands were probably present (Fig. 6A), linked to buried topographic highs that were overstepped by the river in the Mid-Holocene. Similarly to the modern setting, a palaeo-Canning River flowed into the Swan River (Fig. 6A). Channel 2 is in line with the modern thalweg (Fig. 6A), demonstrating that the sedimentation subsequent to the Holocene sea level rise has only partially filled it. The seismic profiles also show evidence of a distributary channel separating southward from the main stream (Fig. 6B). The abandoned palaeochannel was about 300 m wide and up to 12 m deep. The base has a clear erosional contact, indicating that the channel was active and cutting into the underlying Swan River Formation. During Holocene sea level rise (around 10 ky BP), the first areas to be flooded were the old channels, with sediments that started to infill these palaeochannels, levelling the river bed. Similarly to the profile in

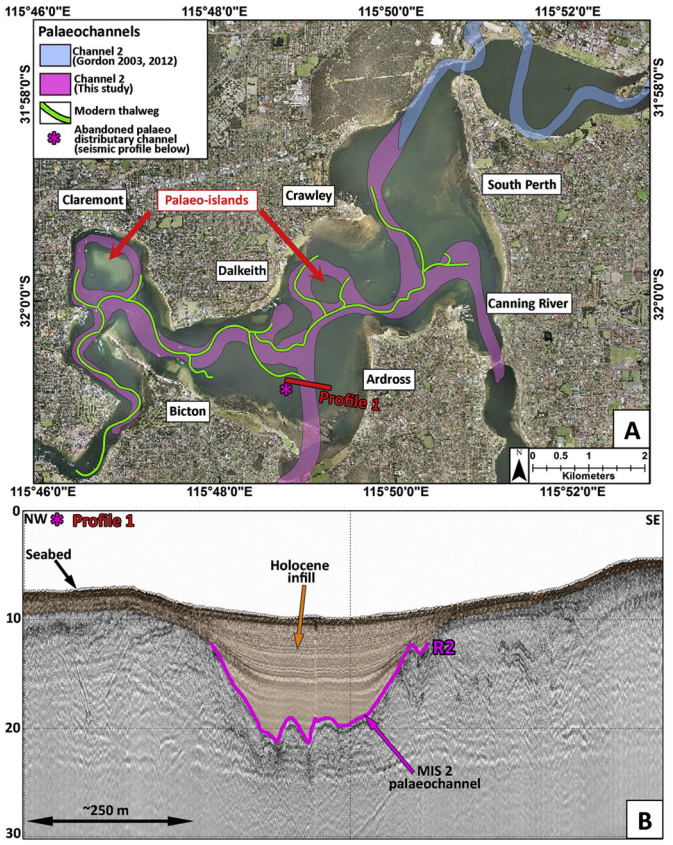


**Fig. 6.** A: sketch map of the palaeomorphology of Channel 2. The modern thalweg is marked in green. Although the modern and palaeo Swan River have a similar trend, the MIS 2 palaeochannel was likely significative narrower than the contemporary one. Aerial photo provided by Landgate (Western Australia). B: acoustic profile of the abandoned tributary. Depths are in metres, below the sea level. (For interpretation of the references to color in this figure legend, the reader is referred to the web version of this article.)

Fig. 3, there is a subdivision of the Holocene infilling sediment. The lower portion (5–7 m thick) appears to be composed of clay, arranged in thick layers and could indicate a phase when the channel was partially abandoned, causing a reduction of the water flow. The upper sediments (~5 m of thickness) appear to be constituted by unconsolidated sandy silty and thinly laminated, possibly corresponding to a stage of intermittent flow, progressively converted to channel abandonment. Considering the amount of deposition, it is likely that a substantial volume of water was flowing in the tributary channel, capable of carrying a large quantity of sediments, until the palaeo-waterway become inactive.

Based on high-resolution topographic (elevation) data of the region (see Fig. 1), it is not possible to locate the alternative pattern of the ancestral tributary channel across the Swan Coastal Plain due to the large eolian dune build-up and extensive urbanisation; however, with a further seismic survey along the coastline, it may be possible to detect where the palaeochannel extended towards the shelf.

*5.1. Fluid blankets*

In some locations, seismic units U1, U2 and U3 appeared partially concealed by an acoustic wipe-out (Fig. 7). The masking is likely to have been caused by absorption of the seismic signal due to fluid escape from underlying deposits. This pattern, called fluid blankets or fluid curtains in relation to the volume of fluid content, is associated with thick sediment deposits in valley bottoms, palaeochannels or buried depressions (Baltzer et al., 2005). The origin and processes of this fluid-flow is still poorly understood, but it could possibly be linked to a

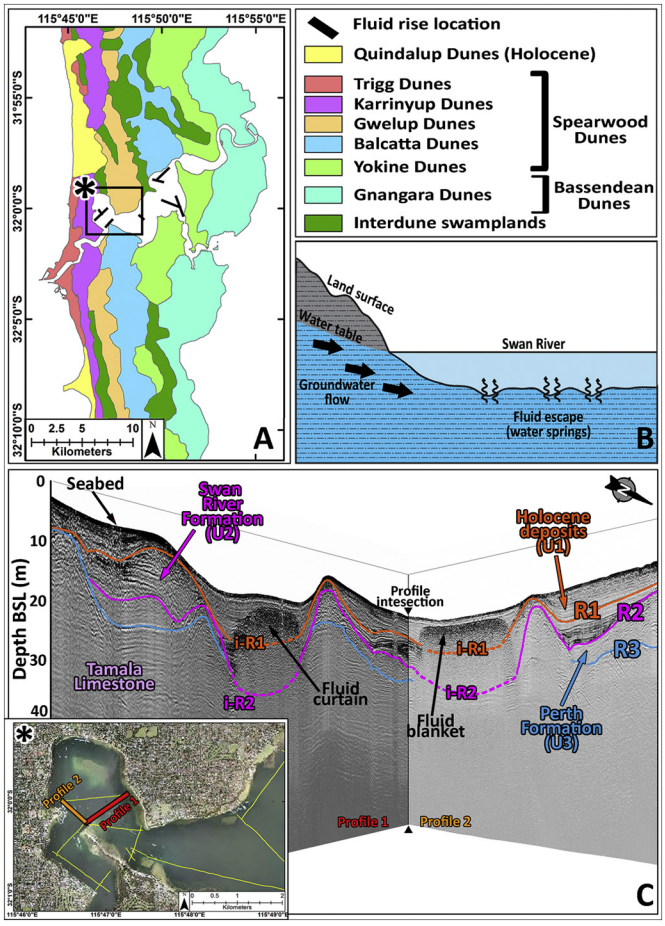


**Fig. 7.** A: Dune systems in the Swan Coastal Plain (re-drawn after Bastian, 1996). Note the north-south trend of the dune system. The locations where fluid rise was recognised in the seismic profiles are marked in black. The rectangle indicates the inset area in Fig. 7C. B: Schematic diagram illustrating the formation of fluid escape in the hypothesis of the presence of subaqueous springs (profile not to scale). In late winter, after heavy rainfall, the water table is higher. These conditions result in the groundwater having a greater pressure of and consequent formation of seepage that flows into the Swan River. Details are discussed in the text. C: Intersecting cross-section between Profiles 1 (length: ~1000 m) and Profile 2 (length: ~650 m). Areas where there is a fluid escape are depicted with dash lines. In this reach, the acoustic basement is likely to be Tamala Limestone. Inset: aerial photo provided by Landgate (Western Australia).

combination of the thickness and nature of the sedimentary deposits in the Swan Coastal Plain and the presence of a high water table.

From the seismic profiles, this kind of structure can be found only in association with the bottom of palaeochannels, masking their base. Plotting the distribution of these features in the coastal dune systems map, they appear to be approximately aligned with the three interdune wetland belts, which run sub-parallel, with a north-south direction in the coastal plain, both north and south of Perth (Fig. 7A). It is likely that the buried fluid-escape structures are linked with freshwater springs, rising from the unconfined, superficial aquifer that, in the Swan estuarine system, rests on the Kings Parks Formation and Tamala Limestone (Davidson, 1995). In addition, it is worth mentioning that Aboriginal people and early European settlers reported running freshwater springs in the area, especially west of the Narrows Bridge (Kennedy Fountain), where the Old Swan Brewery was built and the permanent high quality water was, in the past, used during beverage production (Vinnicombe, 1992). Considering that the survey was carried out at the end of the winter (September), it is expected that, having been recharged by the seasonal rainfall, the water table had risen creating a water pressure gradient that may have initiated a shallow groundwater flow into subaqueous springs or seeps (Fig. 7B).

This kind of acoustic signature could also be linked with the presence of a biogenic gas, such as methane, derived by the decomposition of organic matter, typical in estuarine environments (Baltzer et al., 2005). It is possible that in the area, a combination of the two occurrences is the cause of the limited imaging of the buried sediment structures. Evidence of fluid rise within the sediments have been found also during a seismic investigation carried out in 2008 along the Perth CBD Foreshore (Golder Associated Pty Ltd., 2008), where the presence of gas prevented the imaging of the sediments in approximately 50% of the study area.

## 6. Comparisons with other palaeo-estuarine systems

The Swan River system fits reasonably well to Dalrymple et al.'s (1992) model of a wave-dominated estuary: a funnel-shaped geometry (differing from the model only at the river mouth, where the pre-existing topography significantly controls its shape), a straight-meandering-straight channel morphology (from the source, going seaward) and a tripartite zonation, as a function of water depth and hydrodynamic conditions, that is reflected in the facies distribution. At present, submerged sandy barriers across the river mouth, typical of a wave-dominated system, are not found in the Swan River estuary, as they were dredged for the Fremantle Harbour reclamation during the Nineteenth century (Tutton, 2003).

The Swan River estuary shares several similarities with a number of estuaries worldwide. Table 3 and Fig. 8 compare the Swan River with analogous environments in Australia (Burrill Lake, NSW) and France (Arcachon Lagoon, Bay of Biscay). Despite diversities in size and shape, the three estuarine water bodies have similar environmental settings, lying on a tectonically stable, wave-dominated coastline, with low tidal ranges (micro- to mesotidal). High-resolution seismic profiles carried out in the three locations revealed a complex internal architecture, characterised by three main episodes of cut-and-fill (Sloss et al., 2006; Allard et al., 2009; this study), that record as many transgressive and regressive events (low stand and high stand stages of sea level). Noteworthily, fluid rise is also present in each location. Sets of palaeochannels are clearly recognisable in the seismic data of the Swan River and Arcachon Lagoon, but not identifiable in Burrill Lake. This may be due to the fact that the latter is the narrowest of the considered environments (Fig. 8C), therefore the lowstand river channel has remained confined and could not migrate during the time.

The main differences include the thickness and the age of the sediments over the bedrock. Arcachon Lagoon has the thinnest sediment package. With only ca 10 m section (Allard et al., 2009), the deposits on top of the rock foundation are about 1/3 thinner than in the other 2 locations (Table 3). This difference can be explained by combining annual rates of coastal retreat and relative sea level rise (Klingebiel and Gayet, 1995). According to Klingebiel and Gayet (1995), coastal erosion along the Arcachon Bay is about 1 to 2 m/year, therefore sediments deposited during recent transgressive events may have not be preserved. In addition, dating of sediment cores have shown that from 5.0 to 2.5 ky BP, the sea level in the area was about at −5 to −4 m below the present, then increased to −2 to −1 m below present sea level in the following 1.5 ky, before slowly stabilising at present time (Klingebiel and Gayet, 1995). Conversely, along the Australian coasts, evidence of a Late Holocene highstand is present, with a sea level about 1 m higher than the present, at 6 ky BP, in both the Swan River and Burrill Lake areas (Lambeck and Nakada, 1990). It is likely that sedimentation has been greater and perpetuated for longer in these locations, resulting in thicker deposits.

## 7. Conclusions

This paper reports the results and new insight of the first environmental high-resolution seismic investigation in the middle reach of the Swan River estuary (Melville Waters). Three major acoustic reflectors and 4 seismic units can be recognised within the survey area,

**Table 3**
Summary of characteristics of three wave-dominated estuaries: Burrill Lake (NSW, Australia), Arcachon Lagoon (Aquitaine, France) and Swan River (WA, Australia).

| | Swan River, south western Australia (this study) | Burrill Lake, south eastern Australia (Sloss et al., 2006) | Arcachon Lagoon, south western France (Allard et al., 2009) |
|---|---|---|---|
| Estuary type | Wave-dominated barrier estuary | Wave-dominated barrier estuary | Lagoon |
| Tidal regime | Microtidal | Microtidal | Mesotidal |
| Morphology | Meandering valley upstream, with a wide central basin and narrow corridor downstream | Relatively shallow and narrow bilobate valley, connected to the ocean by a shoaled sinuous channel | Equilateral triangular shape, with 20-km-long sides and connected to the ocean by a tidal inlet |
| Bedrock | Calcarenite and calcareous siltstone | Permian quartz sandstone and monzonite rock | Mesozoic–Cenozoic sedimentary rocks (Leorri and Cearreta, 2004) |
| Total catchment area | ~120,000 $km^2$ (Swan-Avon catchment. Viney and Sivapalan, 2001) | 80 $km^2$ | 4140 $km^2$ (Castel et al., 1996) |
| Sand barrier at the mouth | Dredged | Yes | Yes |
| Tectonic conditions | Stable | Stable | Relatively stable (Klingebiel and Gayet, 1995) |
| Sediment thickness (over bedrock) | From <1 m to at least 27 m (with limitation from acoustic penetration) | From 2 to up to 30 m | ~10 m |
| Sedimentary succession | *Basal unit* (130 to 80 ky BP): interbedded sand, silt and clay<br>*Middle unit* (75 to 18 ky BP): sand, silt and clay<br>*Top unit* (Holocene): silt sand, with clay | *Basal unit* (Late Pleistocene): quartzose sand.<br>*Middle unit* (Holocene): bipartite. Base: quartzose carbonate-rich sand (7.8 and 7.0 ky BP); top: quartzose sand (4.5 ky BP).<br>*Top unit* (ca. 1000 years to present): sand, with seagrass (downstream); estuarine silty clay, with considerable organic material (central basin); organic-rich sandy mud deposits and seagrass (upstream). | *Basal unit* (older than 7.500 ky BP): coarse-grained sand.<br>*Middle unit* 1 (7.5–5.5 ky BP): coarse sand.<br>*Middle unit* 2 (5.5–2.8 ky BP): sand with shells and clay.<br>*Top unit* 1 (2.8–1.5 ky BP): silt and sand, with shell lags.<br>*Top unit* 2 (1.5 ky BP-present): silts and organic debris |

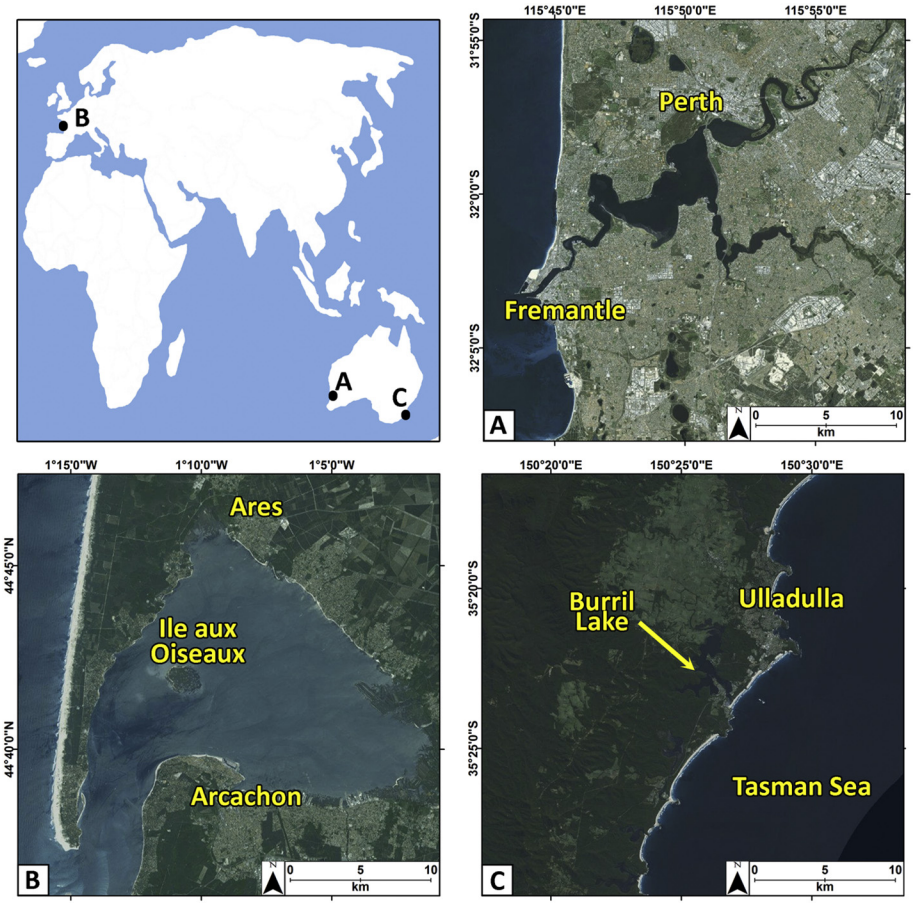


**Fig. 8.** Wave-dominated estuaries of B) Arcachon Lagoon (south western France) and C) Burrill Lake (south eastern Australia) considered for a comparison with the A) Swan River. Note the three locations have been shown with the same scale in order to appreciate better their difference in shape and size, especially between B and C.

forming complex buried cut-and-fill systems (palaeochannels). Combining this data with terrestrial LiDAR data, pre-existing literature and sedimentological analysis, it has been possible to characterise the buried palaeochannels in terms of their seismic architecture, geomorphology and facies, providing a better understanding of the development and evolution of the estuary, as primarily driven by sea level rise and fall during the Late Pleistocene and Holocene. Relative ages of depositional episodes were determined from pre-existing literature and analysis of the sea level curve.

1) *Pre-LIG* (*Mid–Late Pleistocene lowstand*): the palaeo-Swan River flowed through a large valley (acoustic reflector R3), downcutting into the underlying bedrock (acoustic basement), which comprises Tamala Limestone, to the western part of the survey area, and Kings Park Formation, to the east.
2) *LIG to LGM*: a rapid sea level rise (135–127 ky BP, sub-stage MIS-5e) marked the transition from riverine to estuarine setting, with a consequent increment of sediment deposition. The incised palaeovalley was infilled with tripartite deposits of Perth Formation (U3. From bottom to top: clay, silt and alluvial sand). Following the termination of the Last Interglacial highstands (127 to 80 ky, until MIS 5a), an orbitally driven reduction in global temperatures (Last Glacial period) caused a drop in sea level, during which the ancestral Swan River had another episode of downcutting. A narrow and deep palaeochannel incised the Perth Formation and the underlying bedrock (R2) and was successively infilled with estuarine and alluvial deposits of the Swan River Formation (U2), until the sea level reached its lowest position at −130 m below present (LGM), by 21 ky BP.
3) *LGM to Holocene*. During the Last Glacial Maximum, a further palaeochannel (Channel 2, R1) was cut. Through the following transgression, when the sea level was at least 30 m below the present level (~10 ky BP), deposition of Holocene sediments (U1) started to infill Channel 2, till reaching the present conditions and becoming an estuary.

Like several other examples around the world, for instance Burrill Lake (NSW, Australia) and Arcachon Lagoon (Aquitaine, France), the geomorphic record of Late Pleistocene and Holocene sea level fluctuations in the metropolitan area of the Swan River is characterised by a series of palaeochannels, which developed during glacial low sea level stands, and related channel-fill deposits which formed during interglacial highstands.

## Acknowledgments

The Swan River Trust and Dr. Sue Osborne are thanked for approving the survey and providing the vessel support for marine operations; CMST researchers (Curtin University), in particular Chella Armstrong and Chandra Salgado Kent (Marine Mammal Observers), Iain Parnum and Malcolm Perry; Neil MacDonald (AAEngineering Ltd.) and Western Advance for the equipment support; Moataz Kordi and Tubagus Solihuddin (Curtin University) during the seismic survey; Dario Vallini (Fremantle Port Authority), Brendan Wright (Golder Associates Pty Ltd.) for allowing access to the previous survey results; Hery Setiawan (Department of Transport, WA) for providing bathymetric datasets; Giovanni De Vita for his technical advice.

This manuscript was considerably improved by comments from Catena editor Gert Verstraeten, Dr. David Menier and two anonymous reviewers. This research did not receive any specific grant from funding agencies in the public, commercial, or not-for-profit sectors.

## References

Allard, J., Chaumillon, E., Féniès, H., 2009. A synthesis of morphological evolutions and Holocene stratigraphy of a wave-dominated estuary: the Arcachon lagoon, SW France. Cont. Shelf Res. 29 (8), 957–969.

Anderson, J.B., Wallace, D.J., Simms, A.R., Rodriguez, A.B., Milliken, K.T., 2014. Variable response of coastal environments of the northwestern Gulf of Mexico to sea-level rise and climate change: implications for future change. Mar. Geol. 352, 348–366.

Atkinson, R.P., Klemm, V.V., 1987. The effects of discharges, effluents and urbanisation of the Swan River. In: Jacob, J. (Ed.), The Swan River Estuary Ecology and Management. Curtin University of Technology, Bentley, pp. 296–313.

Australian Hydrographic Services (AHS), 1971. Western Australia Fremantle Harbour and Approaches Final report of survey, job no. h.325. (Unpublished).

Baker, G.F.U., 1956. Some Aspects of Quaternary Sedimentation in the Perth Basin W.A. M.Sc Thesis. University of Western Australia.

Baltzer, A., Tessier, B., Nouzé, H., Bates, R., Moore, C., Menier, D., 2005. Seistec seismic profiles: a tool to differentiate gas signatures. Mar. Geophys. Res. 26:235–245. http://dx.doi.org/10.1007/s11001-005-3721-x.

Bastian, L.V., 1996. Residual soil mineralogy and dune subdivision, Swan Coastal Plain, Western Australia. Aust. J. Earth Sci. 43:31–44. http://dx.doi.org/10.1080/08120099608728233.

Berger, W.H., 2008. Sea level in the late quaternary: patterns of variation and implications. Int. J. Earth Sci. 97:1143–1150. http://dx.doi.org/10.1007/s00531-008-0343-y.

Blanco, G.F., Rodríguez, G.F., González, L.A.P., Abanades, J., 2015. Morphodynamics, sedimentary and anthropogenic influences in the San Vicente de la Barquera estuary (north coast of Spain). Geol. Acta 13 (4), 279–295.

Blum, M.D., Tornqvist, T.E., 2000. Fluvial responses to climate and sea-level change: a review and look forward. Sedimentology 47:2–48. http://dx.doi.org/10.1046/j.1365-3091.2000.00008.x.

Blum, M., Martin, J., Milliken, K., Garvin, M., 2013. Paleovalley systems: insights from Quaternary analogs and experiments. Earth Sci. Rev. 116, 128–169.

Bourman, R.P., Murray-Wallace, C.V., Belperio, A.P., Harvey, N., 2000. Rapid coastal geomorphic change in the River Murray Estuary of Australia. Mar. Geol. 170 (1), 141–168.

Brooke, B.P., Olley, J.M., Pietsch, T., Playford, P.E., Haines, P.W., Murray-Wallace, C.V., Woodroffe, C.D., 2014. Chronology of Quaternary coastal aeolianite deposition and the drowned shorelines of southwestern Western Australia — a reappraisal. Quat. Sci. Rev. 93:106–124. http://dx.doi.org/10.1016/j.quascirev.2014.04.007.

Bufarale, G., Collins, L.B., 2015. Stratigraphic architecture and evolution of a barrier seagrass bank in the mid-late Holocene, Shark Bay, Australia. Mar. Geol. 359, 1–21.

Castel, J., Caumette, P., Herbert, R., 1996. Eutrophication gradients in coastal lagoons as exemplified by the Bassin d'Arcachon and the Étang du Prévost. Hydrobiologia 329 (1–3), ix–xxviii.

Chalmer, P.N., Hodgkin, E.P., Kendrick, G.W., 1976. Benthic faunal changes in a seasonal estuary of South-Western Australia. Rec. West. Aust. Mus. 4, 383–410.

Churchill, D.M., 1959. Late Quaternary eustatic changes in the Swan River District. R. Soc. West. Aust. 42 (2), 53–55.

Chaumillon, E., Tessier, B., Reynaud, J.-Y., 2010. Stratigraphic Records and Variability of Incised Valleys and Estuaries Along French Coasts. pp. 75–85.

Coffey Geosciences, 2002. Perth Urban Rail Development South West Metropolitan Railway Geotechnical Desk Study (Unpublished).

Coffey Geosciences, 2010. Perth Flying Squadron Yacht Club Geotechnical Desk Study. Unpublished.

Collins, L.B., 1987. Geological evolution of the Swan-Canning estuarine system. In: Jacob, J. (Ed.), The Swan River Estuary Ecology and Management. Curtin University of Technology, Bentley, pp. 9–20.

Commander, P., 2003. Outline of the geology of the Perth region. Aust. Geomech. 38, 7–16.

Davidson, W.A., 1995. Hydrogeology and groundwater resources of the Perth region. West. Aust.: West. Aust. Geol. Surv., Bull. 142.

Dalrymple, R.W., Zaitlin, B.A., Boyd, R., 1992. Estuarine facies models: conceptual basis and stratigraphic implications: perspective. J. Sediment. Res. 62 (6).

Dalrymple, R.W., Choi, K., 2007. Morphologic and Facies Trends Through the Fluvial — Marine Transition in Tide-dominated Depositional Systems: A Schematic Framework for Environmental and Sequence-stratigraphic Interpretation. 81:pp. 135–174. http://dx.doi.org/10.1016/j.earscirev.2006.10.002.

Eliot, M.J., Travers, A., Eliot, I., 2006. Morphology of a Low-Energy Beach, Como Beach, Western Australia. J. Coast. Res. 221:63–77. http://dx.doi.org/10.2112/05A-0006.1.

Evans, K.G., Stephens, A.W., Shorten, G.G., 1992. Quaternary sequence stratigraphy of the Brisbane River delta, Moreton Bay, Australia. Mar. Geol. 107:61–79. http://dx.doi.org/10.1016/0025-3227(92)90069-T.

Golder Associated Pty Ltd., 2008. Geotechnical Investigation, Perth Waterfront Project, Perth Foreshore Western Australia. (Unpublished).

Golder Associated Pty Ltd., 2012. Interpretive Report, Phase 2 Geotechnical Studies, Perth Waterfront Development, Western Australia (Unpublished).

Gordon, F.R., 2003. Sea level change and paleochannels in the Perth area. Aust. Geomech. 38, 85–90.

Gordon, F.R., 2012. Geology of Quaternary Coastal Limestones of Western Australia. Thesis (Ph.D.). Curtin University.

Gozzard, J.R., 2007. A reinterpretation of the Guildford formation. Aust. Geomech. 42 (3).

Hamilton, D.P., Chan, T., Robb, M.S., Pattiaratchi, C.B., Herzfeld, M., 2001. The hydrology of the upper Swan River Estuary with focus on an artificial destratification trial. Hydrol. Process. 15 (13), 2465–2580.

Hearty, P.J., 2003. Stratigraphy and timing of eolianite deposition on Rottnest Island, Western Australia. Quat. Res. 60:211–222. http://dx.doi.org/10.1016/S0033-5894(03)00063-2.

Hearty, P.J., Hollin, J.T., Neumann, A.C., O'Leary, M.J., McCulloch, M., 2007. Global sea-level fluctuations during the last interglaciation (MIS 5e). Quat. Sci. Rev. 26:2090–2112. http://dx.doi.org/10.1016/j.quascirev.2007.06.019.

Hill, P.J., De Deckker, P., von der Borch, C., Murray-Wallace, C.V., 2009. Ancestral Murray River on the Lacepede Shelf, Southern Australia: late Quaternary migrations of a

major river outlet and strandline development. Aust. J. Earth Sci. 56:135–157. http://dx.doi.org/10.1080/08120090802546993.
Hillman, K., McComb, A.J., Walker, D.I., 1995. The distribution, biomass and primary production of the seagrass *Halophila ovalis* in the Swan/Canning Estuary, Western Australia. Aquat. Bot. 51 (1), 1–54.
Hodgkin, E.P., Hesp, P., 1998. Estuaries to salt lakes: Holocene transformation of the estuarine ecosystems of South–Western Australia. Mar. Freshw. Res. 49 (3), 183–201.
Hori, K., Tanabe, S., Saito, Y., Haruyama, S., Nguyen, V., Kitamura, A., 2004. Delta initiation and Holocene sea-level change: example from the Song Hong (Red River) delta, Vietnam. Sediment. Geol. 164 (3), 237–249.
Hudson-Smith, E., Grinceri, M., 2007. Ground conditions and building protection for the New MetroRail City Project, Perth. Aust. Geomech. 42, 33–58.
Jones, P.H., Marsh, J.G., 1965. Some problems in the construction of embankments for the Mitchell Freeway, Perth W.A. Inst. Eng. Aust. J. Vol. CE 7 (2).
Kendrick, G.W., Wyrwoll, K.-H., Szabo, B.J., 1991. Pliocene–Pleistocene coastal events and history along the western margin of Australia. Quat. Sci. Rev. 10 (5), 419–439.
Kennewell, C., Shaw, B.J., 2008. Perth, Western Australia. Cities 25:243–255. http://dx.doi.org/10.1016/j.cities.2008.01.002.
Klingebiel, A., Gayet, J., 1995. Fluvio-lagoonal sedimentary sequences in Leyre delta and Arcachon bay, and Holocene sea level variations, along the Aquitaine coast (France). Quat. Int. 29, 111–117.
Lambeck, K., Nakada, M., 1990. Late Pleistocene and Holocene sea-level change along the Australian coast. Palaeogeogr. Palaeoclimatol. Palaeoecol. 89, 143–176.
Lambeck, K., Chappell, J., 2001. Sea level change through the last glacial cycle. Science 292 (5517), 679–686.
Lambeck, K., Esat, T.M., Potter, E.-K., 2002. Links between climate and sea levels for the past three million years. Nature 419:199–206. http://dx.doi.org/10.1038/nature01089.
Lambeck, K., Rouby, H., Purcell, A., Sun, Y., Sambridge, M., 2014. Sea level and global ice volumes from the last glacial maximum to the Holocene. Proc. Natl. Acad. Sci. U. S. A. 111:15296–15303. http://dx.doi.org/10.1073/pnas.1411762111.
Leorri, E., Cearreta, A., 2004. Holocene environmental development of the Bilbao estuary, northern Spain: sequence stratigraphy and foraminiferal interpretation. Mar. Micropaleontol. 51 (1), 75–94.
Lisiecki, L.E., Raymo, M.E., 2005. A Pliocene–Pleistocene stack of 57 globally distributed benthic $\delta^{18}O$ records. Paleoceanography 20:1–17. http://dx.doi.org/10.1029/2004PA001071.
Main Roads Western Australia (MRWA), 1998. Narrows Bridge Widening Project Report on Survey of Existing Documents Possibly Relevant to Foundation Conditions (Unpublished).
Mathew, G.V., 2010. Analysis and Interpretation of Ground and Building Movements due to EPB Tunnelling. PhD Thesis. University of Western Australia.
McKimmie Jamieson & Partners (Aust) Pty Ltd., 1987. Fremantle Port Authority Geophysical Investigation (Unpublished).
Menier, D., Tessier, B., Dubois, A., Goubert, E., Sedrati, M., 2011. Geomorphological and hydrodynamic forcing of sedimentary bedforms-example of Gulf of Morbihan (South Brittany, Bay of Biscay). J. Coast. Res. 64, 1530.
Murray-Wallace, C.V., Kimber, R.W.L., 1989. Quaternary marine aminostratigraphy: Perth Basin, Western Australia. Aust. J. Earth Sci. 36:553–568. http://dx.doi.org/10.1080/08120098908729509.
O'Leary, M.J., Hearty, P.J., McCulloch, M.T., 2008. Geomorphic evidence of major sea-level fluctuations during marine isotope substage-5e, Cape Cuvier, Western Australia. Geomorphology 102:595–602. http://dx.doi.org/10.1016/j.geomorph.2008.06.004.
Ove Arup, 2001. Geotechnical Perth Convention Centre Desk Study Report to Multiplex Constructions Pty. Ltd. (Unpublished).
Playford, P.E., Cockbain, A.E., Low, G.H., 1976. Geology of the Perth Basin Western Australia. Geol. Soc. West. Aust., Bull. 124.
Playford, P.E., 1977. Part 1, Geology and groundwater potential. In: Playford, P.E., Leech, R.E.J. (Eds.), Geology and Hydrology of Rottnest Island. Geol. Surv. West. Aust. 6, pp. 1–53.
Quilty, P., 1974. Tertiary stratigraphy of Western Australia. J. Geol. Soc. Aust. 21:37–41. http://dx.doi.org/10.1080/00167617408728853.
Quilty, P.G., Hosie, G., 2006. Modern foraminifera, Swan River Estuary, Western Australia: distribution and controlling factors. J. Foraminifer. Res. 36:291–314. http://dx.doi.org/10.2113/gsjfr.36.4.291.
Radke, L.C., Prosser, I.P., Robb, M., Brooke, B., Fredericks, D., Douglas, G.B., Skemstad, J., 2004. The relationship between sediment and water quality, and riverine sediment loads in the wave-dominated estuaries of south-west Western Australia. Mar. Freshw. Res. 55 (6), 581–596.
Rehman, S.U., Saleem, K., 2014. Forecasting scheme for swan coastal river streamflow using combined model of IOHLN and Niño 4. Asia-Pacific J. Atmos. Sci. 50:1–9. http://dx.doi.org/10.1007/s13143-014-0009-61.
Saqab, M.M., Bourget, J., 2015. Controls on the distribution and growth of isolated carbonate build-ups in the Timor Sea (NW Australia) during the Quaternary. Mar. Pet. Geol. 62:123–143. http://dx.doi.org/10.1016/j.marpetgeo.2015.01.014.
Schumm, S.A., 1993. River response to baselevel change: implications for sequence stratigraphy. sJ. Geol. 279–294.
Sloss, C.R., Jones, B.G., McClennen, C.E., de Carli, J., Price, D.M., 2006. The geomorphological evolution of a wave-dominated barrier estuary: Burrill Lake, New South Wales, Australia. Sediment. Geol. 187 (3), 229–249.
Smith, A.J., Massuel, S., Pollock, D.W., 2012. Geohydrology of the Tamala Limestone Formation in the Perth Region: Origin and Role of Secondary Porosity. CSIRO: Water for a Healthy Country National Research Flagship (63 p.).
Stephens, R., Imberger, J., 1996. Dynamics of the swan river estuary: the seasonal variability. Mar. Freshw. Res. 47:517. http://dx.doi.org/10.1071/MF9960517.
Stephens, R., Imberger, J., 1997. Intertidal motions within deep basin of Swan River estuary. J. Hydraul. Eng. 123 (10), 863–873.
Stirling, C.H., Esat, T.M., Mcculloch, M.T., Lambeck, K., 1995. High-precision U-series dating of corals from Western Australia and implications for the timing and duration gradients in the North Atlantic Ocean (321 to 721N) during the last interglacial period. Paleoceanography 14:23–33. http://dx.doi.org/10.1016/0012-821X(95)00152-3.
Tamura, T., Saito, Y., Sieng, S., Ben, B., Kong, M., Sim, I., Choup, S., Akiba, F., 2009. Initiation of the Mekong River delta at 8 ka: evidence from the sedimentary succession in the Cambodian lowland. Quat. Sci. Rev. 28:327–344. http://dx.doi.org/10.1016/j.quascirev.2008.10.010.
Tanabe, S., Nakanishi, T., Ishihara, Y., Nakashima, R., 2015. Millennial-scale stratigraphy of a tide-dominated incised valley during the last 14 kyr: spatial and quantitative reconstruction in the Tokyo Lowland, central Japan. Sedimentology 62 (7), 1837–1872.
Tutton, M., 2003. Engineering geology of Fremantle harbour. Aust. Geomech. 38 (4), 91–102.
Viney, N.R., Sivapalan, M., 2001. Modelling catchment processes in the Swan–Avon river basin. Hydrol. Process. 15 (13), 2671–2685.
Vinnicombe, P., 1992. An Aboriginal site complex at the foot of Mount Eliza which includes the old Swan Brewery building. Hist. Environ. 9 (1/2), 53.
Woodroffe, C.D., Webster, J.M., 2014. Coral reefs and sea-level change. Mar. Geol. 352: 248–267. http://dx.doi.org/10.1016/j.margeo.2013.12.006.

# Appendix B: Additional publications

***Geomorphic patterns, internal architecture and reef growth in a macrotidal, high-turbidity setting of coral reefs from the Kimberley bioregion***

Lindsay B. Collins[1], Michael O'Leary[2], Alexandra Stevens[1], Giada Bufarale[1], Moataz Kordi[1] & Tubagus Solihuddin[1]

1 Department of Applied Geology, Curtin University, GPO Box U1987, Perth, WA 6845, Australia
2 Department of Environment and Agriculture, Curtin University, Bentley, Western Australia, 6102

This is an Accepted Manuscript of an article published by Taylor & Francis in Australian Journal of Maritime & Ocean Affairs- Issue 1: Coast to Coast Conference 2014: Coastal Knowledge for Coastal Change, on 17/05/2015, available online: https://www.tandfonline.com/doi/abs/10.1080/18366503.2015.1021411

## Abstract

The coral reefs of the Kimberley bioregion are situated in an area that is considered a significant 'biodiversity hotspot' and are poorly known and of recognised international significance. This paper is a review of ongoing research as part of one of the first geoscientific reef studies of the Kimberley Biozone. Remote sensing, sub-bottom profiling and associated sedimentological work have been employed to produce a regional geodatabase of coral reefs and determine the Holocene internal architecture and growth history of the coral reefs. Satellite image analysis has revealed that fringing reefs in the Kimberley bioregion grow very well and differ geomorphologically from planar reefs both inshore and offshore. The acoustic profiles have depicted multiple reef build-ups, demonstrating the reefs' long-term resilience. This research has provided a better understanding of the Kimberley reefs and demonstrated their capacity to succeed in challenging environments and generate habitats characterised by high complexity and species diversity.

## Introduction

The Kimberley region is located on the north-western continental margin of Australia (Figure 1) and is characterised by unique and complex geology and geomorphology, significantly influenced by the macrotidal system (up to 11 m), which result in expansive intertidal zones.[1] The Kimberley coastal region is a large-scale ria coast with a well-developed indented rocky shoreline and many offshore islands with unique geology and geomorphology.[2] Regional structure has determined much of the contemporary landforms and related ecosystem development, and controlled the architecture of the drowned landscapes over which coral reef systems have developed.[3] Thus, there are strong geomorphological controls on reef development. Coral reefs have developed over a broad shelf as shelf edge, inner shelf and coastal inshore reefs for over 800 km across a geomorphically complex coastal zone and, whilst the offshore reefs have been studied,[4] little is known about these inshore coastal reefs.[5]

It is not known whether Kimberley reef morphology conforms to the established geomorphic models, such as those identified from the Great Barrier Reef (GBR),[6] or has developed as distinctive morphologies driven by the extreme environmental conditions unique to the Kimberley. Here, regional reconnaissance mapping was used to assess reef morphology within the complex geophysical environments of the Kimberley coast. Questions such as the impact of extreme tides, high terrestrial sediment loads, exposure of the reefs for long periods during the tidal cycle, and relatively warm waters, all remain to be addressed.

While the offshore reefs have grown vertically as successive sea-level events drowned the shelf during the Quaternary, the inshore reefs have interacted with complex antecedent geomorphology during coastal inundation, as well as intermittent terrestrial inputs, developing around and over rocky islands, headlands and platforms. However, patterns of geomorphology and substrates are poorly understood and little documented regionally.[7] It is not known whether most

Kimberley reefs are veneers over rock platforms or are long-lived features, recording processes and patterns of growth, community composition and structure, hiatuses, sea levels and climate changes through post-glacial time (see note 6). Access to such records is needed to determine long-term adaptive responses of Kimberley coral reefs to oceanographic and coastal processes that are near the environmental limits of coral growth.

The primary aim of this project is to understand the past history of coral reef growth for several Kimberley reef types, using a combination of remote sensing, sub-bottom profiling (SBP) and, where possible, reef stratigraphy in order to provide the first geomorphological analysis of the inshore reefs. The analysis will add value to the many Western Australian Marine Science Institution (WAMSI) biological studies being carried out in parallel to this geological investigation. This paper reviews ongoing research in WAMSI Project 1.3.1 on Coral Reef Geo- morphology and Growth History of Kimberley Reefs.

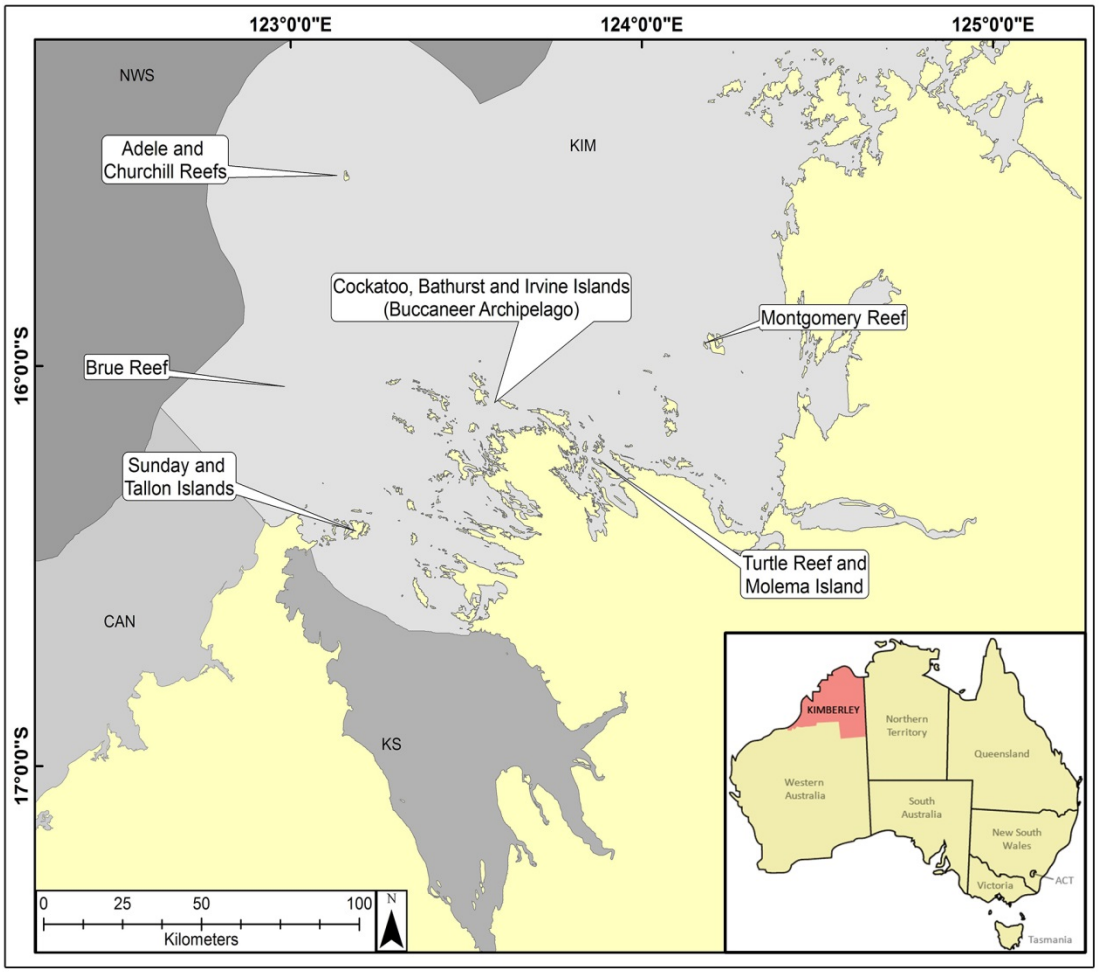


**Figure 1. Map of the Southern Kimberley region. The marine bioregions (Commonwealth of Australia*, A Guide to the Integrated Marine and Coastal Regionalisation of Australia Version 4.0,* Department of the Environment and Heritage, Canberra, Australia, 2006) are shown in grey (NWS: North West Shelf; CAN: Canning; KS: King Sound; KIM: Kimberley). The main reefs studied in this study are labelled, Cock- atoo Reef is in the Buccaneer Archipelago.**

## Materials and methods

In the absence of any previous chronological, stratigraphic and geomorphic data for the inshore Kimberley reefs, three approaches were attempted in related and interactive sub-projects in this study. These were a remote sensing approach used to regionally map the many island and hinterland associated reefs, to analyse geomorphic patterns of reef growth and to determine the living communities and substrates; a targeted stratigraphic and chronologic study of reef growth, using one of the rare reef exposures in a mine pit at Cockatoo Island; and a seismic study to determine reef thickness, the number of stages of reef growth, and an attempt to analyse the regional growth pattern using available chronologic data from the Cockatoo Reef study. These objectives were determined in consultation with agencies responsible for marine park management in the area. The work in this paper is preliminary in nature and ongoing.

### Remote sensing data

Coral reefs occur extensively in the Kimberley Bioregion (KIM), forming major geomorphic features fringing both islands and mainland coasts. Here remotely-sensed images were used to map the spatial distribution of reef habitats and to characterise reef geomorphology. Multiple data sources (see Table 1) were integrated using ESRI's ArcGIS to validate results, which were then verified against ground truth control points in order to produce consistent, accurate habitat and geomorphic maps. Remote sensing data were mainly from Landsat 7 and aerial photography, using unsupervised classification, supported by ground truth whenever available.

**Table 1. Data sources.**

| Data sets | Source of data | Representation |
|---|---|---|
| Kimberley coastline | Satellite images (USGS), Aerial photography (WAMSI) | Polyline |
| Islands | Satellite images (USGS), Aerial photography (DPaW), Bathymetric charts (AHS), Geological maps (GSWA) | Polygon |
| Coral reef | Satellite images (USGS), Aerial photography (DPaW), Bathymetric charts (AHS), Geological maps (GSWA) | |
| | Western Australian Museum Woodside Collection Project (Kimberley) 2008–2011, Brooke, 1995, 1997 and Wilson 2009, 2010 | Polygon, points |
| Seabed geomorphology | Geoscience Australia | Polygon |
| Sea surface temp | NOAA | Polyline |
| Bathymetric map | Geoscience Australia, AHS | Polyline |
| Sub-bottom profiles | Applied Geology Department, CU | Seismic Profiling |
| Weather | Australian Bureau of Meteorology | Vary |

Notes: USGS, U.S. Geological Survey; WAMSI, Western Australian Marine Science Institution; DPaW, Department of Parks and Wildlife; AHS, Australian Hydrographical Service; GSWA, Geological Survey of Western Australia; NOAA, National Oceanic and Atmospheric Administration; AHO, Australian Hydrographic Office; CU, Curtin University.

### Reef and mine pit mapping

The two main iron ore pits on Cockatoo Island have been excavated to a depth of approximately 50 m below sea level and extend out onto the island's modern reef

flat. The fringing reef and the pre-existing substrate have been exposed in a complete vertical section along the face of the pit. Stratigraphic logging, sampling and photographing of the section were completed by Solihuddin, Blakeway, Collins and O'Leary.[8] In order to establish a geochronology of the reef growth, *in situ* coral samples were collected at selected levels and dated using accelerator mass spectrometry radiocarbon dating methods. Dating was recalibrated using CALIB Version 5.0.2, calibration curve Marine04 and calibrated in years Before Present (cal yBP) with 2 σ (68.2%) probability range.

The coral distribution along stratigraphic horizons within the mine pit was compared and correlated with the distribution of living coral communities along the adjacent reef flat and fore-reef slope, using towed camera transects during high tide and on foot during spring low tides (see note 8).

### Sub-bottom profiling

A total of 300km of high-resolution shallow sub-seafloor imaging data was acquired during a sub-bottom profiling (SBP) study, using an AA201 boomer SBP system (Applied Acoustic Engineering Limited, Great Yarmouth, UK). A dual frequency Differential Global Positioning System (DGPS) Fugro SeaSTAR 8200 XP/HP with Trimble Antenna was used to obtain an accurate position (decimetric accuracy). Data were digitally recorded in SegY format (Rev 1), using SonarWiz 5 (Chesapeake Technology Inc., Mountain View, CA) as acquisition and post-processing software.

## Results

### Kimberley reef classification scheme

Before providing an integrated analysis of remotely sensed, stratigraphic and seismic results, it is necessary to propose an organised classification framework for the specialised, macrotidal Kim- berley reefs, which are diverse, and which have unique characteristics.

Previous studies have attempted to apply reef classification schemes developed for the GBR to Kimberley reefs.[9] Although their applicability has been noted, the greater diversity of Kimberley reefs made their use limited. In more recent geoscientific studies,[10] including new reef core data, radiocarbon dating and seismic profiles as well as GIS data allowed the proposal of a new modified classification scheme for the reefs in the Kimberley bioregion (Figure 2).

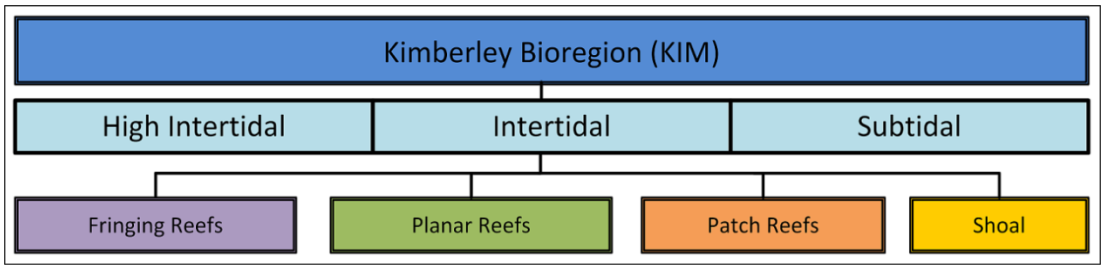

**Figure 2 (previous page). Preliminary reef classification scheme based on adaptation of previous studies and geoscientific data from this study. Modified after Bufarale et al and Kordi et al (see note 10).**

## Geomorphology, habitats and substrates

Preliminary analysis using unsupervised classification of Landsat data, and ground truth observations, of substrate types for the reefs studied to date has shown distinctions between high inter- tidal, fringing, planar and patch reefs. The most striking features of these reefs are the dominance of sand and coral rubble on their reef flat. They are also characterised by a widespread distribution of rhodolith-rich substrates, present as terraces and also near the reef crest. For example, at Montgomery Reef, the reef flat is approximately 30% sand and coral rubble while the reef terraces and crest are about 6% rhodolith dominated substrates (Figure 3).

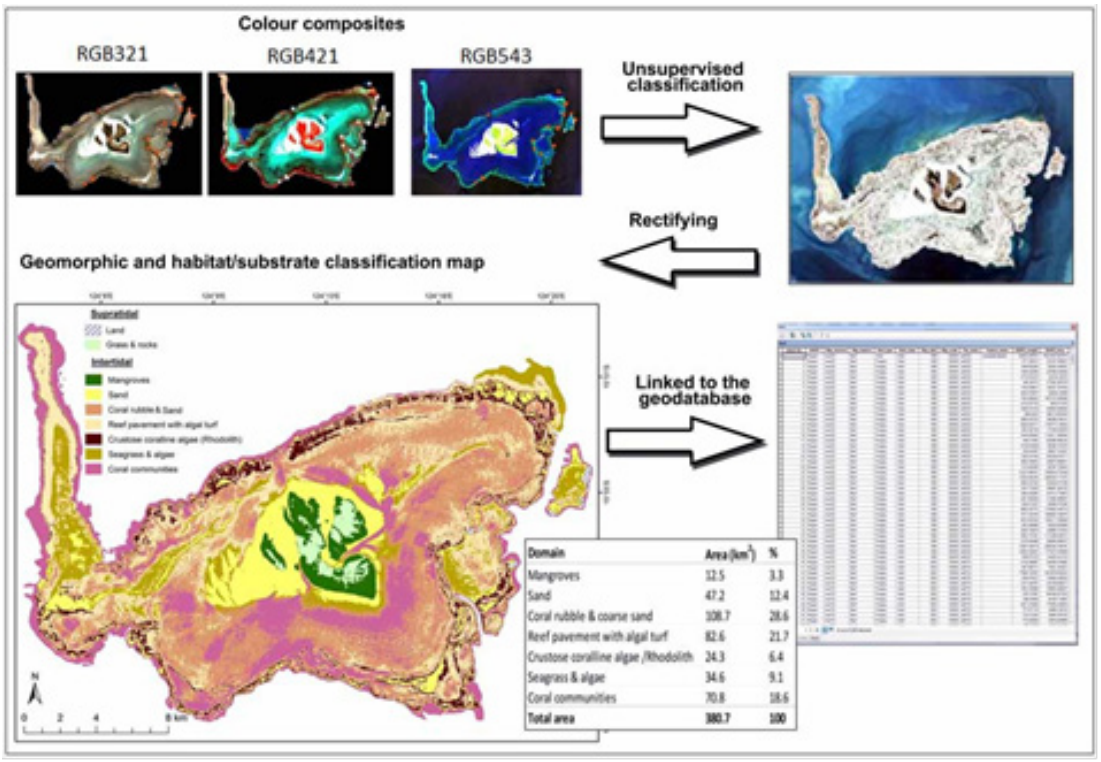


**Figure 3. Example of processing of satellite imagery, for Montgomery Reef (see Figure 1 for location), modified after Kordi et al (see note 10).**

The satellite image analysis has demonstrated that the geomorphic and associated habitats of the inner- to mid-shelf platform reefs have similarities with high intertidal reefs such as the abundance of rhodoliths and coral rubble over the reef platform and the presence of terraced reef flat. The low-gradient fore-reef slope zones in inner- to mid-shelf platform reefs are predominantly colonised by soft and encrusting flat coral and bryozoans, with domal and plate corals becoming significant. This can be seen clearly at Adele Island (see Figure 1 for location), where the coral communities colonising the reef slope represent about 31% of substrates on the platform surface (Figure 4).

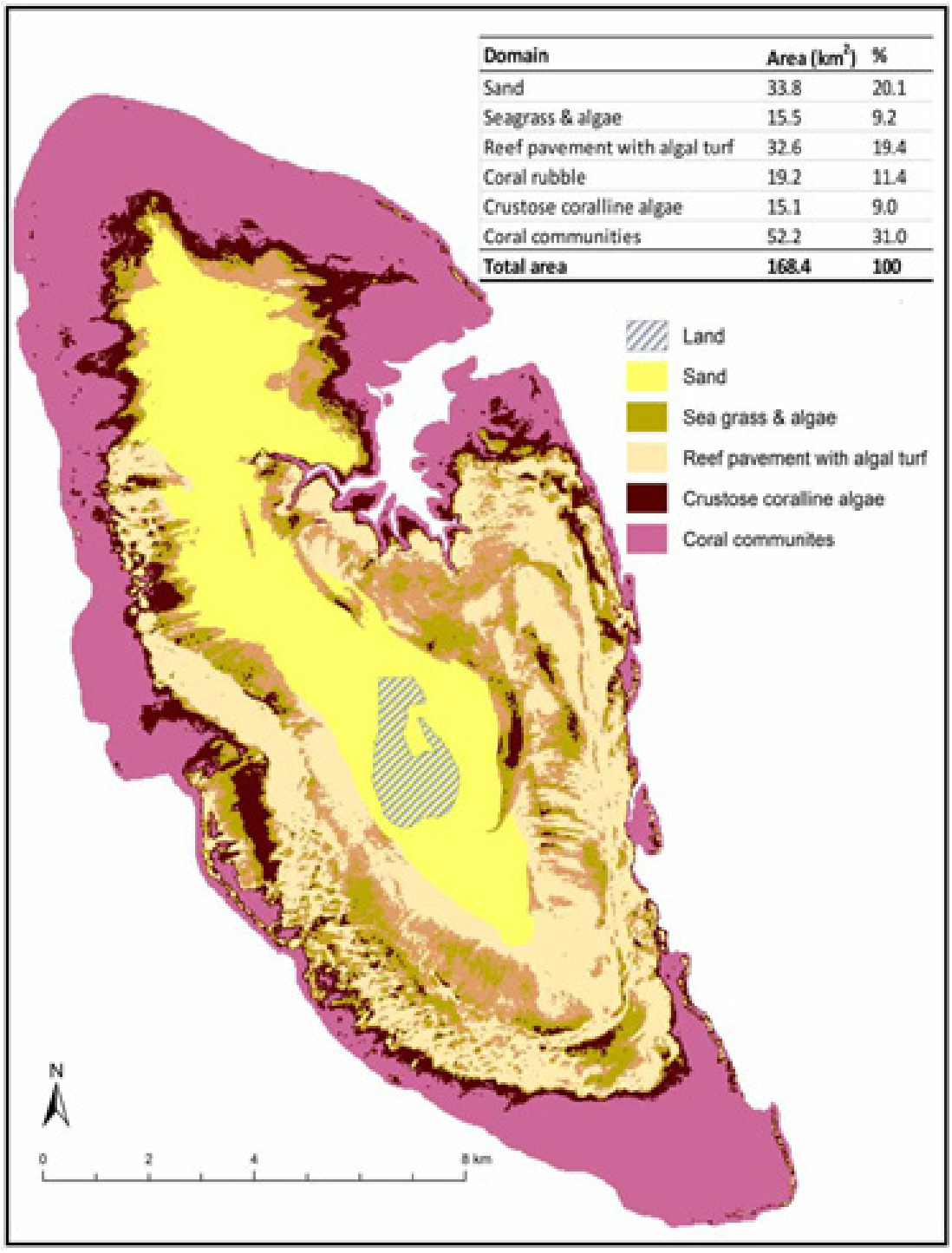


**Figure 4. A preliminarily geomorphic, substrates and habitat map of Adele Reef, surrounding Adele Island. Sample data provided by the REEFKIM database, modified after Kordi et al (see note 10). Coral communities dominate the fore-reef slope. For location, see Figure 1.**

## Stratigraphy and geochronology

Solihuddin, Blakeway, Collins and O'Leary documented stratigraphy and geochronology of mine pits at Cockatoo Island.[11] The following section is based on their results.

Stratigraphic and palaeoecological data, combined with radiometric dates (Figure 5), have revealed that the lower section of the mine pit is Proterozoic basement (Figure 6). A thin layer (1–2 m) of thick sedimentary talus breccia containing haematite boulders separates the basement from a younger coral-rich unit, containing mainly domal corals with minor encrusting and branching forms, dated as belonging to the last interglacial (LIG) (Figure 5). On top of this reef sequence, a second, thinner, haematite boulder breccia layer is present which is overlain by Holocene reef (see note 11). The Holocene reef unit is up to ~13 m thick (Figure 5) and two distinct facies dominate the unit: muddy domal and branching coral framestone. Coral clasts are visually dominated by branching corals mainly of the genus *Acropora* and massive corals including *Porites*; diverse molluscan fauna is also present. Towed camera observations highlighted a few differences between the Holocene and the living reef (see note 11). *Porites* and *Faviids* are the most abundant genus, along with *Sargassum* which sparsely colonises the intertidal coral zone, whilst branching *Millepora* and *Porites cylindrica,* which increase seaward and are not present in the fossil record, have a medium density (see note 11). The contemporary live corals are uncommon in the measured Holocene sections, suggesting that the Holocene reef communities lack reef flat habitat. The Holocene reflects mostly subtidal growth, whereas the present reef is largely intertidal or very shallow subtidal (see note 11).

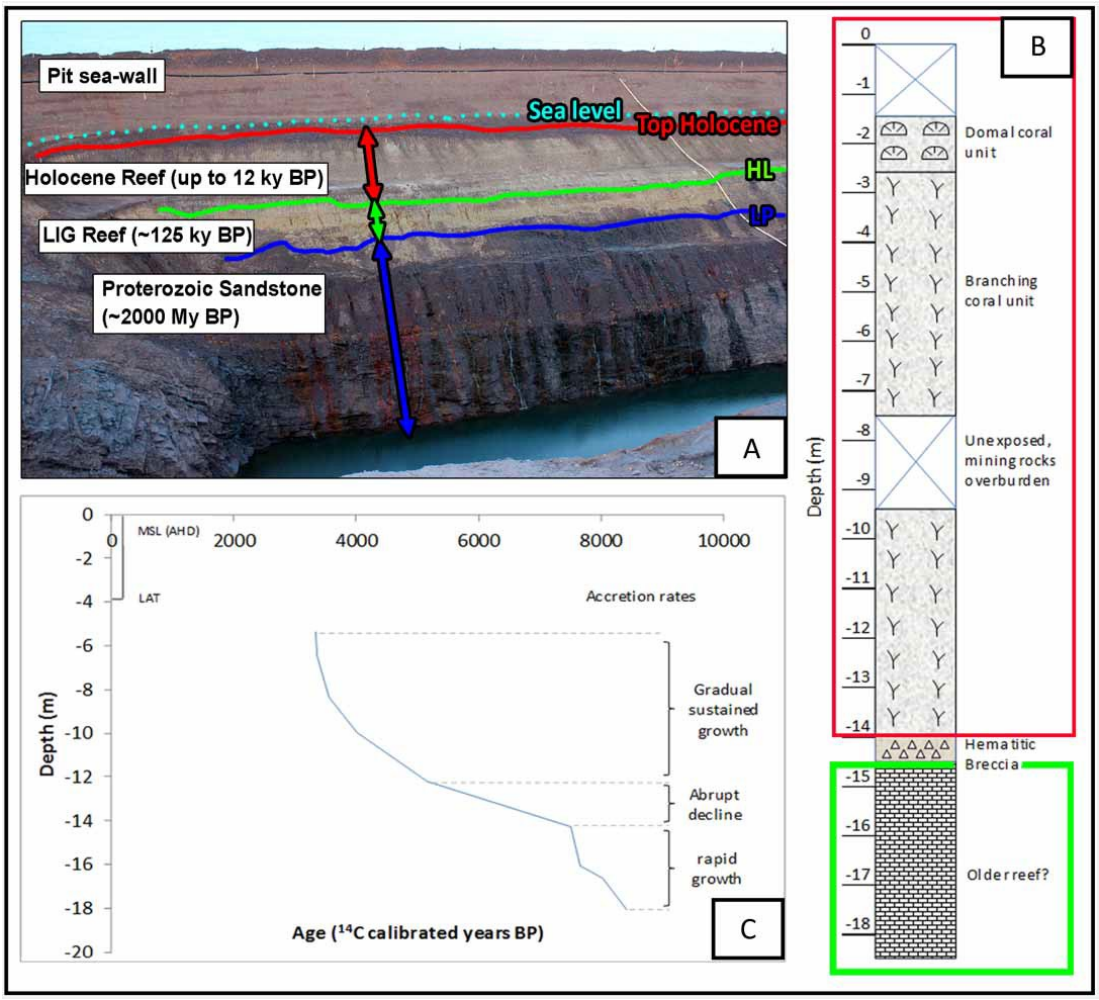

**Figure 5 (previous page). (a) Cockatoo mine pit section, looking SW (refer to Figure 1 for the location). (b) Idealised reef stratigraphic column. (c) Idealised vertical accretion rates. Haematitic breccia marks base of Holocene reef. Older reef is presumed LIG reef. Modified after Solihuddin et al (see note 11).**

Radiocarbon results (see note 11) have indicated that the earliest Holocene reef growth started on the pre-transgressive haematitic breccias, at a depth of ~18 m below mean sea level (bmsl) by approximately nine thousand years before present (ky BP). Vertical accretion rates show initial rapid reef growth after the initial flooding (at 9–8 ky BP), followed by an abrupt decline after about 8ky BP, until about 5ky BP when the accretion rate was low (see note 11). In the following period, the coral accretion showed gradual but sustained growth following sea-level rise closely (Figure 5(c)) (see note 11).

## Seismic facies

New data on Holocene reef growth and its relationship to antecedent foundations of the Kimberley reefs were obtained through a shallow seismic survey. Selected reef sites (Figure 1) were chosen in order to evaluate most of the Kimberley reef morphotypes described in the reef classification scheme (Figure 2). During the post-processing and interpretation of the acoustic data sets, two major acoustic horizons, HL and LP, were recognised based on their relative position, appearance and internal architecture. In mid-ramp reefs (Adele Island), two further deeper seismic reflectors were described. The seismic profiles were calibrated using, for the inner shelf reefs, the mine pit mapping stratigraphy of the proximal part of Cockatoo Island (see note 11)[12] (Figure 6), and for the mid-shelf reefs, palynological and well completion reports for a well drilled in 1982 on the northern tip of Adele Island.[13]

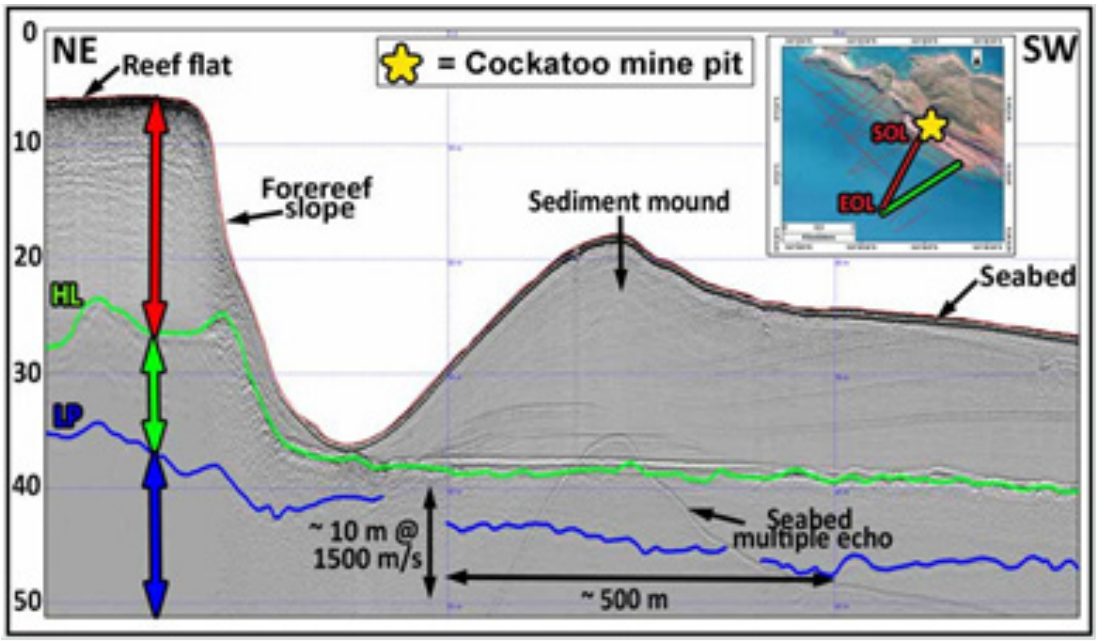


**Figure 6. Seismic profile adjacent to Cockatoo mine pit section (Figure 5(a)) mapped by Solihuddin et al (see note 10) showing the position of Proterozoic (LP, blue), LIG (HL, green) and overlying Holocene reef intervals across the fringing reef (see inset for location of sections. SOL: start of line; EOL: end of line). Note the sediment mound in front of the reef flat. Depth values are in metres, below the sea level. Landgate aerial photography provided by DPaW**

**(modified after Bufarale et al (see note 14)). Note significant subsidence of LIG surface (HL, green).**

The first 150 m of the Adele Island well consists of multiple stacked limestone sequences. Within the equipment range, the seismic profiles (see Figure 7) reveal the presence of four stages of reef build-up, identified as Holocene (Marine Isotope Stage 1 MIS 1, last 12ky BP), LIG (MIS 5e, ~125ky BP), Penultimate Interglacial (MIS 7, ~200 ky BP) and MIS 9 (~300 ky BP), as comparable to the Marine Isotope Curve (Figure 8).

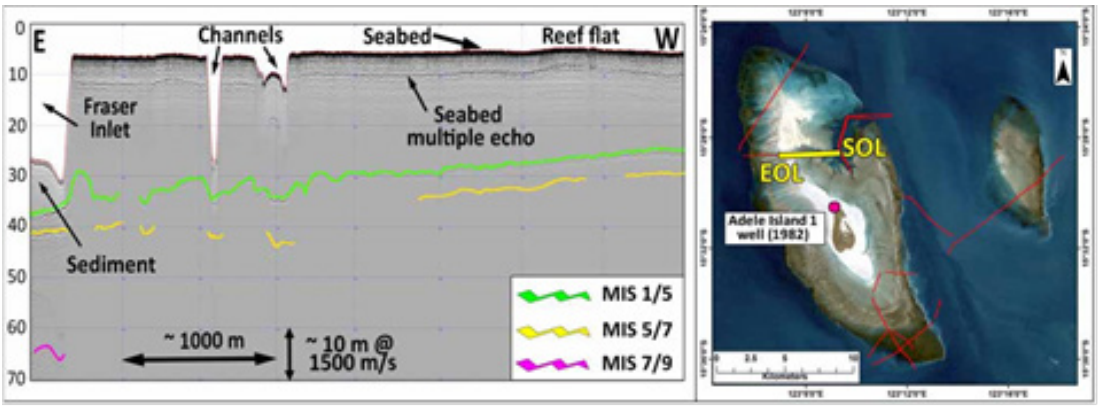


**Figure 7. Left: Profile showing multiple stages of reef build up (MIS 1, 5, 7, 9, respectively) in the northern portion of Adele Reef. Depth values are in metres, below the sea level. Right: Location of the profile (in yellow) and track plot of all the seismic profiles performed in Adele and Churchill reef (in red). Landgate aerial photography provided by DPaW (modified after Bufarale et al (see note 14)).**

Holocene and Pleistocene reef thicknesses vary respectively between 10 and 22 m and 10 and 15 m, in relation to the accommodation locally available (see Bufarale et al[14]): where the Proterozoic rock foundation is shallower, the reef is thinner due to a limited capacity to vertically grow, relative to ultimate sea level (e.g. in Sunday Island). Vice versa, wherever the antecedent substrate is profound, the colonisation could benefit from a greater amount of accommodation (i.e. Montgomery Reef and Cockatoo Reef, Figure 6 and see note 14).

## Conclusion

The Kimberley Coral Reef Geomorphology and Growth History Project researchers are using information and experience gained from participation in WAMSI 1 within the current WAMSI 2 project research. Our data and newly generated products reflect the three areas of activity in the study: remote sensing, SBP and associated sedimentological work.

The work in this paper is preliminary in nature and ongoing. Fringing reefs in the Kimberley bioregion grow very well, despite the inshore Kimberley environment being extremely turbid. Preliminary study using Landsat satellite images reveals that the fringing reefs in the Kimberley bioregion differ geomorphologically from planar reefs both inshore and offshore. The most noticeable distinction is the absence of rhodolith banks and coral rubble over the reef platform as well as reef terraces. The

reef flat which slopes gently seaward consists of intertidal coral, macroalgae and sediment deposits.

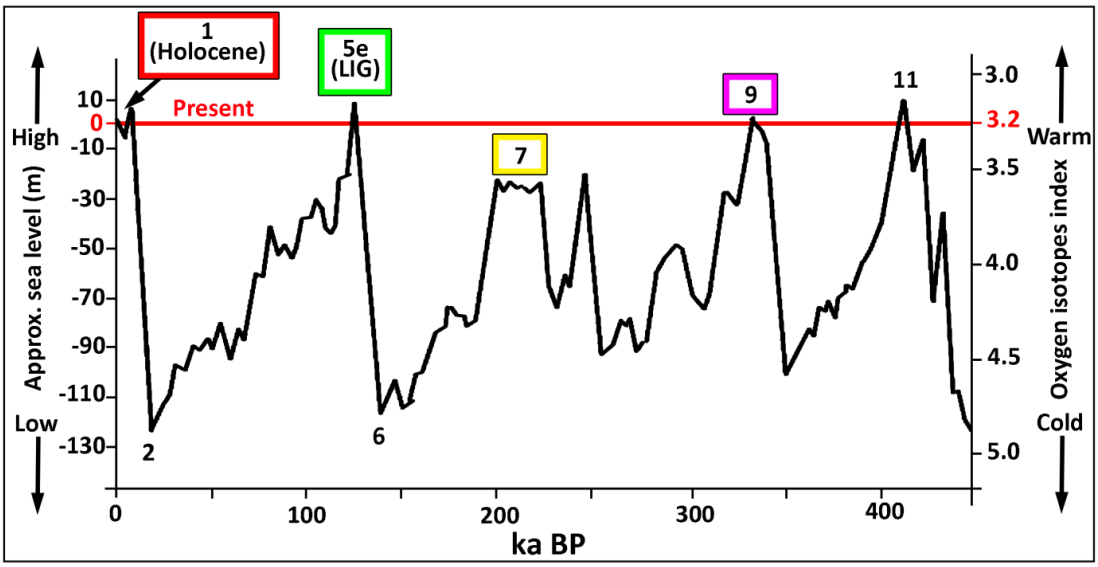


**Figure 8. Marine oxygen isotope index and sea-level changes for the last 500 ky BP (after).15 Inner shelf reefs: Holocene reef (last 12ky BP), LIG reef (~125 ky, MIS 5e) have grown on Proterozoic rock foundation. Mid-shelf reefs: two additional older reef units are identified (~19 ky BP, MIS 7 and ~300 ky, MIS 9).**

The acoustic profiles have depicted two acoustic reflectors across the inner shelf reefs, marking the boundaries between Holocene reef (Marine Isotope Stage 1, MIS1, last 12,000 years) and MIS 5 (last 125,000 years) and an ancient Neoproterozoic rock foundation over which Quaternary reef growth occurred. In the mid-shelf reefs (Adele complex), three acoustic horizons can be characterised. Correlating the seismic data with the reef chronology determined in Cockatoo and Adele Island, it has been possible to highlight the evolution of multiple stages of reef building, stacked by repeated high sea levels (Adele, 3 stages, at least; Sundays Group, Buccaneer Archipelago and Montgomery Reef, 2 stages; some patch reefs, 1 stage). The foundation over which reef growth occurred is the two-billion-year-old land surface seen in many Kimberley islands composed of Neoproterozoic rocks. Thus, Kimberley reefs are not thin growths over bedrock as sometimes postulated recently.

These new data sets have provided a better understanding of reef growth and have demonstrated the reefs' long-term resilience, with multiple reef build-ups, and their capacity to succeed in challenging environments through the late Quaternary. The interaction between complex pre-existing topography, subsidence of the LIG substrates and global sea-level fluctuations, controlled by ice-age fluctuation events, have influenced the successive reef morphology, controlling the available accommodation for reef growth. Simultaneously with these long-term mechanisms, short-term processes such as macrotidal conditions, terrigenous inputs from inland (resulting in high turbidity) and warm ocean temperatures, have contributed to generating a coral-dominated habitat characterised by high complexity and species diversity.

## Acknowledgements

This research was assisted by the Bardi Jawi, Mayala and Dambimangari people through their advice and consent to access their traditional lands and their assistance in some components of the fieldwork. The Cygnet Bay Marine Research Station provided vessel support for marine operations and access to research facilities at Cygnet Bay. James Brown assisted in the planning stage of the project; Dr Erin McGinty capably managed marine operations. Team members wish to thank the following: WA Museum for providing ground truth data through the Woodside Collection Project (Kimberley) 2008 – 2011; Mark Hardman (Fugro Satellite Positioning Pty Ltd) for supplying the DGPS; Neil MacDonald (AAEngineering Ltd) and Western Advance for equipment support; Giovanni De Vita for his technical advice; Richard Costin and Annabelle Sandes (Kimberley Media). Finally, it must be noted that this research was completed in an area where the Traditional Owners have a rich cultural history of climate, land and environment based on thousands of years of habitation. It is important to consider that broad understanding alongside the modern science presented here.

## Funding

The Kimberley Coral Reef Geomorphology and Growth History Project is funded by the Western Australian State Government through the WAMSI.

## Notes

1. GR Cresswell & KA Badcock, ‘Tidal Mixing Near the Kimberley Coast of NW Australia’, Marine Freshwater Research, vol. 51, no. 7, 2000, pp. 641–6; E Wolanski & S Spagnol, ‘Dynamics of the Turbidity Maximum in King Sound, Tropical Western Australia Estuarine’, Coastal and Shelf Science, vol. 56, nos. 5–6, 2003, pp. 877–90; PJ Harris, EK Baker & AR Cole, Physical Sedimentology of the Australian Continental Shelf with Emphasis on Late Quaternary Deposits in Major Shipping Channels, Port Approaches and Choke Points, University of Sydney, Ocean Sciences Institute, Sydney, Report 51, 1991, p. 505.

2. M Brocx & V Semeniuk, ‘The Global Geoheritage Significance of the Kimberley Coast, Western Australia’, Journal of the Royal Society of Western Australia, vol. 94, 2011, pp. 57–88.

3. IM Tyler, RM Hocking & PW Haines, ‘Geological Evolution of the Kimberley Region of Western

Australia’, Episodes – Newsmagazine of the International Union of Geological Sciences, vol. 35, no. 1, 2012, pp. 298–306.

4. LB Collins, V Testa, J Zhao & D. Qu, ‘Holocene Growth History and Evolution of the Scott Reef Car- bonate Platform and Coral Reef’, Journal of the Royal Society of Western Australia, vol. 94, no. 2, 2011, pp. 239–50.

5. M Kordi, LB Collins & AM Stevens, Geomorphic Patterns, Habitats and Substrates of Macrotidal Reefs from the Kimberley, NW Australia, In Prep.

6. BR Wilson, The Biogeography of the Australian North West Shelf: Environmental Change and Life's Response, Elsevier, Burlington, 2013.

7. C Wilkinson, Status of Coral Reefs of the World, Global Coral Reef Monitoring Network, Townsville, 2008, p. 298.

8. T Solihuddin, D Blakeway, LB Collins & MJ O'Leary, 'Holocene Reef Growth and Sea Level in a Macrotidal, High Turbidity Setting: Cockatoo Island, Kimberley Bioregion, Northwest Australia', Marine Geology, vol. 359, pp. 50–60.

9. Wilson, The Biogeography of the Australian North West Shelf.

10. G Bufarale, LB Collins, MJ O'Leary, AM Stevens, M Kordi & T Solihuddin, Geomorphology, Internal Architecture and Growth Patterns of Macrotidal Reefs of the Kimberley Biozone, Northwest Australia, Marine Geology, submitted; Kordi et al, Geomorphic Patterns, Habitats and Substrates of Macrotidal Reefs from the Kimberley.

11. Solihuddin et al, 'Holocene Reef Growth and Sea Level in a Macrotidal, High Turbidity Setting'.

12. Bufarale et al, Geomorphology, Internal Architecture and Growth Patterns of Macrotidal Reefs of the Kimberley Biozone.

13. BS Ingram, Palynological Examination of Samples from Adele Island No. 1 from Well Completion Report, Brunswick Oil NL, 1982; NG Marshall, Adele Island No. 1 Palynological Report, Woodside Offshore Petroleum, Perth, 1995.

14. Bufarale et al, Geomorphology, Internal Architecture and Growth Patterns of Macrotidal Reefs of the Kimberley Biozone.

15. WH Berger, 'Sea Level in the Late Quaternary: Patterns of Variation and Implications', International Journal of Earth Sciences, vol. 97, no. 6, 2008, pp. 1143–50.

***Geomorphology and late Holocene accretion history of Adele Reef: a northwest Australian mid-shelf platform reef***

Tubagus Solihuddin[1], Giada Bufarale[1], David Blakeway[2], Michael J. O'Leary[3]

1 Department of Applied Geology, Curtin University, GPO Box U1987, Perth, WA 6845, Australia

2 Fathom 5 Marine Research, Lathlain, Australia

3 Department of Environment and Agriculture, Curtin University, Bentley, Western Australia, 6102

This is a post-peer-review, pre-copyedit version of an article published in Geo-Marine Letters. The final authenticated version is available online at: http://dx.doi.org/10.1007/s00367-016-0465-3.

## Abstract

The mid-shelf reefs of the Kimberley Bioregion are one of Australia's more remote tropical reef provinces and such have received little attention from reef researchers. This study describes the geomorphology and late Holocene accretion history of Adele Reef, a mid-shelf platform reef, through remote sensing of contemporary reef habitats, shallow seismic profiling, shallow percussion coring and radiocarbon dating. Seismic profiling indicates that the Holocene reef sequence is

25 to 35 m thick and overlies at least three earlier stages of reef build-up, interpreted as deposited during marine isotope stages 5, 7 and 9 respectively. The cored shallow subsurface facies of Adele Reef are predominantly detrital, comprising small coral colonies and fragments in a sandy matrix. Reef cores indicate a *'catch-up*' growth pattern, with the reef flat being approximately 5–10 m deep when sea level stabilised at its present elevation 6,500 years BP. The reef flat is rimmed by a broad low-relief reef crest only 10–20 cm high, characterised by anastomosing ridges of rhodoliths and coralliths. The depth of the Holocene/last interglacial contact (25–30 m) suggests a subsidence rate of 0.2 mm/year for Adele Reef since the last interglacial. This value, incorporated with subsidence rates from Cockatoo Island (inshore) and Scott Reefs (offshore), provides the first quantitative estimate of hinge subsidence for the Kimberley coast and adjacent shelf, with progressively greater subsidence across the shelf.

## Introduction

Adele Reef is a large (200 $km^2$) platform reef located 15.5°S, 123.5°E on Australia's northwest shelf, approximately 80 km from the mainland Kimberley coast and 200 km from the shelf edge (Figure 1). Adele Reef is approximately 22 km long and 9 km wide, and is topped by a 4 $km^2$ vegetated sand cay. Four smaller submerged reefs, Churchill, Albert, Mavis and Beagle reefs, lie to the east. The surrounding shelf is 70-80 m deep and is incised by channels to approximately 90-100 m depth (Figure 1).

The regional climate is semi-arid and monsoonal, with two seasons: a 'wet' season from November to April and 'dry' season from May to October. Monsoon storms in the wet season bring intense rainfall, averaging 800-1,500 mm. The dry season is characterised by warm to hot temperatures and low humidity (DEWHA, 2008). Sea surface temperatures around Adele range from 22 to 28 °C (Pearce and Griffiths, 1991). The predominant swell is from the southwest and the predominant winds are westerly to south-westerly. The region is cyclone-influenced (average three per year. Lough, 1998) and has semidiurnal tides with a maximum range of 7 m.

Previous research on Adele Reef has described its surface geomorphology (Teichert and Fairbridge, 1948; Brooke, 1997), petroleum potential (Ingram, 1982; Marshall, 1995) and reef flat habitats (Richards et al., 2013). The stratigraphic sequence beneath the northern tip of Adele Island was investigated in a petroleum exploration well drilled in 1982 ('Adele Island 1'. Ingram, 1982; Marshall, 1995). The first 156 m of the borehole intersected multiple stacked sedimentary units consisting

of Holocene and Pleistocene limestone, with abundant shell fragments and coral remains in the upper 30 m (Ingram, 1982). Palaeogene sandstone was found below 160 m, overlying a Cretaceous and Upper Jurassic sand/silt sequence; Proterozoic basement was intersected at 798 m (Ingram, 1982).

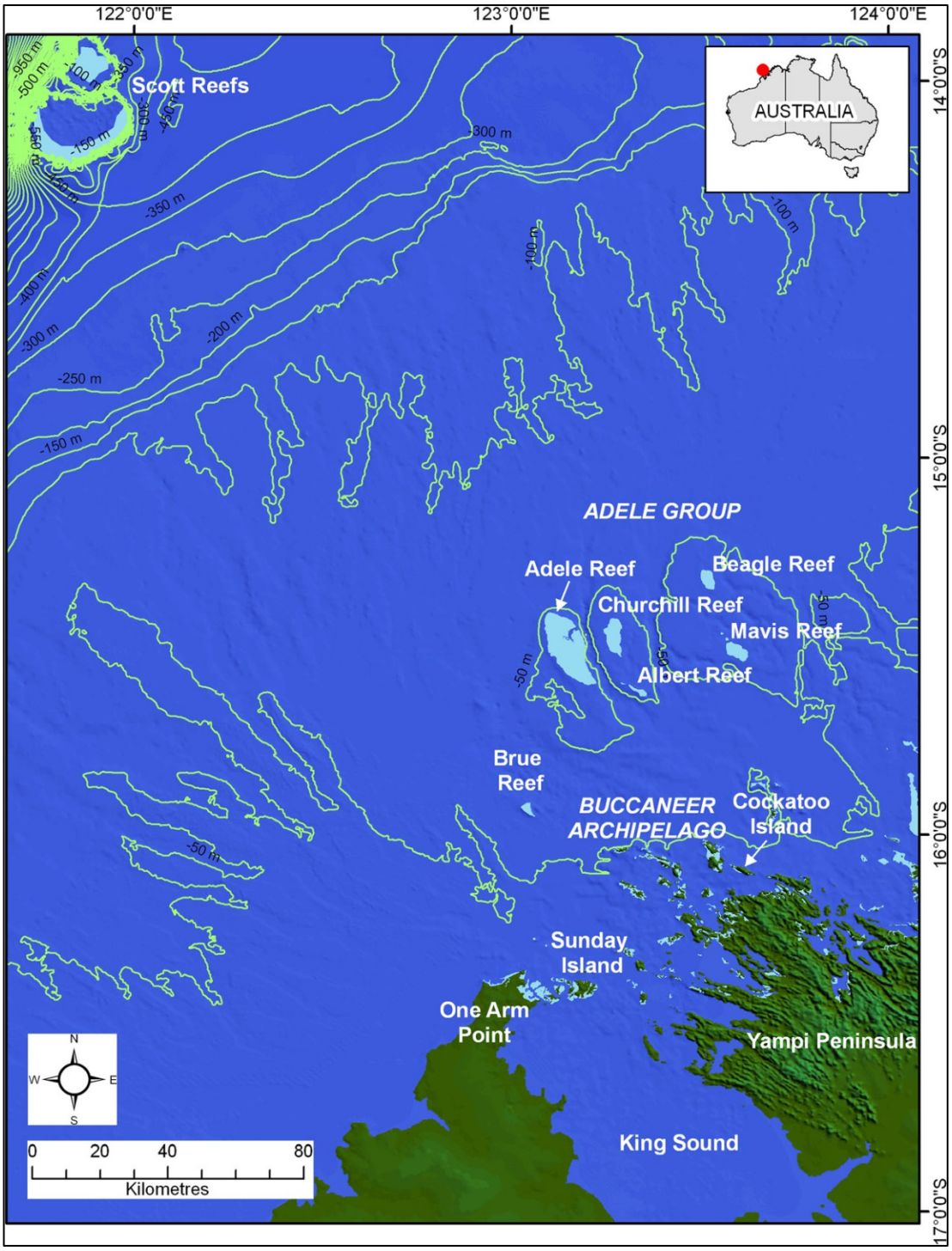


**Figure 1. Map of the study area in the Kimberley Bioregion showing the bathymetry contour derived from 250 m resolution digital elevation model (DEM) sourced from Geoscience Australia (note: there is some uncertainty in the depths due to the coarse nature of the bathymetric grid). Light blue Reef habitat.**

In a recent survey by the Western Australian Museum, Richards et al. (2013) reported the discovery of a unique *rollolith* habitat along the south-western margin of Adele Reef. This includes mobile corals (coralliths) and red crustose coralline algae (rhodoliths) that have coalesced to form low- relief banks on the outer reef flats. This atypical habitat likely formed in response to a combination of wave action and strong surface currents driven by the 7 m macrotidal range (Richards et al., 2013).

Compared to the relatively well-studied oceanic reefs such as Scott Reefs and the Rowley Shoals (Collins, 2011), and the inshore reefs of the Buccaneer Archipelago (Collins et al., 2015; Solihuddin et al., 2015, 2016; Bufarale et al., 2016), the Holocene development of the mid-shelf platform reefs of Australia's northwest shelf remains unknown. The present study attempts to address the information gap by investigating modern habitats, geomorphology and the late Holocene accretion history of Adele Reef through remote sensing, shallow sub-bottom pro- filing, reef core stratigraphy and radiocarbon dating.

## Materials and methods

### Landsat 8 imagery

Contemporary reef communities and associated habitats were mapped using a Landsat 8 multispectral satellite image taken on the 23rd May 2015 (path 110, row 071). This image was corrected geometrically to the WGS 84 reference datum. A digital unsupervised classification from Erdas' ER Mapper utility was used to define reef habitat zones based on a grouping of the reflectance spectra of Landsat 8 bands 2 (0.45-0.52 µm, blue), 3 (0.52-0.60 µm, green) and 4 (0.63-0.68 µm, red). Ground-truth observations of reef habitats from the current study and from the Woodside Collection Project (Kimberley) 2008-2011 (http://www.museum.wa.gov.au/Kimberley/marine-life-kimberley-region; accessed November 2015) were assigned to the corresponding Landsat 30x30 m pixels. All pixels with similar spectral characteristics were then automatically assigned to that ground-truthed habitat.

### Seismic survey

A high-resolution shallow seismic survey of the reef subsurface was undertaken using a boomer/sub-bottom profiler sys- tem (AA201 Applied Acoustic Engineering Limited, Great Yarmouth, UK). A differential global positioning system (DGPS, Fugro Seastar 8200XP/HP) provided accurate positioning (decimetric differential accuracy, typically ±20 cm). Sub-bottom profiling data were digitally acquired, recorded, post-processed and analysed using SonarWiz 5 (Chesapeake Technology Inc., Mountain View, CA). Interpretation of the seismic reflectors depicted in the profiles was performed using a combination of inshore reef seismic data from Bufarale et al. (2016) and petroleum well-log data from Adele Island 1 (Ingram, 1982; Marshall, 1995). Geoscience Australia's 250 m bathymetry dataset was analysed using ESRI's Arc Hydro Tools Terrain Pre-processing toolset to map the position and bathymetry of shelf palaeochannels.

## Reef coring, logging and sampling

Eight percussion cores were collected from Adele Reef. Coring sites were selected to ground-truth the seismic interpretations and to ensure a spatially representative record of reef accretion. A manual slide hammer or a hydraulic post driver was used to drive lengths of a 6 m long, 80 mm diameter aluminium pipe with near-100% core recovery. Compaction was measured onsite and corrected by linear stretching of the core logs. Logs were plotted to local mean sea level (MSL), which is 3.9 m above the lowest astronomical tide (LAT) and referred to metre below sea level (mbsl) in this article. Core locations were recorded by handheld GPS with an accuracy of ±5 m.

Core logging and sampling documented sediment characteristics including (1) the ratio of reef framework to matrix (after Embry and Klovan, 1971), (2) visual assessment of sediment textural characteristics using the Udden-Wentworth nomenclature (Wentworth, 1922) and (3) generic coral identification (after Veron, 2000). Reef framework analysis and facies descriptions followed the terminology proposed by Montaggioni (2005), which highlights the growth forms of the dominant reef builders and environmental indicators. Between 300-500 g samples of matrix sediment were collected for carbonate content analysis using the carbonate bombe technique (weight% loss after treatment with 50% HCL) following guidelines from Müller and Gastner (1971). A pipe dredge was used to collect subtidal sediment samples and these were analysed using the same methods as applied to the core samples.

## Radiocarbon dating

Three to five coral specimens from the top, middle and base of each core were selected, based on size and preservation, for accelerator mass spectrometry (AMS) radiocarbon dating in order to establish a geochronological record of late Holocene reef accretion. Individual coral specimens were ultrasonically cleaned and cut into pieces with minimum weight of 50 mg. All samples were dated at Beta Analytic Inc. USA and recalibrated using the CALIB Version 7.0.4 and the Marine13 calibration curve (http://calib.qub.ac.uk/marine; accessed January 2016). A weighted mean Delta-R (ΔR) value of 58±21 (average calculation from three nearest points: Cape Leveque NE side, King Sound, Port George) was used as the best current estimate of variance in the local open water marine reservoir effect for Adele Reef and adjacent areas (Reimer et al., 2013). Ages discussed in the text are in calibrated years before present (cal years BP) with the 68.2% (2σ) probability range for all dated samples.

# Results

## Contemporary reef biogeomorphic zones

The Landsat-derived reef geomorphology and associated habitat map (Figure 2), supported by ground-truth observations, allowed delineation of six distinct biogeomorphic zones: (1) sand cay, (2) coral rubble and carbonate sand, (3)

coralgal pavement, (4) crustose coralline algae, (5) mixed assemblage of coralliths and rhodoliths and (6) soft and hard corals. Each of these habitats is described in detail below.

*Sand cay*. The sand cay forms a NW-SE elongated, 12x3 km unvegetated island consisting of poorly sorted coarse carbonate sand with approximately 30% coral, 30% mixed shell fragments and foraminifera tests, and 40% unidentified sand to silt grain-size fractions. Comparing the Landsat image with aerial photographs of Teichert and Fairbridge (1948) indicates that the intertidal sand is relatively stable in the south where it encircles Adele Island (the vegetated sand cay), but forms mobile sand waves in the north (Figure 2).

*Coral rubble and carbonate sand*. Coral rubble and coarse carbonate sand is the dominant reef flat sediment facies. This habitat is distributed around the sand cay and on the outer reef flat especially along the north side of the reef platform. The sediments around the sand cay are exposed at every low tide whereas those on the outer reef flat and especially on the NE side are exposed only below mean low water spring (MLWS).

*Coralgal pavement.* An extensive coralgal pavement is distributed over the intertidal reef flat and forms low- relief ridges on the outer reef flat. The pavement is colonised by approximately 10% macroalgae, primarily *Sargassum*, and 20% coral colonies of the genera *Goniastrea, Acropora*, *Porites* and *Favites* (Figure 3, AR1-AR3). A broad 1-2 km wide intertidal coralgal pavement, completely exposed at MLWS, separates the sand cay from the outer reef flat.

*Crustose coralline algae*. Crustose coralline algae occur in a 100-1,000 m wide zone along the outer reef flat, which is broadest on the southern side of the platform and narrows on the eastern (leeward) side. This zone forms a broad low-relief reef crest and intergrades with the coralliths and rhodolith assemblage.

*Mixed assemblage of coralliths and rhodoliths*. Coralliths and rhodoliths with a maximum diameter of (respectively) approximately 8 and 5 cm accumulate in anastomosing ridges approximately 15-20 cm high towards the outer edge of the reef crest (Figure 3, AR4). They are sub-spherical and mobile, and appear to develop where seawater flows off the elevated reef at low tide. Soft and hard corals: On the SW side of the reef, the forereef slope gently dips seawards to a broad submerged terrace at 25-30 m depth, and then dips steeply to the surrounding shelf seafloor at 70-90 m depth. The upper few metres of forereef slope are colonised mainly by soft corals, branching *Acropora* and encrusting *Montipora* up to 1 m in diameter.

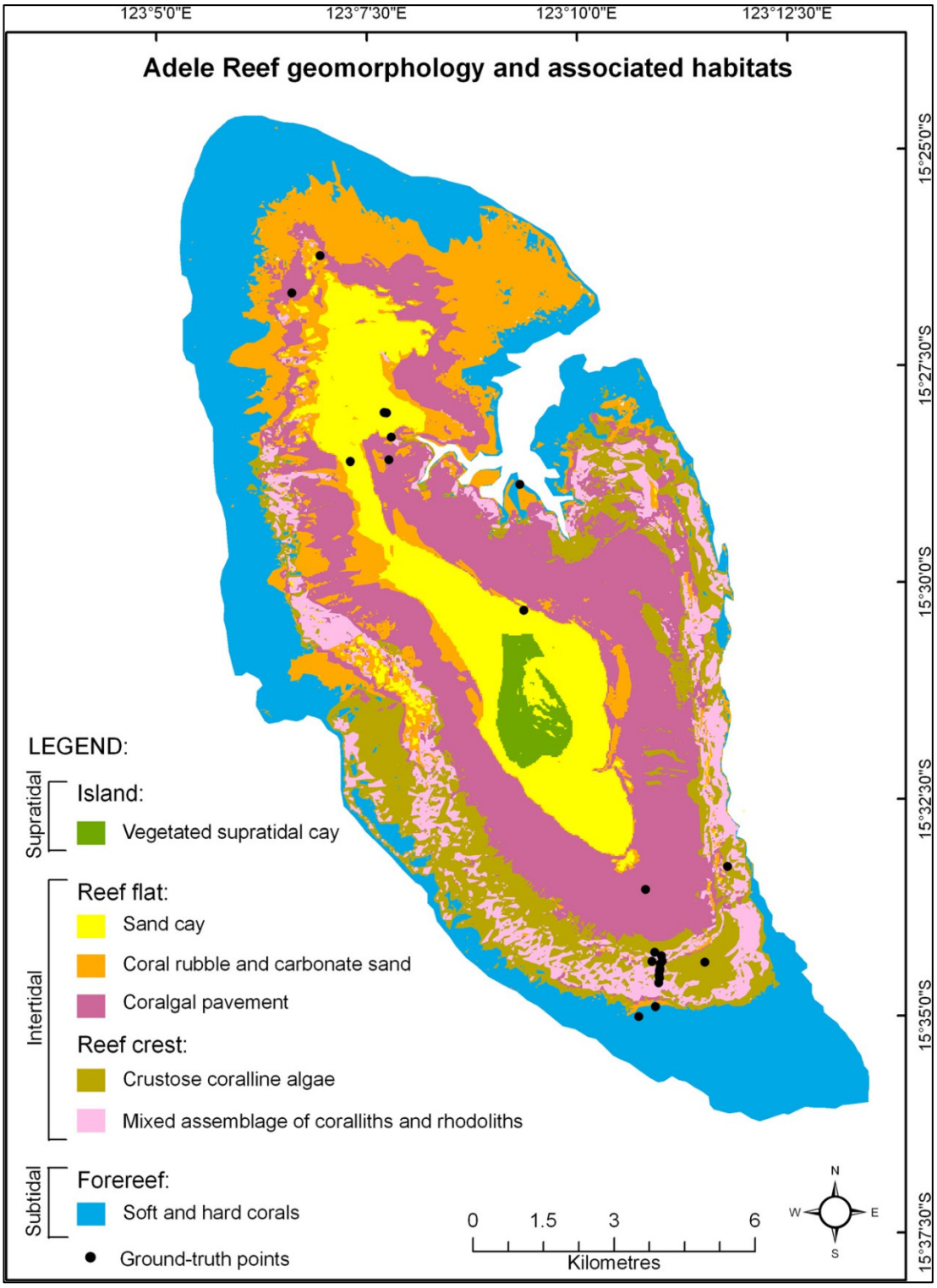


**Figure 2. Map of Adele platform geomorphology and associated habitats, derived from Landsat 8, 23 May 2015.**

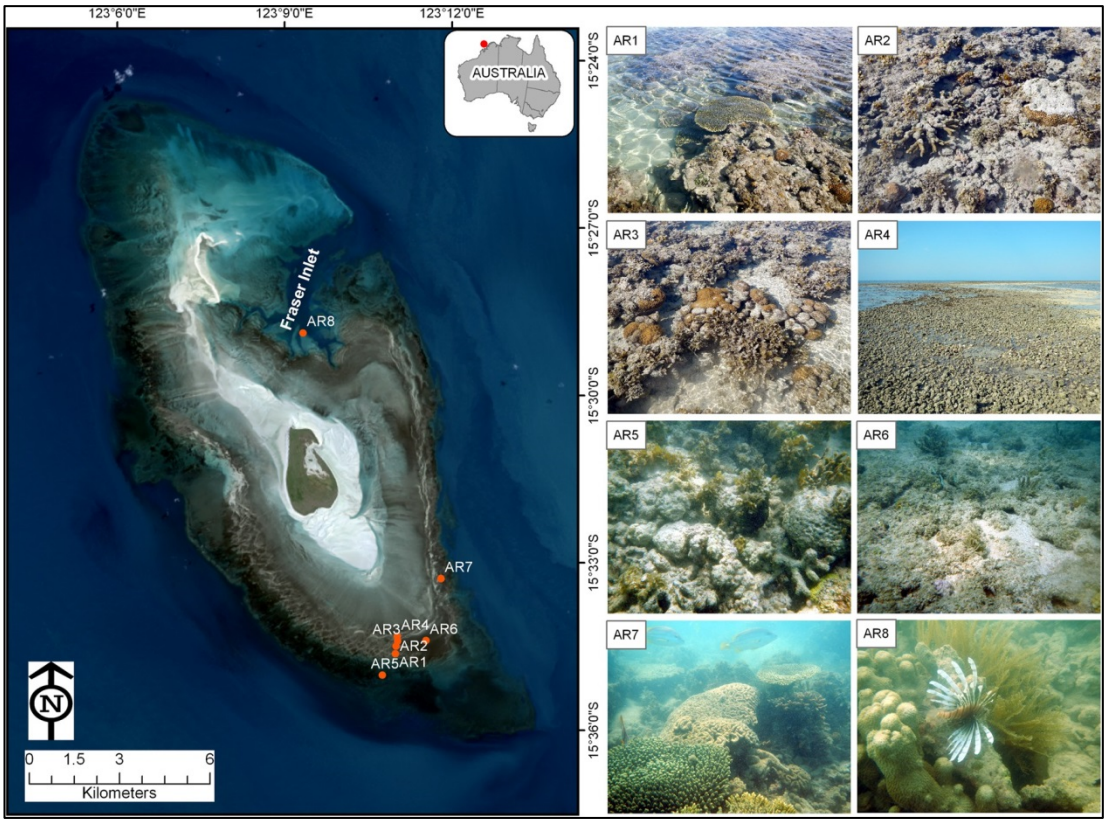


**Figure 3. Contemporary reef habitats of the Adele Reef platform with ground-truth locations. AR1: crustose coralline algae with platy *Acropora*, *Favia*, *Goniastrea* and macroalgae (*Sargassum*). AR2: crustose coralline algae with branching *Porites*, *Goniastrea* and *Sargassum*. AR3: extensive shallow pool on reef flat colonised by *Sargassum*, *Favia* and crustose coralline algae. AR4: rhodolith banks exposed at low spring tides form low-relief reef crest on the SE reef flat. AR5: coral rubble and *Sargassum* on the SE outer reef flat. AR6: *Sargassum* on coral rubble and carbonate sand substrates. AR7: branching *Acropora* and *Lobophyllia* on the SE outer reef flat. AR8: robust branching coral near the narrow drainage channel of Fraser Inlet.**

## Reef architecture and seismic structure

Interpretation of the acoustic horizons across the Adele Reef platform suggests that there are at least three separate stages of reef accretion, bounded by seismic reflectors R1, R2 and R3 (Figure 4).

*R1 reflector*. R1 (Figure 4; depicted in green in Figure 5) is a high-energy reflector, typically expressed as a horizontal surface that parallels the modern surface morphology between 25 and 35 mbsl. The shallowest reef unit (unit 1, or U1) be- tween R1 and the modern reef surface is up to 30 m thick.

*R2 reflector*. R2 (Figure 4; depicted in yellow in Figure 5) is a low to medium amplitude reflector and was encountered in the northern portion of Adele Reef, around 40 mbsl. Unit 2 (U2), between R1 (-30 mbsl) and R2 (-40 mbsl), is mostly acoustically transparent and up to 10 m thick.

| Seismic Unit | Thickness | Limits | Internal Structure | Morphology | Interpretation | Example |
|---|---|---|---|---|---|---|
| U1 | Variable: 20-28 m | **Top:** seabed<br>**Bottom:** unconformity R1 | Moderate to low amplitude. Local discontinuous and sub-parallel reflectors (H1, H2 and H3) | Reef flat, crest forereef slope. Local pinnacle reefs | Reef facies | 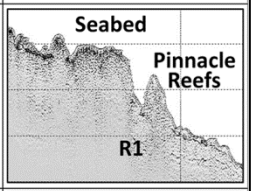 |
| | | | Well-defined, locally parallel to subparallel, prograding layers. Minor disconformities | Channel fill. Sediment mounds or drapes | Sediment Bodies | 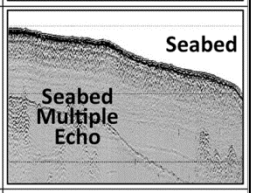 |
| U2 | Variable: 5-10 m | **Top:** unconformity R1<br>**Bottom:** unconformity R2 | Weak to moderate amplitude with discontinuous, subparallel minor reflectors | Reef flat, crest, forereef slope. Local pinnacle reef | Reef facies | 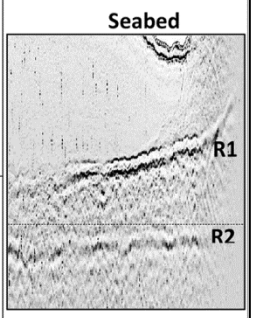 |
| U3 | ~ 22 m | **Top:** unconformity R2<br>**Bottom:** unconformity R3 | Low to medium amplitude, mostly acoustically transparent | Reef flat, crest, forereef slope | Reef facies | |
| U4 | NA | **Top:** unconformity R3<br>**Bottom:** NA | Low amplitude | Reef flat | Reef facies | 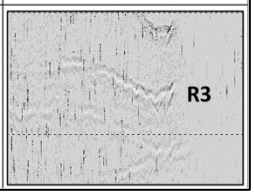 |

**Figure 4 Characteristics of the acoustic features identified in the seismic profiles of Adele Reef (after Bufarale et al., 2016).**

*R3 reflector*. The low amplitude reflector R3 (Figure 4; depicted in pink in Figure 5) was detected only within Fraser Inlet, at a depth of about 65 mbsl. Since the bottom of this channel is relatively deep (~30 mbsl), the substrate that overlies this reflector is thinner than elsewhere, allowing deeper penetration of the acoustic signal. Seismic unit 3 (U3) is constrained between R2 and R3 and it is at least 20 m thick, with no recognisable internal architecture. Reflector R3 covers a deeper seismic unit, the lower limit of which cannot be detected within the acoustic profiles.

The forereef slopes are characterised by an irregular topography (Figure 5A) that likely represents pinnacle reefs, or perhaps linear ridges, rimming the reef platform. These features occur at various depths, typically rising from between 27 and12 mbsl. Most of these structures have an average relief of about 3 m and occur in small groups of three to five pinnacles/ridges. Larger pinnacles/ridges of up to 8 m in height occur in deeper water (>20 mbsl).

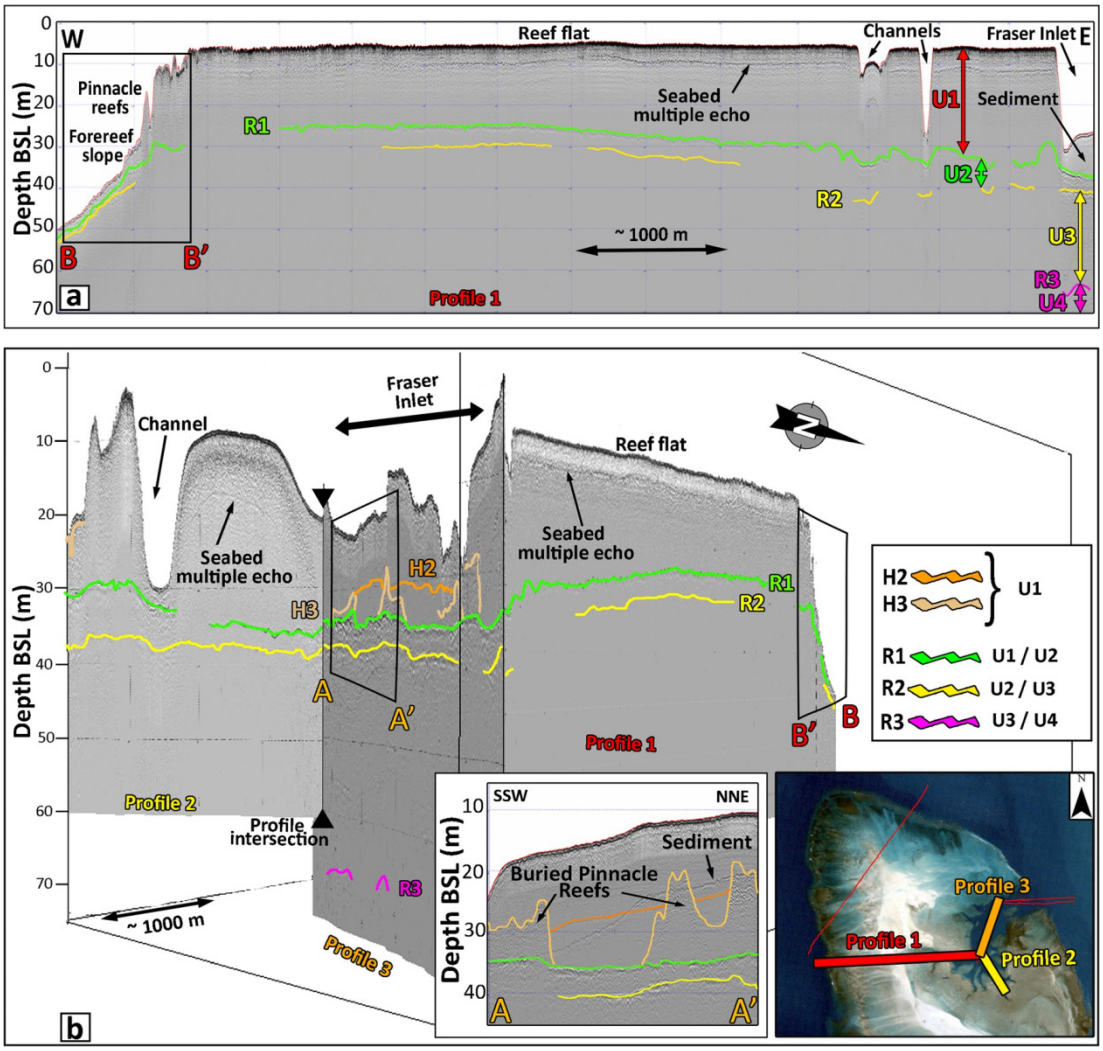


**Figure 5. Cross-sections showing multiple stages of reef build-up (MIS 1, 5,7, 9 or 11 respectively). A) Profile 1, oriented W-E, intersects the northern portion of Adele Reef (modified after Collins et al., 2015). B) Profile 3 runs longitudinally through Fraser Inlet and profile 2 cuts the southern branch of the inlet. The Holocene reef is 25-35 m thick, with drowned pinnacle reefs on the western forereef slope. Along Fraser Inlet, a series of pinnacle reefs are buried within muddy sediments (left insert). The location of the profiles is shown in the insert at lower right.**

Bathymetric and seismic profiles across the Adele group of platform reefs reveal a series of deeply incised channels separating the platforms. The channels are relatively broad (between 7 and 30 km) and are oriented in a north-south to northwest-southeast direction, aligning with the river channels along the mainland coast (Figure 6). The channel separating Adele and Churchill Reef platforms is around 6 km wide and more than 90 m deep. Based on seismic reflection data and the sediments collected with the pipe dredge, the base of this incised channel contains approximately 7 m of thinly bedded fine-grained sediments.

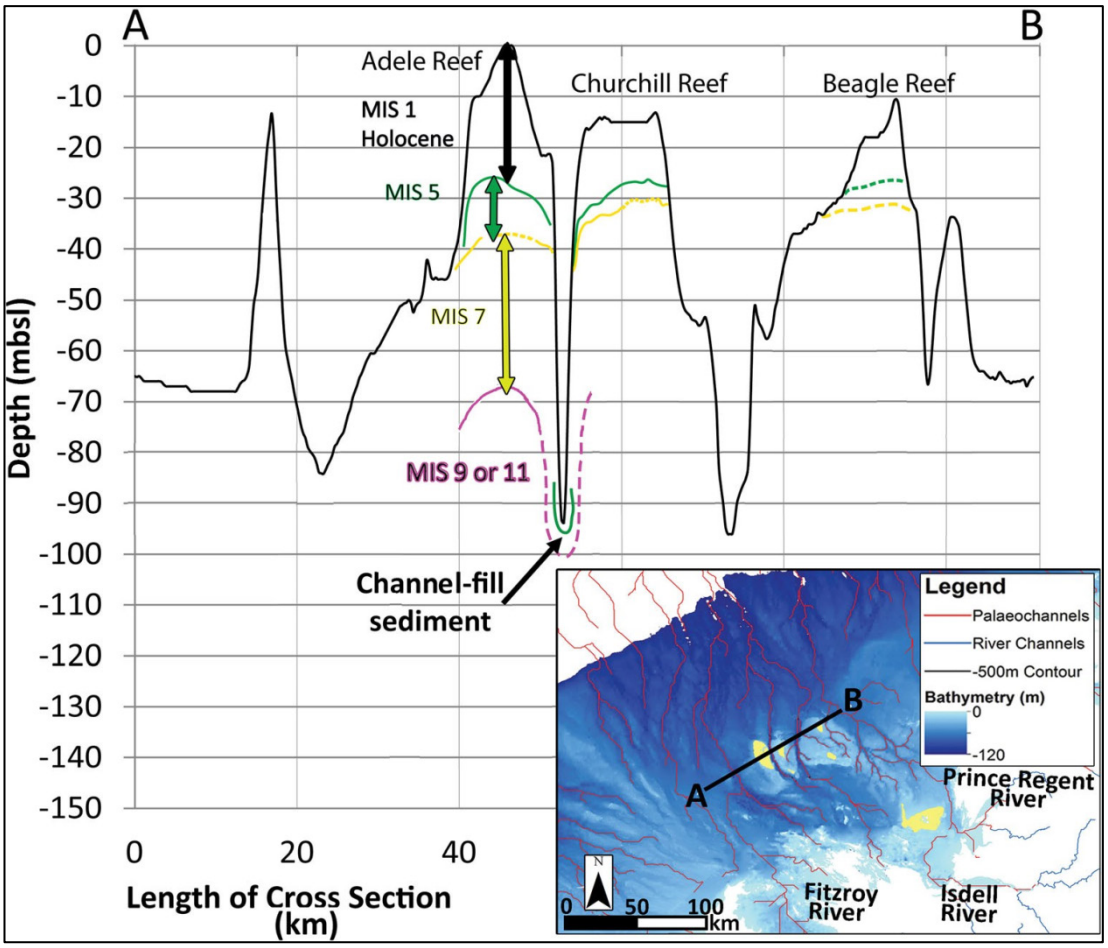


**Figure 6. Bathymetric and seismic profile across Adele Reef and adjacent platforms (see inset for location). Bathymetry data were sourced from Geoscience Australia's 250 m DEM. Note the deep incisions between the platforms. Seismic units within the platforms are interpreted as stacked phases of reef accretion during sea-level highstands (MIS 1, 5, 7 and 9 or 11). Dashed lines are inferred.**

## Reef stratigraphy and geochronology

The eight percussion cores collected around Adele Reef com- prised five on the northwest and three on the southeast sides of the platform. Core penetration ranged from 1.84 to 5.06 m. The cored reef facies are primarily detrital; no reef framework was encountered and few colonies were unequivocally in growth position (Figure 7). However, the predominance of detrital facies is at least partly due to the selection of coring sites; coralline algal pavement was avoided because it could not be penetrated.

The coarser detrital clasts are predominantly coarse gravel to cobble-sized fragments of domal (dome-shaped) corals, with occasional branching coral fragments. Coral genera recorded include, in estimated order of abundance, *Favia*, *Goniopora*, *Porites*, *Galaxea*, *Acropora*, *Cyphastrea*, *Favites*, *Astreopora*, *Heliopora*, *Lobophyllia*, *Fungia* and *Pavona*. Matrix sediment is dominated by carbonate sand with an upward coarsening sequence from mud to coarse sand. The carbonate content ranges from 75% (A08) to 91% (A09), and generally increases up section. The non-carbonate materials are terrigenous mud and organics.

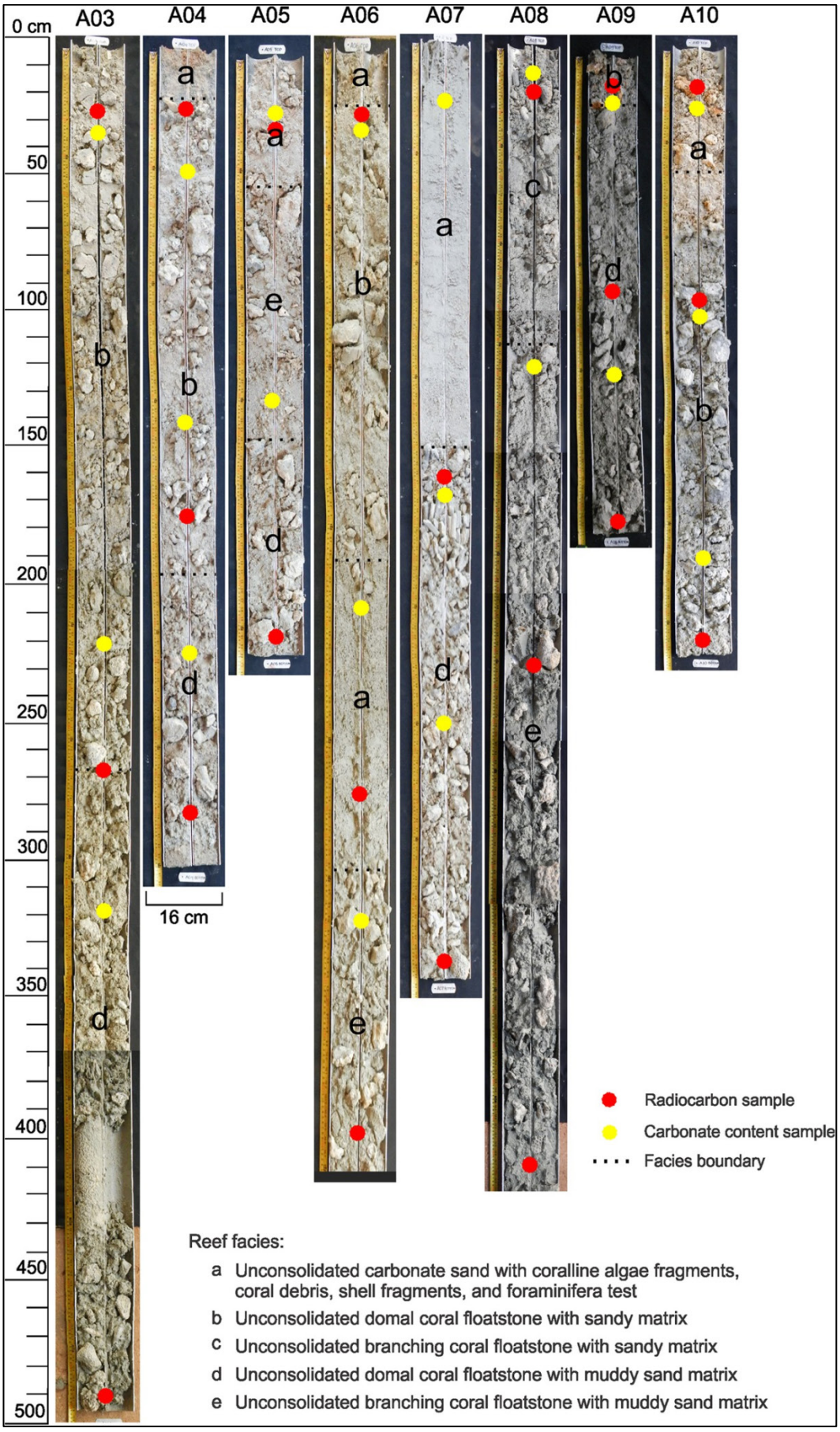
0 cm
A03
A04
A05
A06
A07
A08
A09
A10
50
100
150
200
250
300
350
400
450
500
16 cm
Radiocarbon sample
Carbonate content sample
Facies boundary
Reef facies:
a Unconsolidated carbonate sand with coralline algae fragments, coral debris, shell fragments, and foraminifera test
b Unconsolidated domal coral floatstone with sandy matrix
c Unconsolidated branching coral floatstone with sandy matrix
d Unconsolidated domal coral floatstone with muddy sand matrix
e Unconsolidated branching coral floatstone with muddy sand matrix

**Figure 7 (previous page). Core photograph of Adele Reef showing representative Adele Reef facies where the cores were collected.**

Twenty-two coral samples were collected from the cores for radiometric dating (Figure 8, Table 1). Due to the thick Holocene reef build-up (up to 30 m based on seismic data), the shallow reef coring (maximum core penetration of ~5 m) only penetrated the late Holocene. Therefore, the timing of reef initiation and the style and rates of reef aggradation over the full growth sequence is unknown. The oldest date, ~5,240-4,960 cal years BP, was obtained from the base of core A03 at 7 mbsl on the NW (seaward) side of the island. The reef sequence on the relatively sheltered SE side of the island is apparently younger, the oldest date there being ~3,155-2,940 cal years BP at 5 mbsl in core A08. At both sites, the reef accreted relatively rapidly (mean 4.2 and 3.3 mm/year respectively) until it attained present LAT level (Lowest Astronomical Tide) at approximately 4,000 cal years BP in core A03 and 2,000 cal years BP in core A08, and subsequently decelerated to approximately 1.0 and 2.0 mm/year respectively. Near-surface samples were dated to ~3,225-3,025 cal years BP at 2.9 mbsl in core A04 and ~360-245 cal years BP at 1 mbsl in core A08 (Figure 8, Table 1).

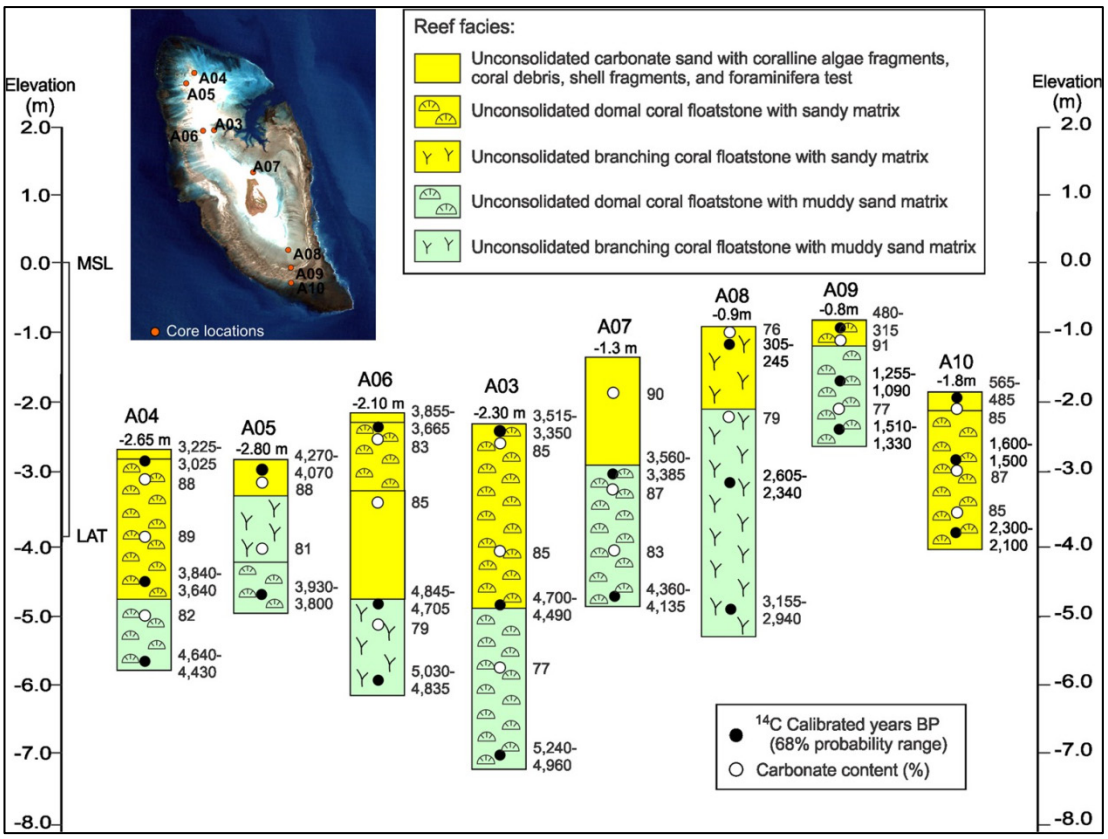


**Figure 8. Lithostratigraphic and chronostratigraphic summary of Holocene reef facies for Adele Reef. The dominant facies was domal coral but the sections also contain fragments and colonies of branching coral.**

**Table 1. AMS Radiocarbon dates from selected samples across Adele Reef.**

| Sample code | Depth (mbsl) | Lab. code | Material | Measured age | $^{13}C/^{12}C$ (‰) | Conventional age (BP) | Calibrated (68% probability, cal yr BP) | Accretion (mm/year) |
|---|---|---|---|---|---|---|---|---|
| A03-43 | –2.33 | Beta-397758 | *Favia* | 3190±30 | +0.3 | 3600 ±30 | 3515–3350 | |
| A03-269 | –4.59 | Beta-397759 | *Goniopora* | 4100±30 | –2.1 | 4480±30 | 4700–4490 | 1.94 |
| A03-492 | –6.82 | Beta-397760 | *Galaxea* | 4500±30 | –2.9 | 4860±30 | 5240–4960 | 4.42 |
| A04-25 | –2.75 | Beta-425803 | *Favia* | 2930±30 | +0.4 | 3350±30 | 3225–3025 | |
| A04-175 | –4.25 | Beta-425791 | *Acropora* | 3490±30 | –2.6 | 3860±30 | 3840–3640 | 0.4 |
| A04-284 | –5.34 | Beta-425792 | *Lobophyllia* | 4040±30 | –0.2 | 4450±30 | 4640–4430 | 1.3 |
| A05-29 | –2.89 | Beta-425793 | *Acropora* | 3780±30 | –1.2 | 4170±30 | 4270–4070 | |
| A05-217 | –4.77 | Beta-425794 | *Favites* | 4270±30 | +0.7 | 4690±30 | 4930–4800 | 2.7 |
| A06-25 | –2.25 | Beta-425795 | *Faviid* | 3460±30 | +0.1 | 3870±30 | 3855–3665 | |
| A06-278 | –4.78 | Beta-425796 | *Acropora* | 4210±30 | +0.4 | 4630±30 | 4845–4705 | 2.5 |
| A06-400 | –6.00 | Beta-425797 | *Acropora* | 4370±30 | –1.1 | 4760±30 | 5030–4835 | 7.7 |
| A07-180 | –1.80 | Beta-425798 | *Lobophyllia* | 3250±30 | –1.0 | 3640±30 | 3560–3385 | |
| A07-341 | –3.41 | Beta-425799 | *Favia* | 3820±30 | –0.5 | 4220±30 | 4360–4135 | 2.1 |
| A08-18 | –1.68 | Beta-397761 | *Favia* | 250±30 | +2.5 | 700±30 | 360–245 | |
| A08-226 | –3.76 | Beta-397762 | *Lobophyllia* | 2450±30 | –3.8 | 2800±30 | 2605–2340 | 0.9 |
| A08-416 | –5.66 | Beta-397763 | Coralline algae | 2880±30 | –0.3 | 3290±30 | 3155–2940 | 3.3 |
| A09-26 | –2.36 | Beta-425800 | *Chypastrea* | 440±30 | –1.4 | 830±30 | 480–315 | |
| A09-100 | –3.10 | Beta-425801 | Coralline algae | 1240±30 | +1.0 | 1670±30 | 1255–1090 | 0.9 |
| A09-177 | –3.87 | Beta-425802 | *Porites* | 1530±30 | –0.4 | 1930±30 | 1510–1330 | 3.1 |
| A10-14 | –2.84 | Beta-425804 | *Rhodoliths* | 580±30 | –0.5 | 980±30 | 565–485 | |
| A10-128 | –3.98 | Beta-425806 | *Porites* | 1650±30 | –0.3 | 2060±30 | 1655–1500 | 1.1 |
| A10-211 | –4.81 | Beta-425805 | *Galaxea* | 2190±30 | –0.8 | 2590±30 | 2300–2110 | 1.3 |
| A03-43 | –2.33 | Beta-397758 | *Favia* | 3190± 30 | +0.3 | 3600±30 | 3515–3350 | |
| A03-269 | –4.59 | Beta-397759 | *Goniopora* | 4100±30 | –2.1 | 4480±30 | 4700–4490 | 1.94 |
| A03-492 | –6.82 | Beta-397760 | *Galaxea* | 4500±30 | –2.9 | 4860±30 | 5240–4960 | 4.42 |
| A04-25 | –2.75 | Beta-425803 | *Favia* | 2930±30 | +0.4 | 3350±30 | 3225–3025 | |
| A04-175 | –4.25 | Beta-425791 | *Acropora* | 3490±30 | –2.6 | 3860±30 | 3840–3640 | 0.4 |

# Discussion

## Reef stratigraphy and sea-level changes

Seismic surveys across Adele Reef reveal multiple stacked seismic units that likely represent distinct phases of reef accretion during sea-level highstands. The seafloor and seismic reflectors R1, R2 and R3 correspond to the top of each seismic unit. Although it is not possible to establish the age of each seismic unit due to the limitations in core penetration (max. depth 5 m), the age can be inferred based on a comparison with seismic, stratigraphic and chronological data from the outer-shelf

Scott Reefs, 200 km NW of Adele Reef (Collins et al., 2011), and the inner-shelf Kimberley reefs 70 km SW of Adele Reef (Solihuddin et al., 2015).

Reflector R1, identified at a depth of 25-35 mbsl on Adele Reef (Figure 5), was also recorded on the inner shelf of Cockatoo Island and the shelf-edge Scott Reefs (see Figure 1 for location). On Cockatoo Island, an open cut iron ore pit has exposed a complete Holocene section, allowing the R1 reflector to be directly correlated with the logged stratigraphic contact. Solihuddin et al. (2015) found that the depth of the R1 reflector at 15 to 20 mbsl corresponded closely with the Holocene/Last Interglacial (LIG) stratigraphic contact in the mine pit, measured at 15 to 18 mbsl. At Scott Reefs, the R1 reflector occurs from 26 mbsl (interpreted as a palaeoreef crest; Collins et al., 2011), a similar depth to Adele, down to 58 mbsl (interpreted as a palaeoreef lagoon; Collins et al., 2011). Shallow boreholes made by Woodside Energy Ltd in 2006/07, and analysed by Collins et al. (2011), found that the Scott Reefs Holocene sequence rested unconformably on a karstified LIG reef exposure surface. U-series analysis of corals beneath the R1 reflector at Scott Reefs returned ages of 125,000 and 130,000 cal years BP. Therefore, it is inferred that R1 on Adele Reef also marks the LIG unconformity surface, and seismic unit U1 is a Holocene reef sequence up to 30 m thick.

Reflector R2 occurs at a depth of 30-40 mbsl on Adele Reef. A similar second reflector was identified on Scott Reefs at a depth of 58 m, and was interpreted as a marine isotope stage (MIS) 7 exposure surface, based on a U-series age of 208,000 cal years BP (Collins et al., 2011). Based on the Scott Reefs observations, R2 at Adele Reef is also interpreted as representing the MIS 7 exposure surface. R2 was not observed in any of the inner shelf seismic surveys (Bufarale et al., 2016) or in the mine pit stratigraphic section of Cockatoo Island (Solihuddin et al., 2015), perhaps indicating that this area remained above sea level during MIS 7.

Reflector R3 is the lowermost unconformity at 65 mbsl (Figure 5). R3 was only observed along seismic lines within the 30 m deep Fraser Inlet. Its apparent absence along the main Adele Reef platform may be due to energy loss with increasing depth, i.e. R3 may be more extensive but not detected. The Adele Island 1 stratigraphic log shows limestone to a depth of 160 mbsl, so it is likely that R3 is a middle to late Pleistocene unconformity surface. It may correlate to the third stratigraphic unconformity at 90 mbsl in Scott Reefs (Collins et al., 2011). A coral sample immediately below this unconformity returned a U-series age of 313,000 cal years BP (Collins et al., 2011), suggesting that the R3 reflector at Scott Reefs, and potentially also at Adele Reef, is the MIS 9 exposure surface.

Fraser Inlet presently has a broad flat sandy mud floor; however, seismic profiling along and across the axis of the channel reveals a buried complex of pinnacle reefs. The pinnacle reefs are considered to be of early Holocene age as they sit atop the R1 reflector. Sedimentation was probably minimal during the early-middle Holocene catch-up phase; however, as the reef platform reached sea level around 3,000 years BP, sediment delivery into Fraser Inlet probably increased, eventually burying the pinnacles.

There is evidence of cross-shelf fluvial incision as seen in a series of deep channels that dissect the main platforms of Adele, Churchill and Beagle reefs. The channel floors have depths of more than 65 mbsl and likely represent glacial lowstand palaeoriver channels, possibly tributaries of the Fitzroy, Isdell and Prince Regent rivers (Figure 6).

## Mode of Holocene growth

The early to mid-Holocene history of Adele Reef remains unknown due to the limited core penetration. Holocene sea level reconstructions (Collins et al., 2006, 2011) suggest that the subaerial LIG surface of Adele Reef would have been transgressed at ~10,000 years BP. Subsequent colonisation and accretion was relatively rapid, as the reef was already up to 20 m thick at the time of the earliest core dates (~5,000 years BP). The internal seismic structure of the Holocene reef appears uniform, consistent with simple vertical aggradation of an extensive low-relief cover of coral and sediment, as inferred for Cockatoo Island where the complete Holocene section was sampled (Solihuddin et al., 2015). Adele Reef at this time may have resembled the coral-rich submerged banks re- ported from the Timor Sea by Heyward et al., (1997). The flanks of the platform are topographically complex and appear to be slowly prograding through pinnacle reef growth and platform-derived sedimentation.

The cores indicate a ‘catch-up’ growth pattern in the late Holocene, with the reef surface being approximately 5-10 m deep when sea level stabilised at its present elevation 6,500 years BP (Collins et al., 2006). The ‘catch-up’ pattern on Adele Reef coincides with a ‘catch-up’ phase from 5,500 years BP at Cockatoo Island, after a short initial period of ‘keep-up’ growth followed by deeper submergence (Solihuddin et al., 2015). Accretion slowed as Adele Reef reached the intertidal zone, probably due to increasing wave energy and periodic emergence at spring low tides, as inferred for Scott Reefs (Collins et al., 2011). The central and northern parts of the platform reached sea level around 3,000 years BP, whereas the southern part of the platform reached sea level only very recently.

## Comparison with other reef systems

The Kimberley Bioregion has abundant inner-shelf fringing reefs but relatively few mid- and outer-shelf reefs. This contrasts with the Great Barrier Reef (GBR), which has more mid- and outer-shelf reefs than inner-shelf reefs. The Kimberley and the GBR reefs also differ in that the Kimberley reefs are generally flat-topped platforms (Brooke 1997; Wilson 2013; Kordi et al., 2016) whereas most GBR reefs have a raised marginal rim surrounding a deeper lagoon (Maxwell 1968; Hopley et al., 2007).

Adele Reef differs from the inshore Buccaneer Archipelago in its relatively exposed oceanic setting, smaller tidal range (7 vs. 11 m), deeper surrounding bathymetry, lower freshwater input and lower turbidity. These contrasts result in obvious differences in the surface features of Adele, including the presence of a sand cay and the absence of mangroves. However, there are also similarities between the mid-shelf and inshore reefs, particularly the abundance of coralline algae and the

development of coralline algal ridges, although these consist largely of uncemented rhodoliths on Adele whereas they are often strongly cemented framework structures on the inshore platform (Richards and O'Leary 2015; Solihuddin et al., 2016).

Subsurface facies of Adele Reef differ from those inshore, consisting predominantly of matrix-supported transported domal coral fragments and sand at Adele versus in-situ branching Acropora-rich muddy units inshore (Solihuddin et al., 2015, 2016). This difference is probably due to the greater exposure of Adele to wave action and cyclones. Reef accretion patterns and rates appear broadly similar between Adele and the inshore reefs, with 'catch-up' growth predominating at both sites and accretion rates averaging <5 mm/year, although some more rapid intervals (up to 27 mm/year) were recorded in the intensively sampled Cockatoo Island sequence (Solihuddin et al., 2015).

## Cross-shelf profile of Holocene reef accretion

Figure 9 portrays a schematic cross-shelf profile of Holocene reef accretion from Cockatoo Island (inner shelf) to Adele Reef (mid-shelf) and Scott Reefs on the edge of the continental shelf (outer shelf). Stratigraphic data from Cockatoo Island and other inner-shelf reefs suggest that the LIG reef beneath the Holocene reef is 15 to 20 mbsl, corresponding to a maximum subsidence rate of 0.12 mm/year (Solihuddin et al., 2015). Collins et al., (2011) reported the upper LIG reef surface of 26 m Scott Reefs, estimating the post-LIG subsidence rate of Scott Reefs to be ~0.2 mm/year. Similarly, seismic profiles at Adele Reef indicate that the upper LIG reef surface is 25 mbsl (Figure 5), giving an inferred subsidence rate of ~0.2 mm/year. So while the subsidence of the NW is well documented, particularly in the petroleum well (Ingram, 1982; Marshall, 1995) and seismic data (Bufarale et al., 2016), this study is able to constrain rates based on the elevation of the Holocene/LIG unconformity surface.

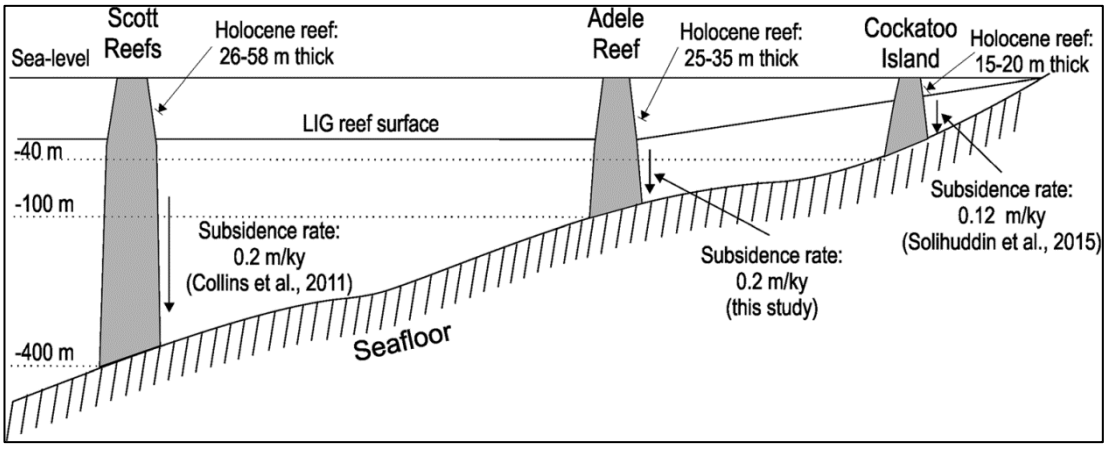


**Figure 9. Diagrammatic cross-shelf profile of Holocene reef growth from Cockatoo Island on the inner shelf to Adele Reef on the mid- shelf and Scott Reefs on the outer shelf, showing estimated post- LIG subsidence rates of 0.12 mm/ year at Cockatoo Island, 0.2 mm/ year at Adele Reef and 0.2 mm/ year at Scott Reefs.**

This cross-shelf dataset of LIG reef elevations provides the first quantitative estimate of neotectonic subsidence rates across the NW shelf of Australia, spanning

the last 120,000 years. Interestingly, subsidence appears to change at a relatively uniform rate of 0.2 m across the mid to outer shelf, with a lower rate of 0.12 along the inner shelf. This difference may be a function of the underlying structural geology bordering the Proterozoic Kimberley basement rocks, and the offshore Browse Basin sediments on which both the Adele and Scott reefs are situated. The higher rate of subsidence across the middle and outer shelf relative to the inner shelf has provided additional accommodation space to build thicker Holocene sequences, as has been recorded on the GBR (Browne et al., 2012).

## Conclusions

This is the first investigation of the Holocene geomorphology and accretion history of a mid-shelf platform reef of the Kimberley Bioregion. Sub-bottom profiles of Adele Reef show at least three stages of reef accretion bounded by reflectors. The shallowest reflector at 25-35 mbsl is interpreted as the Holocene/LIG (MIS 5) contact. Deeper reflectors are interpreted as boundaries between MIS 5 and MIS 7 at depths of 30-40 mbsl, and between MIS 7 and MIS 9 at 65 mbsl.

The Holocene sequence is up to 30 m thick. Cores from the uppermost 5 m of the sequence indicate that the reef accreted in a ‘catch-up’ mode, with accretion rates decreasing as the reef platform approached sea level. The cores were dominated by detrital domal coral colonies and fragments in a sandy matrix, in contrast with the in-situ branching Acropora and mud-rich subsurface facies of inshore reefs. These differences likely reflect Adele’s higher-energy setting and greater exposure to cyclones. Coralline algae are a significant component of the contemporary intertidal and shallow subtidal reef sur- face but were underrepresented in the cores due to the difficulty of percussion coring in this habitat.

The mean post-LIG subsidence rate of the Adele Reef platform was estimated from seismic records to be 0.2 mm/year. This supports a hinge subsidence hypothesis for the Kimberley coast and adjacent shelf, with greater subsidence on the outer shelf (Scott Reefs) and mid-shelf (Adele Reef) than inshore (Cockatoo Island).

## Acknowledgements

The Kimberley Reef Geomorphology Project 1.3.1 was funded by the Western Australian State Government and partners of the Western Australian Marine Science Institution. This paper is dedicated to the memory of our former project leader, the late Prof. Lindsay Collins, for his inspiring ideas and contribution to our knowledge of Western Australia’s seafloor and coral reefs. The research was assisted by the Kimberley Marine Research Station at Cygnet Bay who provided vessel support and access to research facilities. We would like to thank WA Museum for providing ground truth data through the WA Museum/ Woodside Collection Project (Kimberley) 2008-2011. We also thank Geoscience Australia (GA) for providing DEMs data and the United States Geological Survey (USGS) for providing Landsat imagery. Last but not least, special thanks to valued members of the research team at Curtin University: Alexandra Stevens and Moataz Kordi. The

article benefitted from constructive assessments by C.J.R. Braithwaite, L.F. Montaggioni and an anonymous reviewer.

## Compliance with ethical standards

**Conflict of interest.** The authors declare that there is no conflict of interest with third parties.

## References

Brooke B (1997) Geomorphology of the north Kimberley coast. In: Walker D (ed) Marine biological survey of the central Kimberley coast, Western Australia. University of Western Australia, Perth, unpublished report, W.A. Museum Library no UR377, pp 13-39

Browne NK, Smithers SG, Perry CT (2012) Coral reefs of the turbid inner-shelf of the Great Barrier Reef, Australia: an environmental and geomorphic perspective on their occurrence, composition and accretion. Earth-Sci Rev 115(1-2):1–20

Bufarale G, Collins LB, O'Leary MJ, Stevens AM, Kordi M, Solihuddin T (2016) Quaternary onset and evolution of Kimberley coral reefs (Northwest Australia) revealed by high-resolution seismic imaging. Cont Shelf Res 123:80–88

Collins LB (2011) Geological setting, marine geomorphology, sediment and oceanic shoals growth history of the Kimberley Region. J R Soc Western Australia 94(2):89–105

Collins LB, Zhao JX, Freeman H (2006) A high-precision record of mid– late Holocene sea-level events from emergent coral pavements in the Houtman Abrolhos Islands, southwest Australia. Quat Int 145–146: 78–85

Collins LB, Testa V, Zhao J, Qu D (2011) Holocene growth history and evolution of the Scott Reef carbonate platform and coral reef. J R Soc Western Australia 94(2):239–250

Collins LB, O'Leary MJ, Stevens AM, Bufarale G, Kordi M, Solihuddin T (2015) Geomorphic patterns, internal architecture and reef growth in a macrotidal, high-turbidity setting of coral reefs from the Kimberley Bioregion. Aust J Maritime Ocean Affairs 7(1):12–22. doi:10.1080/18366503.2015.1021411

DEWHA (2008) A characterisation of the marine environment of the North-west Marine Region. Perth Workshop Report, A Summary of an Expert Workshop Convened in Perth, Western Australia, 5–6 September 2007. Department of the Environment, Water, Heritage and the Arts, Hobart, Commonwealth of Australia

Embry AF, Klovan JE (1971) A late Devonian reef tract on northeastern Banks Island, N.W.T. Bull Can Petrol Geol 19(4):730–781

Heyward AJ, Pinceratto E, Smith LD (1997) Big Bank Shoals of the Timor Sea: an environmental resource atlas. Australian Institute of Marine Science & BHP Petroleum

Hopley D, Smithers S, Parnell K (2007) The geomorphology of the Great Barrier Reef: Development, diversity, change. Cambridge University Press, Cambridge

Ingram BS (1982) Palynological examination of samples from Adele Island No. 1 from Well Completion Report. Brunswick Oil N.L.

Kordi M, Collins LB, O'Leary M, Stevens A (2016) ReefKIM: an integrated geodatabase for sustainable management of the Kimberley Reefs, North West Australia. Ocean Coastal Manage 119:234–243

Lough JM (1998) Coastal climate of northwest Australia and comparisons with the Great Barrier Reef: 1960 to 1992. Coral Reefs 17(4): 351–367

Marshall NG (1995) Adele Island No. 1 Palynological Report. Woodside Offshore Petroleum

Maxwell WGH (1968) Atlas of the Great Barrier Reef. Elsevier, Amsterdam

Montaggioni LF (2005) History of Indo-Pacific coral reef systems since the last glaciation: development patterns and controlling factors. Earth-Sci Rev 71(1-2):1–75

Müller G, Gastner M (1971) The 'Karbonat-Bombe', a simple device for the determination of carbonate content in sediment, soils, and other materials. Neues Jahrb Mineralogie Monatshefte 10:466–469

Pearce AF, Griffiths RW (1991) The mesoscale structure of the Leeuwin Current: a comparison of laboratory models and satellite imagery. J Geophys Res 96(C9):16739–16757

Reimer PJ, Bard E, Bayliss A, Beck JW, Blackwell PG and 25 others (2013) IntCal13 and Marine13 radiocarbon age calibration curves 0–50,000 years cal BP. Radiocarbon 55(4):1869–1887

Richards ZT, O'Leary MJ (2015) The coralline algal cascades of Tallon Island (Jalan) fringing reef, NW Australia. Coral Reefs 34(2):595

Richards ZT, Bryce M, Bryce C (2013) Bryce C (2013) New records of atypical coral reef habitat in the Kimberley. Australia J Mar Biol. doi:10.1155/2013/363894

Solihuddin T, Collins LB, Blakeway D, O'Leary MJ (2015) Holocene coral reef growth and sea level in a macrotidal, high turbidity setting: Cockatoo Island, Kimberley Bioregion, northwest Australia. Mar Geol 359:50–60

Solihuddin T, O'Leary MJ, Blakeway D, Parnum I, Kordi M, Collins LB (2016) Holocene reef evolution in a macrotidal setting: Buccaneer Archipelago, Kimberley Bioregion. Northwest Australia Coral Reefs. doi:10.1007/s00338-016-1424-1

Teichert C, Fairbridge RW (1948) Some coral reefs of the Sahul Shelf. Geogr Rev 28(2):222–249

Veron JEN (2000) Corals of the world. Australian Institute of Marine Science, vols 1–3

Wentworth CK (1922) A scale of grade and class terms for clastic sediments. J Geol 30(5):377–392

Wilson BR (2013) The biogeography of the Australian North West Shelf: Environmental change and life's response. Elsevier, Burlington, MA

***Geomorphology and Holocene Evolution of Kimberley Coral Reefs***

Giada Bufarale[1, 3], Lindsay B. Collins[1, 3], Michael J. O'Leary[2, 3], Alexandra Stevens[1, 3], Moataz Kordi[1, 3], Tubagus Solihuddin[1, 3]

1 Department of Applied Geology, Curtin University, GPO Box U1987, Perth, WA 6845, Australia
2 Department of Environment and Agriculture, Curtin University, Bentley, Western Australia, 6102
3 The Western Australian Marine Science Institution, Floreat, Western Australia, 6014

This is an Accepted Manuscript of an article published in Proceedings of the 13th International Coral Reef Symposium, Honolulu: 243-253. Session: Coral reef records of sea level, climatic and environmental changes: a tribute to Lucien Montaggioni

## Abstract

The Kimberley Bioregion (NW Australia) is characterised by the largest macrotides of any tropical region in the world (about 11 m), frequent tropical cyclones and high-turbidity. Despite these challenging environmental conditions, the region is also known for extensive and diverse intertidal coral reef habitats. While the area has been recognised as an international biodiversity hotspot, it is still poorly investigated compared to other reefal ecosystems in Australia, primarily due to its extreme remoteness and lack of infrastructure.

A combination of remote sensing, sub-bottom profiling and associated sedimentological work produced a geodatabase of coral reefs, providing the first detailed geospatial study of coral reefs within the bioregion. More than 800 reefs have been documented and a regional reef geomorphic classification scheme, which includes a new “high intertidal” geomorphic class of reef, was developed. Reef coring shows that reef growth began soon after the post-glacial flooding of the antecedent substrate.

High-resolution seismic data, acquired along selected reefs, showed that pre-existing substrate has influenced the successive reef morphology. Global sea-level changes, controlled by ice age fluctuation events, are recorded as successive stages of the reef growth, separated by growth hiatuses. Two seismic reflectors can be distinguished, marking the boundaries between Holocene (Marine Isotope Stage 1, last 12,000, 10-20 m thick) and Last Interglacial (MIS5, 125,000 BP, 12 m thick) reefs and an ancient Neoproterozoic rock foundation.

## Introduction

The Kimberley region is located on the north-west of Australia (Figure 1) and is characterised by unique coastal and marine habitats, rich in biodiversity (Wilson 2013; Collins et al. 2015; Kordi et al. 2016), which endure macrotidal conditions of up to 11 m in range (Cresswell and Badcock, 2000), high turbidity and frequent high-energy cyclonic events (Brocx and Semeniuk, 2011). The geology and geomorphology of the Kimberley is also very complex, influenced by ancient folded and faulted Proterozoic metasedimentary and igneous rocks, resulting in an extremely irregular and indented ria coastline (Tyler et al., 2012). During the Quaternary, tectonism in terms of subsidence has been significant (around 0.11 m/ky during the last 18 ky. Solihuddin et al. 2015), determining much of the modern landforms and shore marine biota (Sandiford, 2007). The progressive drowning of the inner shelf of the region has determined, in particular, the development of coral reef systems. The sea level oscillations during the Last Interglacial and Holocene have also conditioned the reef growth (Wilson, 2013; Collins et al., 2015; Bufarale et al., 2016).

Despite been recognised as one of the most important biodiversity hotspots worldwide (Wilson, 2013), the extensive onshore coral reef systems remained very poorly studied until 2013, when the Western Australian Marine Science Institution (WAMSI) developed the Kimberley Marine Research Program (KMRP) Science

Plan. This research plan aimed to improve the understanding of the marine environment of the Kimberley and close the gap in the scientific knowledge of this area. Since then, a total of 26 projects have been studying different aspects of the biology, geology and ecology in the Kimberley coastal region (WAMSI, 2012). This paper summarises the research that was undertaken to investigate the stratigraphic and geomorphic evolution and distribution of several Kimberley reefs and determine their interaction with different substrates, morphological patterns and coastal processes (WAMSI Project 1.3.1).

## Materials and methods

The research used a combination of three different methods. Remote sensing data were used to map the geomorphological surface cover of the Kimberley Reef and evaluate their extension, in order to create a geodatabase of the main reefs, together with a new reef classification scheme specific for this area. Geomorphic surveys aimed to study the geomorphology, elevation, composition and age of selected reefs. Coring and seismic surveys determined the reef architecture and thickness and determined the growth pattern and stages of reef buildups.

### Remote sensing analysis

Aerial and satellite images were used to produce classification maps of the reef flat geomorphology and substrates and spatial distribution maps of the Kimberley reefs and islands (Kordi and O'Leary 2016a; 2016b). Using GIS Software (Geographic Information System; ArcGIS® by Esri) and ENVI 4.3 Software, unsupervised classification was performed in order to produce consistent data. Existing literature on Kimberley reefs (particularly from Wilson et al., 2011; Richards et al., 2013 and WA Museum Woodside Collection, 2008 – 2012), combined with the information collected during this research project, provided the necessary ground truth information (Kordi et al., 2016).

### Geomorphic surveys

Access to a complete record of coral growth was possible thanks to two large iron ore pits on Cockatoo Island (Buccaneer Archipelago. See location in Figure 1), which have left exposed the whole coral reef stratigraphy and pre-existing substrate to depth of approximately 50 m below sea level. Solihuddin et al. (2015) logged, sampled and recorded the main stratigraphic information (reef framework / matrix ratio, texture, coral identification, matrix carbonate content) of two complete vertical and horizontal sections. These data were compared and correlated with the coral distribution along the reef flat and fore-reef slope of the fringing reef that rims the island, using towed camera and visual observations.

Samples for radiocarbon dating were also collected, in order to establish a geochronology of the reef growth.

Reef elevation was measured using an Odom ES3 multibeam echo sounder combined with a Valeport sound velocimeter, a TSS 355B motion sensor and an iX

Blue Octans gyro compass. A Differential Global Positioning System (DGPS) Trimble Net R9 provided accurate positioning (±2 cm).

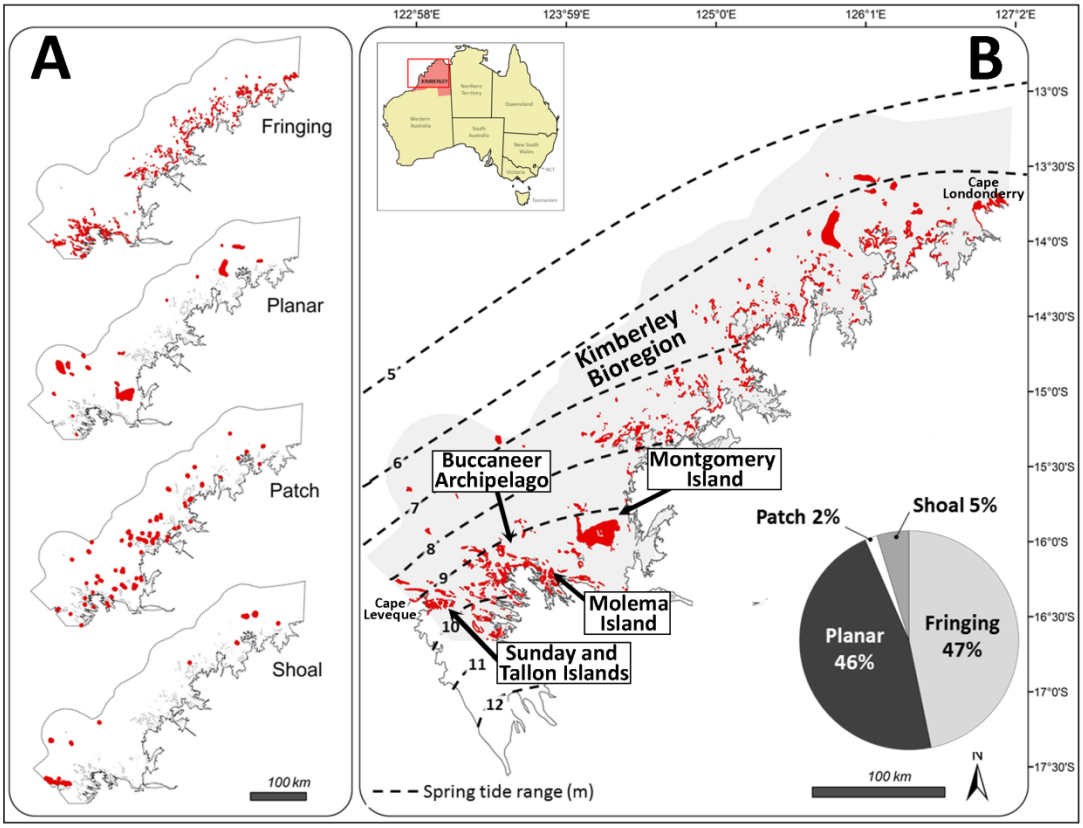


**Figure 1. A) Reef distribution in the Kimberley Bioregion by type: fringing; planar; patch; and shoals. B) Distribution map of reefs with spring tidal range contours (modified after Kordi and O'Leary, 2016b). The reefs seismically surveyed in this study are labelled. The inset shows the percentage of each reef type.**

## Seismic and coring surveys

About 300 km of high-resolution shallow seismic data were acquired, using an AA201 boomer SBP system (Applied Acoustic Engineering Limited, Great Yarmouth, UK), combined with a DGPS Fugro SeaSTAR 8200 XP/HP. The seismic profiles were digitally recorded using SonarWiz 5 (Chesapeake Technology Inc., Mountain View, CA) as acquisition and post-processing software.

The information provided by the Cockatoo Reef study (from Solihuddin et al., 2015) provided a calibration for the acoustic datasets. The reef proximal to the mine pits of Cockatoo Island was examined in detail, serving as a base for the seismic correlation. Within the Buccaneer Archipelago, the neighbouring reefs of Irvine and Bathurst Islands were also surveyed to verify the consistency of the seismic correlation. Montgomery Island was selected as special type of planar reef. Molema, Sunday and Tallon Islands were targeted because of their variety of fringing reef types (see location in Figure 1). The survey lines were planned to target the orientation, internal architecture and morphology of the reefs.

A total of 42 cores, along the seismic lines and up to 6.5 m long, were obtained by percussion coring and rotary drilling. The sediments were logged and dated using the same parameters adopted for the mine pit samples (from Solihuddin et al., 2016).

# Results

## Classification and distribution maps

High-resolution images, combined with other relevant data (such as bathymetric charts and ground-truth information) were used by Kordi et al. (2016) to map the extent of the Kimberley coastline and quantify the distribution of reefs and islands. More than 800 nearshore reefs and 2400 islands were recorded, along 5300 km of coastline (Figure 1), between Cape Leveque and Cape Londonderry. A total of 30 reefs were mapped in detail, producing as many geomorphic maps. In each map five reef geomorphologic zones were defined (land, reef flat, lagoon, reef crest and fore-reef slope, see example in Figure 2). Habitats and substrates maps were also drawn, recording up to seven feature classes (mangroves, sand, seagrass and algae, coral rubble, reef pavement with algal turf, crustose coralline algae and coral communities).

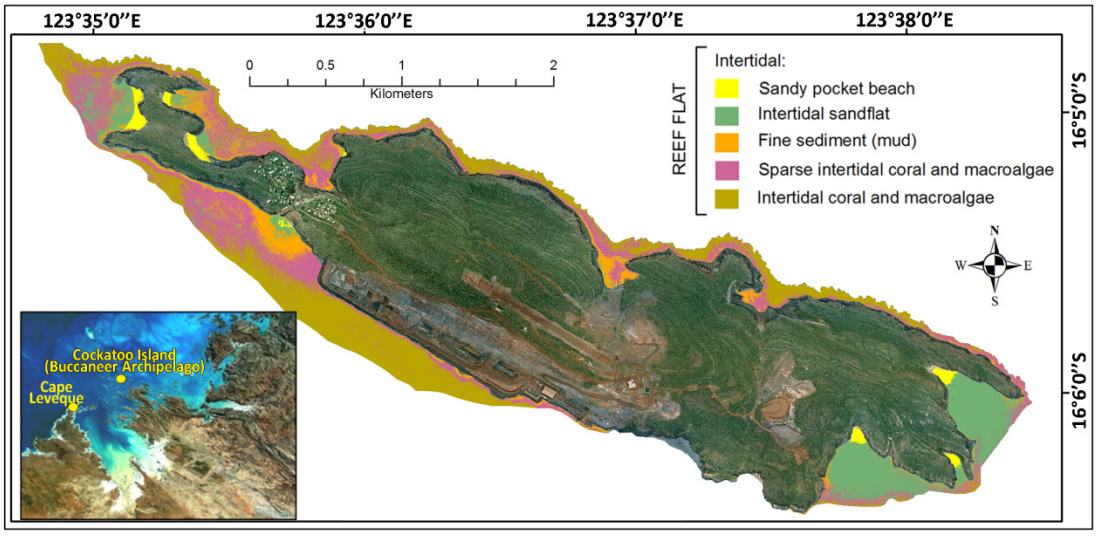


**Figure 2. Map showing Cockatoo Island geomorphic and substrate classification, based on aerial photography interpretation (modified after Solihuddin et al., 2015). Inset: Landgate photography provided by the Department of Parks and Wildlife (DPaW).**

## Geomorphology and geochronology

Solihuddin et al. (2015) documented the lithostratigraphic and chronostratigraphic history of a coral reef exposed in mine pits at Cockatoo Island.

Stratigraphic and palaeoecological data, combined with radiometric dates revealed that the lower section of the mine pit is composed of Proterozoic Elgee Siltstone, which represents the basal substrate for the successive reef deposits (Solihuddin et al., 2015). Atop the basement, a thin layer (1–2 m) of sedimentary talus breccia and

haematite boulders is present. Overlying the haematitic breccia, a sandy coral-rich unit, up to 7 m thick, can be recognised. Dating revealed that the growth of this buildup (mainly composes of *Faviids* domal corals) initiated during the Last Interglacial highstand (Solihuddin et al., 2015). Above this ancient reef formation, a second, thinner, haematite boulder breccia layer divides this unit from an additional reef unit. This shallower reef buildup is at least 9-13 m thick and characterised by muddy domal and branching coral framestone (mainly coral clasts of *Acropora* and *Porites*), with several fragments and whole molluscs (Solihuddin et al., 2015). Results from radiocarbon dating indicated that these are Holocene corals that started colonising the pre-existing topography approximately between 9070 and 8840 years ago.

Towed camera observations provided information about the living reef. Similarly to the mine pit findings, *Porites* and *Faviids* are the most abundant genus, along with *Sargassum* and *Millepora* which are not present in the fossil record.

Coring surveys conducted on the reefs of Tallon Island, Sunday Island and Irvine/Bathurst islands extended the study on reef flat habitats undertaken at Cockatoo Island (Solihuddin et al., 2016). Multibeam echo sounding surveys recorded and measured the seabed elevation, providing further information about these reefs. Low intertidal reefs, where reef flat elevation is approximately mean low water spring, are largely composed of coral colonies and coral fragments in a muddy to sandy matrix. High intertidal reefs, which have a reef flat elevation between mean low water neap and mean high water neap, are dominated by coralline algae terraces.

### Internal reef architecture

The post-processing of the seismic profiles showed that the stratigraphy underneath the modern reef flats is characterised by two main units (U1, U2), overlaying the rock foundation (RF). During the analysis and interpretation of the seismic datasets, the seismic reflectors that define U1 and U2 were considered on the basis of their relative vertical and lateral position and reflection characteristics. The distinctive features of each main reflector can be recognised across the study area and be identified through the correlation with the Cockatoo mine pit sections (Table 1).

## Discussion

These new datasets provided a better understanding of Quaternary reef growth in the Kimberley region of Western Australia. Some of the key interacting factors in coral reef classification and growth include morphology, physical processes, antecedent topography and sea level change. By developing an understanding of seismostratigraphic events, it has been possible to document the subsurface evolution and growth history of diverse reefs in the Kimberley, at the scale of multiple reef building stages correlated to the Marine Isotope Curve. The seismic unit U1 bounded by the seafloor and reflector R1 represents the Holocene reef/sediment buildup (Figure 3). Between the Proterozoic rock foundation (RF) and the Holocene reef buildup, the Pleistocene calcretised reef unit, related to the Last

Interglacial (LIG, MIS 5e, ~ 125 ky BP) sea level highstand, is present (Bufarale et al., 2015; Collins et al., 2015; Bufarale et al., 2016).

A comprehensive geodatabase (ReefKIM) was proposed to organise and integrate the results obtained through the remote sensing analysis and stratigraphic and seismic surveys, together with a new reef classification scheme specific for the Kimberley Bioregion.

**Table 1. Facies identified in the seismic profiles.**

| Seismic unit | Limits | Thickness | Internal structure | Correlation with mine pit stratigraphy |
|---|---|---|---|---|
| U1 | Seafloor to R1 | Variable: 7-22 m | *Under the reef platform*: hard and locally moderately layered (sub-reflectors H1, H2 and H3), locally chaotic. | *Under the reef platform*: Holocene reef |
| | | | *Elsewhere*: very well-layered, with parallel to subparallel continuous laminations | *Elsewhere*: sediment bodies |
| U2 | R1 to RF | Variable: 7-12 m | Mainly without internal structure; locally with discontinuous, sub-parallel minor reflectors | LIG reef |
| Basement | RF-NA | NA | Laminated to massive, locally chaotic. Valley-like depressions and ridges recognisable | Proterozoic metasediments |

## ReefKIM Geodatabase

All the project' findings about the spatial distribution of reefs and islands, the habitat/substrate classification maps and the geological and biological datasets available for the Kimberley reefs were georeferenced and integrated together to create ReefKIM, a data fusion geodatabase (Kordi et al., 2016). This GIS-based database can be considered a significant conservation and decision-support method under several aspects. For instance, it provides researchers with an overview of essential information on many Kimberley reefs, especially those considered "atypical" and it can be used as a main platform for further reef census data. ReefKIM can also be updated with a variety of types of marine environment-related information, sourced from different studies and works in the Kimberley Bioregion including crowdsourcing (Kordi et al., 2016).

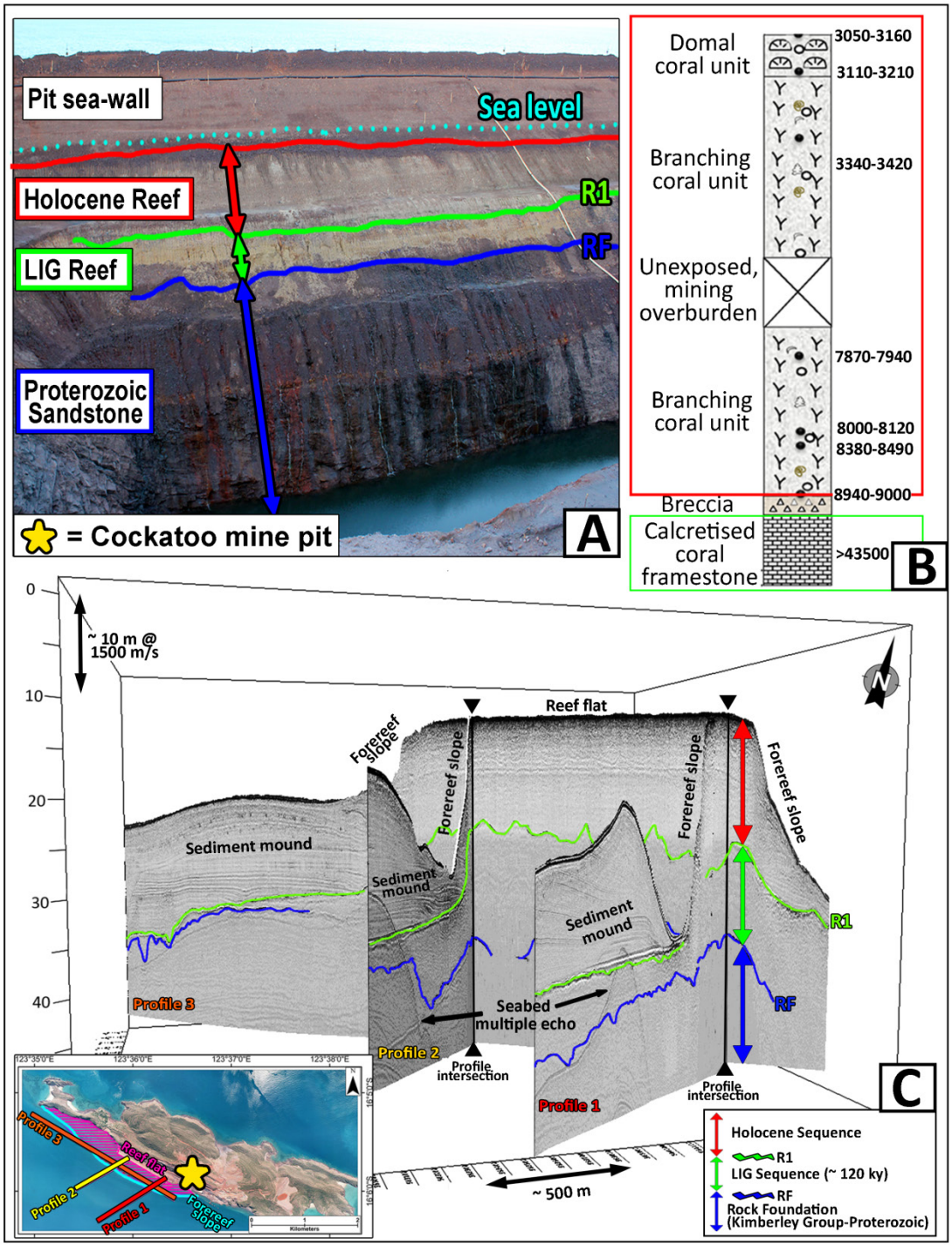


**Figure 3. A) Cockatoo mine pit section looking south west (Photograph credit: Solihuddin T., 2013). The marked lines represent: top of the Holocene reef (red), top of Last Interglacial reef (green) and top of Proterozoic rock (blue). Modified after Collins et al. 2015 and Bufarale et al., 2016. B) Reef lithostratigraphic column, with radiocarbon ages (Solihuddin et al., 2015). C) Intersecting cross-sections (Profiles 1 and 2) and distal longitudinal section (Profile 3) of seismic profiles adjacent to the mine pit. Depth values are in metres, below the sea level. Inset: Landgate aerial photography provided by DPaW.**

## Kimberley reef classification scheme

A number of reef classifications based on geomorphic attributes are present in literature (i.e. Fairbridge, 1950; Hopley et al., 2007; Wilson, 2013) but they all lack the information to enumerate the high intertidal reefs, which are a unique feature of macrotidal reefs and characteristic of the Kimberley. In order to include this highly-specialised type of reef recognised by Wilson (2013) and confirmed by Solihuddin et al. (2016), a revised reef geomorphic classification scheme, specific for this project, was proposed by Bufarale et al. (2016). The classification comprises a hierarchical subdivision of the reefs. In the first order the reefs are divided into high intertidal, intertidal and subtidal on the basis of their elevation. The second rank is based on reef geomorphology and comprises fringing reefs, planar reefs, patch reefs and shoals. The third level further subdivides each reef type according to their configuration in relation to the shoreline and architecture. In this level, five main types of fringing reef are described (bay head, interisland, circum island, headland and narrow beach base) and two for each other reef (planar reefs: sand lagoon or coralgal; patch reefs: irregular or unbroken margins; shoal: sand or coral. Bufarale et al., 2015).

## Acknowledgements

The project was funded by the Western Australian Marine Science Institution and supported by the Western Australian State Government. This research was assisted by the Bardi Jawi, Mayala and Dambimangari people, the Traditional Owners of these lands, Kimberley Marine Research Station and Cygnet Bay Pearl Farm staff, Western Australia Museum, Kimberley Media, Pluton Resources Ltd, Dr David Blakeway (MScience Ltd).

Gilbert Camoin and Jody Webster are thanked for chairing the session “Coral reef records of sea level, climatic and environmental changes: a tribute to Lucien Montaggioni” at the 13th International Coral Reef Symposium and reviewing this manuscript.

## Reference List

Brocx M, Semeniuk V (2011) The global geoheritage significance of the Kimberley coast, Western Australia. J R Soc West Aust 94:57–88

Bufarale G, Collins LB, Leary MO (2015) Sub-bottom profiling and growth patterns of Kimberley coral reefs, North West Australia. J R Soc West Aust. 98: 95–96

Bufarale G, Collins LB, O’Leary MJ, Stevens A, Kordi M, Solihuddin T (2016) Quaternary onset and evolution of Kimberley coral reefs (Northwest Australia) revealed by high-resolution seismic imaging. Cont Shelf Res 123:80–88

Collins LB, O’Leary MJ, Stevens AM, Bufarale G, Kordi M, Solihuddin T (2015) Geomorphic patterns, internal architecture and reef growth in a macrotidal, high-turbidity setting of coral reefs from the Kimberley Bioregion. Australian Journal of Maritime and Ocean Affairs 7:12–22

Cresswell, G. R., Badcock, K. A. (2000). Tidal mixing near the Kimberley coast of NW Australia. Mar. Freshw. Res.51: 641 – 6

Fairbridge RW (1950) Recent and Pleistocene Coral Reefs of Australia. JSTOR 58:330–401

Hopley D, Smithers SG, Parnell KE (2007) The geomorphology of the Great Barrier Reef: development, diversity and change. Cambridge University Press, New York

Kordi MN, Collins LB, O'Leary M, Stevens A (2016) ReefKIM: An integrated geodatabase for sustainable management of the Kimberley Reefs, North West Australia. Ocean Coast Manag 119:234–243

Kordi MN, O'Leary M (2016a) A spatial approach to improve coastal bioregion management of the north western Australia. Ocean Coast Manag 127:26–42

Kordi MN, O'Leary M (2016b) Geomorphic Classification of Reefs in the North Western Australia Shelf. Regional Studies in Marine Science, DOI 10.1016/j.rsma.2016.05.012

Richards ZT, Bryce M, Bryce C (2013) New Records of Atypical Coral Reef Habitat in the Kimberley, Australia. J Mar Biol 2013:1–8

Sandiford M (2007) The tilting continent: A new constraint on the dynamic topographic field from Australia. Earth Planet Sci Lett 261:152–163

Solihuddin T, Collins LB, Blakeway D, O'Leary MJ (2015) Holocene coral reef growth and sea level in a macrotidal, high turbidity setting: Cockatoo Island, Kimberley Bioregion, northwest Australia. Mar Geol 359:50–60

Solihuddin T, O'Leary MJ, Blakeway D, Parnum I, Kordi M, Collins LB (2016) Holocene reef evolution in a macrotidal setting: Buccaneer Archipelago, Kimberley Bioregion, Northwest Australia. Coral Reefs

Tyler IM, Hocking RM, Haines PW (2012) Geological evolution of the Kimberley region of Western Australia. Episodes 35:298–306

Wilson B, Blake S, Ryan D, Hacker J (2011) Reconnaissance of species-rich coral reefs in a muddy, macro-tidal, enclosed embayment, - Talbot Bay, Kimberley, Western Australia. J R Soc West Aust 94:251–265

Wilson BR (2013) The biogeography of the Australian North West Shelf: environmental change and life's response. Elsevier, Burlington MA

Western Australia Marine Science Institute, WAMSI (2012). Kimberley Marine Research Program. http://www.wamsi.org.au/kimberley-marine-research-program-1 (accessed 08.06.2016).

Western Australian Museum Woodside Collection Project (Kimberley) 2008-2012.

## Appendix C: Supervisor and Co-authors Statements

To whom it may concern:

I, **Michael J. O'Leary**, have contributed as supervisor, technical advisor and through mentoring to three research papers as part of a PhD thesis prepared for Curtin University by Giada Bufarale.

I am also listed as co-author of the papers referred to below and did so in my capacity as PhD Supervisor.

List of articles:

Bufarale, G., Collins, L.B., O'Leary, M.J., Stevens, A., Kordi, M., Solihuddin, T., 2016. Quaternary onset and evolution of Kimberley coral reefs (Northwest Australia) revealed by high-resolution seismic imaging. Cont. Shelf Res. 123, 80–88.

Bufarale, G., O'Leary, M., Stevens, A. and Collins, L.B., 2017. Sea level controls on palaeochannel development within the Swan River estuary during the Late Pleistocene to Holocene. CATENA, 153, pp.131-142.

The papers take part of the PhD thesis and first author is Giada Bufarale.

(Supervisor and co-author signature)

Michael J. O'Leary

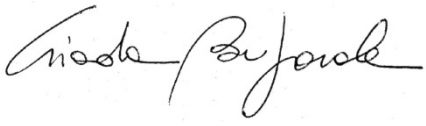

(Candidate signature)

Giada Bufarale

To whom it may concern:

I, **Alexandra Stevens**, have participated in seismic data acquisition and advisor for the articles:

Bufarale, G., Collins, L.B., O'Leary, M.J., Stevens, A., Kordi, M., Solihuddin, T., 2016. Quaternary onset and evolution of Kimberley coral reefs (Northwest Australia) revealed by high-resolution seismic imaging. Cont. Shelf Res. 123, 80–88.

Bufarale, G., O'Leary, M., Stevens, A. and Collins, L.B., 2017. Sea level controls on palaeochannel development within the Swan River estuary during the Late Pleistocene to Holocene. CATENA, 153, pp.131-142.

The papers take part of the PhD thesis and first author is Giada Bufarale

(Co-author signature)

Alexandra Stevens

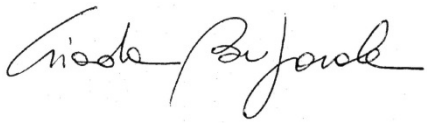

(Candidate signature)

Giada Bufarale

To whom it may concern:

I, **Tubagus Solihuddin** have participated in seismic data acquisition for the article:

Bufarale, G., Collins, L.B., O'Leary, M.J., Stevens, A., Kordi, M., Solihuddin, T., 2016. Quaternary onset and evolution of Kimberley coral reefs (Northwest Australia) revealed by high-resolution seismic imaging. Cont. Shelf Res. 123, 80–88.

The paper takes part of the PhD thesis and first author is Giada Bufarale

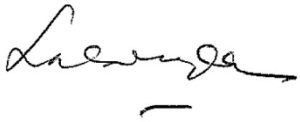

(Co-author signature)

Tubagus Solihuddin

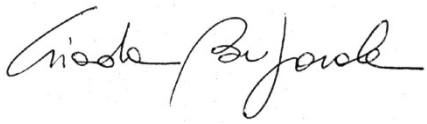

(Candidate signature)

Giada Bufarale

To whom it may concern:

I, **Moataz Kordi** have participated in seismic data acquisition for the article:

Bufarale, G., Collins, L.B., O'Leary, M.J., Stevens, A., Kordi, M., Solihuddin, T., 2016. Quaternary onset and evolution of Kimberley coral reefs (Northwest Australia) revealed by high-resolution seismic imaging. Cont. Shelf Res. 123, 80–88.

The paper takes part of the PhD thesis and first author is Giada Bufarale

(Co-author signature)

Moataz Kordi

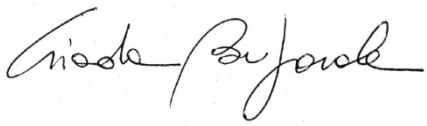

(Candidate signature)

Giada Bufarale

To whom it may concern:

I, **Julien Bourget,** have contributed as advisor for the article:

Bufarale, G., O'Leary, M., Bourget, J. Unpublished. Sea level controls on the geomorphic evolution of Geographe Bay, South-West Australia.

The paper takes part of the PhD thesis and first author is Giada Bufarale

(Co-author signature)

Julien Bourget

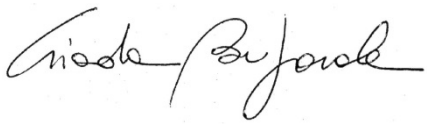

(Candidate signature)

Giada Bufarale